UNIVERSITY OF TURIN

PhD School in Life and Health Sciences

Molecular Medicine

Identification and characterization of host cellular pathways exploited by dsDNA viruses to enhance infection and pathogenesis

Camilla Albano

UNIVERSITY OF TURIN

Department of Molecular Biotechnology and Health Sciences

PhD School in Life and Health Sciences

Molecular Medicine

XXXV cycle

Academic Years 2019-2023

Identification and characterization of host cellular pathways exploited by dsDNA viruses to enhance infection and pathogenesis

Tutor: Candidate:
    Prof. Santo Landolfo (2019-2020)   Camilla Albano
    Prof. Valentina Dell'Oste (2020- 2023)

Coordinator: Student ID:
    Prof. Francesco Novelli   654284

Scientific sector: MED/07

CONTENTS

ACKNOWLEDGEMENT

Lastly, to myself: throughout these years, I have faced numerous challenges, have been overwhelmed and endured considerable pain, yet I have summoned enough strength to achieve this significant milestone in my career.

INTRODUCTION

Viruses are fascinating entities, straddling the line between living and non-living. As obligate intracellular parasites, viruses exploit host cells and manipulate cells' molecular machinery to replicate, amplify, and subsequently spread from cell to cell and from host to host. A profound comprehension of the intricate interactions between viruses and hijacked cellular pathways is essential for the development of efficacious treatments and preventive strategies for viral diseases.

In the present Doctoral Thesis, I illustrate the two primary research topics pursued during my Ph.D., shedding light on cellular pathways exploited by dsDNA viruses.

In the first part, I delve into the role of PAD-mediated citrullination, a post-translational modification, in the context of HPV-driven transformation of epithelial cells.

Subsequently, in the second part, I unveil the manipulation of lipid metabolism by HSV-1, particularly *de novo* lipogenesis, thus uncovering its potential correlation with Alzheimer's Disease and highlighting novel potential therapeutic targets.

PART I

1. CITRULLINATION

1.1 PAD-mediated citrullination

Protein expression undergoes various levels of regulation, encompassing transcriptional, post-transcriptional, and translational mechanisms, which collectively determine whether a protein is expressed within a cell. Post-translational modifications (PTMs) are enzymatic and non-enzymatic processes that chemically modify proteins, determining changes in protein structure, stability, sub-cellular localization, and function, as well as modulating the binding affinity to other proteins, metabolites, and nucleic acids. Protein modifications are tightly regulated, allowing cells to respond to environmental changes such as stress, developmental cues, fluctuations in nutrients or oxygen, and oncogenic insults. To date, over 200 types of PTMs, including citrullination, have been documented[1].

Citrullination, also known as peptidylarginine deimination, is the irreversible post-translational conversion of an arginine residue to citrulline, in which the guanidinium group of a peptidylarginine is hydrolyzed to a ureido group thereby forming the non-genetically coded amino acid citrulline. This enzymatic transformation results in the loss of a positive charge and an increase in molecular mass of 0.984 Da per deimination. The family of cellular enzymes responsible for the calcium-dependent deamination of an arginine to a citrulline is known as peptidylarginine deiminases (PADIs or PADs) (Figure 1). Comprising five PAD isoforms—PAD1, PAD2, PAD3, PAD4, and PAD6—these enzymes share structural similarities but exhibit differences in tissue distribution, subcellular localization, and protein targets, indicating distinct biological roles[2,3].
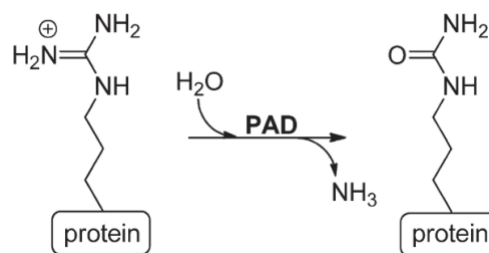

Figure 1. Citrullination (deimination) of peptidylarginine by PAD. The guanidino group of arginine is hydrolyzed yielding a ureido group and ammonia[4].

Depending on the specific site of the conversion within the protein, it has the potential to modify local electrostatic interactions and hydrogen bonding capabilities. This, in turn, induces

alterations in various aspects of protein dynamics, including structure, stability, localization, as well as binding to proteins and nucleic acids, catalytic activity, and the subsequent incorporation of additional post-translational modifications[5]. Through these changes in citrullinated proteins, PADs play a pivotal role in regulating fundamental physiological processes such as gene expression, chromatin compaction, and the innate immune response to bacterial infections.

Notably, the dysregulation of PADs is strongly implicated in the pathogenesis of various diseases, including autoimmune conditions (*i.e.,* rheumatoid arthritis, ulcerative colitis, psoriasis, and type I diabetes), neurodegenerative disorders (*i.e.,* multiple sclerosis, Alzheimer's, and prion diseases), and cancer[6–11]. Conversely, the loss of PADI activity has been associated with compromised neurodevelopment, fertility, and embryo development[12–14].

1.2 PAD family

The presence of citrulline residues in proteins can be traced back to 1939. Subsequently, in the 1950s, citrulline was identified in the red alga Chondrus crispus by Smith and Young[15]. In the early 1960s, for the first time, citrulline residues were discovered in animal proteins, specifically in the polypeptide hydrolysates of hair inner root sheath cells and medullary cells[16,17]. Since there is no citrulline tRNA, the presence of citrulline amino acids in proteins can only result from PTMs. Although the existence of this uncoded amino acid was well-established, the enzymatic process remained unclear until 40 years ago when the first PADI was isolated[18].

In the tree of life, PADIs are widespread across vertebrates, ranging from fish to mammals, absent in yeast, worms, and flies, and present in some bacteria and fungi. However, the function of PADs in these microorganisms is unknown. Phylogenetic and sequence evolution studies suggest that PADIs were introduced into animals by cyanobacteria through horizontal gene transfer. Subsequent duplications along the vertebrate lineage led to five paralogues in mammals (PAD1-4 and PAD6)[19].

The five PAD isoforms are incapable of converting free L-arginine to L-citrulline without the presence of calcium as a cofactor. In physiological conditions, the basal intracellular calcium levels (ranging from 10^{-5} to 10^{-3} mM) are insufficient to activate PADs. This suggests that the citrullination of substrate proteins and PAD activation are intricately linked to biological events characterized by an alteration of calcium homeostasis, such as cell death and epidermal

differentiation. Supraphysiological levels of calcium can be achieved through either extracellular calcium influx or the release from intracellular calcium stores, primarily the endoplasmic reticulum, but also including mitochondria, secretory granules, and the nuclear envelope, where calcium ions are bound to calcium-binding proteins[20].

In humans, the genes encoding PAD isozymes are situated within a single gene cluster spanning 334.7 kb on chromosome 1p36.1 (Figure 2A). These genes share the same exon/intron structure and exhibit a high degree of sequence similarity in their exons. Consequently, the conservation in amino acid sequence among the five paralogues in humans is approximately 50-55% homology. However, when comparing all mammalian PAD isozymes, this homology increases to a range of 70-95%. Notably, the elevated identity levels are not uniformly distributed across the protein sequences[21].
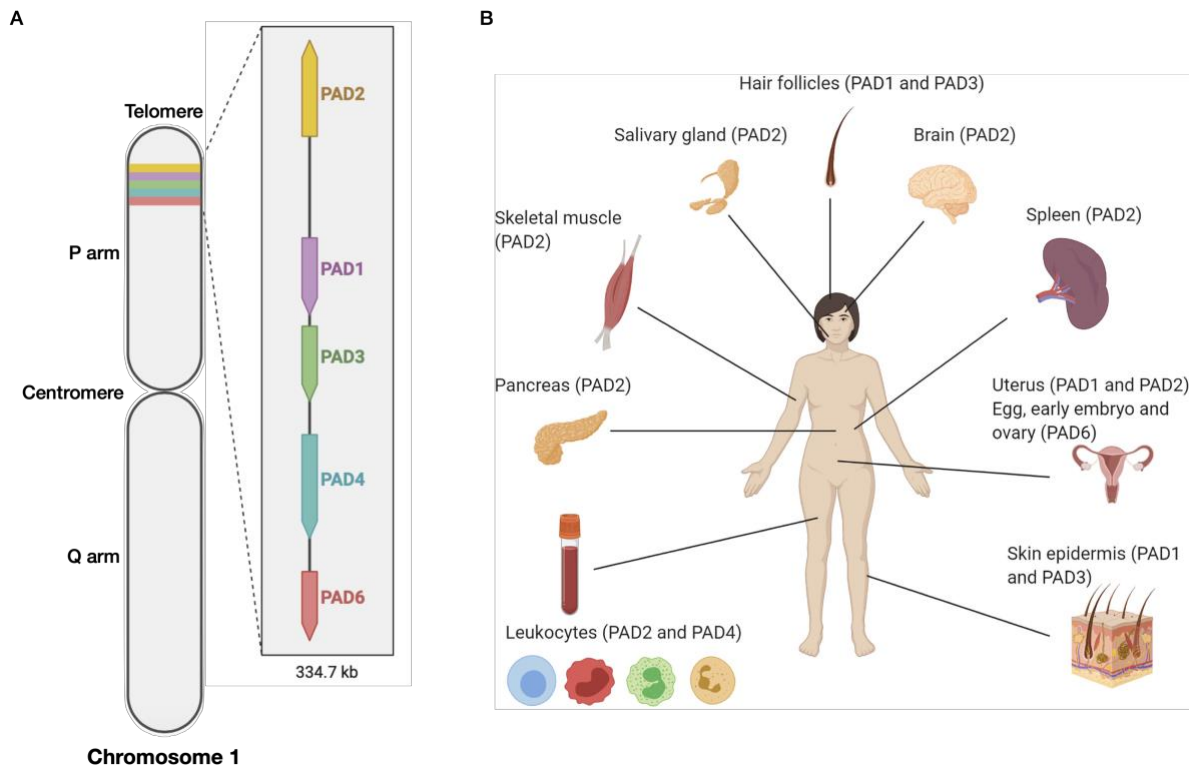
Figure 2. A) Genomic organization of PAD gene clusters. Ideograms of human chromosome 1 showing the location and orientation of the PAD gene clusters[22]. B) Illustration of the organ-specific protein expression of PAD isozymes in humans[23].

PAD proteins consist of three distinct domains: two N-terminal immunoglobulin (IgG)-like domains, IgG1 and IgG2, and a C-terminal catalytic domain, that display greater conservation than the previous ones[24]. Interestingly, PAD4 stands out as the sole isoform featuring a unique nuclear localization signal (NLS) at the N-terminal, enabling its presence in the nucleus where

it catalyses the citrullination of nuclear proteins[25]. Additionally, to PAD4, PAD2 has been identified in the nucleus despite lacking any NLS[26], while all PAD isozymes predominantly reside in the cell cytoplasm.

Currently, crystal structures are available for PAD1 (PDB ID: 5HP5), PAD2 (PDB ID: 4N28), PAD3 (PDB ID: 6CE1), and PAD4 (PDB ID: 3APN), but not for PAD6[27]. While PAD2, PAD3, and PAD4 are observed as homodimeric proteins, forming a head-to-tail dimer where monomers interact with each other (the C-terminal domain is linked to the IgG2 of the N-terminal domain), the structural analysis of PAD1 indicates its existence as a monomer. A crucial finding suggests that a specific residue at position 8 plays a pivotal role in the dimerization process. PAD2, PAD3, and PAD4 feature an arginine residue at position 8, contributing to the stability of the homodimeric structure, whereas PAD1 has a glutamine residue at this position. Moreover, in the absence of a crystal structure for PAD6, it is postulated that PAD6 exists as a monomer, akin to PAD1, primarily due to the lack of an arginine residue at position 16 (also referred to as position 8 in the context of other PAD proteins). Moreover, the homodimerization of PADs is not calcium-dependent but appears to be crucial to maximize the calcium-binding capacity and the enzymatic activity[28].

1.3 Tissue specificity and biological functions of PADs

PADs differ in their subcellular localization, tissue distribution, and substrate specificity (Figure 2B). As mentioned earlier, all PAD proteins are localized in the cytoplasm. However, it is noteworthy that PAD4 and PAD2 exhibit additional localization, with PAD4 expressed on the cellular membrane of neutrophils, PAD2 being released into the extracellular space by neutrophils, and both proteins are found in the cellular nucleus[21].

PAD1 is predominantly expressed in the epidermis, uterus, and hair follicles. In the epidermis, PAD1 plays a crucial role in the terminal differentiation of keratinocytes, citrullinating keratins (K1 and K10), thereby regulating their content, and profilaggrin, which is then cleaved into filaggrin, an important protein in retaining moisture[29]. Although PAD1 is expressed in both male and female reproductive systems, its relevance is particularly pronounced in female fertility. In the uterus, PAD1 expression increases following estradiol injection, contributing to female maturation, and actively citrullinates histone tails during oocyte maturation, influencing the intricate processes of reproductive development. Moreover, PAD1 regulates transcription

by citrullinating histones H4 R3 and H3 R2/8/17 during the early stages of embryonic development, thereby promoting the production of 2- or 4-cell embryos[30].

PAD2 stands out as the ubiquitous member within the family, expressed in diverse tissues such as the brain (including astrocytes, microglia, Schwann cells, and oligodendrocytes), uterus, spleen, pancreas, skeletal muscle, secretory glands, and leucocytes. Within the central nervous system (CNS), PAD2 plays a crucial role in deiminating myelin basic protein (MBP), thereby influencing the organization of myelin. This impacts on the lipid-protein arrangement in the neural plasma membrane resulting in a modulation of myelin structural integrity. While this phenomenon can contribute to plasticity in growing children, it also has implications for compromised saltatory conduction, as observed in conditions such as multiple sclerosis (MS). Additionally, PAD2 targets other cerebral substrates, including two cytoskeletal proteins, glial fibrillary acidic protein (GFAP) and vimentin, with a primary focus on their involvement in neurodegenerative diseases. In skeletal muscle and macrophages, PAD2 exhibits citrullination activity on vimentin, acts on actin in neutrophils, and modifies histones in various cell types. This multifaceted enzymatic activity underscores the diverse and vital roles played by PAD2 across different tissues and cellular contexts[29].

PAD3 is localized in hair follicles and epidermis, where it citrullinates filaggrin, trichohyalin, and vimentin. Additionally, PAD3 is expressed in human neural stem cells, playing a regulating role in apoptosis during neural development by deaminating apoptosis-inducing factor (AIF)[31].

PAD4, formerly known as PAD5, is expressed in leukocytes, monocytes, and macrophages, as well as in bone marrow, brain, lung, and adipose tissue. Distinctively, it is the only PAD isozyme with an NSL, enabling it to target various nuclear proteins, primarily histones. This targeting influences gene expression by directly impacting chromatin organization or recruiting other transcriptional mediators. Furthermore, PAD4 modulates gene expression by citrullinating nonhistone substrates, such as inhibitor growth 4 (ING4), a tumour suppressor that when citrullinated failed to activate p53 transcription. With its high expression in neutrophils, PAD4 plays a crucial role in the generation of neutrophil extracellular traps (NETs), contributing significantly to the first line of defence against bacterial pathogens[32].

PAD6, the least expressed PAD, is predominantly found in eggs, embryos, and ovaries. Despite lacking catalytic activity *in vitro* and having no identified protein substrates to date, PAD6

expression correlates with citrullination in female germ cells. Moreover, it proves to be indispensable in early embryo development, akin to the role played by PAD1[33].

1.4 Physiological role of PAD-citrullination

Under typical physiological calcium concentrations, PADs typically remain inactive. However, these enzymes undergo activation in specific circumstances where calcium levels exceed the normal physiological concentration, as observed in apoptosis and terminal epidermal differentiation. Furthermore, activation is not confined to elevated calcium levels, it can also take place at physiological calcium levels, particularly in processes like gene expression regulation[34].

1.4.1 Apoptosis

PADs play a crucial role in apoptosis, as evidenced by their activation following an increase in calcium levels in cells undergoing apoptosis[35]. Once activated, the mechanism by which PADs determine their substrate specificity is not fully understood. However, it is hypothesized that PADs may selectively target nuclear or structural proteins that are arginine-rich or possess arginine-rich regions within their amino acid sequence, causing structural alterations in these proteins, and thereby facilitating apoptotic cell death.

Supporting this hypothesis, vimentin undergoes citrullination during apoptosis in the arginine-rich non-alpha-helical head domain. The deamination of vimentin by PAD2 causes the disassembly of polymers into monomers, preventing their re-joining. This process leads to cellular structural collapse and the induction of apoptosis, particularly in macrophages[36]. Additionally, the overexpression of PAD2 results in vimentin citrullination and apoptosis in Jurkat cells[37].

PAD4 citrullination is involved in apoptosis through two distinct mechanisms. Firstly, PAD4's ability to deiminate histones and nucleophosmin leads to the collapse of the nucleosome and nuclear lamina, thereby initiating apoptosis. Moreover, when PAD4 is overexpressed, it upregulates p53 and stimulates mitochondrial-associated apoptosis[24,38].

In addition to PAD2 and PAD4, PAD3 has been identified as a key contributor to apoptosis. Specifically, PAD3 is found to be necessary for AIF-mediated apoptosis in human neuronal stem cells[39].

1.4.2 Cellular structural support

One of PADs' main targets is structural proteins, thus PADs play a crucial role in cellular organization, particularly in cells undergoing terminal epidermal differentiation. In the epidermis, the activation of PADs, triggered by elevated calcium concentrations during differentiation, allows them to citrullinate crucial structural proteins such as keratin, filaggrin, and vimentin. This citrullination induces a partial unfolding in these proteins, making them more vulnerable to protease degradation[36].

1.4.3 Gene regulation

PADs, particularly PAD4, play a significant role in governing gene expression. Extensive research has delved into PAD4's role in mediating the regulation of the p53 pathway. By citrullinating the ING4 protein, PAD4 reduces its binding to p53, increasing susceptibility to protease degradation and inhibiting the transcriptional targets of p53, such as p21[40]. Furthermore, PAD4 citrullinates methylated arginine on histones (H4 at R3, H3 at R2, R8, R17), inducing gene repression by altering the charge and hindering protein interactions. In particular, the recruitment of PAD4 to p21 gene promoters results in histone citrullination and the repression of p21 expression, as p53 cannot bind to the promoter region[41]. Moreover, PAD4 binds to the promoter region of p53, repressing gene expression through histone citrullination, surpassingly during periods when damage response pathways are unnecessary[42]. This repression is lifted in response to DNA damage, allowing gene activation. PAD4 also functions as a transcriptional coactivator by citrullinating p300, enhancing its interaction with another coactivator, GRIP1[40].

PAD4 is also involved in pluripotency, where it acts as a transcriptional regulator for key genes. It upregulates pluripotent markers, like Nanog, and downregulates differentiation ones, such as WNT8a, thereby impacting stem cell differentiation during embryonic development[43].

1.4.4 Immune response

PAD2 and PAD4 play pivotal roles in inflammatory immune responses. Specifically, PAD4 exhibits predominant expression in macrophages, neutrophils, and eosinophils, whereas PAD2 is highly expressed in macrophages. In macrophages, the activation of PAD2 is initiated by elevated calcium levels. Upon activation, PAD4 undergoes translocation to the nucleus of neutrophils, triggering hyper-citrullination of histones and initiating the production of neutrophil extracellular traps. These NETs serve to entrap bacteria and pathogens, instigating a pro-inflammatory form of programmed cell death termed "NETosis". Consequently, the release

of NETs can elicit an autoimmune response against NET-associated nuclear antigens and granule proteins, thereby contributing to inflammation[44].

1.5 PADs and diseases

PAD citrullination serves diverse physiological functions but also contributes to pathological conditions. Increased PAD expression and protein citrullination are linked to numerous pathologies, encompassing inflammatory diseases (*i.e.,* psoriasis and inflammatory bowel disease[45]), autoimmune diseases (*i.e.,* rheumatoid arthritis, diabetes[46], systemic lupus erythematosus[47]), cancers, neurodegenerative diseases (*i.e.,* multiple sclerosis, Alzheimer's disease, Parkinson's disease[48], prion disease[49]), and viral infections.

1.5.1 Psoriasis

Psoriasis, a chronic skin ailment, is characterized by the accelerated proliferation of keratinocytes, preventing timely shedding and resulting in the accumulation of thick, dry patches. PAD1 plays a pivotal role in keratinocyte epithelial differentiation. Under normal circumstances, it citrullinates keratin K1, promoting the compaction of keratin filaments—an essential step in the normal cornification process of the epidermis. However, in individuals with psoriasis, reduced or absent PAD1 activity disrupts this process, leading to the formation of hyperproliferative plaques characteristic of psoriatic skin lesions[50].

1.5.2 Rheumatoid arthritis

Rheumatoid arthritis (RA) is a common autoimmune disease marked by chronic inflammation in the synovial joints and infiltration of blood-derived cells, notably activated macrophages. Structural changes induced by citrullination can generate novel epitopes with immunogenic potential, prompting an immune response against the autoantigen itself. In RA, a highly specific family of autoantibodies targets citrullinated proteins (ACPA), detected in 80% of patients, serving as crucial diagnostic, prognostic, and predictive markers. In inflamed joints affected by RA, there is an upregulation in the expression and activity of PAD2 and PAD4. Macrophages and monocytes, rich in PADs and recruited to the joints, ultimately undergo degradation and apoptosis, activating PADs which deaminate cellular and extracellular proteins. This process results in an excessive pool of citrullinated proteins in the joints, contributing to the loss of immune tolerance[51,52].

1.5.3 Multiple sclerosis

Multiple sclerosis (MS) is a complex autoimmune disorder affecting the central nervous system, marked by the destruction of the myelin sheath.

The myelin basic protein (MBP), constituting the second most abundant protein in the myelin sheath, undergoes deamination by PAD2 in six arginine residues, resulting in MBP-cit_6. In young children (up to 2 years old), MBP-cit_6 dominates, comprising 100% of the total MBP, contributing to nervous system development. However, its presence rapidly diminishes to approximately 18% in a few years. In MS patients, the proportion of MBP-cit_6 nearly halves the total MBP, inducing partial unfolding of MBP molecules, rendering the protein more susceptible to degradation, and impacting the lipid-complex-forming ability of MBP. Moreover, antibodies against MBP are detectable in the serum of patients with active demyelinating lesions in MS[53].

1.5.4 Alzheimer's disease

Alzheimer's disease (AD) stands as the most prevalent neurodegenerative condition, characterized by the presence of senile plaques (SP) formed through β-amyloid (Aβ) aggregation, neurofibrillary tangles (NFT) resulting from abnormal tau protein aggregation, and the consequential loss of neurons.

In the context of AD, damaged myelin interacts with Aβ deposits, leading to the identification of antibodies targeting glial-derived antigens. Research indicates that autoantibodies in AD are linked to PAD4 and protein citrullination, with confirmed instances of citrullination in pyramidal neuronal intracellular proteins within the AD hippocampus. This region also exhibits an abnormal accumulation of citrullinated proteins, predominantly structural proteins like vimentin, MBP, and GFAP (glial fibrillary acidic protein), alongside an increased presence of PAD2[54].

1.5.5 Tumour

PAD2 and PAD4 stand out as the most extensively studied PADs in the context of cancer, displaying distinctive expression patterns, activities, and specific effects across various cancer types. Their influence on tumour development involves the modulation of cell signalling, transcription, and the extracellular matrix (ECM), thereby regulating critical processes such as growth, apoptosis, and the epithelial-to-mesenchymal transition[55,56].

Chang et al. revealed that PAD4 expression levels are heightened in a variety of malignancies, including breast carcinomas, lung carcinomas, hepatocellular carcinomas, colorectal

carcinomas, gastric adenocarcinomas, oesophageal squamous cell cancers, ovarian adenocarcinoma, uterine adenocarcinoma, bladder carcinomas, and chondromas, but exhibits low expression or is not expressed in normal tissues and benign tumours. Patients with various malignant tumours, in particular malignant lymphoma, exhibit elevated PAD4 levels in their blood compared to those with chronic inflammation and benign tumors[57,58]. Moreover, PAD4 levels were observed to be higher in metastases than in primary tumours, suggesting that PAD4 may promote a transition of benign tumours into invasive malignancies[59]. This observation suggests that aberrant PAD4 activity is closely associated with tumour progression. Indeed, PAD4 may disrupt gene expression regulation, potentially leading to the transformation of normal cells into cancerous ones, and may induce NETosis triggered by stimuli in the tumour microenvironment, further promoting tumour growth and metastasis.

The PAD2 isoform is also implicated in tumorigenesis processes, contributing to the development of breast, gynaecological, and prostate cancers[60,61]. Notably, abnormal PAD2 expression in colon-rectal cancer is associated with poor prognosis, with lower PAD2 levels in tumours or adjacent mucosal tissue[62]. In prostate cancer, Wang and colleagues highlighted the role of PAD2 in inhibiting the proteasome-mediated degradation of the androgen receptor (AR), while simultaneously promoting AR binding to target genes through histone H3 citrullination. This dual mechanism contributes to the survival and proliferation of tumour cells[60]. In breast cancer, elevated PAD2 expression is observed in tumour samples compared to controls[63] and an increase in PAD2 levels is correlated with tumour progression[64]. In this context, PAD2 exhibits the capability to citrullinate RNA polymerase 2, an enzyme governing gene expression through transcription elongation, thereby initiating the transcription of a multitude of genes and triggering cell proliferation. Additionally, in breast carcinomas, citrullination facilitated by PAD1 and PAD4 instigates the epithelial-to-mesenchymal transition (EMT) by influencing distinct targets. PAD1 impedes MAPK ERK1/2 and P38 signalling via the citrullination of MEK1[65], while PAD4 catalyses the citrullination of the transcription factor glycogen synthase kinase-3-beta (GSK3β). This catalytic activity promotes EMT by elevating vimentin expression while diminishing E-cadherin levels[56].

These findings collectively emphasize the intricate involvement of PAD in cancer progression, shedding light on their potential as therapeutic targets and diagnostic markers across various malignancies[66–68].

1.5.6 Viral infection

Recently, a direct correlation between citrullination and viral infections has been demonstrated, including HIV, human rhinovirus (HRV), respiratory syncytial virus (RSV), human cytomegalovirus (HCMV), β-coronaviruses, and herpes simplex type 1 (HSV-1).

Specifically, Struyf and colleagues showed that, following PAD-mediated citrullination, the physiological activity of the chemokine CXCL12, a crucial inhibitor of HIV and a chemotactic recruiter of leukocytes, gradually weakens, severely reducing the ability of lymphocytes to block retroviral infection[69].

PAD4 activity, as described by Muraro and colleagues, also proved crucial in the mechanism of NETosis commonly induced by RSV, responsible for the development of RSV bronchiolitis that can lead to severe inflammatory consequences. In this context, NETosis induction depends on the signalling of PI3K/AKT, ERK, and p38, which, to be activated, requires histone citrullination by PAD4. Drug inhibition of PAD4 strongly inhibited the release of NETs by neutrophil granulocytes, preventing the formation of an aberrant inflammatory response[70].

Pasquero et al. demonstrated the role of PAD4 in the replication of two human coronaviruses, HCoV-OC43 and SARS-CoV-2. Inhibition of PAD4-mediated citrullination using the pan-PAD inhibitors Cl-amidine (Cl-A) and BB-Cl-amidine (BB-Cl-A) proved effective in inhibiting the replication of both viruses in vitro[71].

Casanova et al. found that the antiviral activity of the LL37 protein is compromised by HRV-induced citrullination. Their study shows that citrullination of LL-37 reduced its antiviral activity directed against HRV44. Furthermore, while the anti-rhinovirus activity of LL-37 results in dampened epithelial cell inflammatory responses, citrullination of the peptide, and a loss in antiviral activity, lessens this effect. Additionally, HRV infection upregulates PAD2 protein expression and increases levels of protein citrullination, including histone H3, in human bronchial epithelial cells, suggesting that PAD citrullination may represent a novel viral evasion mechanism[72].

Griffante and colleagues highlighted HCMV's ability to induce PAD-mediated citrullination of various host proteins, resulting in the loss of their functions. The proteins most involved in this process were found to be two important interferon-inducible proteins, IFIT1 and Mx1, highly expressed during the antiviral immune response. This strategy employed by HCMV plays a key role in supporting virus replication[73].

IFIT1, together with IFIT2, was also found to be deiminated during the infection by another member of the herpesvirus family. Indeed, HSV-1 infection leads to enhanced protein citrullination through transcriptional activation of PAD2, PAD3, and PAD4, with PAD3

playing a pivotal role in supporting viral infection, in fact, inhibition of PAD3 dramatically curbs HSV-1 infection[74].

1.6 PAD inhibitors

Over the years, the association between citrullinated proteins, or antibodies to citrullinated proteins, and various pathological conditions has led to the demand for drugs targeting the citrullination process by acting on the PAD enzymes.

The initial breakthrough in developing bioactive PAD inhibitors occurred in 2006, with Thompson and colleagues unveiling F-amidine. This compound's structure is based on benzoyl arginine amide (BAA), recognized as one of the most effective small molecule substrates for PADs. Given that PADs exhibit a preference for hydrolyzing a positively charged guanidine residue, the introduction of a methylene fluoride in place of one of the amino groups was hypothesized to yield a compound capable of covalently modifying the enzyme. The resultant compound, containing fluoroacetamidine, retains the positive charge and the ability to form most hydrogen bonds of guanidine. However, due to the strongly electrophilic nature of fluorine, it can react with a cysteine residue present in the enzyme's active site. F-amidine proved to be a potent irreversible inhibitor of PAD4 (kinact / KI value of 3000 $M^{-1}s^{-1}$) as further experiments demonstrated its modification of Cys645 and bioavailability[75].

Building on the success of F-amidine, a series of compounds were synthesized, altering the nature of the positively charged head by substituting fluorine with a chlorine or hydrogen atom. Efforts were also made to determine the optimal length of the side chain by synthesizing compounds with side chains ranging from two to four methylene units. Among these, Cl-amidine emerged as the most potent PAD inhibitor, especially for PAD4 (kinact / KI value of 13,000 $M^{-1}s^{-1}$). Structurally resembling F-amidine, Cl-amidine features a chlorine atom in place of fluorine. Similar to F-amidine, Cl-amidine predominantly inhibits the active, calcium-bound conformation of the enzyme. This preference arises because calcium-binding induces a conformational shift that strategically places Cys645 to facilitate substrate catalysis and, consequently, inhibitor binding[76].

To enhance the cellular bioavailability of PAD inhibitors, BB-Cl-amidine was synthesized. While retaining the critical components of Cl-amidine (*i.e.,* the reactive chloroacetamidine head and side chain length), BB-Cl-amidine possesses an N-terminal biphenyl group to increase

hydrophobicity/bioavailability and a C-terminal benzimidazole group that increases proteolytic stability. *In vitro*, Cl-amidine and BB-Cl-amidine exhibit similar potency and selectivity. However, BB-Cl-amidine demonstrates a 20-fold increase in toxicity in cell cultures and a significantly longer *in vivo* half-life than Cl-amidine (1.75 h vs. ~15 min)[76].

Several studies have explored the potential therapeutic applications of PAD inhibitors in conditions where abnormal PAD activation is implicated. For instance, the use of Cl-amidine and BB-Cl-amidine as PAD inhibitors has demonstrated a reduction in NET formation and protection against lupus-related vascular damage in the New Zealand mixed lupus model (MRL/lpr mice)[77].

Given that the five isoforms of PAD exhibit differential expression in tissues under both physiological and pathological conditions, the development of selective inhibitors for each isoform becomes crucial to investigate their specific biological roles. In a recent effort, Thompson and colleagues aimed to design a selective inhibitor for PAD2, a key player in the initiation and progression of multiple sclerosis, rheumatoid arthritis, and breast cancer. This endeavour involved the synthesis of a series of benzimidazole derivatives of Cl-amidine. The alteration of both the N-terminal and the C-terminal led to a remarkable increase in potency and selectivity for PAD2 by over one hundred times[78]. Such a compound holds great promise for unravelling the biological functions of this isoform and may prove valuable in the treatment of diseases where PAD2 activity is dysregulated.

2. HUMAN PAPILLOMAVIRUS
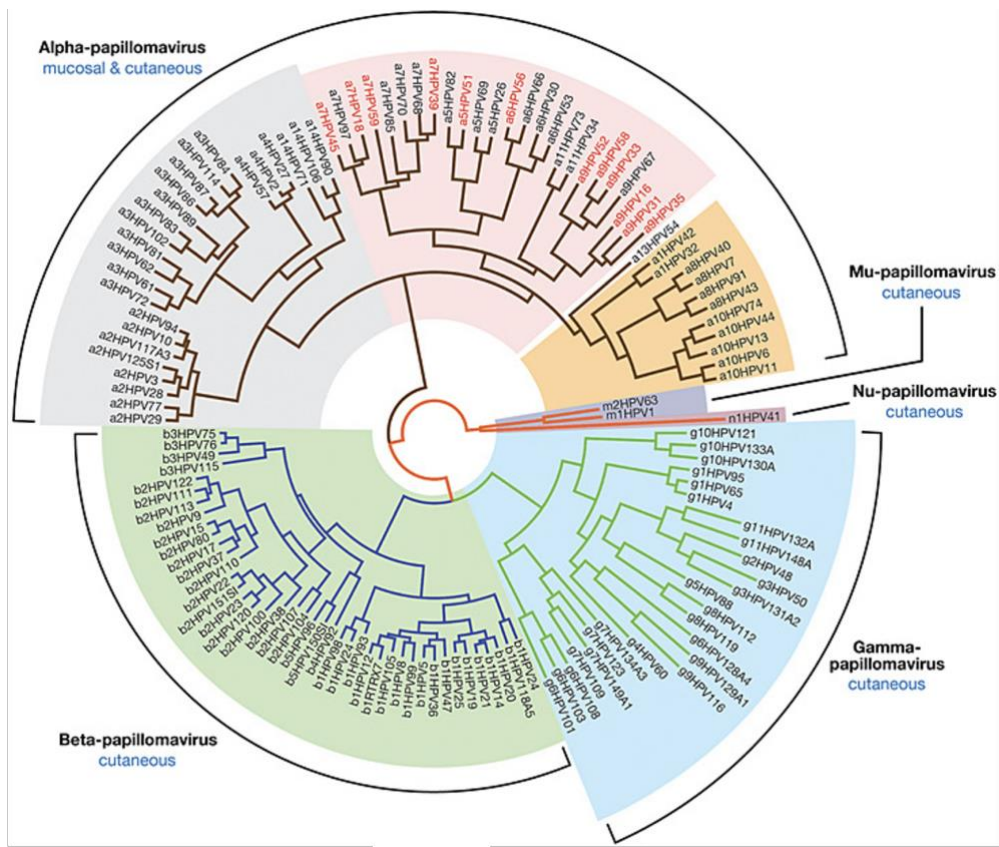
2.1 Classification

Papillomaviruses are a widespread and ancient group of small DNA viruses that have slowly co-evolved with their vertebrate hosts for millions of years. They are highly species-specific and are present in birds, reptiles, marsupials, and mammals, but not in amphibians or lower phylogenetic orders[79].

The discovery of the Human papillomavirus (HPV) genome traces back to the 1970s when it was initially isolated from warts. Later, Harald zur Hausen established the well-recognized correlation between HPV infection and cervical cancer[80]. Currently, the *Papillomaviridae* family encompasses approximately 450 HPV types, organized into five phylogenetic genera: α-papillomaviruses, β-papillomaviruses, γ-papillomaviruses, μ-papillomaviruses, and ν-papillomaviruses (Figure 3). This classification relies on nucleotide sequence homology, particularly within the L1 gene, which encodes the major capsid protein. Genera share over 60% of the nucleotide sequence, species share between 71% and 89%, and types are considered distinct if they differ by more than 10% from their closest known counterpart[81,82]. All five genera of HPVs contain virus types that infect specific regions of the cutaneous epithelium. Notably, the α-papillomavirus genus also includes HPV types that exhibit tropism for oral and genital mucosal epithelium.

Here are the main characteristics of the HPV genera:
1. α-papillomaviruses (α-HPV) produce visible macroscopic lesions. They comprehend low-risk viruses with cutaneous tropism and low- and high-risk viruses with mucosal tropism[83]. Specifically, high-risk HPVs include HPV 16, 18, 31, 33, and 45 and are most frequently associated with malignant genital tumours. HPV-16 and HPV-18, in particular, are responsible for about 70% of cervical carcinoma cases. In contrast, low-risk HPVs, such as HPV-6 and HPV-11, are mostly associated with the development of benign papilloma at the infection site. Besides being linked to cervical and anogenital tumours, persistent HPV infection has also been associated with the onset of head and neck cancers[84].
2. β-papillomaviruses (β-HPV) cause subclinical infections, primarily in childhood, and are particularly involved in the development of skin tumours in immunocompromised patients.

3. γ-papillomaviruses (γ-HPV) are associated with subclinical infections in childhood and clinical lesions in immunocompromised patients.

4. μ-papillomaviruses (μ-HPV) cause skin lesions.

5. ν-papillomaviruses (ν-HPV) are related to skin lesions[83].

Figure 3. Human papillomavirus classification. The human papillomavirus (HPV) types fall into five genera, with the α-HPVs, β-HPVs, and γ-HPVs genera representing the largest groups. α-HPVs are classified as low-risk cutaneous (grey), low-risk mucosal (orange), or high-risk (pink). The high-risk types (in red) are confirmed as human carcinogens based on epidemiological data. The remaining high-risk types are probable or possible carcinogens. The evolutionary tree is based on the alignment of the L1 gene[85].

2.2 Virion structure

HPVs are small, non-enveloped, icosahedral viruses that have a diameter ranging from 52 to 55 nm. The viral particles carry a single double-stranded circular DNA molecule, housed within a protein capsid formed by 72 pentameric capsomers. The capsid comprises two virally encoded structural proteins, L1 (constituting 80% of the total viral protein) and L2 (Figure 4A, B).

Notably, virus-like particles (VLPs) can be produced by the expression of L1, alone or in combination with L2, in mammalian or non-mammalian expression systems[85].

2.3 Genome organization

HPVs have circular double-stranded DNA genomes of ~7–8 kbp that are assembled into chromatin using host histones at all stages of the infectious cycle[86]. The viral genome is composed of three regions: i) an early region (E) with open reading frames (ORFs) that codes for non-structural proteins involved in viral DNA replication (E1), viral expression regulation (E2), virus assembly (E4), and immortalization and transformation of infected epithelial cells (E5, E6, and E7), in the case of HR-HPVs; ii) a late region (L) that encodes for L1 major and L2 minor capsid proteins; iii) and a long control region (LCR), also called as non-coding region (NCR) or upstream regulatory region (URR), which contains the origin of viral replication, viral promoters and various binding sites for cellular and viral transcription factors (Figure 4C)[87]. Viral transcription is meticulously regulated through RNA processing, involving alternative splicing that generates a diverse array of transcripts. In the case of α-papillomaviruses, an additional coding sequence encodes an early protein (E5). Furthermore, in oncogenic α-HPVs, the critical viral oncoproteins E6 and E7, pivotal for neoplastic progression, are transcribed from a polycistronic, alternatively spliced mRNA. In contrast, in low-risk HPVs, these oncoproteins are transcribed from separate promoters[88,89].
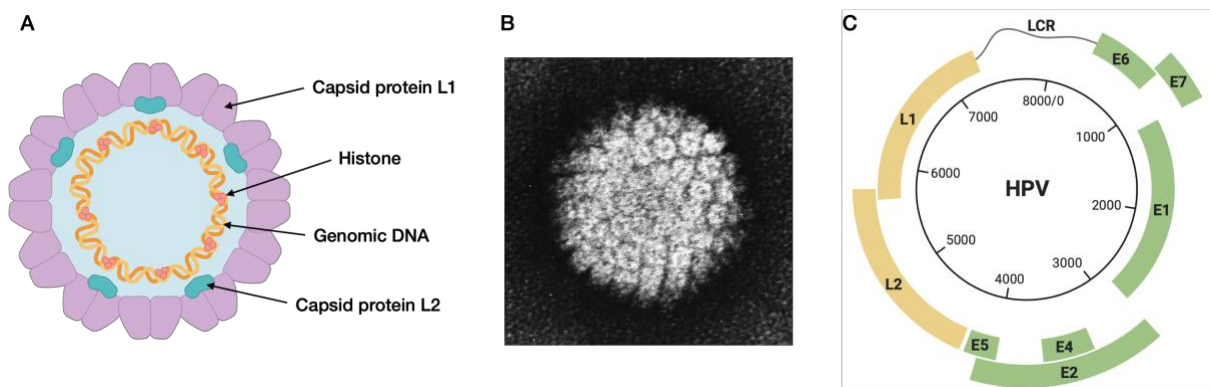
Figure 4. A) HPV virion structure. B) HPV at electron microscopy[90]. C) HPV genome organization[22].

The E1 protein is a highly conserved DNA helicase mainly known for its participation in viral DNA replication. Specifically, E1 binds to the origin of viral replication, engaging with and recruiting various cellular proteins of the replication machinery, including α-DNA polymerase, to initiate, together with E2, HPV replication. Additionally, there is evidence suggesting that E1 may play a crucial role in evading the immune response[91].

E2 can be considered the most pivotal viral protein due to its role in the initiation of viral replication and oncogenesis. E2 meticulously governs the HPV life cycle, functioning as a transcriptional regulator that can either activate or repress viral gene expression by binding to specific E2-binding sites within the viral regulatory regions. Notably, E2 represses the expression of E6 and E7 oncogenes by interacting with p97 and p105 viral promoters, thereby obstructing the access of several transcription factors. Indeed, the HPV DNA integration, during the HPV-driven transformation, causes the loss of the E2, and also E4, gene expression, which triggers a down-replication of the viral genome, a G_2 arrest, and an E6 and E7 overexpression that confers a growth advantage over cells that maintain the HPV DNA episomally. Furthermore, E2 actively contributes to maintaining the HPV genome in dividing cells and facilitates the partitioning of the viral genome to daughter cells by tethering them to host chromosomes, thus allowing persistent infection[92].

The E4 protein, encoded by the E1^E4 spliced mRNA, is expressed in the late stages of infection, preceding L1 and L2. In some wart formations, it can accumulate, constituting up to 30% of the total protein content[93]. During the late phase of the viral cell cycle, E4 appears to play a significant role in the release of newly formed virions. Indeed, E1^E4 interacts with and destabilizes keratin filaments, contributing to the fragility of desquamating cornified cells and facilitating the subsequent release of virions[94]. Despite variations in the primary amino acid sequences of E4 proteins among different HPV types, they share common characteristics, such as the ability to suppress cell proliferation[95].

Mucosal HPVs express a small minor oncoprotein associated with the endoplasmic reticulum called E5, which is crucial in the HPV life cycle by modulating epithelial proliferation and differentiation[96]. Specifically, E5 enhances growth-promoting pathways, including EGFR signalling, while intervening in pathways necessary for keratinocyte differentiation[97]. Additionally, during early carcinogenesis, E5 modulates processes such as survival, adhesion, migration, and invasion. In this context, the E5 protein maintains a balance of cyclin-dependent kinase inhibitor inhibitors (CKI) p21 and p27 to allow cell proliferation. Simultaneously, it activates the PI3K-AKT cascade to promote cell survival and reduce apoptosis by increasing the BCL-2 anti-apoptotic system[98,99]. In contrast to E6 and E7, the E5 open reading frame is lost during the integration of the episomal HPV DNA into the cellular genome, suggesting that E5 acts at the early stages of the transformation process[100].

E6 and E7 are the HPV major oncoproteins of the high-risk HPVs, whose combined effect is required for the neoplastic progression and persistence of HPV-mediated cancer. Abrogation of E6 and E7 in tumours or tumoral cell lines often results in senescence or apoptosis of cancer cells, emphasizing their role in HPV-mediated carcinogenesis[101]. Throughout the viral life cycle, E6 and E7 primarily promote a cellular environment facilitating viral DNA amplification by modulating the balance between proliferation and cellular differentiation while maintaining a reservoir of infected basal cells. To fulfil these tasks, E6 and E7 bind to various host cell factors, differing among HPV types and targeted epithelium.

E7 primarily targets the Rb protein (pRb; a tumour suppressor protein and major G1 checkpoint regulator) and related proteins, p107 and p130. In the case of high-risk viruses, E7 induces pRb degradation, releasing the transcriptional factor E2F from the E2F/pRb repressor complex. This allows transcriptional activation of cyclin E, cyclin A, and p16, stimulating entry into the S-phase[102–104]. In addition, E7 can interact with and abrogate the growth-inhibitory activity of p21, despite p21 being upregulated in E7-expressing cells[105]. Moreover, E7 is known to interact with the DREAM complex, a downstream complex of the p53 pathway, inducing its proteasomal degradation, a process that enhances the cell cycle progression[106].

The mucosal HPV E6 protein forms a complex with the E3 ligase E6-associated protein (E6AP) and disrupts p53 (a crucial tumour suppressor protein) transactivation. However, only the oncogenic E6 proteins present in high-risk HPV coopt E6AP-mediated ubiquitination of p53, leading to p53 degradation. This compels cells to undergo uncontrolled cellular division, promoting carcinogenesis[107–109]. Oncogenic E6 also targets other cellular factors, contributing to E6-induced transformation. It interacts with proteins influencing i) transcription and DNA replication (*i.e.,* p300/CBP, Gps2, IRF-3, hMcm7, E6TP1 and ADA3); ii) apoptosis and immune evasion (*i.e.,* Bak, TNF receptor 1 TNF R1, FADD and c-Myc); iii) epithelial organization and differentiation (*i.e.,* paxillin, E6BP/ERC-55, zyxin and fibulin-1); iv) cell-cell adhesion, polarity, and proliferation control, which contain a PDZ-binding motif (*i.e.,* hDLG, hScrib, PKN, MAGI-1, MAGI-2, MAGI-3 or MUPP1); and v) DNA repair (*i.e.,* XRCC1 and 6-O-methylguanine-DNA methyltransferase)[110,111]. Furthermore, it upregulates telomerase, to maintain telomere length and prevent senescence in continually proliferating cells[112]. Contrastingly, E6 proteins from cutaneous HPVs do not bind to E6AP, altering differentiation by inhibiting the MAML1 transcriptional co-activator downstream from Notch signaling[113,114]. Moreover, E6 proteins from β-HPVs inhibit apoptosis following UV-induced DNA damage and promote the development of squamous cell skin cancer[115].

The L1 major capsid protein forms the entire exterior surface of mature virions, playing a pivotal role in HPV's initial cell attachment during viral entry. After attachment, it facilitates the release of the viral genome into the targeted cell. L1 proteins are expressed late in infection contributing to the generation of novel progeny virions[116]. Notably, L1 possesses a unique characteristic, spontaneously self-assembling into VLPs. These assembled VLPs serve as potent immunogens, likely due to innate B-cell recognition of the regular icosahedrally displayed spacing of surface epitopes[117]. These findings laid the foundation for the development of the current VLP-based vaccines that offer highly effective protection against infection with the cancer-causing HPV types.

L2, the minor capsid protein, is minimally exposed on the surface of the mature virion but it emerges during the HPV entry process. L2 is essential for trafficking the viral DNA to the nucleus and is also involved late in infection, assisting in the packaging of the viral DNA into virion particles[118,119]. The L2 protein is crucial for efficient infection, as VLPs that contain only the L1 protein carry significantly less viral DNA and are non-infectious[120].

2.4 Viral replication

HPV replication is intricately linked to epithelial differentiation. To initiate infection, HPV virions must make contact with the dividing basal cells of the stratified epithelium through micro-abrasions or by entering cells at the squamous cellular junction between the endo- and ectocervix (Figure 5).
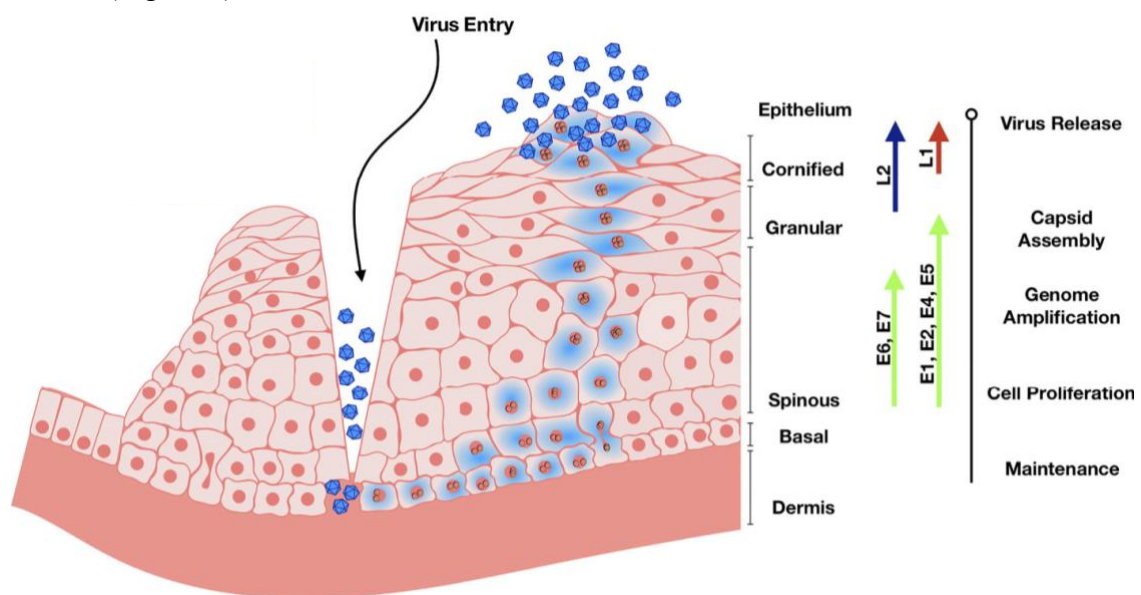

Figure 5. The life cycle of HPV. Abrasion provides HPV access to basal keratinocytes. Viral DNA replication relies on the host DNA replication machinery and is supported by the early viral proteins E1

and E2. The viral genome replicates in the infected basal and stem cells and establishes HPV episome copies, which split between the daughter progeny as cells divide. The early viral proteins E6 and E7 stimulate the continued proliferation. Upon terminal cell differentiation in the upper epithelium, L1 and L2 become activated to package the high number of viral DNA copies. E4 disintegrates the cytokeratin filaments, and the virus is released as keratinocyte remnants are sloughed off at the epithelial surface[121].

The initial interaction of virions with the host cell relies on the binding of the capsid protein L1 to heparan sulphate proteoglycans (HSPG) present on the basal membrane or the surface of basal keratinocytes. This induces conformational changes in the capsid, exposing the minor capsid protein L2 and binding to secondary receptors, leading to virion internalization via caveolae or clathrin-mediated endocytosis[122]. After exiting the endosomes, the L2 minor capsid protein transports the viral DNA into the nucleus to subnuclear promyelocytic leukaemia protein (PML) bodies, where the first steps of viral transcription and replication take place[123].

The E1 and E2 are the first proteins to be expressed and initiate the viral DNA synthesis. The HPV genome is rapidly amplified through the cooptation of the host DNA replication mechanism (since HPV does not express a viral DNA polymerase), but it is maintained at a low copy number in self-renewing cells. At this stage, the viral genome exists in an extrachromosomal (or episomal) form in basal cells, and the expression of other viral proteins remains minimal due to E2-mediated repression on the early promoter p97/p105, thus allowing evasion from the immune response.

Upon division of the infected basal cell, novel genomes are distributed to daughter cells through interaction with the host mitotic chromosomes. One daughter cell remains in the basal layer, acting as a reservoir for episomal DNA, while the other begins migrating toward the upper epithelial layers. Here, the expression of viral oncoproteins E5, E6, and E7 manipulates the balance of cellular proliferation and differentiation, to establish an environment conducive to persistent infection in basal cells and productive infection in differentiated cells. In normal epithelium, only cells in the lower basal layer are mitotically active, and after cell division, one daughter cell is pushed up to replenish the overlying differentiated layers, which eventually shed. However, HPV oncoproteins induce cell cycle re-entry and delay terminal differentiation, to promote further genome amplification[124].

Late viral proteins L1 and L2 are expressed in the upper, terminally differentiated epithelial layers (granular and cornified), where new viral particles are assembled and released during the desquamation of epithelial cells in the cornified layer[86].

2.5 Transmission and tropism

HPV transmission predominantly arises from direct skin-to-skin contact with an infected individual, who may be asymptomatic and unaware of the infection. This virus stands as one of the most prevalent sexually transmitted infections. During sexual activity, HPV can be transmitted through vaginal, anal, and oral sex; despite the use of condoms and dental dams reducing the risk of transmission, their effectiveness is not absolute, given that HPV can infect epithelial areas that remain uncovered by these protective measures. Furthermore, there exists the potential for vertical transmission, as HPV can be passed from an infected mother to her child during childbirth[125].

HPVs are highly specialized viruses. Specifically, HPV primary infection and subsequent progression are limited to distinct layers of the stratified differentiating epithelia. This strategic approach on one hand establishes a viral reservoir with minimal viral activity in cells under immune surveillance, and on the other maximizes virion production in terminally differentiated cells slated for exfoliation.

HPVs belonging to different genera will undergo productive replication exclusively in anatomically distinct regions of the host's cutaneous or mucosal epithelia. This tropism is related to the viral transcription of RNA, which differs in different keratinocytes, rather than viral entry receptors[126]. However, differences in infectivity between cutaneous and mucosal HVPs may be also determined by differences in surface charge distribution of L1 capsid protein[127].

2.6 Pathogenesis

HPV infections manifest across a spectrum of outcomes, spanning from benign lesions, such as warts or papillomas, to potentially severe complications, including cancer. The severity of these outcomes depends on different factors, including the viral genus, the ability of specific HPV types to establish chronic infections, and the effectiveness of the host immune system in controlling or clearing the infection[85].

β-HPVs and γ-HPVs typically induce asymptomatic infections and are considered part of the normal skin microbiome. However, individuals with compromised immune systems, such as those with immunodeficiencies or organ transplant recipients, are highly susceptible to HPV infections. In such cases, normally innocuous commensal β-HPVs can act as cofactors, predisposing individuals to UV-induced squamous cell skin cancer.

μ-HPVs, ν-HPVs, and certain α-HPVs, particularly HPV-1, HPV-2, and HPV-4, cause common warts, a benign lesion that spontaneously resolves, typically appearing on the hands, fingers, and feet.

Mucosal α-HPVs are commonly transmitted through sexual contact and can be classified as high-risk or low-risk based on their potential to induce cancerous transformations. Low-risk HPV types 6 and 11 primarily lead to condyloma acuminata (~90% of cases), also known as anogenital warts. These warts present as soft, cauliflower-like growths on the genital and anal regions. While generally benign, they can cause discomfort and persist for many months before regression, occasionally requiring medical intervention.

Cervical infections caused by high-risk HPVs can be detected in one-third of young women within two years of sexual debut. In the majority of instances (~ 90%), these high-risk HPV infections are transient, resolving completely within 1-2 years. Nevertheless, HPV has developed various strategies to effectively elude the immune response, paving the way for chronic infections and escalating the risk of cervical dysplasia and the progression of cervical intraepithelial neoplasia (CIN). Three prerequisites must be met for this progression: i) integration of viral DNA into the cellular genome, ii) expression of the E6 and E7 genes, and iii) loss of E2 expression.

As discussed earlier, HPV typically avoids integrating its genome into the host cell DNA during its replicative cycle. However, in certain cases, random viral genome integration occurs, leading to the loss of E2 gene expression. Without this crucial regulator of viral transcription, the viral oncogenes E6 and E7 become actively expressed, promoting their pro-proliferative effects, and inducing genomic instability. This, in turn, facilitates the acquisition of genetic aberrations by epithelial cells[86].

Cervical carcinoma, the fourth most common cancer in women, associated with HPV in approximately 95%-100% of cases, usually develops in 10-20 years following infection, but in women with weakened immune systems, such as untreated HIV, this process can be faster and take 5–10 years. The primary high-risk HPV strains linked to these cancers are HPV-16 (50-60% of cases and especially correlated with squamous cell carcinomas) and HPV-18 (10-15% of cases and mostly diagnosed in adenocarcinomas). During the oncogenic progression, the proportion of proliferating cells increases, eventually occupying all layers of the epithelium. Based on the histological progression of CINs, they can be classified into three stages: CIN,

CIN2, and CIN3. Approximately one-third of CIN3 infections progress to invasive carcinoma[84]. Currently, there are no effective strategies for treating low or high-grade cervical lesions apart from surgery[128]. However, preventive measures, including vaccination and regular screening (PAP smears), can significantly reduce the progression of cervical cancer[129].

While high-risk HPVs are prominently linked to cervical cancer, they also play a pivotal role in other malignancies. Notably, HPV is associated with non-cervical anogenital cancers, such as vulva, vagina, penis, and anus cancers, as well as oropharyngeal cancers[126].

In rare instances, vertical transmission of HPV, particularly HPV-6 and HPV-11, from mother to newborns during childbirth can result in genital warts or respiratory papillomatosis, a non-cancerous growth in the respiratory tract in the child[130].

2.7 Vaccines

In the 1980s, the ground-breaking identification of HPV-16 and other high-risk α-HPVs DNA in the majority of cervical cancer specimens marked a pivotal moment. The subsequent revelation that these viruses could transform or immortalize cells *in vitro* established HPV as the first human oncogenic virus[131].

Today, a wealth of compelling evidence underscores the central role of high-risk HPVs, contributing to nearly 100% of cervical cancers and a spectrum of other malignancies, including those affecting the vulva, vagina, penis, anus, and oropharynx. This collective impact accounts for approximately 4.5% of all new cancer cases worldwide[132]. Consequently, the advent of HPV vaccines stands as a potent tool in thwarting neoplastic transformations.

All HPV vaccines share a common composition, featuring purified L1 capsid protein of the relevant HPV type, capable of self-assembling into VLPs. Notably, no viral genes are incorporated into these vaccines[133].

In 2006, a milestone was achieved with the approval of the first HPV vaccine, Gardasil. This vaccine provided protection against HPV-16 and HPV-18, diminishing the risk of virus-related neoplasms by 60-70% with two or three vaccine doses. Additionally, it targeted HPV-6 and HPV-11, responsible for anogenital warts and respiratory papillomatosis.

Subsequent iterations of HPV vaccines, exemplified by Cervarix and Gardasil 9, offer varying spectrums of coverage against HPV serotypes. Cervarix focuses on safeguarding against HPV-

16 and HPV-18, while Gardasil 9 extends its protection to nine of the most pathogenic strains, collectively accounting for approximately 90% of all cervical cancer cases[134].

These vaccines collectively represent crucial tools in the ongoing battle against HPV-related cancers, offering targeted and broad-spectrum defences against the most prevalent and oncogenic strains.

3. OBJECTIVES

As elucidated in preceding chapters, PAD-mediated citrullination exhibits a direct correlation with viral infections, while PADs are involved in human epidermal keratinization, morphogenesis, and pathogenesis of skin tumours, processes intricately intertwined with HPV-induced transformation.

Indeed, the overexpression of PAD2 in transgenic mice resulted in spontaneous skin neoplasia[135], and antibodies targetting citrullinated HPV-47 E2$_{345-362}$ protein were detected in rheumatoid arthritis patients[136]. Furthermore, elevated PAD4 levels were discerned in the bloodstream of individuals afflicted with cervical cancer[137].

Therefore, to gain more insight into the mechanisms through which citrullination fuels disease progression and to identify more effective druggable targets and suitable biomarkers, my research (publication attached in the Pubblications part) endeavours to define the impact of PAD-mediated citrullination on HPV transformation, particularly in the context of cervical cancer progression.

PART II

1. HERPES SIMPLEX VIRUS TYPE 1

1.1 Classification

The *Herpesviridae* family encompasses over 200 species infecting a diverse range of hosts, including mammals, birds, reptiles, amphibians, fish, and bivalves. They are generally characterized by a large double-stranded DNA genome, strict host specificity, and the ability to establish latency and life-long persistence with spontaneous reactivation periods. Within the *Herpesviridae* family, nine species are currently recognized to cause disease in humans, they span all three herpesvirus subfamilies and are grouped based on various criteria such as genome structure, tissue tropism, cytopathologic effect, latent infection site, pathogenesis, and disease manifestations[138].

The herpesvirus subfamilies and the human herpesvirus species are here described (Table 1):

1. The α-herpesvirinae subfamily comprises lytic viruses with short life cycles infecting various cell types. They replicate rapidly and establish latency in the sensory ganglia. This subfamily includes two genera: Simplexvirus, which encompasses herpes simplex virus type 1 (HSV-1) and herpes simplex virus type 2 (HSV-2), and Varicellovirus, which includes varicella-zoster virus (VZV).

2. The β-herpesvirinae subfamily consists of viruses with long replicative cycles and slow progression of infection in cell cultures. Latent infection occurs in secretory glands, lymphoreticular cells, kidneys, and other tissues. This subfamily includes two genera: Cytomegalovirus, encompassing human cytomegalovirus (HCMV), and Roseolovirus, which includes herpesvirus types 6A, 6B, and 7 (HHV-6A, HHV-6B, and HHV-7).

3. The γ-herpesvirinae subfamily comprises viruses that establish latent infections mainly in lymphoblastoid cells. It includes the genera Lymphocryptovirus, which encompasses Epstein-Barr virus (EBV), and Rhadinovirus, which includes herpesvirus type 8 (HHV-8), also known as Kaposi's sarcoma-associated herpesvirus (KSHV)[139].

Over 2500 years ago, Hippocrates coined the term "herpes", derived from the Greek word meaning "to creep", to depict the creeping or crawling nature of skin lesions associated with this contagious ulcerative disease[140]. However, it wasn't until the 1950s that HSV-1 itself was identified[141].

Hence, HSV-1, akin to other herpesviruses, is an ancient pathogen that has co-evolved with the human population for millennia. This prolonged coexistence is evident in HSV-1's development

of multiple evasion strategies against the immune system and its ability to resist eradication from the infected host[142].

Table 1. Classification of human herpesviruses.

Subfamily	Genus	Species	Tropism	Global prevalence (%)
α-herpesvirinae	Simplexvirus	Herpes simplex virus type 1 (HSV-1)	Mucoepithelial cells (mainly oro-facial tract), neurons	40-90
		Herpes simplex virus type 2 (HSV-2)	Mucoepithelial cells (mainly genital tract), neurons	10-60
	Varicellovirus	Varicella zoster virus (VZV)	Mucoepithelial cells, T cells, neurons	50-95
β-herpesvirinae	Cytomegalovirus	Human cytomegalovirus (HCMV)	Epithelial cells, monocytes, lymphocytes, fibroblasts, and more	56-94
	Roseolovirus	Human herpesvirus 6A (HHV-6A)	Epithelial cells, T cells, fibroblasts	60-100
		Human herpesvirus 6B (HHV-6B)	Epithelial cells, T cells, fibroblasts	40-100
		Human herpesvirus 7 (HHV-7)	Epithelial cells, T cells, fibroblasts	44-98
γ-herpesvirinae	Lymphocryptovirus	Epstein-Barr virus (EBV)	Mucoepithelial cells, B cells	80-100
	Rhadinovirus	Human herpesvirus 8 (HHV-8)	Lymphocytes	6-50

1.2 Transmission and tropism

HSV-1 is a neurotropic pathogen that infects a large majority of the human population worldwide (approximately 67%)[143]. The prevalence of HSV-1 increases steadily from childhood to adulthood and is inversely related to socio-economic status[141].

Transmission of HSV-1 typically occurs through direct contact with lesions or infected body fluids, such as saliva, genital fluids, and exudates from active lesions. While salivary contact is the primary route of transmission, sexual, transplacental, or blood-borne transmission can also occur but is less epidemiologically significant[144].

HSV enters through breaks in the skin surface or mucosa via direct contact and quickly establishes acute infections in the skin. After efficient replication in epithelial cells, HSV-1 is transported via nerve endings to the neuronal cell body, where it establishes latent infection in neurons within the trigeminal ganglia (if the primary infection was in the oral/facial district) or sacral dorsal root ganglia (if the primary infection occurred in the genitals)[145,146].

1.3 Virion structure

HSV-1 is an enveloped, spherical virus with a diameter ranging from 186 to 225 nm. Like all members of *Herpesviridae*, mature virions are composed of a linear double-stranded DNA genome, of approximately 152 kb, enclosed by an icosahedral capsid, composed of 162 capsomeres, the capsid is surrounded by the tegument, a pleiomorphic protein compartment, and the envelope (also called pericapsid), a phospholipidic double layer that contains both viral glycoproteins and some host cellular proteins[147] (Figure 6).
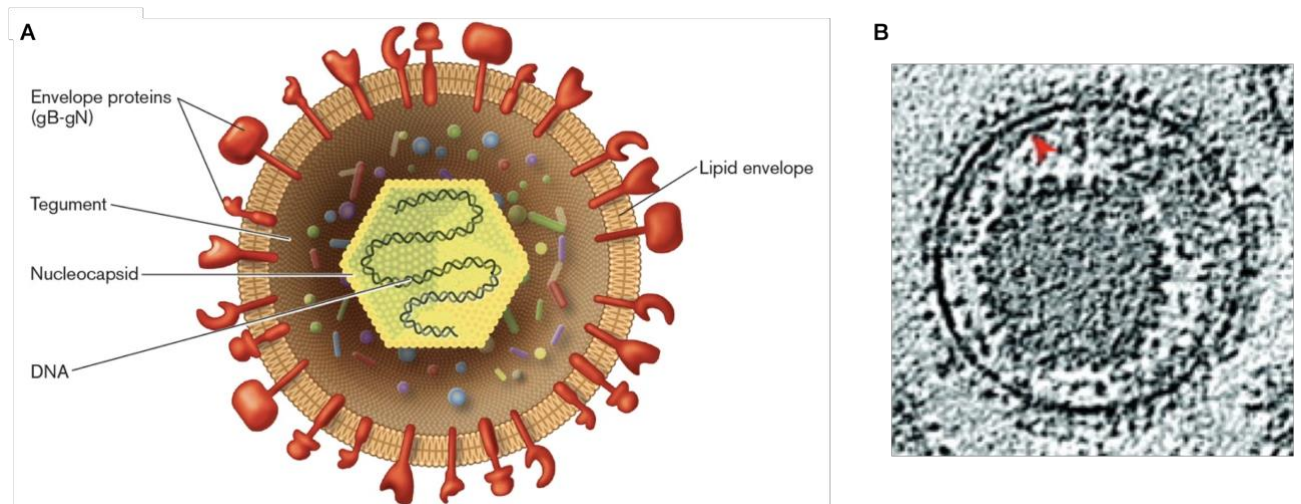

Figure 6. A) HSV-1 virion structure[148]. B) HSV-1 at electron microscopy[149].

The capsid has a diameter of 125 nm and is structured on a T=16 icosahedral lattice. Comprising 162 capsomers, it features 150 hexons shaping the edges and faces of the icosahedron, along with 12 pentons situated at all but one vertex of the capsid. Additionally, the capsid includes 320 triplexes connecting the capsomeres and the portal complex, 150 hexameric rings of small capsomere-interacting proteins (SCPs) covering the outer surface of each hexon, and 5 rod-shaped structures of capsid vertex-specific components (CVSCs) projecting radially outward from each penton[150].

Pentamers and hexamers are composed of five and six copies of the major capsid protein VP5, respectively. The unoccupied vertex accommodates the portal complex, composed of twelve

molecules of pUL6, facilitating DNA entry or exit from the capsid[151]. VP5's interaction with scaffold proteins is pivotal for icosahedral capsid formation, wherein it interacts with VP19C and VP23, crucial proteins in triplex formation, a hallmark of herpesviruses capsids. This triplex, comprising one VP19C protein and two VP23 proteins, aids in shell accretion and protein coat stability[152]. At the tip of each hexamer's VP5 protein lies one copy of VP26, constituting the SCPs. VP26 plays roles in the retrograde transport of viral capsids towards the cell nucleus during infection[153], as well as in viral capsid enveloping and egression[154]. Each CVSC, a heterotrimer of tegument proteins pUL17, pUL25, and pUL36, serves to stabilize the capsid during and after DNA packaging[155,156]. Lastly, VP24, a serine protease, cleaves the scaffolding proteins during capsid maturation[157]. During the process of capsid maturation, three distinct types of capsids can be produced. The A and B capsids are incomplete structures, lacking viral DNA, arising from issues during viral genome packaging. Specifically, the A capsid is single-shelled, while the B capsid (~ 20-30% of capsids) retains the inner scaffold shell. Conversely, the C capsids are fully matured capsids where the inner scaffold shell is replaced by DNA (nucleocapsid) during packaging[158].

HSV-1 tegument layer contains more than 20 proteins crucial for multiple stages of the virus life cycle. These proteins play key roles in various processes such as transporting the capsid to the nucleus and other organelles (UL36, UL37, ICP0), facilitating viral DNA entry into the nucleus (VP1-2, UL36), activating early genes transcription (VP16), suppressing cellular protein biosynthesis, and inducing mRNA degradation (VP22, UL41). Additionally, the tegument includes RNA-binding proteins such as US11, UL47, and UL49, hypothesized to be bound to both viral and cellular transcripts packaged within the virion[139,159].

The outer envelope consists of a double layer of phospholipids and contains 16 membrane proteins, including 12 different glycoproteins (gB, gC, gD, gE, gG, gH, gI, gJ, gK, gL, gM, and gN). Some of them exist as heterodimers (gH/gL and gE/gI), while most exist as monomers. These glycoproteins are of particular importance since their interactions with the host cell surface proteins mediate HSV-1 entry into the cell. However, just four of them (gB, gD, and the heterodimer gH/gL) are necessary and sufficient for viral entry (more detailed in chapter 1.5)[160,161]. Other glycoproteins serve various functions. Although gE is not essential for viral replication, it can interact with other proteins to facilitate the secondary envelope coating of virions, cell-to-cell transmission, and enhance the neurovirulence of the virus. Normally, gE forms a heterodimer with gI (gE/gI) to facilitate viral immune evasion[162]. On the other hand, gC plays a role in viral entry and binds to complement component C3b, inhibiting complement-

mediated immunity[163]. Additionally, gK interacts with UL20 to coordinate intracellular transport, cell surface expression, and membrane fusion. Finally, gM/gN regulates membrane fusion, while gJ protects against CD8+ cytotoxic T lymphocyte killing of infected cells[164,165].

1.4 Genome organization

The genome of HSV-1 consists of a linear molecule of dsDNA with a total length of 152 kb and approximately 68% CG content. It encodes at least 84 protein-coding ORFs, as well as the long non-coding RNA latency-associated transcript and numerous miRNAs. Viral genes are transcribed by cellular RNA polymerase II through a temporal cascade of immediate early (IE or α), early (E or β), and late (L or γ) viral genes[166].

The viral genome is divided into two regions, designated as long (L) and short (S). Each region of the genome contains a unique sequence, UL and US, which is flanked by inverted repetitive elements known as terminal (TRL and TRS) and internal repeats (IRL and IRS). The genome has three copies of the ~400 bp–500 bp "a" sequence located at the edges of the genome and at the L-S junction, which contains the packaging signal. The "a" sequence provides a possible mechanism for the formation of the four isomers of the genome during DNA replication due to the L and S segment inversion. Most wild-type HSV-1 populations contain these four isomers at equal frequencies. The viral genome also has three replication origins: one at the UL region called OriL and two in the short repeat regions RS known as OriS[167,168] (Figure 7).

Comparative studies have indicated that HSV-1 can be clustered into three "phylogroups" associated with geographic origin: I (Europe and America), II (Europe, Asia, and America), and III (Africa) suggesting that the virus codiverged with human migrations out of Africa[169].
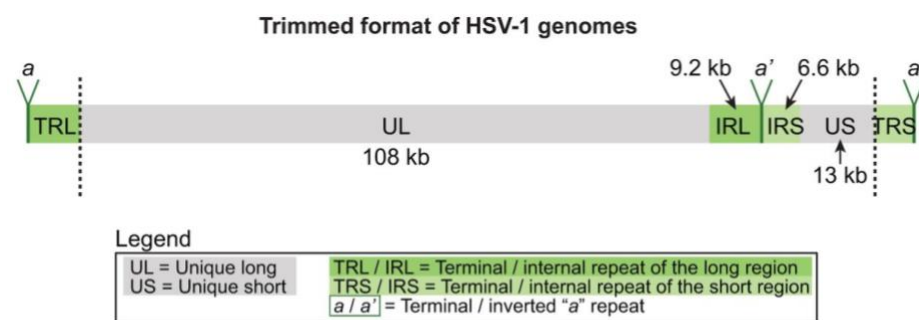

Figure 7. HSV-1 genome. The full structure of the HSV-1 genome includes a unique long region (UL) and a unique short region (US), each of which is flanked by inverted copies of large repeats known as the terminal and internal repeats of the long region (TRL and IRL) and the short region (TRS and IRS). The gene content of each region (UL, US, TRL/IRL, and TRS/IRS) is distinct. A short cleavage and

packaging sequence called a is located as a direct repeat at both genome termini (in TRL and TRS) and as an inverted repeat (a') where IRS and IRL overlap[170].

1.5 Viral replication

The unique aspect of HSV-1's replicative cycle lies in its ability to establish latent infections. Following primary infection, HSV-1 either undergoes lytic replication in epithelial cells, where there is an orchestrated expression of viral genes leading to the production of infectious virions, or latent replication by entering sensory neuron axons and reaching the neuronal cell nucleus. Within the nucleus, the viral DNA remains circular devoid of lytic gene expression, yet latency-associated transcripts (LATs) are expressed and undergo splicing to generate certain mRNAs. Recent research on the functions of LATs has yielded conflicting views, but prevailing theories suggest their primary role is in the generation of miRNAs and siRNAs, which subsequently downregulate the expression of ICP0 and other lytic genes. In response to various stimuli, HSV-1 can reactivate itself, initiating a new round of replication and leading to a recurrent acute infection[171].

1.5.1 HSV-1 lytic cycle

The life cycle of HSV-1 involves several stages: entry into the host cell, expression of viral genes, replication, virion assembly, and the release of newly formed viral particles (Figure 8). In permissive cell lines, this cycle usually takes around 18-20 hours. Two distinct entry pathways have been proposed for HSV-1: i) the primary mechanism involves the fusion of the viral envelope with the host cell's plasma membrane hinged by the interaction between surface glycoproteins of the virus and specific cell surface receptors, followed by the transport of the viral capsid to the nucleus; ii) alternatively, the virus can utilize endocytosis of the enveloped virion, followed by fusion of the envelope with intracellular vesicles[139].

Initial attachment of the virus to cells occurs through the interaction of gB, and/or gC, with cell surface glycosaminoglycans, particularly heparin sulphate portions of proteoglycans (HSPGs). However, this interaction alone is not sufficient for viral entry. Following binding of the virus to the cell surface, cell entry requires that viral gD engage any one of its specific cell surface receptors— nectin-1 and nectin-2, herpesvirus entry mediator (HVEM), and 3-O-sulfated heparan sulphate (3-O-S-HS). This binding event triggers conformational change in gD which transmits an activation signal to gB, and gH/ gL leading to membrane fusion. Thus, fusion requires the formation of a multiprotein complex (a fusogenic complex) comprised of gD, gB,

and gH/gL[161,172]. Specifically, the N-terminal region of gD binds to cellular receptors, leading to the release of its C-terminal domain, which in turn activates gB and the gH/gL complex, initiating membrane fusion. Conversely, when gD is not bound to its ligand, the C-terminal domain remains blocked. Additionally, the interaction between gB and paired immunoglobulin-like type 2 receptor α (PILRα) is essential for viral entry into the cell[160,173].

After fusion, certain tegument proteins, such as VP16, separate from the capsid and travel independently to the nucleus, while others remain attached. Inner tegument proteins facilitate interaction with dynein, dynactin, and kinesin motor proteins, enabling capsid transport on microtubules towards the nucleus. The primary viral proteins responsible for nuclear targeting, which is necessary for genome import into the nucleus, are pUL36 and pUL37[174].

Upon reaching the nuclear membrane, the capsid associates with the nuclear pore complex through the inner tegument protein VP1/2, which contains a nuclear localization signal, and nucleoporins Nup358 and Nup214, which directly or indirectly bind the capsid. The capsid then binds to the nuclear pore complex, positioning its unique portal-containing vertex just above the nuclear pore. The viral linear DNA genome enters the nucleus via the nuclear import pathway, which is mediated by importin-β. The transcription and replication of the viral genome occur within the nucleus. During infection, the nucleus undergoes reorganization, resulting in an increase in size, disruption of the nucleolus and nuclear domain-10 (ND-10), and chromatin condensation. In the late stages of infection, the chromatin and nuclear lamina are destroyed. The infection also blocks key cellular processes, including transcription, splicing of cellular RNA, protein biosynthesis, and cellular response to infection. All of these steps enhance the efficiency of viral replication and transcription[139].

Viral proteins regulate sequential transcriptional cascades of α, β, and γ genes, as well as a series of post-translational modifications. The presence of the tegument protein VP16 is crucial for the transcription of IE genes, as it forms a complex with host cell factor 1 (HCF-1) and octamer binding protein-1 (Oct-1) that binds to the promoter of IE genes, driving their expression[175].

The IE genes, namely ICP0, ICP4, ICP22, ICP27, ICP47, and US1.5, are expressed without de novo viral protein synthesis. Their primary function is to activate the transcription of E genes, many of which produce proteins involved in DNA replication through the rolling circle mechanism. IE proteins perform multiple functions and cause significant reorganization of

cellular processes to benefit the virus. ICP0 contains the E3 domain, which exhibits ubiquitin ligase activity towards a wide range of substrates, including cellular proteins involved in defence against viral infection, such as the interferon-inducible protein 16 (IFI16), a DNA sensor triggering the cascade of the innate immune response. These proteins can be degraded through the proteasome system upon ubiquitination[174,176].

The E genes encode proteins and enzymes that participate in various viral processes, such as genome replication (*e.g.* viral DNA polymerase or UL30), regulation of nucleotide metabolism (*e.g.* thymidine kinase or UL23), suppression of IE genes, and activation of L genes. Thymidine kinase, for example, is essential for viral DNA synthesis and repair, as the corresponding host cell enzyme production is inhibited.

After initiation, viral DNA synthesis switches from a theta replication mechanism to a rolling-circle mechanism. The latter produces concatemeric molecules that are cleaved during the process of nucleocapsid assembly. The UL30 complex, in conjunction with processivity factor UL42, synthesizes the leading and lagging DNA strands. In addition to seven viral proteins, a few cellular proteins appear to participate in replication. These include DNA ligase, topoisomerase II, and various components of the DNA repair and homologous recombination systems. Moreover, the cellular chaperone Hsp90 is crucial for viral replication. Inhibiting it impairs replication and results in viral DNA polymerase mis-localization to the cytoplasm and its proteasome-dependent degradation[174].

After DNA replication, the L genes are expressed, which encode structural proteins involved in virus assembly.

Viral transcription, DNA replication, capsid assembly, and viral genome packaging occur in the nucleus[151]. To ensure specific nuclear import of viral and host components, HSV-1 exploits host transport factors. Importin α1 is specifically required for the nuclear localization of several important HSV1 proteins, capsid assembly, and capsid egress into the cytoplasm[177].

Mature nucleocapsids containing viral DNA exit the nucleus through an envelopment-deenvelopment process. During this process, the capsid acquires a primary envelope from the inner nuclear membrane, which is soon lost upon fusion with the outer nuclear membrane. The capsid is then released into the cytoplasm. The nuclear egress complex, formed by pUL31 and pUL34, mediates this process through interaction with viral and cellular proteins, such as lamin A/C[178]. Once in the cytoplasm, capsids travel along microtubules to reach, dock, and envelope

at cytoplasmic organelles. Specifically, viral proteins UL36 and UL37 participate in transporting the capsids on microtubules in the cytoplasm, where capsids acquire more inner tegument proteins. Outer tegument proteins and viral membrane proteins are incorporated at the membrane compartments of trans-Golgi network vesicles and endosomes, where viral glycoproteins accumulate independently of capsid egress[179], to generate mature infectious HSV-1 particles. Finally, vesicles transporting HSV-1 particles fuse with the plasma membrane leading to the release of enveloped viruses into the extracellular space[180].

In addition to infectious heavy particles (H-particles) or virions, cells infected with HSV-1 produce non-infectious light particles (L-particles). L-particles consist of envelope and tegument proteins but lack capsids and the viral genome because they assemble by budding of condensed tegument into Golgi-delivered vesicles. They deliver functional content to non-infected cells, contributing to viral pathogenesis within the infected host by enhancing virion infectivity and providing immune evasion functions[181].
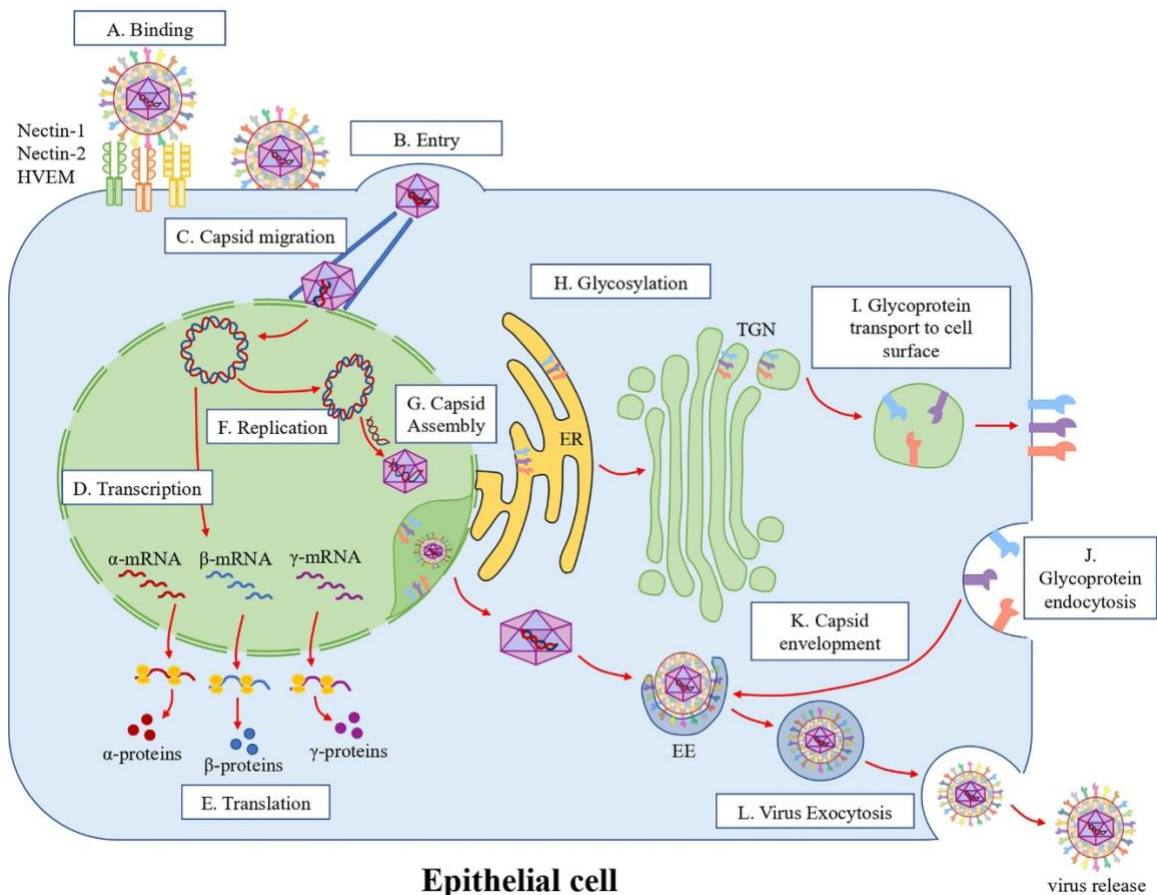

Figure 8. HSV-1 replication cycle in epithelial cells. The HSV-1 replication cycle in epithelial cells begins with the virus attaching to cell surface receptors, where glycoproteins gB and gC recognize and bind to heparan sulfate proteoglycans (HSPGs). Subsequently, gD binds to nectin-1, nectin-2, or HVEM,

activating the gH/gL complex on the virion surface, which in turn activates gB. Acting as a fusion protein, gB facilitates the fusion of viral and cellular membranes. Following membrane fusion, viral capsids and tegument proteins are released into the cytoplasm. Capsids are transported via microtubules to the outer nuclear membrane, where the viral dsDNA genome is injected into the nucleus through nuclear pores. Within the nucleus, the HSV-1 genome undergoes replication via a rolling circle mechanism, with sequential transcription of viral alpha, beta, and gamma genes. Resulting viral mRNAs are exported from the nucleus for translation and viral protein synthesis. Capsid assembly occurs in the host nucleus, where capsid proteins assemble to form viral capsids and encapsulate the viral genome. Newly formed capsids cross the nuclear membrane through envelopment/de-envelopment processes. Viral glycoproteins are synthesized and glycosylated in the rough endoplasmic reticulum (RER), processed in the trans-Golgi network (TGN), and then transported to the cell surface via multivesicular bodies (MVB). Exported glycoproteins are endocytosed, contributing to the formation of viral particle envelopes within the cytoplasm. Concentrated in early endosomes (EE), these glycoproteins then fuse with viral capsids in the cytoplasm. Once the capsids are coated with viral glycoproteins, the virions are ready for release via exocytosis[171].

1.5.2 HSV-1 latent infection

Following lytic replication, the novel infectious viral particles released by epithelial cells can gain access to and enter type-C fibres of sensory neurons that innervate the skin[182]. Capsids, carrying viral genomes, are released into the cytoplasm and retrograde transported by microtubules to the neuronal soma of trigeminal ganglia or dorsal root ganglia, depending on the site of infection, where the viral genome is released in the neuronal nucleus, where a non-productive infection (latency) occurs (Figure 9). One current hypothesis considers the architecture of the innervating neuron to be a key component in the latency process: the extensive trafficking of capsids through long axons results in the inefficient transport of tegument proteins (*e.g.* VP16) to the nucleus, and subsequently in insufficient transcriptional activation of IE gene expression, which favour genome repression by epigenetic regulation[183–185].

During latency, viral DNA persists as a circular episome in the neuronal nucleus. Viral genome transcription is repressed, except for the LAT, an approximately 8.3-kb long noncoding RNA that is spliced to form stable 2.0 and 1.5 introns with lariat structures, and a set of microRNAs, such as miR-H2, which reduce the expression of ICP0, and miR-H6, that inhibit ICP4. The LAT has a neuron-specific enhancer, that promotes its expression in the nucleus of latently

infected cells, is implicated in protecting latently infected neurons from apoptosis, and in contributing to modifications of histones to regulate expression of latent and lytic genes[186–189].

The virus can persist in the latent form forever. However, HSV-1 can reactivate in response to local stimuli, such as injury to the innervated tissue by neurons harbouring latent HSV, or by systemic factors such as physical or emotional stress, fever, exposure to ultraviolet light, menstruation, and hormonal imbalance of stimuli[190]. These stimuli activate different cellular processes to result in increased lytic gene expression and the production of infectious virions within neurons. Novel particles or nucleocapsids travel by anterograde axonal transport to the initial site of infection, causing secondary or recurrent lesions, viral shedding, and transmission to new hosts. Additionally, the newly synthesized viral particles can spread to other cells or tissues. Notably, HSV-1 reactivated from neurons of the trigeminal ganglia is likely the primary source of the virus that causes herpetic encephalitis[191].
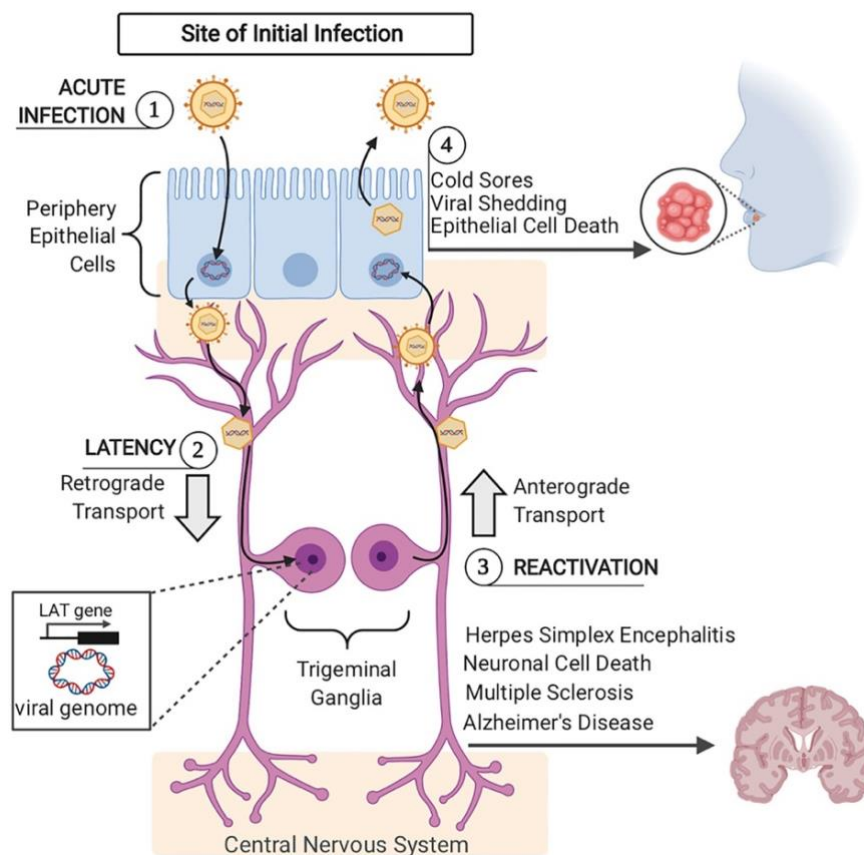

Figure 9. Acute and latent HSV-1 infection. Acute HSV-1 infection begins when infectious virions enter epithelial cells through viral envelope fusion with the plasma membrane. The viral nucleocapsid then enters the nucleus of the epithelial cells, where viral genome replication and viral gene expression occur, producing more infectious virions. Newly formed viral particles are released, some of which infect nearby innervating sensory neurons. Via retrograde trafficking, HSV-1 capsids reach the neuronal

cell body in the sensory ganglia, specifically the trigeminal ganglia. Once in the neuronal nucleus, the viral DNA circularises, leading to the silencing of viral genome transcription, except for the latency-associated transcript (LAT) gene. If viral progeny reaches the central nervous system, it can cause herpes simplex encephalitis, and neuronal cell death, and has more recently been linked to long-term pathogenesis, including Multiple Sclerosis and Alzheimer's Disease. During viral reactivation, viral nucleocapsids exit the neuronal nucleus and return to epithelial cells through anterograde trafficking. Upon arrival at the epithelial cells, the virions initiate viral replication, leading to the assembly and release of viral progeny. This process results in the death of the epithelial cells and the development of clinical manifestations[142].

1.6 Clinical manifestations

HSV-1 infection is often asymptomatic. However, when symptoms do occur, they can range from mild oral and facial lesions to life-threatening pathologies[144].

The infection typically affects the skin and mucosal membranes of the face and mouth, resulting in gingivostomatitis and herpes labialis, the genital organs with genital herpes, or the hands with herpetic whitlow. Serious disorders can occur when the virus infects the eye, leading to episodes of blepharitis, conjunctivitis, retinitis, and epithelial keratitis. In addition, the virus can spread to the central nervous system, causing rapidly progressive, necrotizing, and potentially fatal herpetic encephalitis that damages the brain[192]. Severe complications mainly occur in individuals with an immature or compromised immune system, such as newborns, transplant recipients, and those with AIDS[193].

Neonatal herpes typically occurs when neonates are exposed to HSV-1 during vaginal delivery, although intrauterine and post-partum infections can also occur. In newborns, HSV-1 can cause a disseminated, devastating, and potentially fatal disease[194].

Primary HSV-1 infection of the oropharynx is characterized by vesicular lesions on the buccal and gingival mucosa. The most common manifestation of HSV-1 is cold sores, also known as herpetic fever, on the mouth or lips. In children, symptomatic primary oro-labial HSV-1 infections often present as gingivostomatitis.

The vast majority of genital herpes cases are caused by HSV-2, although the prevalence of HSV-1 is increasing, especially in the young population due to oral sex. Genital herpes is characterised by ulcerative vesicles that resemble those found in cold sores. These vesicles can appear on the penis, cervix, vulva, vagina, or perineum[195]. The reactivation of both orofacial

and genital infections is pre-announced by a prodromal stage in which the patient feels pain, burning sensation, itching, or tingling.

Herpes whitlow is a painful infection of the skin caused by HSV-1 that typically affects the fingers or thumbs. It is most commonly seen in children due to autoinoculation or in dental, medical, and paramedical personnel who do not wear protective gloves. Athletes may also develop a condition known as herpes gladiatorum, which presents as skin ulcerations on the lateral neck, face, and forearms.

Primary ocular HSV-1 can cause blepharitis, conjunctivitis, epithelial keratitis, stromal keratitis, iridocyclitis or retinitis, which may result in visual impairment or blindness.

Herpes encephalitis is a severe and often fatal infection of the brain that primarily affects the temporal lobe, leading to abnormal behaviour and focal neurological deficits localized to that area. Patients may present with fever and altered mental status[144,196].

1.7 Antivirals

The initial antivirals created to treat HSV-1 infection were halogenated nucleoside analogues, such as iododeoxyuridine (IDU) and trifluridine. These compounds hindered viral replication by incorporating their triphosphorylated forms during DNA replication, which resulted in the inhibition of the nascent viral DNA strand. However, their systemic administration was deemed highly toxic due to the lack of selectivity, which also compromised cellular DNA synthesis[138].

The therapy of HSV-1 infection was then revolutionized by the development of nucleoside analogues with a selective mechanism of action, such as acyclovir, penciclovir, and famciclovir. These drugs are also used to treat other herpesvirus infections, such as VZV and HCMV. Although several of these drugs help reduce disease, minimize potential severe damage, and limit the spread of these viruses onto other individuals, they do not affect latent viruses within host neurons and hence, do not cure infection[197,198].

Here are the main HSV-1 antivirals:
- Acyclovir (ACV) is an acyclic guanosine analogue and is the most frequently used compound to treat HSV-1 and HSV-2 manifestations, mainly because of its extremely low toxicity for the host cells. Its selectivity is because it requires intracellular phosphorylation into acyclovir triphosphate to exert its antiviral activity. The viral thymidine kinase (TK) carries out this process by phosphorylating ACV to an ACV-

monophosphate (ACV-MP), which increases the concentration of ACV within infected cells but not in uninfected ones. Subsequently, cellular kinases phosphorylate ACV-MP to ACV-triphosphate (ACV-TP). In its triphosphate form, ACV becomes a substrate for the viral DNA polymerase UL30, thereby interfering with viral DNA synthesis. Unfortunately, HSV-1 has mutated resulting in strains that are resistant to ACV. This is due to mutations in both viral TK, which affect enzyme expression or modify substrate specificity for ACV, and viral DNA polymerase, which allows viral replication in the presence of ACV. Additionally, ACV has poor solubility, low gastrointestinal absorption (oral bioavailability is limited to 20%), and poor membrane permeability, which can lead to severe side effects[199,200].

- Valacyclovir is a prodrug of ACV developed to increase its bioavailability. It is an L-valine ester of ACV targeting hPepT1 peptide transporters present in the intestine, resulting in enhanced absorption at the intestinal level and increased oral bioavailability of the parent ACV to 54%. Because valacyclovir is derived from ACV, cross-resistance between valacyclovir- and ACV-resistant HSV-1 can occur[201].

- Penciclovir is an acyclic guanosine nucleoside analogue and was developed to be phosphorylated more rapidly than ACV, and consequently has a higher half-life than ACV. Like ACV, penciclovir is phosphorylated selectively to monophosphate by viral TK, and subsequently is converted by cellular enzymes into penciclovir triphosphate, which inhibits viral DNA polymerase. However, the oral bioavailability was even lower than that of ACV[202,203].

- Famciclovir is a prodrug developed to increase oral availability and that, after oral administration, is rapidly metabolized to the highly bioavailable antiviral compound penciclovir[204].

- Ganciclovir is a nucleic acid analogue that does not require viral proteins for its activation in the cell and it is primarily used for the treatment of HCMV infections, even though it has antiviral effects against HSV-1. Gancyclovir also demonstrates low bioavailability which can be increased with the addition of a valine ester to yield the prodrug valganciclovir[201].

- Cidofovir is a phosphonate analogue of cytidine, therefore does not require initial phosphorylation by HSV-1 TK. It acts as a nucleotide analogue and polymerase inhibitor with a higher affinity for the viral DNA polymerase than the host one. Cidofovir has been shown to be efficacious against acyclovir-resistant isolates of HSV-1 *in vitro*[197].

- Foscarnet is a pyrophosphate analogue that inhibits the viral DNA polymerase of herpesviruses by binding near the pyrophosphate binding site needed for polymerase activity. It is used in ACV-resistant infections[205].

Currently, there are no available vaccines for HSV-1. However, there are various preventive and therapeutic candidates in both pre-clinical and clinical phases. A prophylactic vaccine would effectively prevent active infection and transmission of the virus, thereby avoiding latent infection of the trigeminal ganglia, reactivation, and the clinical manifestations accompanying it. However, the utility of such a vaccine is in question due to the high prevalence of HSV-1 and early-in-life primary infection. Therapeutic vaccines aim to prevent HSV reactivation, decrease the number of recurrences, or reduce the severity and duration of clinical symptoms[206].

2. ALZHEIMER'S DISEASE

2.1 Alzheimer's disease

Alzheimer's disease (AD) is a chronic neurodegenerative disease characterized by progressive memory loss and cognitive performance deficits. It is the most prevalent form of dementia, accounting for up to 75% of all cases, and affects 10% of individuals over the age of 65 and 50% over the age of 85. The prevalence of AD is increasing annually, making this condition a significant public health issue[207,208].

AD is characterized by identity loss and progressive decline in physical, social, and executive function accompanied by a progressive cognitive decline (episodic memory, linguistic, and spatial orienting)[209]. Most individuals diagnosed with AD experience neuropsychiatric symptoms (NPS): most commonly depression and apathy, although verbal and physical agitation are also highly prevalent. As Alzheimer's progresses, delusions, hallucinations, and aggression become more frequent[210].

From an anatomopathological point of view, AD is characterized by two prototypical lesions that usually rise on the entorhinal cortex, with predictable spread to the hippocampus and eventually throughout the neocortex as the disease progresses. The two lesions are: i) extracellular senile plaques, composed of a nucleus of β-amyloid protein accumulation (Aβ), and ii) intraneuronal neurofibrillary tangles (NFTs) composed of phosphorylated tau protein (P-tau). Deposition of β-amyloid protein can also occur in capillaries walls, arteries, and arterioles causing amyloid cerebral angiopathy worsening blood flow, and predisposing to intraparenchymal haemorrhages[211,212]. Besides the previous key biological features, AD brains are also marked by neuroinflammation, metabolic dysregulation, mitochondria dysfunction, oxidative stress, proteostasis perturbation, and lipid abnormalities[213].

The Aβ peptide is produced through the amyloidogenic proteolysis of amyloid precursor protein (APP), a transmembrane protein that is essential for maintaining brain homeostasis. In the non-amyloidogenic pathway, α-secretase cleaves APP within the Aβ peptide region, while in the amyloidogenic pathway, subsequent processing by β- and γ-secretases (composed of four proteins: presenilin 1 or 2, nicastrin, APH-1, and PEN-2) yields Aβ peptides. Aβ peptides are generated with a predominance of the 40 amino acid form (Aβ 40), followed by 42 (Aβ 42), which is more prone to aggregate. Under physiological conditions, Aβ peptides are produced primarily in monomeric forms that have a synapse-protective function. However, alterations in

the production/clearance of this protein lead to the accumulation of Aβ and the formation of fibrils that aggregate in senile plaques, leading to neuronal toxicity, degeneration, and interfering with the function and survival of neurons. Moreover, Aβ peptide can affect distinct molecular and cellular pathways, thereby facilitating tau phosphorylation, aggregation, mislocalization, and accumulation[214].

Tau protein is a microtubule-associated protein, that stimulates tubulin polymerization, stabilizes microtubules, mediates axonal transport, and modulates synaptic structure and function. However, when hyperphosphorylated, the protein loses its ability to associate with and stabilize microtubules, resulting in neuronal damage and promoting cytotoxicity[212,215].

Both Aβ and P-tau deposits can cause atrophy and death of neurons. This process may involve excitotoxicity, collapse of calcium homeostasis, inflammation, and depletion of energy and growth factors. Consequently, damage to neurons and synapses involved in memory processes, learning, and other cognitive functions leads to cognitive decline[215].

The origins of AD are intricate and not fully understood, but it is estimated that around 70% of the risk of developing AD can be attributed to genetic factors.

Early-onset AD (4-6% of all cases), in other words, individuals in which the onset age is under 65 years, usually are caused by mutations in presenilin 1 (PSEN1), presenilin 2 (PSEN2), or APP. PSEN 1 and 2, membrane proteins belonging to the family of proteases A, regulate γ secretase enzyme functions. Most of APP gene mutations, as well as PSEN1 mutations, lead to an increase in Aβ42: Aβ40 ratio, either by Aβ42 increased expression, reduction of Aβ40, or both, thereby leading to an accumulation of Aβ42.

Late-onset AD, the most common form of AD that affects individuals aged 65 years or older, is mainly associated with apolipoprotein-E (APOE) gene[216]. ApoE is involved in the mobilization and redistribution of lipids and cholesterol during neuronal growth and repair, in the long-distance systemic and cerebrospinal transport of lipids, and in the promotion of synaptic plasticity following neuronal injury. The human APOE gene has three common alleles (ε2, ε3, and ε4), with ε4 allele being the main risk factor for late-onset AD. apoE4 isoform binds to Aβ peptide promoting its polymerization in fibrils and its deposition, while apoE2 and apoE3 are more efficient in promoting Aβ clearance, reducing its deposition in the brain[217,218].

In addition to genetic susceptibility, many theories have been proposed to explain AD pathogenesis, especially for the late-onset sporadic form of the disease. All these theories have led to the conclusion that multiple risk factors, together with genetic predisposition, are likely to be involved in the disease progression, including exacerbation of ageing, exposure to

aluminium, head injury, obesity, diabetes, mitochondrial dysfunction, vascular disease, immune system dysfunction, psychiatric morbidity, and infectious disease[219].

All current AD treatments aim to mitigate the neurotransmitter imbalance resulting from progressive neuronal destruction.

Acetylcholinesterase inhibitors (AChEIs), which include donepezil, galantamine, and rivastigmine, were developed based on the cholinergic hypothesis, which suggests that the progressive loss of limbic and neocortical cholinergic innervation in AD is critically important for memory, learning, attention, and other higher brain functions decline. Furthermore, neurofibrillary degeneration in the basal forebrain is probably the primary cause of the dysfunction and death of cholinergic neurons in this region, giving rise to a widespread presynaptic cholinergic denervation. The AChEIs increase the availability of acetylcholine at synapses and have been proven clinically useful in delaying cognitive decline in AD.

A further therapeutic option available for moderate to severe AD is memantine, an N-methyl-D-aspartate receptor non-competitive antagonist, that binds to open NMDA receptor-operated calcium channels blocking NMDA-mediated ion flux and ameliorating the dangerous effects of pathologically elevated glutamate levels that lead to neuronal dysfunction[220,221].

However, the current clinical trial landscape is more focused on targeting both disease modification, through compounds that cause Aβ and Tau reduction, and potentially modifiable processes that contribute to AD's neuropathology, such as inflammation, oxidative stress, metabolism, and excitotoxicity[222].

2.2 HSV-1 potential role in AD

In the last 40 years, many studies have demonstrated the important role of chronic infection by specific pathogens, including HSV-1, as a risk factor for the development of neurodegenerative diseases, including AD, Parkinson's disease, amyotrophic lateral sclerosis, and multiple sclerosis[223–225]. Specifically, infections of the central nervous system may produce multiple damages in infected and neighbouring cells via different mechanisms: i) activation of inflammatory processes and host immune responses, that can cause chronic damage resulting in alterations of neuronal function and viability; ii) some pathogens can directly trigger neurotoxic pathways; iii) viral and microbial agents can produce molecular hallmarks of neurodegeneration, such as the production and deposit of misfolded protein aggregates, oxidative stress, deficient autophagic processes, synaptopathy and neuronal death[223]. As for

HSV-1, it is gaining greater attention because of its ability to cause recurrent and life-long infections.

In the 80s, Ball first proposed a role for cerebral HSV-1 infection in AD pathogenesis, based on the potential capability of HSV-1 to move from trigeminal ganglia to the brain regions most affected in AD[226]. Subsequently, molecular detection methods on post-mortem brain samples[227] discovered an increase in HSV-1 in AD patients versus control, while serological analysis reported a strong correlation between repeated HSV-1 reactivation and AD incidence[228,229]. However, the cellular and molecular mechanisms underlying the potential role of HSV-1 infection in AD pathogenesis are still to be completely unravelled.

With advanced age, there is an increase in blood-brain-barrier permeability as well as immunosenescence (the gradual dysfunction of the system and overall reduction of immune responses to different perturbations). With the onset of immunosenescence, immune control of HSV-1 latency in peripheral ganglia may diminish, thereby increasing cycling between latency and reactivation. These recurrent reactivations induce an influx of peripheral lymphocytes, recruited by the central nervous system-resident cells (*e.g.,* astrocytes and microglia) that secrete specific cytokines and chemokines in response to virus infection to help virus clearance[230].

In AD, Aβ binds to pattern-recognition receptors (PRRs) on the microglial surface, activating resting microglia, the macrophage-like cells that reside within the parenchyma of the nervous system. In turn, microglia release cytokines to enhance phagocytosis, Aβ uptake, and clearance, inhibit inflammatory processes, and promote tissue repair. The same PRRs recognize the pathogen-associated molecular patterns (PAMPs) in response to viral invasion in the central nervous system. This process, mediated by the PRRs TLR3, 2, and 4 (Toll-like receptor), initiates a series of signalling events that culminate in producing type I interferons (IFN-I) and inflammatory cytokines to establish a potent antiviral state[231,232]. In microglia, HSV-1 infection induces the cGAS-STING pathway that stimulates IFN and inflammatory cytokine production. The activation of this pathway of the innate immune response has a neuroprotective role, as demonstrated by Reinert and collaboratores[233]. However, in the context of periodic HSV-1 reactivation, long-term activation of microglia gives rise to neuroinflammation causing synaptic dysfunction and neurotoxicity that contribute to gradual neuronal loss[213].

As introduced before, the apolipoprotein ApoE4 is a primary genetic risk factor for AD. Linard and colleagues revealed that the frequency of HSV-1 reactivation was correlated with the onset of AD in ApoE4 carriers[234]. In addition, murine experiments discovered that knocking out ApoE4 led to a significantly lower detection of HSV-1 genomes in the nervous system, suggesting that ApoE4 facilitates HSV-1 neuroinvasiveness[235].

Another evidence supporting the hypothesis of the role of HSV-1 in AD pathogenesis is the well-accepted mechanisms that Aβ functions as an antiviral peptide and is induced by HSV-1 infection. To exert its antiviral activity, Aβ deposits on HSV-1 virion particles such that HSV-1 induces the oligomerization and fibrilization of Aβ through physical interaction with its surface glycoprotein B[236,237]. Moreover, HSV-1 was shown to directly induce the accumulation of Aβ42 upregulating the secretases implicated in APP cleavage[238]. Santana and colleagues showed that HSV-1 infection induced Aβ accumulation by impairing the autophagy machinery in human neuroblastoma cells[239]. Inhibition of autophagy, a cellular process that degrades cellular components and allows the clearance of aggregated proteins, in neurons could lead to an accumulation of amyloid proteins and phosphorylated Tau, triggering neuronal cell death and degeneration of the brain of AD patients. Together, these findings demonstrate that HSV-1 infection of neurons activates several distinct mechanisms that can cause Aβ accumulation and consequent neurotoxic events[83].

In addition to Aβ accumulation, HSV-1 infection can trigger tau phosphorylation[240], which in turn increases host DNA damage[241] which can contribute to neuronal cell death and potentially accelerates AD progression.

In AD, different mitochondrial abnormalities have been revealed, such as structural alterations, age-dependent accumulation of oxidized mitochondrial DNA (mtDNA), loss of mitochondrial membrane potential, excessive mitochondrial ROS production, diminished mitochondrial adenosine triphosphate (ATP), disrupted electron transport chain (ETC), and imbalanced mitochondrial fragmentation and fusion[242]. One of the most important functions of mitochondria is oxidative phosphorylation (OXPHOS) via the tricarboxylic acid (TCA) cycle, which provides the energy source to maintain most of the ATP-dependent biological processes. Indeed, neurons are highly dependent on the mitochondrial OXPHOS for synaptic functions. However, Vastag and colleagues discovered that HSV-1 infection reprograms cellular metabolism to aerobic glycolysis to synthesize *de novo* nucleotide crucial for viral replication, while HCMV hijacked cellular metabolism to synthesize fatty acids[243]. Therefore, in neurons,

HSV-1 infection imposes a metabolic switch from mitochondrial oxidative phosphorylation to aerobic glycolysis, which undermines the proper neuronal functions, increases glucose consumption, and leads to inefficient ATP production and excessive lactate secretion, as observed in the early stages of AD[213].

2.3 Lipids, HSV-1, and AD

Lipids play a crucial role in the normal development and functioning of the central nervous system, with sphingolipids and cholesterol being the most prevalent. These lipids serve not only as the fundamental building blocks for membranes but also influence membrane fluidity based on their composition, level of unsaturation, and fatty acyl tail length. Moreover, lipids serve as signalling molecules that regulate various biological processes, including apoptosis, mitochondrial function, immune response, and metabolism, and in some circumstances, they can serve as bioenergetic fuel for the brain[244,245].

Lipids are increasingly recognized as playing a significant role in neurodegenerative diseases. The strong association between lipid metabolism and AD is highlighted by the fact that the most common genetic risk factor for AD is the presence of the ApoE4 allele, responsible for encoding an apolipoprotein essential for transporting cholesterol into the brain. This underscores the close connection between lipid metabolism and AD. Indeed, when APOE4 is expressed in human induced pluripotent stem cell (iPSC)–derived astrocytes and glial cells, it disrupts lipid homeostasis by increasing unsaturated fatty acids and leading to the accumulation of intracellular lipid droplets[246]. Additionally, lipidomic analyses have identified significant alterations in the levels of various lipids, including fatty acids, glycerolipids, glycerophospholipids, sphingolipids, and cholesterol[247,248].

Cellular metabolism reprogramming is a crucial step in viral infections. Upon *de novo* infection or reactivation, HSV-1 redirects cellular metabolism to support viral replication. Specifically, viral replication necessitates the synthesis of nucleic acids, amino acids, and complex lipids, which requires the active transfer of hydrocarbons from complete combustion in the TCA cycle into anabolic pathways.

While several studies have indicated that the fatty acid synthesis pathway remains relatively unchanged during HSV-1 infection[243,249], my preliminary data suggests that *de novo* lipogenesis mediated by FASN (fatty acid synthase) enzyme may play a crucial role in generating infectious viral particles during infection. Furthermore, other studies have investigated how HSV-1

impacts lipid metabolism. For instance, HSV-1 has been shown to stimulate phospholipid synthesis[250], and the viral UL21 protein activates the cellular ceramide transport protein (CERT), facilitating the synthesis of sphingomyelin from ceramide[251]. Additionally, HSV-1 is known to activate the cGAS-STING pathway, which not only triggers the antiviral inflammatory response but also promotes fatty acid desaturase 2 (FADS2)-mediated desaturation to enhance polyunsaturated fatty acid (PUFA) synthesis. Interestingly, PUFA has been found to inhibit STING-mediated signalling, suggesting that HSV-1 may elevate PUFA levels to counteract STING-dependent innate immune defences[252].

3. OBJECTIVES

Emerging research has unveiled an interesting interplay between herpesvirus infection and cellular lipid metabolism. Lipid metabolism, essential for myriad cellular functions, appears to orchestrate pivotal stages of the viral life cycle (*i.e.,* viral entry, replication, and assembly of novel virion particles). Hence, discerning how HSV-1 infection alters cellular lipid metabolism holds promise for uncovering potential targets for viral inhibition.

Moreover, viral hijacking of lipid metabolism is not only crucial for understanding viral replication but also bears implications for associated diseases, including neurodegenerative disorders such as Alzheimer's disease. Mounting experimental evidence suggests that recurrent HSV-1 reactivation could contribute to intracellular damage and subsequent neurodegeneration. Various epidemiological, immunological, and molecular studies have forged a link between HSV-1 infection and the onset of Alzheimer's disease. This correlation is underscored by the pivotal role that perturbations in lipid metabolism play in the aetiology and progression of Alzheimer's disease, prompting speculation about whether these metabolic alterations influence the progression of Alzheimer's disease during HSV-1 infection.

CONCLUSIONS

The research outlined in this thesis has deepened our understanding and revealed new cellular pathways exploited by dsDNA viruses to enhance infection and pathogenesis.

In the first part, I unveiled the role of PAD-mediated citrullination in high-risk HPV pathogenesis within the context of cervical cancer. Specifically, I found a significant association between overall citrullination and PAD4 expression with cervical cancer progression in a cohort of patients exhibiting various stages of cervical lesions. Furthermore, treating CaSki cells, an *in vitro* model of HPV transformation, with the pan-PAD inhibitor BB-Cl-A led to a downregulation of the oncoproteins E6 and E7, accompanied by a robust upregulation of their major cellular targets, p53 and p21. These discoveries introduce a novel element to the complex events associated with HPV-driven transformation, offering potential targets for diagnostic and therapeutic advancements aimed at mitigating HPV transformation in infected patients.

In the second part of my Doctoral Thesis, I demonstrated the essential role of *de novo* lipogenesis in HSV-1 infectivity. Specifically, HSV-1 infection was found to upregulate FASN expression, resulting in a marked increase in lipid concentration and a distinct distribution of lipid species. Conversely, silencing FASN or employing FASN inhibitors CMS121 and C75 reduced viral infectivity, impacting virion structure and host cell entry. Moreover, the provision of lipid-rich external factors from fetal bovine serum significantly augmented HSV-1 infectivity. Notably, in a 3D tissue culture model of herpesvirus-induced Alzheimer's disease, both CMS121 and C75 exhibited potent inhibitory effects on Aβ-like plaque formation, thus linking HSV-1-mediated lipid metabolism dysregulation to Alzheimer's disease etiopathogenesis. These findings underscore the potential of FASN inhibitors to disrupt the progression of Alzheimer's disease by addressing the viral and metabolic components of the disease, offering a novel approach to therapy that could halt or even prevent the development of Alzheimer's disease.

REFERENCES

1. Beltrao P, Krogan NJ, Van Noort V. Evolution and functional cross-talk of protein post-translational modifications. doi:10.1002/msb.201304521

2. Arita K, Hashimoto H, Shimizu T, Nakashima K, Yamada M, Sato M. Structural basis for Ca(2+)-induced activation of human PAD4. *Nat Struct Mol Biol*. 2004;11(8):777-783. doi:10.1038/NSMB799

3. Slade DJ, Fang P, Dreyton CJ, et al. Protein arginine deiminase 2 binds calcium in an ordered fashion: Implications for inhibitor design. *ACS Chem Biol*. 2015;10(4):1043-1053. doi:10.1021/cb500933j

4. Bicker KL, Thompson PR. The protein arginine deiminases: Structure, function, inhibition, and disease. *Biopolymers*. 2013;99(2):155-163. doi:10.1002/bip.22127

5. Slade DJ, Subramanian V, Fuhrmann J, Thompson PR. Chemical and biological methods to detect post-translational modifications of arginine. *Biopolymers*. 2014;101(2):133-143. doi:10.1002/BIP.22256

6. Young C, Russell JR, Van De Lagemaat LN, et al. Intrinsic function of the peptidylarginine deiminase PADI4 is dispensable for normal haematopoiesis. *Biol Open*. 2022;11(6). doi:10.1242/BIO.059143

7. Suzuki A, Yamada R, Chang X, et al. Functional haplotypes of PADI4, encoding citrullinating enzyme peptidylarginine deiminase 4, are associated with rheumatoid arthritis. *Nat Genet*. 2003;34(4):395-402. doi:10.1038/NG1206

8. Musse AA, Zhen L, Ackerley CA, et al. Peptidylarginine deiminase 2 (PAD2) overexpression in transgenic mice leads to myelin loss in the central nervous system. *Dis Model Mech*. 2008;1(4-5):229-240. doi:10.1242/DMM.000729

9. Zhang X, Gamble MJ, Stadler S, et al. Genome-wide analysis reveals PADI4 cooperates with Elk-1 to activate c-Fos expression in breast cancer cells. *PLoS Genet*. 2011;7(6). doi:10.1371/JOURNAL.PGEN.1002112

10. Wang S, Wang Y. Peptidylarginine deiminases in citrullination, gene regulation, health and pathogenesis. *Biochim Biophys Acta - Gene Regul Mech*. 2013;1829(10):1126-1135. doi:10.1016/j.bbagrm.2013.07.003

11. Yuzhalin AE, Gordon-Weeks AN, Tognoli ML, et al. Colorectal cancer liver metastatic growth depends on PAD4-driven citrullination of the extracellular matrix. *Nat Commun*. 2018;9(1). doi:10.1038/S41467-018-07306-7

12. Christophorou MA, Castelo-Branco G, Halley-Stott RP, et al. Citrullination regulates

pluripotency and histone H1 binding to chromatin. *Nature*. 2014;507(7490):104-108. doi:10.1038/NATURE12942

13. Xu Y, Shi Y, Fu J, et al. Mutations in PADI6 Cause Female Infertility Characterized by Early Embryonic Arrest. *Am J Hum Genet*. 2016;99(3):744-752. doi:10.1016/J.AJHG.2016.06.024

14. Falcão AM, Meijer M, Scaglione A, et al. PAD2-Mediated Citrullination Contributes to Efficient Oligodendrocyte Differentiation and Myelination. *Cell Rep*. 2019;27(4):1090-1102.e10. doi:10.1016/J.CELREP.2019.03.108

15. SMITH DG, YOUNG EG. THE COMBINED AMINO ACIDS IN SEVERAL SPECIES OF MARINE ALGAE. *J Biol Chem*. 1955;217(2):845-853. doi:10.1016/S0021-9258(18)65949-6

16. Rogers GE, Simmonds DH. Content of Citrulline and Other Amino-Acids in a Protein of Hair Follicles. *Nat 1958 1824629*. 1958;182(4629):186-187. doi:10.1038/182186a0

17. Lorand L, Fuchs LE, Jacobsen A; R. Occurrence of Citrulline in Proteins. *Nat 1962 1944834*. 1962;194(4834):1149-1151. doi:10.1038/1941149a0

18. Fujisaki M, Sugawara K. Properties of Peptidylarginine Deiminase from the Epidermis of Newborn Rats. *J Biochem*. 1981;89(1):257-263. doi:10.1093/OXFORDJOURNALS.JBCHEM.A133189

19. Cummings TFM, Gori K, Sanchez-Pulido L, et al. Citrullination Was Introduced into Animals by Horizontal Gene Transfer from Cyanobacteria. *Mol Biol Evol*. 2022;39(2). doi:10.1093/MOLBEV/MSAB317

20. Witalison EE, Thompson PR, Hofseth LJ. Protein Arginine Deiminases and Associated Citrullination: Physiological Functions and Diseases Associated with Dysregulation. *Curr Drug Targets*. 2015;16(7):700. doi:10.2174/1389450116666150202160954

21. Christophorou MA. The virtues and vices of protein citrullination. *R Soc Open Sci*. 2022;9(6). doi:10.1098/RSOS.220125

22. Biorender. www.biorender.com.

23. Yang ML, Sodré FMC, Mamula MJ, Overbergh L. Citrullination and PAD Enzyme Biology in Type 1 Diabetes – Regulators of Inflammation, Autoimmunity, and Pathology. *Front Immunol*. 2021;12:678953. doi:10.3389/FIMMU.2021.678953/BIBTEX

24. Vossenaar ER, Zendman AJW, Van Venrooij WJ, Pruijn GJM. PAD, a growing family of citrullinating enzymes: genes, features and involvement in disease. *BioEssays*. 2003;25(11):1106-1118. doi:10.1002/BIES.10357

25. Nakashima K, Hagiwara T, Yamada M. Nuclear Localization of Peptidylarginine Deiminase V and Histone Deimination in Granulocytes. *J Biol Chem*. 2002;277(51):49562-49568. doi:10.1074/JBC.M208795200

26. Cherrington BD, Zhang X, Mcelwee JL, Morency E, Anguish LJ. Potential Role for PAD2 in Gene Regulation in Breast Cancer Cells. *PLoS One*. 2012;7(7):41242. doi:10.1371/journal.pone.0041242

27. The Protein Data Bank. https://www.rcsb.org. Published 2023.

28. Alghamdi M, Al Ghamdi KA, Khan RH, Uversky VN, Redwan EM. An interplay of structure and intrinsic disorder in the functionality of peptidylarginine deiminases, a family of key autoimmunity-related enzymes. *Cell Mol Life Sci*. 2019;76(23):4635-4662. doi:10.1007/S00018-019-03237-8/FIGURES/14

29. Yu K, Proost P. Insights into peptidylarginine deiminase expression and citrullination pathways. *Trends Cell Biol*. 2022;32(9):746-761. doi:10.1016/J.TCB.2022.01.014

30. Zhang X, Liu X, Zhang M, et al. Peptidylarginine deiminase 1-catalyzed histone citrullination is essential for early embryo development OPEN. 2016. doi:10.1038/srep38727

31. Pong K, Subramanian V, Nicholas AP, Thompson PR, Ferretti P. Modulation of calcium-induced cell death in human neural stem cells by the novel peptidylarginine deiminase-AIF pathway. 2014. doi:10.1016/j.bbamcr.2014.02.018

32. Vossenaar ER, Zendman AJW, Van Venrooij WJ, Pruijn GJM. PAD, a growing family of citrullinating enzymes: genes, features and involvement in disease. *BioEssays*. 2003;25:1106-1118. doi:10.1002/bies.10357

33. Esposito G, Vitale AM, Leijten FPJ, et al. Peptidylarginine deiminase (PAD) 6 is essential for oocyte cytoskeletal sheet formation and female fertility. *Mol Cell Endocrinol*. 2007;273(1-2):25-31. doi:10.1016/J.MCE.2007.05.005

34. György B, Tóth E, Tarcsa E, Falus A, Buzás EI. Citrullination: A posttranslational modification in health and disease. *Int J Biochem Cell Biol*. 2006;38(10):1662-1677. doi:10.1016/j.biocel.2006.03.008

35. Mattson MP, Chan SL. Calcium orchestrates apoptosis. *Nat Cell Biol 2003 512*. 2003;5(12):1041-1043. doi:10.1038/ncb1203-1041

36. Witalison E, Thompson P, Hofseth L. Protein Arginine Deiminases and Associated Citrullination: Physiological Functions and Diseases Associated with Dysregulation. *Curr Drug Targets*. 2015;16(7):700-710. doi:10.2174/1389450116661150202160954

37. Hsu PC, Liao YF, Lin CL, Lin WH, Liu GY, Hung HC. Vimentin is involved in

peptidylarginine deiminase 2-induced apoptosis of activated Jurkat cells. *Mol Cells*. 2014;37(5):426-434. doi:10.14348/MOLCELLS.2014.2359

38. Chang X, Fang K. PADI4 and tumourigenesis. *Cancer Cell Int*. 2010;10. doi:10.1186/1475-2867-10-7

39. U KP, Subramanian V, Nicholas AP, Thompson PR, Ferretti P. Modulation of calcium-induced cell death in human neural stem cells by the novel peptidylarginine deiminase-AIF pathway. *Biochim Biophys Acta*. 2014;1843(6):1162-1171. doi:10.1016/J.BBAMCR.2014.02.018

40. Guo Q, Fast W. Citrullination of Inhibitor of Growth 4 (ING4) by Peptidylarginine Deminase 4 (PAD4) disrupts the interaction between ING4 and p53. *J Biol Chem*. 2011;286(19):17069-17078. doi:10.1074/jbc.M111.230961

41. Li P, Yao H, Zhang Z, et al. Regulation of p53 Target Gene Expression by Peptidylarginine Deiminase 4. *Mol Cell Biol*. 2008;28(15):4745-4758. doi:10.1128/mcb.01747-07

42. Zhai Q, Wang L, Zhao P, Li T. Role of citrullination modification catalyzed by peptidylarginine deiminase 4 in gene transcriptional regulation. *Acta Biochim Biophys Sin (Shanghai)*. 2017;49(7):567-572. doi:10.1093/abbs/gmx042

43. Slade DJ, Horibata S, Coonrod SA, Thompson PR. A novel role for protein arginine deiminase 4 in pluripotency: The emerging role of citrullinated histone H1 in cellular programming. *BioEssays*. 2014;36(8):736-740. doi:10.1002/BIES.201400057

44. Liu X, Arfman T, Wichapong K, Reutelingsperger CPM, Voorberg J, Nicolaes GAF. PAD4 takes charge during neutrophil activation: Impact of PAD4 mediated NET formation on immune-mediated disease. *J Thromb Haemost*. 2021;19(7):1607-1617. doi:10.1111/JTH.15313

45. Janssen KMJ, Hop H, Vissink A, et al. Levels of Anti-Citrullinated Protein Antibodies and Rheumatoid Factor, Including IgA Isotypes, and Articular Manifestations in Ulcerative Colitis and Crohn's Disease. *Int J Environ Res Public Health*. 2020;17(21):1-10. doi:10.3390/IJERPH17218054

46. Yang ML, Horstman S, Gee R, et al. Citrullination of glucokinase is linked to autoimmune diabetes. *Nat Commun*. 2022;13(1). doi:10.1038/S41467-022-29512-0

47. Liu Y, Lightfoot YL, Seto N, et al. Peptidylarginine deiminases 2 and 4 modulate innate and adaptive immune responses in TLR-7–dependent lupus. *JCI Insight*. 2018;3(23). doi:10.1172/JCI.INSIGHT.124729

48. Nicholas AP. Dual immunofluorescence study of citrullinated proteins in Parkinson

diseased substantia nigra. *Neurosci Lett*. 2011;495(1):26-29.
doi:10.1016/J.NEULET.2011.03.028

49.   Jang B, Ishigami A, Maruyama N, Carp RI, Choi Y-SK& E-K. Peptidylarginine
deiminase and protein citrullination in prion diseases. *Prion*. 2013;7(1):42-46.
doi:10.4161/pri.22380

50.   Ishida-Yamamoto A, Senshu T, Takahashi H, Akiyama K, Nomura K, Iizuka H.
Decreased deiminated keratin K1 in psoriatic hyperproliferative epidermis. *J Invest
Dermatol*. 2000;114(4):701-705. doi:10.1046/J.1523-1747.2000.00936.X

51.   Damgaard D, Senolt L, Nielsen CH. Increased levels of peptidylarginine deiminase 2
in synovial fluid from anti-CCP-positive rheumatoid arthritis patients: Association with
disease activity and inflammatory markers. *Rheumatology*. 2016;55(5):918-927.
doi:10.1093/RHEUMATOLOGY/KEV440

52.   Darrah E, Andrade F. Rheumatoid arthritis and citrullination. *Curr Opin Rheumatol*.
2018;30(1):72-78. doi:10.1097/BOR.0000000000000452

53.   Yang L, Tan D, Piao H. Myelin Basic Protein Citrullination in Multiple Sclerosis: A
Potential Therapeutic Target for the Pathology. *Neurochem Res*. 2016;41(8):1845-
1856. doi:10.1007/S11064-016-1920-2

54.   Acharya NK, Nagele EP, Han M, et al. Neuronal PAD4 expression and protein
citrullination: Possible role in production of autoantibodies associated with
neurodegenerative disease. *J Autoimmun*. 2012;38(4):369-380.
doi:10.1016/J.JAUT.2012.03.004

55.   Yuzhalin AE. Citrullination in cancer. *Cancer Res*. 2019;79(7):1274-1284.
doi:10.1158/0008-5472.CAN-18-2797

56.   Stadler SC, Vincent CT, Fedorov VD, et al. Dysregulation of PAD4-mediated
citrullination of nuclear GSK3β activates TGF-β signaling and induces epithelialto-
mesenchymal transition in breast cancer cells. *Proc Natl Acad Sci U S A*.
2013;110(29):11851-11856.
doi:10.1073/PNAS.1308362110/SUPPL_FILE/PNAS.201308362SI.PDF

57.   Chang X, Han J, Pang L, Zhao Y, Yang Y, Shen Z. Increased PADI4 expression in
blood and tissues of patients with malignant tumors. *BMC Cancer*. 2009;9(1):1-11.
doi:10.1186/1471-2407-9-40/FIGURES/5

58.   Chang X, Han J. Expression of Peptidylarginine Deiminase Type 4 (PAD4) in Various
Tumors. *Mol Carcinog*. 2006;45:183-196. doi:10.1002/mc.20169

59.   Yuzhalin AE, Gordon-Weeks AN, Tognoli ML, et al. Colorectal cancer liver metastatic

growth depends on PAD4-driven citrullination of the extracellular matrix. doi:10.1038/s41467-018-07306-7

60. Wang L, Song G, Zhang X, et al. PADI2-Mediated Citrullination Promotes Prostate Cancer Progression. *Cancer Res*. 2017;77(21):5755-5768. doi:10.1158/0008-5472.CAN-17-0150

61. Horibata S, Rogers KE, Sadegh D, et al. Role of peptidylarginine deiminase 2 (PAD2) in mammary carcinoma cell migration. *BMC Cancer*. 2017;17(1). doi:10.1186/S12885-017-3354-X

62. Cantarino N, Musulen E, Valero V, et al. Downregulation of the deiminase PADI2 is an early event in colorectal carcinogenesis and indicates poor prognosis. *Mol Cancer Res*. 2016;14(9):841-848. doi:10.1158/1541-7786.MCR-16-0034/176057/AM/DOWNREGULATION-OF-THE-DEIMINASE-PADI2-IS-AN-EARLY

63. Guo W, Zheng Y, Xu B, et al. OncoTargets and Therapy Dovepress investigating the expression, effect and tumorigenic pathway of PaDi2 in tumors. *Onco Targets Ther*. 2017:10-1475. doi:10.2147/OTT.S92389

64. Mcelwee JL, Mohanan S, Griffith OL, et al. Identification of PADI2 as a potential breast cancer biomarker and therapeutic target. 2012. doi:10.1186/1471-2407-12-500

65. Qin H, Liu X, Li F, et al. PAD1 promotes epithelial-mesenchymal transition and metastasis in triple-negative breast cancer cells by regulating MEK1-ERK1/2-MMP2 signaling. 2017. doi:10.1016/j.canlet.2017.08.019

66. Wang Y, Chen R, Gan Y, Ying S. The roles of PAD2- and PAD4-mediated protein citrullination catalysis in cancers. *Int J Cancer*. 2021;148(2):267-276. doi:10.1002/IJC.33205

67. Li F, Miao L, Xue T, et al. Inhibiting PAD2 enhances the anti-tumor effect of docetaxel in tamoxifen-resistant breast cancer cells. *J Exp Clin Cancer Res*. 2019;38(1):1-15. doi:10.1186/S13046-019-1404-8/FIGURES/8

68. Zhu D;, Lu Y;, Wang Y;, et al. PAD4 and Its Inhibitors in Cancer Progression and Prognosis. *Pharm 2022, Vol 14, Page 2414*. 2022;14(11):2414. doi:10.3390/PHARMACEUTICS14112414

69. Struyf S, Noppen S, Loos T, et al. Citrullination of CXCL12 Differentially Reduces CXCR4 and CXCR7 Binding with Loss of Inflammatory and Anti-HIV-1 Activity via CXCR4. *J Immunol*. 2009;182(1):666-674. doi:10.4049/jimmunol.182.1.666

70. Muraro SP, De Souza GF, Gallo SW, et al. Respiratory Syncytial Virus induces the

classical ROS-dependent NETosis through PAD-4 and necroptosis pathways activation. *Sci Rep*. 2018;8(1):1-12. doi:10.1038/s41598-018-32576-y

71. Pasquero S, Gugliesi F, Griffante G, et al. Novel antiviral activity of PAD inhibitors against human beta-coronaviruses HCoV-OC43 and SARS-CoV-2. *Antiviral Res*. 2022;200:105278. doi:10.1016/J.ANTIVIRAL.2022.105278

72. Casanova V, Sousa FH, Shakamuri P, et al. Citrullination Alters the Antiviral and Immunomodulatory Activities of the Human Cathelicidin LL-37 During Rhinovirus Infection. *Front Immunol*. 2020;11(February):1-14. doi:10.3389/fimmu.2020.00085

73. Griffante G, Gugliesi F, Pasquero S, et al. Human cytomegalovirus-induced host protein citrullination is crucial for viral replication. *Nat Commun*. 2021;12(1):1-14. doi:10.1038/s41467-021-24178-6

74. Pasquero S, Gugliesi F, Biolatti M, et al. Citrullination profile analysis reveals peptidylarginine deaminase 3 as an HSV-1 target to dampen the activity of candidate antiviral restriction factors. *PLOS Pathog*. 2023;19(12):e1011849. doi:10.1371/JOURNAL.PPAT.1011849

75. Luo Y, Arita K, Bhatia M, et al. Inhibitors and Inactivators of Protein Arginine Deiminase 4: Functional and Structural Characterization †, ‡. 2006. doi:10.1021/bi061180d

76. Mondal S, Thompson PR. Protein Arginine Deiminases (PADs): Biochemistry and Chemical Biology of Protein Citrullination. *Acc Chem Res*. 2019;52(3):818-832. doi:10.1021/ACS.ACCOUNTS.9B00024/ASSET/IMAGES/LARGE/AR-2019-00024V_0013.JPEG

77. Ledet MM, Anderson R, Harman R, et al. BB-Cl-Amidine as a novel therapeutic for canine and feline mammary cancer via activation of the endoplasmic reticulum stress pathway. doi:10.1186/s12885-018-4323-8

78. Muth A, Subramanian V, Beaumont E, et al. Development of a Selective Inhibitor of Protein Arginine Deiminase 2. *J Med Chem*. 2017;60(7):3198-3211. doi:10.1021/ACS.JMEDCHEM.7B00274/SUPPL_FILE/JM7B00274_SI_002.CSV

79. Antonsson A, Forslund O, Ekberg H, Sterner G, Go¨ran B, Go¨ran Hansson G. The Ubiquity and Impressive Genomic Diversity of Human Skin Papillomaviruses Suggest a Commensalic Nature of These Viruses. *J Virol*. 2000;74(24):11636-11641. doi:10.1128/JVI.74.24.11636-11641.2000

80. H. zur H. Condylomata acuminata and human genital cancer. *Cancer Res*. 1976;(Feb;36(2 pt 2):794).

81.   Papillomavirus Episteme. https://pave.niaid.nih.gov/index.

82.   Lambert PF, McBride A, Ulrich Bernard H. Special issue: The Papillomavirus Episteme. *Virology*. 2013;445(1-2):1. doi:10.1016/J.VIROL.2013.07.017

83.   Magalhães GM, Vieira C, Campos Garcia L, et al. Update on human papilloma virus-part I: epidemiology, pathogenesis, and clinical spectrum. 2020. doi:10.1016/j.abd.2020.11.003

84.   Shanmugasundaram S, You J. Targeting persistent human papillomavirus infection. *Viruses*. 2017;9(8). doi:10.3390/v9080229

85.   Doorbar J, Egawa N, Griffin H, Kranjec C, Murakami I. Human papillomavirus molecular biology and disease association. *Rev Med Virol*. 2015;25(S1):2-23. doi:10.1002/rmv.1822

86.   Scarth JA, Patterson MR, Morgan EL, Macdonald A. The human papillomavirus oncoproteins: A review of the host pathways targeted on the road to transformation. *J Gen Virol*. 2021;102(3):001540. doi:10.1099/JGV.0.001540/CITE/REFWORKS

87.   HOWLEY PM, KNIPE DM. *Fields Virology: Emerging Viruses*. Lippincott Williams & Wilkins; 2020.

88.   McBride AA, Münger K. Expert views on HPV infection. *Viruses*. 2018;10(2). doi:10.3390/v10020094

89.   McBride AA. Human papillomaviruses: diversity, infection and host interactions. *Nat Rev Microbiol*. 2022;20(2):95-108. doi:10.1038/s41579-021-00617-5

90.   Hlectron micrograph of Human Papillomavirus. https://worldofviruses.unl.edu/electron-micrograph-of-human-papillomavirus/.

91.   Josué Castro-Muñoz L, Manzo-Merino J, Omar Muñoz-Bello J, et al. the Human papillomavirus (HpV) E1 protein regulates the expression of cellular genes involved in immune response. doi:10.1038/s41598-019-49886-4

92.   Evande R, Rana A, Biswas-Fiss EE, Biswas SB. Protein–DNA Interactions Regulate Human Papillomavirus DNA Replication, Transcription, and Oncogenesis. *Int J Mol Sci*. 2023;24(10). doi:10.3390/IJMS24108493

93.   Doorbar J, Campbell D, Grand RJ, Gallimore PH. Identification of the human papilloma virus-1a E4 gene products. *EMBO J*. 1986;5(2):355-362. doi:10.1002/J.1460-2075.1986.TB04219.X

94.   Doorbar J., Ely S, Sterling J, McLean C, Crawford L. Specific interaction between HPV-16 E1–E4 and cytokeratins results in collapse of the epithelial cell intermediate filament network. *Nature*. 1991;352:824–827. doi:https://doi.org/10.1038/352824a0

95. Doorbar J. The E4 protein; structure, function and patterns of expression. *Virology*. 2013;445(1-2):80-98. doi:10.1016/J.VIROL.2013.07.008

96. Müller M, Prescott EL, Wasson CW, MacDonald A. Human papillomavirus E5 oncoprotein: Function and potential target for antiviral therapeutics. *Future Virol*. 2015;10(1):27-39. doi:10.2217/FVL.14.99/ASSET/IMAGES/LARGE/FIGURE2.JPEG

97. Wasson CW, Morgan EL, Müller M, et al. Human papillomavirus type 18 E5 oncogene supports cell cycle progression and impairs epithelial differentiation by modulating growth factor receptor signalling during the virus life cycle. *Oncotarget*. 2017;8(61):103581-103600. doi:10.18632/ONCOTARGET.21658

98. Multiple roles of the PI3K/PKB (Akt) pathway in cell cycle progression - PubMed. https://pubmed.ncbi.nlm.nih.gov/12851486/. Accessed March 6, 2024.

99. Zhang B, Spandau DF, Roman A. E5 protein of human papillomavirus type 16 protects human foreskin keratinocytes from UV B-irradiation-induced apoptosis. *J Virol*. 2002;76(1):220-231. doi:10.1128/JVI.76.1.220-231.2002

100. Gutierrez-Xicotencatl L, Pedroza-Saavedra A, Chihu-Amparan L, Salazar-Piña A, Maldonado-Gama M, Esquivel-Guadarrama F. Cellular functions of HPV16 E5 oncoprotein during oncogenic transformation. *Mol Cancer Res*. 2021;19(2):167-179. doi:10.1158/1541-7786.MCR-20-0491/81811/AM/CELLULAR-FUNCTIONS-OF-HPV16-E5-ONCOPROTEIN-DURING

101. Yamato K, Yamada T, Kizaki M, et al. New highly potent and specific E6 and E7 siRNAs for treatment of HPV16 positive cervical cancer. *Cancer Gene Ther 2008 153*. 2007;15(3):140-153. doi:10.1038/sj.cgt.7701118

102. Munger K, Werness BA, Dyson N, Phelps WC, Harlow E, Howley PM. Complex formation of c-myc papillomavirus E7 proteins with the retinoblastoma tumor suppressor gene product. *EMBO J*. 1989;8(13):4099-4105. doi:10.1002/J.1460-2075.1989.TB08594.X

103. McLaughlin-Drubin ME, Münger K. The human papillomavirus E7 oncoprotein. *Virology*. 2009;384(2):335-344. doi:10.1016/J.VIROL.2008.10.006

104. Munger,' K, Yee CL, Phelps WC, Pietenpol JA, Moses HL, Howley' PM. Biochemical and biological differences between E7 oncoproteins of the high- and low-risk human papillomavirus types are determined by amino-terminal sequences. *J Virol*. 1991;65(7):3943-3948. doi:10.1128/JVI.65.7.3943-3948.1991

105. Shin MK, Balsitis S, Brake T, Lambert PF. Human papillomavirus E7 oncoprotein overrides the tumor suppressor activity of p21Cip1 in cervical carcinogenesis. *Cancer*

Res. 2009;69(14):5656-5663. doi:10.1158/0008-5472.CAN-08-3711/654830/P/HUMAN-PAPILLOMAVIRUS-E7-ONCOPROTEIN-OVERRIDES-THE

106. Fischer M, Uxa S, Stanko C, Magin TM, Engeland K. Human papilloma virus E7 oncoprotein abrogates the p53-p21-DREAM pathway. *Sci Rep*. 2017;7(1). doi:10.1038/S41598-017-02831-9

107. Pal A, Kundu R. Human Papillomavirus E6 and E7: The Cervical Cancer Hallmarks and Targets for Therapy. *Front Microbiol*. 2020;10:510168. doi:10.3389/FMICB.2019.03116/BIBTEX

108. Scheffner M, Werness BA, Huibregtse JM, Levine AJ, Howley PM. The E6 oncoprotein encoded by human papillomavirus types 16 and 18 promotes the degradation of p53. *Cell*. 1990;63(6):1129-1136. doi:10.1016/0092-8674(90)90409-8

109. Murakami I, Egawa N, Griffin H, et al. Roles for E1-independent replication and E6-mediated p53 degradation during low-risk and high-risk human papillomavirus genome maintenance. *PLOS Pathog*. 2019;15(5):e1007755. doi:10.1371/JOURNAL.PPAT.1007755

110. Filippova M, Parkhurst L, Duerksen-Hughes PJ. The Human Papillomavirus 16 E6 Protein Binds to Fas-associated Death Domain and Protects Cells from Fas-triggered Apoptosis. *J Biol Chem*. 2004;279(24):25729-25744. doi:10.1074/JBC.M401172200

111. Yim EK, Meoyng J, Namkoong SE, Um SJ, Park JS. Genomic and Proteomic Expression Patterns in HPV-16 E6 Gene Transfected Stable Human Carcinoma Cell Lines. *https://home.liebertpub.com/dna*. 2004;23(12):826-835. doi:10.1089/DNA.2004.23.826

112. Klingelhutz AJ, Foster SA, McDougall JK. Telomerase activation by the E6 gene product of human papillomavirus type 16. *Nat 1996 3806569*. 1996;380(6569):79-82. doi:10.1038/380079a0

113. Meyers JM, Grace M, Uberoi A, Lambert PF, Munger K. Inhibition of TGF-β and NOTCH Signaling by Cutaneous Papillomaviruses. *Front Microbiol*. 2018;9(MAR). doi:10.3389/FMICB.2018.00389

114. Vats A, Trejo-Cerro O, Thomas M, Banks L. Human papillomavirus E6 and E7: What remains? *Tumour Virus Res*. 2021;11:200213. doi:10.1016/J.TVR.2021.200213

115. Dacus D, Wallace NA. Beta-Genus Human Papillomavirus 8 E6 Destabilizes the Host Genome by Promoting p300 Degradation. *Viruses 2021, Vol 13, Page 1662*. 2021;13(8):1662. doi:10.3390/V13081662

116. Buck CB, Day PM, Trus BL. The papillomavirus major capsid protein L1. *Virology*. 2013;445(1-2):169-174. doi:10.1016/J.VIROL.2013.05.038

117. Bachmann MF, Rohrer UH, Kündig TM, Bürki K, Hengartner H, Zinkernagel RM. The influence of antigen organization on B cell responsiveness. *Science*. 1993;262(5138):1448-1451. doi:10.1126/SCIENCE.8248784

118. Wang JW, Roden RBS. L2, the minor capsid protein of papillomavirus. *Virology*. 2013;445(1-2):175-186. doi:10.1016/J.VIROL.2013.04.017

119. Holmgren SC, Patterson NA, Ozbun MA, Lambert PF. The minor capsid protein L2 contributes to two steps in the human papillomavirus type 31 life cycle. *J Virol*. 2005;79(7):3938-3948. doi:10.1128/JVI.79.7.3938-3948.2005

120. Yang R, Day PM, Yutzy WH, Lin K-Y, Hung C-F, Roden RBS. Cell Surface-Binding Motifs of L2 That Facilitate Papillomavirus Infection. *J Virol*. 2003;77(6):3531-3541. doi:10.1128/JVI.77.6.3531-3541.2003

121. Zayats R, Murooka TT, McKinnon LR. HPV and the Risk of HIV Acquisition in Women. *Front Cell Infect Microbiol*. 2022;12:814948. doi:10.3389/FCIMB.2022.814948/BIBTEX

122. McBride AA. Chapter 4 Replication and Partitioning of Papillomavirus Genomes. *Adv Virus Res*. 2008;72:155-205. doi:10.1016/S0065-3527(08)00404-1

123. Day PM, Baker CC, Lowy DR, Schiller JT. Establishment of papillomavirus infection is enhanced by promyelocytic leukemia protein (PML) expression. *Proc Natl Acad Sci U S A*. 2004;101(39):14252-14257. doi:10.1073/PNAS.0404229101

124. McBride AA. Human papillomaviruses: diversity, infection and host interactions. *Nat Rev Microbiol 2021 202*. 2021;20(2):95-108. doi:10.1038/s41579-021-00617-5

125. Wierzbicka M, San Giorgi MRM, Dikkers FG. Transmission and clearance of human papillomavirus infection in the oral cavity and its role in oropharyngeal carcinoma - A review. *Rev Med Virol*. 2023;33(1). doi:10.1002/RMV.2337

126. Egawa N, Egawa K, Griffin H, Doorbar J. Human Papillomaviruses; Epithelial Tropisms, and the Development of Neoplasia. *Viruses*. 2015;7(7):3863-3890. doi:10.3390/V7072802

127. Mistry N, Wibom C, Evander M. Cutaneous and mucosal human papillomaviruses differ in net surface charge, potential impact on tropism. 2008. doi:10.1186/1743-422X-5-118

128. Chen Y, Li S, Zheng J, Xue H, Chen J, Zheng X. Prevalence of multiple human papillomavirus infections and association with cervical lesions among outpatients in

Fujian, China: A cross-sectional study. *J Med Virol*. 2022;94(12):6028-6036. doi:10.1002/JMV.28062

129. Yousefi Z, Aria H, Ghaedrahmati F, et al. An Update on Human Papilloma Virus Vaccines: History, Types, Protection, and Efficacy. *Front Immunol*. 2022;12. doi:10.3389/FIMMU.2021.805695

130. Lee SM, Park JS, Norwitz ER, et al. Risk of Vertical Transmission of Human Papillomavirus throughout Pregnancy: A Prospective Study. 2013. doi:10.1371/journal.pone.0066368

131. Frazer IH. The HPV Vaccine Story. *ACS Pharmacol Transl Sci*. 2019;2(3):210-212. doi:10.1021/ACSPTSCI.9B00032

132. de Martel C, Plummer M, Vignat J, Franceschi S. Worldwide burden of cancer attributable to HPV by site, country and HPV type. *Int J cancer*. 2017;141(4):664-670. doi:10.1002/IJC.30716

133. Zhou J, Sun X, Davies H, Crawford L, Park D, Frazer I. Definition of linear antigenic regions of the HPV16 L1 capsid protein using synthetic virion-like particles. *Virology*. 1992;189(2):592-599. doi:10.1016/0042-6822(92)90582-a

134. Sipp D, Frazer IH, Rasko JEJ. No Vacillation on HPV Vaccination. *Cell*. 2018;172(6):1163-1167. doi:10.1016/J.CELL.2018.02.045

135. Mohanan S, Horibata S, Anguish LJ, et al. PAD2 overexpression in transgenic mice augments malignancy and tumor-associated inflammation in chemically initiated skin tumors. *Cell Tissue Res*. 2017;370(2):275-283. doi:10.1007/s00441-017-2669-x

136. Shi J, Sun X, Zhao Y, Zhao J, Li Z. Prevalence and significance of antibodies to citrullinated human papilloma virus-47 E2345-362 in rheumatoid arthritis. *J Autoimmun*. 2008;31(2):131-135. doi:10.1016/J.JAUT.2008.04.021

137. Chang X, Han J, Pang L, Zhao Y, Yang Y, Shen Z. Increased PADI4 expression in blood and tissues of patients with malignant tumors. *BMC Cancer*. 2009;9:1-11. doi:10.1186/1471-2407-9-40

138. Rechenchoski DZ, Faccin-Galhardi LC, Linhares REC, Nozawa C. Herpesvirus: an underestimated virus. *Folia Microbiol (Praha)*. 2017;62(2):151-156. doi:10.1007/S12223-016-0482-7/METRICS

139. Kukhanova MK, Korovina AN, Kochetkov SN. Human herpes simplex virus: Life cycle and development of inhibitors. *Biochem*. 2014;79(13):1635-1652. doi:10.1134/S0006297914130124

140. Roizman B, Whitley RJ. The nine ages of herpes simplex virus. *Herpes*. 2001;8(1):23-

27.

141. Parks G. Genital Herpes BT - Sexually Transmitted Diseases: A Practical Guide for Primary Care. In: Nelson AL, Woodward J, Wysocki S, eds. Totowa, NJ: Humana Press; 2006:47-70. doi:10.1007/978-1-59745-040-9_3

142. Verzosa AL, McGeever LA, Bhark SJ, Delgado T, Salazar N, Sanchez EL. Herpes Simplex Virus 1 Infection of Neuronal and Non-Neuronal Cells Elicits Specific Innate Immune Responses and Immune Evasion Mechanisms. *Front Immunol*. 2021;12:644664. doi:10.3389/FIMMU.2021.644664/BIBTEX

143. James C, Harfouche M, Welton NJ, et al. Herpes simplex virus: global infection prevalence and incidence estimates, 2016. *Bull World Health Organ*. 2020;98(5):315-329. doi:10.2471/BLT.19.237149

144. Arduino PG, Porter SR. Herpes Simplex Virus Type 1 infection: overview on relevant clinico-pathological features*. *J Oral Pathol Med*. 2008;37(2):107-121. doi:10.1111/J.1600-0714.2007.00586.X

145. Schelhaas M, Jansen M, Haase I, Knebel-Mörsdorf D. Herpes simplex virus type 1 exhibits a tropism for basal entry in polarized epithelial cells. *J Gen Virol*. 2003;84(9):2473-2484. doi:10.1099/VIR.0.19226-0/CITE/REFWORKS

146. Navneet S, C. TD. Herpes Simplex Virus Latency Is Noisier the Closer We Look. *J Virol*. 2020;94(4):10.1128/jvi.01701-19. doi:10.1128/jvi.01701-19

147. Albecka A, Owen DJ, Ivanova L, et al. Dual Function of the pUL7-pUL51 Tegument Protein Complex in Herpes Simplex Virus 1 Infection. *J Virol*. 2017;91(2). doi:10.1128/JVI.02196-16/ASSET/01F98945-C5C7-4322-8FE4-B64D368F82CF/ASSETS/GRAPHIC/ZJV9991822850008.JPEG

148. HSV-1 virion structure. https://microbenotes.com/herpes-simplex-virus-1-hsv-1/.

149. Grünewald K, Desai P, Winkler DC, et al. Three-Dimensional Structure of Herpes Simplex Virus from Cryo-Electron Tomography. *Science (80-)*. 2003;302(5649):1396-1398. doi:10.1126/science.1090284

150. Kosuke T, Jun A, Yuhei M, Naoto K, Akihisa K, Yasushi K. Identification of the Capsid Binding Site in the Herpes Simplex Virus 1 Nuclear Egress Complex and Its Role in Viral Primary Envelopment and Replication. *J Virol*. 2019;93(21):10.1128/jvi.01290-19. doi:10.1128/jvi.01290-19

151. Heming JD, Conway JF, Homa FL. Herpesvirus capsid assembly and DNA packaging. *Adv Anat Embryol Cell Biol*. 2017;223:119-142. doi:10.1007/978-3-319-53168-7_6/COVER

152. Kim HS, Huang E, Desai J, et al. A Domain in the Herpes Simplex Virus 1 Triplex Protein VP23 Is Essential for Closure of Capsid Shells into Icosahedral Structures. *J Virol*. 2011;85(23):12698-12707. doi:10.1128/JVI.05791-11

153. Douglas MW, Diefenbach RJ, Homa FL, et al. Herpes Simplex Virus Type 1 Capsid Protein VP26 Interacts with Dynein Light Chains RP3 and Tctex1 and Plays a Role in Retrograde Cellular Transport*. 2004. doi:10.1074/jbc.M311671200

154. Wang L, Liu L, Che Y, et al. Egress of HSV-1 capsid requires the interaction of VP26 and a cellular tetraspanin membrane protein. *Virol J*. 2010;7(1):1-12. doi:10.1186/1743-422X-7-156/FIGURES/7

155. K. CS, B. HJ, Katerina T, F. CJ, L. HF. Residues of the UL25 Protein of Herpes Simplex Virus That Are Required for Its Stable Interaction with Capsids . *J Virol*. 2011;85(10):4875-4887. doi:10.1128/jvi.00242-11

156. Dai X, Hong Zhou Z. Structure of the herpes simplex virus 1 capsid with associated tegument protein complexes. *Science (80-)*. 2018;360(6384). doi:10.1126/SCIENCE.AAO7298

157. Zhang D, Su C, Zheng C. Herpes Simplex Virus 1 Serine Protease VP24 Blocks the DNA-Sensing Signal Pathway by Abrogating Activation of Interferon Regulatory Factor 3. *J Virol*. 2016;90(12):5824-5829. doi:10.1128/JVI.00186-16

158. Baines JD. Herpes simplex virus capsid assembly and DNA packaging: a present and future antiviral drug target. *Trends Microbiol*. 2011;19(12):606-613. doi:10.1016/J.TIM.2011.09.001

159. Bowman BR, Baker ML, Rixon FJ, Chiu W, Quiocho FA. Structure of the herpesvirus major capsid protein. *EMBO J*. 2003;22(4):757-765. doi:10.1093/EMBOJ/CDG086

160. Madavaraju K, Koganti R, Volety I, Yadavalli T, Shukla D. Herpes Simplex Virus Cell Entry Mechanisms: An Update. doi:10.3389/fcimb.2020.617578

161. Karasneh GA, Shukla D. Herpes simplex virus infects most cell types in vitro: Clues to its success. *Virol J*. 2011;8(1):1-11. doi:10.1186/1743-422X-8-481/TABLES/1

162. Ning Y, Huang Y, Wang M, et al. Alphaherpesvirus glycoprotein E: A review of its interactions with other proteins of the virus and its application in vaccinology. *Front Microbiol*. 2022;13:970545. doi:10.3389/FMICB.2022.970545/BIBTEX

163. Komala Sari T, Gianopulos KA, Nicola A V. Glycoprotein C of Herpes Simplex Virus 1 Shields Glycoprotein B from Antibody Neutralization. *J Virol*. 2020;94(5). doi:10.1128/JVI.01852-19/ASSET/B7673F0B-8103-4310-9FC6-2CCBCBA37668/ASSETS/GRAPHIC/JVI.01852-19-F0006.JPEG

164. Kim I-J, Chouljenko VN, Walker JD, Kousoulas KG. Herpes Simplex Virus 1 Glycoprotein M and the Membrane-Associated Protein UL11 Are Required for Virus-Induced Cell Fusion and Efficient Virus Entry. *J Virol*. 2013;87(14):8029-8037. doi:10.1128/JVI.01181-13/ASSET/96D82986-B4B8-419D-B9B9-C67507F72BBE/ASSETS/GRAPHIC/ZJV9990978430008.JPEG

165. Dogrammatzis C, Waisner H, Kalamvoki M. "Non-Essential" Proteins of HSV-1 with Essential Roles In Vivo: A Comprehensive Review. *Viruses 2021, Vol 13, Page 17*. 2020;13(1):17. doi:10.3390/V13010017

166. Packard JE, Dembowski JA. HSV-1 DNA Replication-Coordinated Regulation by Viral and Cellular Factors. *Viruses*. 2021;13(10). doi:10.3390/V13102015

167. Colgrove RC, Liu X, Griffiths A, et al. History and genomic sequence analysis of the herpes simplex virus 1 KOS and KOS1.1 sub-strains. *Virology*. 2016;487:215-221. doi:10.1016/J.VIROL.2015.09.026

168. Shitrit A, Nisnevich V, Rozenshtein N, et al. Shared sequence characteristics identified in non-canonical rearrangements of HSV-1 genomes. Parrish CR, ed. *J Virol*. November 2023. doi:10.1128/jvi.00955-23

169. Guellil M, van Dorp L, Inskip SA, et al. Ancient herpes simplex 1 genomes reveal recent viral structure in Eurasia. *Sci Adv*. 2022;8(30):4435. doi:10.1126/SCIADV.ABO4435/SUPPL_FILE/SCIADV.ABO4435_DATA_S1_TO_S9.ZIP

170. L. SM, Derek G, Alejandro O, et al. Evolution and Diversity in Human Herpes Simplex Virus Genomes. *J Virol*. 2014;88(2):1209-1227. doi:10.1128/jvi.01987-13

171. Duarte LF, Reyes A, Farías MA, et al. Crosstalk Between Epithelial Cells, Neurons and Immune Mediators in HSV-1 Skin Infection. *Front Immunol*. 2021;12:662234. doi:10.3389/FIMMU.2021.662234/BIBTEX

172. Spear PG. Herpes simplex virus: receptors and ligands for cell entry. *Cell Microbiol*. 2004;6(5):401-410. doi:10.1111/j.1462-5822.2004.00389.x

173. Polpitiya Arachchige S, Henke W, Kalamvoki M, Stephens EB. Analysis of herpes simplex type 1 gB, gD, and gH/gL on production of infectious HIV-1: HSV-1 gD restricts HIV-1 by exclusion of HIV-1 Env from maturing viral particles. *Retrovirology*. 2019;16(1):9. doi:10.1186/s12977-019-0470-5

174. Zhu S, Viejo-Borbolla A. Pathogenesis and virulence of herpes simplex virus. *Virulence*. 2021;12(1):2670-2702. doi:10.1080/21505594.2021.1982373

175. Wysocka J, Herr W. The herpes simplex virus VP16-induced complex: the makings of

a regulatory switch. doi:10.1016/S0968-0004(03)00088-4

176. Orzalli MH, Broekema NM, Knipe DM. Relative Contributions of Herpes Simplex Virus 1 ICP0 and vhs to Loss of Cellular IFI16 Vary in Different Human Cell Types. *J Virol*. 2016;90(18):8351-8359. doi:10.1128/JVI.00939-16/ASSET/6DB2C444-1512-4919-AF73-CBFE69894906/ASSETS/GRAPHIC/ZJV9991819360007.JPEG

177. Döhner K, Ramos-Nascimento A, Bialy D, et al. Importin α1 is required for nuclear import of herpes simplex virus proteins and capsid assembly in fibroblasts and neurons. *PLOS Pathog*. 2018;14(1):e1006823. doi:10.1371/JOURNAL.PPAT.1006823

178. Songfang W, Shuang P, Liming Z, et al. Herpes Simplex Virus 1 Induces Phosphorylation and Reorganization of Lamin A/C through the γ134.5 Protein That Facilitates Nuclear Egress. *J Virol*. 2016;90(22):10414-10422. doi:10.1128/jvi.01392-16

179. Turcotte S, Letellier J, Lippé R. Herpes simplex virus type 1 capsids transit by the trans-Golgi network, where viral glycoproteins accumulate independently of capsid egress. *J Virol*. 2005;79(14):8847-8860. doi:10.1128/JVI.79.14.8847-8860.2005

180. Ahmad I, Wilson DW. Molecular Sciences HSV-1 Cytoplasmic Envelopment and Egress. doi:10.3390/ijms21175969

181. Heilingloh CS, Krawczyk A. Role of L-particles during herpes simplex virus infection. *Front Microbiol*. 2017;8(DEC). doi:10.3389/fmicb.2017.02565

182. Antinone SE, Smith GA. Retrograde Axon Transport of Herpes Simplex Virus and Pseudorabies Virus: a Live-Cell Comparative Analysis. *J Virol*. 2010;84(3):1504-1512. doi:10.1128/JVI.02029-09/ASSET/6BDE3EAA-388A-4747-9D2B-E484847CB25C/ASSETS/GRAPHIC/ZJV0031028480008.JPEG

183. Hafezi W, Lorentzen EU, Eing BR, et al. Entry of Herpes Simplex Virus Type 1 (HSV-1) into the Distal Axons of Trigeminal Neurons Favors the Onset of Nonproductive, Silent Infection. *PLOS Pathog*. 2012;8(5):e1002679. doi:10.1371/JOURNAL.PPAT.1002679

184. Thellman NM, Triezenberg SJ. Herpes Simplex Virus Establishment, Maintenance, and Reactivation: In Vitro Modeling of Latency. *Pathog 2017, Vol 6, Page 28*. 2017;6(3):28. doi:10.3390/PATHOGENS6030028

185. Bloom DC, Giordani N V, Kwiatkowski DL. Epigenetic regulation of latent HSV-1 gene expression. *BBA - Gene Regul Mech*. 2010;1799:246-256. doi:10.1016/j.bbagrm.2009.12.001

186. Nicoll MP, Proença JT, Efstathiou S. The molecular basis of herpes simplex virus

latency. doi:10.1111/j.1574-6976.2011.00320.x

187. Nicoll MP, Hann W, Shivkumar M, et al. The HSV-1 Latency-Associated Transcript Functions to Repress Latent Phase Lytic Gene Expression and Suppress Virus Reactivation from Latently Infected Neurons. *PLOS Pathog*. 2016;12(4):e1005539. doi:10.1371/JOURNAL.PPAT.1005539

188. Phelan D, Barrozo ER, Bloom DC. HSV1 latent transcription and non-coding RNA: A critical retrospective. *J Neuroimmunol*. 2017;308:65,67,71-66. doi:10.1016/J.JNEUROIM.2017.03.002

189. Cohen JI. Herpesvirus latency. *J Clin Invest*. 2020;130(7):3361-3369. doi:10.1172/JCI136225

190. Roizman B, Whitley RJ. An Inquiry into the Molecular Basis of HSV Latency and Reactivation. 2013. doi:10.1146/annurev-micro-092412-155654

191. Suzich JB, Cliffe AR. Strength in diversity: Understanding the pathways to herpes simplex virus reactivation. *Virology*. 2018;522:81-91. doi:10.1016/J.VIROL.2018.07.011

192. Koujah L, Suryawanshi RK, Shukla D. Pathological processes activated by herpes simplex virus-1 (HSV-1) infection in the cornea. *Cell Mol Life Sci 2018 763*. 2018;76(3):405-419. doi:10.1007/S00018-018-2938-1

193. Crimi S, Fiorillo L, Bianchi A, et al. Herpes Virus, Oral Clinical Signs and QoL: Systematic Review of Recent Data. *Viruses*. 2019;11(5). doi:10.3390/v11050463

194. Murray PR, Rosenthal K, Pfaller MA. *Medical Microbiology*.; 2020.

195. Penello AM, Campos BC, Simão MS, et al. Genital herpes. *Brazilian J Sex Transm Dis*. 2010;22(2):64-72.

196. Whitley RJ, Roizman B. Herpes simplex virus infections. *Lancet (London, England)*. 2001;357(9267):1513-1518. doi:10.1016/S0140-6736(00)04638-9

197. Álvarez DM, Castillo E, Duarte LF, et al. Current Antivirals and Novel Botanical Molecules Interfering With Herpes Simplex Virus Infection. *Front Microbiol*. 2020;11:506216. doi:10.3389/FMICB.2020.00139/BIBTEX

198. Poole CL, James SH. Antiviral Therapies for Herpesviruses: Current Agents and New Directions. *Clin Ther*. 2018;40(8):1282-1298. doi:10.1016/J.CLINTHERA.2018.07.006

199. De Clercq E. Selective anti-herpesvirus agents. *Antivir Chem Chemother*. 2013;23(3):93-101. doi:10.3851/IMP2533/ASSET/IMAGES/LARGE/10.3851_IMP2533-FIG16.JPEG

200. Elion GB. Mechanism of action and selectivity of acyclovir. *Am J Med*. 1982;73(1):7-13. doi:10.1016/0002-9343(82)90055-9

201. Chuchkov K, Chayrov R, Hinkov A, Todorov D, Shishkova K, Stankova IG. Modifications on the heterocyclic base of ganciclovir, penciclovir, acyclovir - syntheses and antiviral properties. *Nucleosides Nucleotides Nucleic Acids*. 2020;39(7):979-990. doi:10.1080/15257770.2020.1725043

202. Leary JJ, Wittrock R, Sarisky RT, Weinberg A, Levin MJ. Susceptibilities of herpes simplex viruses to penciclovir and acyclovir in eight cell lines. *Antimicrob Agents Chemother*. 2002;46(3):762-768. doi:10.1128/AAC.46.3.762-768.2002

203. Sarisky RT, Bacon TH, Boon RJ, et al. Profiling penciclovir susceptibility and prevalence of resistance of herpes simplex virus isolates across eleven clinical trials *. *Arch Virol*. 2003;148:1757-1769. doi:10.1007/s00705-003-0124-7

204. Perry CM, Wagstaff AJ. Famciclovir: A Review of its Pharmacological Properties and Therapeutic Efficacy in Herpesvirus Infections. *Drugs*. 1995;50(2):396-415. doi:10.2165/00003495-199550020-00011/METRICS

205. David Hardy W. Foscarnet treatment of acyclovir-resistant herpes simplex virus infection in patients with acquired immunodeficiency syndrome: Preliminary results of a controlled, randomized, regimen-comparative trial. *Am J Med*. 1992;92(2):S30-S35. doi:10.1016/0002-9343(92)90335-9

206. Krishnan R, Stuart PM. Developments in Vaccination for Herpes Simplex Virus. *Front Microbiol*. 2021;12:798927. doi:10.3389/FMICB.2021.798927/BIBTEX

207. Bhushan I, Access O, Kour M, et al. Alzheimer's disease: Causes & treatment-A review 1 MedDocs Publishers Annals of Biotechnology. 2018. http://meddocsonline.org/. Accessed March 8, 2024.

208. Sáiz-Vazquez O, Puente-Martínez A, Pacheco-Bonrostro J, Ubillos-Landa S. Blood pressure and Alzheimer's disease: A review of meta-analysis. *Front Neurol*. 2023;13:1065335. doi:10.3389/FNEUR.2022.1065335/BIBTEX

209. EPPERLY T, DUNAY MA, BOICE JL. Alzheimer Disease: Pharmacologic and Nonpharmacologic Therapies for Cognitive and Functional Symptoms. *Am Fam Physician*. 2017;95(12):771-778. https://www.aafp.org/pubs/afp/issues/2017/0615/p771.html. Accessed March 8, 2024.

210. Lyketsos CG, Carrillo MC, Ryan JM, et al. Neuropsychiatric symptoms in Alzheimer's disease. *Alzheimer's Dement*. 2011;7(5):532-539. doi:10.1016/J.JALZ.2011.05.2410

211. Sun B-L, Li W-W, Zhu C, et al. Clinical Research on Alzheimer's Disease: Progress

and Perspectives. *Neurosci Bull*. 34. doi:10.1007/s12264-018-0249-z

212. Silva MVF, Loures CDMG, Alves LCV, De Souza LC, Borges KBG, Carvalho MDG. Alzheimer's disease: risk factors and potentially protective measures. *J Biomed Sci 2019 261*. 2019;26(1):1-11. doi:10.1186/S12929-019-0524-Y

213. Feng S, Liu Y, Zhou Y, et al. Mechanistic insights into the role of herpes simplex virus 1 in Alzheimer's disease. *Front Aging Neurosci*. 2023;15:1245904. doi:10.3389/FNAGI.2023.1245904/BIBTEX

214. Blurton-Jones M, LaFerla F. Pathways by Which Aβ Facilitates Tau Pathology. *Curr Alzheimer Res*. 2006;3(5):437-448. doi:10.2174/156720506779025242

215. Mucke L. Alzheimer's disease. *Nat 2009 4617266*. 2009;461(7266):895-897. doi:10.1038/461895a

216. Atri A. The Alzheimer's Disease Clinical Spectrum: Diagnosis and Management. *Med Clin North Am*. 2019;103(2):263-293. doi:10.1016/J.MCNA.2018.10.009

217. Lanfranco MF, Ng CA, Rebeck GW. ApoE Lipidation as a Therapeutic Target in Alzheimer's Disease. *Int J Mol Sci 2020, Vol 21, Page 6336*. 2020;21(17):6336. doi:10.3390/IJMS21176336

218. Kim J, Basak JM, Holtzman DM. The Role of Apolipoprotein E in Alzheimer's Disease. *Neuron*. 63:287-303. doi:10.1016/j.neuron.2009.06.026

219. Armstrong RA, Richard P, Armstrong A. Risk factors for Alzheimer's disease. *Folia Neuropathol*. 2019;57(2):87-105. doi:10.5114/FN.2019.85929

220. Yiannopoulou KG, Papageorgiou SG. Current and future treatments for Alzheimer's disease. *Ther Adv Neurol Disord*. 2013;6(1):19-33. doi:10.1177/1756285612461679

221. Yiannopoulou KG, Papageorgiou SG. Current and Future Treatments in Alzheimer Disease: An Update. *J Cent Nerv Syst Dis*. 2020;12. doi:10.1177/1179573520907397

222. Pleen J, Townley R. Alzheimer's disease clinical trial update 2019–2021. *J Neurol*. 1234;269:1038-1051. doi:10.1007/s00415-021-10790-5

223. De Chiara G, Marcocci ME, Sgarbanti R, et al. Infectious Agents and Neurodegeneration. 2012. doi:10.1007/s12035-012-8320-7

224. Duarte LF, Gatica S, Castillo A, et al. Is there a role for herpes simplex virus type 1 in multiple sclerosis? *Microbes Infect*. 2023;25(5):105084. doi:10.1016/J.MICINF.2022.105084

225. Feng Z, Zhou F, Tan M, et al. Targeting m6A modification inhibits herpes virus 1 infection. *Genes Dis*. 2022;9(4):1114-1128. doi:10.1016/J.GENDIS.2021.02.004

226. Ball MJ. Herpesvirus in the Hippocampus as a Cause of Alzheimer's Disease. *Arch*

Neurol. 1986;43(4):313-313. doi:10.1001/ARCHNEUR.1986.00520040003001

227. Readhead B, Haure-Mirande JV, Funk CC, et al. Multiscale Analysis of Independent Alzheimer's Cohorts Finds Disruption of Molecular, Genetic, and Clinical Networks by Human Herpesvirus. *Neuron.* 2018;99(1):64-82.e7. doi:10.1016/J.NEURON.2018.05.023

228. Lövheim H, Gilthorpe J, Adolfsson R, Nilsson LG, Elgh F. Reactivated herpes simplex infection increases the risk of Alzheimer's disease. *Alzheimer's Dement.* 2015;11(6):593-599. doi:10.1016/J.JALZ.2014.04.522

229. Kobayashi N, Nagata T, Shinagawa S, et al. Increase in the IgG avidity index due to herpes simplex virus type 1 reactivation and its relationship with cognitive function in amnestic mild cognitive impairment and Alzheimer's disease. 2012. doi:10.1016/j.bbrc.2012.12.054

230. Mangold CA, Szpara ML. Persistent Infection with Herpes Simplex Virus 1 and Alzheimer's Disease-A Call to Study How Variability in Both Virus and Host may Impact Disease. 2019. doi:10.3390/v11100966

231. Lokensgard JR, Cheeran MCJ, Hu S, Gekker G, Peterson PK. Glial Cell Responses to Herpesvirus Infections: Role in Defense and Immunopathogenesis. *J Infect Dis.* 2002;186(Supplement_2):S171-S179. doi:10.1086/344272

232. Schachtele SJ, Hu S, Little MR, Lokensgard JR. Herpes simplex virus induces neural oxidative damage via microglial cell Toll-like receptor-2. *J Neuroinflammation.* 2010;7(1):35. doi:10.1186/1742-2094-7-35

233. Reinert LS, Lopušná K, Winther H, et al. Sensing of HSV-1 by the cGAS–STING pathway in microglia orchestrates antiviral defence in the CNS. *Nat Commun.* 2016;7(1):13348. doi:10.1038/ncomms13348

234. Linard M, Letenneur L, Garrigue I, Doize A, Dartigues J-F, Helmer C. Interaction between APOE4 and herpes simplex virus type 1 in Alzheimer's disease. doi:10.1002/alz.12008

235. S. BJ, Carlos R, Isabel S, Fernando V. Effect of Apolipoprotein E on the Cerebral Load of Latent Herpes Simplex Virus Type 1 DNA. *J Virol.* 2006;80(11):5383-5387. doi:10.1128/jvi.00006-06

236. Eimer WA, Vijaya Kumar DK, Navalpur Shanmugam NK, et al. Alzheimer's Disease-Associated β-Amyloid Is Rapidly Seeded by Herpesviridae to Protect against Brain Infection. *Neuron.* 2018;100(6):1527-1532. doi:10.1016/J.NEURON.2018.11.043

237. Yirün A, Çakır DA, Sanajou S, et al. Evaluation of the effects of herpes simplex

glycoprotein B on complement system and cytokines in in vitro models of Alzheimer's disease. *J Appl Toxicol*. 2023;43(9):1368-1378. doi:10.1002/JAT.4471

238. Wozniak MA, Itzhaki RF, Shipley SJ, Dobson CB. Herpes simplex virus infection causes cellular β-amyloid accumulation and secretase upregulation. *Neurosci Lett*. 2007;429(2-3):95-100. doi:10.1016/J.NEULET.2007.09.077

239. Santana S, Sastre I, Recuero M, Bullido MJ, Aldudo J. Oxidative Stress Enhances Neurodegeneration Markers Induced by Herpes Simplex Virus Type 1 Infection in Human Neuroblastoma Cells. *PLoS One*. 2013;8(10):e75842. doi:10.1371/JOURNAL.PONE.0075842

240. De Chiara Id G, Piacentini R, Id MF, et al. Recurrent herpes simplex virus-1 infection induces hallmarks of neurodegeneration and cognitive deficits in mice. 2019. doi:10.1371/journal.ppat.1007617

241. Sait A, Angeli C, Doig AJ, Day PJR. Viral Involvement in Alzheimer's Disease. *Cite This ACS Chem Neurosci 2021*. 2021;12. doi:10.1021/acschemneuro.0c00719

242. Misrani A, Tabassum S, Yang L. Mitochondrial Dysfunction and Oxidative Stress in Alzheimer's Disease. *Front Aging Neurosci*. 2021;13:617588. doi:10.3389/FNAGI.2021.617588/BIBTEX

243. Vastag L, Koyuncu E, Grady SL, Shenk TE, Rabinowitz JD. Divergent effects of human cytomegalovirus and herpes simplex virus-1 on cellular metabolism. *PLoS Pathog*. 2011;7(7). doi:10.1371/journal.ppat.1002124

244. Estes RE, Lin B, Khera A, Davis MY. Lipid Metabolism Influence on Neurodegenerative Disease Progression: Is the Vehicle as Important as the Cargo? *Front Mol Neurosci*. 2021;14:788695. doi:10.3389/FNMOL.2021.788695/BIBTEX

245. Yin F. Lipid Metabolism and Alzheimer's Disease: Clinical Evidence, Mechanistic Link and Therapeutic Promise. *FEBS J*. January 2022. doi:10.1111/FEBS.16344

246. Sienski G, Narayan P, Bonner JM, et al. APOE4 disrupts intracellular lipid homeostasis in human iPSC-derived glia. *Sci Transl Med*. 2021;13(583). doi:10.1126/SCITRANSLMED.AAZ4564/SUPPL_FILE/AAZ4564_SM.PDF

247. Mesa-Herrera F, Taoro-González L, Valdés-Baizabal C, Diaz M, Marín R. Lipid and Lipid Raft Alteration in Aging and Neurodegenerative Diseases: A Window for the Development of New Biomarkers. *Int J Mol Sci 2019, Vol 20, Page 3810*. 2019;20(15):3810. doi:10.3390/IJMS20153810

248. Chew H, Solomon VA, Fonteh AN. Involvement of Lipids in Alzheimer's Disease Pathology and Potential Therapies. *Front Physiol*. 2020;11:539026.

doi:10.3389/FPHYS.2020.00598/BIBTEX

249. Huang P, Wang X, Lei M, et al. Metabolomics Profiles Reveal New Insights of Herpes Simplex Virus Type 1 Infection. *Int J Mol Sci*. 2023;24(2):1521. doi:10.3390/IJMS24021521/S1

250. Sutter E, de Oliveira AP, Tobler K, et al. Herpes simplex virus 1 induces de novo phospholipid synthesis. *Virology*. 2012;429(2):124-135. doi:10.1016/J.VIROL.2012.04.004

251. Benedyk TH, Connor V, Caroe ER, et al. Herpes simplex virus 1 protein pUL21 alters ceramide metabolism by activating the interorganelle transport protein CERT. 2022. doi:10.1016/j.jbc.2022.102589

252. Vila IK, Chamma H, Steer A, et al. STING orchestrates the crosstalk between polyunsaturated fatty acid metabolism and inflammatory responses. *Cell Metab*. 2022;34(1):125-139.e8. doi:10.1016/J.CMET.2021.12.007

ABBREVIATION LIST

3-O-S-HS	3-O-sulfated heparan sulphate
Aβ	β-amyloid
AChEI	Acetylcholinesterase inhibitor
ACPA	Anti-citrullinated peptide antibody
ACV	Acyclovir
AD	Alzheimer's Disease
AIDS	Acquired immunodeficiency syndrome
AIF	Apoptosis-inducing factor
APOE	Apolipoprotein-E
APP	Amyloid precursor protein
AR	Androgen receptor
ATP	Adenosine triphosphate
BAA	Benzoyl arginine amide
BB-Cl-A	BB-Cl-amidine
CERT	Ceramide transport protein
CIN	Cervical intraepithelial neoplasia
CKI	Cyclin-dependent kinase inhibitor
Cl-A	Cl-amidine
CNS	Central nervous system
CVSC	Capsid vertex-specific component
E6AP	E6-associated protein
EBV	Epstein-Barr virus
ECM	Extracellular matrix
EMT	Epithelial-to-mesenchymal transition
FADS2	Fatty acid desaturase 2
FASN	Fatty acid synthase
GFAP	Glial fibrillary acidic protein
GSK3β	Glycogen synthase kinase-3-β
HCF-1	Host cell factor 1
HCMV	Human cytomegalovirus
HHV-6A	Herpesvirus types 6A
HHV-6B	Herpesvirus types 6B

HHV-7	Herpesvirus types 7
HHV-8	Herpesvirus types 8
HPV	Human papillomavirus
HRV	Human rhinovirus
HSPG	Heparan sulphate proteoglycans
HSV-1	Herpes simplex virus type 1
HSV-2	Herpes simplex virus type 2
HVEM	Herpesvirus entry mediator
IDU	Iododeoxyuridine
IFI16	Interferon-inducible protein 16
IFN-I	Type I interferon
ING4	Inhibitor growth 4
iPSC	Induced pluripotent stem cell
IRL	Internal repeats of the long region
IRS	Internal repeats of the short region
KSHV	Kaposi's sarcoma-associated herpesvirus
LAT	Latency-associated transcript
LCR	Long control region
MBP	Myelin basic protein
MS	Multiple sclerosis
NCR	Non-coding region
ND-10	Nuclear domain-10
NETs	Neutrophil extracellular traps
NFT	Neurofibrillary tangles
NLS	Nuclear localization signal
NMDA	N-methyl-D-aspartate
Oct-1	Octamer binding protein-1
ORF	Open reading frame
OXPHOS	Oxidative phosphorylation
P-tau	Phosphorylated tau protein
PAD or PADI	Peptidylarginine deaminase
PAMP	Pathogen-associated molecular pattern
PILRα	Immunoglobulin-like type 2 receptor α
PRR	Pattern-recognition receptor

PSEN	Presenilin
PTM	Post-translational modification
PUFA	Polyunsaturated fatty acid
RA	Rheumatoid arthritis
RSV	Respiratory syncytial virus
SCP	Small capsomere-interacting protein
SP	Senile plaques
TCA	Tricarboxylic acid
TK	Thymidine kinase
TLR	Toll-like receptor
TRL	Terminal repeats of the long region
TRS	Terminal repeats of the short region
UL	Unique long region
URR	Upstream regulatory region
US	Unique short region
VLPs	Virus-like particle
VZV	Varicella-zoster virus

MANUSCRIPTS IN PREPARATION

The impact of fatty acid synthase on HSV-1 infectivity unveils the key interconnection with Alzheimer's disease

Albano C, Trifirò L, Hewelt-Belka W, Cairns D. M, Pasquero S, Griffante G, Gugliesi F, Bajetto G, Garwolińska D, Rossi M, Vallino M, De Andrea M, Kaplan D, Dell'Oste V, Biolatti M.

PUBLICATIONS

1. **PAD-mediated citrullination is a novel candidate diagnostic marker and druggable target for HPV-associated cervical cancer.**
   Albano C, Biolatti M, Mazibrada J, Pasquero S, Pugliesi F, Lo Cigno I, Calati I, Bacetto G, Riva G, Griffante G, Landolfo S, Gariglio M, De Andrea M, Dell'Oste V.
   Frontiers in Cellular and Infection Microbiology, 2024.

2. **Antiherpetic Activity of a Root Exudate from *Solanum lycopersicum*.**
   Bajetto G, Arnodo D, Biolatti M, Trifirò L, Albano C, Pasquero S, Gugliesi F, Campo E, Spyrakis F, Prandi C, De Andrea M, Dell'Oste V, Visentin I, Blangetti M.
   Microorganism, 2024.

3. **Citrullination profile analysis reveals peptidylarginine deaminase 3 as an HSV-1 target to dampen the activity of candidate antiviral restriction factors.**
   Pasquero S, Gugliesi F, Biolatti M, Dell'Oste V, Albano C, Bajetto G, Griffante G, Trifirò L, Brugo B, Raviola S, Lacarbonara D, Yang Q, Sudeshna S, Barasa L, Haniff H, Thompson P.R, Landolfo S, De Andrea M.
   Plos Pathogen, 2023.

4. **Strigolactones as Broad-Spectrum Antivirals against β-Coronaviruses through Targeting the Main Protease Mpro.**
   Biolatti M, Blangetti M, Baggieri M, Marchi A, Gioacchini S, Bajetto G, Arnodo D, Bucci P, Fioravanti R, Kojouri M, Bersani M, D'Arrigo G, Siragusa L, Ghinato S, De Andrea M, Gugliesi F, Albano C, Pasquero S, Visentin I, D'Ugo E, Esposito F, Malune P, Tramontano E, Prandi C, Spyrakis F, Magurano F, Dell'Oste V.
   ACS Infectious Diseases, 2023.

5. **IFI16 Impacts Metabolic Reprogramming during Human Cytomegalovirus Infection.**
   Griffante G, Hewelt-Belka W, Albano C, Gugliesi F, Pasquero S, Castillo Pacheco S.F,

Bajetto G, Porporato P.E, Mina E, Vallino M, Krapp C, Jakobsen M.R, Purdy J, von Einem J, Landolfo S, Dell'Oste V, Biolatti M.

mBio, 2022.

6. **Novel antiviral activity of PAD inhibitors against human beta-coronaviruses HCoV-OC43 and SARS-CoV-2.**

Pasquero S, Gugliesi F, Griffante G, Dell'Oste V, Biolatti M, <u>Albano C</u>, Bajetto G, Delbue S, Signorini L, Dolci M, Landolfo S, De Andrea M.

Antiviral Research, 2022.

7. **HPV meets APOBEC: New players in head and neck cancer.**

Riva G, <u>Albano C,</u> Gugliesi F, Pasquero S, Castillo Pacheco S.F, Pecorari G, Landolfo S, Biolatti M, Dell'Oste V.

International Journal of Molecular Sciences, 2021.

8. **Human cytomegalovirus and autoimmune diseases: Where are we?**

Gugliesi F, Pasquero S, Griffante G, Scutera S, <u>Albano C</u>, Riva G, Dell'Oste V, Biolatti M.

Viruses, 2021.

9. **Strigolactone analogs are promising antiviral agents for the treatment of human cytomegalovirus infection.**

Biolatti M, Blangetti M, D'arrigo G, Spyrakis F, Cappello P, <u>Albano C</u>, Ravanini P, Landolfo S, De Andrea M, Prandi C, Dell'oste V.

Microorganisms, 2020.

10. **Where do we stand after decades of studying human cytomegalovirus?**

Gugliesi F, Coscia A, Griffante G, Galitska G, Pasquero S, <u>Albano C,</u> Biolatti M.

Microorganisms, 2020.

1 **The impact of fatty acid synthase on HSV-1 infectivity unveils the key interconnection with**

2 **Alzheimer's disease**

3 Camilla Albano[1,7], Linda Trifirò[1,7], Weronika Hewelt-Belka[2], Dana M. Cairns[3], Selina Pasquero[1],

4 Gloria Griffante[4], Francesca Gugliesi[1], Greta Bajetto[1,5], Dorota Garwolińska[2], Marika Rossi[6], Marta

5 Vallino[6], Marco De Andrea[1,5], David Kaplan[3], Valentina Dell'Oste[1], Matteo Biolatti[1,8,*]

6 [1] Department of Public Health and Pediatric Sciences, University of Turin, Turin, Italy

7 [2] Department of Analytical Chemistry, Faculty of Chemistry, Gdańsk University of Technology,
8 Gdańsk, Poland

9 [3] Department of Biomedical Engineering, Tufts University, Medford, MA, USA

10 [4] IIGM Foundation – Italian Institute for Genomic Medicine, Candiolo, Turin, Italy

11 [5] CAAD Center for Translational Research on Autoimmune and Allergic Disease, Novara, Italy.

12 [6] Institute for Sustainable Plant Protection, CNR, Turin, Italy

13 [7] These authors contributed equally

14 [8] Lead contact

15 * Correspondence: matteo.biolatti@unito.it

16

18

19 **ABSTRACT**

20 Herpes simplex virus type-1 (HSV-1) is a widespread human pathogen that relies on host metabolism

21 to favor its replication. Here, we demonstrated that *de novo* lipogenesis is essential for HSV-1

22 infectivity. Particularly, HSV-1 infection upregulates fatty acid synthase (FASN) expression,

23 accompanied by a marked increase in lipids concentration and a differential lipid species distribution.

24 Conversely, silencing FASN or using FASN inhibitors CMS121 and C75 reduces viral infectivity,

25 affecting virion structure and entry into host cells. Additionally, we show that a source of lipid-rich

26 external factors provided by fetal bovine serum significantly increases HSV-1 infectivity. Lastly, in

27 a 3D tissue culture model of herpesvirus-induced Alzheimer's disease (AD), both CMS121 and C75

28 display a potent inhibitory effect on Aß-like plaque formation, linking HSV-1-mediated lipid

29   metabolism dysregulation to AD etiopathogenesis. Altogether, our findings reveal how HSV-1

30   manipulates lipid metabolism, offering insights into its association with AD and highlighting

31   potential therapeutic targets.

32

33   **INTRODUCTION**

34   Herpes simplex virus type-1 (HSV-1) is a neurotropic double-stranded DNA virus primarily infecting

35   epithelial cells in the oral and nasal mucosa[1]. In these cells, HSV-1 undergoes a lytic replication cycle.

36   Newly produced viral particles can then enter sensory neurons and travel via retrograde axonal

37   transport to the trigeminal ganglion, where they release viral DNA and establish latent infection.

38   Reactivation of the virus leads to the anterograde transportation of newly formed viral particles back

39   to the initial infection site along sensory neurons, resulting in clinical lesions known as cold sores and

40   blisters.

41   Emerging research has unveiled an interesting interplay between herpesvirus infection and

42   cellular lipid metabolism. Indeed, lipid metabolism, crucial for a range of cellular functions, appears

43   to orchestrate key stages of the viral life cycle, ranging from entry and replication to the assembly of

44   new virion particles. Thus, understanding how cellular metabolism is altered after viral infection may

45   reveal potential targets for viral inhibition.

46   While extensive research has explored the interaction between human cytomegalovirus

47   (HCMV)[2,3], a major human pathogenic β-herpesvirus, and host lipid metabolism, the link between α-

48   herpesviruses, such as HSV-1, and lipids remains poorly understood[4–7].

49   Langeland *et al.* (1986) were the first to report that HSV-1 infection alters the synthesis of

50   phosphoinositides, crucial signaling lipids[4]. Furthermore, it is known that phospholipids are

51   synthesized anew for HSV-1 viral envelope formation[5,6]. Conversely, while HCMV relies on *de novo*

52   fatty acid (FA) biosynthesis to produce mature enveloped particles, HSV-1 virions use pre-existing

53   membranes, favoring rapid nucleotide biosynthesis essential for their short replicative cycle[7].

54   Moreover, several viruses, such as hepatitis C virus and rhinovirus, have been shown to alter multiple

55 metabolic pathways in cells, influenced by cellular metabolites. Hepatitis C virus (HCV) infection,

56 for example, disrupts glucose utilization and lipid biosynthesis[8], while rhinovirus-infected cells adjust

57 uptake through a PI3K-dependent mechanism and upregulate the expression of the PI3K-regulated

58 glucose transporter GLUT1, underscoring the critical role of glucose metabolism in viral replication[9].

59 Similarly, Kaposi's sarcoma-associated herpesvirus (KSHV) stimulates FA synthesis, and inhibitors

60 of this pathway can eradicate latently infected KSHV-infected cells, thereby providing novel

61 therapeutic targets for KSHV and associated Kaposi's sarcoma tumors[10]. These findings indicate that

62 viruses can manipulate host metabolism to either enhance or inhibit their replication. Thus, gaining

63 insights into these host metabolic adaptations may help develop effective strategies to counteract viral

64 infections.

65   Against this background, viral hijacking of lipid metabolism is crucial not only for

66 understanding how viruses replicate but also for its potential implications in associated diseases,

67 particularly neurodegenerative disorders like Alzheimer's disease (AD). There is growing

68 experimental evidence suggesting that repeated HSV-1 reactivation may contribute to intracellular

69 damage and subsequent neurodegeneration. Several epidemiological, immunological, and molecular

70 findings have established a link between HSV-1 infection and the development of AD[11–14]. This

71 relationship is evidenced by the critical role that alteration of lipid metabolism plays in the

72 etiopathogenesis of AD[15,16], prompting us to hypothesize whether these metabolic changes impact

73 AD progression in the course of HSV-1 infection. Interestingly, Ates *et al.* have shown that CMS121,

74 a fatty acid synthase (FASN) inhibitor involved in *de novo* lipogenesis, can reduce cognitive loss and

75 inflammation in transgenic AD mice[17]. Furthermore, retrospective cohort studies based on the

76 National Health Insurance Research Database (NHIRD) of Taiwan evidenced that HSV and varicella-

77 zoster virus (VZV) are associated with an elevated risk of AD, which can be counteracted by

78 antiherpetic treatment[18,19].

79   Here, we report that HSV-1 infection triggers an increase of FASN and relies on *de novo*

80 lipogenesis for viral maturation and infectivity. This is also supported by the observation that cellular

81 growth conditions significantly influence viral infectivity. Finally, our research reveals that inhibiting

82 FASN pharmacologically can effectively prevent herpes-induced AD-like phenotypes in a 3D human

83 brain-like tissue model, with potential ramifications in the development of innovative strategies for

84 AD prevention and treatment.

85

86 **RESULTS**

87 ***HSV-1 infection modulates the fatty acid synthase***

88 It has been confirmed that the fatty acid synthase (FASN), the rate-limiting enzyme in FA synthesis

89 and the catalyst of the last step of *de novo* lipid synthesis, is involved in regulating the replication of

90 various viruses[20,21]. To this end, we aimed to determine whether HSV-1 modulates FASN during the

91 infection. We conducted experiments using SH-SY5Y neuron-like cells, a suitable *in vitro* model for

92 HSV-1-associated neurological disorders[22], under fully confluent and serum-free conditions that

93 allowed us to determine whether the observed lipid production is *de novo* rather than derived from

94 external nutrient uptake.

95 Initially, we confirmed that serum-starved SH-SY5Y cells fully support virus replication (Figure 1A

96 and B, respectively). Next, we quantified the FASN mRNA expression levels in SH-SY5Y cells

97 previously infected with HSV-1 at 8, 24, and 32 hpi. We found a significant increase in FASN mRNA

98 in HSV-1-infected *vs.* uninfected cells, especially at 24 hpi, at which time point FASN levels were

99 seven-fold higher than those in mock cells (Figure 1C). Subsequent Western blot analysis provided

100 further confirmation of FASN induction during the progression of infection, indicating an

101 upregulation of lipogenesis (Figure 1D). These results were corroborated in human foreskin

102 fibroblasts (HFFs), another cellular model fully permissive for HSV-1 replication (Figure S1).

103 Furthermore, we observed that a UV-inactivated HSV-1 failed to induce FASN expression indicating

104 that FASN upregulation is contingent upon active virus replication (Figure 1E). Lastly, as depicted

105 in Figure 1F, the analysis of infection kinetics across various MOIs revealed that a higher MOI

106 accelerates the upregulation of FASN protein expression. In particular, at an MOI of 5, we observed

107   a significant increase in FASN protein levels at both 15 and 24 hpi in comparison with the levels seen

108   with an MOI of 1.

109   Altogether, these findings are supportive of the involvement of HSV-1 in disrupting the

110   process of *de novo* lipogenesis.

111   Next, to verify whether the differences in lipogenic enzyme expression between mock and

112   HSV-1-infected cells led to changes in lipid composition, we performed lipidomic analysis by liquid

113   chromatography coupled with high-resolution mass spectrometry (LC-Q-TOF-MS). First, we

114   compared total lipid quantities between uninfected and infected SH-SY5Y cells, as measured by the

115   total MS signal. This comparison included the following lipid classes: glycerophosphocholines (PCs)

116   and ether analogs (PC-Os), glycerophosphoethanolamines (PEs) and ether analogs (PE-Os), and

117   sphingomyelins (SMs). We observed an increase in the overall lipid content of PCs, PC-Os, PEs, PE-

118   Os, and SMs in infected cells compared to their uninfected counterparts. For instance, at 24 hpi, the

119   average fold change (FC) of total lipid amount in infected *vs*. noninfected cells was recorded as 1.28

120   for PCs, 1.41 for PC-Os, 1.46 for PEs, 1.42 for PE-Os, 1.38 for SMs. These differences were

121   statistically significant ($P < 0.005$) across all lipid classes at 24 hpi (Figure S2).

122   Subsequently, we evaluated the differences in lipid composition within specific lipid classes

123   in HSV-1 infected cells *vs*. uninfected SH-SY5Y cells. This comparison, addressing the percentage

124   distribution of lipid species among SMs, PCs, and PEs, along with their ether analogs, revealed

125   significant changes in cell lipid composition during infection, primarily within the PC class and its

126   ether analogs (Figure 1G). Out of the 99 lipid species examined, 45 species, at 24 hpi, and 38, at 48

127   hpi, showed significant changes between infected and uninfected cells ($P < 0.05$, unpaired t-test, false

128   discovery rate - FDR). However, the impact on lipid composition varied. All identified PC-Os were

129   upregulated in HSV-1-infected cells compared to uninfected ones. Conversely, many long-chain (sum

130   of carbon atoms in FAs > 36) and unsaturated PCs (double bonds > 3) were downregulated in HSV-

131   1-infected cells, including PC 40:4, PC 40:5, PC 34:3, and PC 38:4. Unlike PCs, the percentage

132 distribution of PEs and their ether analogs as well as SMs remained largely unchanged between HSV-

133 1 infected and uninfected cells, with only a few exceptions.

134

135 ***FASN modulation impacts HSV-1 replication and infectivity***

136 To investigate the impacts of FASN on HSV-1 infection and, considering the potential role of lipids

137 in ensuring the infectivity of viral particles, we next focused on the interplay between lipid

138 metabolism and HSV-1 replication.

139 For this purpose, SH-SY5Y cells were transduced with previously characterized lentiviral vectors

140 delivering a short hairpin RNA (shRNA) targeting FASN (shFASN) or scramble control RNA

141 (shCTRL) and infected with HSV-1 (MOI 1) in serum-free conditions. We observed reduced FASN

142 protein levels in transfected cells, confirming the knockdown (KD) of FASN (Figure 2A). The

143 expression of HSV-1 ICP27 and gD proteins, along with intracellular and extracellular viral load,

144 were not affected by FASN depletion (Figure 2B-D, respectively). However, FASN silencing

145 significantly decreased both viral progeny production by >1-log (Figure 2E) and the infectivity of

146 newly released HSV-1 virions (Figure 2F), suggesting that HSV-1 exploits FASN for virus

147 production after the synthesis of late proteins, possibly during virion assembly.

148

149 ***FASN inhibition increases fatty acid uptake and alters CD36 expression in HSV-1-infected cells***

150 Given the critical role of lipid metabolism in the life cycle of HSV-1and the potential impact of lipid-

151 rich external factors on this process, we explored the contribution of fetal bovine serum (FBS)—a

152 standard ingredient in cell culture media essential for cell growth and maintenance—in HSV-1

153 replication. Although FBS is essential for cell culture, its role in virus research is complex due to its

154 known effects on virus replication[23,24].

155 To further explore these phenomena, we assessed the expression of viral proteins in shCTRL *vs.*

156 shFASN cells also in the presence of serum. As shown in Figure 3A, FASN depletion considerably

157 augmented the expression levels of both ICP27 and gD proteins. Moreover, intracellular and

158 extracellular viral genome copies, as well as cell infectivity, were significantly increased (Figure 3B-

159 D).

160 The aforementioned results led us to postulate that inhibiting FASN could trigger an increased uptake

161 of FAs from the serum to compensate for the lack of this enzyme. To validate this hypothesis, we

162 initially analyzed the expression of CD36, a key FA transporter [25]. Since CD36 acts at the cell surface,

163 we used flow cytometry to determine its localization in SH-SY5Y cells following HSV-1 infection

164 (Figure 3E). We found that HSV-1 infection enhanced CD36 plasma membrane localization,

165 especially in shFASN cells. To determine whether this increased localization of CD36 correlated with

166 enhanced FA transport activity, we next measured exogenous FA uptake using a fluorescent analog

167 of palmitic acid (BODIPY FL C16) (Figure 3G). Flow cytometry analysis revealed enhanced uptake

168 of the FA analog in HSV-1-infected cells compared to uninfected control cells at 48 hpi, with shFASN

169 cells showing an even greater uptake of BODIPY (Figure 3H), in line with previous reports.

170 Furthermore, to assess the inhibition of FA uptake via CD36, we employed sulfosuccinimidyl oleate

171 (SSO), a compound that can inhibit CD36 function by binding to Lys164 in its hydrophobic cavity

172 [26]. At a non-toxic concentration of 200 μM, as judged by MTT assay (Figure 3G), SSO markedly

173 reduced CD36-mediated FA uptake in both HSV-1-infected shFASN and shCTRL cells. Collectively,

174 these data indicate that HSV-1 infection leads to selective upregulation of CD36 expression and FA

175 uptake, especially in the absence of FASN.

176 Next, we sought to determine whether blocking FA uptake via CD36 would affect HSV-1

177 infectivity. For this purpose, both shCTRL and shFASN cells were treated with SSO or vehicle

178 control (DMSO). In line with our previous results, we observed reduced infectivity of viral particles

179 released in the supernatants of cells treated with SSO compared to those treated with DMSO,

180 indicating a diminished capacity of the virus to form plaques (Figure 3I). Of note, the most significant

181 difference in infectivity was detected between SSO- and DMSO-treated shFASN cells, suggesting

182 that the combined effect of inhibiting lipogenesis and blocking CD36-mediated FA uptake adversely

183 affects viral infectivity.

184

CMS121 and C75 reduce the infectivity of HSV-1 viral particles

186 Given the capability of FASN to impair HSV-1 infectivity, targeting lipid metabolism may constitute

187 an innovative approach to reduce the risk of virus reactivation, an especially critical concern in the

188 context of neurodegenerative diseases, such as Alzheimer's disease (AD). Considering the growing

189 body of evidence linking HSV-1 to the onset of AD and the observed protective effect of CMS121—

190 a derivative of the flavonoid fisetin acting as a FASN inhibitor (FASNi) able to reduce cognitive

191 decline in mice[17,27]—we sought to determine its impact as well as that of C75—a synthetic α-

192 methylene-γ-butyrolactone targeting *de novo* lipogenesis—on HSV-1 replication, ultimately aiming

193 to establish a potential connection between HSV-1 and AD development.

194 In preliminary experiments, we confirmed the non-toxic nature of the CMS121 and C75

195 compounds at the concentrations used by MTT assay (Figure 4A, H). We then treated HSV-1-infected

196 SH-SY5Y cells with the two compounds and examined viral protein expression at 24 and 48 hpi by

197 immunoblotting. While the expression of ICP27 and gD was unaffected by both compounds (Figure

198 5B, I), standard plaque assay showed a dramatic decrease in the accumulation of infectious progeny

199 in CMS121- or C75-treated cells *vs*. untreated controls (Figure 4C, J). Quantification of the

200 intracellular and extracellular genomes of HSV-1-infected SH-SY5Y cells (MOI 1) treated with both

201 drugs at 24 and 48 hpi, respectively, revealed no significant differences from the controls, suggesting

202 that viral replication was not affected (Figure 4D, E, K, L).

203 To determine viral infectivity post-treatment, we measured the number of infectious units/mL

204 by means of viral yield assay. This revealed a considerable reduction in viral infectivity in treated

205 cells compared to untreated ones, indicating a reduced ability of the virus to form plaques (Figure 4F,

206 M). Finally, the genome-infectious unit ratio further confirmed a substantial decrease in viral

207 infectivity in treated cells relative to untreated ones (Figure 4G, N). Thus, CMS121 and C75 exert

208 their inhibitory effects at later stages of virion maturation, specifically affecting the ability of HSV-1

209 to infect new cells.

210   To ascertain whether CMS121 and C75 treatment affects the entry capability of HSV-1

211   virions, we used supernatants from HSV-1-infected SH-SY5Y cells treated with each compound or

212   DMSO for 48 h to infect Vero cells. Following a 2 h HSV-1 entry period, we quantified the viral

213   genome content of these cells. As shown in Figure 5A and B, both treatments significantly hindered

214   the ability of newly formed HSV-1 viral particles to enter the cells. This observation was further

215   substantiated by the reduced mRNA expression of ICP0, an HSV-1 immediate-early gene, and viral

216   DNA polymerase (POL) at 6 hpi observed in similarly treated cells, confirming that CM121 and C75

217   compromise virions integrity, thus impairing entry capability (Figure 5B, C, E, F).

218   To confirm our suspicion regarding viral envelope disruption, we examined HSV-1 virion

219   morphology in post-treatment supernatants using transmission electron microscopy (TEM). We

220   readily noticed morphological alterations in CMS121- or C75-treated HSV-1 virions compared to

221   untreated controls (Figure 5G, H). In particular, numerous virions appeared deformed, likely due to

222   damage to the viral structure that eased the leakage of the envelope, allowing the stain to penetrate

223   the particles.

224   Altogether, these findings indicate that pharmacological inhibition of FASN disrupts the

225   stability of HSV-1 surface structure and virion morphology.

226   Finally, we compared the total lipid amounts, as measured by total MS signal, across different

227   classes between infected cells and infected cells treated with C75 or CMS121. In cells treated with

228   either CMS121 or C75 there was a notable reduction in total lipid content in comparison to merely

229   infected cells, encompassing all lipid classes (Figure S2). For instance, FC of total lipid amount in

230   infected cells treated with CMS121 *vs*. untreated infected cells 24 hpi was 0.75 for PCs, 0.79 for PC-

231   Os, 0.56 for PEs, 0.54 for PE-Os, and 0.8 for SMs. These changes were statistically significant at 24

232   hpi ($P < 0.05$) and 48 hpi ($P < 0.001$) in C75-treated infected cells treated *vs*. untreated infected cells,

233   and at 24 hpi ($P < 0.005$) in CMS121-treated infected cells treated *vs*. untreated infected cells. The

234   significant changes at 48 hpi for CMS121-treated infected cells were limited to SMs, cholesterol, and

235   PCs ($P < 0.05$).

236   When comparing HSV-1 infected cells with CMS121-treated infected cells, 74 lipid species,

237   at 24 hpi, and 63, at 48 hpi, showed significant differences (Figure 6). In CMS121-treated cells, there

238   was a noticeable decrease in the relative amounts of LC-PUFAs in PCs and some SMs, along with a

239   slight increase in short-chained ether analogs of PCs and LPC 18:1. Conversely, in C75-treated cells,

240   we observed an increase in the levels of several LC-PUFA ether analogs of PCs and PEs compared

241   to untreated HSV-1 infected cells, whereas the relative amounts of LC-PUFAs in PCs were reduced.

242   These changes were statistically significant for 67 lipid species at 24 hpi and 70 at 48 hpi ($P < 0.05$,

243   unpaired t-test, FDR).

244

245   *FASN inhibitors prevent AD-like phenotypes in 3D brain human models*

246   To clarify the interplay between HSV-1 and AD and to identify potential therapeutic targets, we

247   evaluated the efficacy of CMS121 and C75 using a 3D human brain-like tissue model of herpes-

248   induced AD, focusing our attention on the formation of Aβ plaques and the mRNA expression of

249   important AD-associated genes, such as like amyloid precursor protein (APP), enzyme β-secretase 1

250   (BACE1), and presenilins 2 (PSEN2). Each compound was administered concurrently with HSV-1

251   infection to enhance its potential anti-plaque effect. In these 3D cortical tissue models, the two FASNi

252   exhibited no toxicity at concentrations of 0.1 and 1 μM.

253   HSV-1-infected cells and treated with C75 or CMS121, at both 0.1 and 1 μM dosages, showed

254   reduced plaque counts compared to those that were infected but left untreated cells (Figure 7A, B).

255   Furthermore, we observed decreased APP mRNA expression levels alongside an upregulation of

256   PSEN2 expression in infected, untreated cells compared to their uninfected counterparts (Figure S3A,

257   B). Interestingly, treatment with C75 or CMS121 normalized the expression of APP and PSEN2 to

258   levels observed in uninfected cells. Overall, these results underscore the potential of FASN inhibitors

259   to mitigate amyloid-related and neuroinflammatory effects in HSV-1-induced AD models.

260

261   **DISCUSSION**

262   Viral infections are known to trigger metabolic changes in host cells to support the increased demand

263   for nutrients, energy, and macromolecular synthesis. This phenomenon has been extensively studied

264   in the context of HCMV, a prominent β-herpesvirus, and its interaction with host lipid metabolism

265   [35–37]. However, the dynamics between α-herpesviruses, such as HSV-1, and lipid metabolism remain

266   less clear, with existing literature often yielding conflicting evidence, likely ascribable to variations

267   in growth conditions across studies that influence virus replication. For instance, an earlier study by

268   Langeland *et al.* (1986) revealed alterations in phosphoinositide synthesis, a pivotal signaling lipid

269   affected by HSV-1[4], providing the first evidence of an interplay between this virus and host lipid

270   metabolism. Subsequent studies demonstrated that phospholipids are synthesized anew in cells

271   infected with HSV-1, serving as essential components for the formation of the viral envelope[5,6]. On

272   the other hand, studies like that of Vastag *et al.* suggested that HSV-1 assembles its virions using pre-

273   existing membranes to expedite nucleotide biosynthesis, essential for its rapid replicative cycle[7].

274   Given these contrasting findings, here we have further investigated the complex interplay between *de*

275   *novo* lipid synthesis and HSV-1 infection in a neuronal-like context.

276   To provide mechanistic insights supporting our hypothesis, we examined *de novo* lipogenesis

277   during HSV-1 infection, both with and without serum. We found a significant, virus-induced

278   upregulation of FASN activity, which correlates with a marked increase in lipid concentrations.

279   Specifically, we observed an increase in PCs, PC-Os, PEs, PE-Os, and SMs, with a notable

280   differentiation in lipid species distribution, particularly in PCs and their ether analogs. Further

281   scrutiny revealed that the changes in lipid composition were not uniform. In particular, all identified

282   PC-Os were upregulated in infected cells. In contrast, long-chain and unsaturated PCs were

283   downregulated, indicating a nuanced virus-induced reprogramming of lipid synthesis pathways.

284   These observations were substantiated by the significant shift in lipid species distribution between

285   infected and uninfected cells, underscoring the complexity of lipid metabolic alterations induced by

286   HSV-1 infection. Importantly, we show that FASN silencing significantly decreases both viral

287   progeny production and the infectivity of newly released HSV-1 particles in serum-starved SH-SY5Y

288 cells, and that this effect is partly rescued by the presence of serum, suggesting that external lipid

289 sources provided by FBS can partially compensate for the lack of endogenous lipid synthesis due to

290 FASN deficiency.

291   Further investigation into the compensatory mechanisms at play reveals that inhibiting FASN

292 triggers an increased uptake of FAs from the serum, mediated by the upregulation of CD36, a key FA

293 transporter. Enhanced CD36 localization on the plasma membrane and subsequent FA transport

294 activity in HSV-1-infected cells, particularly those with silenced FASN, underscore the ability of this

295 virus to adapt its lipid acquisition strategies in response to metabolic restrictions.

296   The augmentation of fatty acid uptake was further validated by employing SSO to inhibit

297 CD36 function, which led to a marked decrease in the infectivity of HSV-1, confirming the essential

298 role of lipid uptake in maintaining viral infectivity, especially when *de novo* lipogenesis is hindered.

299   The central role of FASN in bridging HSV-1 infection and lipid reprogramming is further

300 supported by the observation that treatment of serum-starved SH-SY5Y cells with two FASN

301 inhibitors, CMS121 and C75, substantially reduces the accumulation of infectious progeny and

302 impaired infectivity of viral particles, as evidenced by the decreased ability to form plaques and

303 altered virion integrity, whereas the expression levels of viral proteins remain unaltered. Thus, FASN-

304 mediated lipogenesis not only supports viral replication but also plays a role in maintaining the

305 structural integrity essential for the successful entry of virions into new host cells.

306   Altogether, these findings are consistent with a model in which HSV-1 infection triggers host

307 cell lipid metabolism reprogramming, highlighting the ability of this virus to exploit both endogenous

308 and exogenous lipid sources to overcome metabolic barriers, thereby enhancing its replication and

309 infectivity. This adaptive strategy of HSV-1 underscores the intricate interplay between viral infection

310 and host lipid metabolism, offering novel perspectives on the mechanisms underlying viral replication

311 and the potential therapeutic targets within the host metabolic pathways.

312   The intersection of metabolism with neurodegenerative conditions, particularly dementia, has

313 become increasingly apparent through recent research. Dementia affects over 55 million individuals

314　globally, with a staggering economic burden of 1.3 trillion US dollars. AD is the most prevalent form

315　of dementia, accounting for 60-80% of cases, with most of them (90%) being sporadic (SAD). Among

316　the various environmental risk factors implicated in SAD, persistent brain infections, particularly

317　those caused by HSV-1, have been involved in AD pathogenesis. This points to the importance of

318　gaining mechanistic insights into the link between viral infections and the progression of

319　neurodegenerative conditions.

320　　　　Previous studies have highlighted the potential of targeting lipid metabolism in AD. Recently,

321　Ates et al.[17] have shown that expression levels of FASN protein are significantly increased in AD

322　patients. This finding is complemented by the observation that CMS121 administration enhances

323　memory and cognition in an AD mouse model, echoing the protective effects of fisetin itself as

324　documented in earlier research[27]. Further studies by Ates et al.[17] and Parisi et al.[28] have shown that

325　FASN inhibition safeguards against distinct types of cell death, such as oxytosis/ferroptosis and

326　necroptosis, all implicated in AD pathology. The specific inhibition of FASN has also emerged as a

327　protective strategy against necroptosis[28], further advocating for FASN as a therapeutic target in AD.

328　Finally, the relevance of FASN inhibition extends to a variety of diseases, including cancer, fatty liver

329　disease, obesity, and type 2 diabetes[29–32], highlighting its broad therapeutic potential.

330　　　　Our research advances understanding in this area by showing that the FASN inhibitors

331　CMS121 and C75 effectively prevent the occurrence of an AD-like phenotype in a 3D human brain

332　model. These inhibitors not only significantly reduced Aβ plaque formation—a hallmark of AD—but

333　also preserved high levels of cell viability within our 3D cortical tissue model, effectively

334　counteracting the amyloid-related and neuroinflammatory effects induced by HSV-1 infection.

335　Furthermore, we show that treatment with CMS121 and C75 normalizes the expression of critical

336　AD-associated genes, such as APP and PSEN2, disrupted by viral infection, back to levels

337　comparable to those in uninfected cells. This observation underscores the potential of targeting lipid

338　metabolism as a novel therapeutic strategy to mitigate the progression of AD, particularly in the

339　context of viral infections.

340   Given the established role of lipid-mediated signaling in essential brain functions and its

341   disruption in AD pathogenesis, we propose a framework where HSV-1-induced metabolic

342   dysfunction contributes to AD progression by dysregulating lipid metabolism, thereby enhancing

343   viral fitness and implicating lipid metabolic processes in the progression of neurodegenerative

344   diseases. Within the normal aging process, lipid metabolic homeostasis is crucial for maintaining

345   brain function. However, AD disrupts this equilibrium—a process called dyshomeostasis—resulting

346   in impaired brain function that typifies the disease.

347   This working model is supported by recent evidence suggesting that dysregulation of *de novo*

348   lipogenesis is the probable cause of lipid and FA accumulation, which typifies AD brain pathology[33].

349   Our study, while providing valuable insights into the interplay between HSV-1 infection, lipid

350   metabolism, and AD, has several limitations that warrant mention. Primarily, the 3D brain model

351   employed here, though innovative, only approximates some aspects of the complex human brain

352   architecture: it lacks immune cells and blood vessels and more closely resembles fetal than adult brain

353   tissues[34]. Furthermore, the absence of microglia in our models omits critical aspects of innate

354   immunity and neuroinflammation, precluding the evaluation of therapies targeting these cells.

355   Another limitation is that our research does not account for the full spectrum of cell types present in

356   the central nervous system (CNS), limiting our understanding of the multifaceted nature of AD.

357   Future research should build upon this model of pathogen-induced AD including a broader array of

358   CNS cell types, investigating alternative SAD-associated pathogens, and exploring the interplay

359   between viral infection and genetic AD risk factors like APOE. Additionally, because infection and

360   treatment were concordant in this model, our approach did not allow us to determine whether reduced

361   plaque formation was due to Aβ plaque aggregation or disaggregation activity of each compound.

362   In conclusion, our findings underscore the potential of FASNi to disrupt the progression of

363   AD by addressing the viral and metabolic components of the disease, offering a novel approach to

364   therapy that could halt or even prevent the development of AD. By elucidating how HSV-1 alters

host metabolism, we pave the way for innovative strategies to prevent or treat AD, reinforcing the

critical nexus between viral infection, lipid metabolism, and neurodegeneration.

ACKNOWLEDGMENTS

AUTHOR CONTRIBUTIONS

Conceptualization: M:B.; C.A.; L.T. Methodology and investigation: M.B.; C.A.; L.T.; D.C.; W.B.; S.P.; G.G.; F.G.; G.B.; D.G.; M.R.; M.V. V.D.O. Funding acquisition: M.B.; V.D.O.; M.D.A. Writing original draft: M.B.; C.A.; L.T.; W.B.; D.C.; V.D.O. Critical revision of the manuscript: D.K.; M.D.A.; G.G. All authors read and approved the final manuscript.

DECLARATION OF INTERESTS

We declare no conflicts of interest.

FIGURES

385
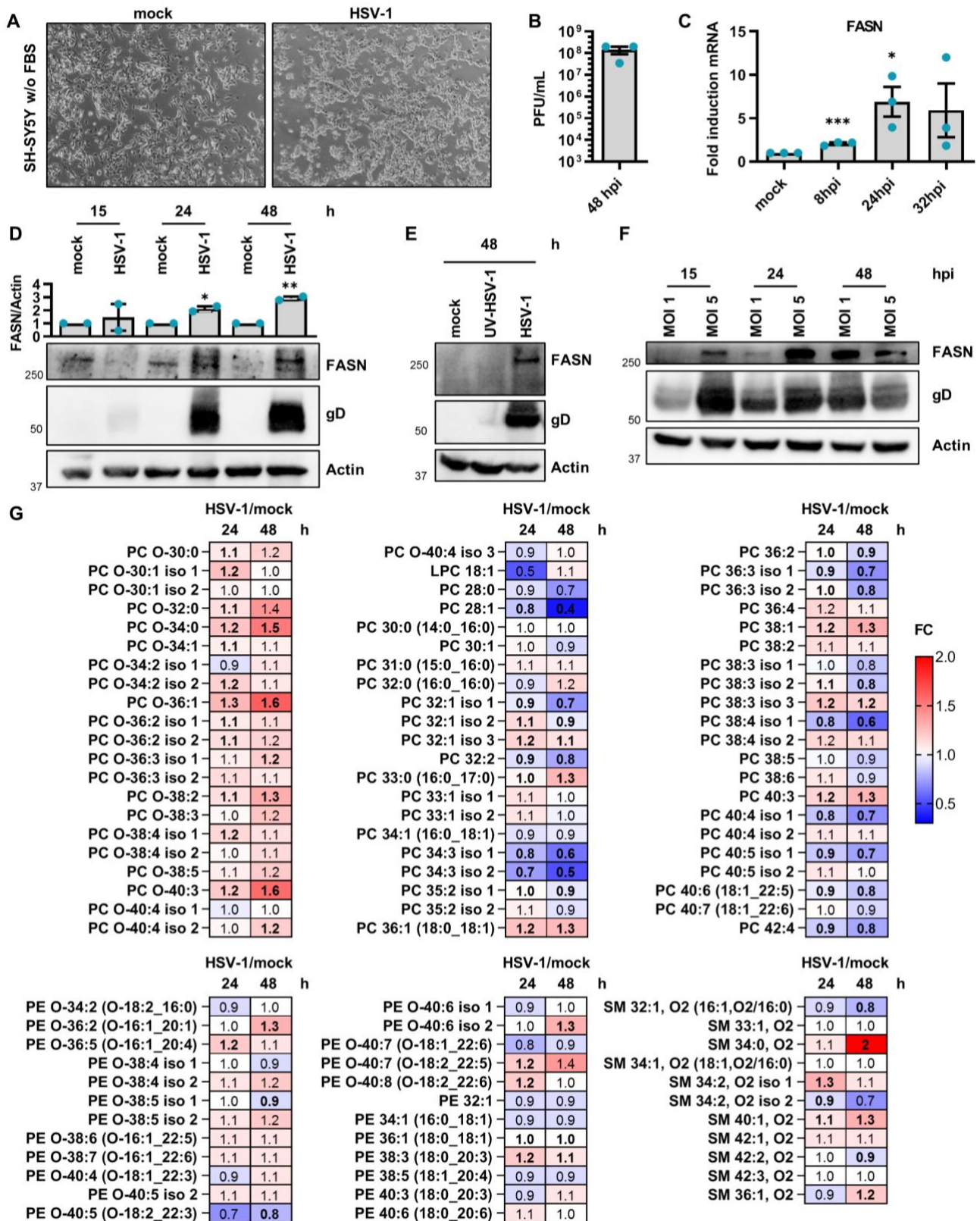
Figure 1. HSV-1 infection modulates the fatty acid synthase. SH-SY5Y cells were infected with HSV-1 (MOI 1) or left uninfected (mock) under serum-free conditions. **(A)** Representative images of mock or HSV-1infected cells at 48 h. **(B)** The extent of HSV-1 replication was assessed by titrating the infectivity of supernatants and cell-associated viruses combined using a standard plaque assay (n = 3). **(C)** At 8, 24, and 32 hpi, total RNA was isolated and subjected to RT-qPCR to quantify FASN mRNA expression levels. The values were normalized against GAPDH mRNA and expressed as fold induction relative to mock-infected cells (set at 1) ($n = 3$; unpaired t-test). **(D)** Western blot analysis of protein lysates from mock- or infected cells using antibodies against FASN, gD, or actin. A representative blot and corresponding

393 densitometric analysis are shown. The values were normalized to actin and expressed as fold induction relative to mock-
394 infected cells (set at 1). ($n = 2$; unpaired t-test). **(E)** SH-SY5Y cells were infected with either HSV-1 or UV-inactivated
395 HSV-1 (UV-HSV-1). Western blot analysis of protein lysates from mock or infected cells using antibodies against FASN,
396 gD, or actin. A representative blot is shown ($n = 2$). **(F)** Western blot analysis using protein lysates from SH-SY5Y cells
397 infected with different MOIs (1 and 5), probing for FASN, gD, or actin. A representative blot is shown ($n = 2$). Data are
398 shown as the mean $\pm$ SEM, *$P < 0.05$, **$P < 0.01$, ***$P < 0.001$. **(G)** Heat map displaying the levels of
399 glycerophosphocholines (PCs) and their ether analogs (PC-Os), glycerophosphoethanolamines (PEs) and their ether
400 analogs (PE-Os), and sphingomyelins (SM) in HSV-infected cells compared to mock cells at 24 h (left column) and 48 h
401 (right column). Upregulated (red, fold change > 1) and downregulated (blue, fold change < 1) lipid species are shown.
402 Bold values indicate statistical significance ($P < 0.05$, unpaired t-test) ($n = 2$).

403
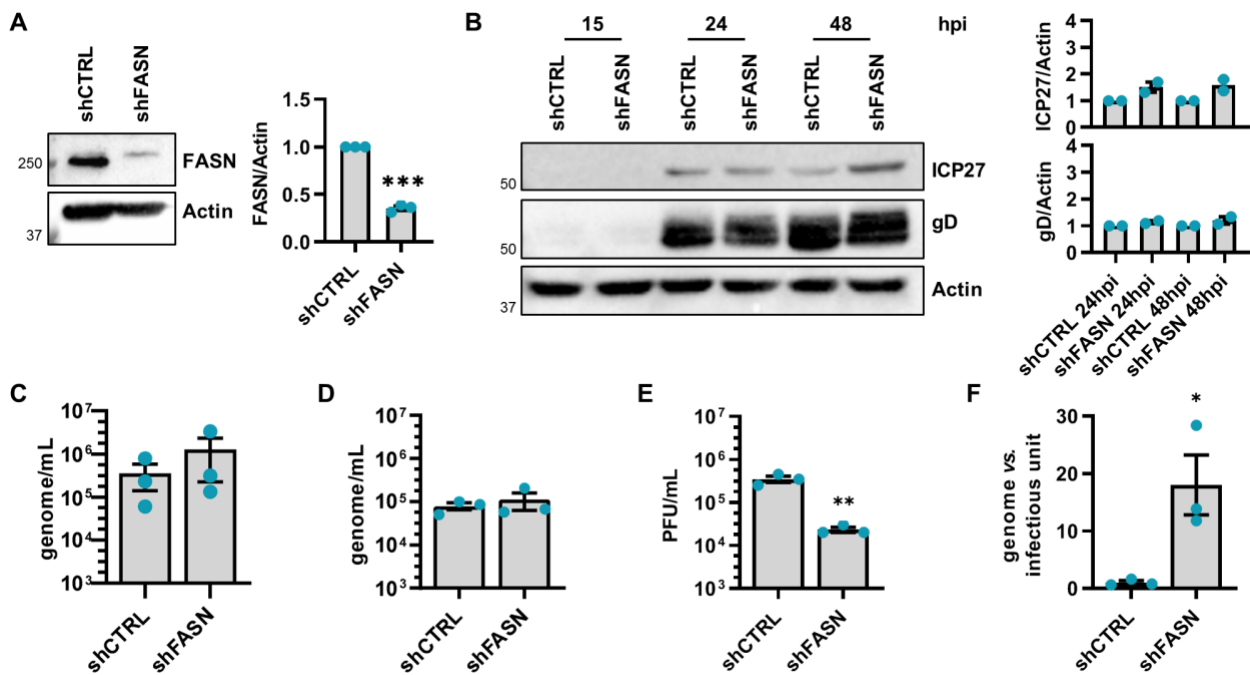
Figure 2. **FASN modulation impacts HSV-1 replication and infectivity.** SH-SY5Y cells were transduced with
lentivirus delivering short hairpin RNA (shRNA) targeting FASN (shFASN) or scramble RNA control (shCTRL). **(A)**
The efficiency of FASN protein depletion was assayed by immunoblotting using antibodies against human FASN or actin
as a loading control. A representative blot and the densitometric analysis are reported ($n = 3$; unpaired t-test). **(B)** shCTRL
and shFASN cells were infected with HSV-1 (MOI 1). Western blot analysis of protein lysates from mock- or infected
cells at the indicated hours post-infection (hpi) using antibodies against ICP27, gD, or actin. A representative blot and the
densitometric analysis are shown. Values were normalized to actin and plotted as fold induction relative to mock-infected
cells (set at 1). ($n = 2$; unpaired t-test). **(C)** At 24 hpi, the number of intracellular HSV-1 genomes was measured by qPCR
($n = 3$; unpaired t-test). **(D)** At 48 hpi, the number of genome-containing particles released by cells was measured by
qPCR ($n = 3$; unpaired t-test). **(E)** The supernatants from panel **D** were used to determine the number of infectious
units/mL by the viral yield test ($n = 3$; unpaired t-test). **(F)** The genome-to-infectious unit ratio has been determined ($n = 3$; unpaired t-test). Data are shown as the mean $\pm$ SEM, *$P < 0.05$, **$P < 0.01$, ***$P < 0.001$.

416
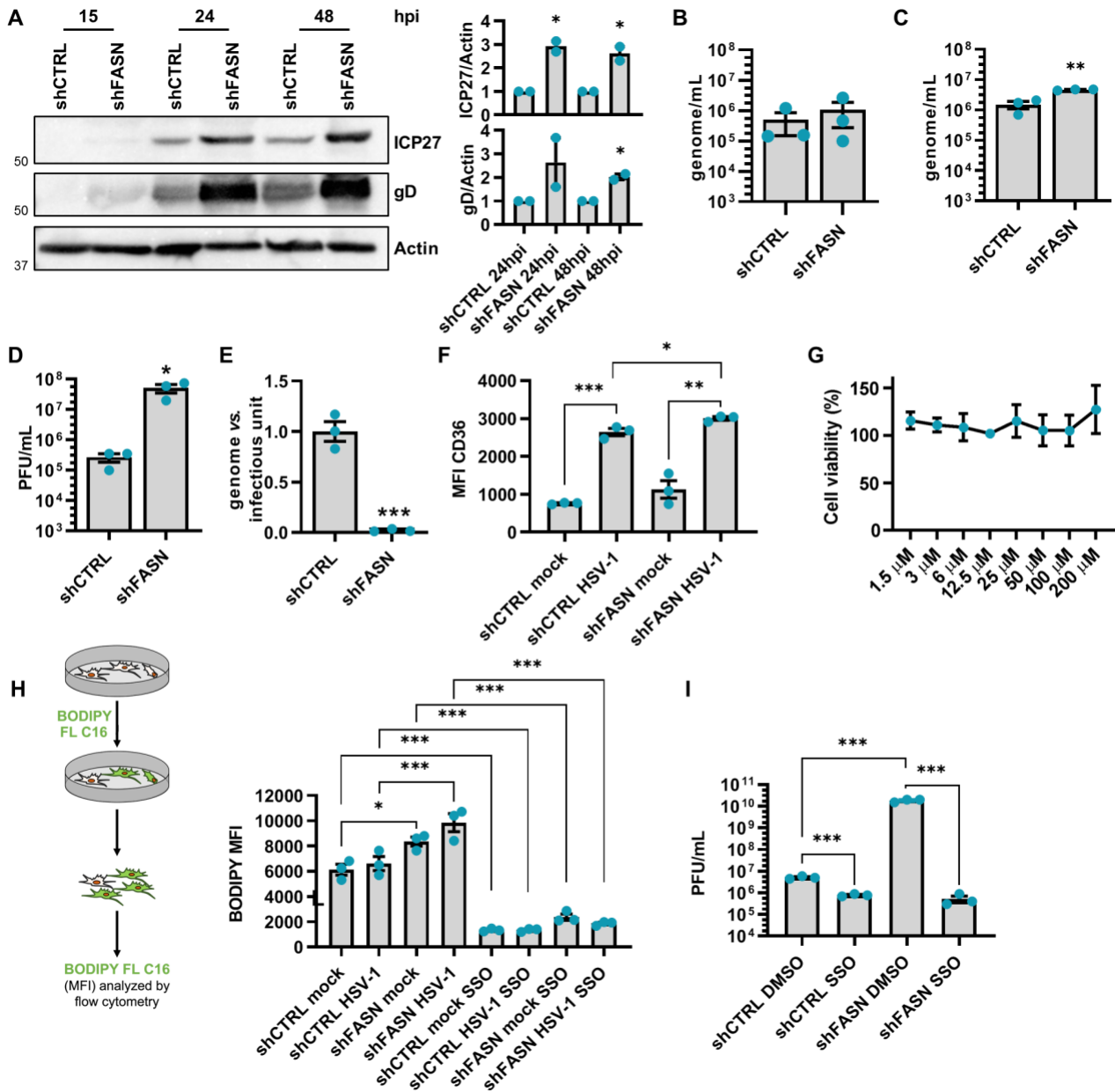
Figure 3. **Effect of FASN knockdown on HSV-1 replication in serum conditions.** shCTRL and shFASN cells were infected with HSV-1 (MOI 1). **(A)** Western blot analysis of protein lysates from mock- or infected cells at the indicated hours post-infection (hpi) using antibodies against ICP27, gD, or actin. A representative blot and the densitometric analysis are shown. Values were normalized to actin and plotted as fold induction relative to mock-infected cells (set at 1). (n = 2; unpaired t-test). **(B)** At 24 hpi, the number of intracellular HSV-1 genomes was measured by qPCR (n = 3; unpaired t-test). **(C)** At 48 hpi, the number of genome-containing particles released by cells was measured by qPCR (n = 3; unpaired t-test). **(D)** The supernatants from panel **C** were used to determine the number of infectious units/mL by the viral yield test (n = 3; unpaired t-test). **(E)** The genome-to-infectious unit ratio has been determined (n = 3; unpaired t-test). **(F)** Surface CD36 protein expression in shCTRL and shFASN cells was assessed by flow cytometry. Results show the mean fluorescence intensity (MFI) (n = 3; unpaired t-test). **(G)** SSO toxicity was determined at 48 h post-treatment (hpt), using the MTT method (n = 3). **(H)** shCTRL and shFASN cells were infected with HSV-1 in serum-free conditions and at 48 hpi treated with DMSO or SSO (200 μM) for 1 h. Then, cells were cultured in the presence of 2 μM BODIPY FL C16 for 30 minutes. (n = 3; one-way ANOVA followed by Bonferroni's post-tests). **(I)** shCTRL and shFASN cells were treated with DMSO or SSO in the presence of serum and then infected with HSV-1 (MOI 1). At 48 hpi, the supernatants were used to determine the number of infectious units/mL by the viral yield test (n = 3; unpaired t-test). Data are shown as the mean ± SEM, *P < 0.05, **P < 0.01, ***P < 0.001.

433
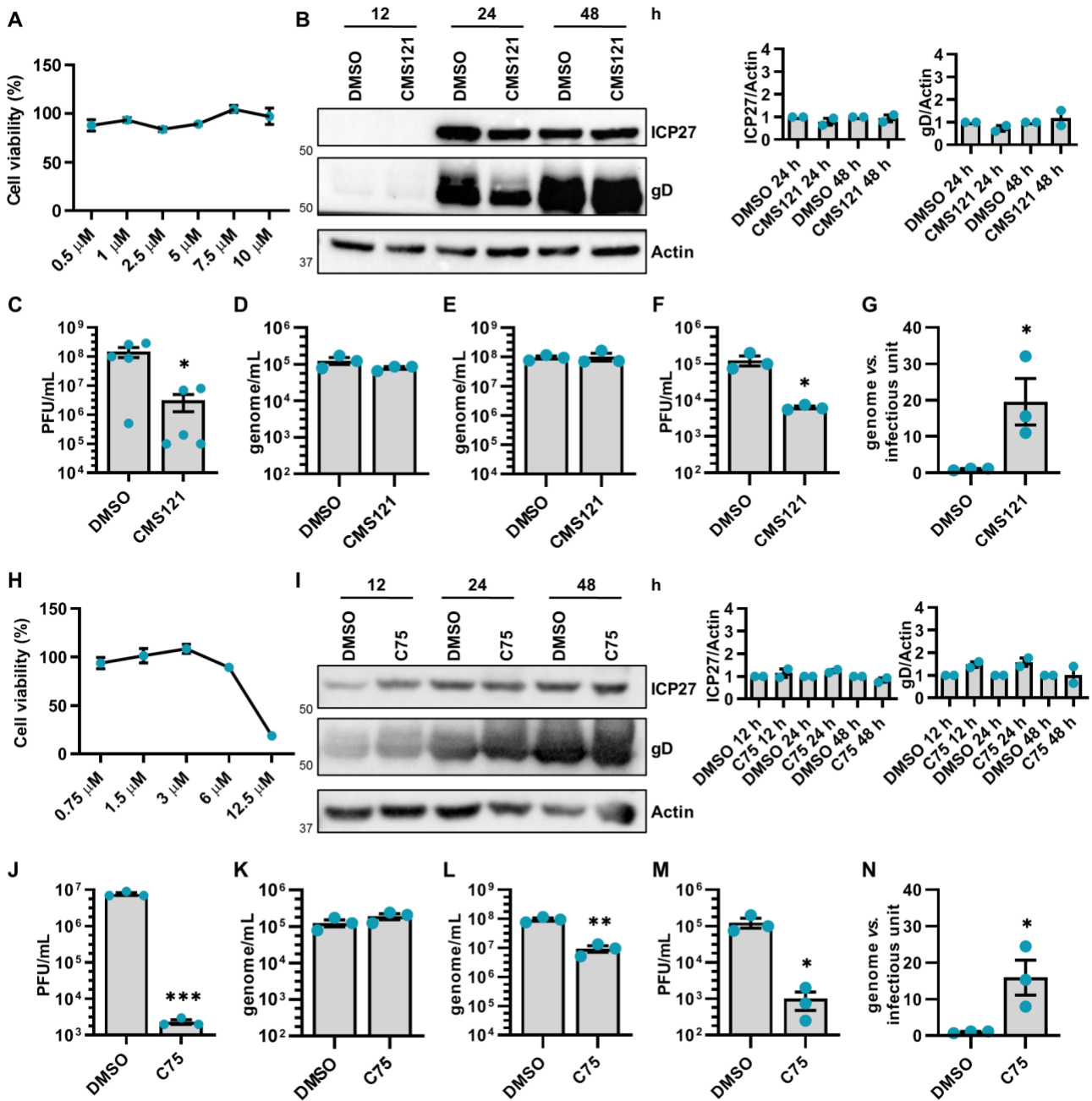
Figure 4. CMS121 and C75 reduce the infectivity of HSV-1 viral particles. **(A,H)** CMS121 and C75 toxicity were assessed by MTT assay at 48 h post-treatment (hpt) (n = 3). **(B,I)** Western blot analysis of protein lysates from cells harvested at different time points using antibodies against ICP27, gD, or actin. For each treatment, a representative blot (left) and relative densitometric analysis (right). Values are expressed as means ± SEM in ICP27 and gD expression normalized to actin (n = 2; unpaired t-test). **(C,J)** The extent of HSV-1 replication was assessed by titrating the infectivity of supernatants and cell-associated viruses from freeze-thaw cycles through standard plaque assay. Bars represent means ± SEM of five **(C)** and three **(J)** independent experiments (unpaired t-test). **(D,K)** At 48 hpi, the number of intracellular HSV-1 genomes was measured by qPCR (n = 3; unpaired t-test). **(E,L)** At 48 hpi, the number of genome-containing particles released by cells was measured by qPCR (n = 3; unpaired t-test). **(F,M)** Infectious units/mL were determined from supernatants in panels **(E)** and **(L)** by viral yield assay (n = 3; unpaired t-test). **(G,N)** The genome-to-infectious unit ratio was calculated as well (n = 3; unpaired t-test). Data are shown as the mean ± SEM, *P < 0.05, **P < 0.01, ***P < 0.001.

446
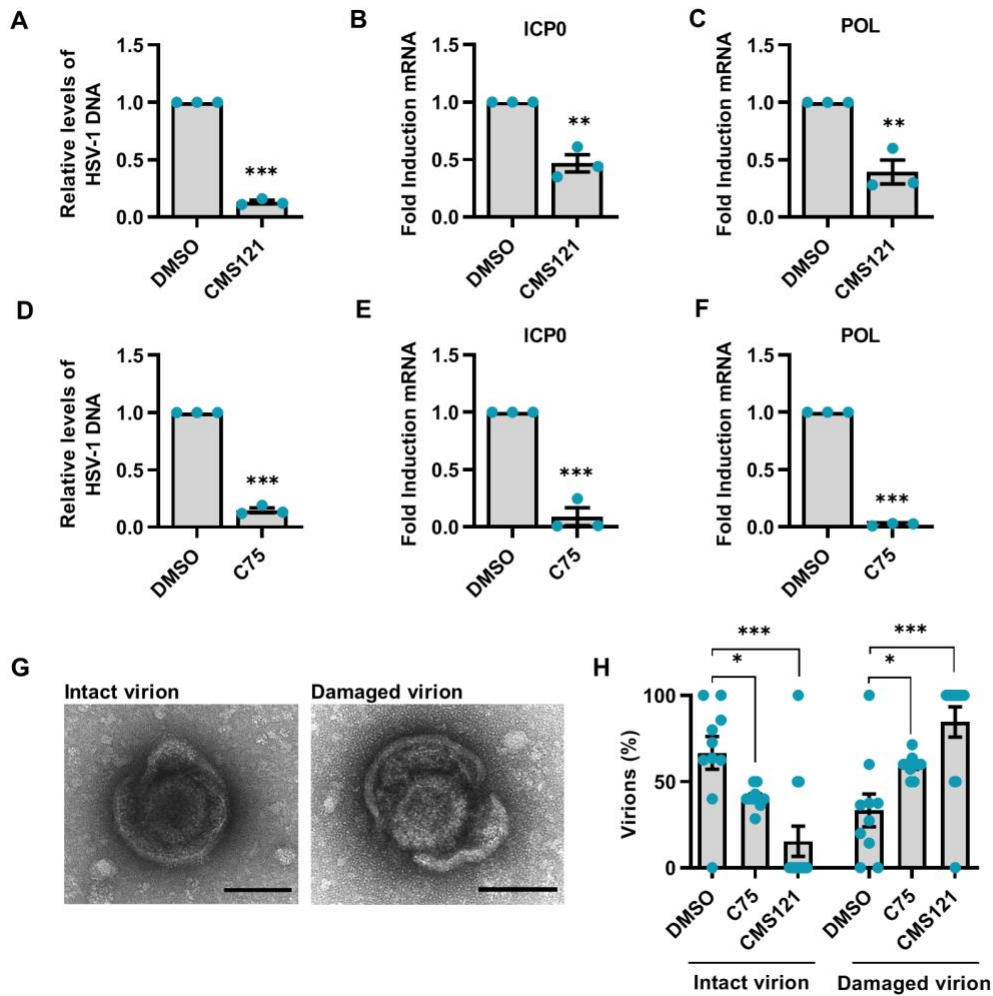
Figure 5. Impact of CMS121 and C75 on HSV-1 entry into Vero cells. Vero cells were infected with the same amount of HSV-1 virions released by SH-SY5Y cells upon treatment with CMS121, C75, or DMSO for 48 h. **(A,D)** After 2 h, the amount of HSV-1 genomes present in infected cells was measured by qPCR using primers for the gE gene, and values were normalized to the housekeeping gene GAPDH ($n = 3$; unpaired t-test). **(B-C,E-F)** At 6 hpi, total RNA was isolated and subjected to RT-qPCR to measure mRNA expression levels of HSV-1 ICP0 **(B,E)** and POL **(C,F)**. Values were normalized to the housekeeping GAPDH and plotted as fold induction relative to DMSO-treated infected cells (set at 1) ($n = 3$; unpaired t-test). **(G)** Representative image of an intact HSV-1 virion showing typical herpesvirus morphology with a prominent outer envelope (left) or a damaged virion displaying compromised envelope integrity (right). Scale bars 100 nm. **(H)** The number of enveloped particles was counted on different frames in DMSO-, C75- or CMS121-treated cells and plotted as a percentage (intact *vs.* damaged) (unpaired t-test). Data are shown as the mean $\pm$ SEM, *P < 0.05, **P < 0.01, ***P < 0.001.

458
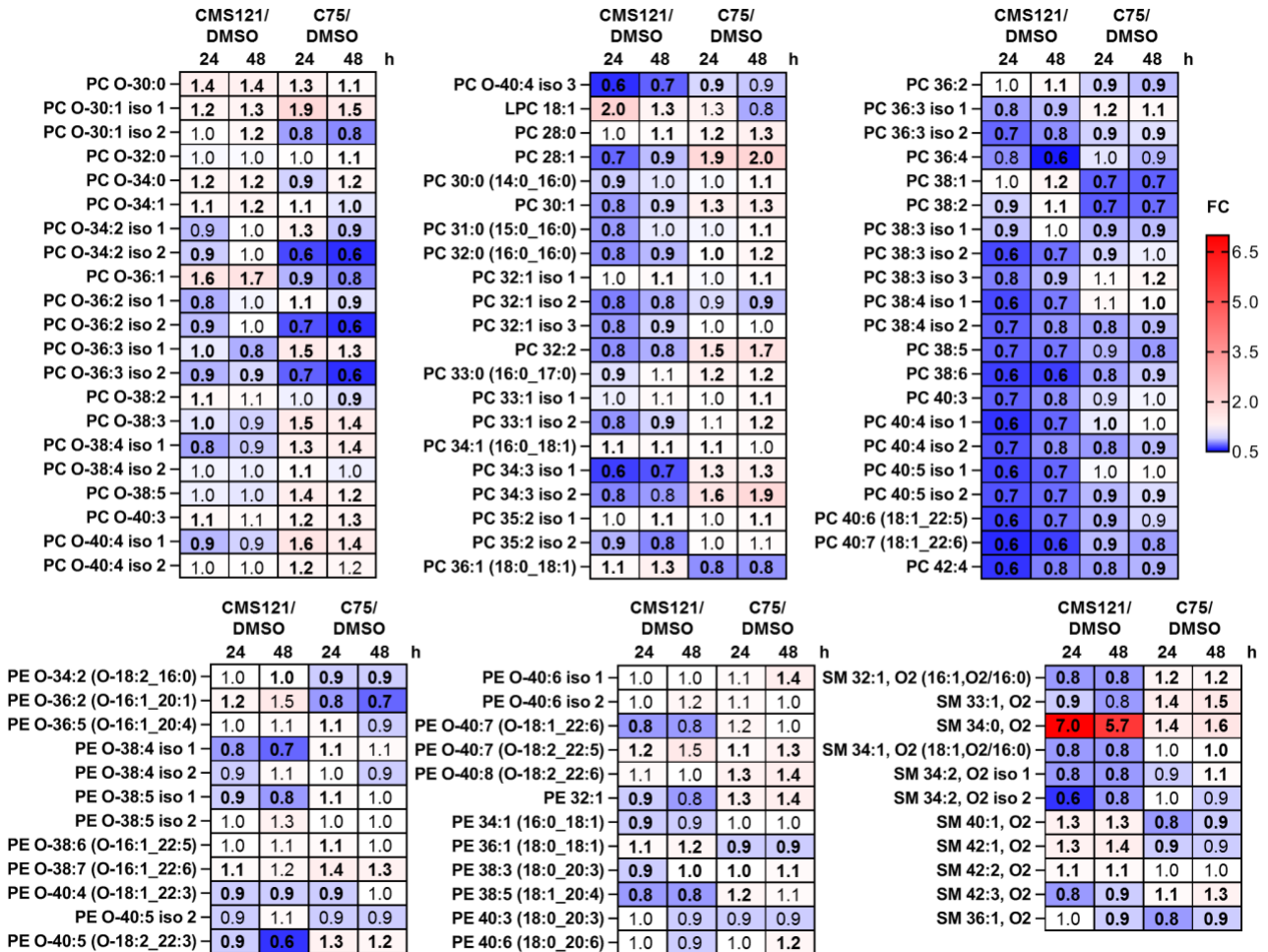
Figure 6. CMS121 and C75 modulate HSV-1-induced lipogenesis. Heat map of glycerophosphocholines (PCs), ether PC (PC-Os), glycerophosphoethanolamines (PEs), ether PE (PE-Os), and sphingomyelins (SMs) in SH-SY5Y cells infected with HSV-1 (MOI 1) and subsequently treated with CMS121, C75 or vehicle (DMSO) (24 h left column/48 h right column). Changes are represented for 24 (left columns) and 48 (right columns) hpi, with upregulation (red, fold change > 1) and downregulation (blue, fold change < 1) highlighted. Statistically significant alterations are denoted in bold (unpaired t-test, $P < 0.05$). Data are derived from two independent experiments.
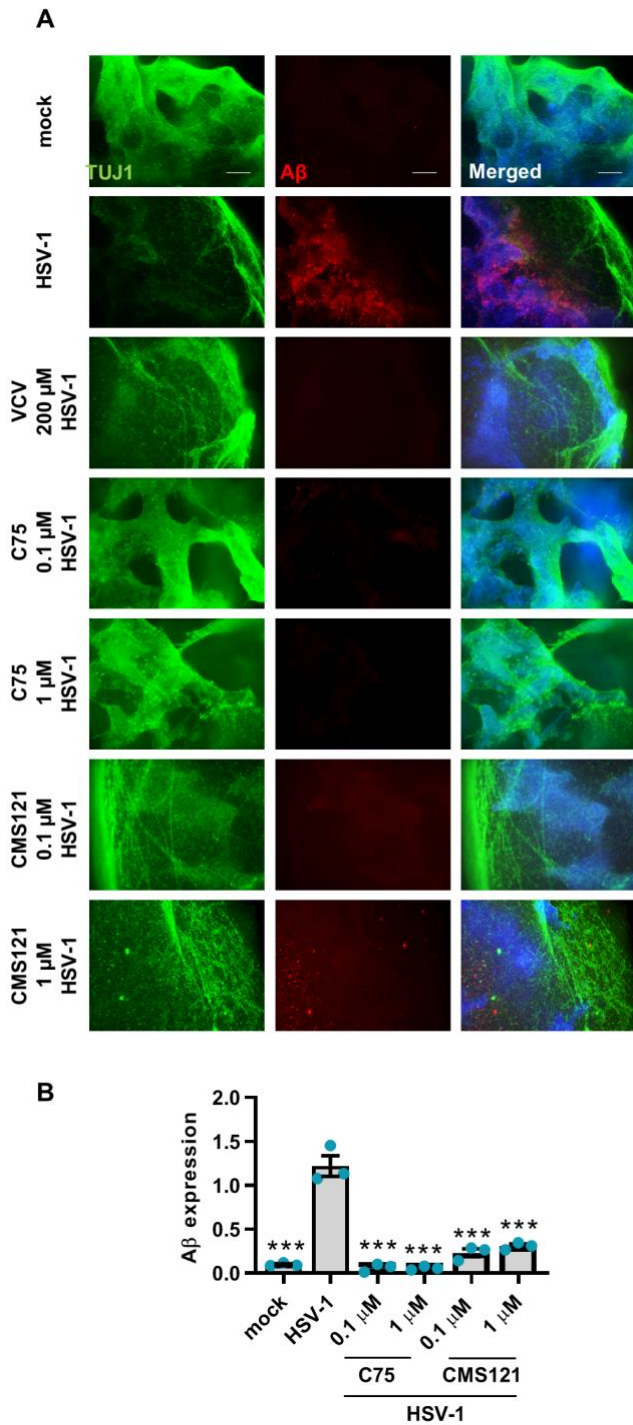
Figure 7. C75 and CMS121 treatment reduces AD-like phenotypes in 3D culture. (A,B) C75 and CMS121 treatment reduces Aβ+ PLFs at 0.1–1 μM to mock-comparable levels. Data are presented as mean ± SEM (***, $P < 0.001$; one-way ANOVA followed by Bonferroni's post-test) for the comparison between mock-/treated- and HSV-1-infected cells. Scale bars 100 μm.

RESOURCE AVAILABILITY
LEAD CONTACT
Further information and requests for resources and reagents should be directed to and will be fulfilled by the Lead Contact, Matteo Biolatti (matteo.bilatti@unito.it).

MATERIALS AVAILABILITY
All materials generated in this study are available from the lead contact upon request.

479 **EXPERIMENTAL MODEL AND STUDY PARTICIPANT DETAILS**
480 **Cells and viruses**

481 SH-SY5Y cells (ATCC CLR-2266), African green monkey kidney cells (Vero; ATCC CCL-81),

482 human foreskin fibroblasts (HFFs; ATCC SCRC-1041), and human embryo kidney 293 cells (HEK

483 293T; ATCC CRL-3216) were maintained at 37°C with 5% CO_2.

484 Cells were cultured in Dulbecco's Modified Eagle's Medium, supplemented with 10% heat-

485 inactivated fetal bovine serum (FBS), 2 mM glutamine, 1 mM sodium pyruvate, 100 U/mL penicillin,

486 and 100 µg/mL streptomycin sulfate (Sigma-Aldrich). HEK 293T and SH-SY5Y cells were

487 supplemented with 1% non-essential amino acids (Sigma-Aldrich).

488 The HSV-1 clinical isolate was a generous gift from Valeria Ghisetti, Amedeo di Savoia

489 Hospital, Turin, Italy. It was propagated and titrated by plaque assay on Vero cells, as previously

490 described[35]. DANA HSV-1 McIntyre strain VR-539 was purchased from ATCC (Manassas, VA).

491 For experiments conducted without serum, cells were initially cultured in a growth medium

492 supplemented with serum. Twenty-four hours prior to infection, cells were subjected to serum

493 starvation and subsequently maintained in serum-free conditions throughout the infection period.

494 Infections were carried out using a multiplicity of infection (MOI) of either 1 or 5 infectious units per

495 cell, tailored to the specific requirements of each experiment.

496 The particle-to-infectious unit ratio was determined by comparing the amount of viral DNA

497 to the infectious virus yield in cell-free supernatants. The determination of virus yields from cell-free

498 supernatants is described elsewhere[36]. Viral DNA in supernatants was quantified by quantitative PCR

499 (qPCR), using primers to amplify gE gene (Fw: 5'-TGTCTGTATCAGCCGCAGC-3'; Rv: 5'-

500 TTCTGGAACACCCCGCGTA-3'). Intracellular HSV-1 DNA copy numbers were normalized to

501 glyceraldehyde 3-phosphate dehydrogenase (GAPDH) (Fw, 5'-AGTGGGTGTCGCTGTTGAAGT-

502 3'; Rv, 5'-AACGTGTCAGTGGTGGACCTG-3'). A standard curve of serially diluted genomic

503 DNA mixed with a gE-encoding plasmid was created in parallel with each analysis.

504   UV-inactivated HSV-1 was prepared using a double pulse of UV-B light (1.2 J/cm^2). The UV-

505   inactivated HSV-1 did not replicate or produce detectable levels of immediate-early (IE) gene

506   products.

507
508   **METHOD DETAILS**
509   **Reagents**

510   CMS121 (HY-135981, MedChemExpress), C75 (HY-12364, MedChemExpress), SSO (11211,

511   Cayman Chemical), and BODIPY FL C16 (D3821; Invitrogen) were used at a concentration of 5 μM,

512   5 μM, 200 μM, and 2 μM, respectively.

513   pLKO.1 puro-humanU6-shRNA FASN was a gift from Elizabeth Stoll (Addgene plasmid

514   #82327; http://n2t.net/addgene:82327; RRID: Addgene_82327). pLKO.1 Puro shRNA Scramble was

515   a gift from A. Follenzi (University of Eastern Piedmont, Novara, Italy). pAcUW51-CgE was a gift

516   from Pamela Bjorkman (Addgene plasmid #13762; http://n2t.net/addgene:13762; RRID:

517   Addgene_13762)

518   **Lentivirus production**

519   Recombinant lentiviruses were packaged in HEK 293T cells by cotransfection of the 3rd Generation

520   Packaging System Mix (kindly provided by A. Follenzi, University of Eastern Piedmont, Novara,

521   Italy) with the above-mentioned vectors to produce viral particles using Lipofectamine 2000 (Thermo

522   Fisher Scientific). Viral supernatants were harvested after 72 h and used to transduce SH-SY5Y cells

523   by infection in the presence of 10 μg/mL polybrene. Transduced cells were selected with puromycin

524   (1 μg/mL) over the course of 14 days post-transduction. After selection, the successful knockout was

525   confirmed by immunoblotting.

526   **Cytotoxicity Assay**

527   To determine the cytotoxicity of cytochalasin, CMS121, C75, and SSO, SH-SY5Y cells were seeded

528   in a 96-well culture plate and exposed to increasing concentrations of either compounds or vehicle

529   dimethyl sulfoxide (DMSO, Sigma-Aldrich) the following day. After 48 h of incubation, the number

530   of viable cells was determined using the 3-(4,5-dimethylthiazol-2-yl)-2,5-diphenyltetrazolium

531   bromide (MTT) (Sigma-Aldrich) assay, as previously described[37].

532   **RNA isolation and RT-qPCR.**

533   Total RNA was extracted using TRI Reagent solution (Life Technologies) according to the

534   manufacturer's instructions, and 1 µg was retrotranscribed using the Revert-Aid H-Minus FirstStrand

535   cDNA synthesis kit (Thermo Fisher Scientific). Comparison of expression between samples was

536   performed by SYBR green-based reverse transcription-qPCR (RT-qPCR) using a CFX96 Real-Time

537   System apparatus (Bio-Rad Laboratories). The housekeeping gene GAPDH was used to normalize

538   for variation in cDNA levels. The following primers were used: FASN Fw, 5'-

539   AGGCTGAGACGGAGGCCATA-3'; FASN Rv, 5'-AAAGCTCAGCTCCTGGCGGT-3'; ICP0

540   Fw, 5'-GGTCCCCACTGACTCATACG-3'; ICP0 Rv, 5'-ATCCCGACCCCTCTTCTTC-3'; Pol Fw

541   5'-CGAGTGCGAAAAGACGTTCA-3'; Pol Rv 5'-TGGAGGTGCGGTTGATAAAC-3'; APP Fw,

542   5'-GTCTCTCCCTGCTCTACAA-3'; APP Rv, 5'-GGCCAAGACGTCATCTGAATAG-3';

543   PSEN2   Fw,   5'-CTGACCGCTATGTCTGTAGTGG-3';   PSEN2   Rv   5'-

544   CTTCGCTCCGTATTTGAGGGT-3'; GAPDH Fw, 5'-AGTGGGTGTCGCTGTTGAAGT-3';

545   GAPDH Rv, 5'-AACGTGTCAGTGGTGGACCTG-3'.

546   **Protein analysis.**

547   Whole-cell protein extracts were examined by Western blot analysis as previously described[38].

548   Briefly, cells were lysed in ice-cold RIPA buffer supplemented with protease inhibitors (Sigma-

549   Aldrich) to obtain total cell lysate. Equal amounts of cell extracts were fractionated by electrophoresis

550   on SDS-polyacrylamide gels and transferred to Immobilon-P membranes (Merck Millipore). After

551   blocking with TBST (Tris-buffered saline containing 0.05% Tween20) containing 5% milk,

552   membranes were incubated overnight at 4°C with the appropriate primary antibodies. Membranes

553   were then washed with TBST and incubated for 2 h at room temperature with HRP-conjugated anti-

554   mouse or anti-rabbit secondary antibodies. Proteins were visualized using ChemiDoc MP Imaging

555   System (Bio-Rad Laboratories) and an enhanced chemiluminescence detection kit (Thermo Fisher

556 Scientific). Scanning densitometry of the bands was performed using Image Lab (version 6.0.1; Bio-

557 Rad Laboratories). The following primary and secondary antibodies were used: anti-actin clone C4

558 (MAB1501; Sigma-Aldrich); anti-FASN (3189S, Cell Signaling Technology), anti-HSV gD (clone

559 2C10, Virusys Corporation), anti-HSV ICP27 (clone H1113, Virusys Corporation), horseradish

560 peroxidase-labeled anti-mouse, and anti-rabbit antibodies (GE Healthcare).

561 **FACS CD36**

562 Cells were seeded at a density of 4×10^5 cells per well in a 12-well plate. Cells were harvested by

563 PBS-EDTA 2mM and stained with CD36 primary antibody (PA1-16813; Invitrogen) combined with

564 Alexa Flour 488 anti-rabbit (Life Technologies) mix solution for 1 h at 37°C. Cells were washed

565 twice in PBS, fixed in PBS containing 1% paraformaldehyde (PAF), and analyzed on a BD

566 FACSCanto II flow cytometer (BD Biosciences). The data were processed and analyzed using FlowJo

567 software (BD Biosciences).

568 **BODIPY-C16 uptake assay**

569 shCTRL and shFASN cells were seeded at a density of 4×10^5 cells/well in a 12-well plate. Cells

570 were infected with HSV-1 (MOI 1) in serum-free media. After 48 h, cells were treated with SSO for

571 1 h or left untreated and then cultured in serum-free media supplemented with 2 μM BODIPY FL

572 C16 (D3821, Invitrogen) for 30 min. Subsequently, cells were harvested by trypsinization, washed

573 twice with PBS, and fixed with PBS-PAF 1% for 20 min at room temperature and finally analyzed

574 by flow cytometry using a BD FACSCanto II flow cytometer (BD Biosciences). The data were

575 processed and analyzed using FlowJo software (BD Biosciences). The mean fluorescence intensity

576 (MFI) was compared between samples.

577 **Transmission electron microscopy**

578 HSV-1 virions were allowed to adsorb onto carbon and Formvar-coated copper grids (Pelco®), left to

579 stand for 5 min, washed with water, and then negatively stained using 0.5% aqueous uranyl acetate.

580 Images were captured using a CM10 electron microscope (Philips) operating at 60 kV. Counting of

581 enveloped or broken virions in each considered grid hole was done during the sample observation.

Lipidomics

Lipid extraction was conducted using a chloroform/methanol/water mixture acidified with formic acid. The procedure consisted of adding 600 µL of chloroform/methanol (1:2 v/v), 10 µL of formic acid, 5 µL of EquiSPLASH™ LIPIDOMIX® (Avanti Polar Lipids), and glass beads to the sample. This mixture was vortexed for 20 s and then shaken for 5 min (2000 rpm, 4 °C). Subsequently, 200 µL of chloroform and 350 µL of deionized water were added, and the mixture was shaken again for 20 min at 2000 rpm and 4 °C. After centrifugation at 3900 x g for 10 min, the lower organic phase was collected and transferred to a chromatographic vial with a glass insert and diluted 10-fold with a 2:8 (v/v) water/methanol mixture. Extraction blanks without cells were also prepared as negative controls.

For lipidome analysis, an Agilent 1290 LC system equipped with a binary pump, online degasser, autosampler, and a thermostated column compartment, coupled to a 6540 Q-TOF–MS with a dual electrospray ionization (ESI) source (Agilent Technologies) was employed. Lipids were separated using a Kinetex EVO C18 reversed-phase column (2.1 × 150 mm, 1.7 µm particle size, Phenomenex, Torrance, CA, USA) with a 0.2-µm in-line filter at 60°C. The mobile phase consisted of component A [5 mM ammonium formate in 20:80 (v/v) water/methanol] and component B (5 mM ammonium formate in 1:99 (v/v) water/methanol), pumped at a flow rate of 0.5 mL/min. The gradient elution started with 20% of component B, ramping to 100% from 0 to 15 min, and held at 100% B for 10 min. The column was then equilibrated with the starting conditions for 10 min. The total run time was 35 min, with an injection volume of 0.25 µL. Each extract was injected in duplicate. The SCAN acquisition mode recorded data in positive ion mode from 200 to 1700 m/z in high-resolution (4 GHz). MS analysis parameters included a capillary voltage of 3500 V, fragmentation voltage of 120 V, nebulizing gas at 35 psig, and a drying gas temperature of 300°C. MS/MS analysis was performed with a collision energy set at 35 V and 80 V. The two most abundant peaks were selected for fragmentation and excluded for the next 0.3 min. MS/MS spectra were acquired in the m/z range of 50–1700. Lipid extracts were randomly injected with a quality control (QC) sample (pooled

608 extracts) introduced after every 4 sample injections to monitor LC–MS system stability. Lipidomic

609 data were processed using Agilent MassHunter Workstation Profinder 10.0 (Agilent Technologies).

610 A list of identified lipids was created and used with the Targeted Molecular Feature Extraction

611 algorithm. The extraction parameters were adjusted for positive ions, with charge carriers (H+ for

612 PC, PC ether analogs, PE, PE ether analogs, SM) and a match of tolerance of 10 ppm, retention time

613 window of 0.1 min, Gaussian smoothing applied before extracting ion chromatograms (EICs) based

614 on a peak height threshold of 1000 counts. Peaks were manually inspected to detect false positive

615 peaks. The .cef files were further processed in Mass Profiler Professional 15.1 software (Agilent

616 Technologies) for data alignment and filtration, with missing values left as is. Alignment was

617 configured with a slope of 0.0% an intercept of 0.1 min, a mass tolerance of 10.0 ppm, and an intercept

618 of 2.0 mDa. Filtration criteria included the %RSD for lipid peak areas in QC samples and %RSD for

619 internal standard peak areas in real samples, retaining molecular features (MFs) with a peak area

620 %RSD below 25%.

621 Lipids were identified through a custom database search, using accurately measured m/z

622 values within a 10 ppm tolerance. The identity of lipids and FA composition were verified manually

623 using MS/MS spectra and Agilent Mass Hunter Workstation Lipid Annotator 1.0 software (Agilent

624 Technologies). Identified lipid species were categorized by lipid class, total carbon atoms, and

625 unsaturation level in fatty acyl groups, following LipidMaps classification standards[39]. Diagnostic

626 ions for lipid class identification included m/z 184.0726 for SM and PC identity, a neutral loss of

627 141.02 Da for PE, and m/z 264.27 for the C18 sphingoid base backbone.

628 **3D human brain-like tissue model of herpes-induced AD**

629 Human-induced neural stem cells (hiNSCs) were generated as previously described[40,41]. hiNSCs were

630 expanded on mouse embryonic fibroblast (MEF) feeder layers that had been previously inactivated

631 by mitomycin C, using hiNSC media: Knockout (KO) DMEM supplemented with 20% KO xeno-

632 free serum replacement, 20 ng/mL recombinant bFGF, 1% Glutamax, 1% antibiotic-antimycotic, and

633 0.1 mM β-mercaptoethanol.

634   Human 3D brain tissues were engineered by generating silk protein sponges using a 6% (wt/vol)

635   Bombyx mori-derived silk solution, achieving a pore size range of 500–600 μm. These sponges were

636   then shaped into 6-mm diameter discs, 2-mm thick, with central 2-mm holes to create donut-shaped

637   scaffolds, which were sterilized by autoclaving and coated with 0.5 mg/ml laminin (Roche,

638   Indianapolis, IN). Dissociated hiNSCs were seeded into the silk porous scaffolds at a density of 10^6

639   cells per scaffold and allowed to adhere overnight. The following day, collagen gels were prepared

640   using type I rat tail collagen (Corning, Bedford, MA, USA) as previously described[40,41]. 3D human

641   brain tissue constructs were then cultured in neurobasal media (Invitrogen, Carlsbad, CA)

642   supplemented with 2% B27 (Invitrogen, Carlsbad, CA), 0.5 mM Glutamax, and 1% antibiotic-

643   antimycotic (Invitrogen, Carlsbad, CA) for 6 weeks to allow for mature network formation, with

644   medium changes every 3 days. HSV-1 McIntyre strain VR-539 was purchased from ATCC

645   (Manassas, VA). We used purified HSV-1 to directly infect hiNSCs at an MOI of 0.0001 based on

646   our previous studies[40,41], which was calculated according to initial seeding density. For mock

647   infections, an equal volume of control culture medium from uninfected viral production cells was

648   used (ATCC). All virus work was approved by Tufts Institutional Biosafety Committee.

649   **Immunofluorescence**

650   Human 3D brain scaffolds were fixed in 4% paraformaldehyde and washed with 1X phosphate-

651   buffered saline (PBS). Samples were incubated with blocking buffer (PBS, 10% goat serum, and

652   0.1% Triton X-100). Primary antibodies used were against amyloid beta (anti-Amyloid Fibril,

653   Abcam, mOC87) and beta III tubulin (anti-Tuj1, Sigma, T8578), which were added to the blocking

654   buffer and incubated with samples overnight at 4ºC. The next day, samples were washed several times

655   with PBS, and incubated with a corresponding fluorescently conjugated secondary antibody in a

656   blocking buffer for 1 h at room temperature (Alexa Fluor 488 anti-mouse, Alexa Fluor 594 anti-

657   rabbit). Nuclei were counterstained with DAPI (Invitrogen).

658   **Microscopy**

659 Brightfield and fluorescent images were obtained using a Keyence BZ-X700 microscope and

660 associated software.

661

662 **QUANTIFICATION AND STATISTICAL ANALYSIS**
663 **Statistical analysis**

664 Statistical tests were performed using GraphPad Prism version 8.00 for Windows (GraphPad

665 Software), Mass Profiler Professional 15.1 software (Agilent Technologies), or MetaboAnalyst5.0

666 (https://www.metaboanalyst.ca/home.xhtml). The data are presented as means and standard errors of

667 the means (SEM) or standard deviation (SD). Differences were considered statistically significant

668 when the p-value was < 0.05. Statistical details for each experiment including statistical significance

669 and n value were provided in the figure legends.

670

671 **SUPPLEMENTAL INFORMATION TITLES AND LEGENDS**
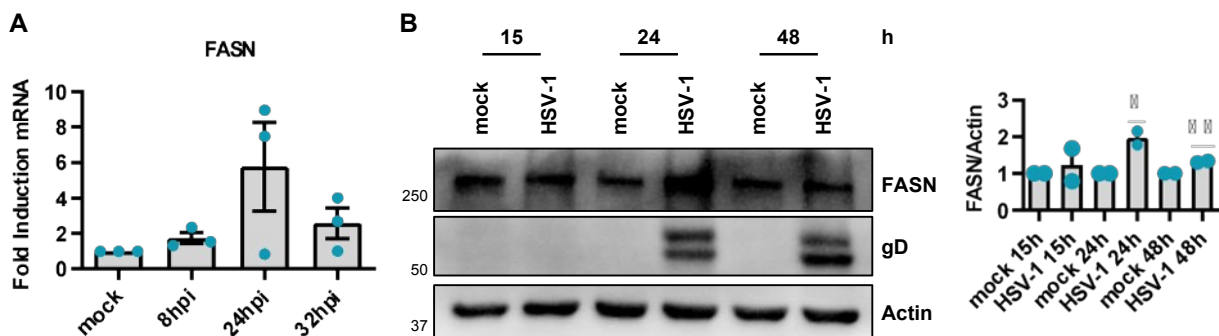
672

673 **Figure S1. FASN upregulation induced by HSV-1 is cell type-independent.** HFFs were infected with HSV-1 (MOI
674 1). **(A)** At 8, 24, and 32 hpi, total RNA was isolated and subjected to RT-qPCR to measure mRNA expression levels of
675 FASN. The values were normalized to GAPDH and expressed as fold induction relative to mock-infected cells (set at 1).
676 ($n = 3$; unpaired t-test) for the comparison between infected and uninfected cells (mock). **(B)** Western blot analysis of
677 protein lysates from mock- or infected cells using antibodies against FASN, gD, or actin. A representative blot and the
678 densitometric analysis are shown. Values were normalized to actin and plotted as fold induction relative to mock-infected
679 cells (set at 1) ($n = 2$; unpaired t-test). Data are shown as the mean ± SEM, *P < 0.05, **P < 0.01, ***P < 0.001.

680
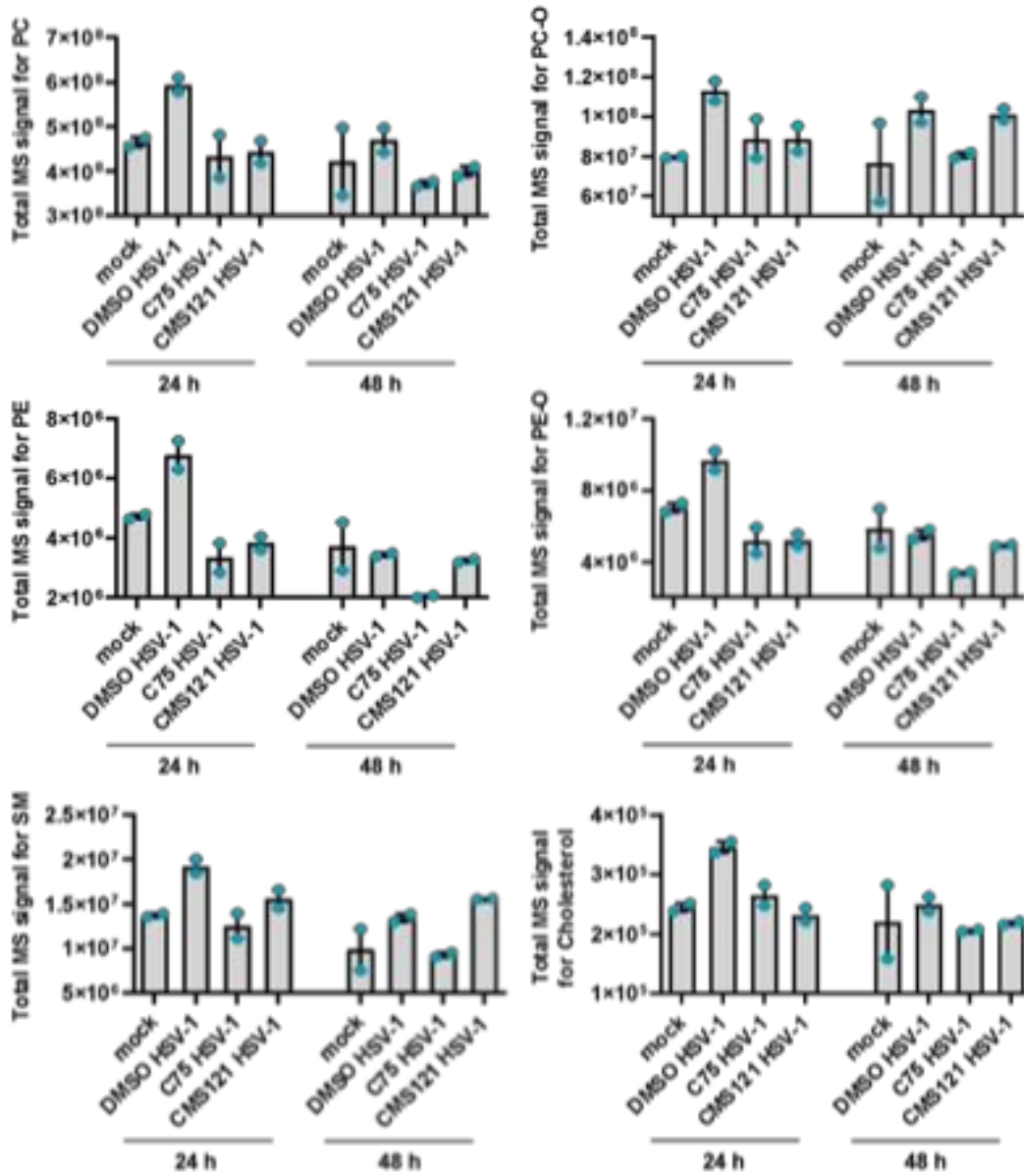
Figure S2. HSV-1 increases *de novo* lipogenesis. The total amount of all examined lipid classes has increased in HSV-1 infected cells in comparison to uninfected cells, and decreased in CMS121 or C75 treated HSV-1 infected cells in comparison to untreated HSV-1 infected cells. Total lipid content is the sum of all lipids belonging to a specific lipid class. Bars show mean ± SEM ($n = 2$).
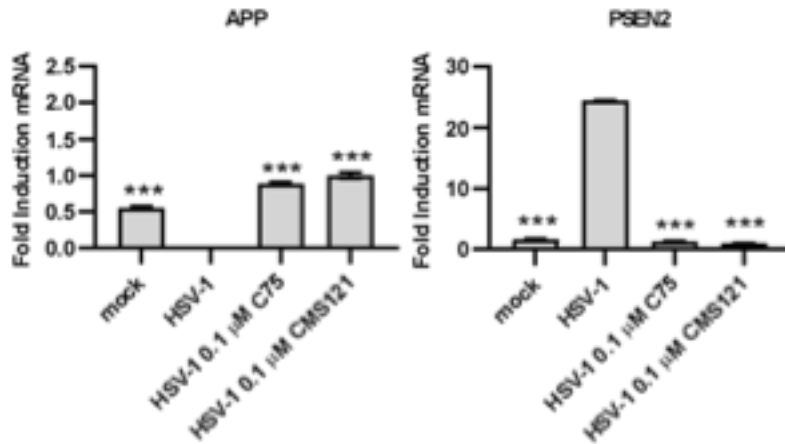
Figure S3. C75 and CMS121 treatment modulates AD-factors in 3D culture. FASNi treatments protected against HSV-1-induced downregulation of APP **(A)**, and upregulation of PSEN2 **(B)** mRNA transcripts. RT-qPCR data are presented as mean ± SD (**, $P < 0.01$; ***, $P < 0.001$; unpaired t-test) for the comparison between mock-/treated- and HSV-1-infected cells.

REFERENCES

1. Whitley, R.J., and Roizman, B. (2001). Herpes simplex virus infections. Lancet *357*, 1513–1518. 10.1016/S0140-6736(00)04638-9.

2. Rodríguez-Sánchez, I., and Munger, J. (2019). Meal for Two: Human Cytomegalovirus-Induced Activation of Cellular Metabolism. Viruses *11*, 273. 10.3390/v11030273.

3. Thaker, S.K., Ch'ng, J., and Christofk, H.R. (2019). Viral hijacking of cellular metabolism. BMC Biol *17*, 59. 10.1186/s12915-019-0678-9.

4. Langeland, N., Haarr, L., and Holmsen, H. (1986). Polyphosphoinositide metabolism in baby-hamster kidney cells infected with herpes simplex virus type 1. Biochem J *237*, 707–712. 10.1042/bj2370707.

5. Sutter, E., de Oliveira, A.P., Tobler, K., Schraner, E.M., Sonda, S., Kaech, A., Lucas, M.S., Ackermann, M., and Wild, P. (2012). Herpes simplex virus 1 induces de novo phospholipid synthesis. Virology *429*, 124–135. 10.1016/j.virol.2012.04.004.

6. Asher, Y., Heller, M., and Becker, Y. (1969). Incorporation of lipids into herpes simplex virus particles. J Gen Virol *4*, 65–76. 10.1099/0022-1317-4-1-65.

7. Vastag, L., Koyuncu, E., Grady, S.L., Shenk, T.E., and Rabinowitz, J.D. (2011). Divergent effects of human cytomegalovirus and herpes simplex virus-1 on cellular metabolism. PLoS Pathog *7*, e1002124. 10.1371/journal.ppat.1002124.

8. Blackham, S., Baillie, A., Al-Hababi, F., Remlinger, K., You, S., Hamatake, R., and McGarvey, M.J. (2010). Gene expression profiling indicates the roles of host oxidative stress, apoptosis, lipid metabolism, and intracellular transport genes in the replication of hepatitis C virus. J Virol *84*, 5404–5414. 10.1128/JVI.02529-09.

9. Gualdoni, G.A., Mayer, K.A., Kapsch, A.-M., Kreuzberg, K., Puck, A., Kienzl, P., Oberndorfer, F., Frühwirth, K., Winkler, S., Blaas, D., et al. (2018). Rhinovirus induces an anabolic reprogramming in host cell metabolism essential for viral replication. Proc Natl Acad Sci U S A *115*, E7158–E7165. 10.1073/pnas.1800525115.

10. Delgado, T., Sanchez, E.L., Camarda, R., and Lagunoff, M. (2012). Global metabolic profiling of infection by an oncogenic virus: KSHV induces and requires lipogenesis for survival of latent infection. PLoS Pathog *8*, e1002866. 10.1371/journal.ppat.1002866.

11. Piacentini, R., De Chiara, G., Li Puma, D.D., Ripoli, C., Marcocci, M.E., Garaci, E., Palamara, A.T., and Grassi, C. (2014). HSV-1 and Alzheimer's disease: more than a hypothesis. Front Pharmacol *5*, 97. 10.3389/fphar.2014.00097.

12. Itzhaki, R.F. (2014). Herpes simplex virus type 1 and Alzheimer's disease: increasing evidence for a major role of the virus. Front Aging Neurosci *6*, 202. 10.3389/fnagi.2014.00202.

13. Protto, V., Marcocci, M.E., Miteva, M.T., Piacentini, R., Li Puma, D.D., Grassi, C., Palamara, A.T., and De Chiara, G. (2022). Role of HSV-1 in Alzheimer's disease pathogenesis: A challenge for novel preventive/therapeutic strategies. Curr Opin Pharmacol *63*, 102200. 10.1016/j.coph.2022.102200.

14. Feng, S., Liu, Y., Zhou, Y., Shu, Z., Cheng, Z., Brenner, C., and Feng, P. (2023). Mechanistic insights into the role of herpes simplex virus 1 in Alzheimer's disease. Front Aging Neurosci *15*, 1245904. 10.3389/fnagi.2023.1245904.

15. Chew, H., Solomon, V.A., and Fonteh, A.N. (2020). Involvement of Lipids in Alzheimer's Disease Pathology and Potential Therapies. Front Physiol *11*, 598. 10.3389/fphys.2020.00598.

16. Kosicek, M., and Hecimovic, S. (2013). Phospholipids and Alzheimer's disease: alterations, mechanisms and potential biomarkers. Int J Mol Sci *14*, 1310–1322. 10.3390/ijms14011310.

17. Ates, G., Goldberg, J., Currais, A., and Maher, P. (2020). CMS121, a fatty acid synthase inhibitor, protects against excess lipid peroxidation and inflammation and alleviates cognitive loss in a transgenic mouse model of Alzheimer's disease. Redox Biol *36*, 101648. 10.1016/j.redox.2020.101648.

18. Chen, V.C.-H., Wu, S.-I., Huang, K.-Y., Yang, Y.-H., Kuo, T.-Y., Liang, H.-Y., Huang, K.-L., and Gossop, M. (2018). Herpes Zoster and Dementia: A Nationwide Population-Based Cohort Study. J Clin Psychiatry *79*, 16m11312. 10.4088/JCP.16m11312.

19. Tzeng, N.-S., Chung, C.-H., Lin, F.-H., Chiang, C.-P., Yeh, C.-B., Huang, S.-Y., Lu, R.-B., Chang, H.-A., Kao, Y.-C., Yeh, H.-W., et al. (2018). Anti-herpetic Medications and Reduced Risk of Dementia in Patients with Herpes Simplex Virus Infections-a Nationwide, Population-Based Cohort Study in Taiwan. Neurotherapeutics *15*, 417–429. 10.1007/s13311-018-0611-x.

20. Gao, Y., Hu, J.-H., Liang, X.-D., Chen, J., Liu, C.-C., Liu, Y.-Y., Cheng, Y., Go, Y.Y., and Zhou, B. (2021). Curcumin inhibits classical swine fever virus replication by interfering with lipid metabolism. Vet Microbiol *259*, 109152. 10.1016/j.vetmic.2021.109152.

21. Aweya, J.J., Zheng, X., Zheng, Z., Wang, W., Fan, J., Yao, D., Li, S., and Zhang, Y. (2020). The sterol regulatory element binding protein homolog of Penaeus vannamei modulates fatty acid metabolism and immune response. Biochim Biophys Acta Mol Cell Biol Lipids *1865*, 158757. 10.1016/j.bbalip.2020.158757.

22. Shipley, M.M., Mangold, C.A., Kuny, C.V., and Szpara, M.L. (2017). Differentiated Human SH-SY5Y Cells Provide a Reductionist Model of Herpes Simplex Virus 1 Neurotropism. J Virol *91*, e00958-17. 10.1128/JVI.00958-17.

23. Iki, S., Yokota, S., Okabayashi, T., Yokosawa, N., Nagata, K., and Fujii, N. (2005). Serum-dependent expression of promyelocytic leukemia protein suppresses propagation of influenza virus. Virology *343*, 106–115. 10.1016/j.virol.2005.08.010.

24. Quinteros, J.A., Browning, G.F., Noormohammadi, A.H., Stevenson, M.A., Coppo, M.J.C., Loncoman, C.A., Ficorilli, N., Lee, S.-W., and Diaz-Méndez, A. (2021). Serum-free medium increases the replication rate of the avian coronavirus infectious bronchitis virus in chicken embryo kidney cells. Preprint at bioRxiv, 10.1101/2021.04.30.442100 10.1101/2021.04.30.442100.

25. Xu, S., Jay, A., Brunaldi, K., Huang, N., and Hamilton, J.A. (2013). CD36 enhances fatty acid uptake by increasing the rate of intracellular esterification but not transport across the plasma membrane. Biochemistry *52*, 7254–7261. 10.1021/bi400914c.

26. Kuda, O., Pietka, T.A., Demianova, Z., Kudova, E., Cvacka, J., Kopecky, J., and Abumrad, N.A. (2013). Sulfo-N-succinimidyl oleate (SSO) inhibits fatty acid uptake and signaling for intracellular calcium via binding CD36 lysine 164: SSO also inhibits oxidized low density lipoprotein uptake by macrophages. J Biol Chem *288*, 15547–15555. 10.1074/jbc.M113.473298.

27. Currais, A., Prior, M., Dargusch, R., Armando, A., Ehren, J., Schubert, D., Quehenberger, O., and Maher, P. (2014). Modulation of p25 and inflammatory pathways by fisetin maintains cognitive function in Alzheimer's disease transgenic mice. Aging Cell *13*, 379–390. 10.1111/acel.12185.

28. Parisi, L.R., Li, N., and Atilla-Gokcumen, G.E. (2017). Very Long Chain Fatty Acids Are Functionally Involved in Necroptosis. Cell Chem Biol *24*, 1445-1454.e8. 10.1016/j.chembiol.2017.08.026.

29. Menendez, J.A., and Lupu, R. (2017). Fatty acid synthase (FASN) as a therapeutic target in breast cancer. Expert Opin Ther Targets *21*, 1001–1016. 10.1080/14728222.2017.1381087.

30. Yoshii, Y., Furukawa, T., Oyama, N., Hasegawa, Y., Kiyono, Y., Nishii, R., Waki, A., Tsuji, A.B., Sogawa, C., Wakizaka, H., et al. (2013). Fatty acid synthase is a key target in multiple essential tumor functions of prostate cancer: uptake of radiolabeled acetate as a predictor of the targeted therapy outcome. PLoS One *8*, e64570. 10.1371/journal.pone.0064570.

31. Angeles, T.S., and Hudkins, R.L. (2016). Recent advances in targeting the fatty acid biosynthetic pathway using fatty acid synthase inhibitors. Expert Opin Drug Discov *11*, 1187–1199. 10.1080/17460441.2016.1245286.

32. Buckley, D., Duke, G., Heuer, T.S., O'Farrell, M., Wagman, A.S., McCulloch, W., and Kemble, G. (2017). Fatty acid synthase - Modern tumor cell biology insights into a classical oncology target. Pharmacol Ther *177*, 23–31. 10.1016/j.pharmthera.2017.02.021.

33. Khan, M.A., Khan, Z.A., Shoeb, F., Fatima, G., Khan, R.H., and Khan, M.M. (2023). Role of de novo lipogenesis in inflammation and insulin resistance in Alzheimer's disease. Int J Biol Macromol *242*, 124859. 10.1016/j.ijbiomac.2023.124859.

34. Qian, X., Song, H., and Ming, G.-L. (2019). Brain organoids: advances, applications and challenges. Development *146*, dev166074. 10.1242/dev.166074.

35. Biolatti, M., Blangetti, M., D'Arrigo, G., Spyrakis, F., Cappello, P., Albano, C., Ravanini, P., Landolfo, S., De Andrea, M., Prandi, C., et al. (2020). Strigolactone Analogs Are Promising Antiviral Agents for the Treatment of Human Cytomegalovirus Infection. Microorganisms *8*. 10.3390/microorganisms8050703.

36. Griffante, G., Hewelt-Belka, W., Albano, C., Gugliesi, F., Pasquero, S., Castillo Pacheco, S.F., Bajetto, G., Porporato, P.E., Mina, E., Vallino, M., et al. IFI16 Impacts Metabolic Reprogramming during Human Cytomegalovirus Infection. mBio *0*, e00435-22. 10.1128/mbio.00435-22.

37. Toscani, A., Denaro, R., Pacheco, S.F.C., Biolatti, M., Anselmi, S., Dell'Oste, V., and Castagnolo, D. (2021). Synthesis and Biological Evaluation of Amidinourea Derivatives against Herpes Simplex Viruses. Molecules *26*, 4927. 10.3390/molecules26164927.

38. Griffante, G., Gugliesi, F., Pasquero, S., Dell'Oste, V., Biolatti, M., Salinger, A.J., Mondal, S., Thompson, P.R., Weerapana, E., Lebbink, R.J., et al. (2021). Human cytomegalovirus-induced host protein citrullination is crucial for viral replication. Nat Commun *12*, 3910. 10.1038/s41467-021-24178-6.

39. Liebisch, G., Fahy, E., Aoki, J., Dennis, E.A., Durand, T., Ejsing, C.S., Fedorova, M., Feussner, I., Griffiths, W.J., Köfeler, H., et al. (2020). Update on LIPID MAPS classification, nomenclature, and shorthand notation for MS-derived lipid structures. J Lipid Res *61*, 1539–1555. 10.1194/jlr.S120001025.

40. Cairns, D.M., Itzhaki, R.F., and Kaplan, D.L. (2022). Potential Involvement of Varicella Zoster Virus in Alzheimer's Disease via Reactivation of Quiescent Herpes Simplex Virus Type 1. J Alzheimers Dis *88*, 1189–1200. 10.3233/JAD-220287.

41. Cairns, D.M., Rouleau, N., Parker, R.N., Walsh, K.G., Gehrke, L., and Kaplan, D.L. (2020). A 3D human brain-like tissue model of herpes-induced Alzheimer's disease. Sci Adv *6*, eaay8828. 10.1126/sciadv.aay8828.

Check for updates

PAD-mediated citrullination is a novel candidate diagnostic marker and druggable target for HPV-associated cervical cancer

Camilla Albano[1], Matteo Biolatti[1], Jasenka Mazibrada[2],
Selina Pasquero[1], Francesca Gugliesi[1], Irene Lo Cigno[3],
Federica Calati[3], Greta Bajetto[1,3,4], Giuseppe Riva[5],
Gloria Griffante[6,7], Santo Landolfo[1], Marisa Gariglio[3],
Marco De Andrea[1,4] and Valentina Dell'Oste[1]*

[1]Department of Public Health and Pediatric Sciences, University of Turin, Turin, Italy, [2]Department of
Cellular Pathology, The Cotman Centre Norfolk and Norwich University Hospital, Norwich, United
Kingdom, [3]Department of Translational Medicine, University of Eastern Piedmont, Novara, Italy,
[4]Center for Translational Research on Autoimmune and Allergic Disease-CAAD, Novara, Italy,
[5]Department of Surgical Sciences, University of Turin, Turin, Italy, [6]IIGM Foundation – Italian Institute
for Genomic Medicine, Turin, Italy, [7]Candiolo Cancer Institute, FPO-IRCCS, Turin, Italy

Citrullination is an emerging post-translational modification catalyzed by peptidyl-arginine deiminases (PADs) that convert peptidyl-arginine into peptidyl-citrulline. In humans, the PAD family consists of five isozymes (PADs 1-4, 6) involved in multiple diseases, including cancer. Given that high-risk (hr) human papillomaviruses (HPVs) are the etiological agents of cervical cancer, in this study, we sought to determine whether PAD-mediated protein citrullination would play a functional role in the HPV-driven transformation of epithelial cells. Here we show that both total protein citrullination and PAD4 expression levels are significantly associated with cervical cancer progression. Specifically, epithelial immunostaining for PAD4 revealed an increasingly higher histoscore from low-grade (CIN1) to high-grade (CIN2, CIN3) cervical intraepithelial neoplasia, and invasive squamous cell carcinoma (SCC) lesions, raising the attractive possibility that PAD4 may be used as tumor staging markers. Furthermore, taking advantage of the epidermoid cervical cancer cell line CaSki, which harbors multiple copies of the integrated HPV16 genome, we show that the expression of E6 and E7 HPV oncoproteins is impaired by treatment with the pharmacological pan-PAD inhibitor BB-Cl-amidine. Consistently, p53 and p21, two targets of HPV oncoproteins, are upregulated by the PAD inhibitor, which undergoes cell growth arrest and apoptosis. Altogether, these findings highlight a novel mechanism by which hrHPVs alter host regulatory pathways involved in cell cycle and survival to gain viral fitness, raising the possibility that PADs may represent an attractive target for developing novel host-targeting antivirals effective in preventing cervical cancer progression.

KEYWORDS

human papillomaviruses, cervical cancer, citrullination, peptidylarginine deiminases, BB-cl-Amidine

1 Introduction

Human papillomaviruses (HPVs) are a major cause of human cancer, especially cervical cancer (Schiffman et al., 2016; McBride, 2022). Indeed, high-risk (hr) HPVs, in particular HPV16, are the etiological agents of almost 80% of all cervical cancer cases (de Villiers, 2013; Van Doorslaer et al., 2017). The development of HPV-associated cancers relies on the expression of two oncoproteins, E6 and E7, which are the only viral gene products consistently found in these tumors (Hoppe-Seyler et al., 2018; Scarth et al., 2021). Transformative capabilities have been demonstrated also for the HPV16 E5 oncoprotein. Nevertheless, the precise molecular mechanisms underlying its activity remain poorly understood. Unlike E6 and E7, the integration of episomal HPV DNA into the cellular genome results in the loss of the E5 open reading frame. Recent studies highlighted that E5 influences the initial phases of the transformation process rather than the later steps of malignant progression. It accomplishes this by modulating cellular processes like proliferation, differentiation, apoptosis, and energy metabolism through interactions with cell growth factor receptors and other cellular proteins (Gutierrez-Xicotencatl et al., 2021). As E6 and E7 do not possess intrinsic enzymatic activities, their transforming activity is thought to be predominantly exerted through direct or indirect interactions with cellular proteins, which ultimately favors the formation of the tumor environment (Mittal and Banks, 2017; Rasi Bonab et al., 2021). Recent evidence has shown that besides acting through the tumor suppressors p53 and retinoblastoma protein (pRb) (Vats et al., 2021), respectively, E6 and E7 can drive tumorigenesis through chromatin remodeling by altering the expression or the enzymatic activity of several epigenetic modifiers, such as histone deacetylases, histone demethylases, histone acetyltransferases, and histone methyltransferases (Durzynska et al., 2017; Burley et al., 2020). Concomitantly, HPVs have evolved strategies to subvert antiviral immunity and hamper cancer immunosurveillance, thereby favoring carcinogenesis (Zhou et al., 2019; Lo Cigno et al., 2020a, 2023; Girone et al., 2023). Even though the widespread implementation of vaccines has clear potential (Yousefi et al., 2021), no effective strategy for the treatment of low- or high-grade cervical lesions other than surgery is currently available (Zheng et al., 2022).

Citrullination, also called deimination, is a post-translational conversion of peptidyl-arginine to the non-genetically encoded amino acid peptidyl-citrulline, catalyzed by Ca^{2+}-dependent, phylogenetically conserved, peptidyl-arginine deiminase (PAD) family of enzymes (Gudmann et al., 2015; Mondal and Thompson, 2021; Yu and Proost, 2022). In humans, the PAD family is composed of five highly-homologous isozymes (i.e., PADs 1-4 and 6), with different tissue-specific expression and substrate specificities (Bicker and Thompson, 2013; Witalison et al., 2015). Citrullination is particularly relevant to many human diseases, such as rheumatoid arthritis (Darrah and Andrade, 2018; Alghamdi and Redwan, 2021; Catrina et al., 2021), systemic lupus erythematosus (Singh et al., 2011), Alzheimer's disease (Ishigami and Maruyama, 2010), Parkinson's disease (Sancandi et al., 2020), and multiple sclerosis (Tu et al., 2016; Bruggeman et al., 2021). Higher expression of PAD genes has also been observed in various malignant tumors (Yuzhalin, 2019; Beato and Sharma, 2020; Zhu et al., 2021), suggesting their involvement in cancer pathogenesis.

A direct correlation between citrullination and viral infections has only recently emerged (Struyf et al., 2009; Muraro et al., 2018; Casanova et al., 2020). In this context, our group has recently unveiled the role of citrullination in promoting human cytomegalovirus (HCMV) and herpes simplex virus 1 (HSV-1) infection through the deimination of several cellular proteins, which promotes viral fitness (Griffante et al., 2021; Pasquero et al., 2023).

PADs are also involved in human epidermal keratinization and morphogenesis as well as skin tumorigenesis, processes closely linked to HPV transformation (Ying et al., 2009). Indeed, PAD2 overexpression in transgenic mice resulted in spontaneous skin neoplasia (Mohanan et al., 2017), and antibodies to citrullinated HPV-47 $E2_{345-362}$ protein were found in patients affected by rheumatoid arthritis (Shi et al., 2008). Finally, *PADI4* levels were found to be significantly increased in the blood of patients with cervical cancer (Chang et al., 2009). However, how HPV induces protein citrullination in the host and whether citrullinated proteins can support viral replication in the host is currently unknown.

To gain more insights into the mechanisms of citrullination favoring disease progression and to identify more effective druggable targets and suitable biomarkers, the present study aimed to define the impact of PAD-mediated citrullination on HPV transformation. Our results reveal a significant association between PAD4 expression and cervical cancer progression. Accordingly, the pan-PAD-inhibitor BB-Cl-amidine (Ledet et al., 2018) downregulates the expression of HPV16 E6/E7, indicating that the process driven by PADs could be involved in HPV pathogenesis.

2 Materials and methods

2.1 Patients' samples and data

Tissue sections were obtained from 100 formalin-fixed paraffin-embedded (FFPE) blocks, previously collected from surgically treated cervical lesions, and stored in the Norwich University Hospital material archives. The cervical lesions were obtained from high-risk HPV-positive women with abnormal cytology on cervical screening. In cases of high-grade (HG) cervical intraepithelial neoplasia (CIN)—at different stages (see below)—or invasive squamous cell carcinoma (SCC), tumor specimens were obtained by large loop excision of the transformation zone (LLETZ) or by hysterectomy. CIN is classified on a scale from one to three. CIN1 refers to abnormal cells affecting about one-third of the thickness of the epithelium, whereas CIN2 and 3 define abnormal cells present in one- to two-thirds or more than two-thirds of the epithelium, respectively (Table 1).

All procedures were performed in accordance with the ethical standards of the institutional Research Committee and with the 1964 Helsinki Declaration and its later amendments or comparable ethical standards.

All human tissues derived from biopsied cervical lesions were classified according to the 8th Edition of the American Joint Committee on Cancer (AJCC-TNM) Staging Manual (TNM8) (Brierley et al., 2017).

Hematoxylin and eosin (H&E)-stained slides were reviewed to confirm the diagnosis and to assess the cytological and histomorphological features of each specimen.

2.2 HPV detection

HPV detection was performed using the cobas® HPV Test (Roche Molecular Systems). Positive results were subcategorized into HPV16, HPV18, and other hrHPV types. p16 was used as a surrogate for hrHPV infection (Table 1).

2.3 Immunohistochemistry

Serial 5-μm sections from FFPE tissues were processed using the automated immunostainer Leica Bond III (Leica Biosystems). The primary antibodies employed are reported in Supplementary Table S1. Immunohistochemical expression of PAD4, PAD2, and anti-citrulline was evaluated by histo (H) score. For each histological section, the staining intensity was scored as 0 (negative), 1 (weak), 2 (moderate), and 3 (strong). The H-score was calculated by multiplying the intensity score (0-3) and the percentage of positive cells (0-100%), with a maximum of 300.

2.4 Cell cultures

CaSki cells (ATCC CRL-1550™) were cultured in RPMI-1640 medium and HeLa cells (ATCC CCL-2™) in Dulbecco's Modified Eagle's medium, both supplemented with 10% heat-inactivated fetal bovine serum (FBS), 2 mM glutamine, 1 mM sodium pyruvate, 100 U/mL penicillin, and 100 μg/mL streptomycin sulfate (Sigma-Aldrich). HPV-negative normal oral keratinocytes (NOKs) were kindly provided by Frank Rösl (Germany) and were cultured as previously described (Yang et al., 2019).

2.5 Transfection

CaSki and HeLa cells were transiently transfected with small interfering RNAs (siRNAs) using a Neon™ Transfection System (Life Technologies) according to the manufacturer's instructions (1005 V, 35 ms pulse width, two impulses). The following siRNAs were used: control siRNA (siCTRL; 1027292) was purchased from Qiagen; siRNAs against HPV16 E6/E7#1, HPV16 E6/E7#2, HPV18 E6/E7#1, and HPV18 E6/E7#2 were synthesized by Eurofins Genomics. The indicated siRNAs were previously characterized (Lo Cigno et al., 2020b), and the specific sequences are reported in Supplementary Table S2.

2.6 Compounds

BB-Cl-amidine (BB-Cl-A; HY-111347A) (Ledet et al., 2018) was purchased by MedChemExpress and dissolved in dimethyl sulfoxide (DMSO; Sigma-Aldrich) at stock concentrations of 25 mM.

2.7 Cell viability assay

CaSki viability upon exposure to increasing concentrations of BB-Cl-A or DMSO was determined by 3-(4,5-dimethylthiazol-2-yl)-2,5diphenyltetrazolium bromide (MTT) method (Toscani et al., 2021).

2.8 Quantitative nucleic acid analysis

Total RNA was extracted using TRI Reagent (Sigma-Aldrich), and 1 μg was retrotranscribed using the Revert-Aid H-Minus First Strand cDNA Synthesis Kit (Thermo Fisher Scientific), according to the manufacturer's instructions. Comparison of mRNA expression between samples was performed by SYBR green-based RT-qPCR using Mx3000P apparatus (Stratagene). The housekeeping gene glyceraldehyde 3-phosphate dehydrogenase (GAPDH) was used to normalize for variation in cDNA levels. The primer sequences used are reported in Supplementary Table S2.

2.9 Western blot analysis

Protein extracts were prepared in RIPA buffer and subjected to immunoblotting. The primary antibodies used are reported in Supplementary Table S1. Scanning densitometry was performed using Image Lab (version 6.0.1; Bio-Rad).

2.10 Detection of citrullination with rhodamine–phenylglyoxal

Equal amounts of protein were diluted with 80% trichloroacetic acid and incubated with Rh–PG (final concentration 0.1 mM; Cayman Chemical) for 30 min. The reaction was quenched with 100 mM L-citrulline (Sigma-Aldrich), centrifuged at 21,100×g for 10 min, washed with ice-cold acetone, resuspended in PBS supplemented with L-arginine and analyzed through gel electrophoresis. Gels were imaged (excitation = 532 nm, emission = 580 nm) using a ChemiDoc MP Imaging System (Bio-Rad Laboratories), stained with brilliant blue G-colloidal solution (Sigma-Aldrich).

2.11 Cell cycle analysis

CaSki cells were seeded in 6-well plates and treated with BB-Cl-A (3 μM) for 24 or 48 h. After treatment, cells were pelleted down and fixed with 70% methanol for 30 min at 4°C. After washing with PBS twice, cells were incubated with a DNA staining solution consisting of propidium iodide (PI; Sigma-Aldrich) and RNase (Merck Millipore) for 15 min at 37°C in the dark. The proportion

TABLE 1 Patient characteristics.

Lesions	Age (years)	Menopause	hrHPVs		p16		Follow-up (After 2 years)
			Positive	Negative	Positive	Negative	
NILM (n=20)	Mean=39.4 Range=22-83	3/20 (15%)	9/17 (52.9%) HPV16: 2/17 (11.8%) HPV18: 3/17 (17.6%) Others: 4/17 (23.5%)	8/17 (47.1%)	2/19 (10.5%)	17/19 (89.5%)	N.a.
CIN1 (n=20)	Mean=37.5 Range=25-62	2/19 (10.5%)	20/20 (100%) HPV16: 2/20 (10%) HPV18: 2/20 (10%) Others: 16/20 (80%)	0/20 (0%)	4/20 (20%)	16/20 (80%)	2/18 (11.1%) hrHPV persistence (no CIN)
CIN2 (n=20)	Mean=31 Range=24-44	0/20 (0%)	20/20 (100%) HPV16: 4/20 (20%) HPV18: 1/20 (5%) Others: 15/20 (75%)	0/20 (0%)	18/20 (90%)	2/20 (10%)	2/20 (10%) hrHPV persistence (no CIN)
CIN3 (n=20)	Mean=34.3 Range=24-53	2/20 (10%)	20/20 (100%) HPV16: 7/20 (35%) HPV18: 0/20 (0%) Others: 13/20 (65%)	0/20 (0%)	20/20 (100%)	0/20 (0%)	19/19 (100%) hrHPV negative
SCC (n=20)	Mean=42.8 Range=25-63	5/18 (27.8%)	18/18 (100%) HPV16: 6/18 (33.3%) HPV18: 4/18 (22.2%) Others: 8/18 (44.4%)	0/18 (0%)	20/20 (100%)	0/20 (0%)	1/14 (7.1%) Recurrence after 2 years

of cells in each phase of the cell cycle was determined by DNA content stained with PI using a BD FACSCanto II flow cytometer (BD Biosciences). Data obtained were analyzed with FlowJo software (BD Biosciences).

2.12 Apoptosis detection

To distinguish apoptotic from necrotic cells, double staining was performed for exposed phosphatidylserine and PI exclusion using the annexin V-FITC Apoptosis Detection Kit (Calbiochem). Experiments were performed according to the manufacturer's instructions. Briefly, CaSki cells were seeded in 6-well plates and treated with BB-Cl-A (3 µM) for 24 or 48 h. After treatment, cells were washed with PBS twice, trypsinized, and then resuspended in a binding buffer (10 mM HEPES/NaOH, pH 7.4, 140 mM NaCl, 2.5 mM $CaCl_2$). Annexin V-FITC was added to a final concentration of 100 ng/mL, and the cells were incubated in the dark for 10 min, then washed again in PBS, and resuspended in 300 µL of the binding buffer. In total, 40 µg/mL of PI was added to each sample before the flow cytometric analyses. Cells were analyzed using a BD FACSCanto II flow cytometer (BD Biosciences). Data obtained were analyzed with FlowJo software (BD Biosciences). Unstained cells and cells only stained with annexin V-FITC or PI were used as controls to establish compensation and quadrants. Cells were gated according to their light-scatter properties to exclude cell debris.

2.13 Statistical analysis

All statistical tests were performed using GraphPad Prism version 7.04 for Windows (GraphPad Software). Data are presented as means ± SEM or medians ± interquartile. Means were compared using an unpaired t-test, meanwhile, medians were compared using a one-way analysis of variance (ANOVA) with Bonferroni's post-tests. The two-tailed Pearson correlation was employed to assess the correlation between PAD4 and citrulline expression in immunohistochemistry. Differences were considered statistically significant at $P < 0.05$ (*, $P < 0.05$; **, $P < 0.01$; ***, $P < 0.001$).

3 Results

3.1 Enhanced total protein citrullination and PAD4 expression in cervical intraepithelial neoplasia and invasive squamous cell carcinoma

To evaluate the role of citrullination in the context of hrHPV-related lesions, we assessed the citrullination profiles of FFPE biopsies from samples negative for intraepithelial lesion or malignancy (NILM) vs. cervical intraepithelial neoplasia (CIN) at different stages — from CIN (CIN1 > CIN2 > CIN3, see Materials and Methods) to invasive SCC. Information about patients' age, menopausal status (yes/no), and follow-up is presented in Table 1. The mean age of the cohort was 47

years, ranging from 22 to 63 years, with 12.2% of women in a menopausal state. HrHPV and p16 positivity are also reported and agree with previous findings (Kombe Kombe et al., 2021; Shafique et al., 2023). A recurrence of carcinoma has been reported after 2 years in 1 out of 14 SCC cases with available follow-up data.

As shown in Figure 1A and Supplementary Table S3, disease progression was paralleled by a significant increase in total protein citrullination levels in cells with aberrant proliferative capacity, and this effect is more pronounced in CIN2 and CIN3 lesions, while in the SCC group, there was significant variability in citrulline staining. Specifically, keratinocytes with high and abnormal levels of citrullinated proteins in the cytoplasm were localized throughout the mucosal layers, whereas in the normal epithelium, they were predominantly found in the basal and parabasal layers (Supplementary Table S3).

Since PADs are the enzymes catalyzing citrullination, we next sought to determine their expression according to tumor stage. To rule out bias due to allelic loss in tumors, we first examined PAD expression in a squamous cervical carcinoma data set curated by TCGA (Gao et al., 2013; Ciriello et al., 2015). We found the PAD genomes rarely mutated—less than 1.2% out of 278 tumors, considering all PAD isoforms (Figure 1B)—indicating that loss of PAD expression is a rare event.

Next, we assessed cervical cancer *vs.* NILM for protein expression levels of PADs 2 and 4, the two PAD isozymes most broadly expressed in human cancer (Yuzhalin, 2019; Sarnik and Makowska, 2022). In NILM, PAD4 expression was limited to the nuclei in basal and parabasal layers of the squamous epithelium and in sparse stromal and inflammatory cells within the stromal compartment (Figure 1C). On the other hand, PAD4 staining of both the atypical squamous epithelium and the stromal compartment significantly increased as the cancer progressed to more advanced stages (Figure 1C). Interestingly, this increase was significantly correlated with enhanced citrullinated protein expression levels in CIN2 and CIN3 lesions but not CIN1 and SCC (Supplementary Table S3). No signal was observed in negative controls that were incubated with either the primary or secondary antibody alone (data not shown). Of note, koilocytes in low-grade CIN exhibited a very weak PAD4 immunoreactivity in comparison with high-grade lesions, which suggests differential expression of this marker according to the integration status of HPV in squamous cells. Moreover, mature squamous cells in the upper epithelial layers were PAD4 negative, which implies that PAD4 expression can be detected only in immature squamous phenotypes.

Collectively, these results argue in favor of PAD4-mediated citrullination as a critical event in cervical tumorigenesis. In contrast, PAD2, whose expression is restricted to the glandular epithelium and absent in the squamous epithelium in both normal mucosa and hrHPV-related lesions (Supplementary Figure S1), does not seem to be involved in disease progression.

3.2 Impact of hrHPV E6/E7 on PAD expression profile

To investigate whether HPV trigger PAD-mediated citrullination to promote viral fitness, we first evaluate the protein citrullination profile in CaSki cells, which contain about 600 copies of HPV16

genomes per cell (Mincheva et al., 1987). Protein lysates obtained from either siRNA E6/E7- or siRNA CTRL-transfected CaSki were exposed to the citrulline-specific probe Rh-PG (Bicker et al., 2012). Even though the expression of the viral proteins was almost completely suppressed upon gene silencing (Figure 2A), as demonstrated by immunoblotting with antibodies raised against HPV E6 and E7, we did not notice any significant differences between the citrullination profiles of cells lacking E6 and E7 (siE6/E7) and their controls (siCTRL) (Figure 2B, left panel), neither the overall amount of proteins was modified (Figure 2B, middle panel). The same results were obtained when membranes were probed with an anti-cyclic citrullinated peptide (CCP) antibody (Figure 2B, right panel). We detected the same citrullination pattern in HeLa cells transfected with siRNA E6/E7 or siRNA CTRL (Supplementary Figures S2A, B), confirming that the overall citrullination profile is not markedly affected by the absence of hrHPV E6/E7. Furthermore, RT-qPCR analysis of RNAs from the same cells revealed that *PADI* genes were all expressed in CaSki and HeLa, but not profoundly modulated by E6 and E7 compared to the controls (Figure 2C, Supplementary Figure S2C). When we analyzed PAD protein expression, we only observed a slight downregulation of PAD2 in CaSki and HeLa cells lacking E6 and E7 (24% and 22%, respectively), while PAD3 and PAD4 were not significantly modulated. Other PAD isoforms (PAD1 and 6) were expressed at undetectable levels in CaSki and HeLa cells and did not vary upon E6/7 gene silencing (Figure 2D, Supplementary Figure S2D).

3.3 The pan-PAD inhibitor BB-Cl-amidine subverts hrHPV E6/E7-related pathways

To conclusively elucidate the impact of PAD-mediated citrullination on hrHPV pathogenesis, we took advantage of the cell-permeable pan-PAD inhibitor BB-Cl-amidine (BB-Cl-A). However, before assessing BB-Cl-A activity on CaSki cells, we performed a standard MTT viability assay to rule out the possibility that the drug may have cytotoxic effects. Indeed, our screening indicated that the cytotoxicity of BB-Cl-A was low or undetectable at concentrations of up to 3 μM, as ~90% of the cells were viable after 48 h of treatment (Figure 3A).

We then evaluated E6 and E7 protein expression levels in CaSki cells treated or not with BB-Cl-A. As shown in Figure 3B, we observed a dramatic downregulation of both E6 and E7 expression in BB-Cl-A-treated cells, with a more pronounced effect after 24 h. Conversely, an expected increase in p53 protein expression, a known target of E6 (Mittal and Banks, 2017), was detected at 24 and 48 h post-BB-Cl-A treatment (15 and 2.4 folds at 24 and 48 h *vs.* vehicle control, respectively). Fittingly, at the same time points, we also recorded a 9.2 (24 h) and 4.5 (48 h) fold increase of the cyclin-dependent kinase inhibitor p21 (Harris and Levine, 2005), a p53, and E7 target gene. Overall, these results demonstrate that the inhibitory activity of the BB-Cl-A compound against hrHPV E6 and E7 is associated with the upregulation of p53 and p21 expression. This effect is specific, as p53 and p21 were not modulated by BB-Cl-A in HPV-negative NOKs (Supplementary Figure S3).

Finally, since p53 target genes, such as p21, are involved in the regulation of cell cycle progression (Xiong et al., 1993), we sought to
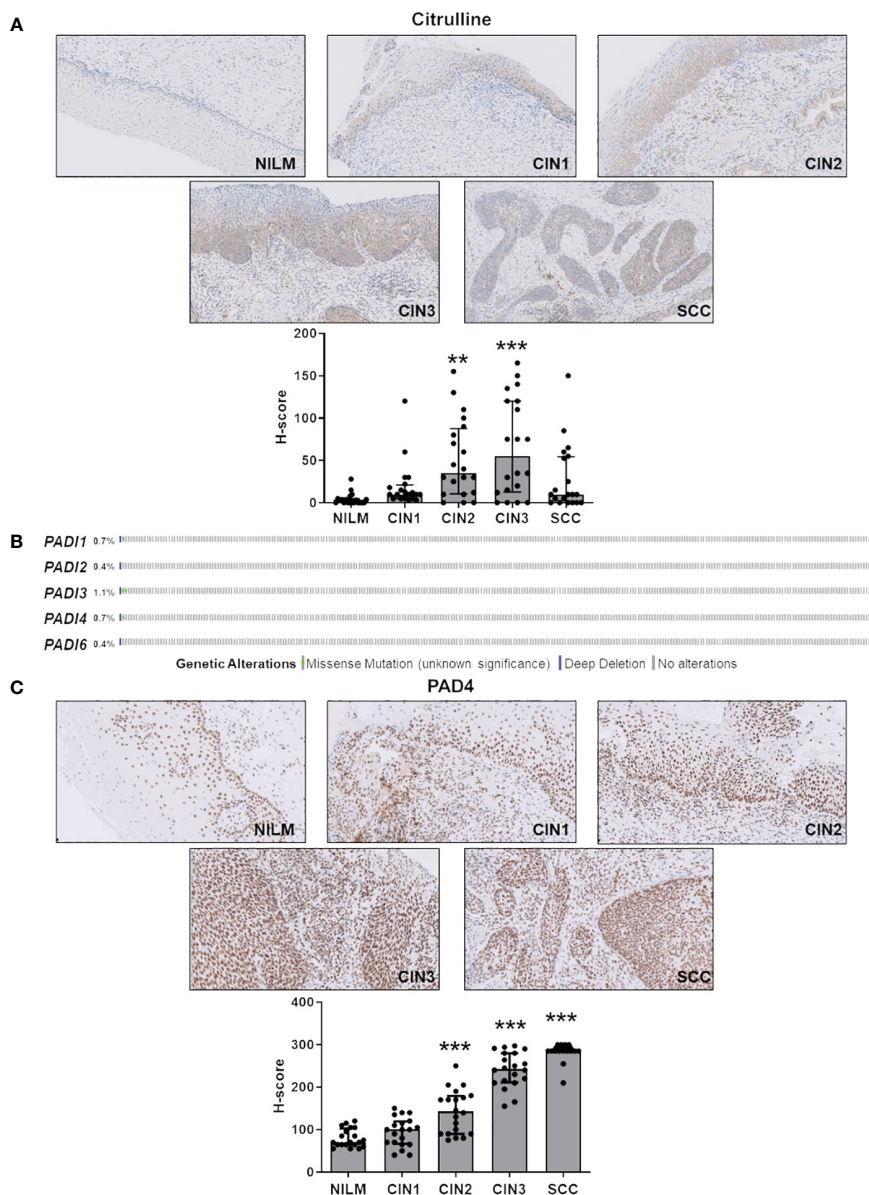
FIGURE 1

Citrulline and PAD4 expression in CINs and SCC. **(A)** Citrulline immunohistochemical photomicrographs of representative biopsies of mucosa negative for intraepithelial lesion or malignancy (NILM) and different stages of cervical carcinogenesis (CIN1, CIN2, CIN3, and SCC). Hematoxylin was used for counterstaining. Original magnification: 20X. In the lower histogram, the collective presentation of quantified anti-citrulline IHC score in NILM (n=20), CIN1 (n=20), CIN2 (n=20), CIN3 (n=20), and SCC (n=20). The H-score median and interquartile range for each group are shown. Medians were compared using a one-way analysis of variance (ANOVA) with Bonferroni's post-tests. $P < 0.05$ (**, $P < 0.01$; ***, $P < 0.001$). **(B)** TCGA-curated clinical data set of cervical squamous cell carcinoma (n=278) was assessed for samples harboring genomic *PADI* gene loss (solid blue) and/or missense mutations (green dot). **(C)** PAD4 immunohistochemical photomicrographs of representative biopsies of normal mucosa and different stages of cervical carcinogenesis as above. Hematoxylin was used for counterstaining. Original magnification: 20X. In the lower histogram, the collective presentation of quantified PAD4 IHC scores in NILM (n=20), CIN1 (n=20), CIN2 (n=20), CIN3 (n=20), and SCC (n=20). The H-score median and interquartile range for each group are shown. Medians were compared using a one-way analysis of variance (ANOVA) with Bonferroni's post-tests. $P < 0.05$ (**, $P < 0.01$; ***, $P < 0.001$).

determine the effect of BB-Cl-A treatment on the cell cycle. Flow cytometry analyses showed that upon 48 h of treatment, BB-Cl-A significantly increased the population of CaSki cells in the sub-G_0 phase, while decreasing in the G_0-G_1 phase, compared to control, indicating that PAD inhibition leads to cell cycle arrest (Figure 3C). To further strengthen this observation and given that apoptosis is one of the major mechanisms by which hosts evade viral infections, including HPV (Shimada et al., 2020; Gusho and Laimins, 2022), we assessed the

ability of BB-Cl-A to drive cell-death pathways in CaSki cells by dual staining with annexin V and PI. As shown in Figure 3D, at 48 hpt (hours post-treatment), a significant increase in apoptosis (annexin V +/PI−) was detected in cells treated with BB-Cl-A compared to vehicle-treated cells (33.9% *vs.* 12.73%, respectively), while necrosis (annexin V +/PI+) barely occurred in every condition tested.

Altogether, our findings indicate that the inhibition of protein citrullination by BB-Cl-A halts cell cycle progression at the sub-G_0
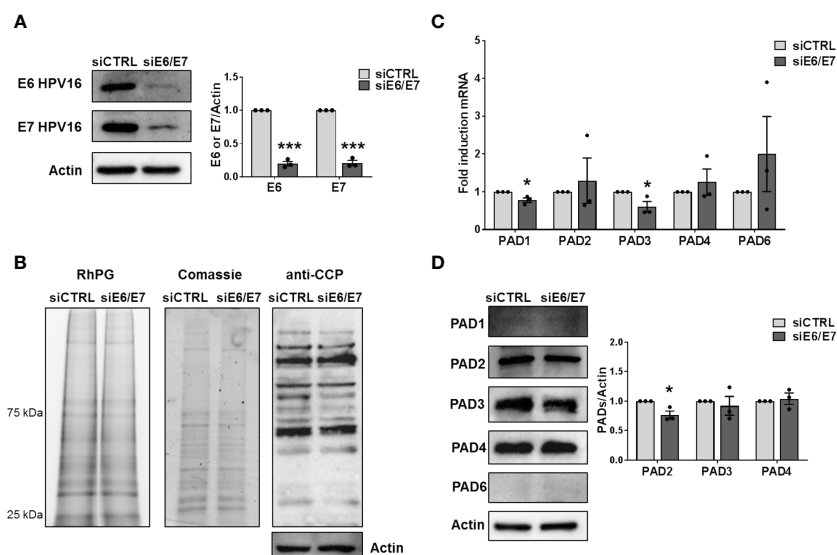
FIGURE 2

Citrullination analysis. **(A)** CaSki cells were transfected with siRNA E6/E7 or siRNA CTRL and processed at 72 h post-transfection. The efficiency of E6 and E7 protein depletion was determined by immunoblotting using antibodies against E6 and E7 and Actin as control. Values are expressed as means $\pm$ SEM (error bars) of three independent experiments. $P < 0.05$ (*, $P < 0.05$; **, $P < 0.01$; ***, $P < 0.001$, unpaired t-test). **(B)** Detection of citrullinated proteins in lysates obtained from siRNA E6/E7- or siRNA CTRL-transfected CaSki cells at 72 h post-transfection. *Left panels:* lysates were exposed to an Rh-PG citrulline-specific probe and subjected to gel electrophoresis to detect total proteins. Equal loading was assessed by Coomassie blue staining. *Right panel:* the indicated samples were analyzed by immunoblotting, and citrullinated proteins were detected using an anti-CCP antibody and Actin as a loading control. **(C)** mRNA expression levels of *PADI* isoforms by RT-qPCR of siRNA E6/E7- or siRNA CTRL-transfected CaSki cells were normalized to the housekeeping gene GAPDH and expressed as mean fold change $\pm$ SEM over siRNA CTRL. $P < 0.05$ (*, $P < 0.05$; ***, $P < 0.001$, unpaired t-test). **(D)** Western blot analysis of protein lysates from siRNA E6/E7- or siRNA CTRL-transfected CaSki cells using antibodies against PAD1, PAD2, PAD3, PAD4, PAD6, or Actin. One representative blot and densitometric analysis relative to three independent experiments are shown. Values are expressed as mean fold change $\pm$ SEM normalized to Actin. $P < 0.05$ (*, $P < 0.05$; ***, $P < 0.001$, unpaired t-test).

phase and drives CaSki cells to apoptosis, suggesting that BB Cl-A is a promising pharmacological agent to treat HPV-infected cells.

4 Discussion

In the present study, we report for the first time that citrullination plays a role in hrHPV pathogenesis in the context of cervical cancer. Indeed, we find a significant association between the overall citrullination pattern, PAD expression, and cervical cancer progression in a cohort of patients with different stages of cervical lesions. Accordingly, in an *in vitro* model of persistent hrHPV transformation - i.e. CaSki cells - the expression of E6 and E7 HPV oncoproteins is downregulated by the pan-PAD inhibitor BB-Cl-A, followed by robust upregulation of p53 and p21, the main targets of HPV oncoproteins. Conversely, total protein citrullination and PAD expression do not seem to be affected by E6 and E7 expression *in vitro*, in both CaSki and HeLa cells (Supplementary Figure S4).

Increasing evidence is emerging about the relevance of citrullination to human diseases. Indeed, besides the upregulation of PAD isozymes in many autoimmune disorders (Bicker and Thompson, 2013; Bruggeman et al., 2021), recent studies highlighted a modulation of citrullination in the context of viral infections (Griffante et al., 2021; Pasquero et al., 2022, 2022).

Our group has previously shown that HCMV infection induces citrullination in human fibroblasts and that PAD2, the isoform mainly induced upon infection, is essential for HCMV replication

(Griffante et al., 2021). This might represent an alternative strategy for efficient inhibition of HCMV replication even in the presence of drug resistance mechanisms due to viral DNA polymerase mutations. Furthermore, we have recently found the same ability to exploit PAD-mediated citrullination in order to achieve enhanced viral growth in *in vitro* models of β-coronavirus infection, i.e., HCoV-OC43 and SARS-CoV-2 (Pasquero et al., 2022) and HSV-1 replication (Pasquero et al., 2023). Interestingly, we failed to observe a robust modulation of the citrullination profile or PAD expression in the context of hrHPV transformation *in vitro*, even upon silencing the E6 and E7 viral oncoproteins. This could be ascribed to an already mutated cellular phenotype due to HPV integration, with citrullination and PAD expression levels already saturated. As such, it is likely that citrullination was not altered *per se* but might influence cellular pathways linked to HPV-induced transformation. Fittingly, the pan-PAD inhibitor BB-Cl-A impairs E6 and E7 expression. As a consequence, p53 and p21, targeted by E6 and E7, are restored, leading to a sub-G_0 cell cycle block in cells treated with BB-Cl-A and an increased rate of apoptotic cells. The impact of BB-Cl-A is more evident at 24 h, while at 48 h, E7 protein levels increase, albeit remaining significantly downregulated compared to the control. This phenomenon may be attributed to various factors, such as feedback mechanisms, adaptive responses, protein turnover, or alternative regulatory pathways. However, determining these factors precisely extends beyond the scope of the current study. PAD inhibitors have already been successfully employed in preclinical and *in vitro* studies for various
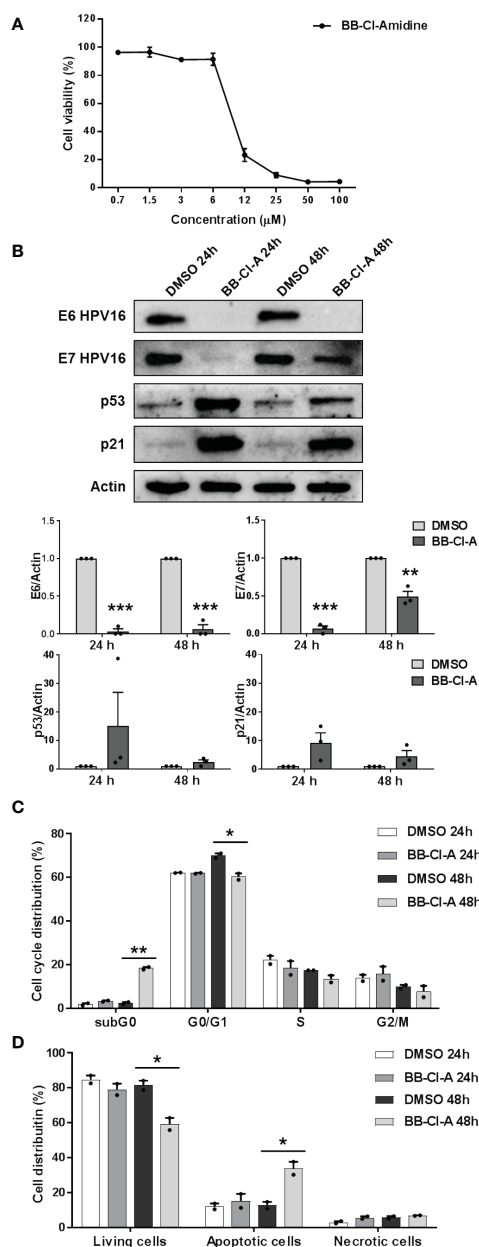
FIGURE 3

Antiviral activity of the pan-PAD inhibitor BB-Cl-amidine against HPV transformation. **(A)** CaSki cells were treated with increasing concentrations of the cell-permeable pan-PAD inhibitor BB-Cl-amidine (BB-Cl-A). At 48 h post-treatment (hpt), the number of viable cells was determined for each BB-Cl-A concentration by MTT. Values are expressed as means $\pm$ SEM (error bars) of three independent experiments. **(B)** Protein lysates from CaSki cells treated with 3 μM BB-Cl-A were subjected to immunoblotting using antibodies against E6, E7, p53, p21, or Actin. One representative blot and predictive densitometric analysis relative to three independent experiments are shown. Values are expressed as means $\pm$ SEM. Differences were considered statistically significant for $P < 0.05$ (*, $P < 0.05$; **, $P < 0.01$; ***, $P < 0.001$, unpaired t-test). **(C)** Cell cycle analysis of BB-Cl-A-treated cells by flow cytometry. CaSki cells were treated with 3 μM of BB-Cl-A or DMSO for 24 and 48 (h) Values were plotted as the percentage of cell distribution across the different cell cycle phases (SubG$_0$, G$_0$/G$_1$, S, and G$_2$/M). Each bar represents the mean of data obtained from two independent experiments. Differences were considered statistically significant for $P < 0.05$ (*, $P < 0.05$; **, $P < 0.01$; ***, $P < 0.001$, unpaired t-test). **(D)** CaSki cells were treated with 3 μM of BB-Cl-A or with equal volumes of DMSO. After 24 and 48 h, cells were processed for Annexin V/propidium iodide (PI) flow cytometric analysis. Annexin−/PI− cells indicated living cells, Annexin+/PI− apoptotic cells, and Annexin+/PI+ necrotic cells. Values were plotted as the percentage of cell distribution across the two different conditions. Fold changes were calculated after the normalization of BB-Cl-A *vs.* DMSO-treated cells. Differences were considered statistically significant for $P < 0.05$ (*, $P < 0.05$, unpaired t-test).

inflammatory conditions, such as arthritis, colitis, and sepsis, showing a good safety profile (Chumanevich et al., 2011; Willis et al., 2011). This represents an important aspect that supports the repurposing of these compounds as antivirals to counteract HPV-related carcinogenesis.

Our findings that citrullinated proteins and PAD4 are overexpressed in HPV-positive cervical cancers support the role of citrullination in HPV transformation, in agreement with the higher expression of *PADI4* genes found in various malignant tumor tissues, as well as in the blood of patients with some cancers (Chang et al., 2009;

Yuzhalin, 2019). Interestingly, we showed that citrulline and PAD4 H-scores correlated significantly in CIN2 and CIN3, while in the carcinoma group, there was significant variability in the expression of citrullinated proteins. This observation is consistent with previous results obtained with lung cancer, demonstrating that citrullination was a less specific marker for the tumor (Baka et al., 2011). Alternatively, we could speculate that even though high levels of PAD4 are detectable in invasive cancer, we do not know whether the protein still retains its enzymatic activity. Interestingly, a single recurrence was observed in a carcinoma with low detectedcitrullinated proteins (H-score 10), suggesting a possible protective role of citrulline during cervical carcinogenesis. Variation in citrullinated protein levels may therefore be used as an adjunctive criterion to predict the biological behavior of tumor in addition to other clinical and surgical criteria (e.g. completeness of excision, stage, grade, age of patients, risk factors, etc). This warrants further studies, however, on a larger number of specimens.

Another evidence of citrullination involvement in HPV-driven carcinogenesis arises from the observation that p53 is strongly upregulated in BB-Cl-A-treated CaSki cells, in line with previous findings indicating that the expression of p53 target genes is reduced in cells overexpressing PAD4, resulting in the perturbation of the normal cell cycle (Li et al., 2008). Of note, PADs are also involved in human epidermal keratinization and morphogenesis, as well as in skin tumorigenesis, a process closely linked to HPV infection. For instance, differential expression of the four genes encoding PAD1, together with laminin-γ2 (LAMC 2), collagen type IV α1 (COL4A 1), and collagen type I α1 (COL1A 1), has been proposed to be a predictive biomarker of squamous cell carcinomas of the oral cavity and oropharynx (Chen et al., 2008). Finally, stromal CD66b^{+} neutrophils and myeloperoxidase/citrullinated histone H3 (MPO/H3Cit)-labeled neutrophil extracellular trap (NETs) have been recently identified as an independent prognostic factor for recurrence-free survival (RFS) in cervical cancer (Yan et al., 2021).

Surprisingly, our immunohistochemical analysis of cervical carcinoma tissue specimens found that PAD2, unlike PAD4, is not linked to cervical cancer progression and that its expression is restricted to the glandular epithelium of both normal mucosa and hrHPV-related lesions. This is somewhat surprising given that PAD2 overexpression in transgenic mice promotes skin neoplasia (McElwee et al., 2014; Mohanan et al., 2017). In addition, PAD2 was found to be overexpressed in patients with many types of tumor tissues, such as castration-resistance prostate cancer (CRPC) (Wang et al., 2017), invasive breast ductal carcinoma, cervical squamous cell carcinoma, colon adenocarcinoma, liver hepatocellular carcinoma, lung cancer, ovarian serous papillary adenocarcinoma, and papillary thyroid carcinoma samples (McElwee et al., 2012; Guo et al., 2017). However, and in good agreement with our results, downregulation of PAD2 is an early event in the pathogenesis of colorectal cancer associated with poor prognosis (Cantariño et al., 2016), suggesting that PAD expression is strictly dependent on the tumor microenvironment, while their tumorigenic effects and mechanisms are still controversial.

Overall, our findings provide a new paradigm of hrHPV-host interplay based on PAD-mediated citrullination that could ultimately be exploited for further diagnostic and therapeutic development to curb HPV transformation in infected patients.

Data availability statement

The raw data supporting the conclusions of this article will be made available by the authors, without undue reservation.

Ethics statement

This research was approved by the Cambridge East Research Ethics Committee (Ethics application ID: BAC.007.22; ref EE/19/0089) and adhered to the principles of the Declaration of Helsinki. The studies were conducted in accordance with the local legislation and institutional requirements. Written informed consent for participation was not required from the participants or the participants' legal guardians/next of kin because The investigations were conducted in compliance with local legislation and institutional requirements. Written informed consent for participation was not required from the participants or the participants' legal guardians/next of kin. The study, involving the use of paraffin-embedded material from existing records, was sanctioned by the Cambridge East Research Ethics Committee. In the UK, oral consent was deemed sufficient for cervical biopsies performed after abnormal HPV results.

Author contributions

CA: Writing – original draft, Methodology, Investigation, Data curation, Conceptualization. MB: Writing – original draft, Supervision, Investigation, Funding acquisition, Data curation. JM: Writing – original draft, Methodology, Investigation, Data curation, Conceptualization. SP: Writing – review & editing, Investigation. FG: Writing – review & editing, Investigation, Funding acquisition. IC: Writing – review & editing, Supervision, Investigation. FC: Writing – review & editing, Methodology. GB: Writing – review & editing, Methodology. GG: Writing – review & editing, Investigation. GR: Writing – review & editing, Conceptualization. SL: Writing – review & editing. MG: Writing – review & editing, Project administration, Funding acquisition. MD: Writing – review & editing, Funding acquisition. VD: Writing – original draft, Supervision, Project administration, Funding acquisition, Data curation, Conceptualization.

Funding

study design, data collection, and interpretation, as well as in the decision to submit this work for publication.

Acknowledgments

We would sincerely like to thank Marcello Arsura for his critical reading of our manuscript.

Conflict of interest

The authors declare that the research was conducted in the absence of any commercial or financial relationships that could be construed as a potential conflict of interest.

Publisher's note

All claims expressed in this article are solely those of the authors and do not necessarily represent those of their affiliated organizations, or those of the publisher, the editors and the reviewers. Any product that may be evaluated in this article, or claim that may be made by its manufacturer, is not guaranteed or endorsed by the publisher.

Supplementary material

The Supplementary Material for this article can be found online at: https://www.frontiersin.org/articles/10.3389/fcimb.2024.1359367/full#supplementary-material

References

Alghamdi, M. A., and Redwan, E. M. (2021). Interplay of microbiota and citrullination in the immunopathogenesis of rheumatoid arthritis. *Probiotics Antimicrob. Proteins*. 14 (1), 99–113. doi: 10.1007/s12602-021-09802-7

Baka, Z., Barta, P., Losonczy, G., Krenács, T., Pápay, J., Szarka, E., et al. (2011). Specific expression of PAD4 and citrullinated proteins in lung cancer is not associated with anti-CCP antibody production. *Int. Immunol.* 23, 405–414. doi: 10.1093/intimm/dxr026

Beato, M., and Sharma, P. (2020). Peptidyl arginine deiminase 2 (PADI2)-mediated arginine citrullination modulates transcription in cancer. *Int. J. Mol. Sci.* 21, E1351. doi: 10.3390/ijms21041351

Bicker, K. L., Subramanian, V., Chumanevich, A. A., Hofseth, L. J., and Thompson, P. R. (2012). Seeing citrulline: development of a phenylglyoxal-based probe to visualize protein citrullination. *J. Am. Chem. Soc.* 134, 17015–17018. doi: 10.1021/ja308871v

Bicker, K. L., and Thompson, P. R. (2013). The protein arginine deiminases: Structure, function, inhibition, and disease. *Biopolymers* 99, 155–163. doi: 10.1002/bip.22127

Brierley, J., Gospodarowicz, M. K., and Wittekind, C. (2017). *American Joint Committee on Cancer (AJCC-TNM) Staging Manual (TNM8). 8th Edition* (Oxford, UK: Wiley Blackwell).

Bruggeman, Y., Sodré, F. M. C., Buitinga, M., Mathieu, C., Overbergh, L., and Kracht, M. J. L. (2021). Targeting citrullination in autoimmunity: insights learned from preclinical mouse models. *Expert Opin. Ther. Targets* 25, 269–281. doi: 10.1080/14728222.2021.1918104

Burley, M., Roberts, S., and Parish, J. L. (2020). Epigenetic regulation of human papillomavirus transcription in the productive virus life cycle. *Semin. Immunopathol.* 42, 159–171. doi: 10.1007/s00281-019-00773-0

Cantariño, N., Musulén, E., Valero, V., Peinado, M. A., Perucho, M., Moreno, V., et al. (2016). Downregulation of the deiminase PADI2 is an early event in colorectal carcinogenesis and indicates poor prognosis. *Mol. Cancer Res.* 14, 841–848. doi: 10.1158/1541-7786.MCR-16-0034

Casanova, V., Sousa, F. H., Shakamuri, P., Svoboda, P., Buch, C., D'Acremont, M., et al. (2020). Citrullination alters the antiviral and immunomodulatory activities of the human cathelicidin LL-37 during rhinovirus infection. *Front. Immunol.* 11. doi: 10.3389/fimmu.2020.00085

Catrina, A., Krishnamurthy, A., and Rethi, B. (2021). Current view on the pathogenic role of anti-citrullinated protein antibodies in rheumatoid arthritis. *RMD Open* 7, e001228. doi: 10.1136/rmdopen-2020-001228

Chang, X., Han, J., Pang, L., Zhao, Y., Yang, Y., and Shen, Z. (2009). Increased PADI4 expression in blood and tissues of patients with Malignant tumors. *BMC Cancer* 9, 40. doi: 10.1186/1471-2407-9-40

Chen, C., Méndez, E., Houck, J., Fan, W., Lohavanichbutr, P., Doody, D., et al. (2008). Gene expression profiling identifies genes predictive of oral squamous cell carcinoma. *Cancer Epidemiol. Biomarkers Prev.* 17, 2152–2162. doi: 10.1158/1055-9965.EPI-07-2893

Chumanevich, A. A., Causey, C. P., Knuckley, B. A., Jones, J. E., Poudyal, D., Chumanevich, A. P., et al. (2011). Suppression of colitis in mice by Cl-amidine: a novel peptidylarginine deiminase inhibitor. *Am. J. Physiol. Gastrointest Liver Physiol.* 300, G929–G938. doi: 10.1152/ajpgi.00435.2010

Ciriello, G., Gatza, M. L., Beck, A. H., Wilkerson, M. D., Rhie, S. K., Pastore, A., et al. (2015). Comprehensive molecular portraits of invasive lobular breast cancer. *Cell* 163, 506–519. doi: 10.1016/j.cell.2015.09.033

Darrah, E., and Andrade, F. (2018). Rheumatoid arthritis and citrullination. *Curr. Opin. Rheumatol* 30, 72–78. doi: 10.1097/BOR.0000000000000452

de Villiers, E.-M. (2013). Cross-roads in the classification of papillomaviruses. *Virology* 445, 2–10. doi: 10.1016/j.virol.2013.04.023

Durzynska, J., Lesniewicz, K., and Poreba, E. (2017). Human papillomaviruses in epigenetic regulations. *Mutat. Research/Reviews Mutat. Res.* 772, 36–50. doi: 10.1016/j.mrrev.2016.09.006

Gao, J., Aksoy, B. A., Dogrusoz, U., Dresdner, G., Gross, B., Sumer, S. O., et al. (2013). Integrative analysis of complex cancer genomics and clinical profiles using the cBioPortal. *Sci. Signal* 6, pl1. doi: 10.1126/scisignal.2004088

Girone, C., Calati, F., Lo Cigno, I., Salvi, V., Tassinari, V., Schioppa, T., et al. (2023). The RIG-I agonist M8 triggers cell death and natural killer cell activation in human papillomavirus-associated cancer and potentiates cisplatin cytotoxicity. *Cancer Immunol. Immunother.* 72, 3097–3110. doi: 10.1007/s00262-023-03483-7

Griffante, G., Gugliesi, F., Pasquero, S., Dell'Oste, V., Biolatti, M., Salinger, A. J., et al. (2021). Human cytomegalovirus-induced host protein citrullination is crucial for viral replication. *Nat. Commun.* 12, 3910. doi: 10.1038/s41467-021-24178-6

Gudmann, N. S., Hansen, N. U. B., Jensen, A. C. B., Karsdal, M. A., and Siebuhr, A. S. (2015). Biological relevance of citrullinations: diagnostic, prognostic and therapeutic options. *Autoimmunity* 48, 73–79. doi: 10.3109/08916934.2014.962024

Guo, W., Zheng, Y., Xu, B., Ma, F., Li, C., Zhang, X., et al. (2017). Investigating the expression, effect and tumorigenic pathway of PADI2 in tumors. *Onco Targets Ther.* 10, 1475–1485. doi: 10.2147/OTT.S92389

Gusho, E., and Laimins, L. A. (2022). Human papillomaviruses sensitize cells to DNA damage induced apoptosis by targeting the innate immune sensor cGAS. *PloS Pathog.* 18, e1010725. doi: 10.1371/journal.ppat.1010725

Gutierrez-Xicotencatl, L., Pedroza-Saavedra, A., Chihu-Amparan, L., Salazar-Piña, A., Maldonado-Gama, M., and Esquivel-Guadarrama, F. (2021). Cellular functions of HPV16 E5 oncoprotein during oncogenic transformation. *Mol. Cancer Res.* 19, 167–179. doi: 10.1158/1541-7786.MCR-20-0491

Harris, S. L., and Levine, A. J. (2005). The p53 pathway: positive and negative feedback loops. *Oncogene* 24, 2899–2908. doi: 10.1038/sj.onc.1208615

Hoppe-Seyler, K., Bossler, F., Braun, J. A., Herrmann, A. L., and Hoppe-Seyler, F. (2018). The HPV E6/E7 oncogenes: key factors for viral carcinogenesis and therapeutic targets. *Trends Microbiol.* 26, 158–168. doi: 10.1016/j.tim.2017.07.007

Ishigami, A., and Maruyama, N. (2010). Importance of research on peptidylarginine deiminase and citrullinated proteins in age-related disease. *Geriatr. Gerontol Int.* 10 Suppl 1, S53–S58. doi: 10.1111/j.1447-0594.2010.00593.x

Kombe Kombe, A. J., Li, B., Zahid, A., Mengist, H. M., Bounda, G.-A., Zhou, Y., et al. (2021). Epidemiology and burden of human papillomavirus and related diseases, molecular pathogenesis, and vaccine evaluation. *Front. Public Health* 8. doi: 10.3389/fpubh.2020.552028

Ledet, M. M., Anderson, R., Harman, R., Muth, A., Thompson, P. R., Coonrod, S. A., et al. (2018). BB-Cl-Amidine as a novel therapeutic for canine and feline mammary cancer via activation of the endoplasmic reticulum stress pathway. *BMC Cancer* 18, 412. doi: 10.1186/s12885-018-4323-8

Li, P., Yao, H., Zhang, Z., Li, M., Luo, Y., Thompson, P. R., et al. (2008). Regulation of p53 target gene expression by peptidylarginine deiminase 4. *Mol. Cell Biol.* 28, 4745–4758. doi: 10.1128/MCB.01747-07

Lo Cigno, I., Calati, F., Albertini, S., and Gariglio, M. (2020a). Subversion of host innate immunity by human papillomavirus oncoproteins. *Pathogens* 9, E292. doi: 10.3390/pathogens9040292

Lo Cigno, I., Calati, F., Borgogna, C., Zevini, A., Albertini, S., Martuscelli, L., et al. (2020b). Human papillomavirus E7 oncoprotein subverts host innate immunity via SUV39H1-mediated epigenetic silencing of immune sensor genes. *J. Virol.* 94, e01812–e01819. doi: 10.1128/JVI.01812-19

Lo Cigno, I., Calati, F., Girone, C., Borgogna, C., Venuti, A., Boldorini, R., et al. (2023). SIRT1 is an actionable target to restore p53 function in HPV-associated cancer therapy. *Br. J. Cancer* 129, 1863–1874. doi: 10.1038/s41416-023-02465-x

McBride, A. A. (2022). Human papillomaviruses: diversity, infection and host interactions. *Nat. Rev. Microbiol.* 20, 95–108. doi: 10.1038/s41579-021-00617-5

McElwee, J. L., Mohanan, S., Griffith, O. L., Breuer, H. C., Anguish, L. J., Cherrington, B. D., et al. (2012). Identification of PADI2 as a potential breast cancer biomarker and therapeutic target. *BMC Cancer* 12, 500. doi: 10.1186/1471-2407-12-500

McElwee, J. L., Mohanan, S., Horibata, S., Sams, K. L., Anguish, L. J., McLean, D., et al. (2014). PAD2 overexpression in transgenic mice promotes spontaneous skin neoplasia. *Cancer Res.* 74, 6306–6317. doi: 10.1158/0008-5472.CAN-14-0749

Mincheva, A., Gissmann, L., and zur Hausen, H. (1987). Chromosomal integration sites of human papillomavirus DNA in three cervical cancer cell lines mapped by in situ hybridization. *Med. Microbiol. Immunol.* 176, 245–256. doi: 10.1007/BF00190531

Mittal, S., and Banks, L. (2017). Molecular mechanisms underlying human papillomavirus E6 and E7 oncoprotein-induced cell transformation. *Mutat. Res. Rev. Mutat. Res.* 772, 23–35. doi: 10.1016/j.mrrev.2016.08.001

Mohanan, S., Horibata, S., Anguish, L. J., Mukai, C., Sams, K., McElwee, J. L., et al. (2017). PAD2 overexpression in transgenic mice augments Malignancy and tumor-associated inflammation in chemically initiated skin tumors. *Cell Tissue Res.* 370, 275–283. doi: 10.1007/s00441-017-2669-x

Mondal, S., and Thompson, P. R. (2021). Chemical biology of protein citrullination by the protein A arginine deiminases. *Curr. Opin. Chem. Biol.* 63, 19–27. doi: 10.1016/j.cbpa.2021.01.010

Muraro, S. P., De Souza, G. F., Gallo, S. W., Da Silva, B. K., De Oliveira, S. D., Vinolo, M. A. R., et al. (2018). Respiratory Syncytial Virus induces the classical ROS-dependent NETosis through PAD-4 and necroptosis pathways activation. *Sci. Rep.* 8, 14166. doi: 10.1038/s41598-018-32576-y

Pasquero, S., Gugliesi, F., Biolatti, M., Dell'Oste, V., Albano, C., Bajetto, G., et al. (2023). Citrullination profile analysis reveals peptidylarginine deaminase 3 as an HSV-1 target to dampen the activity of candidate antiviral restriction factors. *PloS Pathog.* 19, e1011849. doi: 10.1371/journal.ppat.1011849

Pasquero, S., Gugliesi, F., Griffante, G., Dell'Oste, V., Biolatti, M., Albano, C., et al. (2022). Novel antiviral activity of PAD inhibitors against human beta-coronaviruses HCoV-OC43 and SARS-CoV-2. *Antiviral Res.* 200, 105278. doi: 10.1016/j.antiviral.2022.105278

Rasi Bonab, F., Baghbanzadeh, A., Ghaseminia, M., Bolandi, N., Mokhtarzadeh, A., Amini, M., et al. (2021). Molecular pathways in the development of HPV-induced cervical cancer. *EXCLI J.* 20, 320–337. doi: 10.17179/excli2021-3365

Sancandi, M., Uysal-Onganer, P., Kraev, I., Mercer, A., and Lange, S. (2020). Protein deimination in plasma and plasma-EVs and protein deimination in the brain vasculature in a rat model of pre-motor Parkinson's disease. *Int. J. Mol. Sci.* 21, E2743. doi: 10.3390/ijms21082743

Sarnik, J., and Makowska, J. S. (2022). Highlighting the versatility of the citrullination process. *Immunobiology* 227, 152233. doi: 10.1016/j.imbio.2022.152233

Scarth, J. A., Patterson, M. R., Morgan, E. L., and Macdonald, A. (2021). The human papillomavirus oncoproteins: a review of the host pathways targeted on the road to transformation. *J. Gen. Virol.* 102 (3), 001540. doi: 10.1099/jgv.0.001540

Schiffman, M., Doorbar, J., Wentzensen, N., de Sanjosé, S., Fakhry, C., Monk, B. J., et al. (2016). Carcinogenic human papillomavirus infection. *Nat. Rev. Dis. Primers* 2, 16086. doi: 10.1038/nrdp.2016.86

Shafique, M., Shoaib, I., Aslam, B., Khalid, R., Tanvir, I., Rasool, M. H., et al. (2023). Detection of high-risk human papillomavirus infected cervical biopsies samples by immunohistochemical expression of the p16 tumor marker. *Arch. Microbiol.* 206, 17. doi: 10.1007/s00203-023-03736-0

Shi, J., Sun, X., Zhao, Y., Zhao, J., and Li, Z. (2008). Prevalence and significance of antibodies to citrullinated human papilloma virus-47 E2345-362 in rheumatoid arthritis. *J. Autoimmun* 31, 131–135. doi: 10.1016/j.jaut.2008.04.021

Shimada, M., Yamashita, A., Saito, M., Ichino, M., Kinjo, T., Mizuki, N., et al. (2020). The human papillomavirus E6 protein targets apoptosis-inducing factor (AIF) for degradation. *Sci. Rep.* 10, 14195. doi: 10.1038/s41598-020-71134-3

Singh, U., Singh, S., Singh, N. K., Verma, P. K., and Singh, S. (2011). Anticyclic citrullinated peptide autoantibodies in systemic lupus erythematosus. *Rheumatol Int.* 31, 765–767. doi: 10.1007/s00296-010-1374-9

Struyf, S., Noppen, S., Loos, T., Mortier, A., Gouwy, M., Verbeke, H., et al. (2009). Citrullination of CXCL12 differentially reduces CXCR4 and CXCR7 binding with loss of inflammatory and anti-HIV-1 activity via CXCR4. *J. Immunol.* 182, 666–674. doi: 10.4049/jimmunol.182.1.666

Toscani, A., Denaro, R., Pacheco, S. F. C., Biolatti, M., Anselmi, S., Dell'Oste, V., et al. (2021). Synthesis and biological evaluation of amidinourea derivatives against herpes simplex viruses. *Molecules* 26, 4927. doi: 10.3390/molecules26164927

Tu, R., Grover, H. M., and Kotra, L. P. (2016). Peptidyl arginine deiminases and neurodegenerative diseases. *Curr. Med. Chem.* 23, 104–114. doi: 10.2174/0929867323666151118120710

Van Doorslaer, K., Li, Z., Xirasagar, S., Maes, P., Kaminsky, D., Liou, D., et al. (2017). The Papillomavirus Episteme: a major update to the papillomavirus sequence database. *Nucleic Acids Res.* 45, D499–D506. doi: 10.1093/nar/gkw879

Vats, A., Trejo-Cerro, O., Thomas, M., and Banks, L. (2021). Human papillomavirus E6 and E7: What remains? *Tumour Virus Res.* 11, 200213. doi: 10.1016/j.tvr.2021.200213

Wang, L., Song, G., Zhang, X., Feng, T., Pan, J., Chen, W., et al. (2017). PADI2-mediated citrullination promotes prostate cancer progression. *Cancer Res.* 77, 5755–5768. doi: 10.1158/0008-5472.CAN-17-0150

Willis, V. C., Gizinski, A. M., Banda, N. K., Causey, C. P., Knuckley, B., Cordova, K. N., et al. (2011). N-α-benzoyl-N5-(2-chloro-1-iminoethyl)-L-ornithine amide, a protein arginine deiminase inhibitor, reduces the severity of murine collagen-induced arthritis. *J. Immunol.* 186, 4396–4404. doi: 10.4049/jimmunol.1001620

Witalison, E. E., Thompson, P. R., and Hofseth, L. J. (2015). Protein arginine deiminases and associated citrullination: physiological functions and diseases associated with dysregulation. *Curr. Drug Targets* 16, 700–710. doi: 10.2174/1389450116666150202160954

Xiong, Y., Hannon, G. J., Zhang, H., Casso, D., Kobayashi, R., and Beach, D. (1993). p21 is a universal inhibitor of cyclin kinases. *Nature* 366, 701–704. doi: 10.1038/366701a0

Yan, B., Dai, X., Ma, Q., and Wu, X. (2021). Stromal neutrophil extracellular trap density is an independent prognostic factor for cervical cancer recurrence. *Front. Oncol.* 11. doi: 10.3389/fonc.2021.659445

Yang, R., Klimentová, J., Göckel-Krzikalla, E., Ly, R., Gmelin, N., Hotz-Wagenblatt, A., et al. (2019). Combined transcriptome and proteome analysis of immortalized human keratinocytes expressing human papillomavirus 16 (HPV16) oncogenes reveals novel key factors and networks in HPV-induced carcinogenesis. *mSphere* 4, e00129–e00119. doi: 10.1128/mSphere.00129-19

Ying, S., Dong, S., Kawada, A., Kojima, T., Chavanas, S., Méchin, M.-C., et al. (2009). Transcriptional regulation of peptidylarginine deiminase expression in human keratinocytes. *J. Dermatol. Sci.* 53, 2–9. doi: 10.1016/j.jdermsci.2008.09.009

Yousefi, Z., Aria, H., Ghaedrahmati, F., Bakhtiari, T., Azizi, M., Bastan, R., et al. (2021). An update on human papilloma virus vaccines: history, types, protection, and efficacy. *Front. Immunol.* 12. doi: 10.3389/fimmu.2021.805695

Yu, K., and Proost, P. (2022). Insights into peptidylarginine deiminase expression and citrullination pathways. *Trends Cell Biol.* 32 (9), 746–761. doi: 10.1016/j.tcb.2022.01.014

Yuzhalin, A. E. (2019). Citrullination in cancer. *Cancer Res.* 79, 1274–1284. doi: 10.1158/0008-5472.CAN-18-2797

Zheng, K., Egawa, N., Shiraz, A., Katakuse, M., Okamura, M., Griffin, H. M., et al. (2022). The reservoir of persistent human papillomavirus infection; strategies for elimination using anti-viral therapies. *Viruses* 14, 214. doi: 10.3390/v14020214

Zhou, C., Tuong, Z. K., and Frazer, I. H. (2019). Papillomavirus immune evasion strategies target the infected cell and the local immune system. *Front. Oncol.* 9. doi: 10.3389/fonc.2019.00682

Zhu, D., Zhang, Y., and Wang, S. (2021). Histone citrullination: a new target for tumors. *Mol. Cancer* 20, 90. doi: 10.1186/s12943-021-01373-z

Article

Antiherpetic Activity of a Root Exudate from *Solanum lycopersicum*

Greta Bajetto [1,2,†], Davide Arnodo [3,†], Matteo Biolatti [1], Linda Trifirò [1], Camilla Albano [1], Selina Pasquero [1], Francesca Gugliesi [1], Eva Campo [4], Francesca Spyrakis [5], Cristina Prandi [3], Marco De Andrea [1,2], Valentina Dell'Oste [1,*], Ivan Visentin [4] and Marco Blangetti [3,*]

[1] Department of Public Health and Pediatric Sciences, University of Turin, 10126 Turin, Italy; greta.bajetto@unito.it (G.B.); matteo.biolatti@unito.it (M.B.); linda.trifiro@unito.it (L.T.); camilla.albano@unito.it (C.A.); selina.pasquero@unito.it (S.P.); francesca.gugliesi@unito.it (F.G.); marco.deandrea@unito.it (M.D.A.)

[2] Center for Translational Research on Autoimmune and Allergic Disease (CAAD), 28100 Novara, Italy

[3] Department of Chemistry, University of Turin, 10125 Turin, Italy; davide.arnodo@unito.it (D.A.); cristina.prandi@unito.it (C.P.)

[4] Department of Agricultural, Forestry, and Food Sciences, University of Turin, 10095 Turin, Italy; eva.campo@unito.it (E.C.); ivan.visentin@unito.it (I.V.)

[5] Department of Drug Science and Technology, University of Turin, 10125 Turin, Italy; francesca.spyrakis@unito.it

* Correspondence: valentina.delloste@unito.it (V.D.); marco.blangetti@unito.it (M.B.); Tel.: +39-011-6705631 (V.D.); +39-011-6708033 (M.B.)

† These authors contributed equally to this work.

Abstract: The rise of drug resistance to antivirals poses a significant global concern for public health; therefore, there is a pressing need to identify novel compounds that can effectively counteract strains resistant to current antiviral treatments. In light of this, researchers have been exploring new approaches, including the investigation of natural compounds as alternative sources for developing potent antiviral therapies. Thus, this work aimed to evaluate the antiviral properties of the organic-soluble fraction of a root exudate derived from the tomato plant *Solanum lycopersicum* in the context of herpesvirus infections. Our findings demonstrated that a root exudate from *Solanum lycopersicum* exhibits remarkable efficacy against prominent members of the family *Herpesviridae*, specifically herpes simplex virus type 1 (HSV-1) (EC_{50} 25.57 µg/mL, SI > 15.64) and human cytomegalovirus (HCMV) (EC_{50} 9.17 µg/mL, SI 32.28) by inhibiting a molecular event during the herpesvirus replication phase. Moreover, the phytochemical fingerprint of the *Solanum lycopersicum* root exudate was characterized through mass spectrometry. Overall, these data have unveiled a novel natural product with antiherpetic activity, presenting a promising and valuable alternative to existing drugs.

Keywords: antivirals; herpesviruses; natural compounds; tomatoes; plant specialized metabolites; rhizosphere

1. Introduction

Herpesviruses pose a significant threat to human health, causing chronic and recurring infections that profoundly impact the quality of life for affected individuals. Notable members of this viral family include herpes simplex virus type 1 (HSV-1) and human cytomegalovirus (HCMV) [1,2]. Many members of the *Herpesviridae* family exhibit high seroprevalence globally; HCMV reaches more than 50% of the general population, and HSV, more than 60%. Around 500 million people worldwide, aged 15 to 50, have genital infections caused by HSV-1 or HSV-2, while the incidence of cold sores is second globally only to the common cold. HCMV infection stands as the prevailing congenital infection globally, with an estimated occurrence in developed nations ranging from 0.6% to 0.7% of all live births. This translates to around 60,000 neonates born annually with HCMV infection in the Western world. Notably, in developing countries, the prevalence is even more pronounced, affecting between 1% and

5% of all live births [2–4]. The efficacy of existing treatments is compromised by resistant strains of herpesviruses, highlighting the pressing need to explore alternative compounds and formulations [5–7]. Therefore, the quest for new antiherpetic drugs is a critical global challenge not only to alleviate the suffering caused by herpesvirus, but also to counter drug-resistant herpesvirus strains, improve treatment outcomes, and tackle the evolving challenges exacerbated by the emergence of viral escape mutants.

Within this framework, herbal medicines and purified natural products derived from plants, marine organisms, and other natural sources have garnered considerable attention as a rich resource for the development of innovative antiviral drugs. This includes a diverse array of substances, including essential oils, plant extracts, small peptides from animal sources, bacteriocins, and several categories of plant compounds (such as alkaloids, triterpenoids, flavonoids, and phenols) renowned for their antimicrobial and antiviral properties [8–10]. The use of natural compounds as antivirals presents several advantages over synthetic drugs. Indeed, they are often derived from renewable sources, making them more sustainable and environmentally friendly. Moreover, these compounds may have fewer adverse side effects compared to synthetic drugs, as they have evolved alongside living organisms and are more compatible with human biology [11,12].

Solanum lycopersicum, commonly referred to as the tomato plant, is a species of flowering plant that belongs to the *Solanaceae* family. It ranks as the second most widely cultivated and consumed vegetable worldwide, making it both an essential model organism for plant research and a significant commercial crop. In addition to its noteworthy nutritional value, *Solanum lycopersicum* has been studied for its potential medicinal properties which have been recognized and utilized for centuries [13–16]. Notably, tomato extracts contain a diverse array of bioactive compounds, such as flavonoids and carotenoids. These specialized metabolites accumulate in various tissues of the tomato plant and are released as root exudates and volatiles [17]. Tomato root exudates are rich in organic acids, sugars, and amino acids. Among these, glucose and fructose stand out as the primary sugars; malic, citric, and succinic acids are the predominant organic acids [18]; and glutamic acid, aspartic acid, leucine, isoleucine, and lysine are the main amino acids [19]. The secretion levels differ based on the growth phase of the tomato and the presence of particular microorganisms [20].

These compounds impart a significant nutraceutical value to tomatoes, positioning them as functional foods that can positively impact various pathological conditions [16]. One notable example is their ability to reduce the production of pro-inflammatory molecules, thereby mitigating inflammation and potentially avoiding the onset of chronic inflammatory diseases [21]. Furthermore, tomatoes have also garnered attention for their potential cardiovascular benefits. The abundant potassium content found in *Solanum lycopersicum* assists in regulating blood pressure by counteracting the effects of sodium, thus supporting a healthy cardiovascular system. Lastly, in terms of medicinal properties, it is suggested that it may contribute to a reduction in cancer risks, particularly for lung and prostate cancers [22,23].

Despite numerous investigations into the therapeutic properties of tomatoes, there is a lack of studies exploring their potential antiviral effects, particularly those of root exudates. Interestingly, the antiviral efficacy of tomatidine, a steroidal alkaloid obtained from the stem and leaves of unripe, green tomatoes, has been demonstrated against all four dengue virus (DENV) serotypes and Zika virus (ZIKV) in the Huh7 in vitro model. It disrupts various stages of DENV replication, especially post-virus–cell binding and internalization. The cellular activating transcription factor 4 (ATF4) may enhance the antiviral effect, yet it is not entirely responsible for it. Notably, no antiviral activity was detected for West Nile virus (WNV), another mosquito-borne flavivirus [24]. Tomatidine and its structural derivatives solasodine and sarsasapogenin were also effective against multiple chikungunya virus (CHIKV) strains, primarily during the early stages of infection [25]. In the context of DNA viruses, tomatine displayed inhibitory activity against HSV-1, possibly through the interaction of the sugar moiety of the glycosidic chain with the viral envelope [26].

In this study, recognizing the need to continue searching for novel antiviral agents, we aimed to investigate the in vitro antiviral activity of a root exudate derived from *Solanum lycopersicum* against two members of the herpesvirus family (specifically HSV-1 and HCMV). Additionally, the phytochemical fingerprint of the exudate was determined by ESI-MS analyses, disclosing the occurrence of several bioactive compounds (carotenoids, phytosterols, and polyphenols) which might play a synergic role in determining the antiviral activity of the tomato root exudate. In summary, these data highlight *Solanum lycopersicum* as a natural product with the potential to serve as a valuable alternative to existing antiviral drugs.

2. Materials and Methods

2.1. Plant Material and Tomato Extract Preparation

Tomato (*Solanum lycopersicum* cv. M82) seeds were surfaced-sterilized in 4% sodium hypochlorite containing 0.02% (*v/v*) Tween 20, washed thoroughly with sterile water, and germinated for 2 days in a plate on moistened filter paper at 25 °C in the darkness. Subsequently, 4-week-old plants were transferred in an aeroponic system and grown with Hogland nutrient solution (0.2 μM $ZnSO_4$, 0.2 μM $CuSO_4$, 1 mM $Ca(NO_3)_2$, 80 μM KH_2PO_4, 250 μM KNO_3, 20 μM FeNa EDTA, 1.8 μM $MnCl_2$, 0.2 μM $Co(NO_3)_2$, 9 μM H_3BO_3, 0.2 μM $NiSO_4$, 1 mM $MgSO_4$, pH 6.0). The plants were cultured in a growth chamber set at the following parameters: 16/8 h day/night cycle, 25 °C, 65% humidity, and 200 μmol s^{-1} m^{-2} of photosynthetic photon flux density (PPFD). The nutrient solution was renewed and alternated with a version containing an equimolar quantity of KCl instead of KH_2PO_4. The nutrient solution containing the root exudates was collected and filtered twice a week by a 0.2 mm sieve. Subsequently, the root exudate was loaded onto the preequilibrated column (Grace Pure C18-Fast 500 mg/3 mL SPE) and eluted with 5 mL of 1:1 water/acetone solution. Finally, the eluted solution was dried with a rotary evaporator and stocked at −20 °C (Figure 1) [27]. At the time of use, 10 mg of lyophilized root exudate was dissolved in 1 mL of DMSO/H_2O mixture (1:1) and subsequently diluted in the culture medium.
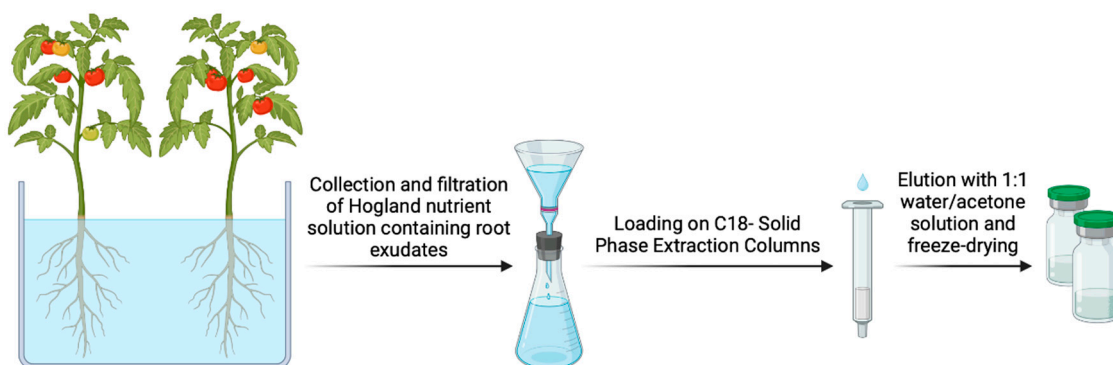
Figure 1. Strategy for the preparation of extracts from tomato root exudates (created with BioRender).

2.2. Phytochemical Analysis

Acetonitrile (HPLC-grade) and formic acid (mass-spectrometry-grade, 98%) were purchased from Sigma Aldrich. The tomato root exudate sample was diluted in acetonitrile (1.0 mg/mL) with 0.1% formic acid as a charge carrier.

Direct-infusion positive ESI-MS analysis was performed on a 3200 QTRAP® LC-MS/MS System (AB Sciex) equipped with a syringe pump. The sample was infused at a flow rate of 10 μL/min. The paramete, rs adopted for the ESI source were as follows: source voltage 5.0 kV; heated capillary temperature 350 °C; N_2 curtain gas flow rate 20 (arbitrary units); declustering potential 20 V; entrance potential 10 V. Total ion current (TIC) mode was used to record the abundances of the ionized adducts. In the full-scan mode, masses were scanned as centroid data from *m/z* 100 to 700 at a rate of 1 scan/s (averaged over 5 min). Data acquisition and processing and instrumental control were performed using the Analyst®® software package version 1.7 (AB Sciex).

2.3. Cells and Viruses

African green monkey kidney cells (VERO, ATCC CCL-81™) and primary human foreskin fibroblasts (HFFs, ATCC SCRC-1041™) were propagated in Dulbecco's Modified Eagle Medium (DMEM; Sigma-Aldrich, Milan, Italy) complemented with 1% streptomycin/penicillin solution (Sigma-Aldrich) and 10% fetal bovine serum (heat-inactivated) (Sigma-Aldrich).

The clinical isolate of HSV-1 (obtained from Valeria Ghisetti, "Amedeo di Savoia" Hospital, Turin, Italy) and the AD169 HCMV strain (ATCC VR538) were grown and titrated by a standard plaque assay on VERO and HFF cells, respectively, on a 96-well plate (~30,000 cells/well), as previously described [28,29].

2.4. Cytotoxicity Assay

VERO and HFF cells were seeded in a 96-well culture plate (~30,000 cells/well) and exposed to increasing concentrations of either tomato extract or vehicle control (DMSO/H_2O mixture 1:1). After 48 h (for VERO) or 144 h (for HFF) of incubation, cell viability was determined using the 3-(4,5-dimethylthiazol-2-yl)-2,5-diphenyltetrazolium bromide (MTT) (Sigma-Aldrich) assay, as previously described [30].

2.5. Virus Yield Reduction Assay

VERO and HFF cells were plated in 24-well plates (~200,000 cells/well) and pre-treated with different concentrations of tomato extracts, vehicle, or the reference drugs Acyclovir (ACV, Sigma-Aldrich) for HSV-1 and Ganciclovir (GCV, Sigma-Aldrich) for HCMV for 1 h at 37 °C. They were then infected with HSV-1 (VERO) or HCMV (HFF) at an MOI of 0.1 plaque-forming units per cell (PFU/cell) in the presence of treatments. Following virus adsorption (2 h at 37 °C), the viral inoculum was removed, and the cultures were maintained in a medium that contained the extract for 48 h (HSV-1) or 144 h (HCMV). Cells and supernatants (combined) were then collected and lysed using three freeze (liquid nitrogen)/thaw (37 °C) cycles. Virus replication was assessed by titrating the infectivity of the samples obtained from the virus yield reduction assay with a standard plaque assay on VERO (HSV-1) and HFF (HCMV) previously plated in a 96-well plate (~30,000 cells/well). After 48 h (HSV-1) or 144 h (HCMV), cells were fixed and stained with a crystal violet solution (0.1% crystal violet, 20% ethanol). Plaques were microscopically counted, and the mean plaque counts for each drug concentration were expressed as PFU/mL. The concentration that produced a 50% reduction in plaque formation (EC_{50}) was determined for each test by nonlinear regression (curve fitting analysis) in GraphPad Prism software version 8.02 for Windows. The selectivity index (SI) reflects the CC_{50}-to-EC_{50} ratio.

2.6. Time of Addition Assay

VERO and HFF cells were seeded in 24-well plates (~200,000 cells/well) and treated with various concentrations of tomato extract or vehicle solution at different time points: (i) 1 h pre-infection as pre-treatment, (ii) only during the 2 h of viral adsorption, (iii) post-infection until sample collection. In all conditions, cells were infected with HSV-1 or HCMV (MOI 0.1 PFU/cell). After 48 h (VERO) or 144 h (HFF), cells and supernatants were collected and disrupted using three freeze (liquid nitrogen)/thaw (37 °C) cycles. The level of virus replication was then assessed by titrating the infectivity of the samples by a plaque assay as described in the virus yield reduction assay section.

2.7. Western Blot Analysis

VERO and HFF cells were seeded in 6-well plates (~10^6 cells/well), treated as described in the virus yield reduction assay section, and infected at an MOI of 1. Cells were collected at different time points, and whole-cell protein extracts were prepared using Radioimmunoprecipitation Assay (RIPA) buffer. Then, 30 μg of protein extracts were subjected to electrophoresis on sodium dodecyl sulfate–polyacrylamide (SDS) gels and transferred to Immobilon-P membranes (Biorad). Membranes were blocked with 5% nonfat dry milk in TBS-Tween 0.05%

and incubated overnight at 4 °C with the primary antibodies. The following mouse monoclonal primary antibodies were used: anti-HSV-1 ICP4 (clone 10F1, H1A021-100, Virusys Corporation, Taneytown, MD, USA), anti-HSV-1/2 gD (clone 2C10, HA025-100, Virusys Corporation), anti-HCMV IEA (clone CH160, P1215, Virusys Corporation), pp65 (clone 3A12, CA003-100, Virusys Corporation), pp28 (clone 5C3, CA004-100, Virusys Corporation), anti-Actin (clone C4, MAB1501, Sigma-Aldrich) (all at 1:1000 dilution in 5% nonfat dry milk, TBS-Tween 0.05%). After washing with TBST buffer (500 mM NaCl, 20 mM Tris pH 7.4, 0.05% Tween 20), the membranes were incubated with an HRP-conjugated anti-mouse secondary antibody (1:3000 diluted, Sigma-Aldrich) for 2 h at room temperature, and immunocomplexes were visualized using an enhanced chemiluminescence detection kit (SuperSignal West Pico Chemiluminescent Substrate, Thermo SCIENTIFIC, Waltham, MA, USA).

2.8. DNA Extraction and Viral Load

VERO and HFF cells were seeded in 24-well plates (~200,000 cells/well), treated as described in the virus yield reduction assay section, and infected at an MOI of 1. After 24 (HSV-1) or 72 (HCMV) hours, cells were collected, and the cellular-associated DNA was isolated using the TRI Reagent solution (Sigma-Aldrich) according to the manufacturer's instructions. The extracted viral DNA was quantified by quantitative real-time PCR (qPCR) analysis using a CFX Touch Real-Time PCR Detection System (BioRad, Hercules, CA, US). The viral DNA copy numbers were quantified using primers to amplify a segment of the IE1 gene for HCMV (Fw, 5′-TCAGTGCTCCCCTGATGAGA-3′; Rv, 5′-GATCAATGTGCGTGAGCACC-3′) or gE for HSV (Fw, 5′-TGTCTGTATCAGCCGCAGC-3′; Rv, 5′-TTCTGGAACACCCCGCGTA-3′). Intracellular viral DNA copy numbers were normalized to GAPDH (Fw, 5′-AGTGGGTGTCGCTGTTGAAGT-3′; Rv, 5′-AACGTGTCAGTGGTGG ACCTG-3′). To create a standard curve for each analysis, genomic DNA mixed with a gE2- or IE1-encoding plasmid (pAcUW51-CgE, a gift from Pamela Bjorkman; Addgene plasmid #13762, http://n2t.net/addgene:13762 accessed on 31 December 2023, RRID: Addgene_13762 [31] (Addgene, Watertown, MA, USA; pSG-IE72, available at the Department of Public Health and Pediatric Sciences, Turin, Italy) was serially diluted and analyzed in parallel.

2.9. Statistical Analysis

The statistical tests were performed using GraphPad Prism version 8.0.2 for Windows (GraphPad, Boston, MA, USA. Data were presented as the mean value and standard error of the mean (SEM). Differences were considered statistically significant for $p < 0.05$ ($p < 0.05$ *; $p < 0.01$ **; $p < 0.001$ ***; $p < 0.0001$ ****).

3. Results and Discussion

In this work, we aimed to study the antiherpetic activity of a root exudate of *Solanum lycopersicum* in vitro (named tomato extract). Initially, we focused on HSV-1, an alpha-herpesvirus highly transmissible and widespread in the population [32,33]. First, the organic extract was prepared from the root exudates of the plants, as described in the materials and methods section. Subsequently, its impact on cellular viability was assessed using a standard MTT assay on uninfected VERO cells, treated with increasing extract concentrations (10–400 μg/mL) or an equal volume of control vehicle (CTRL, DMSO/H_2O mixture 1:1). The results, depicted in Figure 2A, revealed that the half-maximal cytotoxic concentration (CC_{50}) after 48 h of treatment exceeded 400 μg/mL, indicating a lack of significant cytotoxicity at the tested concentrations. To evaluate the potential antiviral activity of the tomato root exudate, we first performed a virus yield reduction assay by treating VERO cells in the presence of serial dilutions of the exudate before, during, and after viral infection to generate a dose–response curve. The extent of HSV-1 replication was then assessed by titrating the infectivity of both supernatants and cell-associated viruses combined through a standard plaque assay in VERO cells. The results presented in Figure 2B demonstrated that the exudate was endowed with anti-HSV-1 activity with the half-maximal inhibitory concentration (EC_{50}) value of 25.57 (±8.51) μg/mL.

Based on the above results, the SI for HSV-1 is >15.64. Noteworthily, at the highest non-toxic concentration of tomato extract (400 μg/mL), the infectious virus titer was reduced to $\sim10^5$ PFU/mL, which corresponds to a reduction of over 99% when compared to the vehicle control. Therefore, this concentration was employed in the subsequent experiments. The widely employed antiviral drug ACV was included as a positive control (44.4 μM [34]). As expected, its presence resulted in a complete reduction in viral replication (Figure 2B). To further confirm the antiviral activity, we examined the impact of the treatment on viral protein expression by Western blot analysis. Immunoblotting with specific antibodies was performed to analyze the expression patterns of viral proteins, particularly immediate early/early (ICP4) and late (gD) viral products. A noticeable decrease in viral protein levels was observed at each time point in cells treated with tomato exudate or ACV (Figure 2C). These results suggest that the root exudate interferes with a molecular event that occurs in the early stages of the HSV-1 replication cycle. To further analyze the impact of the tomato exudate on viral DNA replication and the production of new viral genomes, we performed a quantitative real-time PCR (qPCR) analysis. As depicted in Figure 2D, a significant reduction in intracellular copies of the HSV-1 genome was observed after 24 h of treatment, providing additional evidence for the inhibitory impact of the root exudate on viral replication.
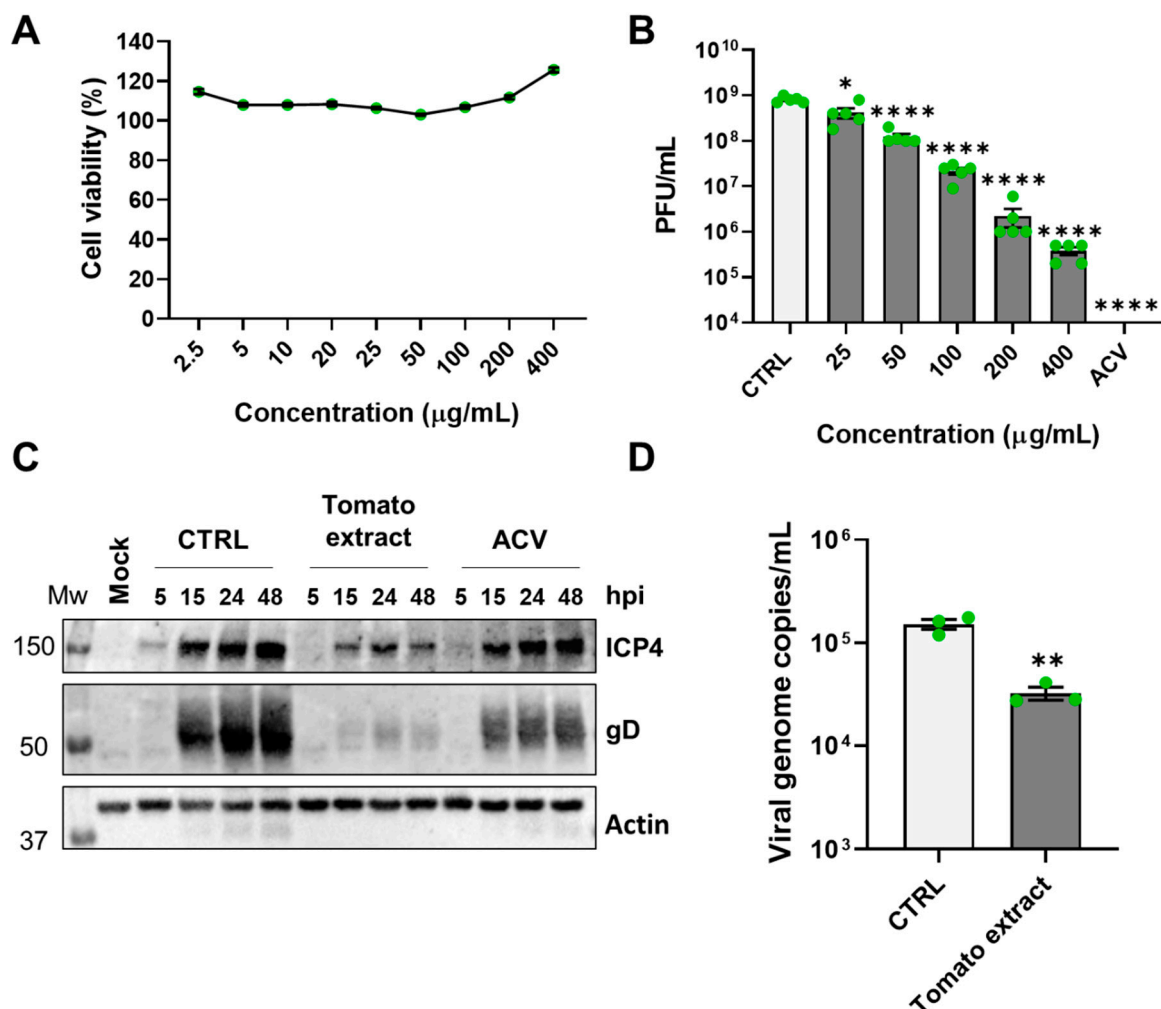
Figure 2. Antiviral activity of tomato extract against HSV-1. (**A**) VERO cells were treated with different concentrations of the exudate or the same amount of vehicle solution (CTRL). Forty-eight hours after treatment, cell viability was determined using the MTT assay. Data are expressed as mean value percent cell viability vs. vehicle control cells (set at 100%). Bars represent the means ± SEM from three independent experiments. (**B**) VERO cells were pre-treated with serial concentrations of tomato extract or

CTRL for 1 h. Subsequently, cells were infected with HSV-1 (MOI 0.1), and after the virus adsorption, the viral inoculum was removed; cultures were exposed to the extract or ACV during the infection and for 48 h thereafter. The extent of HSV-1 replication was then assessed by titrating the infectivity of the cell extracts and supernatants combined using a standard plaque assay. Histograms were obtained by plotting the mean plaque counts for each dilution expressed as PFU/mL. Bars represent the means and $\pm$ SEM from five independent experiments ($p < 0.05$ *, $p < 0.0001$ ****, unpaired *t*-test tomato extract vs. CTRL). (**C**) VERO cells were treated with the exudate (400 µg/mL) or with an equal volume of CTRL 1 h before infection and for the entire duration of the infection and infected with HSV-1 at an MOI of 1. Samples were collected at the indicated time points, lysed, and subjected to Western blot analyses. ACV was used as a reference drug. Membranes were stained with the indicated antibodies. (**D**) VERO cells were treated with the tomato extract (400 µg/mL) or with the same volume of CTRL and infected with HSV-1 (MOI 1). After 24 h, DNA was extracted from infected cells, and the number of HSV-1 genomes was quantified by qPCR. To determine the number of viral DNA genomes, the primers were used to amplify a segment of the gE gene, and the cellular housekeeping gene GAPDH was used to normalize viral genome counts. Bars represent the means $\pm$ SEM from three independent experiments ($p < 0.01$ **, unpaired *t*-test tomato extract vs. CTRL).

To determine whether the antiviral activity of *Solanum lycopersicum* was limited to HSV-1 or encompassed other herpesviruses, we investigated its efficacy on the replication of HCMV, which belongs to the *Betaherpesvirinae* subfamily (Figure 3). An MTT viability assay was conducted on HFF cells after 144 h of treatment to establish the CC_{50} dose, which was calculated to be 296.00 ($\pm$80) µg/mL (Figure 3A). Through a virus yield reduction assay, performed with serial dilutions of root exudate, we confirmed the antiviral activity of the compound also against HCMV, with an EC_{50} value of 9.17 ($\pm$0.65) µg/mL (Figure 3B). The SI for HCMV is 32.28. GCV (25 µM [35]) was included as a positive control.

Similarly to the approach taken for HSV-1, cells underwent Western blot and qPCR analysis after exposure to the extract at concentrations of 100 µg/mL (highly effective non-toxic concentrations, over 99% inhibition). Western blot analysis revealed a decrease in viral protein expression, including immediate early (IEA), early–late (pp65), and late (pp28) proteins, suggesting an overall inhibitory effect on HCMV replication (Figure 3C). Finally, we assessed the extent of intracellular viral genome replication upon treatment with the extract by a qPCR analysis at 72 hpi. Consistently, the results shown in Figure 3D highlight a significant reduction in the viral genome copy number compared to vehicle-treated samples.

Next, to identify which phase of the viral replication cycle was mainly affected by the treatment, serial dilutions of extract were added to VERO or HFF cells at different time schedules: (i) one hour before infection (pre-adsorption stage), (ii) for 2 h during viral adsorption and then removed (adsorption stage), (iii) after the removal of viral inoculum (post-adsorption stage). For each condition, the infected samples were collected at 48 hpi for HSV-1 and 144 hpi for HCMV. Plaque assay titration revealed that the most substantial antiviral effect occurred when the root extract was added after the infection (Figure 4C), compared to the pre-adsorption (Figure 4A) or the adsorption (Figure 4B) conditions.
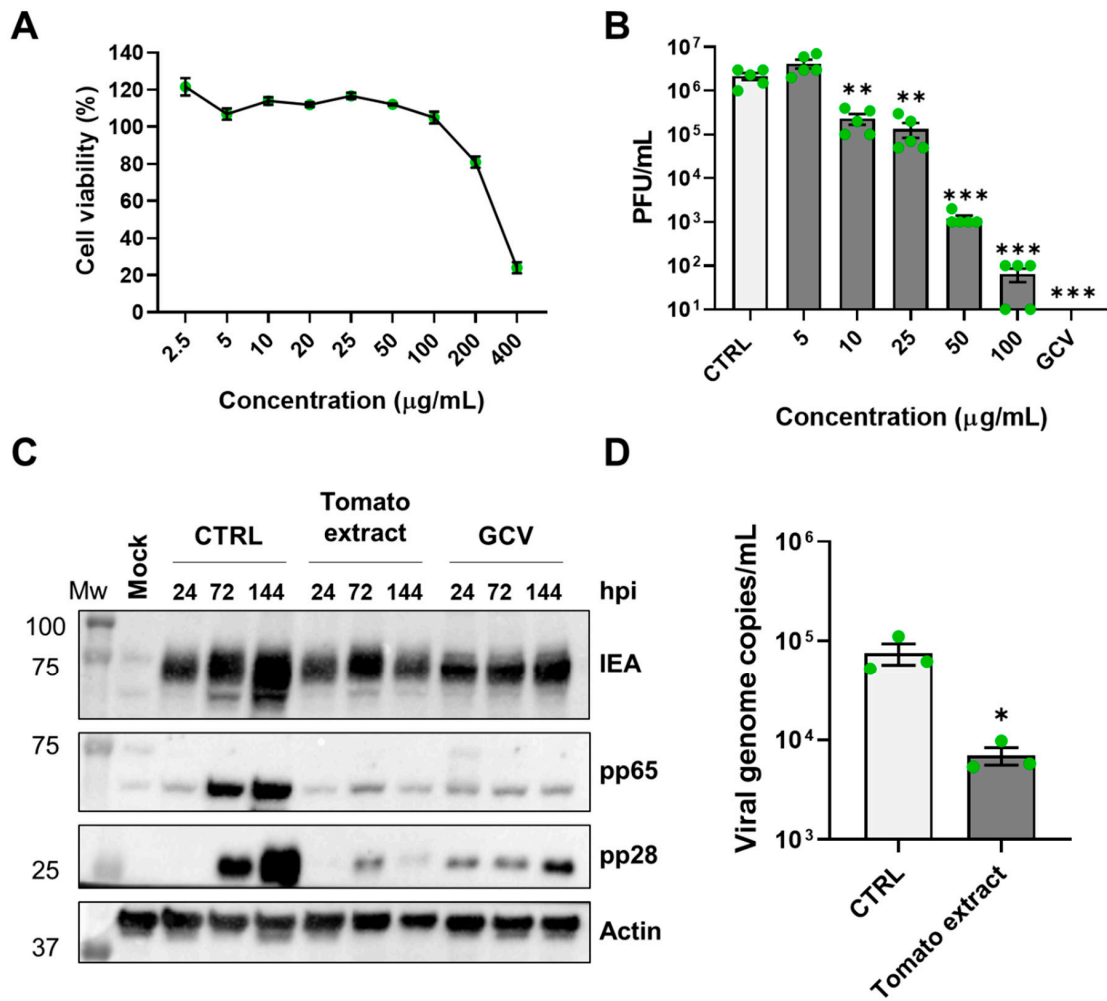
Figure 3. Antiviral activity of the tomato extract against HCMV. (**A**) HFF cells were treated with different concentrations of the exudate or with the same amount of vehicle solution (CTRL). After six days, cell viability was determined using the MTT assay. Data are expressed as mean value percent cell viability vs. CTRL (set at 100%). Bars represent the means $\pm$ SEM from three independent experiments. (**B**) HFF cells were pre-treated with serial concentrations of tomato extract for 1 h. Subsequently, cells were infected with HCMV (MOI 0.1), and after the virus adsorption, the viral inoculum was removed; cultures were exposed to the extract, GCV, or CTRL during the infection and for 144 h thereafter. The extent of HCMV replication was then assessed by titrating the infectivity of cell extract and supernatants combined using a standard plaque assay. Histograms were obtained by plotting the mean plaque counts for each dilution expressed as PFU/mL. Bars represent the means $\pm$ SEM from five independent experiments ($p < 0.01$ **, $p < 0.001$ ***, unpaired t-test tomato extract vs. CTRL). (**C**) HFF cells were treated with tomato extract (100 μg/mL) or with an equal volume of vehicle 1 h before infection and for the entire duration of the infection and infected with HCMV at an MOI of 1. Samples were collected at the indicated time points, lysed, and subjected to Western blot analyses. GCV was used as a reference drug. Membranes were stained with the indicated antibodies. (**D**) HFF cells were treated with the root extract (100 μg/mL) or with the same volume of CTRL and infected with HCMV (MOI 1). After 72 h, DNA was extracted, and the number of HCMV genomes was quantified by qPCR. To determine the number of viral DNA genomes, the primers were used to amplify a segment of the IE1 gene, and the cellular housekeeping gene GAPDH was used to normalize viral genome counts. Bars represent the means $\pm$ SEM from three independent experiments ($p < 0.05$ *, unpaired t-test tomato extract vs. CTRL).
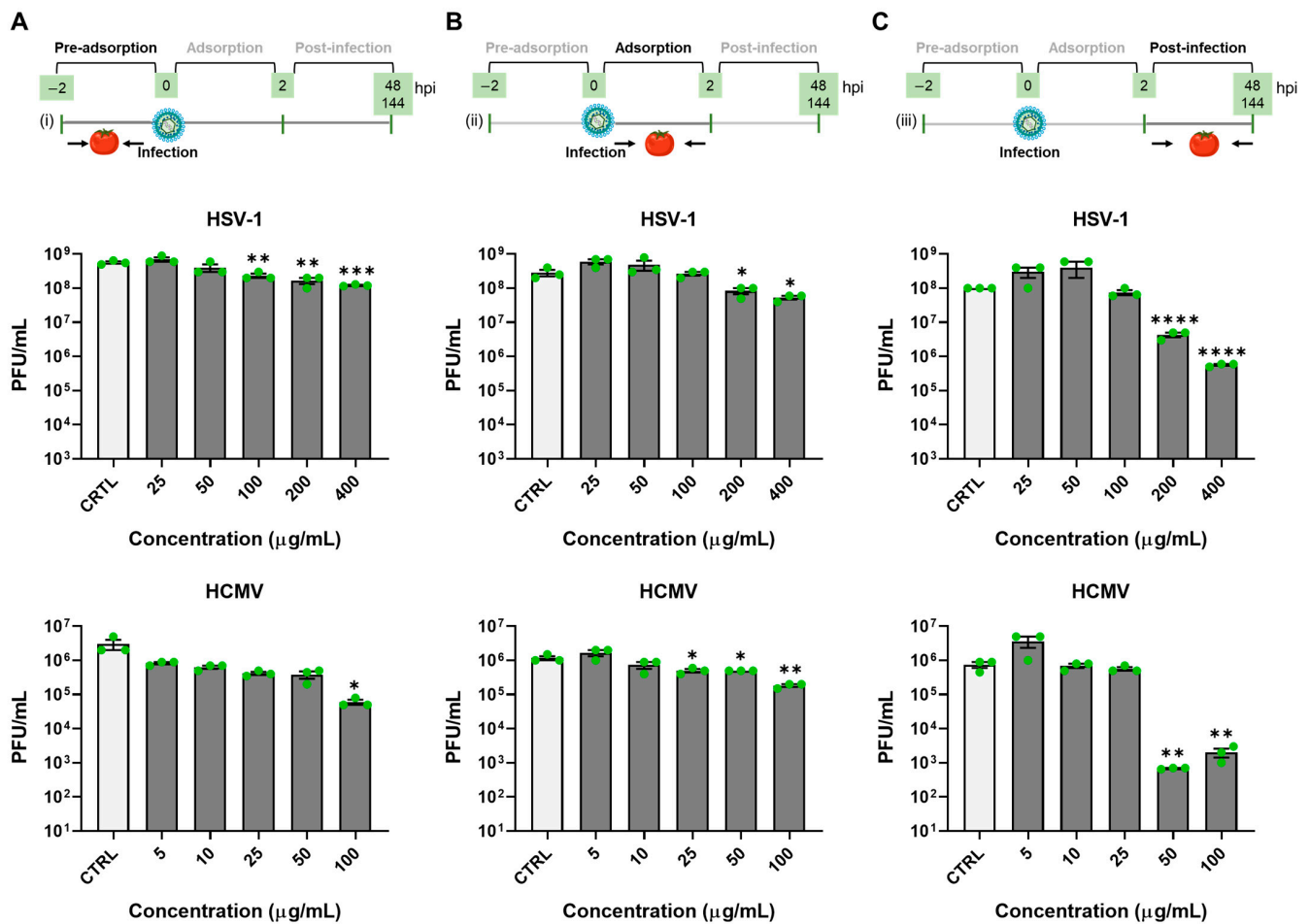
Figure 4. Time of addition assay. VERO or HFF cells were (**A**) pretreated with serial dilutions of tomato extract for 1 h, after which, treatments were removed and cells were infected with HSV-1 (VERO) or HCMV (HFF) (MOI 0.1); (**B**) infected and treated simultaneously for 2 h, after which treatments and viral inoculum were removed; (**C**) infected as described above and, after the removal of inoculum, treated with increasing concentrations of the compound. For all the conditions, cells were incubated for 48 h (VERO) or 144 h (HFF); then, samples were harvested, and infectivity titers were determined by a standard plaque assay. Histograms were obtained by plotting the mean plaque counts for each dilution expressed as PFU/mL. Bars represent the means $\pm$ SEM from three independent experiments ($p < 0.05$ *, $p < 0.01$ **, $p < 0.001$ ***, $p < 0.0001$ ****, unpaired t-test tomato extract vs. CTRL).

Our results align with prior research that underscores the use of various Solanum-genus plants, including *Solanum dulcamara*, *Solanum lyratum*, and *Solanum nigrum*, as traditional anti-herpes agents since ancient times [36]. Importantly, our study extends this activity for the first time to HCMV, representing another member of the *Herpesviridae* family. Studies indicate that Solanum steroidal glycosides, particularly spirostanol glycosides, inhibit HSV-1. It has been suggested that the activity is influenced by the type of oligosaccharide moiety, but the underlying mechanism remains unclear [36]. Additionally, extracts from *S. paniculatum* leaves demonstrated efficacy against HSV-1 in a VERO cell in vitro model, albeit with a lower SI compared to our product. In this context, the mechanism of action has not been elucidated [37]. Notably, *Solanaceae* glycoalkaloids insert glycones into the viral envelope, causing HSV-1 virion leakage [26]. While we cannot completely rule out a similar mechanism for root exudate extracts, our observations suggest only minimal inhibition when the compound is added during viral pre-adsorption and adsorption (i.e., attachment and entry phases). Since the primary inhibitory effect of the extract

was prominently observed when added post-infection, we can infer that the root extract interferes with a molecular event during the herpesvirus replication stage. These findings are consistent with viral protein expression and qPCR results (Figures 2 and 3, panels C and D) and align with earlier studies on DENV [24] and CHIKV [25] viral models.

Finally, the phytochemical composition of the *Solanum lycopersicum* root exudate was investigated through mass spectrometry. Specifically, electrospray ionization (ESI-MS) was employed, enabling the acquisition of mass spectra with a low degree of fragmentation and the qualitative characterization of the complex mixture, consisting of small chemicals and biomolecular components [38]. The full-scan positive ion ESI-MS spectrum is depicted in Figure 5, with detailed information on the major components presented in Table 1.
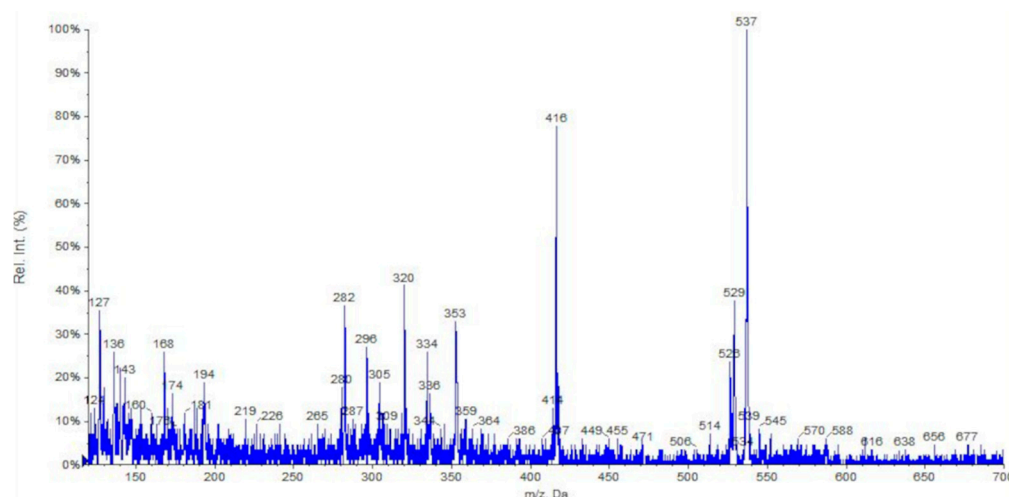
Figure 5. Full-scan positive ion ESI-MS spectrum of a solution of tomato root exudate. Solution infused: 1.0 mg/mL in acetonitrile + 0.1% formic acid.

Table 1. Identification of phytochemicals of tomato root exudate components. Analytically significant ions (*m/z*) are reported.

Compound	Molecular Formula	M.W. (g/mol)	Ionized Adduct	Signal (*m/z*)
Lycopene	$C_{40}H_{56}$	536.88	$[M + H]^+$	537
β-Carotene	$C_{40}H_{56}$	536.88	$[M + H]^+$	537
α-Tomatine	$C_{50}H_{83}NO_{21}$	1034.18	$[M + H + Na]^{2+}$	529
Lycoperoside H	$C_{50}H_{83}NO_{22}$	1049.54	$[M + 2H]^{2+}$	525
β-Sitosterol	$C_{29}H_{50}O$	414.72	$[M + H]^+$	416
Tomatidine	$C_{27}H_{45}NO_2$	415.66	$[M + H]^+$	416
Glc*N*Ac-(1→*N*)-Asn	$C_{12}H_{21}N_3O_8$	335.31	$[M + NH_4]^+$	353
Myricetin	$C_{15}H_{10}O_8$	318.04	$[M + NH_4]^+$	336 [a]
			$[M + H + NH_4]^{2+}$	168
Isorhamnetin	$C_{16}H_{12}O_7$	316.26	$[M + NH_4]^+$	334
Quercetin	$C_{15}H_{10}O_7$	302.24	$[M + NH_4]^+$	320
Lutein	$C_{40}H_{56}O_2$	568.87	$[M + H + Na]^{2+}$	296
Kaempferol	$C_{15}H_{10}O_6$	286.23	$[M + H]^+$	287 [a]
Phytoene	$C_{40}H_{64}$	544.95	$[M + H + NH_4]^{2+}$	282
Phytofluene	$C_{40}H_{62}$	542.94	$[M + H + NH_4]^{2+}$	280 [a]
AHYP	$C_7H_{11}NO_4$	173.17	$[M + H]^+$	174 [a]
Homocysteine	$C_4H_9NO_2S$	135.18	$[M + H]^+$	136

[a] Low-abundance ions.

Five main classes of biologically derived compounds were identified in the ESI-MS spectrum belonging to different substances (see Table 1) commonly found in tomato extracts: carotenoids, glycoalkaloids, phytosterols, flavonoids, and amino acids [39,40]. The

first class, carotenoids, includes the typical fragment of ionized tetraterpene derivatives lycopene and β-carotene (M.W. 536.88 g/mol, m/z = 537 [M + H]$^+$), while doubly charged adducts can be found for lutein (M.W. 568.87 g/mol, m/z = 296 [M + H + Na]$^{2+}$), phytoene (M.W. 544.95 g/mol, m/z = 282 [M + H + NH$_4$]$^{2+}$), and phytofluene (M.W. 542.94 g/mol, m/z = 280 [M + H + NH$_4$]$^{2+}$). Glycoalkaloid derivatives identified were α-tomatine, with the molecular fragment at m/z = 529 which might result from the formation of a doubly charged adduct (M.W. 1034.18 g/mol, [M + H + Na]$^{2+}$), its corresponding aglycone tomatidine (M.W. 415.66 g/mol, m/z = 416 [M + H]$^+$), and lycoperoside H (M.W. 1049.54 g/mol, m/z = 525 [M + 2H]$^{2+}$). The ionized adduct at m/z = 416 can be assigned to the phytosterol derivative β-sitosterol (M.W. 414.72 g/mol, [M + H]$^+$). The fourth class of polyphenolic compounds (flavonoids) identified in the tomato root exudate includes myricetin (M.W. 318.04 g/mol, m/z = 336 [M + NH$_4$]$^+$ and m/z = 168 [M + H + NH$_4$]$^{2+}$), isorhamnetin (M.W. 316.26 g/mol, m/z = 334 [M + NH$_4$]$^+$), quercetin (M.W. 302.24 g/mol, m/z = 320 [M + NH$_4$]$^+$), and kaempferol (M.W. 286.23 g/mol, m/z = 287 [M + H]$^+$). Lastly (glyco)amino acid derivatives *N*-acetylglucosamine-asparagine (Glc*N*Ac-(1→*N*)-Asn, M.W. 335.31 g/mol, m/z = 353 [M + NH$_4$]$^+$), *N*-acetyl-L-hydroxyproline (AHYP, M.W. 173.17 g/mol, m/z = 174 [M + H]$^+$), and homocysteine (M.W. 135.18 g/mol, m/z = 136 [M + H]$^+$) were identified.

The results of this qualitative analysis show that the root exudate of *Solanum lycopersicum* contains a number of phytochemicals with recognized antiviral activity. In particular, some key identified phytochemicals in the root exudate possess antiherpetic properties, as demonstrated for lycopene (EC$_{50}$ = 22.86 μg/mL for HSV-1) [41], β-sitosterol (EC$_{50}$ = 2.7 μg/mL for HSV-2) [42], tomatidine [26], and several flavonoids [43,44], including quercetin (EC$_{50}$ = 52.90 μg/mL for HSV-1 and EC$_{50}$ = 70.01 μg/mL for HSV-2) [45,46], kaempferol [47], and myricetin [44]. Furthermore, natural antioxidants, such as bioactive carotenoids (lycopene, β-carotene, lutein, phytoene, phytofluene), phytosterols (β-sitosterol), and flavonoids (quercetin, kaempferol, myricetin,) have a beneficial role in human health and chronic diseases owing to their ability to modulate the activity of specific enzymes or inhibit the production of reactive oxygen species (ROS) acting as free radical scavengers [48–50]. Additionally, it is well known that the pharmacological profile of flavonoids, carotenoids, glycoalkaloids, and phytosterols includes anticancer, anti-inflammatory, anti-allergenic, antithrombotic, antimicrobial, antioxidant, vasodilator, and cardioprotective effects [51–55].

Since phytoextracts are mixtures of secondary metabolites, the pharmacological behavior of plant extracts is often due to the synergic effect of two or more active constituents rather than a single component. Indeed, the results presented in this work can be rationalized assuming that the biologically active compounds detected in the *Solanum lycopersicum* root exudate might play a synergic role in the antiviral activity against herpesviruses. The combination of the antiherpetic activity of the detected phytochemicals with their antioxidant properties and other pharmacological profiles make this extract a promising candidate for the development of the root exudate of *Solanum lycopersicum* as a new combined phytomedicine. Overall, these findings could potentially contribute to progress in the field of antiviral phytotherapy, which has experienced a resurgent interest in the field of antiviral drug discovery owing to the increasing urge to contest the development of drug resistance [56].

4. Conclusions

In conclusion, our research highlights the potential of tomato plants as a natural product exhibiting antiviral activity against herpesviruses. The exudate from *Solanum lycopersicum* root significantly inhibited HSV-1 and HCMV replication in VERO and HFF cells, with EC$_{50}$ values of 25.57 and 9.17 μM, respectively. The SIs of >15.64 for HSV-1 and 32.28 for HCMV imply a substantial therapeutic window, indicating that the drug can effectively inhibit the target while maintaining a relatively low cytotoxic impact on host cells, making it a promising candidate for further preclinical and clinical development. Subsequent protein expression analysis and time-of-addition experiments revealed that the antiviral effect is mainly produced in post-infection conditions, during the viral replication

phase, as no or a limited antiviral effect was detectable for the pre-infection and during-infection treatments. These findings suggest that *Solanum lycopersicum* could be a promising alternative to current antiviral drugs. Further investigation is necessary to understand the specific mechanisms of action, the efficacy in vivo, and the pharmacokinetics of the extract. Finally, it will be crucial to identify the more active molecules within the root exudate responsible for the observed antiviral effects. Nevertheless, this study offers valuable insights into the potential of *Solanum lycopersicum* as a source of natural antiviral agents in the ongoing efforts to combat viral infections and uphold public health safety.

References

1. Zhu, S.; Viejo-Borbolla, A. Pathogenesis and Virulence of Herpes Simplex Virus. *Virulence* **2021**, *12*, 2670–2702. [CrossRef]
2. Gugliesi, F.; Coscia, A.; Griffante, G.; Galitska, G.; Pasquero, S.; Albano, C.; Biolatti, M. Where Do We Stand after Decades of Studying Human Cytomegalovirus? *Microorganisms* **2020**, *8*, E685. [CrossRef]
3. Chayavichitsilp, P.; Buckwalter, J.V.; Krakowski, A.C.; Friedlander, S.F. Herpes Simplex. *Pediatr. Rev.* **2009**, *30*, 119–129, quiz 130. [CrossRef] [PubMed]
4. James, S.H.; Kimberlin, D.W. Neonatal Herpes Simplex Virus Infection: Epidemiology and Treatment. *Clin. Perinatol.* **2015**, *42*, 47–59, viii. [CrossRef]
5. Walti, C.S.; Khanna, N.; Avery, R.K.; Helanterä, I. New Treatment Options for Refractory/Resistant CMV Infection. *Transpl. Int.* **2023**, *36*, 11785. [CrossRef] [PubMed]
6. Chen, S.-J.; Wang, S.-C.; Chen, Y.-C. Antiviral Agents as Therapeutic Strategies Against Cytomegalovirus Infections. *Viruses* **2019**, *12*, 21. [CrossRef] [PubMed]
7. Piperi, E.; Papadopoulou, E.; Georgaki, M.; Dovrat, S.; Bar Illan, M.; Nikitakis, N.G.; Yarom, N. Management of Oral Herpes Simplex Virus Infections: The Problem of Resistance. A Narrative Review. *Oral Dis.* **2023**. [CrossRef] [PubMed]
8. Boswell, Z.; Verga, J.U.; Mackle, J.; Guerrero-Vazquez, K.; Thomas, O.P.; Cray, J.; Wolf, B.J.; Choo, Y.-M.; Croot, P.; Hamann, M.T.; et al. In-Silico Approaches for the Screening and Discovery of Broad-Spectrum Marine Natural Product Antiviral Agents against Coronaviruses. *IDR* **2023**, *16*, 2321–2338. [CrossRef] [PubMed]
9. Newman, D.J.; Cragg, G.M. Natural Products as Sources of New Drugs over the Nearly Four Decades from 01/1981 to 09/2019. *J. Nat. Prod.* **2020**, *83*, 770–803. [CrossRef] [PubMed]
10. Musarra-Pizzo, M.; Pennisi, R.; Ben-Amor, I.; Mandalari, G.; Sciortino, M.T. Antiviral Activity Exerted by Natural Products against Human Viruses. *Viruses* **2021**, *13*, 828. [CrossRef]
11. Lin, L.-T.; Hsu, W.-C.; Lin, C.-C. Antiviral Natural Products and Herbal Medicines. *J. Tradit. Complement. Med.* **2014**, *4*, 24–35. [CrossRef] [PubMed]
12. Stan, D.; Enciu, A.-M.; Mateescu, A.L.; Ion, A.C.; Brezeanu, A.C.; Stan, D.; Tanase, C. Natural Compounds With Antimicrobial and Antiviral Effect and Nanocarriers Used for Their Transportation. *Front. Pharmacol.* **2021**, *12*, 723233. [CrossRef] [PubMed]

13. Shamshirgaran, M.; Maleki, A.; Askari, P.; Yousefi, M.; Malaki Moghadam, H.; Aramjoo, H.; Zare_Bidaki, M. Antibacterial Effects of the Aqueous Extract of Lycopersicon Esculentum Mill Native in South Khorasan of Iran against Four Species Associated with Gastrointestinal Infections. *J. Basic Res. Med. Sci.* **2020**, *7*, 1–6.

14. Heber, D.; Lu, Q.-Y. Overview of Mechanisms of Action of Lycopene. *Exp. Biol. Med.* **2002**, *227*, 920–923. [CrossRef] [PubMed]

15. Tilahun, S.; Park, D.S.; Seo, M.H.; Jeong, C.S. Review on Factors Affecting the Quality and Antioxidant Properties of Tomatoes. *AJB* **2017**, *16*, 1678–1687. [CrossRef]

16. Kumar, M.; Tomar, M.; Bhuyan, D.J.; Punia, S.; Grasso, S.; Sá, A.G.A.; Carciofi, B.A.M.; Arrutia, F.; Changan, S.; Singh, S.; et al. Tomato (*Solanum lycopersicum* L.) Seed: A Review on Bioactives and Biomedical Activities. *Biomed. Pharmacother.* **2021**, *142*, 112018. [CrossRef]

17. Nakayasu, M.; Takamatsu, K.; Yazaki, K.; Sugiyama, A. Plant Specialized Metabolites in the Rhizosphere of Tomatoes: Secretion and Effects on Microorganisms. *Biosci. Biotechnol. Biochem.* **2022**, *87*, 13–20. [CrossRef]

18. Kamilova, F.; Kravchenko, L.V.; Shaposhnikov, A.I.; Azarova, T.; Makarova, N.; Lugtenberg, B. Organic Acids, Sugars, and l-Tryptophane in Exudates of Vegetables Growing on Stonewool and Their Effects on Activities of Rhizosphere Bacteria. *MPMI* **2006**, *19*, 250–256. [CrossRef]

19. Simons, M.; Permentier, H.P.; de Weger, L.A.; Wijffelman, C.A.; Lugtenberg, B.J.J. Amino Acid Synthesis Is Necessary for Tomato Root Colonization by Pseudomonas Fluorescens Strain WCS365. *MPMI* **1997**, *10*, 102–106. [CrossRef]

20. Zboralski, A.; Filion, M. Genetic Factors Involved in Rhizosphere Colonization by Phytobeneficial *Pseudomonas* Spp. *Comput. Struct. Biotechnol. J.* **2020**, *18*, 3539–3554. [CrossRef]

21. Sahlin, E.; Savage, G.P.; Lister, C.E. Investigation of the Antioxidant Properties of Tomatoes after Processing. *J. Food Compos. Anal.* **2004**, *17*, 635–647. [CrossRef]

22. Miller, E.C.; Giovannucci, E.; Erdman, J.W.; Bahnson, R.; Schwartz, S.J.; Clinton, S.K. Tomato Products, Lycopene, and Prostate Cancer Risk. *Urol. Clin. N. Am.* **2002**, *29*, 83–93. [CrossRef] [PubMed]

23. Story, E.N.; Kopec, R.E.; Schwartz, S.J.; Harris, G.K. An Update on the Health Effects of Tomato Lycopene. *Annu. Rev. Food Sci. Technol.* **2010**, *1*, 189–210. [CrossRef] [PubMed]

24. Diosa-Toro, M.; Troost, B.; van de Pol, D.; Heberle, A.M.; Urcuqui-Inchima, S.; Thedieck, K.; Smit, J.M. Tomatidine, a Novel Antiviral Compound towards Dengue Virus. *Antivir. Res.* **2019**, *161*, 90–99. [CrossRef] [PubMed]

25. Troost, B.; Mulder, L.M.; Diosa-Toro, M.; van de Pol, D.; Rodenhuis-Zybert, I.A.; Smit, J.M. Tomatidine, a Natural Steroidal Alkaloid Shows Antiviral Activity towards Chikungunya Virus in Vitro. *Sci. Rep.* **2020**, *10*, 6364. [CrossRef] [PubMed]

26. Thorne, H.V.; Clarke, G.F.; Skuce, R. The Inactivation of Herpes Simplex Virus by Some Solanaceae Glycoalkaloids. *Antivir. Res.* **1985**, *5*, 335–343. [CrossRef] [PubMed]

27. Santoro, V.; Schiavon, M.; Visentin, I.; Constán-Aguilar, C.; Cardinale, F.; Celi, L. Strigolactones Affect Phosphorus Acquisition Strategies in Tomato Plants. *Plant Cell Environ.* **2021**, *44*, 3628–3642. [CrossRef]

28. Pasquero, S.; Gugliesi, F.; Biolatti, M.; Dell'Oste, V.; Albano, C.; Bajetto, G.; Griffante, G.; Trifirò, L.; Brugo, B.; Raviola, S.; et al. Citrullination Profile Analysis Reveals Peptidylarginine Deaminase 3 as an HSV-1 Target to Dampen the Activity of Candidate Antiviral Restriction Factors. *PLoS Pathog.* **2023**, *19*, e1011849. [CrossRef]

29. Biolatti, M.; Blangetti, M.; D'Arrigo, G.; Spyrakis, F.; Cappello, P.; Albano, C.; Ravanini, P.; Landolfo, S.; De Andrea, M.; Prandi, C.; et al. Strigolactone Analogs Are Promising Antiviral Agents for the Treatment of Human Cytomegalovirus Infection. *Microorganisms* **2020**, *8*, E703. [CrossRef]

30. Biolatti, M.; Blangetti, M.; Baggieri, M.; Marchi, A.; Gioacchini, S.; Bajetto, G.; Arnodo, D.; Bucci, P.; Fioravanti, R.; Kojouri, M.; et al. Strigolactones as Broad-Spectrum Antivirals against β-Coronaviruses through Targeting the Main Protease M^{pro}. *ACS Infect. Dis.* **2023**, *7*, 1310–1318. [CrossRef]

31. Sprague, E.R.; Reinhard, H.; Cheung, E.J.; Farley, A.H.; Trujillo, R.D.; Hengel, H.; Bjorkman, P.J. The Human Cytomegalovirus Fc Receptor gp68 Binds the Fc C_H2-C_H3 Interface of Immunoglobulin G. *J. Virol.* **2008**, *82*, 3490–3499. [CrossRef] [PubMed]

32. Cole, S. Herpes Simplex Virus: Epidemiology, Diagnosis, and Treatment. *Nurs. Clin. N. Am.* **2020**, *55*, 337–345. [CrossRef] [PubMed]

33. Whitley, R.J.; Roizman, B. Herpes Simplex Virus Infections. *Lancet* **2001**, *357*, 1513–1518. [CrossRef] [PubMed]

34. Kumar, A.; De, S.; Moharana, A.K.; Nayak, T.K.; Saswat, T.; Datey, A.; Mamidi, P.; Mishra, P.; Subudhi, B.B.; Chattopadhyay, S. Inhibition of Herpes Simplex Virus-1 Infection by MBZM-N-IBT: In Silico and in Vitro Studies. *Virol. J.* **2021**, *18*, 103. [CrossRef] [PubMed]

35. Gentry, B.G.; Drach, J.C. Metabolism of Cyclopropavir and Ganciclovir in Human Cytomegalovirus-Infected Cells. *Antimicrob. Agents Chemother.* **2014**, *58*, 2329–2333. [CrossRef]

36. Ikeda, T.; Ando, J.; Miyazono, A.; Zhu, X.H.; Tsumagari, H.; Nohara, T.; Yokomizo, K.; Uyeda, M. Anti-Herpes Virus Activity of Solanum Steroidal Glycosides. *Biol. Pharm. Bull.* **2000**, *23*, 363–364. [CrossRef]

37. Valadares, Y.M.; Brandão'a, G.C.; Kroon, E.G.; Filho, J.D.S.; Oliveira, A.B.; Braga, F.C. Antiviral Activity of Solanum Paniculatum Extract and Constituents. *Z. Naturforsch C J. Biosci.* **2009**, *64*, 813–818. [CrossRef]

38. Kumar, B.R. Application of HPLC and ESI-MS Techniques in the Analysis of Phenolic Acids and Flavonoids from Green Leafy Vegetables (GLVs). *J. Pharm. Anal.* **2017**, *7*, 349–364. [CrossRef]

39.   Ali, M.Y.; Sina, A.A.I.; Khandker, S.S.; Neesa, L.; Tanvir, E.M.; Kabir, A.; Khalil, M.I.; Gan, S.H. Nutritional Composition and Bioactive Compounds in Tomatoes and Their Impact on Human Health and Disease: A Review. *Foods* **2020**, *10*, 45. [CrossRef] [PubMed]

40.   Moco, S.; Bino, R.J.; Vorst, O.; Verhoeven, H.A.; de Groot, J.; van Beek, T.A.; Vervoort, J.; de Vos, C.H.R. A Liquid Chromatography-Mass Spectrometry-Based Metabolome Database for Tomato. *Plant Physiol.* **2006**, *141*, 1205–1218. [CrossRef] [PubMed]

41.   Sánchez-Fidalgo, S.; Villegas, I.; Aparicio-Soto, M.; Cárdeno, A.; Rosillo, M.Á.; González-Benjumea, A.; Marset, A.; López, Ó.; Maya, I.; Fernández-Bolaños, J.G.; et al. Effects of Dietary Virgin Olive Oil Polyphenols: Hydroxytyrosyl Acetate and 3, 4-Dihydroxyphenylglycol on DSS-Induced Acute Colitis in Mice. *J. Nutr. Biochem.* **2015**, *26*, 513–520. [CrossRef]

42.   Toujani, M.M.; Rittà, M.; Civra, A.; Genovese, S.; Epifano, F.; Ghram, A.; Lembo, D.; Donalisio, M. Inhibition of HSV-2 Infection by Pure Compounds from Thymus Capitatus Extract in Vitro. *Phytother. Res.* **2018**, *32*, 1555–1563. [CrossRef]

43.   Zakaryan, H.; Arabyan, E.; Oo, A.; Zandi, K. Flavonoids: Promising Natural Compounds against Viral Infections. *Arch. Virol.* **2017**, *162*, 2539–2551. [CrossRef]

44.   Lyu, S.-Y.; Rhim, J.-Y.; Park, W.-B. Antiherpetic Activities of Flavonoids against Herpes Simplex Virus Type 1 (HSV-1) and Type 2 (HSV-2) in Vitro. *Arch. Pharm. Res.* **2005**, *28*, 1293–1301. [CrossRef] [PubMed]

45.   Lee, S.; Lee, H.H.; Shin, Y.S.; Kang, H.; Cho, H. The Anti-HSV-1 Effect of Quercetin Is Dependent on the Suppression of TLR-3 in Raw 264.7 Cells. *Arch. Pharm. Res.* **2017**, *40*, 623–630. [CrossRef]

46.   Hung, P.-Y.; Ho, B.-C.; Lee, S.-Y.; Chang, S.-Y.; Kao, C.-L.; Lee, S.-S.; Lee, C.-N. Houttuynia Cordata Targets the Beginning Stage of Herpes Simplex Virus Infection. *PLoS ONE* **2015**, *10*, e0115475. [CrossRef] [PubMed]

47.   Periferakis, A.; Periferakis, A.-T.; Troumpata, L.; Periferakis, K.; Scheau, A.-E.; Savulescu-Fiedler, I.; Caruntu, A.; Badarau, I.A.; Caruntu, C.; Scheau, C. Kaempferol: A Review of Current Evidence of Its Antiviral Potential. *Int. J. Mol. Sci.* **2023**, *24*, 16299. [CrossRef] [PubMed]

48.   Hossen, M.S.; Ali, M.Y.; Jahurul, M.H.A.; Abdel-Daim, M.M.; Gan, S.H.; Khalil, M.I. Beneficial Roles of Honey Polyphenols against Some Human Degenerative Diseases: A Review. *Pharmacol. Rep.* **2017**, *69*, 1194–1205. [CrossRef] [PubMed]

49.   Agarwal, S.; Rao, A.V. Tomato Lycopene and Its Role in Human Health and Chronic Diseases. *CMAJ* **2000**, *163*, 739–744. [PubMed]

50.   Navarro-González, I.; García-Alonso, J.; Periago, M.J. Bioactive Compounds of Tomato: Cancer Chemopreventive Effects and Influence on the Transcriptome in Hepatocytes. *J. Funct. Foods* **2018**, *42*, 271–280. [CrossRef]

51.   Imran, M.; Ghorat, F.; Ul-Haq, I.; Ur-Rehman, H.; Aslam, F.; Heydari, M.; Shariati, M.A.; Okuskhanova, E.; Yessimbekov, Z.; Thiruvengadam, M.; et al. Lycopene as a Natural Antioxidant Used to Prevent Human Health Disorders. *Antioxidants* **2020**, *9*, 706. [CrossRef]

52.   Zhu, R.; Chen, B.; Bai, Y.; Miao, T.; Rui, L.; Zhang, H.; Xia, B.; Li, Y.; Gao, S.; Wang, X.-D.; et al. Lycopene in Protection against Obesity and Diabetes: A Mechanistic Review. *Pharmacol. Res.* **2020**, *159*, 104966. [CrossRef]

53.   Saini, R.K.; Rengasamy, K.R.R.; Mahomoodally, F.M.; Keum, Y.-S. Protective Effects of Lycopene in Cancer, Cardiovascular, and Neurodegenerative Diseases: An Update on Epidemiological and Mechanistic Perspectives. *Pharmacol. Res.* **2020**, *155*, 104730. [CrossRef] [PubMed]

54.   Sakemi, Y.; Sato, K.; Hara, K.; Honda, M.; Shindo, K. Biological Activities of Z-Lycopenes Contained in Food. *J. Oleo Sci.* **2020**, *69*, 1509–1516. [CrossRef] [PubMed]

55.   Zhang, Z.; Li, Q.; Liu, F.; Wang, D. Lycoperoside H Protects against Diabetic Nephropathy via Alteration of Gut Microbiota and Inflammation. *J. Biochem. Mol. Toxicol.* **2022**, *36*, e23216. [CrossRef] [PubMed]

56.   Thomas, E.; Stewart, L.E.; Darley, B.A.; Pham, A.M.; Esteban, I.; Panda, S.S. Plant-Based Natural Products and Extracts: Potential Source to Develop New Antiviral Drug Candidates. *Molecules* **2021**, *26*, 6197. [CrossRef]
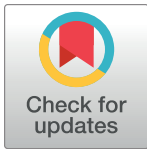
PLOS PATHOGENS

Citrullination profile analysis reveals peptidylarginine deaminase 3 as an HSV-1 target to dampen the activity of candidate antiviral restriction factors

Selina Pasquero[1]°, Francesca Gugliesi[1]°, Matteo Biolatti[1], Valentina Dell'Oste[1], Camilla Albano[1], Greta Bajetto[1,2], Gloria Griffante[3], Linda Trifirò[1], Bianca Brugo[1], Stefano Raviola[2,3], Davide Lacarbonara[2,3], Qiao Yang[1,4], Sen Sudeshna[5], Leonard Barasa[5], Hafeez Haniff[5], Paul R. Thompson[5], Santo Landolfo[1], Marco De Andrea[1,2] *

1 Department of Public Health and Pediatric Sciences, University of Turin – Medical School, Turin, Italy, 2 CAAD Center for Translational Research on Autoimmune and Allergic Disease, University of Piemonte Orientale, Novara Medical School, Novara, Italy, 3 Department of Translational Medicine, University of Piemonte Orientale, Novara, Italy, 4 Avian Disease Research Center, College of Veterinary Medicine, Sichuan Agricultural University, Wenjiang, Chengdu City, P.R. China, 5 Department of Biochemistry and Molecular Pharmacology, UMass Medical School, Worcester, Massachusetts, United States of America

° These authors contributed equally to this work.
* marco.deandrea@unito.it

Abstract

Herpes simplex virus 1 (HSV-1) is a neurotropic virus that remains latent in neuronal cell bodies but reactivates throughout an individual's life, causing severe adverse reactions, such as herpes simplex encephalitis (HSE). Recently, it has also been implicated in the etiology of Alzheimer's disease (AD). The absence of an effective vaccine and the emergence of numerous drug-resistant variants have called for the development of new antiviral agents that can tackle HSV-1 infection. Host-targeting antivirals (HTAs) have recently emerged as promising antiviral compounds that act on host-cell factors essential for viral replication. Here we show that a new class of HTAs targeting peptidylarginine deiminases (PADs), a family of calcium-dependent enzymes catalyzing protein citrullination, exhibits a marked inhibitory activity against HSV-1. Furthermore, we show that HSV-1 infection leads to enhanced protein citrullination through transcriptional activation of three PAD isoforms: PAD2, PAD3, and PAD4. Interestingly, PAD3-depletion by specific drugs or siRNAs dramatically inhibits HSV-1 replication. Finally, an analysis of the citrullinome reveals significant changes in the deimination levels of both cellular and viral proteins, with the interferon (IFN)-inducible proteins IFIT1 and IFIT2 being among the most heavily deiminated ones. As genetic depletion of IFIT1 and IFIT2 strongly enhances HSV-1 growth, we propose that viral-induced citrullination of IFIT1 and 2 is a highly efficient HSV-1 evasion mechanism from host antiviral resistance. Overall, our findings point to a crucial role of citrullination in subverting cellular responses to viral infection and demonstrate that PAD inhibitors efficiently suppress HSV-1 infection *in vitro*, which may provide the rationale for their repurposing as HSV-1 antiviral drugs.

Author summary

HSV-1 is a common human pathogen that infects approximately 70% of the population for life. After infection, the virus remains dormant in sensory neurons but reactivates periodically, releasing virus particles that move down the axon to infect skin epithelial cells, where it can be spread to other individuals. Depending on the recipient's immune condition, primary infection or reactivation can cause a wide range of symptoms. However, accessible HSV-1 antivirals are currently limited, and most of them target viral DNA polymerase, thus leading to the emergence of drug-resistant viral infections. Citrullination, an irreversible protein alteration driven by peptidylarginine deiminases (PADs), has been linked to various inflammation-related events, including viral infections. In our study, we provide evidence that HSV-1 triggers citrullination of multiple proteins, some of which possess anti-viral properties, thereby promoting viral fitness. Notably, we show that specifically targeting the PAD3 isoform dramatically reduces viral replication. Overall, our study sheds light on the potential of using host PAD inhibitors for developing antiviral agents against HSV-1.

Introduction

Herpes simplex virus 1 (HSV-1) is a widespread and highly infectious alpha-herpesvirus, with seroprevalence reaching up to 75% in the adult population [1]. Primarily transmitted by oral-oral contact and often causing orolabial herpes, commonly known as "cold sores", HSV-1 can persist latently and lifelong in the local ganglia of its host. In response to a variety of diverse stimuli, the virus can reactivate to produce new virus progeny. Reactivation results in clinical signs and symptoms ranging from painful, but self-limited, infections of the oral or genital mucosa to severe infections of the eye or life-threatening infections in immuno-compromised hosts or newborns [2]. Additionally, recent evidence suggests that HSV-1 may be involved in the etiology of Alzheimer's disease (AD) [3,4]. Although numerous vaccine candidates have been investigated in clinical trials, no licensed vaccine is available to prevent HSV infections [5].

Acute HSV infections can be treated with antiviral drugs that inhibit its DNA-polymerase. Even though these drugs have been approved and used for decades, their effectiveness has been hampered by the emergence of drug resistant HSV strains [6]. A new strategy to develop antiviral drugs that can overcome these obstacles is to target the host cell factors that participate in viral replication. These drugs are known as host-targeting antivirals (HATs) [7,8].

An example of a host cell factor that can be targeted by HATs is peptidylarginine deiminases (PADs). PADs are a family of enzymes that need calcium to work and can change the structure of proteins by a process called citrullination. This post-translational modification (PTM), also called deimination, is a process in which the guanidinium group of a peptidyl-arginine is hydrolyzed to form peptidyl-citrulline, a non-genetically coded amino acid [9,10]. Five PAD isozymes (PADs 1–4 and 6) are expressed in humans, with a unique distribution in various tissues [9,11,12], and their dysregulation has been associated with various inflammatory conditions and neurodegenerative disorders, such as multiple sclerosis (MS) and AD [13–18]. Given the involvement of PADs in several pathological settings, several PAD inhibitors have been synthesized in recent years. Some of these compounds, such as Cl-amidine (Cl-A) and its derivative BB-Cl-amidine (BB-Cl) [19–21], can inhibit the activity of all the different isoforms and, as such, are called pan-PAD inhibitors [19,22]. Other available inhibitors are

highly specific for the different PAD-isozymes, like AFM-30 for PAD2, CAY10727, and HF4 for PAD3, and GSK199 for PAD4 [23,24].

There is growing evidence of a link between PAD dysregulation and viral infections. Specifically, Arisan and colleagues [25] have recently shown that SARS-CoV-2 infection can modulate PADI gene expression, especially in lung tissues. In addition, we have recently demonstrated an *in vitro* antiviral activity of PAD inhibitors against betacoronaviruses [26]. It has also been found that the antiviral activity of the LL37 protein is weakened by human rhinovirus-induced citrullination [27], and that sera from rheumatoid arthritis (RA) patients specifically recognize artificially citrullinated Epstein-Barr virus proteins [28,29]. Finally, we have demonstrated that another member of the *Herpesviridae* family, human cytomegalovirus (HCMV), upregulates two members of the PAD family (*i.e.*, PAD2 and PAD4) to promote viral fitness, while PAD-inhibitors significantly dampen HCMV replication *in vitro* [30].

Here we report that HSV-1 can alter the protein citrullination profile in different cell lines upon infection, and that this function is mediated by the specific activation of PAD3. Furthermore, by analyzing the citrullinome profile, we also identify IFIT1 and IFIT2 as potential restriction factors for HSV-1 replication. Our findings suggest that: i) HSV-1 replication can be blocked by a new type of HTAs, namely PAD inhibitors, with PAD3 and its specific inhibitor being key players, and ii) HSV-1 manipulates IFIT1/2 to enhance its replication rate.

The potential impact of peptidylarginine deiminases as novel targets for antiviral therapy against HSV-1 are further discussed below.

Results

Pan-PAD inhibitors block HSV-1 replication

We have previously shown that HCMV triggers PAD-mediated citrullination to enhance its replication [30]. To test whether this feature would apply to other herpesviruses, we first measured total protein citrullination in human foreskin fibroblasts (HFFs) upon HSV-1 infection (MOI 1) at different time points. We used electrophoresis to analyze the protein lysates incubated with the citrulline-specific probe Rh-PG. HSV-1-infection increased and altered the pattern of total protein citrullination in lysates from infected *vs* uninfected mock cells, starting from 16 h post-infection (hpi) (Fig 1A, left panel). In particular, we observed a specific enrichment of bands corresponding to proteins with molecular weights higher than 75 kDa, whereas the total amount of proteins remained unchanged, as shown by the similar blue Coomassie staining at different time points (Fig 1A, right panel).

Since citrullination is catalyzed by the PAD family of enzymes [31], we tested whether the cell-permeable pan-PAD inhibitors Cl-amidine (Cl-A) and BB-Cl-amidine (BB-Cl) would affect HSV-1 replication. For this purpose, we assessed viral plaque formation in HSV-1-infected HFFs (MOI 1) treated for 1 h before infection with increasing concentrations of Cl-A (25–200 μM; Fig 1B) or BB-Cl (0.6–5 μM; Fig 1C). After 24 h of continuous exposure to the inhibitors, we observed a dose-dependent decrease in the number of viral particles in all treated cells. The IC50 values of Cl-A and BB-Cl were ~61 μM and ~0.7 μM, respectively, which is consistent with our previous results [30]. Notably, 100 μM Cl-A and 2.5 μM BB-Cl were able to significantly reduce the virus yield by approximately 1 log. We also assessed cell viability using the 3-(4,5-dimethylthiazol-2-yl)-2,5-diphenyl tetrazolium bromide (MTT) assay in cells treated under the same conditions and found that the drugs were not cytotoxic at these concentrations (S1A and S1B Fig). To confirm these results in other cell types, we repeated the experiments in adult retinal pigment epithelial (ARPE-19) and neuroblastoma (SH-SY5Y) cells. We observed similar antiviral effects of Cl-A in both cell lines (S1C and S1D Fig), with only a slight cytotoxic effect in SH-SY5Y cells at higher concentrations (S1A Fig). These

Fig 1. The pan-PAD inhibitors Cl-A and BB-Cl inhibit HSV-1 replication in human fibroblasts. (A) Protein lysates from HFFs infected with HSV-1 (MOI 1 PFU/cell) at different hours post-infection (hpi) or from uninfected HFFs (Mock) were exposed to an Rh-PG citrulline-specific probe (left panel) and subjected to gel electrophoresis to detect citrullinated proteins. An

anti-gD antibody was used to assess HSV-1 infection, while β-actin cellular expression was used for protein loading control. Equal loading was also assessed by Coomassie blue staining (right panel). One representative gel of three independent experiments is shown. (**B, C**) Dose-response curves of the cell-permeable pan-PAD inhibitors Cl-A (B) and BB-Cl (C) in HFFs infected with HSV-1 (MOI 1). Inhibitors were given 1 h prior to virus adsorption and kept throughout the whole experiment. 24 hpi viral plaques were microscopically counted and the number of plaques was plotted as a function of inhibitor concentration. Values are expressed as mean ± SEM of three independent experiments, *P < 0.05, **P < 0.01, ***P < 0.001; one-way ANOVA followed by Bonferroni's post test. (**D**) Protein lysates from uninfected (mock) or infected HFFs (24 hpi) at an MOI of 1 PFU/cell treated with Cl-A (100 μM), BB-Cl (2.5 μM), or vehicle (DMSO) were analyzed by immunoblotting for viral expression (gD) and normalized to β-actin. (**E**) To determine the number of viral DNA genomes in HSV-1-infected HFFs, viral DNA was isolated at 24 hpi and analyzed by qPCR using primers amplifying a region of the gE gene. GAPDH was used to normalize HSV-1 genome counts. Values are expressed as mean ± SEM of three independent experiments. HFFs were infected with HSV-1 (MOI 1 PFU/cell) and then treated with Cl-A (100 μM), BB-Cl (2.5 μM), or vehicle (DMSO), which were given at four different time points as indicated (**F**). At 24 hpi, viral plaques were microscopically counted and expressed as PFU/mL (**G**). Values are expressed as mean ± SEM of three independent experiments, *P < 0.05, **P < 0.01; one-way ANOVA followed by Bonferroni's post test.

findings suggest that citrullination is a common and important event for HSV-1 replication in different cell models.

We next examined the effect of Cl-A and BB-Cl on HSV-1 protein expression and citrullination in HFFs. We treated HSV-infected cells with the same concentrations of the drugs as before and collected them at 24 hpi. We found that both drugs significantly reduced the expression of gD, a late viral protein, compared to the vehicle control (Fig 1D). We also observed that the drugs restored the normal citrullination profile of the cells, which was altered by the infection (S1E Fig). Moreover, the drugs prevented the cytopathic effect caused by the virus (S1F Fig).

To measure viral DNA replication, we performed qPCR analysis on the same cell samples. We detected a slight decrease in viral DNA copies in the drug-treated cells, albeit not as pronounced as that observed in the plaque assay (Fig 1E), suggesting that PAD inhibitors may target multiple stages of the HSV-1 life cycle.

To further investigate this possibility, we tested tree different treatment schedules using Cl-A and BB-Cl (Fig 1F). We either added the drugs before infection and washed them away prior to viral addition (pre-treatment, Pre) or removed them at 2 hpi (pre-treatment + infection, Pre+). We observed only a slight difference in the number of viral particles counted by plaque assay between Pre and Pre+ cells, with neither group achieving a notable reduction in the number of viral particles when compared to Post cells (Fig 1G).

These data suggest that PAD activity plays a less important role in the early phases of infection, such as binding and entry, but becomes essential during the later stages of viral replication.

HSV-1 infection upregulates PAD expression

To determine whether HSV-1-enhanced citrullination was modulated by any of the five known PAD isoforms (*i.e.*, PADs 1–4 and PAD6) and if they played a role in this process, we conducted RT-qPCR analysis in infected HFFs. The results revealed that the *PADI2*, *3*, and *4* genes were all expressed at significantly higher levels in HSV-1-infected HFFs at 16 hpi compared to mock-infected controls (Fig 2A). By contrast, the other PAD isoforms (*PADI1* and *6*) were expressed at very low levels and did not significantly change following HSV-1 infection (S2A Fig). Consistent with their mRNA expression, PAD2, 3, and 4 protein levels were increased upon HSV-1 infection, albeit with different kinetics (Fig 2B). Compared to uninfected cells, HSV-1-infected HFFs showed a significant increase in PAD2 and PAD4 protein expression (at 16 and 24 hpi, respectively) but returned to basal conditions soon after (S2B Fig). Of note, PAD3 protein was undetectable in mock-infected HFFs, but it was strongly
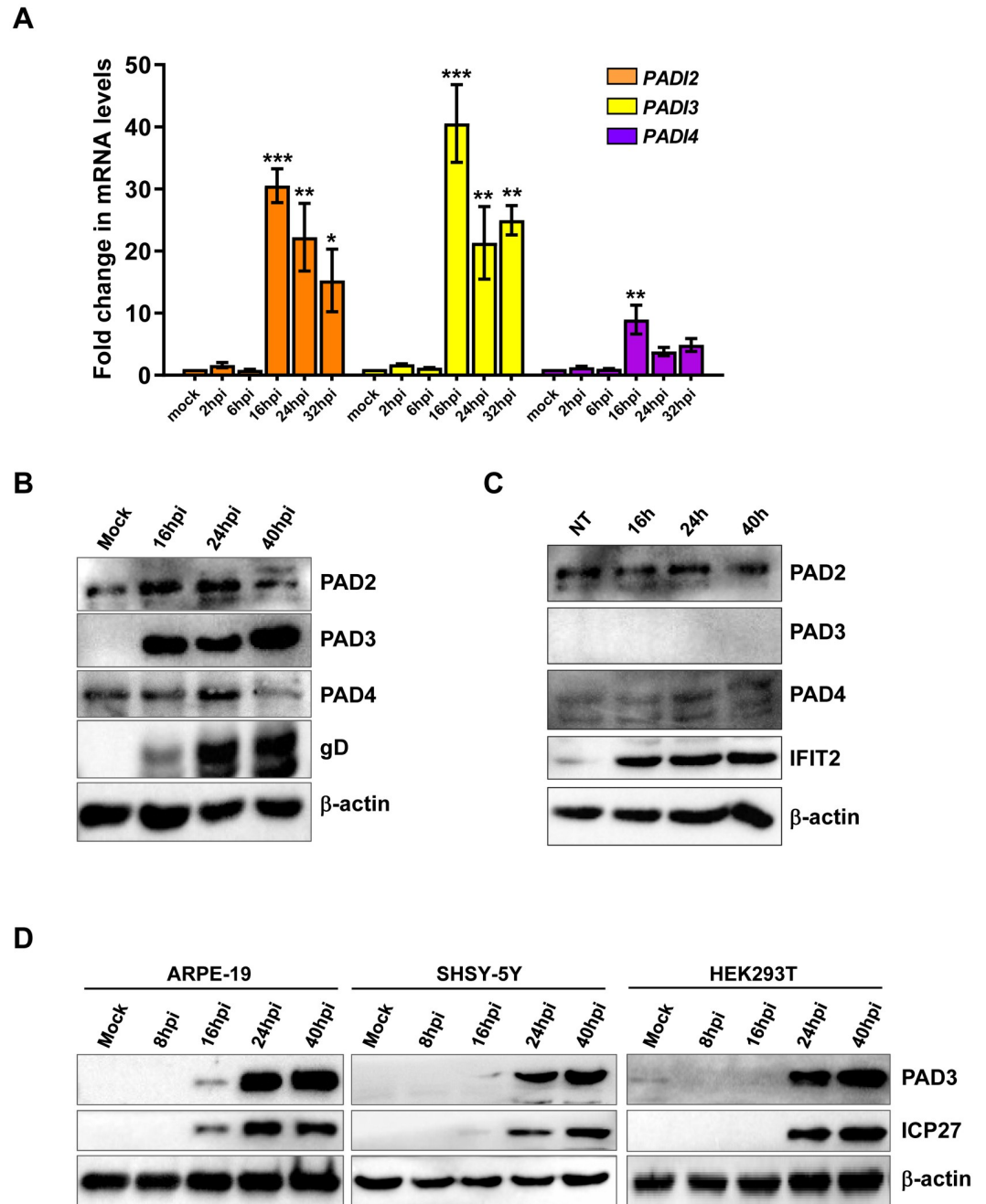
Fig 2. HSV-1 infection upregulates PAD expression in human fibroblasts. (A) mRNA expression levels of *PADI* isoforms by RT-qPCR of HSV-1-infected (8 and 16 hpi) *vs* uninfected (mock) HFFs were normalized to the housekeeping gene glyceraldehyde-3-phosphate dehydrogenase (GAPDH) and expressed as mean fold change ± SEM over mock-infected cells. *$P < 0.05$, **$P < 0.01$, ***$P < 0.001$; one-way ANOVA followed by Bonferroni's post test. (**B**) Western blot analysis of protein lysates from uninfected (mock) or infected HFFs (MOI 1) at different time points using antibodies against PAD2, PAD3, and PAD4. An anti-gD antibody was used to assess HSV-1 infection, while β-actin cellular expression was used for protein loading control. (**C**) Western blot analysis of protein lysates from untreated (NT) or IFN-β-treated (500 U/mL) HFFs using antibodies against PAD2, PAD3, and PAD4. An anti-ICP27 antibody was used to assess HSV-1 infection, while β-actin cellular expression was used for protein loading control. (**D**) Western blot analysis of protein lysates from uninfected (mock) or HSV-1-infected (MOI 1) cells at different time points using antibody against PAD3. An anti-ICP27 antibody was used to assess HSV-1 infection, while β-actin cellular expression was used for protein loading control. Representative blots of three independent experiments are shown.

expressed in HSV-1-infected cells starting from 16 hpi and persisted at later time points, with a pattern similar to that of the late gD viral protein. Moreover, to rule out the possibility that increased PAD expression in HFFs was induced by an interferon (IFN) response to viral infection rather than HSV-1 infection *per se*, cells were treated with IFN-β (500 U/mL) and harvested at different time points after treatment. IFN-β treatment failed to change the basal expression of PAD proteins at any time compared to untreated cells, whereas the interferon-inducible IFIT2 protein showed a significant increase (Figs 2C and S2E).

Finally, to ascertain whether this phenomenon was restricted to HFFs, we extended our RT-qPCR and Western blot analyses of PAD3 to include ARPE-19 and SHSY-5Y cells. HEK293 cells, which are known to basally express PAD3 [32], were analyzed as well. In all the cell lines tested, PAD3 was upregulated during HSV-1 infection (MOI 1), with minor variations between the cell lines (Fig 2D and S2C Fig). This pattern contrasts with our earlier findings in HCMV-infected HFFs [30] and HCoV-43-infected MRC-5 fibroblasts [26], where PAD3 was undetectable under basal conditions and did not show any signs of upregulation, suggesting that different viruses may induce different PAD isoforms.

PAD3 protein levels are induced through a calcium-independent HSV-1-early mechanism

Having established that PAD3 was the most significantly impacted PAD family member by HSV-1 infection, we sought to determine the mechanism underlying *PADI3* transcriptional upregulation in response to viral infection. To this end, we assessed the promoter activity of *PADI3* gene by transiently transfecting HFFs with luciferase reporter plasmids carrying the wild-type promoter region of *PADI3*. At 24 h post transfection, cells were infected with HSV-1. As shown in Fig 3A, HSV-1 infection led to a robust induction of the luciferase activity driven by *PADI3* promoter (~6 fold) and upregulated viral ICP27 expression at 24 hpi (Fig 3B), indicating once more than early stages of infection are critical for the transcriptional activation of *PADI3* gene. As expected, UV-inactivated HSV-1 infection failed to induce both PAD3 and ICP27 protein expression in HFFs compared to cells infected with wild-type HSV-1 (Fig 3B). Furthermore, treatment of HSV-1-infected HFFs with the protein synthesis inhibitor CHX curbed the induction of PAD2, 3, and 4, as well as ICP27, protein expression and total levels of protein citrullination at 24 hpi, without altering total protein levels (Fig 3C and S2E Fig), indicating that *de novo* gene expression is required for PAD protein upregulation and citrullination profile modification during infection. In contrast, treatment with the viral DNA synthesis inhibitor phosphonoformic acid (PFA) only marginally affected the upregulation of PAD3 despite resulting in a dramatic reduction in the synthesis of the late viral protein gD (Fig 3D). Altogether, these data indicate that one or more viral proteins synthetized during the initial stages of infection are involved in PAD3 transcriptional upregulation.

Finally, as HSV-1 infection is known to increase intracellular calcium levels [33], we asked whether PAD3 overexpression could be ascribable to this calcium influx rather than being a direct consequence of upregulated gene expression induced by HSV-1 viral proteins. To rule out this possibility, we employed thapsigargin (TG), an endoplasmic reticulum (ER) stressor known to elevate intracellular calcium levels by interfering with the sarcoplasmic/endoplasmic reticulum Ca^{2+}-ATPase [34]. Specifically, we treated mock-infected HFFs with two concentrations of TG (1.5 and 5 μM) and evaluated PAD3 expression at both the mRNA (Fig 3E) and protein (Fig 3F) levels after 16 h. We found that, in comparison with HSV-1-infected cells (MOI 1; 16 hpi), TG treatment failed to upregulate PAD3 expression at any of the concentrations tested, whereas it significantly upregulated *ATF-6* gene expression (Fig 3F), confirming its efficacy as an ER stressor at both concentrations.
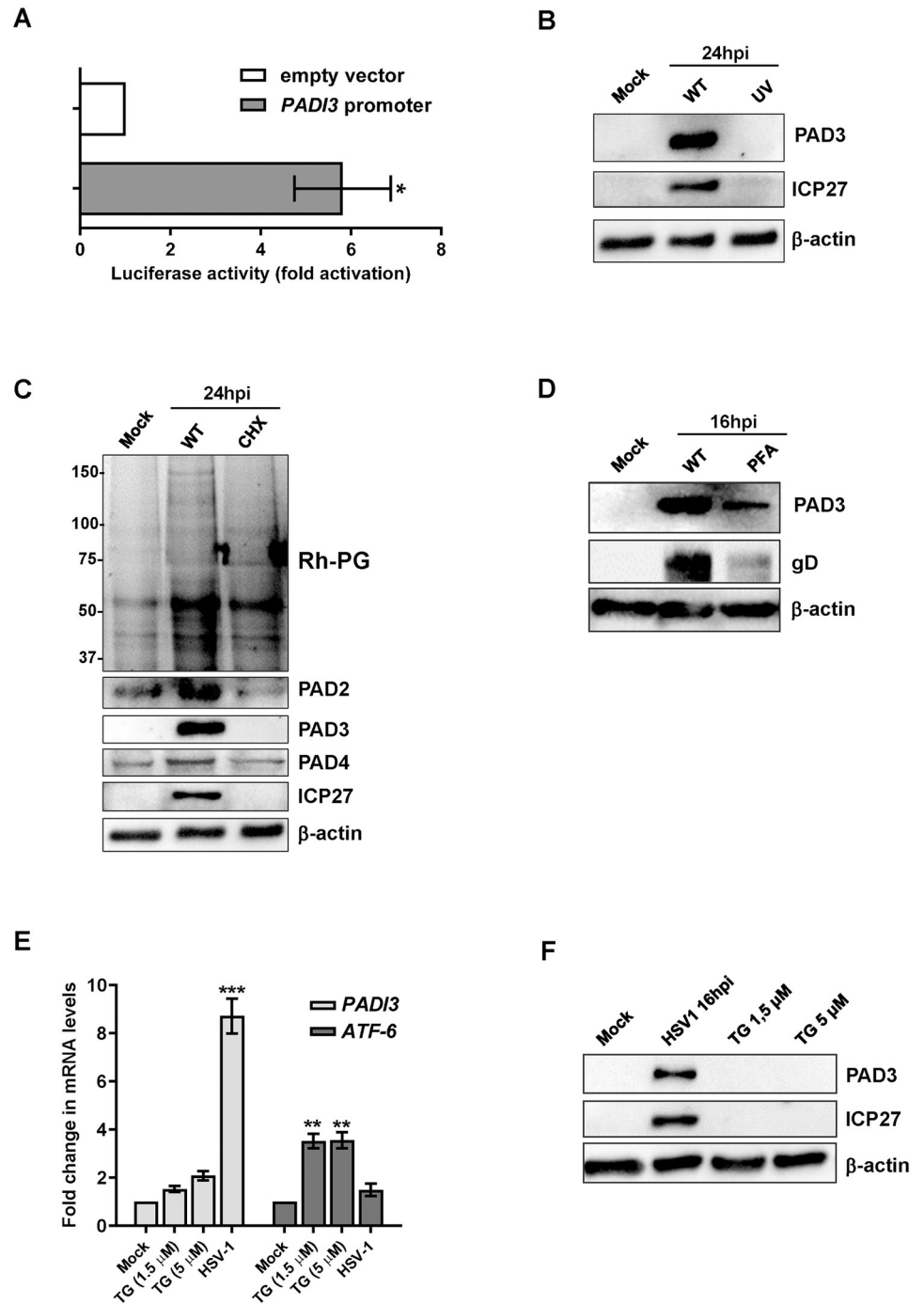
Fig 3. PAD3 induction by HSV-1 early mechanism. (A) HFFs were transiently transfected with luciferase plasmid encoding the wild-type PADI3 promoter region (pGL4.20-PADI3) or the pGL4.20 empty vector. Twenty-four h later, the cells were mock-infected or infected with HSV-1 at an MOI of 1. At 24 hpi, firefly and *Renilla* luciferase activities were measured. Luciferase activity in whole-cell lysates was normalized to *Renilla* luciferase activity and plotted as folds induction relative to infected HFFs carrying the pGL4.20 empty vector (set at 1). Results are shown as means of fold change ± SEM (error bars) of three independent experiments. **(B)** Western blot analysis of protein lysates from uninfected (mock) or infected HFFs with HSV-1 wild-type (WT) or UV-inactivated HSV1 (UV), at 24 hpi (MOI 1). Analysis was performed using antibodies against PAD3, ICP27, or β-actin. One representative blot of three independent experiments is shown. **(C)** Western blot and Rh-PG analysis of protein lysates from uninfected (mock) or HSV1-infected HFFs (MOI 1), treated with 150 μg/ml CHX or left untreated. Analysis was performed using antibodies against PAD2, PAD3, PAD4, ICP27, or β-actin to assess for equal loading. One representative blot of three

independent experiments is shown. **(D)** Protein lysates from uninfected (mock) or infected HFFs (16 hpi) at an MOI of 1 PFU/cell treated with (PFA 250 μM) or vehicle were analyzed by immunoblotting for PAD3, viral protein gD, or β-actin. **(E)** *PAD3* and *ATF-6* mRNA expression levels by RT-qPCR of HSV-1-infected (16 hpi, MOI 1) or mock-infected HFFs treated or not with the indicated amounts of thapsigargin (TG). The results were normalized to the housekeeping gene glyceraldehyde-3-phosphate dehydrogenase (GAPDH) and expressed as mean fold change ± SEM over mock-infected cells. $*P < 0.05$, $**P < 0.01$, $***P < 0.001$; one-way ANOVA followed by Bonferroni's post test. **(F)** Western blot analysis of protein lysates from uninfected (mock), HSV-1-infected (16 hpi, MOI 1) or mock-infected HFFs treated with TG for 16 h. Analysis was performed using antibodies against PAD3, ICP27, or β-actin. Representative blots of three independent experiments are shown.

https://doi.org/10.1371/journal.ppat.1011849.g003

PAD3 targeting impairs HSV-1 replication

Having observed that PAD2, 3, and 4 protein levels increased during HSV-1 infection, we asked whether inhibiting the enzymatic activity of these proteins would affect viral replication. To this end, HFFs were treated with increasing concentrations of the specific inhibitors of the three isoforms (AFM30a for PAD2, HF4 for PAD3, and GSK199 for PAD4) or with equal volumes of vehicle control (DMSO) 1 h before HSV-1 infection (MOI 1) and for the entire duration of the infection. After 24 h of continuous exposure to the PAD inhibitors, we measured total virus production by plaque assay. While AFM30a and GSK199 treatment had no or minimal effect on HSV-1 replication rate at high doses (S3A and S3B Fig, respectively), exposure to HF4 strongly inhibited viral production in a dose-dependent manner, achieving a reduction of almost 3 logs at 5 μM (Fig 4A). To rule out the possibility that this antiviral activity was related to any off-target effects, we confirmed these results with another PAD3-specific inhibitor, namely CAY10727 [35], which showed a very similar efficacy in reducing viral production (Fig 4B). MTT assay excluded cytotoxic effect of drugs under the same treatment conditions (S3C, S3D and S3E Fig). In line with these results, at 24 hpi, infected carrier-treated cells showed a dramatic cytopathic effect, while HF4 and CAY10727 treatments restored a phenotype more similar to that of uninfected cells (Fig 4C). Moreover, immunoblot analysis of total protein extracts showed downregulation of viral late gD protein expression levels at 24 hpi in treated cells, particularly evident in the presence of HF4 and consistent with the inhibition observed in the plaque assay (Fig 4D). To corroborate these findings, we tested the PAD3 specific inhibitors HF4 and CAY10727 in the other cell types included in this study. As shown in Fig 4E and 4F, we observed a reduction in the count of viral particles in all cell lines in a dose-dependent manner, with the concentrations used being non-toxic for the cells (S3C and S3D Fig).

Finally, to confirm these results we knocked down PAD3 expression in HFF cells with a specific cocktail of PAD3-siRNAs and with siRNA control (siCtrl). At 24 h post-electroporation, cells were infected with HSV-1 (MOI 1). Protein lysates were harvested from siRNA-transfected cells at 24 hpi, and the efficiency of cellular gene expression reduction was evaluated at the protein level by Western blot analysis. We noted that PAD3 depletion was accompanied by a significant decrease in gD expression compared to control (Fig 4G). Moreover, the plaque assay on infected and PAD3-silenced HFFs showed a significant reduction of the virus yield by more than 2 logs compared to siCtrl HFFs (Fig 4H), which was confirmed by the complete recovery from the cytopathic effect upon PAD3 silencing (Fig 4I).

Overall, these data suggest that PAD3 activity plays a key role in supporting HSV-1 replication, and that PAD3 might be a promising target for anti-HSV-1 therapy.

Citrullinome analysis reveals IFIT proteins as restriction factors for HSV-1 replication

Next, to identify which cellular and/or viral proteins were citrullinated during infection, we used a citrulline specific probe (biotin-PG) and enriched the HSV-1-associated citrullinome in
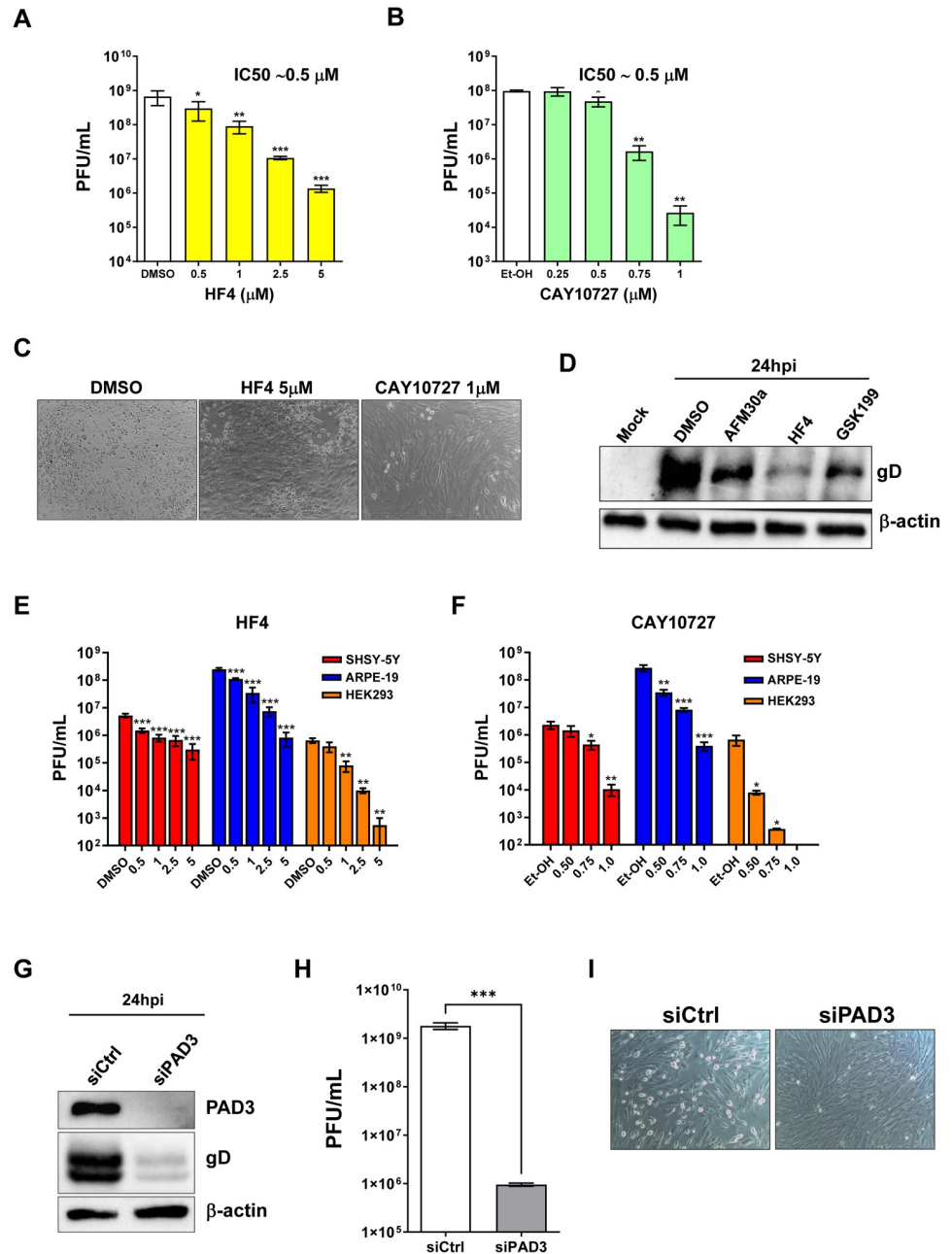
Fig 4. PAD3 targeting impairs HSV-1 replication in human cells. HFFs were infected with HSV-1 (MOI 1) and then treated with increasing concentrations of HF4 (**A**) or CAY10727 (**B**), two PAD3-specific inhibitors, which was given 1 h prior to virus adsorption and kept throughout the whole experiment. At 24 hpi, viral plaques were microscopically counted, and the number of plaques was plotted as a function of inhibitor concentration. Values are expressed as means ± SEM (error bars) of three independent experiments. Values are expressed as mean ± SEM of three independent experiments, *$P < 0.05$, **$P < 0.01$, ***$P < 0.001$; one-way ANOVA followed by Bonferroni's post test. (**C**) Representative images of infected HFFs (24 hpi) at an MOI of 1 PFU/cell and treated with HF4 (5 μM), CAY10727 (1 μM), or vehicle (DMSO). (**D**) Protein lysates from uninfected (mock) or infected HFFs (24 hpi) at an MOI of 1 PFU/cell treated with AFM30a (20 μM), HF4 (5 μM), GSK199 (20 μM) or vehicle (DMSO) were analyzed by immunoblotting to assess for viral expression with an anti-gD antibody; β-actin cellular expression was used for protein loading control. SH-SY5Y, ARPE-19, and HEK293 cells were infected with HSV-1 (MOI 1 PFU/cell) and then treated with increasing concentrations of HF4 (**E**) or CAY10727 (**F**), which were given 1 h prior to virus adsorption and kept throughout the whole experiment. At 24 hpi, viral plaques were microscopically counted, and the number of plaques was plotted as a function of inhibitor concentration. Values are expressed as means ± SEM (error bars) of four independent experiments, *$P < 0.05$, **$P < 0.01$, ***$P < 0.001$; one-way ANOVA followed by Bonferroni's post test.

(G) HFFs were silenced for PAD3 using specific siRNAs (siPAD3), as negative control cells were also similarly transfected with scrambled siRNA (siCTRL). At 24 h post-treatment (hpt), cells were infected with HSV-1 at an MOI of 1 PFU/cell. The efficiency of PAD3 protein depletion at 24 hpi was assessed by immunoblotting using antibodies against PAD3 or β-actin for equal loading. An anti-gD antibody was used to verify HSV-1 infection. Representative blots of three independent experiments are shown. (H) PAD3-silenced cells were infected with HSV-1 at an MOI of 1 PFU/cell. Viral supernatants were collected at 24 hpi and analyzed by standard plaque assay. Values are expressed as means ± SEM. Values are expressed as mean ± SEM of three independent experiments, ***$P < 0.001$; one-way ANOVA followed by Bonferroni's post test. (I) Representative images of infected HFFs (24 hpi) at an MOI of 1 PFU/ cell and transfected with the same siCTRL and siPAD3 described in the legend to Fig 3D.

https://doi.org/10.1371/journal.ppat.1011849.g004

HFFs harvested at 16 and 24 hpi through streptavidin-agarose beads. As shown in Fig 5A, and consistent with our earlier findings, we observed a massive increase in overall protein citrulli-nation in HSV-1-infected cells compared to uninfected control cells. In detail, database searches using the SEQUEST algorithm allowed us to identify 297 (126 significant) and 287 (125 significant) citrullinated cellular proteins at 16 and 24 hpi, respectively (S1 Data). In addi-tion, a total of 39 and 35 (28 and 25 significant, respectively) citrullinated viral proteins were also detected at the indicated time points (Fig 5B and S2 Data). Of note, at 16 hpi most of the citrullinated viral proteins were immediate early (IE) genes and enzymes involved in the syn-thesis of viral DNA, whereas at 24 hpi mainly structural capsid and tegument proteins or enve-lope glycoproteins were detected. Moreover, through PANTHER software, we were able to identify a wide range of citrullinated host proteins falling into various functional classes, including metabolite interconversion enzymes, RNA and DNA metabolism proteins, chaper-ones, cytoskeletal proteins, protein-binding activity modulators, protein modifying enzymes, membrane traffic proteins, transporters, and defense/immunity proteins (Fig 5C).

Previously, we demonstrated that during HCMV infection several members of the inter-feron (IFN)-induced protein with tetratricopeptide repeat (*IFIT*) family were heavily citrulli-nated, and that IFIT1 lost its restriction factor activity when citrullinated *in vitro* [30]. Consistently, here we found that IFIT1 and IFIT2 were also significantly citrullinated in the HSV-1-associated citrullinome at both 16 and 24 hpi (Fig 5A). Unlike IFIT1 and IFIT2, IFIT3 showed only a slight increase in citrullination during infection, which was not statistically sig-nificant ($p = 0.06$). Therefore, we decided to focus on the other two isoforms for further investigation.

To validate these findings, total proteins from mock or HSV-1-infected HFFs at 16 and 24 hpi (MOI 1) were immunoprecipitated with an anti-citrulline antibody and subjected to immunoblotting using antibodies against IFIT1, IFIT2, or the viral protein ICP27. As shown in Fig 5D, IFIT1, IFIT2 and ICP27 proteins were upregulated and, consistent with previous results, citrullinated following infection with HSV-1, especially at 16 hpi. Considering that IFIT family members are significantly upregulated by IFNs, we sought to investigate whether the observed increase in citrullination was a direct consequence of the infection or resulted from the IFN-mediated upregulation in response to the infection. To test whether interferon alone could induce deimination of IFIT1 and IFIT2, we treated HFFs with IFN-β (500 U/mL) for 16 h and 24 h and immunoprecipitated the total proteins with the anti-citrulline antibody. Successively, we performed immunoblotting using antibodies against IFIT1 and IFIT2. As shown in Fig 5E, we found that both proteins were strongly upregulated by IFN treatment, but they did not bind to the anti-citrulline antibody, suggesting that interferon itself is not suffi-cient to cause deimination of IFIT proteins.

Next, to gain further insight into the role of these genes during HSV-1 infection, we mea-sured viral production in HSV-1-infected HFFs after siRNA-mediated depletion of IFIT1 and IFIT2. Following transfection with specific siRNAs (siIFIT1 and siIFIT2, respectively) and
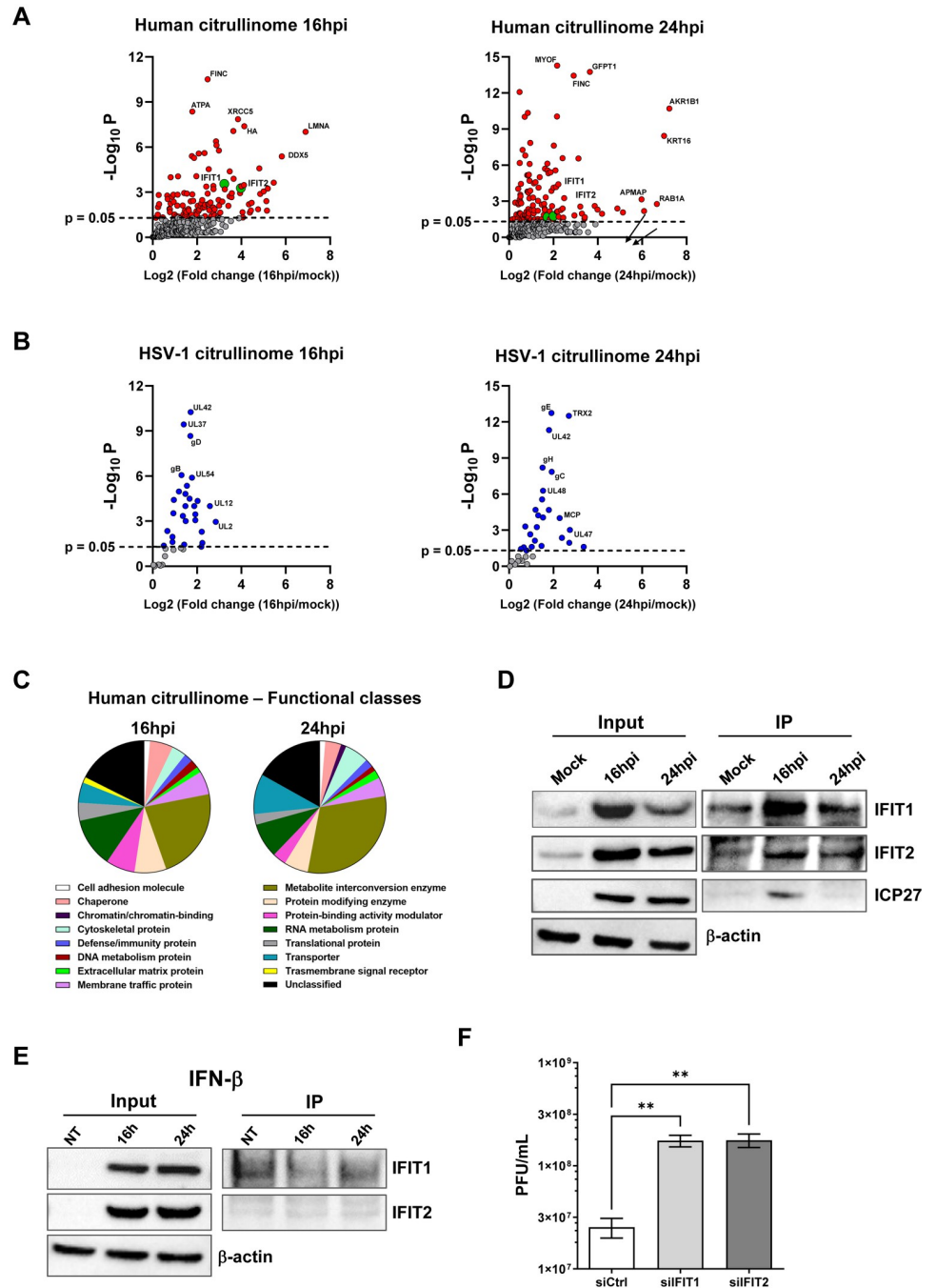
Fig 5. Citrullinome analysis reveals IFIT proteins as restriction factors for HSV-1 replication. (A-B) Volcano plot depicting the host (**A**, red dots) and viral (**B**, blue dots) citrullinated proteins of infected cells *vs* mock-infected cells at 16 hpi (left panels) and 24 hpi (right panels). Cell lysates from uninfected (mock) or HSV-1-infected HFFs (MOI 1) were exposed to a biotin-PG to isolate citrullinated proteins on streptavidin agarose. Bound proteins were then subjected to on-bead tryptic digestion and analyzed by LC-MS/MS—in the graph, every identified citrullinated protein corresponds to a dot. The x-axis represents the ratio of citrullination between mock and infected cells at the indicated time points, while the y-axis indicates the statistical significance. Both variables were plotted on a logarithmic scale (*n* = 3). IFIT1 and IFIT2 proteins are reported as green dots, while grey dots represent proteins that do not reach statistical significance. **(C)** The pie charts show the classification of citrullinated cellular proteins at 16 hpi (left) and 24 hpi (right) based on protein classes. Only classes with a representation exceeding 1% are reported. **(D)** Immunoprecipitation (IP) of total cell extracts (Input) from mock or infected HFFs at 24 hpi using an anti-peptidylcitrulline antibody. The IP complexes were analyzed by Western blotting using antibodies against IFIT1 and

IFIT2. An anti-ICP27 antibody was used to assess HSV-1 infection, while β-actin cellular expression was used for protein loading control. The blot shown is representative of three independent experiments. (**E**) Immunoprecipitation (IP) of total cell extracts (input) from untreated (NT) or IFN-β-treated (500U/ml) HFFs using an anti-peptidylcitrulline antibody. The IP complexes were analyzed by Western blot using antibodies against IFIT1 and IFIT2. Equal loading was assessed by β-actin immunoblotting. The blot shown is representative of three independent experiments. (**F**) HFFs were silenced for IFIT1 and IFIT2 using specific siRNAs (siIFIT1 and siIFIT2, respectively). As negative control cells were also similarly transfected with scrambled siRNA (siCtrl. At 24 hpt, cells were infected with HSV-1 at an MOI of 1 PFU/cell. Viral supernatants were collected at 24 hpi and analyzed by standard plaque assay. Values are expressed as means ± SEM of three independent experiments. Representative blots of three independent experiments are shown.

https://doi.org/10.1371/journal.ppat.1011849.g005

subsequent infection with HSV-1 for 24 h, we achieved a nearly complete silencing of both proteins, without affecting the ability of the virus to replicate, as demonstrated by the expression of the ICP27 viral marker (S4A Fig). Rather, silencing either IFIT1 or IFIT2 resulted in significantly higher levels of virus production compared to siCtrl-transfected cells (Fig 5F), suggesting that IFIT1 and IFT2 are potential restriction factors for HSV-1, whose activity can be overcome by virus-induced citrullination.

Discussion

Viruses, unlike other infectious agents, require the molecular machinery of the host to complete their replication cycle. As a result, these pathogens have evolved multiple mechanisms to promote the translation of their transcripts, evade the immune system, and induce host gene expression alterations during infection. These mechanisms are indispensable for the viral life cycle, but they are particularly sophisticated in viruses, such as herpesviruses, that establish latency and persist throughout the host's lifespan. Recent research has unveiled the potential involvement of host-cellular environment manipulation mechanisms in the pathogenesis of autoimmune diseases, as well as tumors and neurodegenerative disorders. A promising strategy to target these evasion mechanisms is to employ host-targeting antiviral agents (HTAs) that interfere with the host factors required for viral replication [36].

Citrullination, a post-translational modification mediated by PAD enzymes, is emerging as a key mechanism that viruses exploit during their replication in host cells. This is supported by an association between viral infection and PAD-mediated upregulation of citrullination, which we and others have reported in various viral and cellular models [25–27,30]. In particular, we have shown that one such virus, HCMV, induces PAD-mediated citrullination of several cellular proteins endowed with antiviral activity, including the IFN-stimulated genes (ISGs) IFIT1 and Mx1, and that blocking this process with the PAD inhibitor Cl-amidine can inhibit viral replication [30]. Here, we extend those findings to a different member of the *Herpesviridae* family, HSV-1, which we demonstrate to be capable of promoting PAD-mediated citrullination *in vitro*. Specifically, we show that HSV-1 infection of human fibroblasts upregulates total protein citrullination, and that this process is required for optimal viral replication.

Despite various viruses being capable of upregulating PAD enzyme expression, which is crucial for optimal viral replication, our findings suggest that each virus displays a preference for specific PAD isoforms. This challenges the assumption that PAD upregulation is a general response to viral infection. For instance, PAD4 is the main isoform regulated by human rhinovirus (HRV) and HCoV [26,27], while PAD2 and PAD4 cooperate in supporting HCMV replication [30]. In the present work, we show that during HSV-1 infection three different PAD isoforms are upregulated: PAD2, 3, and 4. Although PAD2 and PAD4 are also induced upon HSV-1 replication, PAD3 seems to play a major role, as shown by the fact that its promoter is robustly induced by HSV-1 infection and that its targeted inactivation

through specific inhibitors or silencing by siRNAs has a detrimental effect on HSV-1 replication. Noteworthy, during HSV-1 infection PAD3 consistently displayed similar kinetics to that of the viral protein ICP27, regardless of the cell model used, suggesting that the variations in permissiveness among cells, and consequently, the different kinetics of viral replication, rather than the different basal expression of PAD3, influence the kinetics of PAD expression. Hence, developing specific inhibitors for this particular isoform could improve the efficacy and mitigate the toxicity of HSV-1 antiviral treatments. This underscores the overarching need to identify which isoforms are specifically involved in different viral infections to design more effective HTAs [37].

In this study, we have also identified the cellular and viral proteins deiminated during HSV-1 infection, thus determining the citrullinome of the infected cells. We show that several members of the interferon (IFN)-induced protein with tetratricopeptide repeat (*IFIT*) family, such as IFIT1 and IFIT2, are robustly citrullinated, similar to what we observed in HCMV-infected cells. This is of particular interest because IFIT family members, primarily known for their antiviral activity against RNA viruses [38,39], have recently been linked to the innate immune response against DNA viruses, including two other members of the herpesvirus family, namely KSHV and HCMV [30,40]. More specifically, the antiviral function of IFIT3— which in our analysis was not significantly citrullinated—against HSV-1 is known, as is the ability of the virus to evade this function via the UL41 protein [41]. However, the roles of the other two members, IFIT1 and IFIT2, in HSV-1 infection have not been previously reported. Our research shows that silencing of either IFIT1 or IFIT2 results in increased virus production, while ectopic expression of IFIT1 inhibits viral growth, which agrees with previous findings in KSHV and HCMV-infected cells [30,40]. In terms of viral proteins, our study reveals that citrullination follows the natural replication cycle of the virus, with IE, E, and L proteins undergoing citrullination in a sequential order. Importantly, both viral structural and catalytic proteins show citrullination, underscoring the need to understand how this modification impacts their functions and whether it is involved in the assembly of new virions. In this regard, the substantial presence of citrullinated cellular and viral proteins observed in our analysis indicates that infection-induced citrullination is critically involved in multiple stages of HSV-1 replication throughout its life cycle. Therefore, PAD family members represent promising candidates for antiviral drug targeting, as their inhibitors can effectively block the replication of HSV-1 through various mechanisms.

It is however worth pointing out that although some substrates of PADs are IFN-inducible proteins, citrullination *per se* is not an IFN-dependent phenomenon. We show that, in mock-infected cells exposed to interferon, IFIT1 and IFIT2 proteins are upregulated but not over-citrullinated, and that the expression levels of PAD enzymes are unchanged. These findings, along with the fact that PADs are only upregulated in cells infected with functional HSV-1 but not in cells infected with UV-treated HSV-1, imply that viral IE protein production regulates PAD protein expression, as we observed in HCMV-infected cells [30].

Overall, our results clearly demonstrate that PAD induction and subsequent citrullination profile alteration are virus-specific phenomena. However, it is highly likely that the over-citrullinated host proteins in the course of infection are closely dependent on the infected tissue, just as the citrullinome is strictly linked to the gene expression profile of host cells prior to infection [42]. Consequently, it is highly probable that the effects of citrullination induced by an infection will vary depending on the specific tissue and organ affected, rather than simply being influenced by the type of virus involved.

Altogether, our findings suggest the intriguing scenario that conditions where citrullination contributes to a pathological state may be triggered by a viral infection that initially disrupts PAD activity.

Materials and methods

Cell lines and viruses

Human foreskin fibroblasts (HFFs; ATCC, SCRC-1041), African green monkey kidney Vero cells (Sigma-Aldrich, 84113001), the human neuroblastoma cell line SH-SY5Y (ATCC, CRL-2266), human embryonic kidney cells HEK293 (ATCC, CRL-1573) and retinal pigment epithelial cell (ARPE-19; ATCC, CRL-2302) were grown in Dulbecco's Modified Eagle Medium (DMEM; Sigma-Aldrich) supplemented with 1% (v/v) penicillin/streptomycin solution (Euroclone) and heat-inactivated 10% (v/v) fetal bovine serum (FBS) (Sigma-Aldrich). The medium of SH-SY5Y cells was also supplemented with non-essential amino acids (NEAA, Sigma-Aldrich). The clinical isolate of HSV-1 was grown in Vero cells and titrated by standard plaque assay as described previously [43].

Reagents and treatments

The PAD inhibitors Cl-amidine (Cl-A), BB-Cl-amidine (BB-Cl), GSK199, CAY10727, and AFM30a—also known as CAY10723—were obtained from Cayman Chemical (Ann Arbor). CHX and foscarnet (phosphonoformic acid, PFA) were from Sigma-Aldrich. All these compounds were reconstituted in dimethyl sulfoxide (DMSO) or ethanol accordingly to their solubility. HF4 and Thapsigargin were kindly provided by Dr. P. Thompson and Dr. M. Corazzari, respectively. Immediately before use, the inhibitors were diluted in the cell medium to their final concentrations. For the PADs inhibitors experiments, cells were pre-treated with the inhibitors for 1 h and then infected (MOI 1) by adding the virus without changing the medium. Following virus adsorption (2 h), the viral inoculum was removed, and a new medium with fresh inhibitor was added. After that, no more medium or inhibitor was added until the samples were collected.

Cell viability assay

Cells were seeded at a density of $3*10^4$/well in a 96-well plate. After 24 h, the cells were treated with the indicated concentration of the different inhibitors or mock-treated using the vehicle alone (DMSO or ethanol). After 48 h, cell viability was determined using the 3-(4,5-dimethylthiazol-2-yl)-2,5-diphenyltetrazolium bromide (MTT, Sigma) method as described previously [30].

In vitro antiviral assay

Cells were cultured in a 24-well plate for 1 day and then treated as described in 3.2. Briefly, they were incubated with the aforementioned PAD inhibitors at the indicated concentration for 1 h and subsequently infected with HSV-1 at a MOI of 1. Following virus adsorption (2 h at 37°C), the viral inoculum was removed, and the cell cultures were maintained in a medium containing the indicated treatment for 24 h. DMSO or ethanol were used as a negative control. Next, the cells and supernatants were harvested, pooled, and then lysed by two freeze-thaw cycles. The extent of virus replication was then assessed by titrating the infectivity of the sample by standard plaque assay on Vero cells.

Plaque assay

Vero cells were seeded at a density of $3*10^4$/well in a 96-well plate and inoculated 24 h later with 10-fold serial dilutions of the HSV-1 production. After 48 h, cells were fixed and stained with crystal violet solution, and plaques were counted on each well to determine the virus titer,

which was determined by counting the number of immunostained foci on each well using the following formula: virus titer (PFU/ml) = number of plaques * 0.1 ml/dilution fold.

DNA and RNA isolation and quantitative nucleic acid analysis

Total DNA and RNA were extracted using the NucleoSpin RNA kit (Macherey-Nagel, Düren, Germany), and 1 μg of RNA was retrotranscribed using the Revert-Aid H-Minus FirstStrand cDNA Synthesis Kit (Thermo Fisher Scientific, Waltham, USA), according to the manufacturer's instructions. Comparison of mRNA expression between samples (*i.e*., infected *vs*. untreated) was performed by SYBR green-based RT-qPCR using a Biorad CFX96 apparatus, using the primers reported in S1 Table. To determine the number of viral DNA genomes, viral DNA levels were measured by quantitative PCR on a Biorad CFX96 apparatus (Stratagene, San Diego, USA). To create a standard curve for each analysis, genomic DNA mixed with a gE2-encoding plasmid (Addgene pAcUW51-gE2) was serially diluted from 109 to 1 copy and analyzed in parallel. The amount of human GAPDH gene amplified per reaction mixture was used to normalize the HSV-1 DNA copy numbers.

Western blot analysis

Cells were treated with the indicated compound or equal volumes of DMSO solvent 1 h before infection and throughout the entire duration of the infection as previously described in point 2.2. Cells were infected with HSV-1 at an MOI of 1 and harvested at the indicated time points. Cell lysates were prepared with RIPA buffer, quantified by Bradford method, and subjected to Western blot analysis. The primary antibodies were as follows: anti-PAD1 (Abcam, ab181791); anti-PAD2 (Cosmo Bio, SML-ROI002-EX); anti-PAD3 (Abcam, ab50246); anti-PAD4 (Abcam, ab128086); anti-PAD6 (Abcam ab16480); anti-actin (Sigma-Aldrich, A2066), anti-gD (Virusys, HA025-1), anti-ICP27 (Virusys, P1113), anti-IFIT1 (Invitrogen PA5-31254), anti-IFIT2 (Proteintech, 12604-1-AP), anti-IFIT3 (Proteintech 15201-1-AP).

Detection of citrullination with rhodamine-phenylglyoxal (Rh-PG)

Whole-cell protein extracts were prepared as described in the previous paragraph. Equal amounts of protein were diluted with 80% trichloroacetic acid and incubated with Rh-PG (final concentration 0.1 mM) for 30 min [44]. The reaction was quenched with 100 mM L-citrulline, then centrifuged at 21,100xg for 10 min, washed with ice-cold acetone, and resuspended in 2X SDS loading dye for gel electrophoresis. Gels were imaged (excitation = 532 nm, emission = 580 nm) using a Biorad Chemidoc Imaging System, stained with brilliant blue G-colloidal solution (Sigma-Aldrich).

PAD3 vector construction

The 5' flanking region of *PADI3* gene was amplified by PCR using the Q5 High-Fidelity DNA polymerase (New England Biolabs, Ipswich, USA), the human genomic DNA from HFFs as a template, and the PAD3 primers containing *Xho* I and *Hind* III restriction enzymes sites (see primers sequences listed in S1 Table). The resulting amplification products were digested with *Xho* I and *Hind* III (Thermo Fisher Scientific, Waltham, USA) and cloned into the pGL4.20 [luc2/Puro] vector (Promega, Madison, USA), which encodes the luciferase reporter gene *luc2* (*Photinus pyralis*) with no other regulatory elements. The resulting pGL4.20-PADI3prom construct was purified using the PureYield Plasmid Miniprep System (Promega, Madison, USA) and verified by restriction mapping and complete sequencing. The resulting chromatograms were analyzed using Chromas software 2.6.6 (Technolysium Ltd.).

Dual-luciferase reporter assay

HFFs were seeded into 12-well plates and, after 24 h of incubation, transiently transfected with 1 μg of pGL4.20 or pGL4.20-PADI3 plasmids together with 0.1 μg of Renilla reporter plasmid (pRL-SV40, to correct for transfection efficiency) using Lipofectamine 2000 Transfection Reagent kit (Thermo), according to the manufacturer's instruction. After 24h, cells were infected with HSV-1 (MOI of 1 PFU/ml), and 24 hpi the Dual-luciferase Reporter Assay System (Promega, USA) was used to detect Firefly and *Renilla* luciferase activities and recorded using GloMax 96 Microplate Luminometer (Promega, USA). Firefly luciferase activity from the luciferase reporter vector was normalized to *Renilla* luciferase activity from the pRL-SV40 vector and plotted as folds of induction relative to infected HFFs expressing the pGL4.20 empty vector (set at 1).

Pull-down experiments

Uninfected or HSV-1-infected cells (MOI of 1 PFU/ml) were washed with 1X PBS and lysed in radioimmunoprecipitation assay (RIPA) buffer (50 mM Tris pH 7.4; 150 mM NaCl; 1 mM EDTA; 1% nonidet P-40; 0.1% SDS; 0.5% deoxycholate; protease inhibitors). Proteins (200 μg) were then incubated with 2 μg of anti-citrulline monoclonal antibody (Cayman Chemical, 30773) or with an isotype antibody as negative control (62–6820; Thermo Fischer Scientific, Waltham, USA) for 1 h at room temperature with rotation followed by overnight incubation at 4˚C with protein G-sepharose (Sigma-Aldrich, Milan, Italy). Immune complexes were collected by centrifugation and washed with RIPA buffer. The sepharose beads were pelleted and washed three times with RIPA buffer, resuspended in reducing sample buffer (50 mM Tris pH 6.8; 10% glycerol; 2% SDS; 1% 2- mercaptoethanol), boiled for 5 min and resolved on an SDS-PAGE gel to assess protein binding by immunoblotting.

Citrullinome analysis by mass spectrometry: Sample preparation

Sample preparation in technical triplicates followed the procedure outlined in [45]. Equal amounts of cell lysates from each experimental group (300 μg) were diluted in buffer (100 mM HEPES pH 7.6) to a final concentration of 1 μg/μL and incubated with 20% trichloroacetic acid (TCA) and 0.5 mM biotin-PG [46] for 30 min at 37 ˚C. Labeled proteomes were precipitated on ice for 30 min. Samples were pelleted through tabletop centrifugation (21,100xg, 15 min) at 4 ˚C. The supernatants were discarded, and the pellets were washed with cold acetone (300 μL). After drying for 5 min, the pellets were resuspended in 1.2% SDS in PBS by bath sonication and heating. Samples were then transferred to 15 mL screw cap tubes and diluted in 1X PBS to a 0.2% SDS final concentration. Samples were incubated with streptavidin agarose slurry (Sigma Aldrich, 170 μL) overnight at 4 ˚C and for an additional 3 h at 25 ˚C. After discarding the flow through, the streptavidin beads were washed with 0.2% SDS in PBS (5 mL) for 10 min at 25 ˚C. The beads were then washed three times with 1X PBS (5 mL) and three times with water (5mL) to remove any unbound proteins. Beads were then transferred to a screw cap microcentrifuge tube and heated in 1X PBS with 500 μL 6 M urea and 10 mM DTT (65 ˚C, 20 min). Proteins bound to the beads were then alkylated with iodoacetamide (20 mM, 37 ˚C for 30 min). The beads were successively pelleted by centrifugation (1,400 x *g* for 3 min) and the supernatant was removed. The pellet was resuspended in a premixed solution of 2 M urea, 1 mM CaCl₂ and 2 μg Trypsin Gold (Promega, Madison, USA) in PBS. These were shaken overnight at 37 ˚C. The supernatant was collected, and the beads were washed twice with water (50 μL), each time collecting the supernatant. The fractions were combined, acidified with formic acid (5% final concentration) and stored at -20 ˚C until use.

Mass spectrometry

Liquid chromatography-mass spectrometry/mass spectrometry (LC-MS/MS) analysis was performed with an LTQ-Orbitrap Discovery mass spectrometer (Thermo Fisher Scientific, Waltham, MA, USA) coupled to an Easy-nLC HPLC (Thermo Fisher Scientific, Waltham, MA, USA). Samples were pressure loaded onto a 250-μm fused-silica capillary hand packed with 4-cm Aqua C18 reverse phase resin (Phenomenex). Samples were separated on a hand packed 100-μm fused-silica capillary column with a 5-μm tip packed with 10 cm Aqua C18 reverse phase resin (Phenomenex). Peptides were eluted using a 10-h gradient of 0–100% Buffer B in Buffer A (Buffer A: 95% water, 5% acetonitrile, 0.1% formic acid; Buffer B: 20% water, 80% acetonitrile, 0.1% formic acid). The flow rate through the column was set to ~400 nL/min, and the spray voltage was set to 2.5 kV. One full MS scan (FTMS) was followed by 7 data-dependent MS2 scans (ITMS) of the nth most abundant ions. The tandem MS data were searched by the SEQUEST algorithm using a concatenated target/decoy variant of the human and viral UniProt database. A static modification of +57.02146 on cysteine was specified to account for alkylation by iodoacetamide. SEQUEST output files were filtered using DTASelect 2.0.

Database search

Raw data were processed and searched using Maxquant 1.6.14 and its integrated Andromeda search engine using the Swiss-Prot human (downloaded 04/09/2019) and Uniprot HCMV (downloaded 02/27/2021). Search parameters were as follows: tryptic digestion with up to 2 missed cleavages; peptide N-terminal acetylation, methionine oxidation, N-terminal glutamine to pyroglutamate conversion were specified as variable modifications. The monoisotopic mass increment of the triplex dimethyl labels, light, medium and heavy dimethyl label at 28.0313, 32.0564 and 36.0757 Da, respectively, were set as variable modification on the peptide N-termini and lysine residues. Carbamidomethylation of cysteines was set as static modification. Main search tolerance was 6 ppm, and the first search tolerance was 50 ppm. Both the protein and peptides identification false discovery rates (FDR) were < 1%. Protein grouping, dimethyl ratio calculations and downstream statistics were performed in Scaffold Q+S 4.8.9 (Proteome Software, Portland, OR).

siRNA-mediated knockdown

HFFs were transiently transfected with a Neon Transfection System (Thermo Fischer Scientific) according to the manufacturer's instructions (1200 V, 30 ms pulse width, one impulse) with a pool of small interfering RNAs targeting PAD3 (Sigma-Aldrich, EHU012711), IFIT1 (Qiagen S102660777), IFIT2 (Invitrogen AM16708) or control siRNA (siCTRL, Qiagen 1027292) as negative control.

Statistical analysis

All statistical tests were performed using GraphPad Prism version 9.5.1 for Windows (GraphPad Software, San Diego, USA). The data were presented as means ± standard error of mean (SEM). Statistical significance was determined by using unpaired t test (two-tailed), one-way or two-way analysis of variance (ANOVA) with Bonferroni's, or Dunnett's post-tests. Differences were considered statistically significant for $P < 0.05$ (*$P < 0.05$; **$P < 0.01$; ***$P < 0.001$). The half-maximal inhibitory concentration (IC_{50}) was calculated by Quest Graph IC50 Calculator (AAT Bioquest, Inc, https://www.aatbio.com/tools/ic50-calculator).

Supporting information

S1 Fig. Uninfected HFFs, ARPE-19, and SHSY-5Y were treated with the indicated concentrations of Cl-A (**A**) and BB-Cl (**B**) for 24 h, and the number of viable cells was determined for each concentration using the MTT assay. Values are expressed as means ± SEM of three independent experiments. SH-SY5Y (**C**) and ARPE-19 (**D**) were infected with HSV-1 (MOI 1 PFU/cell) and then treated with increasing concentrations of Cl-A, which were given 1 h prior to virus adsorption and kept throughout the whole experiment. At 24 hpi, viral plaques were microscopically counted, and the number of plaques was plotted as a function of inhibitor concentration. Values are expressed as means ± SEM (error bars) of three independent experiments, $*P < 0.05$, $**P < 0.01$, $***P < 0.001$; one-way ANOVA followed by Bonferroni's post-test. (**E**) Protein lysates from uninfected (mock) or infected HFFs (24 hpi) at an MOI of 1 PFU/cell treated with Cl-A (100 μM), BB-Cl (2.5 μM) or vehicle (DMSO) were exposed to an Rh-PG citrulline-specific probe (left panel) and subjected to gel electrophoresis to detect citrullinated proteins. Equal loading was assessed by Coomassie blue staining (right panel). (**F**) Representative images of infected HFFs (24 hpi) at an MOI of 1 PFU/cell and treated with Cl-A (100 μM), BB-Cl (2.5 μM), or vehicle (DMSO).
(TIF)

S2 Fig. (**A**) mRNA expression levels of *PADI* isoforms by RT-qPCR of HSV-1-infected (8 and 16 hpi) *vs* uninfected (mock) HFFs were normalized to the housekeeping gene glyceraldehyde-3-phosphate dehydrogenase (GAPDH) and expressed as mean fold change ± SEM over mock-infected cells. $*P < 0.05$, $**P < 0.01$, $***P < 0.001$; one-way ANOVA followed by Bonferroni's post test. (**B**) Densitometric analysis of three independent experiments, values are expressed as fold change in PAD2 and PAD4 expression normalized to α-tubulin. (**C**) mRNA expression levels of *PADI3* isoforms by RT-qPCR of HSV-1-infected (6, 16 and 24 hpi) *vs* uninfected (mock) cells were normalized to GAPDH and expressed as mean fold change ± SEM over mock-infected cells. $*P < 0.05$, $**P < 0.01$, $***P < 0.001$; one-way ANOVA followed by Bonferroni's post test. (**D**) Western blot analysis of protein lysates from untreated (NT) or IFN-β treated (500 U/mL) HFFs using antibodies against PAD1 or PAD6. β-actin cellular expression was used for protein loading control. One representative gel of three independent experiments is shown. (**E**) Blu Coomassie staining of the same protein extracts used in the experiments shown in Fig 2D (protein lysates from uninfected (mock) or HSV1-infected HFFs, treated with 150 μg/ml CHX or left untreated).
(TIF)

S3 Fig. (**A-B**) HFFs were infected with HSV-1 (MOI 1 PFU/cell) and then treated with increasing concentrations of AFM30a (A), GSK199 (B) and CAY10727 (C), which were given 1 h prior to virus adsorption and kept throughout the whole experiment. At 24 hpi, viral plaques were microscopically counted, and the number of plaques was plotted as a function of inhibitor concentration. Values are expressed as means ± SEM (error bars) of three independent experiments, $*P < 0.05$, $**P < 0.01$, $***P < 0.001$; one-way ANOVA followed by Bonferroni's post test. (**C-E**) Uninfected HFF, SHSY-5Y, ARPE-19 or HEK293 cells were treated with the indicated concentrations of HF4 (C), CAY10727 (D), AFM30a, or GSK199 (E) for 24 h and the number of viable cells was determined for each concentration by MTT assay. Values are expressed as means ± SEM of three independent experiments.
(TIF)

S4 Fig. (**A**) The efficiency of IFIT1 or IFIT2 protein depletion at 24 hpi was assessed by immunoblotting using antibodies against IFIT1 or IFIT2, or against β-actin to check for equal loading. An anti-ICP27 antibody was also used to verify HSV-1 infection. Representative blots of

three independent experiments are shown.
(TIF)

S1 Table. Oligonucleotide primer sequences for qPCR and PADI3 promoter cloning.
(PDF)

S1 Data. List of the host citrullinated proteins of infected *vs* mock-infected HFFs at 16 hpi and 24 hpi.
(XLSX)

S2 Data. List of the viral citrullinated proteins of infected *vs* mock-infected HFFs at 16 hpi and 24 hpi.
(XLSX)

Acknowledgments

Author Contributions

Conceptualization: Selina Pasquero, Francesca Gugliesi, Paul R. Thompson, Santo Landolfo, Marco De Andrea.

Data curation: Selina Pasquero, Francesca Gugliesi, Camilla Albano, Stefano Raviola, Sen Sudeshna, Marco De Andrea.

Formal analysis: Camilla Albano, Greta Bajetto, Linda Trifirò, Bianca Brugo, Qiao Yang, Sen Sudeshna, Leonard Barasa, Hafeez Haniff.

Funding acquisition: Francesca Gugliesi, Matteo Biolatti, Valentina Dell'Oste, Marco De Andrea.

Investigation: Selina Pasquero, Francesca Gugliesi, Camilla Albano, Greta Bajetto, Gloria Griffante, Linda Trifirò, Bianca Brugo, Davide Lacarbonara, Qiao Yang, Sen Sudeshna, Leonard Barasa.

Methodology: Selina Pasquero, Francesca Gugliesi, Matteo Biolatti, Valentina Dell'Oste, Camilla Albano, Greta Bajetto, Bianca Brugo, Stefano Raviola, Sen Sudeshna.

Project administration: Marco De Andrea.

Resources: Paul R. Thompson.

Software: Selina Pasquero, Francesca Gugliesi, Greta Bajetto, Gloria Griffante, Linda Trifirò, Davide Lacarbonara, Qiao Yang, Sen Sudeshna, Leonard Barasa, Hafeez Haniff, Paul R. Thompson.

Supervision: Matteo Biolatti, Valentina Dell'Oste, Paul R. Thompson, Marco De Andrea.

Validation: Selina Pasquero, Francesca Gugliesi, Matteo Biolatti, Valentina Dell'Oste, Stefano Raviola, Sen Sudeshna, Hafeez Haniff.

Visualization: Selina Pasquero, Francesca Gugliesi, Gloria Griffante, Leonard Barasa, Hafeez Haniff.

Writing – original draft: Selina Pasquero, Francesca Gugliesi, Valentina Dell'Oste.

Writing – review & editing: Paul R. Thompson, Santo Landolfo, Marco De Andrea.

References

1. Yousuf W, Ibrahim H, Harfouche M, Abu Hijleh F, Abu-Raddad L. Herpes simplex virus type 1 in Europe: Systematic review, meta-analyses and meta-regressions. BMJ Global Health. 2020; 5: 1–15. https://doi.org/10.1136/bmjgh-2020-002388 PMID: 32675066

2. Rechenchoski DZ, Faccin-Galhardi LC, Linhares REC, Nozawa C. Herpesvirus: an underestimated virus. Folia Microbiologica. 2017; 62: 151–156. https://doi.org/10.1007/s12223-016-0482-7 PMID: 27858281

3. Itzhaki RF. Herpes and Alzheimer's Disease: Subversion in the Central Nervous System and How It Might Be Halted. Journal of Alzheimer's Disease. 2016; 54: 1273–1281. https://doi.org/10.3233/JAD-160607 PMID: 27497484

4. De Chiara G, Piacentini R, Fabiani M, Mastrodonato A, Marcocci ME, Limongi D, et al. Recurrent herpes simplex virus-1 infection induces hallmarks of neurodegeneration and cognitive deficits in mice. PLoS Pathogens. 2019; 15: 1–30. https://doi.org/10.1371/journal.ppat.1007617 PMID: 30870531

5. Krishnan R, Stuart PM. Developments in Vaccination for Herpes Simplex Virus. Frontiers in Microbiology. 2021; 12. https://doi.org/10.3389/fmicb.2021.798927 PMID: 34950127

6. Sadowski LA, Upadhyay R, Greeley ZW, Margulies BJ. Current drugs to treat infections with herpes simplex viruses-1 and -2. Viruses. 2021; 13:1–12. https://doi.org/10.3390/v13071228 PMID: 34202050

7. Badia R, Garcia-Vidal E, Ballana E. Viral-Host Dependency Factors as Therapeutic Targets to Overcome Antiviral Drug-Resistance: A Focus on Innate Immune Modulation. Frontiers in Virology. 2022; 2: 1–17. https://doi.org/10.3389/fviro.2022.935933

8. Cakir M, Obernier K, Forget A, Krogan NJ. Target Discovery for Host-Directed Antiviral Therapies: Application of Proteomics Approaches. mSystems. 2021; 6. https://doi.org/10.1128/mSystems.00388-21 PMID: 34519533

9. Witalisom E, Thompson R, Hofseth L. Protein Arginine Deiminases and Associated Citrullination: Physiological Functions and Diseases Associated with Dysregulation. Curr Drug Targets. 2015; 16:700–10. https://doi.org/10.2174/1389450116666150202160954 PMID: 25642720

10. Mondal S, Thompson PR. Protein Arginine Deiminases (PADs): Biochemistry and Chemical Biology of Protein Citrullination. Accounts of Chemical Research. 2019; 52: 818–832. https://doi.org/10.1021/acs.accounts.9b00024 PMID: 30844238

11. Valesini G, Gerardi MC, Iannuccelli C, Pacucci VA, Pendolino M, Shoenfeld Y. Citrullination and autoimmunity. Autoimmunity Reviews. 2015; 14: 490–497. https://doi.org/10.1016/j.autrev.2015.01.013 PMID: 25636595

12. Vossenaar ER, Zendman AJW, Van Venrooij WJ, Pruijn GJM. PAD, a growing family of citrullinating enzymes: Genes, features and involvement in disease. BioEssays. 2003; 25: 1106–1118. https://doi.org/10.1002/bies.10357 PMID: 14579251

13. Acharya NK, Nagele EP, Han M, Coretti NJ, DeMarshall C, Kosciuk MC, et al. Neuronal PAD4 expression and protein citrullination: Possible role in production of autoantibodies associated with neurodegenerative disease. Journal of Autoimmunity. 2012; 38: 369–380. https://doi.org/10.1016/j.jaut.2012.03.004 PMID: 22560840

14. Sokolove J, Brennan MJ, Sharpe O, Lahey LJ, Kao AH, Krishnan E, et al. Brief Report: Citrullination Within the Atherosclerotic Plaque: A Potential Target for the Anti-Citrullinated Protein Antibody Response in Rheumatoid Arthritis. Arthritis & Rheumatism. 2013; 65: 1719–1724. https://doi.org/10.1002/art.37961 PMID: 23553485

15. Yang L, Tan D, Piao H. Myelin Basic Protein Citrullination in Multiple Sclerosis: A Potential Therapeutic Target for the Pathology. Neurochemical Research. 2016; 41: 1845–1856. https://doi.org/10.1007/s11064-016-1920-2 PMID: 27097548

16. Yuzhalin AE. Citrullination in Cancer. Cancer Research. 2019; 79: 1274–1284. https://doi.org/10.1158/0008-5472.CAN-18-2797 PMID: 30894374

17. Masutomi H, Kawashima S, Kondo Y, Uchida Y, Jang B, Choi EK, et al. Induction of peptidylarginine deiminase 2 and 3 by dibutyryl cAMP via cAMP-PKA signaling in human astrocytoma U-251MG cells. Journal of Neuroscience Research. 2017; 95: 1503–1512. https://doi.org/10.1002/jnr.23959 PMID: 27704563

18. Ishigami A, Masutomi H, Handa S, Nakamura M, Nakaya S, Uchida Y, et al. Mass spectrometric identification of citrullination sites and immunohistochemical detection of citrullinated glial fibrillary acidic protein in Alzheimer's disease brains. Journal of Neuroscience Research. 2015; 93: 1664–1674. https://doi.org/10.1002/jnr.23620 PMID: 26190193

19. Knight JS, Subramanian V, O'Dell AA, Yalavarthi S, Zhao W, Smith CK, et al. Peptidylarginine deiminase inhibition disrupts NET formation and protects against kidney, skin and vascular disease in lupus-prone MRL/ *lpr* mice. Annals of the Rheumatic Diseases. 2015; 74: 2199–2206. https://doi.org/10.1136/annrheumdis-2014-205365 PMID: 25104775

20. Willis VC, Gizinski AM, Banda NK, Causey CP, Knuckley B, Cordova KN, et al. N-α-Benzoyl-N5-(2-Chloro-1-Iminoethyl)-l-Ornithine Amide, a Protein Arginine Deiminase Inhibitor, Reduces the Severity of Murine Collagen-Induced Arthritis. The Journal of Immunology. 2011; 186: 4396–4404. https://doi.org/10.4049/jimmunol.1001620 PMID: 21346230

21. Causey CP, Jones JE, Slack J, Kamei D, Jones LE, Subramanian V, et al. The development of o-F-amidine and o-Cl-amidine as second generation PAD inhibitors. J Med Chem. 2011; 54: 6919–6935. https://doi.org/10.1021/jm2008985.The

22. Falcão AM, Meijer M, Scaglione A, Rinwa P, Agirre E, Liang J, et al. PAD2-Mediated Citrullination Contributes to Efficient Oligodendrocyte Differentiation and Myelination. Cell Reports. 2019; 27: 1090–1102.e10. https://doi.org/10.1016/j.celrep.2019.03.108 PMID: 31018126

23. Muth A, Subramanian V, Beaumont E, Nagar M, Kerry P, McEwan P, et al. Development of a Selective Inhibitor of Protein Arginine Deiminase 2. Journal of Medicinal Chemistry. 2017; 60: 3198–3211. https://doi.org/10.1021/acs.jmedchem.7b00274 PMID: 28328217

24. Lewis HD, Liddle J, Coote JE, Atkinson SJ, Barker MD, Bax D, et al. HHS Public Access. 2015; 11: 189–191. https://doi.org/10.1038/nchembio.1735.Inhibition

25. Arisan ED, Uysal-Onganer P, Lange S. Putative roles for peptidylarginine deiminases in COVID-19. International Journal of Molecular Sciences. 2020; 21: 1–29. https://doi.org/10.3390/ijms21134662 PMID: 32629995

26. Pasquero S, Gugliesi F, Griffante G, Dell'Oste V, Biolatti M, Albano C, et al. Novel antiviral activity of PAD inhibitors against human beta-coronaviruses HCoV-OC43 and SARS-CoV-2. Antiviral Research. 2022; 200: 105278. https://doi.org/10.1016/j.antiviral.2022.105278 PMID: 35288208

27. Casanova V, Sousa FH, Shakamuri P, Svoboda P, Buch C, D'Acremont M, et al. Citrullination Alters the Antiviral and Immunomodulatory Activities of the Human Cathelicidin LL-37 During Rhinovirus Infection. Frontiers in Immunology. 2020; 11. https://doi.org/10.3389/fimmu.2020.00085 PMID: 32117246

28. Trier NH, Holm BE, Heiden J, Slot O, Locht H, Lindegaard H, et al. Antibodies to a strain-specific citrullinated Epstein-Barr virus peptide diagnoses rheumatoid arthritis. Scientific Reports. 2018; 8: 3684. https://doi.org/10.1038/s41598-018-22058-6 PMID: 29487382

29. Pratesi F, Tommasi C, Anzilotti C, Puxeddu I, Sardano E, Di Colo G, et al. Antibodies to a new viral citrullinated peptide, VCP2: fine specificity and correlation with anti-cyclic citrullinated peptide (CCP) and anti-VCP1 antibodies. Clinical & Experimental Immunology. 2011; 164: 337–345. https://doi.org/10.1111/j.1365-2249.2011.04378.x PMID: 21413944

30. Griffante G, Gugliesi F, Pasquero S, Dell'Oste V, Biolatti M, Salinger AJ, et al. Human cytomegalovirus-induced host protein citrullination is crucial for viral replication. Nature Communications. 2021; 12: 1–14. https://doi.org/10.1038/s41467-021-24178-6 PMID: 34162877

31. Bicker KL, Thompson PR. The protein arginine deiminases: Structure, function, inhibition, and disease. Biopolymers. 2013; 99: 155–163. https://doi.org/10.1002/bip.22127 PMID: 23175390

32. U KP, Subramanian V, Nicholas AP, Thompson PR, Ferretti P. Modulation of calcium-induced cell death in human neural stem cells by the novel peptidylarginine deiminase-AIF pathway. Biochim Biophys Acta. 2014; 1843: 1162–1171. https://doi.org/10.1016/j.bbamcr.2014.02.018 PMID: 24607566

33. Cheshenko N, Del Rosario B, Woda C, Marcellino D, Satlin LM, Herold BC. Herpes simplex virus triggers activation of calcium-signaling pathways. J Cell Biol. 2003; 163: 283–293. https://doi.org/10.1083/jcb.200301084 PMID: 14568989

34. Quynh Doan NT, Christensen SB. Thapsigargin, Origin, Chemistry, Structure-Activity Relationships and Prodrug Development. Curr Pharm Des. 2015; 21: 5501–5517. https://doi.org/10.2174/1381612821666151002112824 PMID: 26429715

35. Jamali H, Khan HA, Stringer JR, Chowdhury S, Ellman JA. Identification of Multiple Structurally Distinct, Nonpeptidic Small Molecule Inhibitors of Protein Arginine Deiminase 3 Using a Substrate-Based Fragment Method. 2015.

36. Hartenian E, Nandakumar D, Lari A, Ly M, Tucker JM, Glaunsinger BA. The molecular virology of coronaviruses. J Biol Chem. 2020; 295: 12910–12934. https://doi.org/10.1074/jbc.REV120.013930 PMID: 32661197

37. Martín Monreal MT, Rebak AS, Massarenti L, Mondal S, Šenolt L, Ødum N, et al. Applicability of Small-Molecule Inhibitors in the Study of Peptidyl Arginine Deiminase 2 (PAD2) and PAD4. Frontiers in Immunology. 2021; 12: 1–11. https://doi.org/10.3389/fimmu.2021.716250 PMID: 34737738

38. Vladimer GI, Górna MW, Superti-Furga G. IFITs: Emerging roles as key anti-viral proteins. Frontiers in Immunology. 2014; 5: 1–6. https://doi.org/10.3389/fimmu.2014.00094 PMID: 24653722

39. Mears H V., Sweeney TR. Better together: The role of IFIT protein-protein interactions in the antiviral response. Journal of General Virology. 2018; 99: 1463–1477. https://doi.org/10.1099/jgv.0.001149 PMID: 30234477

40. Li D, Swaminathan S. Human IFIT proteins inhibit lytic replication of KSHV: A new feed-forward loop in the innate immune system. PLoS Pathogens. 2019; 15: 1–27. https://doi.org/10.1371/journal.ppat.1007609 PMID: 30779786

41. Jiang Z, Su C, Zheng C. Herpes Simplex Virus 1 Tegument Protein UL41 Counteracts IFIT3 Antiviral Innate Immunity. Journal of Virology. 2016; 90: 11056–11061. https://doi.org/10.1128/JVI.01672-16 PMID: 27681138

42. Lee CY, Wang D, Wilhelm M, Zolg DP, Schmidt T, Schnatbaum K, et al. Mining the human tissue proteome for protein citrullination. Molecular and Cellular Proteomics. 2018; 17: 1378–1391. https://doi.org/10.1074/mcp.RA118.000696 PMID: 29610271

43. Luganini A, Caposio P, Landolfo S, Gribaudo G. Phosphorothioate-modified oligodeoxynucleotides inhibit human cytomegalovirus replication by blocking virus entry. Antimicrob Agents Chemother. 2008; 52: 1111–1120. https://doi.org/10.1128/AAC.00987-07 PMID: 18180342

44. Bicker KL, Subramanian V, Chumanevich AA, Hofseth LJ, Thompson PR. Seeing citrulline: development of a phenylglyoxal-based probe to visualize protein citrullination. J Am Chem Soc. 2012; 134: 17015–17018. https://doi.org/10.1021/ja308871v PMID: 23030787

45. Tilvawala R, Nguyen SH, Maurais AJ, Nemmara VV., Nagar M, Salinger AJ, et al. The Rheumatoid Arthritis-Associated Citrullinome. Cell Chemical Biology. 2018; 25: 691–704.e6. https://doi.org/10.1016/j.chembiol.2018.03.002 PMID: 29628436

46. Lewallen DM, Bicker KL, Subramanian V, Clancy KW, Slade DJ, Martell J, et al. Chemical Proteomic Platform To Identify Citrullinated Proteins. ACS Chemical Biology. 2015; 10: 2520. https://doi.org/10.1021/acschembio.5b00438 PMID: 26360112

Strigolactones as Broad-Spectrum Antivirals against β-Coronaviruses through Targeting the Main Protease M^pro

Matteo Biolatti, Marco Blangetti, Melissa Baggieri, Antonella Marchi, Silvia Gioacchini, Greta Bajetto, Davide Arnodo, Paola Bucci, Raoul Fioravanti, Maedeh Kojouri, Matteo Bersani, Giulia D'Arrigo, Lydia Siragusa, Simone Ghinato, Marco De Andrea, Francesca Gugliesi, Camilla Albano, Selina Pasquero, Ivan Visentin, Emilio D'Ugo, Francesca Esposito, Paolo Malune, Enzo Tramontano, Cristina Prandi, Francesca Spyrakis,* Fabio Magurano,* and Valentina Dell'Oste*

Cite This: *ACS Infect. Dis.* 2023, 9, 1310–1318

Read Online

ACCESS | Metrics & More | Article Recommendations | Supporting Information

ABSTRACT: The current SARS-CoV-2 pandemic and the likelihood that new coronavirus strains will emerge in the immediate future point out the urgent need to identify new pan-coronavirus inhibitors. Strigolactones (SLs) are a class of plant hormones with multifaceted activities whose roles in plant-related fields have been extensively explored. Recently, we proved that SLs also exert antiviral activity toward herpesviruses, such as human cytomegalovirus (HCMV). Here we show that the synthetic SLs TH-EGO and EDOT-EGO impair β-coronavirus replication including SARS-CoV-2 and the common cold human coronavirus HCoV-OC43. Interestingly, *in silico* simulations suggest the binding of SLs in the SARS-CoV-2 main protease (M^pro) active site, and this was further confirmed by an *in vitro* activity assay. Overall, our results highlight the potential efficacy of SLs as broad-spectrum antivirals against β-coronaviruses, which may provide the rationale for repurposing this class of hormones for the treatment of COVID-19 patients.

KEYWORDS: antiviral screening, strigolactones, HCoV-OC43, SARS-CoV-2, M^pro
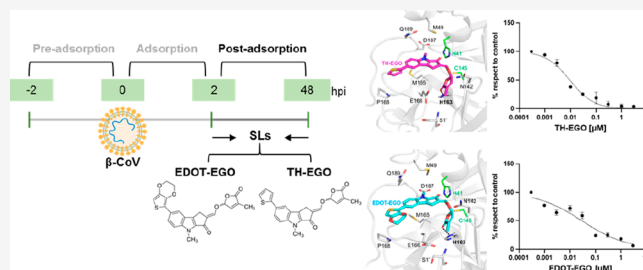
Emerging coronaviruses (CoVs) have recently raised global concerns, due to their high spillover potential and transmissibility rate, worsened by the limited availability of effective treatments.[1] Although a series of drugs approved for clinical use effectively inhibits severe acute respiratory syndrome coronavirus-2 (SARS-CoV-2) infection *in vitro*,[2] there is an urgent requirement for broad-spectrum antivirals.

Recently, the use of traditional medicines as an adjuvant in the treatment of COVID-19 has been demonstrated.[3] Strigolactones (SLs) are an emerging class of plant hormones with many functions.[4,5] They are made up of a tricyclic ABC core linked through an enol ether bridge to a fourth butenolide ring, commonly known as the D-ring, responsible for the bioactivity of SLs.[5] While their role in plant-related fields has been exhaustively investigated, the effects of SLs on human cells and their potential use in medicine are still poorly defined. So far, the most significant data on SLs suggest they have the ability to induce G2/M arrest and apoptosis in various types of human cancer cells.[6,7] Additionally, recent research shows that SLs may have promising anti-inflammatory properties by inhibiting the release of inflammatory molecules and the migration of neutrophils and macrophages in zebrafish larvae, as well as by increasing detoxifying enzymes.[8−10] Recently, we proved that SLs also exert an antiviral activity toward herpesviruses.[11]

Based on this background, this work aimed to ascertain whether SLs might constitute a new class of broad-spectrum compounds against β-CoVs.

We employed two indole-based SL analogues, named TH-EGO and EDOT-EGO (Figure 1A), derived from the potent antioxidant and neuroprotectant tryptophan metabolite indole-3-propionic acid.[12] The hydrolytic stability of TH-EGO and EDOT-EGO in prototypical DMEM/FBS 10% culture medium was evaluated (Figure 1B). Both compounds follow an exponential model decay and show comparable hydrolytic stabilities with estimated half-life times of 11.96 h for TH-EGO and 10.54 h for EDOT-EGO.

Initial screening to assess the antiviral activity of TH-EGO and EDOT-EGO was performed using HCoV-OC43 due to its
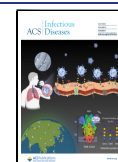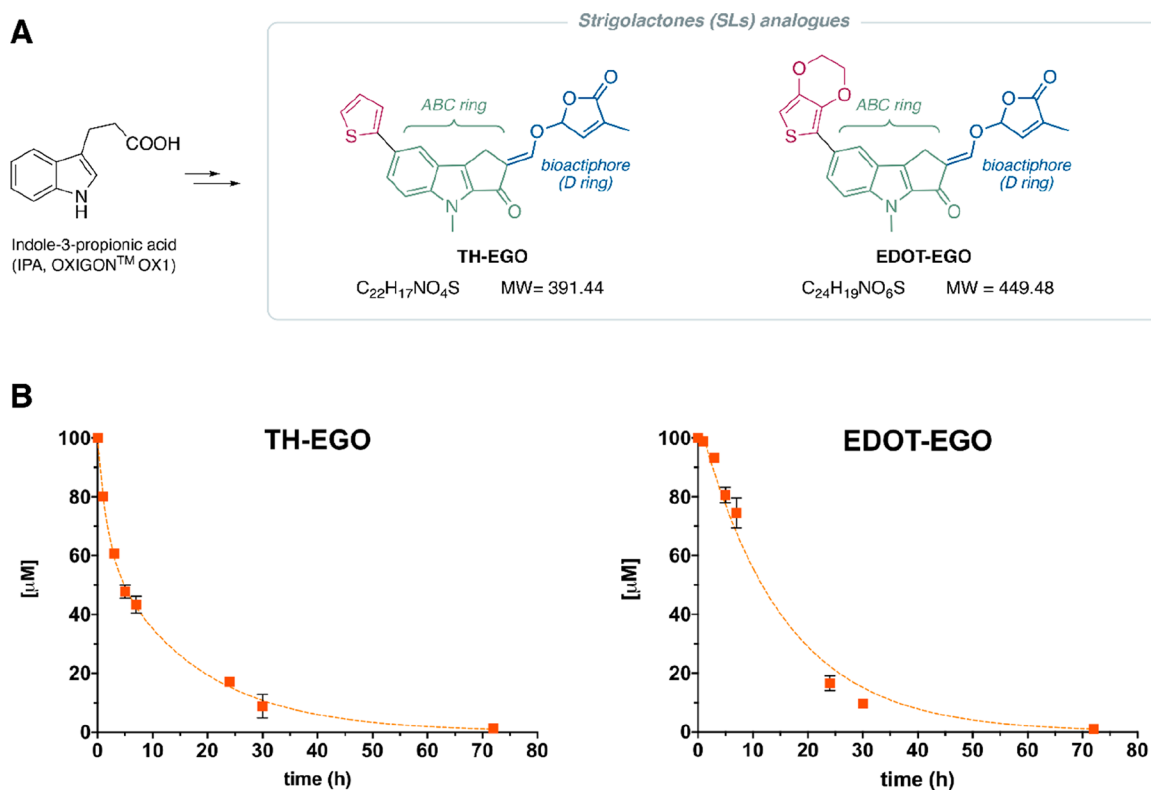
Figure 1. Indole-derived SL analogues. (A) Chemical structures of TH-EGO and EDOT-EGO. (B) Stability analyses of TH-EGO and EDOT-EGO in a culture medium. $[SL]_0 = 100 \ \mu M$ in DMEM/FBS + 0.5% DMSO. RP-HPLC analyses were run on an end-capped C18 (150×4.6 mm ID, 5 μM) column, using acetonitrile/H_2O (60/40 v/v) as a solvent mixture (1 mL/min flow rate) and analyzed at 295 nm (TH-EGO) and 326 nm (EDOT-EGO). Bars show means $\pm$ SEM of three independent experiments.

low biosafety concerns. First, a standard MTT viability assay was employed to rule out any cytotoxic effects of the compounds on MRC-5 cells. Both compounds' cytotoxicity for MRC-5 was low or undetectable at concentrations up to 25 μM, since ~90% of cells were viable after 48 h of treatment (Figure 2A).

Then, TH-EGO and EDOT-EGO were analyzed for their antiviral activity against HCoV-OC43 at a concentration of 25 μM, which was the minimum effective dose that did not show remarkable cytotoxicity. The antiviral activity was first measured on infected MRC-5 cells by RT-PCR. In this test, the inhibitory effect of a compound on viral replication is calculated by relative quantitation of the viral RNA genome released in supernatants in the presence of the compound vs the vehicle control (DMSO). As shown in Figure 2B, both tested SLs demonstrated significant inhibitory activity against HCoV-OC43. According to the results obtained by measuring viral RNA released in the supernatants, SLs also reduced the intracellular viral genome (Figure 2C), suggesting they act during the replication of the virion and not in the maturation step. Additionally, we investigated the effects of TH-EGO and EDOT-EGO on the HCoV-OC43 nucleocapsid protein (N) expression by Western blotting. Interestingly, both compounds significantly reduced the level of HCoV-OC43 N protein expression, thus confirming their inhibitory activity during the replication phase (Figure 2D).

Finally, a more detailed analysis with serial dilutions of the two compounds revealed that both TH-EGO and EDOT-EGO specifically inhibited HCoV-OC43 replication in a dose-dependent manner when the compounds were added to the cells 2 h before, during, and after infection (Figure 2E, panel i). To deeply understand which phase of the viral replication cycle

is targeted by SL analogues, the compounds were added to the cells during the adsorption stage (Figure 2E, panel ii) or after the removal of inoculum (postadsorption stage) (Figure 2E, panel iii). The virus yield reduction assay revealed that TH-EGO and EDOT-EGO retained a significant activity against HCoV-OC43 when added after the infection but not during the adsorption stage, suggesting that SL analogues interfere with a late molecular event during the HCoV-OC43 replication cycle.

To verify if SL derivatives maintain their antiviral activity toward other β-CoVs, we examined the impact of SL treatment on SARS-CoV-2 replication. The cytotoxicity of TH-EGO and EDOT-EGO for VERO E6 was low or undetectable at concentrations up to 200 μM (Figure 3A). First, TH-EGO and EDOT-EGO were analyzed for their antiviral activity against SARS-CoV-2 at a concentration of 25 μM (i.e., the same doses used for HCoV-OC43 experiments) by RT-PCR. As shown in Figure 3B, both tested SLs retained their antiviral activity also against SARS-CoV-2. Then, a more detailed analysis with serial dilutions of the two compounds revealed that the two compounds impair SARS-CoV-2 replication on VERO E6 cells in a dose-dependent manner when the compounds were added to the cells 2 h before, during, and after infection (Figure 3C, panel i). It is worth noting that, also in the SARS-CoV-2 model, SLs demonstrate sustained antiviral effects when added after the removal of inoculum during the postadsorption stage (Figure 3C, panel iii). This observation is consistent with our findings for HCoV-OC43 (Figure 2E). Conversely, SLs do not exhibit efficacy when inoculated during the adsorption stage (Figure 3C, panel ii), providing further evidence that a late step of β-CoV replication is targeted by SLs.
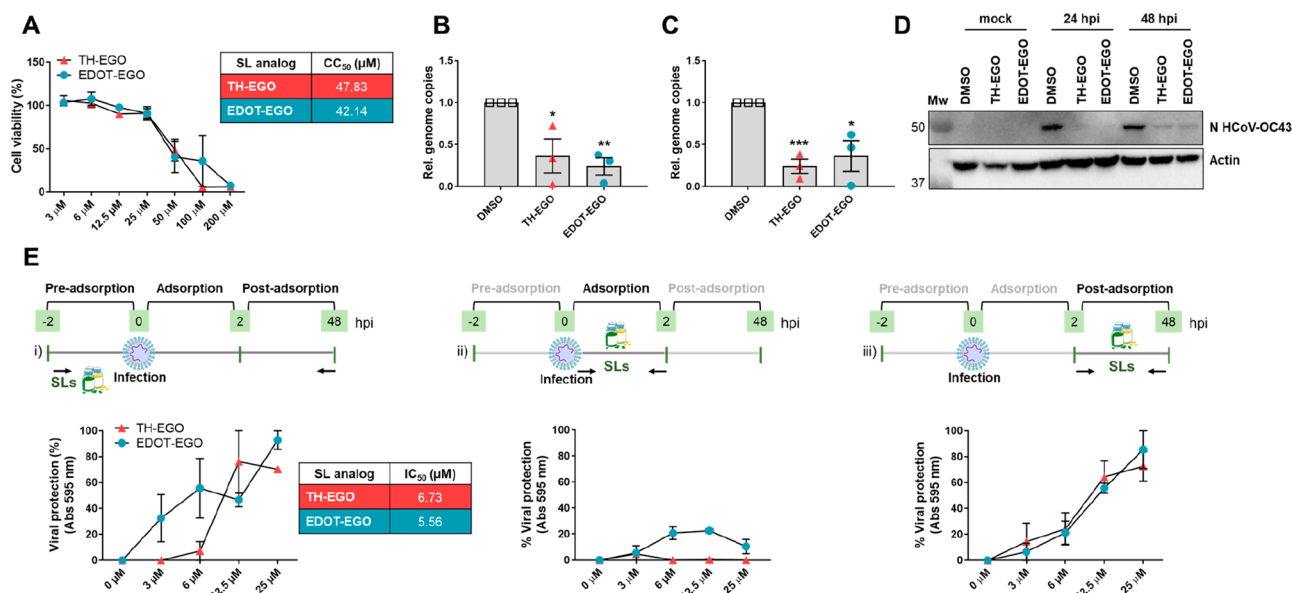
Figure 2. SL analogues as antivirals against HCoV-OC43. (A) Cell viability was measured by using the MTT assay. Confluent MRC-5 cultures were incubated with different concentrations of the indicated SLs for 48 h. Bars show means $\pm$ SEM of three independent experiments. CC_{50} values are reported in the table. (B) MRC-5 cells were pretreated with 25 μM of the indicated SLs or vehicle (DMSO) for 2 h. Later, MRC-5 cultures were infected with HCoV-OC43 (MOI 0.1), and following virus adsorption (2 h at 33 °C), the viral inoculum was removed and cultures were exposed to the compounds. At 48 hpi the number of HCoV-OC43 genomes released in the supernatants of infected cells was measured by RT-PCR. The mean value of DMSO-treated cells was arbitrarily set to 1. Bars show means $\pm$ SEM of three independent experiments ($P < 0.05$*; $P < 0.01$**; unpaired t test, for comparison of SL vs DMSO-treated cells). (C) The cells from (B) were also used to determine the relative intracellular number of viral RNA genomes in infected cells. The mean value of DMSO-treated cells was arbitrarily set to 1. Bars show means $\pm$ SEM of three independent experiments ($P < 0.05$*; $P < 0.001$***; unpaired t test, for comparison of SL vs DMSO-treated cells). (D) Western blot analysis of protein lysates from uninfected (mock) or infected cells using antibodies against the HCoV-OC43 N protein or actin. One representative blot (left panel) and densitometric analysis (right panel) are shown. Values are expressed as the percentage of inhibition of HCoV-OC43 N protein expression normalized to actin (DMSO-treated cells were arbitrarily set to 100). (E) Time-of-addition assays. (i) MRC-5 cells were pretreated with serial dilutions of SLs for 2 h. Later, MRC-5 were infected with HCoV-OC43 (MOI 0.1) in the presence of the compounds, and following virus adsorption (2 h at 33 °C), the viral inoculum was removed and cultures were exposed to increasing dilutions of SLs or vehicle (DMSO) and incubated for 48 h. IC_{50} values are reported in the table. (ii) The compounds and the virus were added simultaneously on cells (2 h at 33 °C) and then removed. (iii) MRC-5 were infected with HCoV-OC43 as described above, and after the removal of inoculum, they were treated with increasing concentrations of the compound and incubated for 48 h. Supernatants were harvested, and infectivity titers were determined by a colorimetric plaque assay. Bars show means $\pm$ SEM of three independent experiments.

To investigate which SARS-CoV-2 protein could be targeted by the analyzed SLs, we screened both SLs toward all the structures of coronavirus proteins present in CROMATIC at the time of the analyses,[14] using the screening procedure that allows evaluating the possible interaction of a series of ligands with several protein pockets. Overall, a total amount of 67 proteins and 124 pockets, belonging to the viruses MERS-CoV, SARS-CoV-1, and SARS-CoV-2, were considered.[14] Pockets were ranked according to the Glob-Prod score and selected for having a score higher than 1.

Among the highest-scored pockets of SARS-CoV-2, we noticed the presence of the 3-chymotrypsin-like protease (3CL^pro) or main protease (M^pro) orthosteric site, characterized by a Cys−His catalytic dyad. In particular, M^pro was identified at the fourth position among SARS-CoV-2 proteins, after the nucleoprotein C terminal domain, Nsp12, and Nsp14 (Table S1). Preliminary *in silico* docking simulations showed the most promising poses of both SLs in M^pro, in terms of the number of interactions and the stability of the poses.

These findings align with the observation that M^pro is currently one of the primary targets of several antivirals, including Nirmatrelvir (the active component of Paxlovid),[15] Ensitrelvir,[16] and Simnotrelvir,[17] which have already received clinical approval in certain countries and regions worldwide. Moreover, M^pro is a promising target also considering the SL

mechanism of action. Indeed, the natural target of SLs in plants, and specifically in rice, is an α/β-fold hydrolase named DWARF 14 (D14),[18] which hydrolyzes SLs into the active form of hormone (CLIM), covalently binds CLIM to trigger SL signaling, and finally releases an inactive hydrolysis product. The hydrolysis is performed by a Ser/His/Asp catalytic triad, which operates a nucleophilic attack on the ring D cyclic ester, as proposed by Scaffidi et al.[19] Similarly, M^pro could hydrolyze SLs by a nucleophilic attack performed by the deprotonated catalytic cysteine.[20]

We, thus, performed a more accurate docking simulation of EDOT-EGO and TH-EGO in the M^pro binding site with GOLD, obtaining similar and reasonable poses for both ligands (Figure 4A,C). In particular, for both compounds, a H-bond is formed between His163 and the lactone D-ring carbonyl group, while several hydrophobic contacts involve Met49, Met165, and Pro168 and the other SL rings. Interestingly, the interaction with His163 appears to be crucial for properly targeting the M^pro active site,[21] and the lactone functionality of the D-ring is close to the catalytic Cys145, thus supporting the hypothesis of a subsequent possible covalent attack. The docking score, provided by the PLP scoring function for the reported EDOT-EGO and TH-EGO, was over 60, thus supporting the prediction reliability.[22] Similar results were obtained when the compounds were docked in M^pro from HCoV-OC43 (Figure S1).
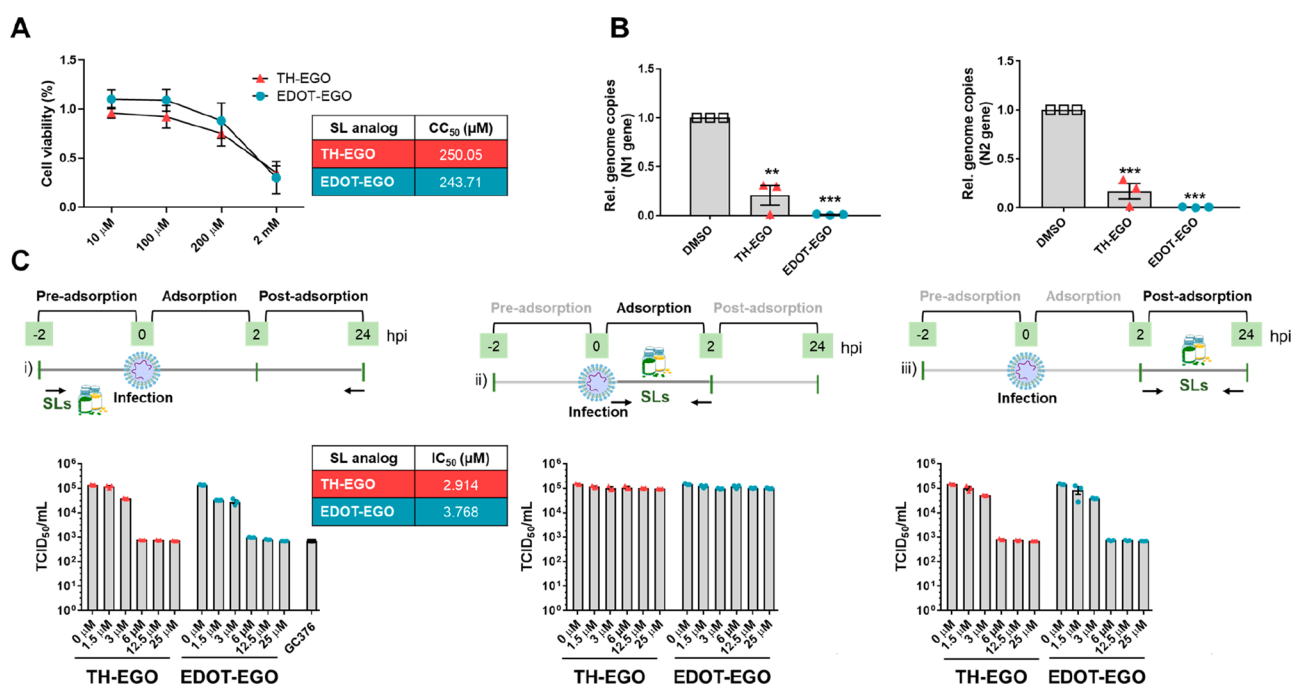
Figure 3. SL analogues as antivirals against SARS-CoV-2. (A) Cell viability was determined using the XTT assay. Confluent VERO E6 cultures were incubated with different concentrations of the indicated SLs for 24 h. Bars show means ± SD of three independent experiments. CC_{50} values are reported in the table. (B) VERO E6 cells were pretreated with the indicated SLs (25 μM) or vehicle (DMSO) for 2 h and then infected with SARS-CoV-2 (MOI 0.01). Following virus adsorption (2 h at 37 °C), the viral inoculum was removed, and cultures were exposed to SLs or DMSO. At 24 hpi the number of SARS-CoV-2 genomes leased in the supernatants of infected cells was measured by RT-PCR (N1, left panel; N2, right panel). The mean value of DMSO-treated cells was arbitrarily set to 1. Bars show means ± SEM of three independent experiments ($P < 0.05$*; $P < 0.01$**; $P < 0.001$***; unpaired t test, for comparison of SL vs DMSO-treated cells). (C) VERO E6 cells were (i) treated with serial dilutions of SLs for 2 h. Later, cells were infected with SARS-CoV-2 in the presence of the compounds, and following virus adsorption (2 h at 37 °C), the viral inoculum was removed, and cultures were exposed to increasing dilutions of SLs or vehicle (DMSO) and incubated for 24 h. IC_{50} values are reported in the table. (ii) The compounds and the virus were added simultaneously on cells (2 h at 37 °C) and then removed. (iii) VERO E6 cultures were infected with SARS-CoV-2, and after the removal of inoculum, they were treated with increasing concentrations of the compounds and incubated for 24 h. Supernatants were harvested, and the 50% end-point titers ($TCID_{50}$) were determined by using the Spearman−Karber method. Bars show means ± SEM of three independent experiments. GC376 (5 μM)[13] was used as a positive control of antiviral activity.

We then simulated covalent docking for both SLs in M^pro with Glide, obtaining the adducts reported in Figure 4B,D and Figure S2. In particular, we simulated the catalytic mechanism proposed by Scaffidi et al.,[19] in which the cysteine attacked the lactone moiety (Figure S3), the ABC ring has been released and a receptor−ligand covalent intermediate, stabilized by an additional H-bond, has formed (Figure 4B,D).

We thus hypothesized that both SLs could recognize the M^pro binding site to form a non-covalent complex, subsequently transforming into a covalent intermediate.

To validate the computational results, we tested EDOT-EGO and TH-EGO on SARS-CoV-2 M^pro activity using a biochemical assay. Serial dilutions of compounds were incubated with M^pro, and a substrate peptide was added. The resulting fluorescence resonance energy transfer (FRET) signal was acquired after 15 min of cleaving reaction at room temperature. GC376 was used as a positive control.[23]

Both compounds TH-EGO and EDOT-EGO were able to inhibit the activity of the SARS-CoV-2 M^pro and showed an IC_{50} value in the nanomolar range (0.008 and 0.048 μM, respectively) (Figure 5). To assess the broad-spectrum effect of SL analogues, we tested EDOT-EGO and TH-EGO on MERS-CoV M^pro activity. MERS-CoV is another β-coronavirus that shares 50.3% of M^pro sequence identity with SARS-CoV-2.[21] Both compounds were able to inhibit also the activity of the MERS M^pro but with less potency (Figure S4). For clarity, it

should be noted that the IC_{50} of GC376 is 0.00013 μM, while the concentration of M^pro enzyme used in the reaction is 15 nM, which represents the optimal enzyme concentration based on enzyme kinetics for the assay. However, it is worth noting that this concentration exceeds the inhibitor concentration by more than 10-fold. Hence, it is reasonable to speculate that only a fraction of the enzyme molecules are active during evaluation of the compound inhibition capability. Consequently, it can be inferred that the concentration of GC376 required to inhibit 50% enzyme activity is less than 50% of the total protein concentration. To further confirm the predicted inhibitory mechanism of action of EDOT-EGO and TH-EGO on SARS-CoV-2 M^pro activity, we performed the biochemical assay as previously described, with different preincubation times of the enzyme in the reaction mix in the presence of compounds, before the addition of the substrate. Results in Figure 5, panel D, show an increase in the IC_{50} value when increasing the preincubation time, similarly to what was observed for the control GC376, suggesting a covalent reversible inhibitory mode of action for both tested compounds.[24]

Overall, our findings show that the SLs TH-EGO and EDOT-EGO inhibit the replication of both HCoV-OC43 and SARS-CoV-2. Importantly, *in silico* simulations and activity experiments revealed that SARS-CoV-2 M^pro is targeted and inhibited by both molecules. Our studies allowed the discovery of potential antiviral compounds for further testing *in vivo* to
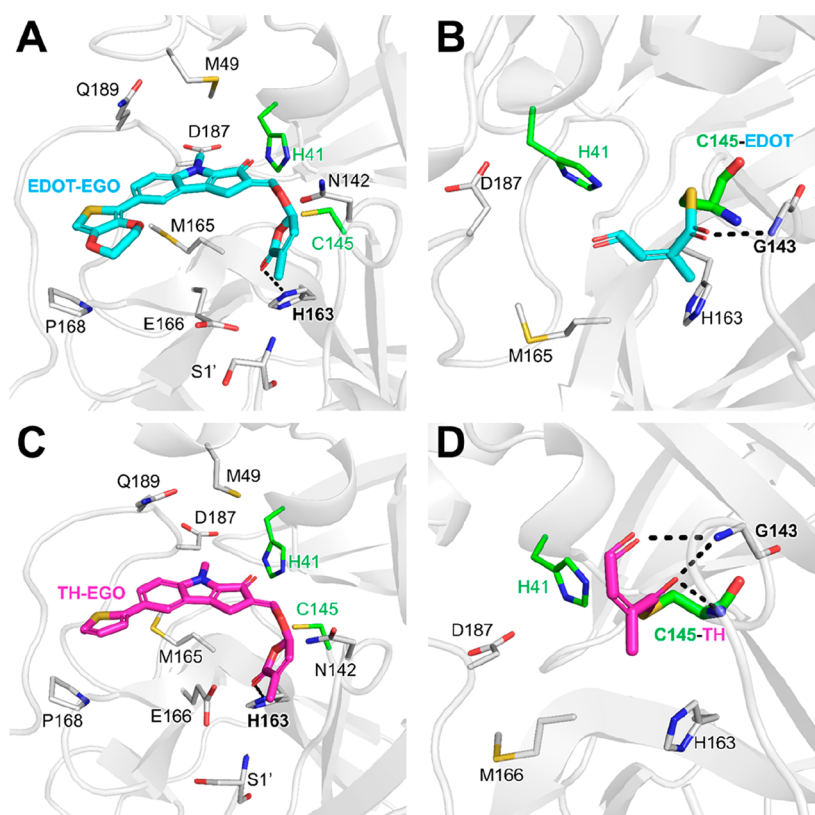
Figure 4. SARS-CoV-2 M^{pro} is targeted by SLs. (A, C) Docking poses of EDOT-EGO (A) and TH-EGO (C) in M^{pro}. (B, D) Second intermediate covalent adducts of EDOT-EGO (B) and TH-EGO (D) in M^{pro} obtained by covalent docking. The protein is shown as a cartoon, and the ligand and the key residues in the binding site are labeled and shown as capped sticks. H-bonds are displayed as black dashed lines.
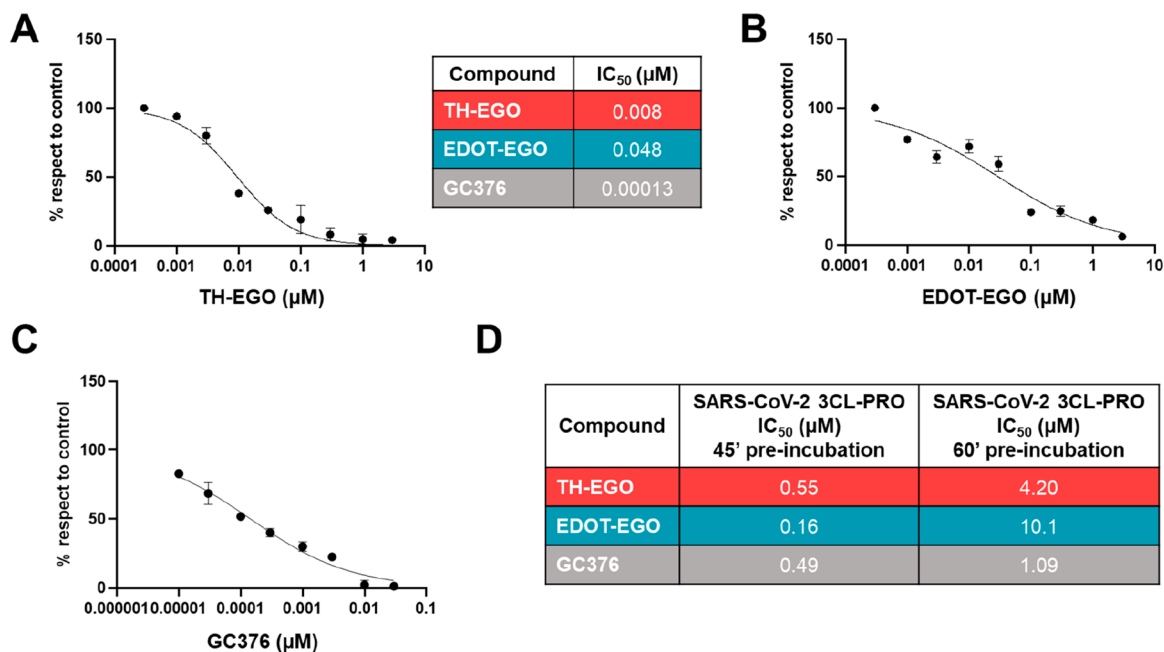

Figure 5. Inhibitory effect of SL analogues on SARS-CoV-2 M^{pro} activity. Inhibition curves of SARS-CoV-2 M^{pro} were obtained by TH-EGO (A), EDOT-EGO (B), and GC376 (C). (D) Influence of longer preincubation times of the SL analogues on SARS-CoV-2 M^{pro} activity. GC376 was used as a positive control. IC$_{50}$ values are reported in the table.

contain the current outbreak. Additionally, it may aid in the development of pan-anti-CoV inhibitors/treatments that can quickly and effectively respond to future pandemics.

■ METHODS

Compounds. The SL analogues TH-EGO and EDOT-EGO, synthesized as previously described,[25] were dissolved in dimethyl sulfoxide (DMSO) (Sigma-Aldrich) at a stock

concentrations of 20 mM and used as racemic mixtures. The GC376 compound (DBA Italia) was dissolved in DMSO and used as a positive control in SARS-CoV-2 antiviral assays and M^{pro} *in vitro* activity assays.

Hydrolytic Stability of SL Analogues. The hydrolytic stabilities of TH-EGO and EDOT-EGO were evaluated by incubation in Dulbecco's Modified Eagle Medium (DMEM; Sigma-Aldrich) supplemented with 10% (v/v) fetal bovine serum (FBS; Sigma-Aldrich). The stock solution of the compound (20 mM in DMSO) was diluted in preheated (37 °C) DMEM/FBS (10%) to a final concentration of 100 μM. The solution was incubated at 37 ± 0.5 °C, and at appropriate time intervals, a 300 μL aliquot of mixture was withdrawn and added to 300 μL of acetonitrile (+0.1% HCOOH) to deproteinize the serum. The sample was sonicated, vortexed, filtered through 0.45 μm PTFE filters (Alltech), and analyzed by RP-HPLC. All experiments were performed in triplicate. RP-HPLC analyses were performed with a Waters 1500 chromatograph system (Waters, Milford, MA, USA) equipped with a manual injector (Rheodyne, Cotati, CA, USA), a binary pump (model 1525), and a diode-array detector (DAD, model 2998) integrated into the Waters system. The injection volume was 20 μL. Analyses were performed on a SunFire endcapped C18 column (150 × 4.6 mm ID, 5 μM) using an acetonitrile/water mobile phase (60/40 v/v, 1 mL/min flow rate). The column effluent was monitored at 295 nm (TH-EGO) and 326 nm (EDOT-EGO), referenced against a 700 nm wavelength. The data were processed by using a Breeze software package (Waters). The compounds were quantified using a calibration curve obtained with standard solutions chromatographed under the same experimental conditions, with a concentration range of 1−100 μM (r^2 > 0.99).

Cell Lines and Virus Propagation. Human lung fibroblast MRC-5 (ATCC CCL-171) and VERO E6 cells (*Cercopithecus aethiops* derived epithelial kidney, C1008; ATCC CRL-1586) were propagated at 37 °C in a humidified 5% CO$_2$ atmosphere in DMEM (Sigma-Aldrich) supplemented with 1% (v/v) penicillin/streptomycin solution (Sigma-Aldrich) and heat-inactivated, 10% (v/v) FBS (Sigma-Aldrich).

The human coronavirus HCoV-OC43 strain (ATCC VR-1558) was grown as reported in Milewska et al.[26] The human β-coronavirus SARS-CoV-2, strain BetaCov/Italy/CDG1/2020| EPI ISL 412973|2020-02-20 (GISAID accession ID: EPI_-ISL_412973), was propagated on VERO E6 cells, and the infectious titer was determined by a plaque assay. Virus propagation was conducted under biosafety level 3 facilities at the "Istituto Superiore di Sanità" (Rome, IT).

Cytotoxicity Assays. SL cytotoxicity was determined by standard 2,3-bis-(2-methoxy-4-nitro-5-sulfophenyl)-2*H*-tetrazolium-5-carboxanilide (XTT) for VERO E6 (Roche) or the 3-(4,5-dimethylthiazol-2-yl)-2,5-diphenyltetrazolium bromide (MTT) (Sigma-Aldrich) assay for MRC-5.

Antiviral Assays against HCoV-OC43. *Plaque Assay.* MRC-5 cells were seeded in 24-well plates and subjected to the time of addition assays with different concentrations of SL analogues or the vehicle control (DMSO), as described in the Results section. Cells were infected with HCoV-OC43 (MOI 0.1) for 2 h at 33 °C, and the supernatants were then collected at 48 hpi. The extent of virus replication was subsequently assessed by titrating the infectivity of the supernatants by standard plaque assay. Cells were fixed and stained with crystal violet solution, and the absorbance readings were measured at 595 nm using a Victor X4 multilabel plate reader. Histograms were obtained by

plotting the values of the 10^{-4} dilution, expressed for each compound concentration as a percentage of the mean absorbance of the uninfected control (mock) (set as 100%).

Real-Time PCR. MRC-5 cells were treated as described in the standard plaque assay section. Forty-eight hours later cells or supernatants were collected, and RNA was isolated from 200 μL of supernatants or cell pellets, respectively, using the TRI Reagent solution (Sigma-Aldrich), according to the manufacturer's instructions. Extracted viral RNA was retrotranscribed and amplified by the Sensi Fast Probe No Rox One step kit (Bioline). The primers and probe for N gene amplification (Eurofins Genomics) are reported in Table S1.

Western Blot Analysis. Whole-cell protein extracts were prepared and subjected to Western blot analysis. The following primary antibodies were used: anti-Coronavirus mouse monoclonal antibody, HCoV-OC43 strain, clone 541-8F (MAB9012, Sigma-Aldrich), and anti-actin (A2066, Sigma Aldrich) (both at 1:1000 dilution in 5% nonfat dry milk, TBS-Tween 0.05%). Immunocomplexes were detected using appropriate secondary antibodies conjugated with horseradish peroxidase (HRP) (GE Healthcare Europe GmbH) and visualized by enhanced chemiluminescence (Super Signal West Pico; Thermo Fischer Scientific).

Antiviral Activity against SARS-CoV-2. *Plaque Assay.* VERO E6 cells were seeded in 24-well plates and subjected to the time of addition assays with different dilutions of SL analogues or the vehicle control (DMSO), as described in Figure 2E. Cells were infected with SARS-CoV-2 (MOI 0.01) for 2 h at 37 °C. After 24 h, a cytopathic effect was observed, and culture supernatants were collected for virus titration by standard TCID$_{50}$ assay, as previously described.[27]

Real-Time PCR. The RNAs were tested by TaqMan RT-PCR (Bio-Rad) to target the N genes of SARS-CoV-2, based on protocols developed by the Centers for Disease Control and Prevention (CDC; 2019-Novel Coronavirus (2019-nCoV) rRT-PCR Panel Primers and Probes. Updated: May 29, 2020). Primers and probes used (Eurofins Genomics) are reported in Table S1.

Virtual screening. EDOT-EGO and TH-EGO were evaluated by means of a structure-based virtual screening approach against all cavities of a database composed of 67 proteins and 124 corresponding pockets.[14] The FLAP structure-based approach[28] was applied to evaluate the molecular interaction field (MIF) complementarity between the template molecule and the cavity MIFs. The MIF superposition is reported as a complementarity score: the higher the score, the better the ligand fits into the cavity. EDOT-EGO and TH-EGO were screened against the entire database of cavities. The score values were considered for ranking the database cavities according to their complementarity with the two templates. Cavities were selected to have a Glob-prod higher than 1. Among the selected pocket, we identified the orthosteric site of SARS-CoV-2 M^{pro}, which was subsequently used for docking simulations, according to the possibility of hydrolyzing SL and forming a nucleophilic adduct.

Docking Simulations. Docking simulations were performed for EDOT-EGO and TH-EGO in the SARS-CoV-2 M^{pro} catalytic site (PDB code: 6Y2G), using GOLD[29] and Glide docking from Maestro.[30] Static docking experiments were carried out with GOLD in both chains of the M^{pro} dimer using a spherical region of 12 Å radius and the oxygen atom of His164 as the centroid, generating a maximum of 50 docking poses. According to the first catalytic step hypothesized for D14

(Figure S3), the possible covalent binding mode of the two SL in M^pro was further investigated through the Glide CovDock procedure.[31] In this simulation, a single pose was generated for each SL, using a 22 Å cubic box region of the same previously mentioned centroid.

Static docking simulations were also performed in the OC43 M^pro catalytic site, maintaining settings similar to those previously described. Given the absence of three-dimensional information, the structure of the protein was modeled with Swiss Model, using as template 6Y2G.[32] Indeed, the primary sequence of the protease is quite similar, with a global identity equal to 50% but a high similarity at the binding site level. All residues lining the pocket are conserved with the only exception of Asn142, Met165, and Pro168, respectively, substituted in OC43 M^pro by Cys142, Leu165, and Ser168. Moreover, in SARS-CoV-2 M^pro (and not in OC43), Glu166 is salt-bridged to the N-terminal serine of the other monomer. With the orientation of the mentioned amino acids being biased by the conformations of 6Y2G template residues, we performed docking simulations allowing the flexibility at these residue side-chains, by means of library rotamers implemented in GOLD.

SARS-CoV-2 and MERS M^pro Purification. The SARS-CoV-2 and the Middle-East Respiratory Syndrome Coronavirus (MERS) M^pro proteins were expressed in the *E. coli* cells BL21 (DE3) strain, the pellets were clarified by ultracentrifugation, and the proteins were purified using two purification steps. Eluted fractions containing the SARS-CoV-2 M^pro were pooled and subjected to buffer exchange (20 mM Tris−HCl, 150 mM NaCl, 1 mM EDTA, 1 mM DTT, pH 7.8) by using Amicon Ultra 15 centrifugal filters at 4000g, at 4 °C. The protein purity was checked by SDS-PAGE analysis.

SARS-CoV-2 and MERS M^pro *in Vitro* Activity Assays. The SARS-CoV-2 and MERS M^pro enzyme inhibition FRET assays[15,33] were performed in a buffer containing 20 mM Tris (pH 7.3), 100 mM NaCl, 5 mM TCEP, 0.1% BSA, and 1 mM EDTA.

After preincubation with 15 nM protein (a quantity below saturation for the enzymatic assay, as determined by an enzyme activity curve for M^pro) and different concentrations of the tested compounds for 30 min (or 45 and 60 min in the case of longer-time experiments) at 37 °C, the substrate was added (peptide DABCYL-KTSAVLQ↓SGFRKM-EDANS) and the fluorescent signal (em/ex 320/480) was monitored after 15 and 30 min of incubation at room temperature with the substrate, for SARS-CoV-2 and MERS M^pro, respectively.

Statistical Analysis. The statistical tests were performed using GraphPad Prism ver. 5.00 for Windows (GraphPad Software). The data were presented as means ± the standard error of the mean (SEM). Differences were considered statistically significant for $P < 0.05$ ($P < 0.05$*; $P < 0.01$**; $P < 0.001$***). CC_{50} and IC_{50} values were calculated by nonlinear regression (curve fitting analysis) in GraphPad Prism software.

■ ASSOCIATED CONTENT

Ⓢ Supporting Information

The Supporting Information is available free of charge at https://pubs.acs.org/doi/10.1021/acsinfecdis.3c00219.

> Supplementary figures with additional docking analyses and the proposed mechanism of SL hydrolysis (Figures S1−S3), supplementary figure reporting the inhibitory effect of SL analogues on MERS-CoV M^pro activity (Figure S4), and tables with the extract of the virtual screening analysis (Table S1) and with the oligonucleotide sequences (Table S2) (PDF)

■ AUTHOR INFORMATION

Corresponding Authors

Francesca Spyrakis − *Department of Drug Science and Technology, University of Turin, 10125 Turin, Italy;* ⓞ orcid.org/0000-0002-4016-227X; Email: francesca.spyrakis@unito.it

Fabio Magurano − *Department of Infectious Diseases, Istituto Superiore di Sanità, 00161 Rome, Italy;* Email: fabio.magurano@iss.it

Valentina Dell'Oste − *Department of Public Health and Pediatric Sciences, University of Turin, 10126 Turin, Italy;* ⓞ orcid.org/0000-0002-9336-7906; Email: valentina.delloste@unito.it

Authors

Matteo Biolatti − *Department of Public Health and Pediatric Sciences, University of Turin, 10126 Turin, Italy;* ⓞ orcid.org/0000-0001-7675-0762

Marco Blangetti − *Department of Chemistry, University of Turin, 10125 Turin, Italy;* ⓞ orcid.org/0000-0001-6553-8846

Melissa Baggieri − *Department of Infectious Diseases, Istituto Superiore di Sanità, 00161 Rome, Italy*

Antonella Marchi − *Department of Infectious Diseases, Istituto Superiore di Sanità, 00161 Rome, Italy*

Silvia Gioacchini − *Department of Infectious Diseases, Istituto Superiore di Sanità, 00161 Rome, Italy*

Greta Bajetto − *Department of Public Health and Pediatric Sciences, University of Turin, 10126 Turin, Italy; Center for Translational Research on Autoimmune and Allergic Disease-CAAD, 28100 Novara, Italy*

Davide Arnodo − *Department of Chemistry, University of Turin, 10125 Turin, Italy;* ⓞ orcid.org/0000-0002-0294-2750

Paola Bucci − *Department of Infectious Diseases, Istituto Superiore di Sanità, 00161 Rome, Italy*

Raoul Fioravanti − *Department of Infectious Diseases, Istituto Superiore di Sanità, 00161 Rome, Italy;* ⓞ orcid.org/0000-0002-0151-0331

Maedeh Kojouri − *Department of Infectious Diseases, Istituto Superiore di Sanità, 00161 Rome, Italy*

Matteo Bersani − *Department of Drug Science and Technology, University of Turin, 10125 Turin, Italy*

Giulia D'Arrigo − *Department of Drug Science and Technology, University of Turin, 10125 Turin, Italy*

Lydia Siragusa − *Molecular Discovery Ltd., Borehamwood WD6 4PJ Hertfordshire, United Kingdom; Molecular Horizon s.r.l., 06084 Bettona, PG, Italy;* ⓞ orcid.org/0000-0003-4596-7242

Simone Ghinato − *Department of Chemistry, University of Turin, 10125 Turin, Italy*

Marco De Andrea − *Department of Public Health and Pediatric Sciences, University of Turin, 10126 Turin, Italy; Center for Translational Research on Autoimmune and Allergic Disease-CAAD, 28100 Novara, Italy*

Francesca Gugliesi − *Department of Public Health and Pediatric Sciences, University of Turin, 10126 Turin, Italy*

Camilla Albano − *Department of Public Health and Pediatric Sciences, University of Turin, 10126 Turin, Italy;* ⓞ orcid.org/0000-0002-0847-6332

Selina Pasquero — *Department of Public Health and Pediatric Sciences, University of Turin, 10126 Turin, Italy;* ● orcid.org/0000-0002-3815-2494

Ivan Visentin — *Department of Agricultural, Forestry, and Food Sciences, University of Turin, 10095 Turin, Italy*

Emilio D'Ugo — *Department of Infectious Diseases, Istituto Superiore di Sanità, 00161 Rome, Italy*

Francesca Esposito — *Department of Life and Environmental Sciences, University of Cagliari, 09042 Cagliari, Italy*

Paolo Malune — *Department of Life and Environmental Sciences, University of Cagliari, 09042 Cagliari, Italy*

Enzo Tramontano — *Department of Life and Environmental Sciences, University of Cagliari, 09042 Cagliari, Italy;* ● orcid.org/0000-0002-4849-0980

Cristina Prandi — *Department of Chemistry, University of Turin, 10125 Turin, Italy;* ● orcid.org/0000-0001-9510-8783

Complete contact information is available at:
https://pubs.acs.org/10.1021/acsinfecdis.3c00219

Notes

The authors declare no competing financial interest.

■ **ACKNOWLEDGMENTS**

■ **ABBREVIATIONS**

CoV, coronavirus; CC_{50}, compound concentration that produces 50% of cytotoxicity; DAD, diode-array detector; DMSO, dimethyl sulfoxide; FRET, fluorescence resonance energy transfer; HCMV, human cytomegalovirus; IC_{50}, 50% inhibitory concentration at half-maximal response; MERS, Middle-East respiratory syndrome coronavirus; MIFs, molecular interaction fields; M^{pro}, main protease; SARS-CoV-2, severe acute respiratory syndrome coronavirus-2; SLs, strigolactones

■ **REFERENCES**

(1) Ruiz-Aravena, M.; McKee, C.; Gamble, A.; Lunn, T.; Morris, A.; Snedden, C. E.; Yinda, C. K.; Port, J. R.; Buchholz, D. W.; Yeo, Y. Y.; Faust, C.; Jax, E.; Dee, L.; Jones, D. N.; Kessler, M. K.; Falvo, C.; Crowley, D.; Bharti, N.; Brook, C. E.; Aguilar, H. C.; Peel, A. J.; Restif, O.; Schountz, T.; Parrish, C. R.; Gurley, E. S.; Lloyd-Smith, J. O.; Hudson, P. J.; Munster, V. J.; Plowright, R. K. Ecology, Evolution and Spillover of Coronaviruses from Bats. *Nat Rev Microbiol* **2022**, *20*, 299.

(2) Xiong, H.-L.; Cao, J.-L.; Shen, C.-G.; Ma, J.; Qiao, X.-Y.; Shi, T.-S.; Ge, S.-X.; Ye, H.-M.; Zhang, J.; Yuan, Q.; Zhang, T.-Y.; Xia, N.-S. Several FDA-Approved Drugs Effectively Inhibit SARS-CoV-2 Infection in Vitro. *Frontiers in Pharmacology* **2021**, *11*, 609592.

(3) Chapman, R. L.; Andurkar, S. V. A Review of Natural Products, Their Effects on SARS-CoV-2 and Their Utility as Lead Compounds in the Discovery of Drugs for the Treatment of COVID-19. *Med Chem Res* **2022**, *31* (1), 40−51.

(4) Dell'Oste, V.; Spyrakis, F.; Prandi, C. Strigolactones, from Plants to Human Health: Achievements and Challenges. *Molecules* **2021**, *26* (15), 4579.

(5) *Strigolactones - Biology and Applications*; Koltai, H., Prandi, C., Eds.; Springer International Publishing: 2019. DOI: 10.1007/978-3-030-12153-2.

(6) Mayzlish-Gati, E.; Laufer, D.; Grivas, C. F.; Shaknof, J.; Sananes, A.; Bier, A.; Ben-Harosh, S.; Belausov, E.; Johnson, M. D.; Artuso, E.; Levi, O.; Genin, O.; Prandi, C.; Khalaila, I.; Pines, M.; Yarden, R. I.; Kapulnik, Y.; Koltai, H. Strigolactone Analogs Act as New Anti-Cancer Agents in Inhibition of Breast Cancer in Xenograft Model. *Cancer Biol. Ther.* **2015**, *16* (11), 1682−1688.

(7) Pollock, C. B.; McDonough, S.; Wang, V. S.; Lee, H.; Ringer, L.; Li, X.; Prandi, C.; Lee, R. J.; Feldman, A. S.; Koltai, H.; Kapulnik, Y.; Rodriguez, O. C.; Schlegel, R.; Albanese, C.; Yarden, R. I. Strigolactone Analogues Induce Apoptosis through Activation of P38 and the Stress Response Pathway in Cancer Cell Lines and in Conditionally Reprogrammed Primary Prostate Cancer Cells. *Oncotarget* **2014**, *5* (6), 1683−1698.

(8) Tumer, T. B.; Yılmaz, B.; Ozleyen, A.; Kurt, B.; Tok, T. T.; Taskin, K. M.; Kulabas, S. S. GR24, a Synthetic Analog of Strigolactones, Alleviates Inflammation and Promotes Nrf2 Cytoprotective Response: In Vitro and in Silico Evidences. *Comput Biol Chem* **2018**, *76*, 179−190.

(9) Zheng, J.-X.; Han, Y.-S.; Wang, J.-C.; Yang, H.; Kong, H.; Liu, K.-J.; Chen, S.-Y.; Chen, Y.-R.; Chang, Y.-Q.; Chen, W.-M.; Guo, J.-L.; Sun, P.-H. Strigolactones: A Plant Phytohormone as Novel Anti-Inflammatory Agents. *Medchemcomm* **2018**, *9* (1), 181−188.

(10) Antika, G.; Cinar, Z. Ö.; Seçen, E.; Özbil, M.; Tokay, E.; Köçkar, F.; Prandi, C.; Tumer, T. B. Strigolactone Analogs: Two New Potential Bioactiphores for Glioblastoma. *ACS Chem Neurosci* **2022**, *13* (5), 572−580.

(11) Biolatti, M.; Blangetti, M.; D'Arrigo, G.; Spyrakis, F.; Cappello, P.; Albano, C.; Ravanini, P.; Landolfi, S.; De Andrea, M.; Prandi, C.; Dell'Oste, V. Strigolactone Analogs Are Promising Antiviral Agents for the Treatment of Human Cytomegalovirus Infection. *Microorganisms* **2020**, *8* (5), No. 703.

(12) Bendheim, P. E.; Poeggeler, B.; Neria, E.; Ziv, V.; Pappolla, M. A.; Chain, D. G. Development of Indole-3-Propionic Acid (OXIGON) for Alzheimer's Disease. *J Mol Neurosci* **2002**, *19* (1−2), 213−217.

(13) Resnick, S. J.; Iketani, S.; Hong, S. J.; Zask, A.; Liu, H.; Kim, S.; Melore, S.; Lin, F.-Y.; Nair, M. S.; Huang, Y.; Lee, S.; Tay, N. E. S.; Rovis, T.; Yang, H. W.; Xing, L.; Stockwell, B. R.; Ho, D. D.; Chavez, A. Inhibitors of Coronavirus 3CL Proteases Protect Cells from Protease-Mediated Cytotoxicity. *Journal of Virology* **2021**, *95* (14), e02374−20.

(14) Siragusa, L.; Menna, G.; Buratta, F.; Baroni, M.; Desantis, J.; Cruciani, G.; Goracci, L. CROMATIC: Cross-Relationship Map of Cavities from Coronaviruses. *J Chem Inf Model* **2022**, *62* (12), 2901−2908.

(15) Owen, D. R.; Allerton, C. M. N.; Anderson, A. S.; Aschenbrenner, L.; Avery, M.; Berritt, S.; Boras, B.; Cardin, R. D.; Carlo, A.; Coffman, K. J.; Dantonio, A.; Di, L.; Eng, H.; Ferre, R.; Gajiwala, K. S.; Gibson, S. A.; Greasley, S. E.; Hurst, B. L.; Kadar, E. P.; Kalgutkar, A. S.; Lee, J. C.; Lee, J.; Liu, W.; Mason, S. W.; Noell, S.; Novak, J. J.; Obach, R. S.; Ogilvie, K.; Patel, N. C.; Pettersson, M.; Rai, D. K.; Reese, M. R.; Sammons, M. F.; Sathish, J. G.; Singh, R. S. P.; Steppan, C. M.; Stewart, A. E.; Tuttle, J. B.; Updyke, L.; Verhoest, P. R.; Wei, L.; Yang, Q.; Zhu, Y. An Oral SARS-CoV-2 Mpro Inhibitor Clinical Candidate for the Treatment of COVID-19. *Science* **2021**, *374* (6575), 1586−1593.

(16) Unoh, Y.; Uehara, S.; Nakahara, K.; Nobori, H.; Yamatsu, Y.; Yamamoto, S.; Maruyama, Y.; Taoda, Y.; Kasamatsu, K.; Suto, T.; Kouki, K.; Nakahashi, A.; Kawashima, S.; Sanaki, T.; Toba, S.; Uemura, K.; Mizutare, T.; Ando, S.; Sasaki, M.; Orba, Y.; Sawa, H.; Sato, A.; Sato, T.; Kato, T.; Tachibana, Y. Discovery of S-217622, a Noncovalent Oral SARS-CoV-2 3CL Protease Inhibitor Clinical Candidate for Treating COVID-19. *J. Med. Chem.* **2022**, *65* (9), 6499−6512.

(17) Huang, C.; Shuai, H.; Qiao, J.; Hou, Y.; Zeng, R.; Xia, A.; Xie, L.; Fang, Z.; Li, Y.; Yoon, C.; Huang, Q.; Hu, B.; You, J.; Quan, B.; Zhao,

X.; Guo, N.; Zhang, S.; Ma, R.; Zhang, J.; Wang, Y.; Yang, R.; Zhang, S.; Nan, J.; Xu, H.; Wang, F.; Lei, J.; Chu, H.; Yang, S. A New Generation Mpro Inhibitor with Potent Activity against SARS-CoV-2 Omicron Variants. *Sig Transduct Target Ther* **2023**, *8* (1), 1−13.

(18) Yao, R.; Wang, L.; Li, Y.; Chen, L.; Li, S.; Du, X.; Wang, B.; Yan, J.; Li, J.; Xie, D. Rice DWARF14 Acts as an Unconventional Hormone Receptor for Strigolactone. *J Exp Bot* **2018**, *69* (9), 2355−2365.

(19) Scaffidi, A.; Waters, M. T.; Sun, Y. K.; Skelton, B. W.; Dixon, K. W.; Ghisalberti, E. L.; Flematti, G. R.; Smith, S. M. Strigolactone Hormones and Their Stereoisomers Signal through Two Related Receptor Proteins to Induce Different Physiological Responses in Arabidopsis. *Plant Physiol* **2014**, *165* (3), 1221−1232.

(20) Ramos-Guzmán, C. A.; Ruiz-Pernía, J. J.; Tuñón, I. Unraveling the SARS-CoV-2 Main Protease Mechanism Using Multiscale Methods. *ACS Catal* **2020**, *10*, 12544−12554.

(21) Gossen, J.; Albani, S.; Hanke, A.; Joseph, B. P.; Bergh, C.; Kuzikov, M.; Costanzi, E.; Manelfi, C.; Storici, P.; Gribbon, P.; Beccari, A. R.; Talarico, C.; Spyrakis, F.; Lindahl, E.; Zaliani, A.; Carloni, P.; Wade, R. C.; Musiani, F.; Kokh, D. B.; Rossetti, G. A Blueprint for High Affinity SARS-CoV-2 Mpro Inhibitors from Activity-Based Compound Library Screening Guided by Analysis of Protein Dynamics. *ACS Pharmacol Transl Sci* **2021**, *4* (3), 1079−1095.

(22) Spyrakis, F.; Felici, P.; Bayden, A. S.; Salsi, E.; Miggiano, R.; Kellogg, G. E.; Cozzini, P.; Cook, P. F.; Mozzarelli, A.; Campanini, B. Fine Tuning of the Active Site Modulates Specificity in the Interaction of O-Acetylserine Sulfhydrylase Isozymes with Serine Acetyltransferase. *Biochim. Biophys. Acta* **2013**, *1834* (1), 169−181.

(23) Ma, C.; Sacco, M. D.; Hurst, B.; Townsend, J. A.; Hu, Y.; Szeto, T.; Zhang, X.; Tarbet, B.; Marty, M. T.; Chen, Y.; Wang, J. Boceprevir, GC-376, and Calpain Inhibitors II, XII Inhibit SARS-CoV-2 Viral Replication by Targeting the Viral Main Protease. *Cell Res* **2020**, *30* (8), 678−692.

(24) Costanzi, E.; Kuzikov, M.; Esposito, F.; Albani, S.; Demitri, N.; Giabbai, B.; Camasta, M.; Tramontano, E.; Rossetti, G.; Zaliani, A.; Storici, P. Structural and Biochemical Analysis of the Dual Inhibition of MG-132 against SARS-CoV-2 Main Protease (Mpro/3CLpro) and Human Cathepsin-L. *Int J Mol Sci* **2021**, *22* (21), 11779.

(25) Prandi, C.; Occhiato, E. G.; Tabasso, S.; Bonfante, P.; Novero, M.; Scarpi, D.; Bova, M. E.; Miletto, I. New Potent Fluorescent Analogues of Strigolactones: Synthesis and Biological Activity in Parasitic Weed Germination and Fungal Branching. *Eur. J. Org. Chem.* **2011**, *2011* (20−21), 3781−3793.

(26) Milewska, A.; Kaminski, K.; Ciejka, J.; Kosowicz, K.; Zeglen, S.; Wojarski, J.; Nowakowska, M.; Szczubiałka, K.; Pyrc, K. HTCC: Broad Range Inhibitor of Coronavirus Entry. *PLoS One* **2016**, *11* (6), No. e0156552.

(27) Magurano, F.; Baggieri, M.; Marchi, A.; Rezza, G.; Nicoletti, L. SARS-CoV-2 Infection: The Environmental Endurance of the Virus Can Be Influenced by the Increase of Temperature. *Clin Microbiol Infect* **2021**, *27* (2), 289.e5−289.e7.

(28) Siragusa, L.; Luciani, R.; Borsari, C.; Ferrari, S.; Costi, M. P.; Cruciani, G.; Spyrakis, F. Comparing Drug Images and Repurposing Drugs with BioGPS and FLAPdock: The Thymidylate Synthase Case. *ChemMedChem* **2016**, *11* (15), 1653−1666.

(29) Jones, G.; Willett, P.; Glen, R. C.; Leach, A. R.; Taylor, R. Development and Validation of a Genetic Algorithm for Flexible Docking. *J. Mol. Biol.* **1997**, *267* (3), 727−748.

(30) Friesner, R. A.; Murphy, R. B.; Repasky, M. P.; Frye, L. L.; Greenwood, J. R.; Halgren, T. A.; Sanschagrin, P. C.; Mainz, D. T. Extra Precision Glide: Docking and Scoring Incorporating a Model of Hydrophobic Enclosure for Protein-Ligand Complexes. *J. Med. Chem.* **2006**, *49* (21), 6177−6196.

(31) Zhu, K.; Borrelli, K. W.; Greenwood, J. R.; Day, T.; Abel, R.; Farid, R. S.; Harder, E. Docking Covalent Inhibitors: A Parameter Free Approach to Pose Prediction and Scoring. *J Chem Inf Model* **2014**, *54* (7), 1932−1940.

(32) Waterhouse, A.; Bertoni, M.; Bienert, S.; Studer, G.; Tauriello, G.; Gumienny, R.; Heer, F. T.; de Beer, T. A. P.; Rempfer, C.; Bordoli, L.; Lepore, R.; Schwede, T. SWISS-MODEL: Homology Modelling of Protein Structures and Complexes. *Nucleic Acids Res.* **2018**, *46* (W1), W296−W303.

(33) Pelliccia, S.; Cerchia, C.; Esposito, F.; Cannalire, R.; Corona, A.; Costanzi, E.; Kuzikov, M.; Gribbon, P.; Zaliani, A.; Brindisi, M.; Storici, P.; Tramontano, E.; Summa, V. Easy Access to α-Ketoamides as SARS-CoV-2 and MERS Mpro Inhibitors via the PADAM Oxidation Route. *Eur. J. Med. Chem.* **2022**, *244*, 114853.

IFI16 Impacts Metabolic Reprogramming during Human Cytomegalovirus Infection

Gloria Griffante,[a]* Weronika Hewelt-Belka,[b] Camilla Albano,[a] Francesca Gugliesi,[a] Selina Pasquero,[a] Sergio Fernando Castillo Pacheco,[a§] Greta Bajetto,[a◇] Paolo Ettore Porporato,[c] Erica Mina,[c] Marta Vallino,[d] Christian Krapp,[e] Martin Roelsgaard Jakobsen,[e] John Purdy,[f] Jens von Einem,[g] Santo Landolfo,[a] Valentina Dell'Oste,[a] Matteo Biolatti[a]

aDepartment of Public Health and Pediatric Sciences, University of Turin, Turin, Italy
bDepartment of Analytical Chemistry, Faculty of Chemistry, Gdańsk University of Technology, Gdańsk, Poland
cDepartment of Molecular Biotechnology and Health Sciences, University of Turin, Turin, Italy
dInstitute for Sustainable Plant Protection, CNR, Turin, Italy
eDepartment of Biomedicine, Aarhus University, Aarhus, Denmark
fDepartment of Immunobiology, University of Arizona, Tucson, Arizona, USA
gInstitute of Virology, Ulm University Medical Center, Ulm, Germany

ABSTRACT Cellular lipid metabolism plays a pivotal role in human cytomegalovirus (HCMV) infection, as increased lipogenesis in HCMV-infected cells favors the envelopment of newly synthesized viral particles. As all cells are equipped with restriction factors (RFs) able to exert a protective effect against invading pathogens, we asked whether a similar defense mechanism would also be in place to preserve the metabolic compartment from HCMV infection. Here, we show that gamma interferon (IFN-γ)-inducible protein 16 (IFI16), an RF able to block HCMV DNA synthesis, can also counteract HCMV-mediated metabolic reprogramming in infected primary human foreskin fibroblasts (HFFs), thereby limiting virion infectivity. Specifically, we find that IFI16 downregulates the transcriptional activation of the glucose transporter 4 (GLUT4) through cooperation with the carbohydrate-response element-binding protein (ChREBP), thereby reducing HCMV-induced transcription of lipogenic enzymes. The resulting decrease in glucose uptake and consumption leads to diminished lipid synthesis, which ultimately curbs the *de novo* formation of enveloped viral particles in infected HFFs. Consistently, untargeted lipidomic analysis shows enhanced cholesteryl ester levels in IFI16 KO versus wild-type (WT) HFFs. Overall, our data unveil a new role of IFI16 in the regulation of glucose and lipid metabolism upon HCMV replication and uncover new potential targets for the development of novel antiviral therapies.

IMPORTANCE Human cytomegalovirus (HCMV) gathers all the substrates and enzymes necessary for the assembly of new virions from its host cell. For instance, HCMV is known to induce cellular metabolism of infected cells to favor virion assembly. Cells are, however, equipped with a first-line defense represented by restriction factors (RFs), which after sensing viral DNA can trigger innate and adaptive responses, thereby blocking HCMV replication. One such RF is IFN-γ-inducible protein 16 (IFI16), which we have shown to downregulate viral replication in human fibroblasts. Thus, we asked whether IFI16 would also play a role in preserving cellular metabolism upon HCMV infection. Our findings highlight an unprecedented role of IFI16 in opposing the metabolic changes elicited by HCMV, thus revealing new promising targets for antiviral therapy.

KEYWORDS IFI16, glucose and lipid metabolism, human cytomegalovirus, lipidomics, virus-host interactions

1

Human cytomegalovirus (HCMV) is a betaherpesvirus with a worldwide seroprevalence of up to 90% (1). It is often asymptomatic in immunocompetent adults, but it can cause severe and sometimes fatal diseases in immunocompromised individuals and neonates (2–5).

Due to its ability to establish a lifelong latent or chronic/permanent infection, HCMV may also lead to other unexpected long-term health sequelae. For example, HCMV infection was first associated with atherosclerosis in 1987 (6), a connection further supported by a number of studies showing HCMV infection of endothelial cells (ECs) to be a crucial event for atherosclerosis development. Indeed, once aortic ECs are infected with HCMV, they become a source of viral spread, further infecting the vascular tissue, altering cellular processes, and eventually leading to atherosclerosis (7).

The aforementioned events are not surprising in light of numerous strategies devised by HCMV to exploit cellular pathways for its own benefit (8, 9). One such strategy consists of inducing metabolic reprogramming of host cells to improve its replication and release (10–14). An overall increase in metabolites from glycolysis, tricarboxylic acid (TCA) cycle, and pyrimidine synthesis pathways was in fact observed following HCMV-mediated upregulation of enzymes involved in these pathways (15). In particular, HCMV-infected fibroblasts displayed enhanced glucose consumption and lactate production, while glucose withdrawal impaired virus replication in these cells (16–19).

Glucose transporter 4 (GLUT4) has long been known to be one of the main targets of HCMV activity (20). In particular, increased GLUT4 levels were found in infected fibroblasts, whereas GLUT1, whose glucose transport capacity is lower than that of GLUT4, was inhibited through a mechanism involving the HCMV major immediate early protein IE72 (20). HCMV-mediated GLUT4 upregulation relies on carbohydrate response element binding protein (ChREBP) (21) and AMP-activated protein kinase (AMPK) (22, 23), both of which are induced during infection. Conversely, inhibition of ChREBP or AMPK signaling counteracts the metabolic changes induced by HCMV, thus curbing viral replication (21–23). Finally, GLUT4 translocation to the cell surface has been observed in infected cells, accompanied by an increase in cytoplasmic glucose for *de novo* fatty acid biosynthesis (20), which will then be available for viral envelopment (24).

It is widely established that HCMV can persist in the host thanks to its multilayered ability to escape from immune surveillance. One of the key players in this process is gamma interferon (IFN-γ)-inducible protein 16 (IFI16), which we have previously shown to act as a restriction factor (RF) for HCMV replication through transcriptional downregulation of the DNA polymerase UL54 (25). However, HCMV has evolved several strategies to escape from the restriction activity of IFI16, one of which relies on IFI16 nuclear delocalization, followed by incorporation into newly formed virions and expulsion from the cell (26, 27). Thus, we asked whether IFI16 could also act as an RF against HCMV within the metabolic compartment, which is essential to achieve a productive HCMV infection (12).

Here, we provide the first evidence of IFI16 acting as an inhibitor of lipid synthesis in HCMV-infected primary human foreskin fibroblasts (HFFs), whose ultimate effect is the release of virus particles with reduced infectivity. Overall, our findings reveal an unprecedented function of IFI16 based on its ability to keep HCMV replication in check by regulating HCMV-induced metabolic reprogramming.

RESULTS

IFI16 hampers glucose uptake upon HCMV infection. As IFI16 mediates intrinsic resistance to HCMV (25, 28), we asked whether it might counteract the metabolic rewiring promoted by HCMV infection. To this end, we generated gene knockout (KO) variants of HFFs through clustered regularly interspaced short palindromic repeat (CRISPR)/Cas9 technology. Primary cell lines carrying mutations in genes encoding IFI16 (IFI16 KO) were generated based on two different guide RNAs (gRNAs). Targeting effectiveness was verified by Western blotting (Fig. 1A) and tracking of indels by
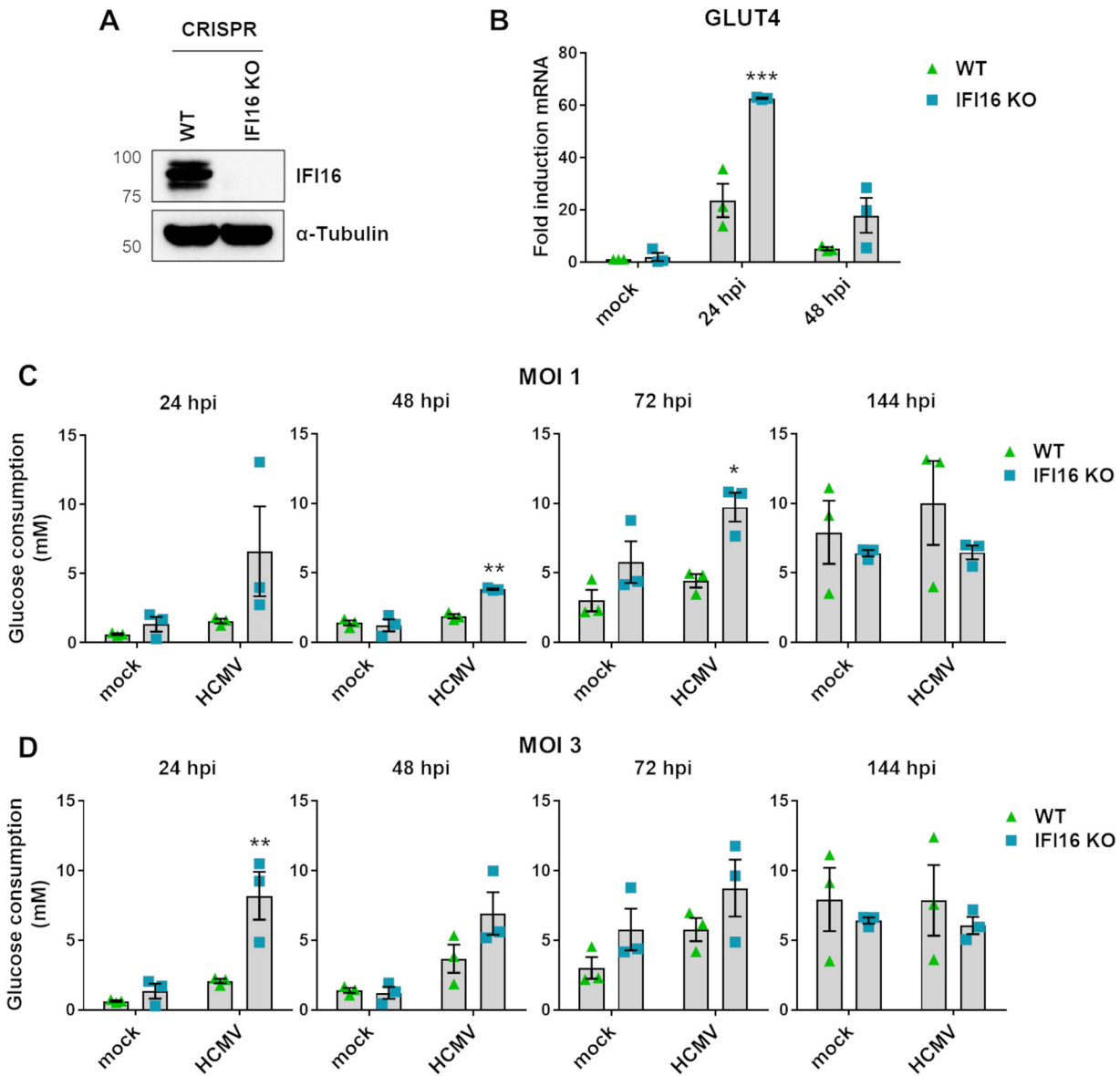
FIG 1 IFI16 involvement in glucose consumption. (A) A knockout gene variant of IFI16 (IFI16 KO) was generated from HFFs using CRISPR/Cas9 technology. Wild-type HFFs (WT) were used as controls. The efficiency of IFI16 protein depletion was assayed by Western blotting using a monoclonal antibody against human IFI16 or α-tubulin as a loading control. (B) WT and IFI16 KO HFFs were infected with HCMV (MOI, 1). To measure GLUT4 expression levels, total RNA was isolated at 24 and 48 hpi and subjected to RT-qPCR. Values were normalized to the housekeeping GAPDH gene mRNA and plotted as fold induction relative to mock-infected WT HFFs (set at 1). Bars show means and SEM from three independent experiments (***, $P < 0.001$; two-way analysis of variance [ANOVA] followed by Bonferroni's posttests, for comparison of WT versus IFI16 KO cells). (C and D) Culture medium was collected from mock- or HCMV-infected IFI16 KO or WT HFFs (MOI of 1 [C] and 3 [D]) at 24, 48, 72, or 144 hpi. Glucose concentration in the supernatants was measured as described in Materials and Methods. Bars show means and SEM from two independent experiments (*, $P < 0.05$; **, $P < 0.01$; two-way ANOVA followed by Bonferroni's posttests, for comparison of WT versus IFI16 KO HFFs).

decomposition (TIDE) analysis in comparison with the parental cell line (WT), as we reported previously (27).

Since HCMV exploits GLUT4 to carry hexose sugars across the membrane (20), we first sought to determine whether IFI16 expression would affect GLUT4 expression and GLUT4-mediated glucose uptake in HCMV-infected HFFs. As shown in Fig. 1B, HCMV (laboratory strain AD169) infection of WT HFFs triggered lower levels of GLUT4 mRNA expression compared to those observed in IFI16 KO cells at 24 and 48 h postinfection (hpi). Particularly, the levels of GLUT4 transcript at 24 hpi in IFI16 KO HFFs were significantly higher (2.6-fold) than those observed in WT HFFs. Thus, IFI16 expression is
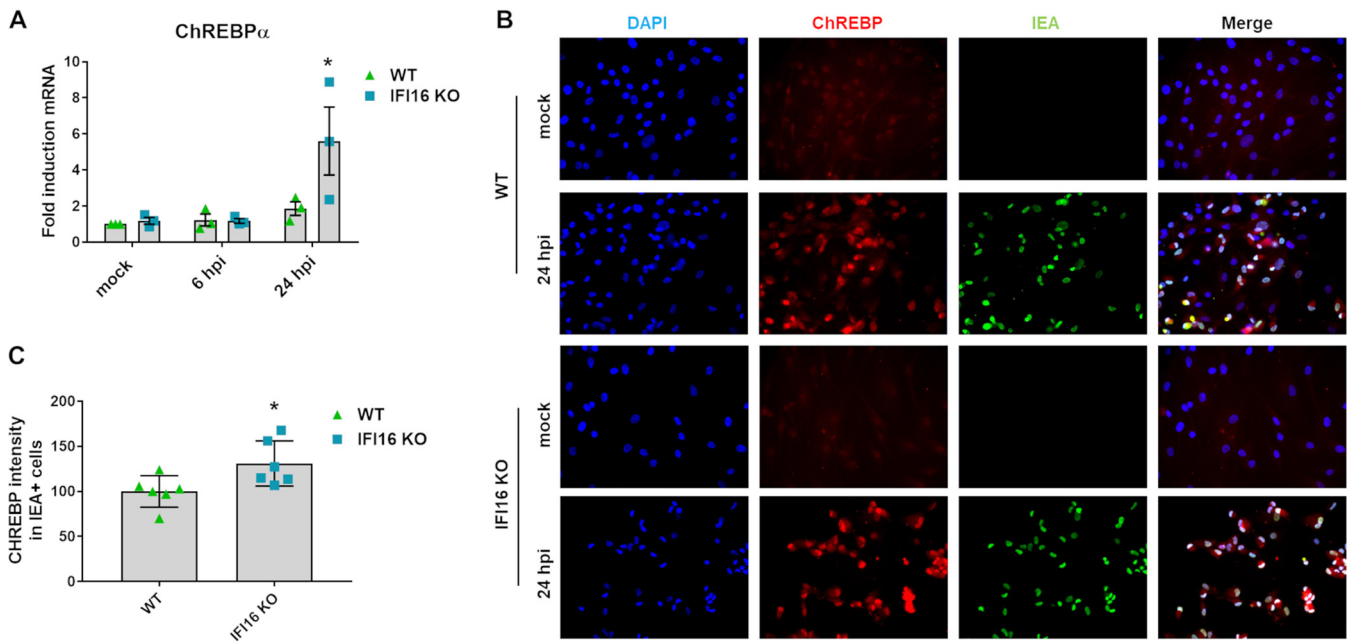
FIG 2 ChREBP modulation in HCMV WT- and IFI16 KO-infected cells. WT and IFI16 KO HFFs were infected with HCMV (MOI, 1), for the indicated times. (A) Total RNA was isolated, and ChREBPα mRNA levels were measured by RT-qPCR, normalized to GAPDH mRNA, and plotted as fold induction relative to mock-infected WT cells (set at 1). Bars show means and SEM from three independent experiments (*, $P < 0.05$; two-way ANOVA followed by Bonferroni's posttests, for comparison of WT versus IFI16 KO cells). (B) Representative immunofluorescence (IF) images of HCMV-infected HFFs in the presence of 10% HCMV-negative human serum. The ChREBP protein is stained in red, whereas the HCMV protein immediate early antigen (IEA) is stained in green. Cell nuclei are visualized by DAPI (blue). (C) Amount of ChREBP localized in the nucleus of HCMV IEA-positive IFI16 KO cells compared to WT cells calculated from 2 different fields for each experiment. IF staining intensity is represented as fold induction relative to WT-infected cells (set at 100%). Bars show means and SEM from three independent experiments (*, $P < 0.05$; unpaired t test).

required to tackle HCMV-mediated GLUT4 mRNA upregulation in the early stages of viral infection.

Given that enhanced GLUT4 expression results in increased glucose uptake (20), we sought to assess glucose consumption in IFI16 KO versus WT HFFs following HCMV infection. For this purpose, we measured glucose concentrations in supernatants from WT and IFI16 KO HFFs (mock or HCMV infected) following infection kinetics from 24 to 144 hpi, using multiplicities of infection (MOI) of 1 and 3 (Fig. 1C and D, respectively). As shown in Fig. 1C and D, glucose consumption was much faster in the cell culture medium of HCMV-infected IFI16 KO HFFs than in that of HCMV-infected WT cells in an MOI-dependent manner. Particularly, a significant enhancement of glucose consumption in IFI16 KO cells was observed at 48 and 72 hpi at an MOI of 1, followed by later pairing (Fig. 1C). A similar and earlier trend of glucose utilization was also recorded at 24 hpi in IFI16 KO cells incubated with HCMV at an MOI of 3 (Fig. 1D).

Taken together, these results confirm that IFI16 acts as a transcriptional repressor of GLUT4, thereby reducing glucose consumption in HCMV-infected cells during the early stages of viral infection.

ChREBP is induced in the absence of IFI16. As Yu et al. (20) showed previously that ChREBP is a critical regulator of HCMV-induced metabolic alterations by acting directly on GLUT4 and GLUT2 expression, we assessed the ability of IFI16 to modulate ChREBP expression during HCMV infection. For this purpose, we measured the mRNA levels of ChREBPα, the canonical ChREBP isoform (29), in WT and IFI16 KO cells at 6 and 24 hpi. At the 6-h time point, ChREBPα mRNA expression levels remained basically unchanged in both cell lines. In contrast, after 24 h of HCMV infection, we recorded a 6-fold induction of ChREBPα expression in cells lacking IFI16, which was almost three times as high as that seen in WT cells that were similarly infected (Fig. 2A). Furthermore, immunofluorescence of HCMV-infected cells at 24 hpi showed enhanced ChREBP nuclear localization (Fig. 2B), indicating that, in response to HCMV infection, ChREBP translocates from the cytoplasm to the nucleus, where it normally acts as a transcription factor (29–31). In particular, the nuclear
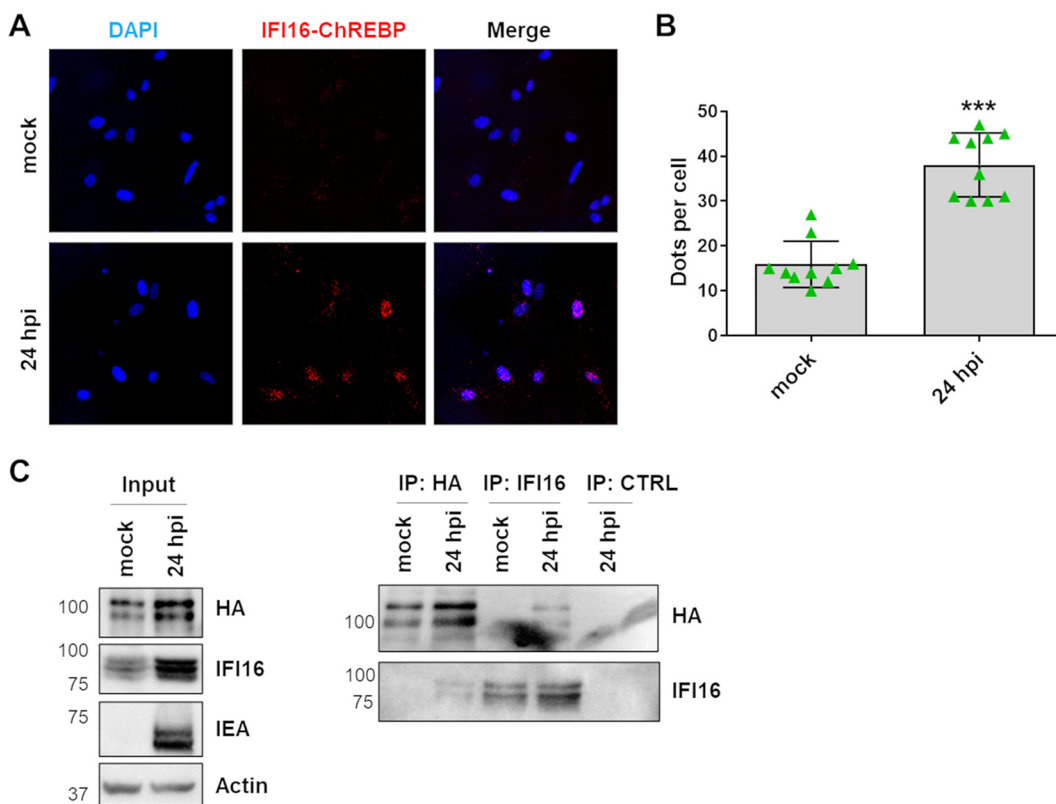
FIG 3 Interplay between ChREBP and IFI16. (A) Representative confocal images of *in situ* PLA between IFI16 and ChREBP in HFFs infected with HCMV (MOI, 1) for the indicated time. The signal was detected as distinct fluorescent dots in the Texas Red channel. Cell nuclei were visualized by DAPI (blue). (B) PLA dots per cell were counted in 5 cells from each sample using ImageJ software and plotted as means and SEM from two independent experiments (***, $P < 0.001$; unpaired *t* test). (C) Immunoprecipitation (IP) from HFF lysates. HFFs were transiently transfected with a ChREBP-HA-tagged plasmid and, 24 h later, infected with HCMV (MOI of 1). IPs were performed at 24 hpi using antibodies against an HA tag, IFI16, or the appropriate control antibody (CTRL). Immunoprecipitated and nonimmunoprecipitated (input) proteins were detected by immunoblot analysis using antibodies against IFI16 and HA-tag. Antibodies against actin and HCMV IEA were used as loading and infection controls, respectively.

signal of ChREBP was significantly enhanced in HCMV-infected IFI16 KO cells (Fig. 2C). Thus, IFI16 appears to downregulate ChREBP activity during HCMV infection.

IFI16 selectively interacts with ChREBP. To better understand how IFI16 affected ChREBP activity, we next examined the possibility that IFI16 could form a complex with ChREBP that would interfere with ChREBP-mediated GLUT4 transcriptional activation. To this end, we measured IFI16/ChREBP interaction in HCMV-infected HFFs by *in situ* proximity ligation assay (PLA). This assay provides a positive signal or dot on confocal pictures when the distance between two molecules is less than 40 nm (32). When we performed PLA on cell cultures at 24 hpi using both anti-ChREBP and anti-IFI16 antibodies, we noticed an increased number of dots per cell in HCMV-infected versus mock-infected HFFs (Fig. 3A and B), indicating close proximity between the two proteins. To further assess the specificity of the IFI16/ChREBP interaction, we performed coimmunoprecipitation (co-IP) experiments using HFFs that had been transiently transfected with a vector carrying a hemagglutinin (HA)-tagged human ChREBP protein and then infected with HCMV for 24 h. As shown in Fig. 3C, IFI16 was detectable in lysates from HCMV-infected cells immunoprecipitated with the anti-HA antibody but not in the negative control. Moreover, reciprocal IPs corroborate these results, establishing that IFI16 selectively interacts with ChREBP during HCMV infection.

GLUT4 promoter activation is enhanced in the absence of IFI16. To ascertain whether IFI16-driven GLUT4 transcriptional regulation requires ChREBP, we first sought to assess the association of IFI16 with the carbohydrate response element (ChoRE) motif of the GLUT4 promoter in HCMV-infected HFFs in the presence or absence of
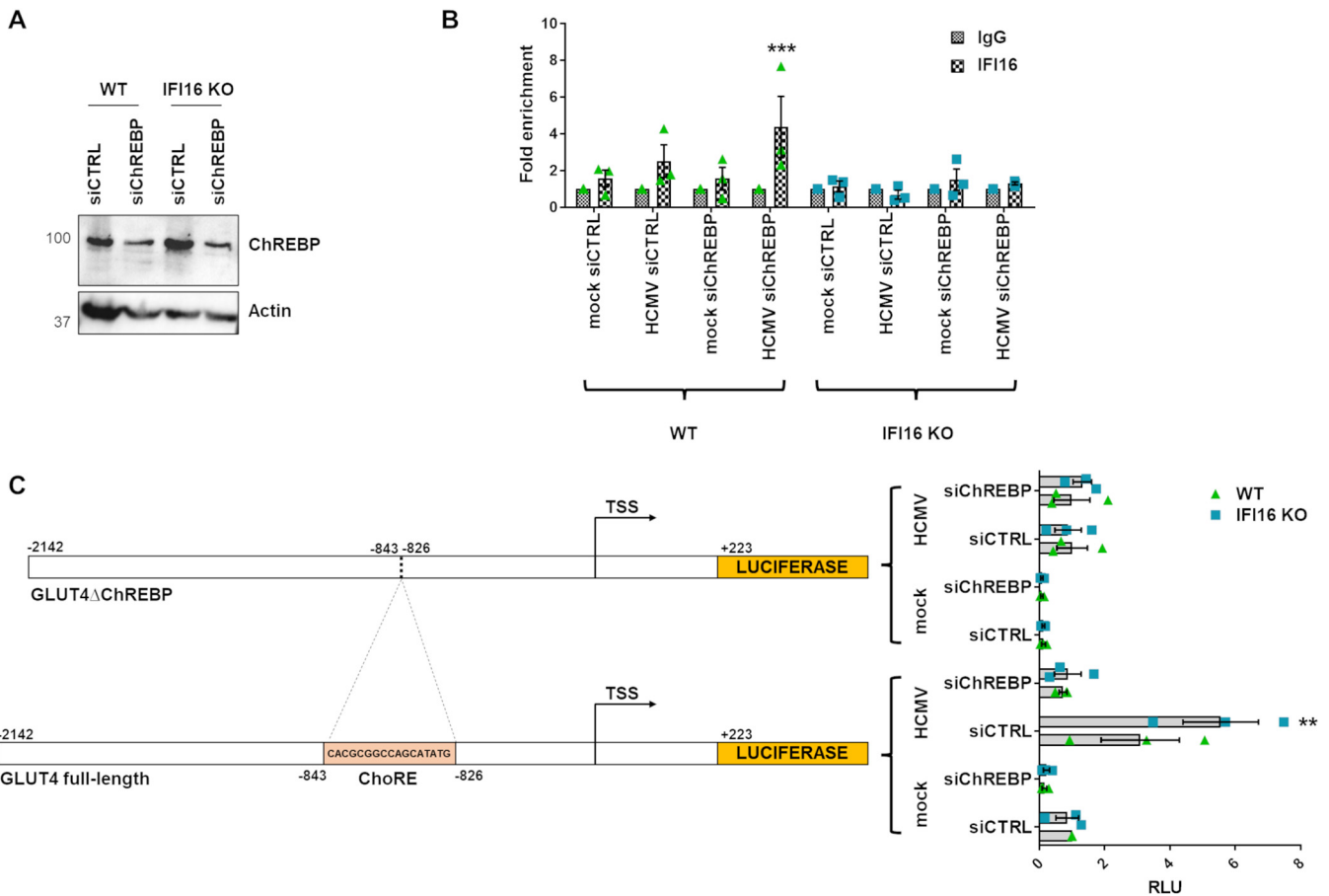
FIG 4 Modulation of GLUT4 promoter activation by IFI16. (A) Efficiency of ChREBP depletion assayed by Western blotting using a polyclonal antibody against human ChREBP. Actin was used as a loading control. (B) WT and IFI16 KO HFFs were electroporated with a mixture of 3 different small interfering RNAs targeting ChREBP (siChREBP) or scrambled control siRNA (siCTRL) and then infected with HCMV at an MOI of 1. After 24 h, cells were cross-linked with formaldehyde, and then IFI16 immune complexes were isolated by immunoprecipitation. Purified ChIP DNA was analyzed by qPCR for the presence of the GLUT4 DNA promoter sequence. The control antibody (IgG) baseline was arbitrarily set at a value of 1. Bars show means and SEM from three independent experiments (***, $P < 0.001$; two-way ANOVA followed by Bonferroni's posttests, for comparison of IFI16 antibody versus IgG control). (C) Schematic model of GLUT4 promoter (nucleotides -2142 to $+223$). The ChoRE-responsive site is shown (nucleotides -843 to -826). The transcription start site (TSS) is marked by the black arrow. WT and IFI16 KO HFFs were electroporated with siChREBP or siCTRL and with luciferase reporter plasmids containing either the full-length GLUT4 promoter or a promoter harboring a ChoRE site deletion (GLUT4ΔChREBP). Cells were infected with HCMV (MOI, 1) or left uninfected, and luciferase activity was assayed after 24 h. Luciferase activity in whole-cell lysates was normalized to *Renilla* luciferase activity. The mean value of siCTRL-WT mock-infected cells was arbitrarily set to 1. Bars show means and SEM from three independent experiments (**, $P < 0.01$; two-way ANOVA followed by Bonferroni's posttests, for comparison of WT versus IFI16 KO cells).

ChREBP. To this end, WT or IFI16 KO HFFs were first silenced for ChREBP expression through specific small interfering RNAs (siRNAs) (siChREBP) or scrambled control (siCTRL) and then infected with HCMV (MOI, 1) for 24 h. As shown in Fig. 4A, ChREBP expression levels were efficiently inhibited in siChREBP- versus siCTRL-treated cells. Cell extracts were then cross-linked with formaldehyde, sonicated, and subjected to chromatin immunoprecipitation (ChIP) using anti-IFI16 or anti-IgG polyclonal antibodies (28). The DNA released from the immunocomplexes was then analyzed by quantitative PCR (qPCR) for the presence of GLUT4. As shown in Fig. 4B, the GLUT4 DNA promoter was detectable in the IFI16-specific immune complexes from HCMV-infected WT but not IFI16 KO HFFs. In particular, a significant enhancement was seen in HCMV-infected siChREBP WT cells. As expected, we did not detect GLUT4 DNA promoter in uninfected WT or IFI16 KO HFFs.

To further define the functional role of IFI16 on GLUT4 promoter activity, we used two luciferase reporter plasmids driven by the full-length GLUT4 gene promoter or by a mutant lacking the ChREBP responsive element (from -843 to -826, named ChoRE) (GLUT4ΔChREBP) (Fig. 4C).
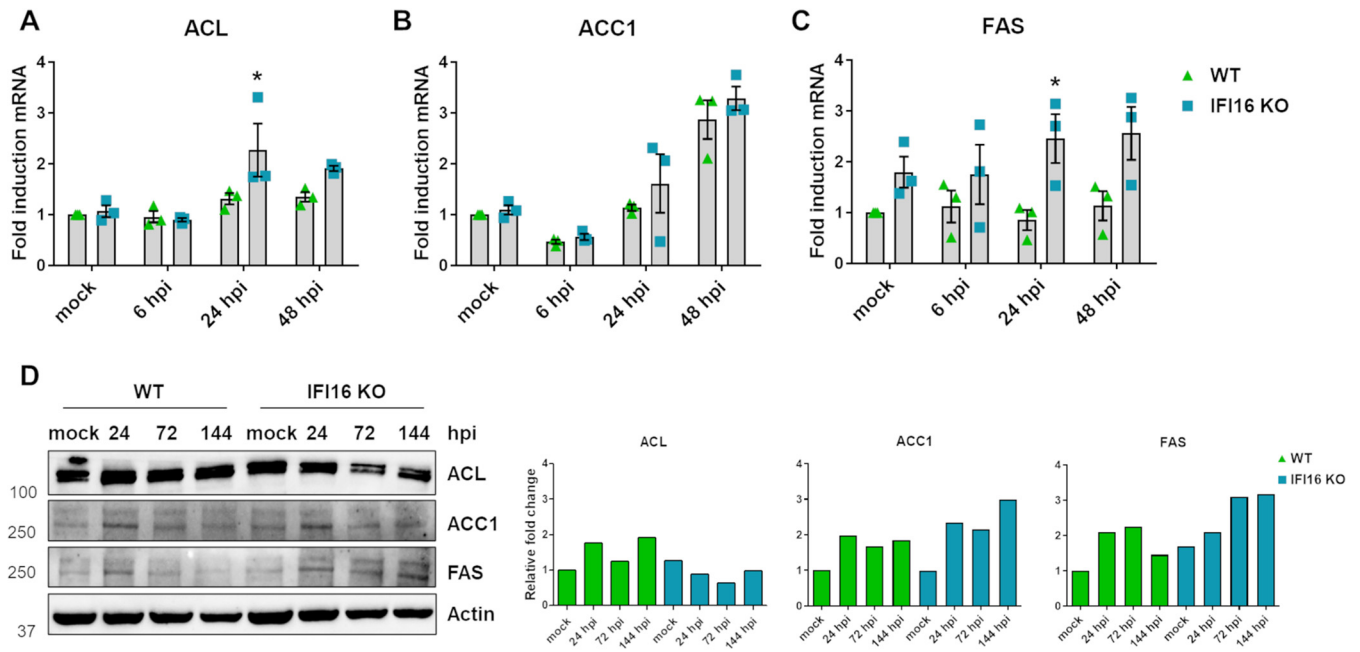
FIG 5 Effects of IFI16 silencing on HCMV-induced lipogenesis. IFI16 KO and WT HFFs were infected with HCMV (MOI 1). At 6, 24, and 48 hpi, total RNA was isolated and subjected to RT-qPCR to measure mRNA expression levels of the lipogenic enzymes ACL (A), ACC1 (B), and FAS (C). Values were normalized to the housekeeping gene GAPDH mRNA and plotted as fold induction relative to mock-infected WT cells (set at 1). Bars show means and SEM from three independent experiments (*, $P < 0.05$; two-way ANOVA followed by Bonferroni's posttests, for comparison of WT versus IFI16 KO cells). (D) Western blot analysis of protein lysates from uninfected (mock) or infected cells using antibodies against ACL, ACC1, FAS, or actin. One representative blot (left) and densitometric analysis (right) are shown. Values are expressed as fold change in ACL, ACC1, and FAS expression normalized to actin.

To understand if HCMV-mediated modulation of GLUT4 expression requires ChREBP and/or IFI16, cells were again silenced for ChREBP (siChREBP) or scrambled control (siCTRL) and electroporated with luciferase reporter plasmids. WT and IFI16 KO HFFs were then infected with HCMV or left uninfected (mock infected). Luciferase activity was then assessed after 24 h of incubation.

As shown in Fig. 4C, we observed a robust induction of luciferase activity in cells transfected with the GLUT4 construct and infected with HCMV for 24 h, while cells transfected with the GLUT4ΔChREBP reporter plasmid displayed a reduced increase in luciferase activity, indicating that the ChoRE site is crucial for GLUT4 transcriptional activation by HCMV. HCMV-infected IFI16 KO cells transfected with the GLUT4 construct for 24 h showed a much higher luciferase activity than WT cells (~2-folds), underscoring a robust inhibitory activity of IFI16 on the GLUT4 promoter. Importantly, siChREBP-treated HFFs were not responsive to HCMV-mediated GLUT4 promoter activation, regardless of the presence of IFI16, suggesting that ChREBP is required for GLUT4 promoter activation.

IFI16 limits HCMV-mediated cholesteryl ester accumulation. ChREBP is a transcription factor known to activate the transcription of lipogenic enzymes upon HCMV infection in a sterol regulatory element-binding protein (SREBP)-independent way (29). The transcriptional targets of ChREBP include the *de novo* lipogenesis (DNL) genes acetyl-coenzyme A (CoA), carboxylase 1 (ACC1), and fatty acid synthase (FAS), each containing a ChoRE element in their promoter/regulatory region (33, 34).

As ChREBP translocation to the nucleus induces lipogenic enzyme transcription, and HCMV infection increases *de novo* fatty acid synthesis through transactivation of lipogenic enzymes (35, 36), we asked whether IFI16 would also play an inhibitory role in these processes. To answer this question, we first analyzed mRNA and protein expression of ATP-citrate lyase (ACL), ACC1, and FAS in HCMV-infected IFI16 KO and WT cells. As shown in Fig. 5, mRNA and protein expression levels of FAS were upregulated in either mock or HCMV-infected IFI16 KO compared to similarly treated WT HFFs (Fig. 5C and D). A similar trend, albeit less pronounced, was also observed for ACC1

(Fig. 5B to D), while ACL induction was not affected by the presence of IFI16 (Fig. 5A to D). Thus, these results support the hypothesis that IFI16 may play an inhibitory role in HCMV-induced lipogenesis.

To verify whether the differences in lipogenic enzyme expression between WT and IFI16 KO HFFs corresponded to differences in lipid composition, we performed lipidomic analysis by reversed-phase liquid chromatography coupled with quadrupole-time-of-flight mass spectrometry (RP-LC-Q-TOF-MS). For these experiments, cells were grown to confluence in serum-free medium to limit lipid or metabolite contamination from the bovine serum (19, 24).

First, we estimated the amounts of the phospholipids with very-long-chain-fatty-acid tails (PL-VLCFAs) in HCMV-infected versus uninfected WT HFFs. As shown in Fig. 6A, PL-VLCFAs were generally increased in HCMV-infected WT cells compared to uninfected cells, in good agreement with previous results by Purdy et al. (24).

When we compared the MS patterns of the various glycerophospholipid species, we noticed that the lipid fingerprint of IFI16 KO HFFs was different from that of WT cells, even though not all lipid classes were equally affected (Fig. 6B, left column). The majority of tested glycerophospholipids were upregulated in uninfected IFI16 KO cells in comparison with uninfected WT cells. However, we observed that some lipid species were downregulated (e.g., glycerophosphocholines [PCs] and glycerophosphoethanolamines [PEs]), in particular lipids species containing medium-chain fatty acids with up to 2 double bonds, such as $PC_{28:0}$, $PC_{30:0}$, and $PC_{30:1}$.

The lipid types that were most significantly modulated upon infection between IFI16 KO and WT cells are listed in Fig. 6B (middle and right columns). Interestingly, a major fraction of long-chain and unsaturated (37) PCs, PEs, and glycerophosphoinositols (PIs) (e.g., $PE_{38:6}$, $PE_{38:3}$, and $PI_{38:4}$) were upregulated in infected IFI16 KO cells with respect to WT cells. Finally, lipids containing medium-chain fatty acid substituents with up to 2 double bonds (e.g., $PC_{32:0}$, $PC_{32:1}$, and $PC_{34:0}$), lysoglycerophosphocholines (lysoPCs), and some diacylglycerolphosphoserines (PSs) were significantly downregulated in IFI16 KO versus WT HFFs following HCMV infection.

Given that HCMV upregulates host fatty acid elongase 7 (ELOVL7) expression to catalyze fatty acid elongation (24), we decided to investigate whether IFI16 would also play a role in ELOVL7 gene expression. Interestingly, we observed a slight upregulation in ELOVL7 expression in cells depleted of IFI16 and infected with HCMV, indicating that IFI16 protein is partially responsible for HCMV-induced ELOVL7 expression (Fig. 6C) (38).

Due to the relevance and implications of cholesterol esters (CEs) for viral replication (39–42), we also measured CE accumulation in IFI16 KO versus WT HFFs. The fold change (FC) difference in total CE lipids between HCMV-infected IFI16 KO and WT HFFs is shown in Fig. 7A (FC = 2.2 [$P < 0.001$] at an MOI of 3 and 2.0 [$P < 0.001$] at an MOI of 1). Interestingly, all CEs were significantly upregulated ($P < 0.005$) in IFI16 KO cells in comparison with WT at both MOI (Fig. 7B). The most affected CE species were $CE_{20:5}$ (FC = 2.7 for an MOI of 1 and 3.5 for an MOI of 3) and $CE_{18:2}$ (FC = 2.3 for an MOI of 1 and 3.0 for an MOI of 3) (Fig. 7C).

Intracellular CE biosynthesis is mediated by sterol O-acyl transferase 1 (SOAT; also known as acyl-CoA:cholesterol acyltransferase [ACAT]). To determine whether SOAT1 gene expression was affected by HCMV replication and/or IFI16 sensor activity, we examined its mRNA expression pattern during a time course of HCMV infection of WT and IFI16 KO HFFs. As shown in Fig. 7D, SOAT1 gene expression increased upon HCMV infection, confirming previous studies (43). Importantly, SOAT1 reached a 2-fold-greater expression in IFI16 KO than WT infected cells, reflecting the lipidomic analysis (Fig. 7D).

Taken together, these results support the notion that HCMV can reprogram the cellular lipid environment through modulation of lipid metabolic enzymes and reveal a novel functional role of IFI16 in this process.

IFI16 affects HCMV infectivity. In addition to being a source of energy, enhanced fatty acid biosynthesis is crucial for HCMV budding because it increases the amount of the
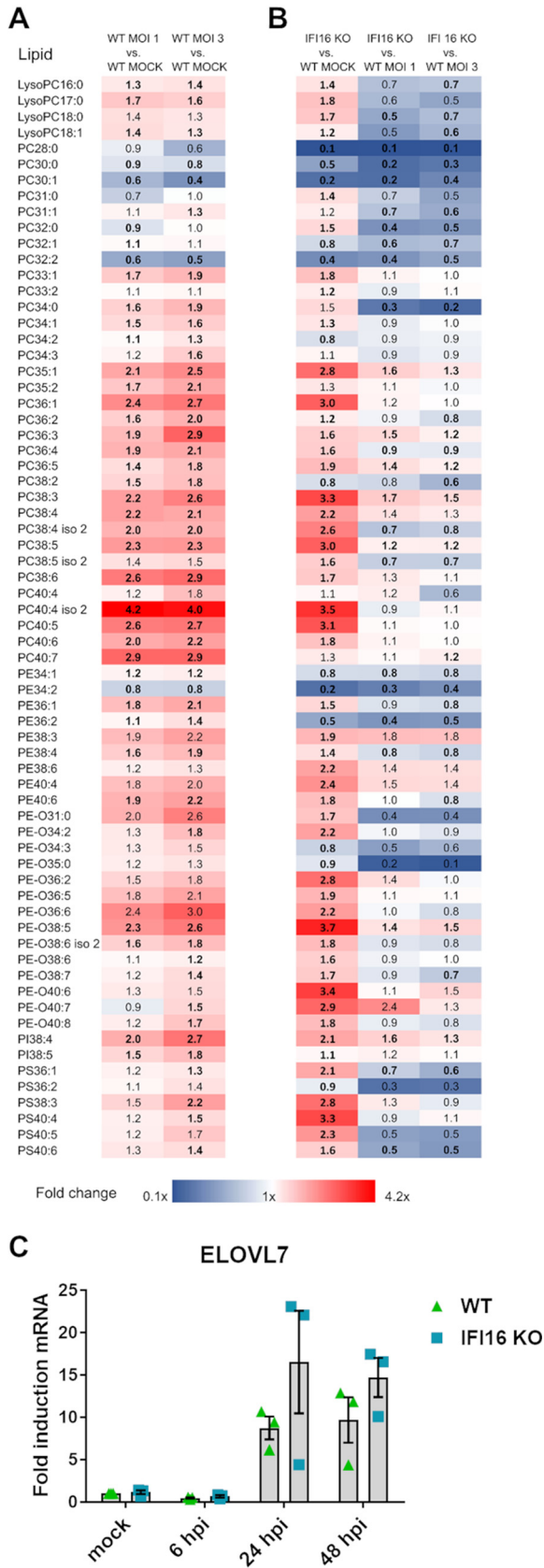
FIG 6 Lipidomic comparison of WT and IFI16 KO HFFs. WT and IFI16 KO HFF cells were infected with HCMV (MOI of 1 or 3) or left uninfected (mock) and maintained in serum-free medium. At 96 hpi,

main constituents necessary for viral envelope formation (37, 44). To explore the role of IFI16 in this process, we first quantified the amount of viral enveloped particles—i.e., double-layered particles formed by tegumentation and secondary envelopment in the secretory pathway—in the cytoplasm of WT versus IFI18 KO HFFs (Fig. 8A). Transmission electron microscopy (TEM) revealed that the number of enveloped particles was reduced in the cytoplasm of WT HFFs in comparison with IFI16 KO HFFs (Fig. 8B), suggesting that IFI16 diminishes virion maturation by subverting HCMV-induced reprogramming of lipid metabolism. Of note, these results are in line with previous findings from our lab (25) showing that IFI16 restricts HCMV replication (25, 28).

Finally, to support and complement the EM results and to further strengthen the role of IFI16 in modulating lipid reprogramming, we assessed the role of IFI16 in restricting HCMV replication in our stable KO model under serum-free conditions. For this purpose, we assessed the accumulation of viral proteins in HCMV-infected WT versus IFI16 KO HFFs at a low MOI (0.5). As shown in Fig. 9A, we observed reduced expression of viral proteins in cells harboring IFI16, confirming our previous findings that IFI16 restricts HCMV replication (25). Consistently, the intracellular number of HCMV genome copies at 48 and 72 hpi was increased in IFI16 KO cells compared to WT cells (Fig. 9B), supporting a role of IFI16 in suppressing viral replication (25).

This increase in intracellular viral genomes in IFI16 KO cells was not reflected by the total number of HCMV genomes released into the supernatants at later times (Fig. 9C), which was similar for IFI16 KO and WT cells. To explain this discrepancy, we measured the release of infectious progeny. Surprisingly, as reported in Fig. 9D, IFI16 KO cells released infectious HCMV progeny with an increased infectivity than similarly infected WT HFFs. The ratio of HCMV genomes to infectious units (i.e., genome-to-IU ratio) was approximately $168\times$ for WT HFF, whereas it was $39\times$ for IFI16 KO cells (Fig. 9E). Because a higher genome-to-IU ratio implies lower particle infectivity, IFI16 KO cells released four times more infectious viral particles, suggesting that IFI16 impairs HCMV-induced lipogenesis and thus impairs maturation and release of infectious viral particles.

Altogether, our findings support a model where IFI16 not only restricts HCMV replication but also can curb virion infectivity by acting as a metabolism regulator.

DISCUSSION

The interplay between HCMV and the host cell metabolism is a crucial aspect of this virus' life cycle, as its replication largely depends on the energy and biosynthetic precursors supplied by the infected cell (10, 38). In this regard, glucose uptake has been shown to be significantly increased in HCMV-infected cells (16, 45), corroborating the evidence that HCMV, like other viruses, exploits glucose metabolism for its own benefit.

Glucose uptake mainly involves specific carriers belonging to the family of glucose transporters (GLUTs). There are 13 different GLUTs in mammalian cells, GLUT1 to -12 plus the proton (H$^+$)-myoinositol cotransporter (HMIT) (46, 47). Structurally, GLUTs can be divided into three classes: GLUT1 to -4 (class I); GLUT5, -7, -9, and -11 (class II); and GLUT6, -8, -10, and -12 and HMIT (class III) (46, 47), each with different tissue specificities and affinities for glucose. For example, in HCMV-infected human fibroblasts, the

FIG 6 Legend (Continued)

total lipids from cells were extracted and analyzed by LC-MS/MS. The fold changes of lipid species peak area are visualized as a heat map showing the levels of upregulated (red, fold change > 1) and downregulated (blue, fold change < 1) glycerophospholipids. Boldface shows statistically significant values (Mann-Whitney unpaired test, $P < 0.05$). PC, glycerophosphocholine; PE, glycerophosphoethanolamine; PE-O, ether analogue of glycerophosphoethanolamine; PS, glycerophosphoserine, PI, glycerophosphoinositol. $n = 2$ independent determinations. (A) Infected WT (MOI of 1 [left] and 3 [right]) versus uninfected HFFs. (B) IFI16 KO versus WT HFFs, mock (left), and HCMV-infected IFI16 KO versus HCMV-infected WT HFFs (MOI of 1 [middle] and 3 [right]). (C) WT and IFI16 KO HFFs were infected with HCMV (MOI, 1), and at 6, 24, and 48 hpi, total RNA was isolated and subjected to RT-qPCR to measure mRNA expression levels of the fatty acid elongase 7 (ELOVL7). Values were normalized to the housekeeping gene GAPDH mRNA and plotted as fold induction relative to WT mock-infected cells (set at 1). Bars show means and SEM from three independent experiments (not significant; two-way ANOVA followed by Bonferroni's posttests, for comparison of WT versus IFI16 KO cells).
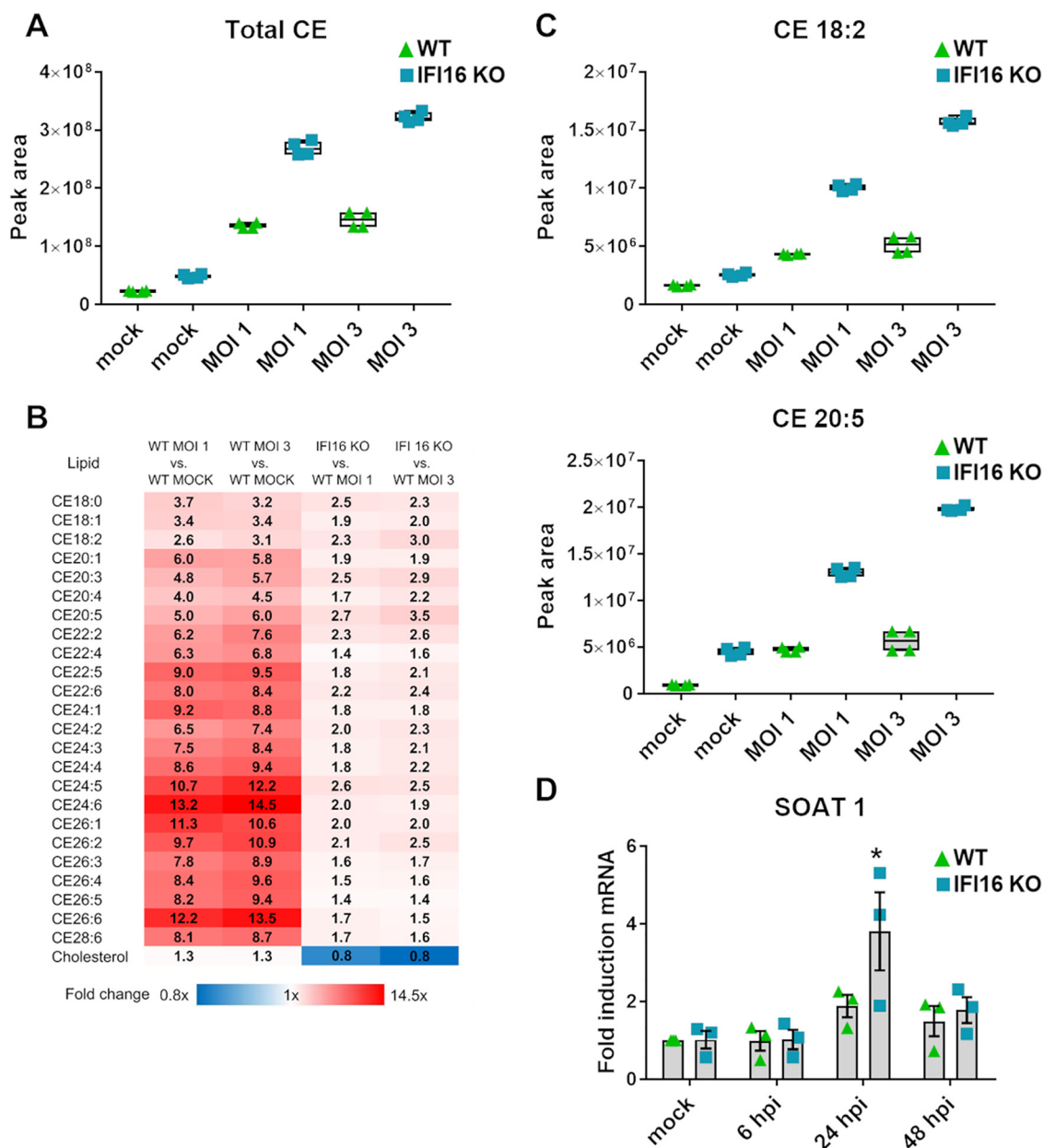
FIG 7 IFI16 is partially responsible for HCMV-mediated CE accumulation. CE comparison in mock- or HCMV-infected IFI16 KO versus WT HFFs. Cells were infected with HCMV (MOI of 1 or 3) and maintained in serum-free medium. At 96 hpi, total lipids from cells were extracted and analyzed by LC-MS/MS. (A) Comparison of total CE content measured as the sum of the peak area for all CE species. (B) Heat map of CE species showing the levels of upregulated (red, fold change > 1) and downregulated (blue, fold change < 1) CE species in HCMV-infected relative to uninfected HFFs (two left panels) and HCMV-infected IFI16 KO relative to HCMV-infected WT cells (two right panels). Boldface shows statistically significant values (nonparametric Student's t test, $P < 0.05$). (C) Levels—measured by the peak area—of the significantly modulated CE species in HCMV-infected or uninfected WT and IFI16 KO HFFs. Center lines show the medians; box limits indicate the 25th and 75th percentiles as determined by R software; whiskers extend 1.5 times the interquartile range from the 25th and 75th percentiles; crosses represent sample means. $n = 2$ independent determinations. (D) WT and IFI16 KO HFFs were infected with HCMV (MOI, 1). At 6, 24, and 48 hpi, total RNA was isolated and subjected to RT-qPCR to measure SOAT1 expression levels. Values were normalized to GAPDH mRNA and plotted as fold induction relative to WT mock-infected cells (set at 1). Bars show means and SEM from three independent experiments (*, $P < 0.05$; two-way ANOVA followed by Bonferroni's posttests, for comparison of WT versus IFI16 KO cells).

HCMV IE72 protein can simultaneously suppress GLUT1 mRNA and induce GLUT4, which has a greater glucose transport capacity (20). This switching of glucose transporters appears to be essential for successful HCMV infection and replication, as inhibition of glucose uptake via GLUT4 by indinavir impedes viral production (20).

In the course of evolution, HCMV has evolved a number of strategies aimed at the
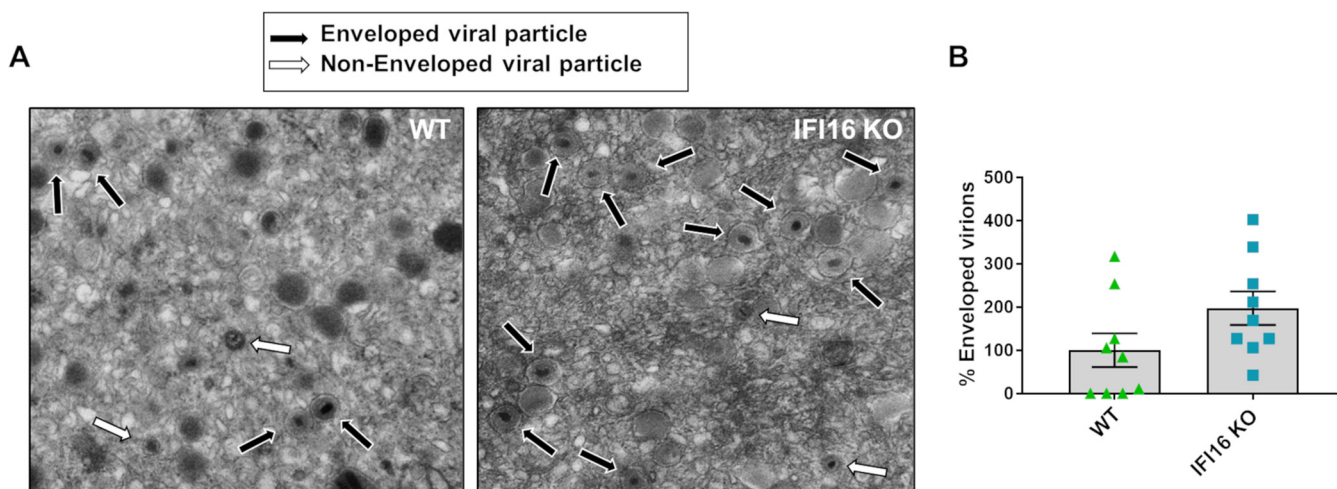
FIG 8 Transmission electron micrographs of HCMV-infected WT and IFI16 KO HFFs. (A) Monolayers were infected with HCMV (MOI, 1) and processed for electron microscopy at 7 dpi. Multiple frames from each sample were imaged and photographed. (Left) WT; (right) IFI16 KO. Particles from a representative cell are shown. White and black arrows indicate representative nonenveloped and enveloped particles, respectively. (B) The number of enveloped particles was counted on 9 frames from different cells and plotted as fold induction relative to WT-infected cells (set at 100%). Data are mean percentages of the enveloped particles and SEM (not significant; unpaired t test).

modulation of host metabolic pathways to favor virion production. Conversely, the host has long tried to counteract this hijacking threat through innate immunity. In this regard, we have previously demonstrated that IFI16 acts as a cellular restriction factor of HCMV replication (25) and plays a key role in HCMV-related innate immunity (26, 28).

In the present study, we add another layer of complexity to the restriction activity of IFI16 by showing that this pathogen sensor can counteract HCMV-induced metabolic reprogramming, as summarized schematically in Fig. 10. In particular, we show that IFI16 decreases HCMV-induced glucose uptake through inhibition of GLUT4 mRNA expression in HFFs, leading to decreased glucose uptake and consumption. We also show that GLUT4 inhibition relies on the cooperation between IFI16 and ChREBP, which form a complex that inhibits HCMV-induced transcriptional activation of the GLUT4 promoter in HFFs.

ChREBP is a key regulator of lipogenic gene expression. In synergy with SREBP, it can in fact regulate the expression of genes involved in the conversion of glucose to fatty acids and nucleotides. Furthermore, ChREBP deficiency has been shown to impair glucose uptake and glycolysis in HCMV-infected cells, thereby decreasing the glucose-carbon flux for anabolic processes, such as lipid synthesis, NADPH generation, and nucleotide biosynthesis (21, 48). Here, we unveil an unprecedented selective interaction between IFI16 and ChREBP to modulate GLUT4 expression during HCMV infection, resulting in decreased glycolytic and lipogenic gene expression.

We also report an overall increase in lipid concentration, especially of CE species, in HCMV-infected IFI16 KO versus WT HFFs, indicating that IFI16 is a negative regulator of lipogenesis. However, the fact that metabolic reprogramming still occurs in HCMV-infected WT HFFs despite the presence of IFI16 indicates that while IFI16 may play an important role in lipid transcriptional downregulation, its activity is not sufficient to completely overcome the metabolic changes induced by HCMV. Nevertheless, our findings are in line with the notion that herpesviruses rely on host lipid metabolism to replicate, which is also supported by our lipidomic analysis of HCMV-infected cells.

The finding of CE accumulation upon HCMV infection did not come as a surprise, as it had already been reported by Fabricant et al. in the early 1980s while they were studying other herpesviruses (40). In contrast, in a more recent study by Low et al. (49), no CE lipid accumulation in HCMV-infected fibroblasts was observed. This discrepancy may be ascribable to the presence of fetal bovine serum (FBS)—and therefore lipids— in the growth medium, which may have led to bias in the normalization step. Interestingly, previous screenings revealed that increased CE levels may also occur in
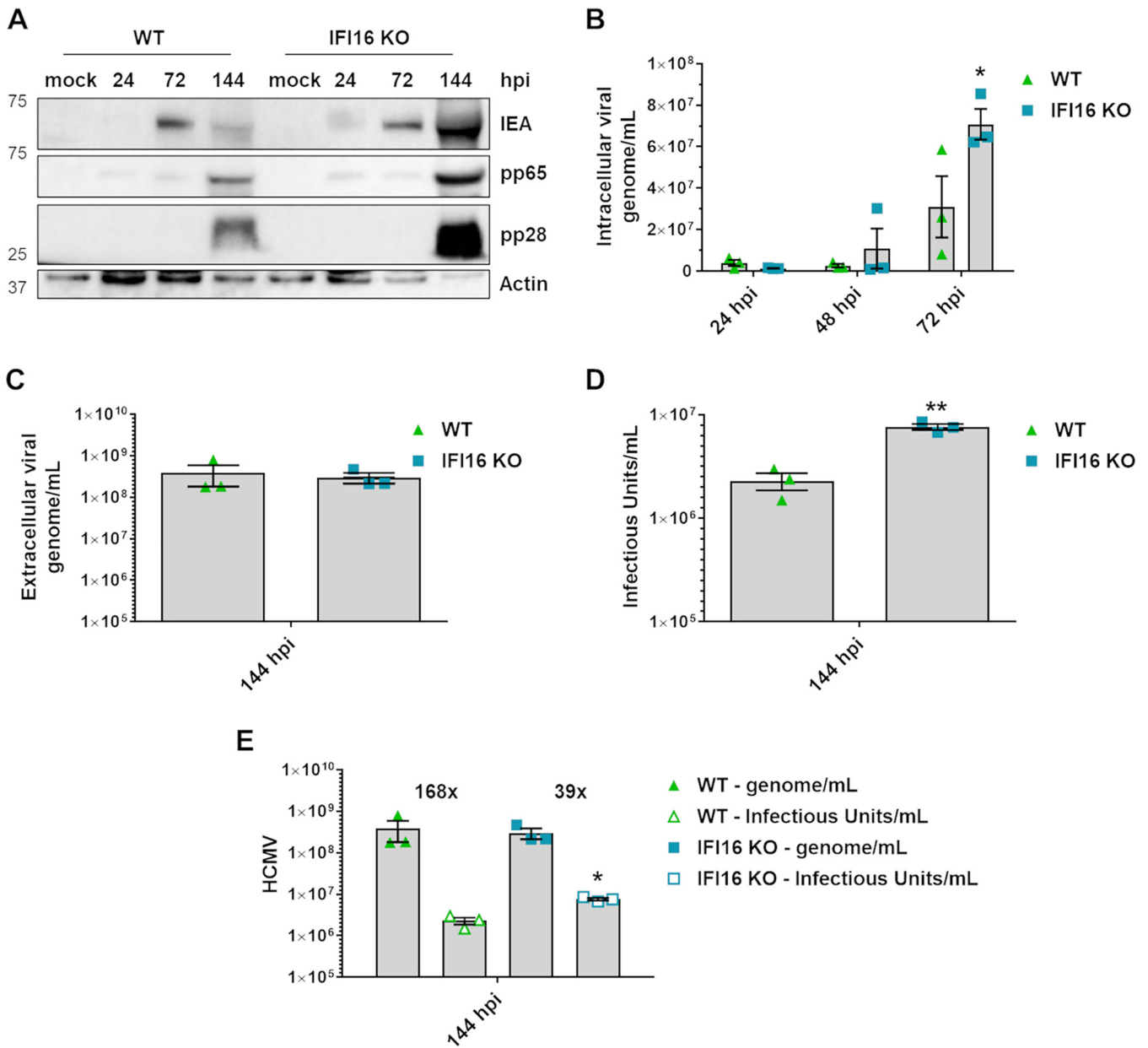
FIG 9 IFI16 impairs the infectivity of HCMV viral particles. (A) WT and IFI16 KO HFFs were infected with HCMV (MOI, 0.5). At the indicated time points, cells were harvested and subjected to Western blot analysis using monoclonal antibodies against HCMV IEA, pp65, pp28, or actin as the loading control. (B) WT and IFI16 KO HFFs were infected with HCMV (MOI, 0.5). At the indicated time points, the DNA was extracted from infected cells, and the number of HCMV genomes was measured by qPCR. The primers amplified a segment of the IE1 gene to determine the number of viral DNA genomes per nanogram of cellular reference DNA (GAPDH gene). Bars represent the means and SEM from three independent experiments (*, $P < 0.05$; two-way ANOVA followed by Bonferroni's posttests, for comparison of WT versus IFI16 KO cells). (C) The number of HCMV genomes released in the supernatants of infected cells was measured by qPCR (not significant; unpaired t test). (D) The supernatants used for panel C were used to determine the number of infectious units/mL by virus yield assay. Bars represent means and SEM from three independent experiments (**, $P < 0.01$; unpaired t test). (E) The genome-to-infectious unit ratio was determined, and the values are above the bars (*, $P < 0.05$, unpaired t test).

cells infected with RNA viruses, such as HCV (42, 50). Accordingly, SOAT1, responsible for intracellular CE biosynthesis from cholesterol and fatty acyl-CoA, was shown to be upregulated early upon HCMV infection, and its inhibition restrained viral replication (43). Our findings of increased CE levels in HCMV-infected IFI16 KO cells, which are further accompanied by more robust SOAT1 upregulation than in similarly infected WT HFFs, support our hypothesis that IFI16 is a negative regulator of lipid synthesis.

The final outcome of IFI16 restriction activity on HCMV enhanced metabolic pathways is a significant and highly reproducible decrease in the release of infectious
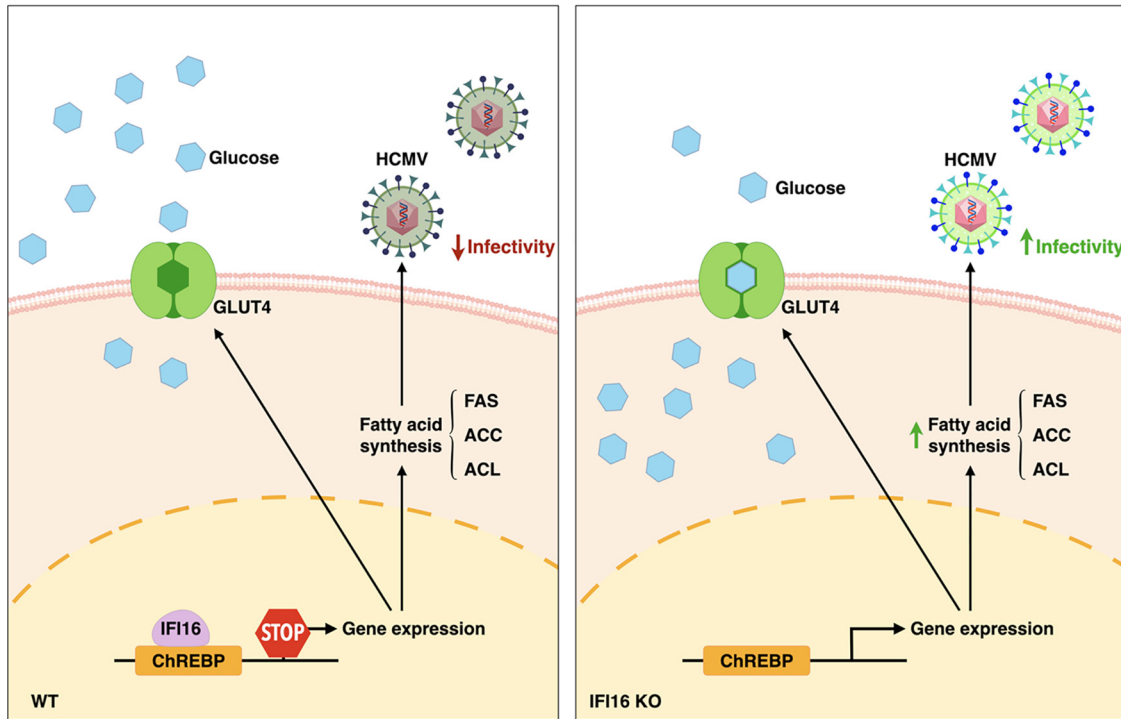
FIG 10 Proposed model of IFI16 control on HCMV-induced metabolic changes. Upon HCMV infection, IFI16 forms an inhibitory complex with the transcription factor ChREBP, thereby downmodulating the expression of GLUT4 and reducing glucose consumption. Furthermore, IFI16-ChREBP cooperation leads to decreased expression of genes involved in HCMV-induced lipogenesis, which leads to impaired lipid synthesis and reduced infectivity of viral particles.

virions. HCMV virion assembly is a complex process involving initial envelopment at the inner nuclear membrane and de-envelopment at the outer nuclear membrane to release partially tegumented nucleocapsids into the cytoplasm (44, 51). There, nucleocapsids obtain their envelope in a secondary envelopment process by budding into vesicles of the secretory pathway prior to their release into supernatant (52). In this context, our electron microscopy experiments show no obvious defect in virion morphogenesis between WT and IFI16 KO cells, but we found that the number of enveloped nucleocapsids is slightly decreased in WT HFFs. It is reasonable to assume that the reduction in viral protein expression and restriction of viral replication in WT HFFs compared with IFI16 KO cells results in the production of fewer viral particles, which explains our electron-microscopic observations. The IFI16-dependent restriction of viral replication shown in this work is in complete agreement with our previous results (25). Despite the difference intracellular virion number, the release of viral particles from infected cells did not appear to be affected, as there was no difference in extracellular genome copy number between WT and IFI16-KO cells. The infectivity of released virus particles, however, was decreased by a factor of 4 in WT-HFF. This may well be related to IFI16 restriction activity on the lipid metabolic pathway, since selective impairment of lipid metabolism, e.g., by knockdown of ELOVL7 or PERK, was associated with reduced infectivity of virus particles in previous work (14, 24).

Together, these results not only confirm IFI16 as a restriction factor of HCMV replication, but also identify IFI16 as a metabolism regulator affecting virion infectivity.

Another implication of our findings involves the potential interplay among lipid metabolic disorders, HCMV, and atherosclerosis, whose pathogenetic mechanism is not fully understood (53). In this regard, the possible infectious etiology of atherosclerosis has recently gained increasing attention (54–56), with HCMV being proposed as the main culprit (53, 57, 58). Indeed, several studies have shown a correlation between HCMV seropositivity and increased risk of coronary atherosclerosis (59, 60), and HCMV

DNA and viral protein have been detected in atherosclerotic lesions (61). Moreover, animal models have provided evidence that HCMV infection promotes atherogenesis (62). Last, CE metabolism has long been linked to the development of atherosclerosis (63, 64). Thus, based on the results of this study, experiments are ongoing to explore the potential contribution of HCMV-driven metabolic reprogramming to the pathogenesis of atherosclerosis.

Altogether, our findings strengthen the idea that IFI16 is a global regulator of HCMV-induced modulation of lipid metabolism, which may pave the way to the discovery of new therapeutic targets for HCMV therapy.

MATERIALS AND METHODS

Cells and viruses. Primary HFFs (American Type Culture Collection; ATCC SCRC-1041) were cultured in Dulbecco's modified Eagle's medium (Sigma-Aldrich) supplemented with 10% fetal calf serum (FCS; Sigma-Aldrich) according to ATCC specifications. HFFs with IFI16 silenced (IFI16 KO) were generated by the CRISPR/Cas9 system, as previously described (27, 65). The HCMV laboratory strain AD169 (ATCC-VR538) was propagated and titrated by standard plaque assay (25). Prior to infection, cells were maintained at full confluence for 24 h in serum-containing growth medium and switched to serum-free medium the day before the infection. Infections were performed at a MOI of 1 or 3 infectious units per cell, depending on the experiment.

Plasmids. The GLUT4 promoter was kindly provided by K. T. Dalen (University of Oslo, Norway) and generated according to Dalen et al. (66). The plasmid expressing HA-tagged human ChREBPα was kindly provided by Y. Yu (University of Pennsylvania, Philadelphia, PA, USA) (21). The mutant construct of the GLUT4 promoter lacking the ChREBP binding site (GLUT4ΔChREBP) was cloned starting from a pGL3-Basic vector carrying the GLUT4 promoter previously described, using the following primers: GLUT4ΔChREBP Fw, AGGATCCAAACCC GGAGCAGCCTCCAGAGAGCGTGTCGTTCTCAGAGACCTCAGAGGCTC; GLUT4ΔChREBP Rv, CCACCAGCCCTGAGG TCTCTGAGCCTCTGAGGTCTCTGAGAACGACACGCTCTCTGGAGG. Mutations were confirmed by DNA sequencing. The IE1-encoding plasmid pSGIE72 was used in the quantitative nucleic acid analysis.

RNA isolation and semiquantitative RT-qPCR. Total RNA was extracted using TRI Reagent solution (Life Technologies) according to the manufacturer's instructions, and 1 μg was retrotranscribed using the Revert-Aid H-Minus FirstStrand cDNA synthesis kit (Thermo Fisher Scientific). Comparison of mRNA expression between samples (i.e., WT versus IFI16 KO) was performed by SYBR green-based reverse transcription-qPCR (RT-qPCR) using an Mx3000P apparatus (Stratagene) with the following primers: GLUT4 Fw, GGAGCTGGTGTGGTCAACACA; GLUT4 Rv, GGAGCAGAGCCACAGTCATCA; ACL Fw, TGTAACAGAGCC AGGAACCC; ACL Rv, CTGTACCCCAGTGGCTGTTT; ACC1 Fw, TTAACAGCTGTGGAGTCTGGCTGT; ACC1 Rv, AACACTCGATGGAGTTTCTCGCCT; FAS Fw, AGGCTGAGACGGAGGCCATA; FAS Rv, AAAGCTCAGCTCCTGG CGGT; CHREBPα Fw, AGTGCTTGAGCCTGGCCTAC; CHREBPα Rv, TTGTTCAGGCGGATCTTGTC; ELOVL7 Fw, GGCCAGCCTACCAGAAGTATTTG; ELOVL7 Rv, GGCGACAATAACAAACTGGACAAG; SOAT1 Fw, CCACTG GTCCAGATGAGTTTAG; SOAT1 Rv, GGGAACATGCAGAGTACCTTT; GAPDH (the housekeeping gene encoding glyceraldehyde-3-phosphate dehydrogenase) Fw, AGTGGGTGTCGCTGTTGAAGT; GAPDH Rv, AACGTG TCAGTGGTGGACCTG.

Inhibition of ChREBP expression. HFFs were transiently transfected using a MicroPorator (Digital Bio) according to the manufacturer's instructions (1,200 V, 30-ms pulse width, one impulse), with a pool of ChREBP small interfering RNAs (siChREBP; CHREBP [MLXIPL] human siRNA oligonucleotide duplex; OriGene SR309520) or control siRNA (siCTRL) as a negative control, according to the manufacturer's protocols. siRNA-induced blockade of ChREBP expression was checked by Western blotting.

DNA extraction and viral load determination. Intracellular DNA was extracted using TRI Reagent solution (Life Technologies) according to the manufacturer's instructions. Quantification of intracellular and extracellular HCMV copy numbers was evaluated via quantitative real-time PCR (qPCR) analysis on an Mx 3000 P apparatus (Stratagene), using primers to amplify a segment of the IE1 gene (Fw, 5'-TCAGTGCTCCCCTGATGAGA-3'; Rv, 5'-GATCAATGTGCGTGAGCACC-3'), as described by Biolatti et al. (28). Intracellular HCMV DNA copy numbers were normalized to GAPDH. A standard curve of serially diluted genomic DNA mixed with an IE1-encoding plasmid (from 10^7 copies to 1 copy) was created in parallel with each analysis.

Western blot analysis. Whole-cell protein extracts were prepared and subjected to Western blot analysis as previously described (26, 67). The primary antibodies against the following proteins were used: actin clone C4 (MAB1501; Sigma-Aldrich), α-tubulin (39527; Active Motif), IFI16 (Santo Landolfo, University of Turin, Italy), IFI16 (sc-8023; Santa Cruz Biotechnology), HA (3724; Cell Signaling), immediate early antigen (IEA) (P1215; Virusys), pp65 (CA003; Virusys), and pp28 (P1207; Virusys). Immunocomplexes were detected using appropriate secondary antibodies conjugated with horseradish peroxidase (HRP) (GE Healthcare Europe GmbH) and visualized by enhanced chemiluminescence (Super Signal West Pico; Thermo Fisher Scientific).

Immunoprecipitation. Uninfected or HCMV-infected cells (MOI, 1) were washed with 1$\times$ phosphate-buffered saline (PBS) and lysed in Triton buffer (50 mM Tris, pH 7.4; 150 mM NaCl; 1 mM EDTA; 1% Triton; protease inhibitors). Proteins (400 μg) were incubated with 4 μg of specific antibodies against IFI16 (Santo Landolfo, University of Turin, Italy) or HA (3724; Cell Signaling), or with rabbit IgG preimmune antibody (NRI01; Cell Sciences) as a negative control, for 2 h at 4°C with rotation, followed by an overnight incubation at 4°C with protein G-Sepharose (Sigma-Aldrich). Immune complexes were collected by centrifugation, washed three times with PBS, resuspended in reducing sample buffer (50 mM

Tris, pH 6.8; 10% glycerol; 2% SDS; 1% 2-mercaptoethanol), boiled for 5 min, and resolved on an SDS-PAGE gel to assess protein binding by Western blotting.

ChIP assay. ChIP assays were performed using a shearing optimization kit and a OneDay ChIP kit (Diagenode Europe), according to the manufacturer's instructions. Extracts were cross-linked with 1% paraformaldehyde for 15 min and then processed with OneDay ChIP (Diagenode Europe), according to the manufacturer's instructions. DNA fragments were sonicated with a BioruptorH Twin (Diagenode Europe) for 10 cycles (30 s on, 30 s off) on the high-power setting. Immunoprecipitation was performed using 5 μg of anti-IFI16 antibody (Santo Landolfo, University of Turin, Italy). Rabbit IgG was used as a negative control. The DNA solution (1 μL per reaction mixture) was used for qPCR using HCMV- or human-specific primers: ChREBP responsive element Fw, CTCCAGAGAGCGTGTCGTTC; ChREBP responsive element Rv, CGAGGGACAAGTGGTCACAA.

Luciferase assay. Cells were electroporated with siChREBP or siCTRL and with a luciferase reporter plasmid driven by the GLUT4 gene promoter and with pRL-SV40 (Promega Italia) plasmid as previously described (25). HFFs were then infected with HCMV (MOI, 1). At 24 hpi, firefly and *Renilla* luciferase activities were measured using the dual-luciferase reporter assay system kit (Promega Italia) and a Lumino luminometer (Stratec Biomedical Systems), as previously described (68). The firefly luciferase activity from the luciferase reporter vector was normalized to that of the *Renilla* luciferase vector (pRL-SV40). Data are expressed as the ratio of relative light units (RLU) measured for firefly luciferase activity to the RLU measured for *Renilla* luciferase activity.

Immunofluorescence microscopy. Indirect immunofluorescence analysis was performed as previously described (26). The primary antibodies were those against IEA (P1215; Virusys) and ChREBP (ab92809; Abcam). Signals were detected using goat anti-rabbit or goat anti-mouse conjugated secondary antibodies (Thermo Fisher Scientific). Nuclei were counterstained with 4′,6-diamidino-2-phenylindole (DAPI). Samples were observed using a fluorescence microscope (Olympus IX70) equipped with cellSens standard microscopy imaging software. The percentage of cells showing ChREBP nuclear translocation in IEA-positive nuclei was calculated using ImageJ software.

Proximity ligation assay. The PLA was performed using the DuoLink (Sigma-Aldrich) PLA kit to detect protein-protein interactions using fluorescence microscopy according to the manufacturer's instructions. Briefly, HFFs were cultured and infected with HCMV at an MOI of 1 for 24 h, fixed for 15 min at room temperature with 4% paraformaldehyde, permeabilized with 0.2% Triton X-100, and blocked with 10% HCMV-negative human serum for 30 min at RT. Cells were then incubated with the primary antibodies diluted in Tris-buffered saline (TBS)–0.05% Tween for 1 h, washed, and then incubated for an additional h at 37°C with species-specific PLA probes under hybridization conditions and in the presence of 2 additional oligonucleotides to facilitate the hybridization only in close proximity (40 nm). A ligase was then added to join the two hybridized oligonucleotides, forming a closed circle. Using the ligated circle as the template, rolling-circle amplification was initiated by adding an amplification solution, generating a concatemeric product extending from the oligonucleotide arm of the PLA probe. Last, a detection solution consisting of fluorophore-labeled oligonucleotides was added, and the labeled oligonucleotides were hybridized to the concatemeric products. The signal was detected as distinct fluorescent dots in the Texas Red channel and analyzed by confocal microscope (Leica Microsystem). Negative controls consisted of mock-infected cells that were otherwise treated in the same way as the infected cells.

Glucose metabolic assays. For glucose assays, HFFs were plated in 24-well cell plates and cultured in serum-free DMEM. Cells were infected at an MOI of 1 and 3. The culture medium was harvested at 24, 48, 72, and 144 hpi, and the glucose concentration in the culture medium was measured by means of a Biosen C-line analyzer (EKF Diagnostics).

Electron microscopy. HFFs were infected with HCMV at an MOI of 1 and examined by electron microscopy at 7 days postinfection (dpi). Briefly, the cells were fixed with 2.5% glutaraldehyde and postfixed with 1% osmium tetroxide. Cells were then stained with 2% uranyl acetate, dehydrated with a graded series of acetone, infiltrated, and embedded in Epon. Seventy nanometer sections were stained with lead citrate and examined using a CM10 electron microscope (Philips).

Lipidomics. For lipidomic analysis, lipids were extracted from WT and IFI16 KO HFFs under fully confluent serum-free medium and infected or not with HCMV for 96 h (MOI of 1 or 3) using an acidified chloroform-methanol-water mixture and glass beads. Briefly, 600 μL of chloroform-methanol (1:2 [vol/vol]) and 10 μL of formic acid and glass beads were added to the cells, vortexed for 20 s, and shaken for 5 min (2,000 rpm, 4°C). Next, 200 μL of chloroform and 350 μL of deionized water were added and shaken for an additional 20 min (2,000 rpm at 4°C). Subsequently, extracts were centrifuged (10 min, 3,900 × *g*), and the lower organic phase was collected and transferred to a chromatographic vial with a glass insert. In parallel with the biological samples, extraction was carried out with samples without cells to obtain extraction blanks to be used as negative controls.

After extraction, cells were analyzed using an Agilent 1290 LC system equipped with a binary pump, online degasser, autosampler, and a thermostated column compartment coupled to a 6540 Q-TOF–MS with a dual electrospray ionization (ESI) source (Agilent Technologies). Lipids were separated using reversed-phase column (Poroshell 120 EC-C8, 2.1 by 150 mm, 1.9-μm particle size; Agilent InfinityLab; Agilent Technologies) with a 0.2-μm in-line filter. The column was maintained at 60°C. The mobile phase comprised component A (5 mM ammonium formate in water-methanol [20/80, vol/vol]) and component B (2-propanol). The mobile phase was pumped at a flow rate of 0.3 mL/min. The gradient elution program was initiated with 20% of component B, which was ramped to 30% from 0 to 20 min and then from 30% to 100% from 20 to 30 min and kept for 1 min at 100% B. The column was then equilibrated with the starting conditions for 10 min. The total run time was 41 min, and the injection volume was set

to 1.5 μL. Each extract was injected in duplicate. The data were collected in the positive-ion mode using the SCAN acquisition mode in a range from 100 to 1,700 m/z in the high-resolution mode (4 GHz).

MS analysis was carried out using the following parameters: capillary voltage, 3,500 V; fragmentation voltage, 120 V; nebulizing gas, 35 psi; drying gas temperature, 300℃. MS/MS analysis was performed using identical chromatographic and ion source conditions. The collision energy was set to 35 V and 80 V. The two most abundant peaks were selected for fragmentation and excluded for the next 0.3 min. The MS/MS spectra were acquired in the m/z range of 50 to 1,700. Lipid extracts were injected randomly using one quality control (QC) sample (pooled extracts) injected every 4 real samples for the LC-MS stability control.

Lipidomic data were prepared in the Agilent MassHunter Workstation Profinder 10.0 (Agilent Technologies). The MFE algorithm was used to extract the total molecular features (MFs) from the raw LC-MS data using the following parameters: ion threshold, >1,000 counts; ion type, H$^+$; isotope model, common organic (no halogens); charge state range, 1 to 2; MFE score, ≥70. Next, the list of identified lipids was used for the Targeted Molecular Feature Extraction step with the following parameters: positive ions, charge carriers, H+, Na$^+$, NH$_4^+$; match tolerance, 20 ppm; retention time, 0.2 min; Gaussian smoothing before extracted ion chromatogram extraction (EIC) filtering on peak height, 1,000 counts. The .cef files were exported and imported to Mass Profiler Professional 15.1 software (Agilent Technologies) for data alignment and filtration. Missing values were exported as missing. The alignment parameters were set as follows: alignment slope, 0.0%; alignment intercept, 0.2 min; mass tolerance slope, 20.0 ppm; intercept, 2.0 mDa. Filtration was based on frequency—the MFs remained in the data set if they were present in 80% of the samples in at least one specified group—and on the QC %RSD—MFs remained if the %Relative Standard Deviation (RSD) was <25% in all the QC samples. The MFs present in the extraction blank with an average peak volume higher than 10% of the average peak volume in the real samples were removed.

The statistical analysis and fold change calculation were conducted using Mass Profiler Professional 15.1 software (Agilent Technologies) and MetaboAnalyst5.0 (https://www.metaboanalyst.ca/home.xhtml). The parameters in the statistical test (Mann-Whitney unpaired test or Student's t test were a P value of ≤0.05 and asymptotic P value computation, and only detectable values were used for the calculation of fold change and P value). Lipid identification was carried out using the two-step procedure: (i) a custom lipid database (containing the mass of theoretical lipid structures) search based on an accurately measured m/z value (Δ5 ppm tolerance) and (ii) manual interpretation of the obtained MS/MS spectra. The identified lipid species were described according to the lipid class, number of carbon atoms, and number of double bonds in fatty acyl substituents. The diagnostic ions for the lipid class confirmation were as follows: m/z 184.0726 for confirmation of the PC identity, neutral loss of 141.02 Da for the confirmation of the PE identity, neutral loss of 185.01 Da for the confirmation of PS identity, and m/z 369.3536 for confirmation of CE.

Statistical analysis. Statistical tests were performed using GraphPad Prism version 5.00 for Windows (GraphPad Software), Mass Profiler Professional 15.1 software (Agilent Technologies), or MetaboAnalyst5.0 (https://www.metaboanalyst.ca/home.xhtml). The data are presented as means and standard errors of the means (SEM). Differences were considered statistically significant when the P value was <0.05.

REFERENCES

1. Adland E, Klenerman P, Goulder P, Matthews PC. 2015. Ongoing burden of disease and mortality from HIV/CMV coinfection in Africa in the antiretroviral therapy era. Front Microbiol 6:1016. https://doi.org/10.3389/fmicb.2015.01016.

2. Griffiths PD. 2001. Cytomegalovirus therapy: current constraints and future opportunities. Curr Opin Infect Dis 14:765–768. https://doi.org/10.1097/00001432-200112000-00016.

3. Britt WJ. 2018. Maternal immunity and the natural history of congenital human cytomegalovirus infection. Viruses 10:405. https://doi.org/10.3390/v10080405.

4. Coscia A, Leone A, Rubino C, Galitska G, Biolatti M, Bertino E, Peila C, Cresi F. 2020. Risk of symptomatic infection after non-primary congenital cytomegalovirus infection. Microorganisms 8:786. https://doi.org/10.3390/microorganisms8050786.

5. Gugliesi F, Coscia A, Griffante G, Galitska G, Pasquero S, Albano C, Biolatti M. 2020. Where do we stand after decades of studying human cytomegalovirus? Microorganisms 8:685. https://doi.org/10.3390/microorganisms8050685.

6. Adam E, Melnick JL, Probtsfield JL, Petrie BL, Burek J, Bailey KR, McCollum CH, DeBakey ME. 1987. High levels of cytomegalovirus antibody in patients requiring vascular surgery for atherosclerosis. Lancet 2:291–293. https://doi.org/10.1016/s0140-6736(87)90888-9.

7. Fish KN, Soderberg-Naucler C, Mills LK, Stenglein S, Nelson JA. 1998. Human cytomegalovirus persistently infects aortic endothelial cells. J Virol 72:5661–5668. https://doi.org/10.1128/JVI.72.7.5661-5668.1998.

8. Cohen Y, Stern-Ginossar N. 2014. Manipulation of host pathways by human cytomegalovirus: insights from genome-wide studies. Semin Immunopathol 36:651–658. https://doi.org/10.1007/s00281-014-0443-7.

9. Dell'Oste V, Biolatti M, Galitska G, Griffante G, Gugliesi F, Pasquero S, Zingoni A, Cerboni C, De Andrea M. 2020. Tuning the orchestra: HCMV vs. innate immunity. Front Microbiol 11:661. https://doi.org/10.3389/fmicb.2020.00661.

10. Shenk T, Alwine JC. 2014. Human cytomegalovirus: coordinating cellular stress, signaling, and metabolic pathways. Annu Rev Virol 1:355–374. https://doi.org/10.1146/annurev-virology-031413-085425.

11. Mayer KA, Stöckl J, Zlabinger GJ, Gualdoni GA. 2019. Hijacking the supplies: metabolism as a novel facet of virus-host interaction. Front Immunol 10:1533. https://doi.org/10.3389/fimmu.2019.01533.

12. Rodríguez-Sánchez I, Munger J. 2019. Meal for two: human cytomegalovirus-induced activation of cellular metabolism. Viruses 11:273. https://doi.org/10.3390/v11030273.

13. Thaker SK, Ch'ng J, Christofk HR. 2019. Viral hijacking of cellular metabolism. BMC Biol 17:59. https://doi.org/10.1186/s12915-019-0678-9.

14. Xi Y, Lindenmayer L, Kline I, von Einem J, Purdy JG. 2021. Human cytomegalovirus uses a host stress response to balance the elongation of saturated/monounsaturated and polyunsaturated very-long-chain fatty acids. mBio 12:e00167-21. https://doi.org/10.1128/mBio.00167-21.

15. Munger J, Bajad SU, Coller HA, Shenk T, Rabinowitz JD. 2006. Dynamics of the cellular metabolome during human cytomegalovirus infection. PLoS Pathog 2:e132. https://doi.org/10.1371/journal.ppat.0020132.

16. Landini MP. 1984. Early enhanced glucose uptake in human cytomegalovirus-infected cells. J Gen Virol 65:1229–1232. https://doi.org/10.1099/0022-1317-65-7-1229.

17. Yu Y, Alwine JC. 2002. Human cytomegalovirus major immediate-early proteins and simian virus 40 large T antigen can inhibit apoptosis through activation of the phosphatidylinositide 3′-OH kinase pathway and the cellular kinase Akt. J Virol 76:3731–3738. https://doi.org/10.1128/jvi.76.8.3731-3738.2002.

18. Chambers JW, Maguire TG, Alwine JC. 2010. Glutamine metabolism is essential for human cytomegalovirus infection. J Virol 84:1867–1873. https://doi.org/10.1128/JVI.02123-09.

19. Vastag L, Koyuncu E, Grady SL, Shenk TE, Rabinowitz JD. 2011. Divergent effects of human cytomegalovirus and herpes simplex virus-1 on cellular metabolism. PLoS Pathog 7:e1002124. https://doi.org/10.1371/journal.ppat.1002124.

20. Yu Y, Maguire TG, Alwine JC. 2011. Human cytomegalovirus activates glucose transporter 4 expression to increase glucose uptake during infection. J Virol 85:1573–1580. https://doi.org/10.1128/JVI.01967-10.

21. Yu Y, Maguire TG, Alwine JC. 2014. ChREBP, a glucose-responsive transcriptional factor, enhances glucose metabolism to support biosynthesis in human cytomegalovirus-infected cells. Proc Natl Acad Sci U S A 111:1951–1956. https://doi.org/10.1073/pnas.1310779111.

22. McArdle J, Moorman NJ, Munger J. 2012. HCMV targets the metabolic stress response through activation of AMPK whose activity is important for viral replication. PLoS Pathog 8:e1002502. https://doi.org/10.1371/journal.ppat.1002502.

23. Terry LJ, Vastag L, Rabinowitz JD, Shenk T. 2012. Human kinome profiling identifies a requirement for AMP-activated protein kinase during human cytomegalovirus infection. Proc Natl Acad Sci U S A 109:3071–3076. https://doi.org/10.1073/pnas.1200494109.

24. Purdy JG, Shenk T, Rabinowitz JD. 2015. Fatty acid elongase 7 catalyzes lipidome remodeling essential for human cytomegalovirus replication. Cell Rep 10:1375–1385. https://doi.org/10.1016/j.celrep.2015.02.003.

25. Gariano GR, Dell'Oste V, Bronzini M, Gatti D, Luganini A, De Andrea M, Gribaudo G, Gariglio M, Landolfo S. 2012. The intracellular DNA sensor IFI16 gene acts as restriction factor for human cytomegalovirus replication. PLoS Pathog 8:e1002498. https://doi.org/10.1371/journal.ppat.1002498.

26. Dell'Oste V, Gatti D, Gugliesi F, De Andrea M, Bawadekar M, Lo Cigno I, Biolatti M, Vallino M, Marschall M, Gariglio M, Landolfo S. 2014. Innate nuclear sensor IFI16 translocates into the cytoplasm during the early stage of in vitro human cytomegalovirus infection and is entrapped in the egressing virions during the late stage. J Virol 88:6970–6982. https://doi.org/10.1128/JVI.00384-14.

27. Biolatti M, Dell'Oste V, Pautasso S, Gugliesi F, von Einem J, Krapp C, Jakobsen MR, Borgogna C, Gariglio M, De Andrea M, Landolfo S. 2018. Human cytomegalovirus tegument protein pp65 (pUL83) dampens type I interferon production by inactivating the DNA sensor cGAS without affecting STING. J Virol 92:e01774-17. https://doi.org/10.1128/JVI.01774-17.

28. Biolatti M, Dell'Oste V, Pautasso S, von Einem J, Marschall M, Plachter B, Gariglio M, De Andrea M, Landolfo S. 2016. Regulatory interaction between the cellular restriction factor IFI16 and viral pp65 (pUL83) modulates viral gene expression and IFI16 protein stability. J Virol 90:8238–8250. https://doi.org/10.1128/JVI.00923-16.

29. Herman MA, Peroni OD, Villoria J, Schön MR, Abumrad NA, Blüher M, Klein S, Kahn BB. 2012. A novel ChREBP isoform in adipose tissue regulates systemic glucose metabolism. Nature 484:333–338. https://doi.org/10.1038/nature10986.

30. Davies MN, O'Callaghan BL, Towle HC. 2008. Glucose activates ChREBP by increasing its rate of nuclear entry and relieving repression of its transcriptional activity. J Biol Chem 283:24029–24038. https://doi.org/10.1074/jbc.M801539200.

31. Leclerc I, Rutter GA, Meur G, Noordeen N. 2012. Roles of Ca2+ ions in the control of ChREBP nuclear translocation. J Endocrinol 213:115–122. https://doi.org/10.1530/JOE-11-0480.

32. Everett RD. 2016. Dynamic response of IFI16 and promyelocytic leukemia nuclear body components to herpes simplex virus 1 infection. J Virol 90:167–179. https://doi.org/10.1128/JVI.02249-15.

33. Filhoulaud G, Guilmeau S, Dentin R, Girard J, Postic C. 2013. Novel insights into ChREBP regulation and function. Trends Endocrinol Metab 24:257–268. https://doi.org/10.1016/j.tem.2013.01.003.

34. Grønning-Wang LM, Bindesbøll C, Nebb HI. 2013. The role of liver X receptor in hepatic de novo lipogenesis and cross-talk with insulin and glucose signaling. In Baez RV (ed), Lipid metabolism. InTechOpen, London, United Kingdom.

35. Spencer CM, Schafer XL, Moorman NJ, Munger J. 2011. Human cytomegalovirus induces the activity and expression of acetyl-coenzyme A carboxylase, a fatty acid biosynthetic enzyme whose inhibition attenuates viral replication. J Virol 85:5814–5824. https://doi.org/10.1128/JVI.02630-10.

36. Yu Y, Maguire TG, Alwine JC. 2012. Human cytomegalovirus infection induces adipocyte-like lipogenesis through activation of sterol regulatory element binding protein 1. J Virol 86:2942–2949. https://doi.org/10.1128/JVI.06467-11.

37. Koyuncu E, Purdy JG, Rabinowitz JD, Shenk T. 2013. Saturated very long chain fatty acids are required for the production of infectious human cytomegalovirus progeny. PLoS Pathog 9:e1003333. https://doi.org/10.1371/journal.ppat.1003333.

38. Xi Y, Harwood S, Wise LM, Purdy JG. 2019. Human cytomegalovirus pUL37x1 is important for remodeling of host lipid metabolism. J Virol 93:e00843-19. https://doi.org/10.1128/JVI.00843-19.

39. Dahlmann EA. 2019. HCMV manipulation of host cholesteryl ester metabolism. PhD thesis. University of Arizona, Tucson, AZ.

40. Fabricant CG, Hajjar DP, Minick CR, Fabricant J. 1981. Herpesvirus infection enhances cholesterol and cholesteryl ester accumulation in cultured arterial smooth muscle cells. Am J Pathol 105:176–184.

41. Hajjar DP, Pomerantz KB, Falcone DJ, Weksler BB, Grant AJ. 1987. Herpes simplex virus infection in human arterial cells. Implications in arteriosclerosis. J Clin Invest 80:1317–1321. https://doi.org/10.1172/JCI113208.

42. Read SA, Tay E, Shahidi M, George J, Douglas MW. 2014. Hepatitis C virus infection mediates cholesteryl ester synthesis to facilitate infectious particle production. J Gen Virol 95:1900–1910. https://doi.org/10.1099/vir.0.065300-0.

43. Harwood SJ. 2019. Human cytomegalovirus use and manipulation of host phospholipids. MS thesis. University of Arizona, Tucson, AZ.

44. Tandon R, Mocarski ES. 2012. Viral and host control of cytomegalovirus maturation. Trends Microbiol 20:392–401. https://doi.org/10.1016/j.tim.2012.04.008.

45. Munger J, Bennett BD, Parikh A, Feng X-J, McArdle J, Rabitz HA, Shenk T, Rabinowitz JD. 2008. Systems-level metabolic flux profiling identifies fatty acid synthesis as a target for antiviral therapy. Nat Biotechnol 26:1179–1186. https://doi.org/10.1038/nbt.1500.

46. Joost H-G, Bell GI, Best JD, Birnbaum MJ, Charron MJ, Chen YT, Doege H, James DE, Lodish HF, Moley KH, Moley JF, Mueckler M, Rogers S, Schürmann A, Seino S, Thorens B. 2002. Nomenclature of the GLUT/SLC2A family of sugar/polyol transport facilitators. Am J Physiol Endocrinol Metab 282:E974–976. https://doi.org/10.1152/ajpendo.00407.2001.

47. Uldry M, Thorens B. 2004. The SLC2 family of facilitated hexose and polyol transporters. Pflugers Arch 447:480–489. https://doi.org/10.1007/s00424-003-1085-0.

48. Ortega-Prieto P, Postic C. 2019. Carbohydrate sensing through the transcription factor ChREBP. Front Genet 10:472. https://doi.org/10.3389/fgene.2019.00472.

49. Low H, Mukhamedova N, Cui HL, McSharry BP, Avdic S, Hoang A, Ditiatkovski M, Liu Y, Fu Y, Meikle PJ, Blomberg M, Polyzos KA, Miller WE, Religa P, Bukrinsky M, Soderberg-Naucler C, Slobedman B, Sviridov D. 2016. Cytomegalovirus restructures lipid rafts via US28/CDC42 mediated pathway enhancing cholesterol efflux from host cells. Cell Rep 16:186–200. https://doi.org/10.1016/j.celrep.2016.05.070.

50. Merz A, Long G, Hiet M-S, Brügger B, Chlanda P, Andre P, Wieland F, Krijnse-Locker J, Bartenschlager R. 2011. Biochemical and morphological properties of hepatitis C virus particles and determination of their lipidome. J Biol Chem 286:3018–3032. https://doi.org/10.1074/jbc.M110.175018.

51. Sanchez V, Britt W. 2021. Human cytomegalovirus egress: overcoming barriers and co-opting cellular functions. Viruses 14:15. https://doi.org/10.3390/v14010015.

52. Schauflinger M, Villinger C, Mertens T, Walther P, von Einem J. 2013. Analysis of human cytomegalovirus secondary envelopment by advanced electron microscopy. Cell Microbiol 15:305–314. https://doi.org/10.1111/cmi.12077.

53. Zhu W, Liu S. 2020. The role of human cytomegalovirus in atherosclerosis: a systematic review. Acta Biochim Biophys Sin (Shanghai) 52:339–353. https://doi.org/10.1093/abbs/gmaa005.

54. Campbell LA, Rosenfeld ME. 2015. Infection and atherosclerosis development. Arch Med Res 46:339–350. https://doi.org/10.1016/j.arcmed.2015.05.006.

55. Kearns A, Gordon J, Burdo TH, Qin X. 2017. HIV-1-associated atherosclerosis: unraveling the missing link. J Am Coll Cardiol 69:3084–3098. https://doi.org/10.1016/j.jacc.2017.05.012.

56. Peretz A, Azrad M, Blum A. 2019. Influenza virus and atherosclerosis. QJM 112:749–755. https://doi.org/10.1093/qjmed/hcy305.

57. Dummer S, Lee A, Breinig MK, Kormos R, Ho M, Griffith B. 1994. Investigation of cytomegalovirus infection as a risk factor for coronary atherosclerosis in the explanted hearts of patients undergoing heart transplantation. J Med Virol 44:305–309. https://doi.org/10.1002/jmv.1890440316.

58. Nieto FJ, Adam E, Sorlie P, Farzadegan H, Melnick JL, Comstock GW, Szklo M. 1996. Cohort study of cytomegalovirus infection as a risk factor for carotid intimal-medial thickening, a measure of subclinical atherosclerosis. Circulation 94:922–927. https://doi.org/10.1161/01.CIR.94.5.922.

59. Jeong SJ, Ku NS, Han SH, Choi JY, Kim CO, Song YG, Kim JM. 2015. Anti-cytomegalovirus antibody levels are associated with carotid atherosclerosis and inflammatory cytokine production in elderly Koreans. Clin Chim Acta 445:65–69. https://doi.org/10.1016/j.cca.2015.03.015.

60. Zhang J, Liu Y, Sun H, Li S, Xiong H, Yang Z, Xiang G, Jiang X. 2015. High human cytomegalovirus IgG level is associated with increased incidence of diabetic atherosclerosis in type 2 diabetes mellitus patients. Med Sci Monit 21:4102–4110. https://doi.org/10.12659/msm.896071.

61. Tanaka S, Toh Y, Mori R, Komori K, Okadome K, Sugimachi K. 1992. Possible role of cytomegalovirus in the pathogenesis of inflammatory aortic diseases: a preliminary report. J Vasc Surg 16:274–279. https://doi.org/10.1067/mva.1992.37474.

62. Hsich E, Zhou YF, Paigen B, Johnson TM, Burnett MS, Epstein SE. 2001. Cytomegalovirus infection increases development of atherosclerosis in apolipoprotein-E knockout mice. Atherosclerosis 156:23–28. https://doi.org/10.1016/s0021-9150(00)00608-0.

63. Leitinger N. 2003. Cholesteryl ester oxidation products in atherosclerosis. Mol Aspects Med 24:239–250. https://doi.org/10.1016/s0098-2997(03)00019-0.

64. Ghosh S, Zhao B, Bie J, Song J. 2010. Macrophage cholesteryl ester mobilization and atherosclerosis. Vascul Pharmacol 52:1–10. https://doi.org/10.1016/j.vph.2009.10.002.

65. Jønsson KL, Laustsen A, Krapp C, Skipper KA, Thavachelvam K, Hotter D, Egedal JH, Kjolby M, Mohammadi P, Prabakaran T, Sørensen LK, Sun C, Jensen SB, Holm CK, Lebbink RJ, Johannsen M, Nyegaard M, Mikkelsen JG, Kirchhoff F, Paludan SR, Jakobsen MR. 2017. IFI16 is required for DNA sensing in human macrophages by promoting production and function of cGAMP. Nat Commun 8:14391. https://doi.org/10.1038/ncomms14391.

66. Dalen KT, Ulven SM, Bamberg K, Gustafsson J-A, Nebb Hl. 2003. Expression of the insulin-responsive glucose transporter GLUT4 in adipocytes is dependent on liver X receptor alpha. J Biol Chem 278:48283–48291. https://doi.org/10.1074/jbc.M302287200.

67. De Meo S, Dell'Oste V, Molfetta R, Tassinari V, Lotti LV, Vespa S, Pignoloni B, Covino DA, Fantuzzi L, Bona R, Zingoni A, Nardone I, Biolatti M, Coscia A, Paolini R, Benkirane M, Edfors F, Sandalova T, Achour A, Hiscott J, Landolfo S, Santoni A, Cerboni C. 2020. SAMHD1 phosphorylation and cytoplasmic relocalization after human cytomegalovirus infection limits its antiviral activity. PLoS Pathog 16:e1008855. https://doi.org/10.1371/journal.ppat.1008855.

68. Baggetta R, De Andrea M, Gariano GR, Mondini M, Rittà M, Caposio P, Cappello P, Giovarelli M, Gariglio M, Landolfo S. 2010. The interferon-inducible gene IFI16 secretome of endothelial cells drives the early steps of the inflammatory response. Eur J Immunol 40:2182–2189. https://doi.org/10.1002/eji.200939995.

Novel antiviral activity of PAD inhibitors against human beta-coronaviruses HCoV-OC43 and SARS-CoV-2

Selina Pasquero [a], Francesca Gugliesi [a], Gloria Griffante [b], Valentina Dell'Oste [a], Matteo Biolatti [a], Camilla Albano [a], Greta Bajetto [a,c], Serena Delbue [d], Lucia Signorini [d], Maria Dolci [d], Santo Landolfo [a], Marco De Andrea [a,c,*]

[a] *Department of Public Health and Pediatric Sciences, University of Turin – Medical School, Turin, Italy*
[b] *Department of Translational Medicine, University of Piemonte Orientale, Novara, Italy*
[c] *CAAD Center for Translational Research on Autoimmune and Allergic Disease, University of Piemonte Orientale, Novara Medical School, Italy*
[d] *Department of Biomedical, Surgical and Dental Sciences, University of Milan, Milan, Italy*

ARTICLE INFO

ABSTRACT

The current SARS-CoV-2 pandemic, along with the likelihood that new coronavirus strains will appear in the nearby future, highlights the urgent need to develop new effective antiviral agents. In this scenario, emerging host-targeting antivirals (HTAs), which act on host-cell factors essential for viral replication, are a promising class of antiviral compounds. Here we show that a new class of HTAs targeting peptidylarginine deiminases (PADs), a family of calcium-dependent enzymes catalyzing protein citrullination, is endowed with a potent inhibitory activity against human beta-coronaviruses (HCoVs). Specifically, we show that infection of human fetal lung fibroblasts with HCoV-OC43 leads to enhanced protein citrullination through transcriptional activation of PAD4, and that inhibition of PAD4-mediated citrullination with either of the two pan-PAD inhibitors Cl-A and BB-Cl or the PAD4-specific inhibitor GSK199 curbs HCoV-OC43 replication. Furthermore, we show that either Cl-A or BB-Cl treatment of African green monkey kidney Vero-E6 cells, a widely used cell system to study beta-CoV replication, potently suppresses HCoV-OC43 and SARS-CoV-2 replication. Overall, our results demonstrate the potential efficacy of PAD inhibitors, in suppressing HCoV infection, which may provide the rationale for the repurposing of this class of inhibitors for the treatment of COVID-19 patients.

1. Introduction

In recent years, emerging zoonotic RNA viruses have raised serious public health concerns worldwide. Among them, novel coronaviruses (CoVs) deserve special attention due to their high spillover potential and transmissibility rate, often leading to deadly epidemics across multiple countries, worsened by the lack of effective therapies (Fan et al., 2019).

The *Coronaviridae* family consists of enveloped single-stranded, positive-sense RNA viruses classified into four coronavirus genera: alpha, beta, gamma, and delta. To date, seven human coronaviruses (HCoVs), belonging to the alpha and beta genera, have been identified (Su et al., 2016). HCoV-229E and HCoV-OC43 were first described in 1966 and 1967, respectively, followed by HCoV-NL63 in 2004 and HCoV-HKU1 in 2005. HCoVs generally establish infections in the upper respiratory district—responsible for about 10–30% of common cold cases—, but in vulnerable patients they can also cause bronchiolitis and pneumonia (Leao et al., 2020; Paules et al., 2020).

Even though HCoVs have long been recognized as human pathogens, effective treatments against these viruses have only started to be developed after the severe acute respiratory syndrome CoV (SARS-CoV) outbreak in 2002 (Ksiazek et al., 2003; Weiss and Navas-Martin, 2005). Since then, recurrent spillover events from wildlife have led to the appearance of two other highly pathogenic beta-CoV strains associated with severe respiratory diseases in humans: the Middle East respiratory syndrome coronavirus (MERS-CoV) in 2011, which causes MERS (De Wit et al., 2016; Zaki et al., 2012), and the severe acute respiratory syndrome CoV-2 (SARS-CoV-2) in 2019, the etiological agent of the ongoing pandemic of coronavirus disease 2019 (COVID-19) (Lu et al., 2020; Wu et al., 2020).

In this scenario, the widespread vaccine hesitancy, the growing

---

number of breakthroughs among the vaccinated population, the emergence of increasingly infectious SARS-CoV-2 variants, and the likelihood that new CoV strains will continue to appear in the future have all led to the urgent need to develop new antiviral agents able to tackle ongoing SARS-CoV-2 outbreaks. Consistent with this emergency status, HCoV-OC43 has often been used as a surrogate of—or together with—SARS-CoV-2 to test potential inhibitors of HCoV replication in both cell-based assays and *in silico* analysis (Milani et al., 2021).

Most of the approved antiviral drugs are the so-called direct-acting antiviral agents (DAAs), compounds designed against viral proteins deemed essential for infection. For example, remdesivir, whose efficacy against SARS-CoV-2 is highly controversial (Hsu, 2020), and molnupiravir, a new oral antiviral highly effective in preventing severe disease based on the results of a recent Phase 2a trial (Fischer et al., 2021), are nucleoside analogue prodrugs acting as competitive substrates for virally-encoded RNA-dependent RNA polymerase (RdRp) (Beigel et al., 2020; Warren et al., 2016). Another emerging class of antiviral agents named host-targeting antivirals (HTAs) consists of drugs acting on host-cell factors involved in viral replication. To date, most studies have focused on the analysis of viral proteins and the identification of potential DAAs. However, viruses encode a limited number of proteins, and those suitable as drug targets are only a subset of them. Therefore, targeted disruption of the mechanisms devised by HCoVs to manipulate the host cellular environment during infection, such as those leading to immune evasion and host gene expression alterations (Hartenian et al., 2020), holds great promise for the treatment of COVID-19 patients.

Peptidyl-arginine deiminases (PADs) are a family of calcium-dependent enzymes that catalyze a posttranslational modification (PTM) named citrullination, also known as deimination, a process during which the guanidinium group of a peptidyl-arginine is hydrolyzed to form peptidyl-citrulline, an unnatural amino acid (Mondal and Thompson, 2019; Witalison et al., 2015). Five PAD isozymes (PAD 1-4 and 6) are expressed in humans, with a unique distribution in various tissues (Table 1) (Darrah and Andrade, 2018; György et al., 2006; Kanno et al., 2000; Nachat et al., 2005; Slack et al., 2011; Valesini et al., 2015; Vossenaar et al., 2003; Wang and Wang, 2013; Witalison et al., 2015). PAD dysregulation leads to aberrant citrullination, which is a typical biomarker of various inflammatory conditions, suggesting that it may play a pathogenic role in inflammation-related diseases (Acharya et al., 2012; Knight et al., 2015; Sokolove et al., 2013; van Venrooij et al., 2011; Yang et al., 2016; Yuzhalin, 2019).

Given the involvement of PAD in several pathological settings, a number of PAD inhibitors have been synthesized in recent years. Some of these compounds, such as Cl-amidine (Cl-A) and its derivative BB-Cl-amidine (BB–Cl)—in this latter compound the C-terminus is replaced by a benzimidazole to prevent proteolysis of the C-terminal amide, and the N-terminal benzoyl group is replaced by a biphenyl moiety to enhance cellular uptake (Knight et al., 2015)—, can inhibit the activity of all the different isoforms and, as such, are called pan-PAD inhibitors (Falcão et al., 2019; Knight et al., 2015; Knuckley et al., 2010). Other available inhibitors are highly specific for the different PAD-isozymes, like AFM-30 for PAD2 and GSK199 for PAD4 (Table S1) (Lewis et al., 2015; Muth et al., 2017).

In this scenario, a correlation between PAD dysregulation and viral infections has recently emerged. In particular, the antiviral activity of the LL37 protein appears to be compromised upon human rhinovirus (HRV)-induced citrullination (Casanova et al., 2020), and sera from RA patients can specifically recognize artificially citrullinated Epstein-Barr virus (EBV) proteins (Pratesi et al., 2006, 2011; Trier et al., 2018). Consistently, we have recently shown that human cytomegalovirus (HCMV) induces PAD-mediated citrullination of several cellular proteins endowed of antiviral activity, including the two IFN-stimulated genes (ISGs) IFIT1 and Mx1, and that the inhibition of this process by the PAD inhibitor Cl-A blocks viral replication (Griffante et al., 2021). Finally, another recent study has shown that SARS-CoV-2 infection can modulate PADI gene expression, particularly in lung tissues, leading to the intriguing possibility that PAD enzymes may play a critical role in COVID-19 (Arisan et al., 2020).

Based on this evidence, the aim of this work was to ascertain whether PAD inhibitors might constitute a new class of HTAs against HCoVs. For this purpose, we performed cell based-assays to measure the antiviral activity of the previously mentioned both pan- or specific-PAD inhibitors against two members of the beta-CoV genus: HCoV-OC43, the first one to have been discovered, and SARS-CoV-2, the last one to have emerged so far.

Overall, our results show that both HCoV-OC43 and SARS-CoV-2 infections are significantly associated with PAD-mediated citrullination *in vitro*. Importantly, pharmacological inhibition of PAD enzymes through Cl-A treatment led to ~50% reduction of SARS-CoV-2 NP protein expression and 1 log in SARS-CoV-2 yield, suggesting that PAD inhibitors may be considered for repurposing to treat COVID-19.

2. Materials and methods

2.1. Ethics approval statement

Nasal pharyngeal swabs were collected upon approval of the Local Ethics Committee and signature of the informed consent. The

Table 1
Properties of the different human peptidylarginine deiminases (PADs).

	Tissue distribution	Citrullination substrate	Biological process	Disease associated with aberrant citrullination	Reference
PAD1	All living skin layers, hair follicle, uterus, stomach	Keratin and filaggrin	Cornification of epidermal tissue	Psoriasis	Nachat et al. (2005); Senshu et al. (1999); Ying et al. (2009); Zhang et al. (2016)
PAD2	Skeletal muscle, salivary gland, brain, immune cells, bone marrow, skin, peripheral nerves, uterus, spleen, secretory gland, pancreas, kidney, inner ear.	Actin, vimentin, histone, myelin basic protein	Plasticity of the CNS, transcription, regulation, innate immunity and fertility	Multiple sclerosis, rheumatoid arthritis, Alzheimer disease, prion disease	Falcão et al. (2019); Jang et al. (2008); Musse et al. (2008); Vossenaar et al. (2003)
PAD3	Hair follicle, skin, peripheral nerves, CNS	Vimentin, filaggrin, apoptosis inducing factor	Regulation of epidermal function	Unknown	Kanno et al. (2000); Nachat et al. (2005)
PAD4	Immune cells, brain, uterus, joints, bone marrow	Histones, collagen type I, ING4, p300, p21, lamin C, nucleophosmin	Chromatin decondensation, transcription regulation, tumor formation, innate immune response and NETosis process	Rheumatoid arthritis, multiple sclerosis, and cancers	Acharya et al. (2012); Chang et al. (2009); Willis et al. (2017)
PAD6	Ovary, egg cells, embryo, testicle		Oocyte, sperm chromatin decondensation, female productivity, cytoskeleton formation, early fetal growth, and target for contraceptive drugs	Unknown	Esposito et al. (2007); Kan et al. (2011)

Fondazione Ca' Granda, Ospedale Maggiore, Milano, Italy, approved the protocol No. 456_2020 in May 2020.

2.2. Cell lines and viruses

Human lung fibroblast MRC-5 cells (ATCC® CCL-171) and African green monkey kidney Vero-E6 cells (ATCC®-1586) were propagated in Dulbecco's Modified Eagle Medium (DMEM; Sigma) supplemented with 1% (v/v) penicillin/streptomycin solution (Euroclone) and heat-inactivated 10% (v/v) fetal bovine serum (FBS) (Sigma). The human coronavirus strain OC43 (HCoV-OC43) (ATCC® VR-1558) was kindly provided by David Lembo (Department of Clinical and Biological Sciences, University of Turin, Turin, Italy). HCoV-OC43 was propagated on MRC-5 cells at 33 °C in a humidified 5% CO_2 incubator and titrated by standard plaque method on MRC-5 cells, as described elsewhere (Marcello et al., 2020). SARS-CoV-2 was isolated from a nasal-pharyngeal swab positive for SARS-CoV-2. The isolated SARS-CoV-2 strain belongs to the B.1 lineage, carrying the characteristic spike mutation D614G. The B.1 lineage is the large European lineage, the origin of which roughly corresponds to the Northern Italian outbreak in early 2020. The complete nucleotide sequence has been deposited at GenBank and GISAID (accession Nos. MT748758.1 and EPI_ISL 584051, respectively).

2.3. Reagents and treatments

The PAD inhibitors Cl-A, BB-Cl, GSK199, and AFM30a—also known as CAY10723—were purchased from Cayman Chemical (Ann Arbor). All the compounds were solubilized in DMSO according to the manufacturer's instructions. Immediately before use, the inhibitors were diluted in the culture medium to the desired concentrations (Table S1).

2.4. Cell viability assay

MRC-5 or Vero-E6 cells were seeded at a density of 3×10^4/well in a 96-well plate. After 24 h, cells were treated with different PAD inhibitors at the indicated concentrations or with an equal volume of the vehicle alone (DMSO). After 72 h, cell viability was determined by 3-(4,5-dimethylthiazol-2-yl)-2,5-diphenyltetrazolium bromide assay (MTT, Sigma), as previously described (Griffante et al., 2021).

2.5. In vitro antiviral assay

MRC-5 and Vero-E6 cells were cultured in 24-well plates for 1 day and then, 1 h before infection, pre-treated with PAD inhibitors or vehicle alone at the indicated concentrations. Subsequently, cells were infected with HCoV-OC43 at a multiplicity of infection (MOI) of 0.1 or 1. Following virus adsorption (2 h at 33 °C) and viral inoculum removal, new medium with fresh PAD inhibitors or DMSO alone was added to the plates and kept for further 72 h. The extent of HCoV-OC43 replication in MRC-5 cells was assessed by titrating the infectivity of supernatants using plaque assay and comparative real-time RT-PCR. For Vero-E6 cells, the extent of HCoV-OC43 replication was assessed by titrating the infectivity of supernatants using comparative real-time RT-PCR.

SARS-CoV-2 *in vitro* infection of Vero-E6 cells and the anti-viral inhibition assay were conducted as described previously (Parisi et al., 2021).

2.6. Plaque assay

MRC-5 cells were inoculated with 10-fold serial dilutions of the HCoV-OC43. After 24 h, cells were fixed with cold acetone-methanol (50:50) and subjected to indirect immunostaining with an anti-NP-HCoV-OC43 monoclonal antibody (Millipore MAB9012). To determine the virus titer, the number of immunostained foci was counted on each well using the following formula: virus titer (PFU/ml) = number of plaques * 0.1 ml/dilution fold. SARS-CoV-2 plaque assay were performed on VERO-E6 cells as described previously (Parisi et al., 2021).

2.7. Comparative real-time RT-PCR (viral load)

All molecular analyses were performed according to Milewska et al. (2016). Briefly, viral nucleic acids were isolated from 200 μl of sample using the TRI Reagent solution (Sigma-Aldrich), according to the manufacturer's instructions. Extracted viral RNA (4 μl per sample) was retrotranscribed and amplified in a 20 μl reaction mixture containing Sensi Fast Probe No Rox One step kit (Bioline) using a CFX Touch Real Time PCR Detection System (BioRad). The primers and probe for N gene amplification (Eurofins) are reported below:

HCoV-OC43 Fw: AGCAACCAGGCTGATGTCAATACC;
HCoV-OC43 Rv: AGCAGACCTTCCTGAGCCTTCAAT;
Probe (HCoV-OC43P_rt): TGACATTGTCGATCGGGACCCAAGTA (5′ FAM and 3′TAMRA labeled).

The reaction conditions were as follows: 10 min at 45 °C and 20 min at 95 °C, followed by 40 cycles of 5 s at 95 °C and 1 min at 60 °C.

Quantification of SARS-CoV-2 copy numbers in cell supernatants was evaluated *via* specific real time RT-PCR of the *N1* gene, according to the protocols "Coronavirus disease (COVID-19) technical guidance: Laboratory testing for 2019-nCoV in humans" and "CDC 2019-Novel Coronavirus (2019-nCoV) Real-Time RT-PCR Diagnostic Panel", available at: https://www.who.int/emergencies/diseases/novel-corona virus-2019/technical-guidance/laboratory-guidance and https://www.fda.gov/media/134922/download [last access 25 October 2021]), respectively.

2.8. Cell-associated RNA isolation and quantitative nucleic acid analysis

Total RNA was extracted using the TRI Reagent solution (Sigma-Aldrich), and 1 μg of it retrotranscribed using the RevertAid H-Minus FirstStrand cDNA Synthesis Kit (Thermo Fisher Scientific) according to the manufacturer's instructions. Comparison of mRNA expression between treated and untreated samples was performed by SYBR green-based real time RT-qPCR by Mx3000P apparatus (Santa Clara), using the primers reported previously. As cellular reference, we amplified the housekeeping gene glyceraldehyde-3-phosphate dehydrogenase (GADPH) with the following primers: GAPDH Fw: AGTGGGTGTCGCTGTTGAAGT; GADPH Rv: AACGTGTCAGTGGTG-GACCTG. The reaction conditions were as follows: 2 min at 95 °C, followed by 40 cycles of 5 s at 95 °C and 1 min at 60 °C.

2.9. Western blot analysis

MRC-5 or Vero-E6 cells were treated as described in 2.5 and infected at an MOI of 1. The cells were harvested at 48 and 72 hpi, lysed in RIPA buffer (50 mM Tris-HCl, pH 8.0, 1 mM EDTA, 1% Nonidet P-40, 0.1% sodium deoxycholate, 0.1% SDS, 150 mM NaCl), quantified by the Bradford method, and subjected to Western blot analysis. The primary antibodies were as follows: anti-HCoV-OC43 (Millipore MAB9012); anti-PAD1 (ABCAM ab181791); anti-PAD2 (Cosmo Bio SML-ROI002-EX); anti-PAD3 (ABCAM ab50246); anti-PAD4 (ABCAM ab128086); anti-PAD6 (ABCAM ab16480); anti-actin (Sigma Aldrich A2066), anti-SARS-CoV-2 (GeneTex GTX36802).

2.10. Detection of citrullination with rhodamine-phenylglyoxal (Rh-PG)

Whole-cell protein extracts were prepared as described in 2.9. Protein citrullination detection was performed as described previously (Griffante et al., 2021). Briefly, equal amounts of protein were resuspended with 80% trichloroacetic acid and incubated with a rhodamine phenylglyoxal (Rh-PG, Cayman) probe, at a final concentration 0.1 mM, for 30 min. The reaction was quenched with 100 mM L-citrulline for 30 min at 4 °C and then centrifuged at 21100×*g* for 10 min. The pellet was washed with ice-cold acetone and resuspended in 2 X SDS loading dye

for gel electrophoresis. Upon staining with brilliant blue G-colloidal solution (Sigma-Aldrich), gels were imaged (excitation = 532 nm, emission = 580 nm) using Chemidoc Imaging System (Biorad).

2.11. Statistical analysis

All data were analyzed using GraphPad Prism (GraphPad Software, San Diego, CA). All results are presented as means ± SEM. The half-maximal inhibitory concentrations (IC_{50}) and half-maximal cytotoxic concentration (CC_{50}) values were calculated by Quest Graph™ IC50 Calculator (AAT Bioquest, Inc, https://www.aatbio.com/tools/ic50-calculator). The selectivity index (SI) values were calculated as the ratio of CC_{50} and IC_{50} (SI= CC_{50}/IC_{50}). The P-value was calculated by comparing between % inhibition of infected-treated samples and % inhibition of infected-untreated samples. One-tailed Student's t-test was used to compare groups. Differences were considered statistically
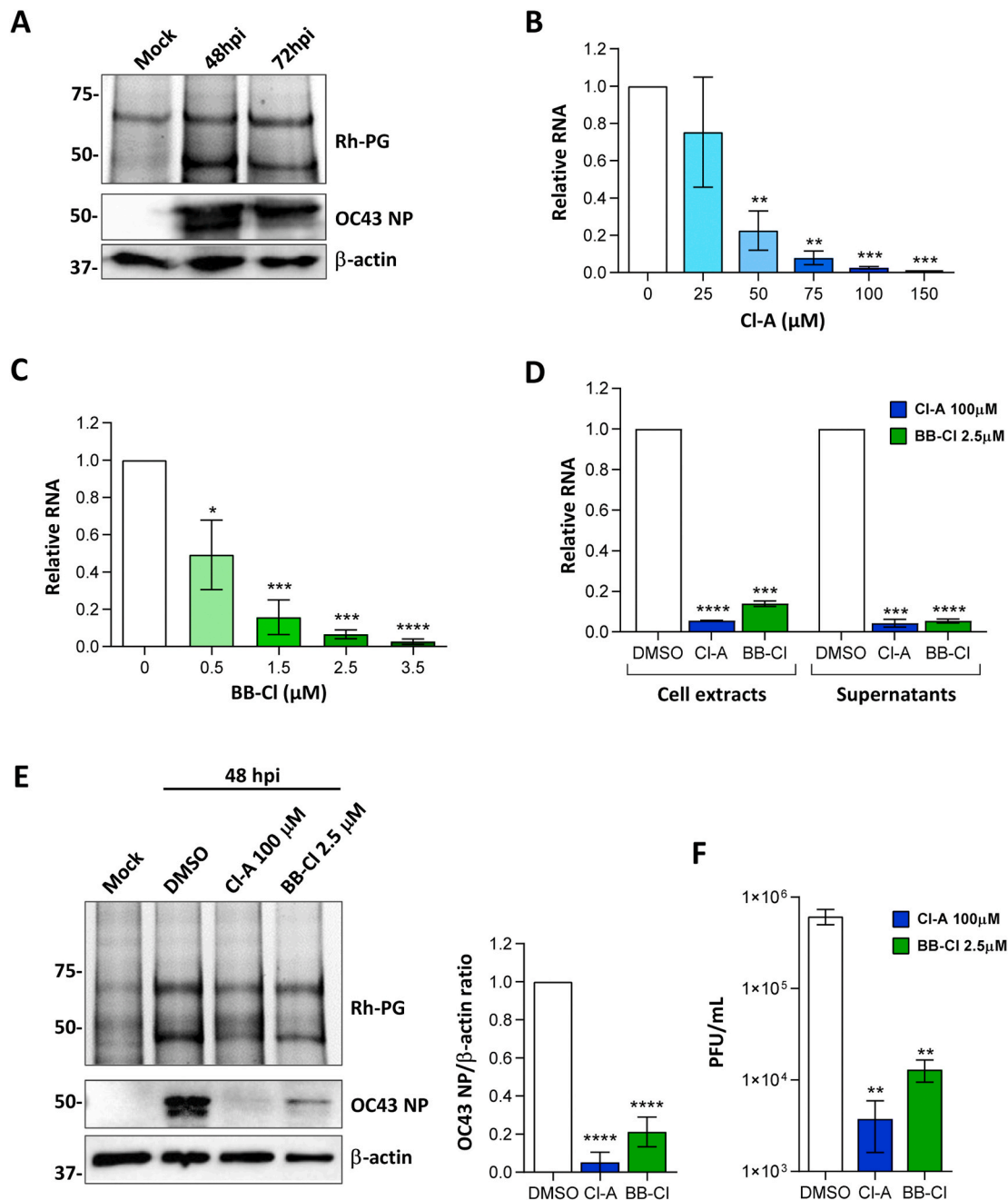
Fig. 1. The pan-PAD inhibitors Cl-A and BB-Cl hamper HCoV-OC43 replication in MRC-5 cells. (A) Rh-PG and Western blot analysis of total protein extract of mock- or HCoV-OC43-infected MRC5 cells (MOI 1). One representative gel of three independent experiments is shown. (B, C) Dose-response curves of the cell-permeable pan-PAD inhibitors Cl-A (B) and BB-Cl (C) in MRC-5 cells infected with HCoV-OC43 (MOI 0.1). After 72 hpi, the viral load was determined by real-time PCR and values were normalized to those for DMSO-treated cells value (0 in the x axis) set to 1. Values are expressed as mean ± SEM of three independent experiments. (D) RT-PCR of viral RNA in cell extracts or supernatants from HCoV-OC43-infected MRC5 cells (MOI 0.1) treated with Cl-A (100 μM), BB-Cl (2.5 μM), or DMSO. Values are expressed as mean ± SEM of three independent experiments. (E) Rh-PG and Western blot analysis of protein extract of mock- or HCoV-OC43-infected MRC5 cells (MOI 1) treated with pan-PAD inhibitors as in D. One representative gel of three independent experiments is shown. (F) Viral productions were collected at 72 hpi and analyzed by plaque-forming assay. Values are expressed as mean ± SEM of three independent experiments. $P < 0.05$ (*), <0.01 (**), <0.001 (***) and <0.0001 (****).

significant if $P < 0.05$ (*), $P < 0.01$ (**), $P < 0.001$ (***), and $P < 0.0001$ (****).

3. Results

3.1. Pan-PAD inhibitors block HCoV-OC43 replication in MRC-5 cells

We previously demonstrated that HCMV triggers PAD-mediated citrullination to promote its replication (Griffante et al., 2021). To evaluate whether the protein citrullination profile would also be altered during HCoV infection, we first performed an electrophoresis analysis of protein lysates obtained from MRC-5 lung fibroblasts infected with HCoV-OC43 (MOI 1) incubated with the citrulline-specific probe Rh-PG. At 48 and 72 h post infection (hpi), HCoV-OC43-infected MRC5 cells, but not mock-infected cells, showed a robust increase in total protein citrullination (Fig. 1A). Of note, the expression of the OC43 nucleocapsid protein (OC43 NP) was only detected in HCoV-OC43-infected MRC5 cells, confirming the successful infection of these cells (Fig. 1A).

Next, to test whether PAD enzymatic activity played a functional role in HCoV-OC43 replication, we treated infected cells with the two pan-PAD inhibitors Cl-A and BB-Cl and assessed viral RNA synthesis by real time RT-PCR. Incubation of HCoV-OC43-infected MRC5 cells with increasing amounts of these inhibitors led to a dose-dependent reduction of viral genome copies, a drop that became statistically significant at 50 μM for Cl-A and 0.5 μM for BB-Cl (Fig. 1B and C). The calculated IC50s for Cl-A and BB-Cl were 34.76 μM and 0.54 μM, respectively. To rule out compound cytotoxicity, HCoV-OC43-infected MRC-5 cells were subjected to MTT assay. The results shown in Figs. S1A and B demonstrate that none of the PAD inhibitors significantly reduced cell viability at either IC50. Table 2 shows the CC50s for Cl-A (949.14 μM) and BB-Cl (10.12 μM). Based on the calculated IC50 and CC50, the SIs of Cl-A and BB-Cl in HCoV-OC43-infected MRC-5 were quite similar and both greater than 10 (27.3 and 18.6, respectively). Consistent with the results obtained measuring viral RNA, Cl-A and BB-Cl drastically reduced both intra- and extra-cellular viral genome copy numbers (Fig. 1D), confirming the key role of citrullination in HCoV-OC43 replication and viral cycle.

To determine whether PAD inhibition would prevent viral replication and/or production of infectious viral particles, we assessed HCoV-OC43 NP protein expression by Western blotting. We also measured the virus yield by plaque assay using cell extracts and supernatants from HCoV-OC43-infected MRC-5 cells treated with 100 μM Cl-A or 2.5 μM BB-Cl, as previously described. Interestingly, both Cl-A and BB-Cl treatments significantly reduced HCoV-OC43 NP expression in the very same total protein extracts in which a partial suppression of the citrullination profile was also observed by Rh-PG (Fig. 1E). Moreover, consistent with our previous results (Griffante et al., 2021), DMSO treatment alone didn't affect total protein citrullination in uninfected cells nor OC43 N gene expression in infected cells (Figs. S2A and B). Finally, the two drugs significantly reduced PFUs per mL of supernatant by more than 2 and 1 logs, respectively (Fig. 1F).

3.2. PAD4 plays a central role in HCoV-OC43 replication

To gain more insight into the mechanism of HCoV-OC43-induced cellular citrullination, we asked which of the five known PAD isoforms (PAD1-4 and PAD6) would be preferentially modulated following HCoV-OC43 infection. To answer this question, we performed immunoblot analysis on whole protein lysates obtained from mock and HCoV-OC43-infected MRC5 cells collected at different time points after infection (Fig. 2A). PAD2 and PAD4 were the only two PAD isoforms expressed in these cells, with PAD4 being the only one increased upon infection, as judged by densitometry. By contrast, PAD1, 3, and 6 were neither detectable in mock cells nor did they appear upon infection (Figs. 2A and S5). Given the above results, we next sought to determine whether targeting the enzymatic activity of PAD4 would affect viral replication. To this end, OC43-infected MRC-5 cells were treated with increasing concentrations of the PAD4-specific inhibitor GSK199 or the PAD2-specific inhibitor AFM30a, and assessed for their antiviral activity. Whereas AFM30a treatment only marginally suppressed the HCoV-OC43 replication rate—never exceeding 40% inhibition within the range of concentrations tested (Fig. 2B), exposure of cells to GSK199 robustly inhibited viral genome production in a dose-dependent manner (IC50 = 0.6 μM), achieving a complete blockade of viral replication at 20 μM (Fig. 2C). Furthermore, MRC-5 cells treated with 20 μM GSK199 were viable, ruling out any unspecific effect due to compound toxicity (Fig. S3). Of note, we could only observe significant cytotoxicity of both compounds at concentrations above 100 μM (Fig. S2). This conferred them an SI > 10, which was particularly robust in the case of GSK199 (224.94) (Table 2).

To confirm these results, we measured the number of viral genome copies in cell lysates and supernatants from MRC-5 cells treated with 20 μM AFM30a or GSK199 and infected with HCoV-OC43. As expected, inhibition of PAD4 by GSK199 drastically reduced the relative viral genome copy number in both compartments compared to vehicle-treated cells, while PAD2 inhibition by AFM30a led to a much less pronounced reduction of viral genome (Fig. 2D). Consistently, immunoblot analysis of total protein extracts from HCoV-OC43-infected MRC-5 cells treated with GSK199 showed a dramatic downregulation of OC43 NP protein expression levels in comparison with vehicle-treated infected cells (Fig. 2E). In contrast, treatment with the PAD2 inhibitor AFM30a only led to a slight decrease in NP protein levels. Fittingly, plaque assay on these cells confirmed a significant reduction of the viral titer in the presence of GSK199 (~2-log reduction), while the inhibitory activity of AFM30a at the same concentration was barely detectable (Fig. 2F).

Taken together, these results suggest that PAD4 plays a major role in HCoV-OC43 replication, and that PAD4 inhibitors are promising anti-HCoV compounds.

3.3. PAD inhibitors affect HCoV-OC43 and SARS-CoV-2 replication in Vero-E6 cells

Since Vero-E6 cells represent a widely used cellular system to study beta-CoV replication in the presence of candidate antiviral compounds, we sought to extend our analysis also to this cell model. Initially, we performed a quantitative analysis of HCoV-OC43 viral RNA production at 72 hpi using different concentrations of Cl-A (50–300 μM) and BB-Cl (5–20 μM). As depicted in Fig. 3, we observed a marked reduction of viral genome replication in Vero-E6 cells treated with either 150–300 μM Cl-A (panel A) or 20 μM BB-Cl (panel B) compared to their vehicle-treated counterparts. These pronounced effects were not a consequence of an intrinsic cytotoxicity of the PAD inhibitors as none of the screened compounds significantly reduced cell viability at the same concentrations as those used in the antiviral assays (Figs. S4A and B and Table 2).

Next, to evaluate whether HCoV-OC43 infection would also trigger protein citrullination in Vero-E6 cells, we performed electrophoresis analysis of protein lysates from HCoV-OC43-infected cells using the Rh-PG probe. As shown in Fig. 3C, cellular protein citrullination in these

Table 2
CC50, IC50, and SI of PAD inhibitors against beta-CoVs.

Cell/virus	Compound	IC50[μM]	CC50[μM]	SI
MRC-5/OC43	Cl-amidine	34.80	949.14	27.30
	BB-Cl-amidine	0.53	10.12	18.62
	GSK199	0.60	133.08	224.94
	AFM30a	>20	320.92	>16
Vero-E6/OC43	Cl-amidine	44.15	>1000	>22
	BB-Cl-amidine	10.68	33.06	3.10
Vero-E6/SARS-CoV-2	Cl-amidine	95.17	>1000	>10
	BB-Cl-amidine	17.78	33.06	1.86

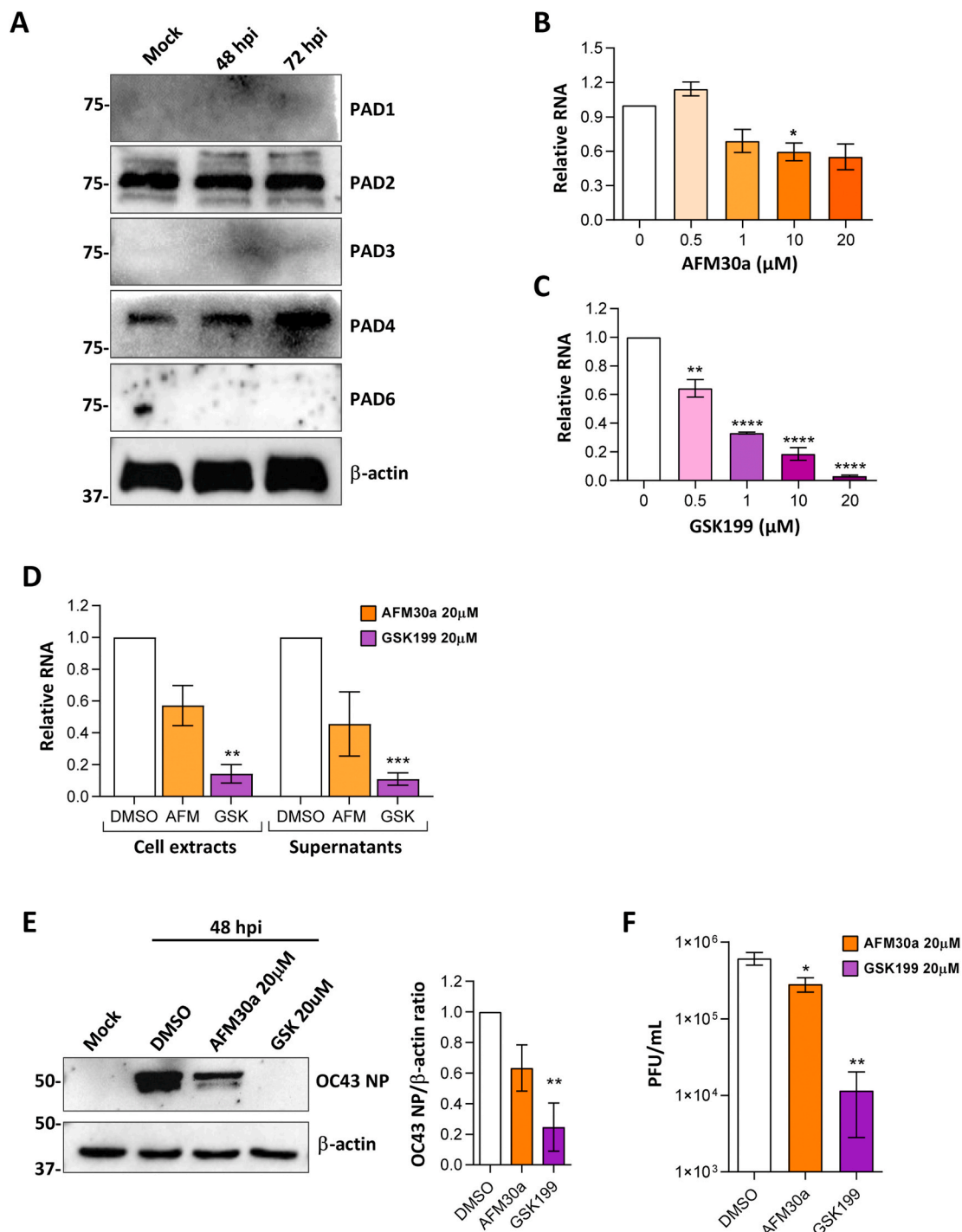**Fig. 2.** Effect of PAD2-or PAD4-specific inhibitors on HCoV-OC43 replication in MRC-5 cells. (A) Western blot analysis of protein lysates from mock- or HCoV-OC43-infected MRC5 cells (MOI 1) using antibodies against PAD1, PAD2, PAD3, PAD4, PAD6, or β-actin. The blot shown is representative of three independent experiments. (B–C) Dose-response curves of the cell-permeable pan-PAD inhibitors AFM30a (B) and GSK199 (C) in HCoV-OC43-infected MRC-5 cells (MOI 0.1). After 72 hpi, the viral load was determined by real-time PCR and values were normalized to those for DMSO-treated cells value (0 in the *x* axis) set to 1. Values are represented as mean ± SEM of three independent experiments. (D) Real time RT-PCR on supernatants or cell-associated viral RNA collected from HCoV-OC43-infected MRC5 cells (MOI 0.1) treated with AFM30a (20 μM), GSK199 (20 μM), or DMSO. Values are expressed as mean ± SEM of three independent experiments. (E) Western blot analysis of protein extract of mock- or HCoV-OC43-infected MRC5 cells (MOI 1) treated with AFM30a (20 μM), GSK199 (20 μM), or DMSO. One representative gel of three independent experiments is shown. (F) Viral productions were collected at 72 hpi and analyzed by plaque assay. Values are expressed as mean ± SEM of three independent experiments. $P < 0.05$ (*), <0.01 (**), <0.001 (***) and <0.0001 (****).

infected cells was significantly induced at 48 hpi, whereas it remained almost unchanged in infected cells treated with 300 μM of the Cl-A inhibitor.

To extend our findings to other beta-CoVs, we examined the impact of PAD inhibitors treatment on SARS-CoV-2 viral genome replication. As shown in Fig. 3D and E, both Cl-A and BB-Cl treatments suppressed SARS-CoV-2 viral genome replication in a dose-dependent manner, albeit to a lower extent than that observed for HCoV-OC43.
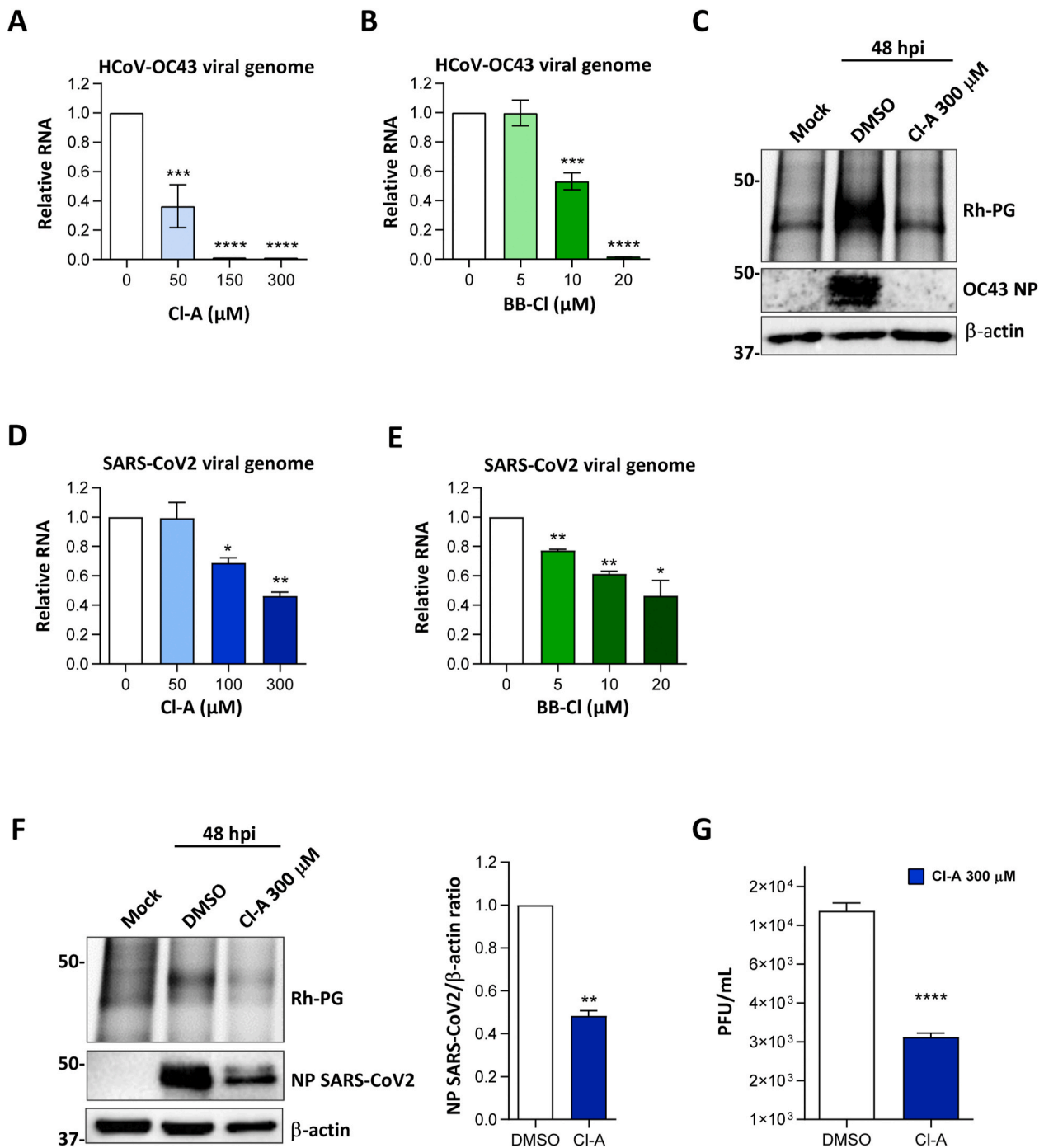
Fig. 3. The pan-PAD inhibitors Cl-A and BB-Cl block β-coronavirus replication in Vero-E6 cells. (A, B) Dose-response curves of the pan-PAD inhibitors Cl-A (A) and BB-Cl (B) in VERO-E6 cells infected with HCoV-OC43 (MOI 0.1). After 72 hpi, the viral load was determined by real-time RT-PCR and values were normalized to those for DMSO-treated cells value (0 in the *x* axis) set to 1. Values represent the mean ± SEM of three independent experiments. (C) Rh-PG and Western blot analysis of total protein extract from mock – or HCoV-OC43-infected VERO-E6 cells (MOI 1) treated with Cl-A (300 μM) or DMSO. One representative gel of three independent experiments is shown. (D, E) Dose-response curves of Cl-A (D) or BB-Cl (E) treatment of SARS-CoV2-infected VERO-E6 cells (MOI 0.1). After 72 hpi, the viral load was determined by real-time RT-PCR and values were normalized to those for DMSO-treated cells value (0 in the *x* axis) set to 1. Values are expressed as mean ± SEM of three independent experiments. (F) Rh-PG and Western blot analysis of total protein extract of mock- or SARS-CoV- infected VERO-E6 cells (MOI 1) and with Cl-A (300 μM) or DMSO. One representative gel of three independent experiments is shown. (G) Viral productions from the same experiment described in F were collected at 72 hpi and analyzed by plaque assay. Values are expressed as mean ± SEM of three independent experiments. $P < 0.05$ (*), <0.01 (**), <0.001 (***) and <0.0001 (****).

To characterize the protein citrullination profile during SARS-CoV-2 infection, protein lysates obtained from Vero-E6 cells infected with SARS-CoV-2, treated with or without Cl-A, were analyzed by Rh-PG (Fig. 3F). The citrullination profile of these SARS-CoV-2-infected cells was consistent with that observed upon HCoV-OC43 infection, both displaying a signal lower than 50 kDa, which specifically appeared after the infection. However, unlike what we observed in HCoV-OC43-infected cells, the citrullination signal, albeit strongly reduced, it never completely disappeared following Cl-A treatment. In line with this observation, Cl-A treatment led to ~50% reduction of SARS-CoV-2 NP

protein expression (Fig. 3F). To corroborate these results, we carried out plaque reduction assays in SARS-CoV-2-infected Vero-E6 cells treated with 300 μM Cl-A as described above. Consistent with our previous results, the inhibition of PAD catalytic activity resulted in a reduction of 1 log in SARS-CoV-2 yield (Fig. 3G).

Altogether, our results demonstrate that beta-CoV infection is associated with protein citrullination. Moreover, treatment of HCoV-OC43 and SARS-CoV-2-infected cells with PAD pan-inhibitors inhibits virus replication restoring the physiological citrullination profile.

4. Discussion

We have recently shown that HCMV infection triggers PAD-mediated citrullination of several host proteins in primary human fibroblasts, and that this activity enhances viral fitness *per se* (Griffante et al., 2021). Here, we extend those findings to two RNA viruses, HCoV-OC43 and SARS-CoV-2, which we demonstrate to be both capable of promoting PAD-mediated citrullination *in vitro*. In particular, we show that HCoV-OC43 infection of MRC-5 lung fibroblasts upregulates total protein citrullination, and that this process is required for optimal viral replication. A similar induction in citrullination levels was also found in CoV-infected Vero-E6 cells, a non-human model system widely used to study HCoVs, especially SARS-CoV-2 (Dittmar et al., 2021; Ghosh et al., 2021; Milani et al., 2021; Wing et al., 2021), suggesting that HCoVs can modulate citrullination across species.

Citrullination is a posttranslational modification mediated by PAD family members, whose distribution and expression patterns are modulated by inflammatory signals in a tissue-specific manner (Table 1) (Acharya et al., 2012; Esposito et al., 2007; Falcão et al., 2019; Kan et al., 2011; Knight et al., 2015; Nachat et al., 2005; Vossenaar et al., 2003; Willis et al., 2011; Yang et al., 2016). Fittingly, we and others have recently reported a positive association between viral infection and PAD-mediated upregulation of citrullination in different cellular models (Arisan et al., 2020; Casanova et al., 2020; Griffante et al., 2021), raising the important question as to whether pharmacological inhibition of PAD activity can be used to reduce viral replication in infected patients. In the present study, we provide additional evidence supporting the use of PAD inhibitors to curb viral growth. Specifically, we show that treatment of HCoV-OC43-infected MRC-5 cells with either of the two pan-PAD inhibitors Cl-A and BB-Cl (Biron et al., 2016; Knight et al., 2015; Ledet et al., 2018; Willis et al., 2011) or the specific PAD4 inhibitor GSK199, but not the PAD2 inhibitor AFM30a, can not only efficiently inhibit viral replication but also reduce the production of infectious particles in the supernatant. This finding is consistent with our observation that MRC-5 cells express basal levels of both PAD2 and PAD4, but only PAD4 is significantly increased upon viral infection. Of note, the considerable reduction in viral replication and titer by the GSK199 compound was achieved at concentrations that do not affect cell viability. Indeed, the high SI of GSK199 (224.94, Table 2) along with its potent antiviral activity makes this PAD4 inhibitor an attractive target for further therapeutic development, a possibility further supported by results showing that targeting PAD4 led to a significant improvement of the clinical and histopathological end-points in a preclinical model of murine arthritis (Willis et al., 2017). This potential therapeutic usefulness would also be supported by a recent study by Arisan and co-workers showing that SARS-CoV-2 infection can modulate PADI gene expression in lung tissues (Arisan et al., 2020). In good agreement, here we show that the inhibitory activity of Cl-A and BB-Cl is not just restricted to HCoV-OC43-infected fibroblasts, but it can also be extended to SARS-CoV-2-infected Vero-E6 cells, highly permissive cells commonly used to propagate and study beta-CoV strains (Ogando et al., 2020). In these cells, both compounds efficiently suppress SARS-CoV-2 genome replication in a dose-dependent manner, albeit at higher concentrations than those used to inhibit HCoV-OC43 replication.

In the past two years, much research has attempted to assess the impact of interferon inducible proteins (ISGs) on SARS-CoV2 infection.

In this regard, Banerjee and colleagues have shown that many ISG proteins, including IFIT1 and MX1, are induced during infection, and that their expression reduces virus replication (Banerjee et al., 2021). Interestingly, we have recently shown that the same ISGs are citrullinated by PAD2 and PAD4 during HCMV infection, which hampers their biological activity (Griffante et al., 2021). Therefore, it is possible that PAD inhibitors act by blocking the inactivating citrullination of ISGs by PADs in response to beta-CoV infection, thus restoring the viral restriction activity of ISGs. Nevertheless, it is important to point out that this mechanism would only partially explain the antiviral activity of PAD inhibitors. Indeed, VERO cells have lost the ability to produce IFN due to spontaneous gene deletions (Desmyter et al., 1968, Mosca and Pitha, 1986) and consequently do not express ISG proteins. This loss of IFN responsiveness would however be consistent with the lower efficacy of PAD inhibitors in Vero-E6 *vs.* MRC-5 cells. Experiments are ongoing to test whether this difference is virus- or cell line-dependent.

Another implication of our findings revealing a strong induction of citrullination levels in SARS-CoV-2-infected Vero-E6 cells is that PAD inhibitors may be used to treat COVID-19 patients. It is in fact conceivable to envisage an association between SARS-CoV-2 infection and aberrant citrullination as a way to induce an inflammatory state in different tissues (Delorey et al., 2021).

Another important aspect that supports the repurposing of PAD inhibitors for antiviral therapy is that their efficacy in treating various inflammatory conditions, such as arthritis, colitis, and sepsis, has already been confirmed in preclinical and *in vitro* studies, all showing a good safety profile of such compounds (Chumanevich et al., 2011; Willis et al., 2011; Zhao et al., 2016). Of note, a recent review by Elliot and coworkers explores the possibility that PAD inhibitors, especially PAD4 inhibitors, may be used to resolve SARS-CoV2-induced thrombotic complications (Elliott et al., 2021). Indeed, neutrophil extracellular traps (NETs) and their constituents, including citrullinated histones, display a linear connection with thrombotic manifestations in COVID-19 patients. This intriguing scenario fits quite well with the results presented in the present study since, in a clinical context, the antiviral activity of the PAD inhibitors described here could potentially synergize with their inhibitory effect on immunothrombosis.

In the current pandemic of COVID-19, it is more important than ever that the most promising anti-SARS-CoV-2 drug candidates enter clinical development. Based on some similarities between the clinical outcome observed in autoimmune/autoinflammatory disease and COVID-19, including lung involvement and aberrant cytokine release, pan- and specific-PAD inhibitors—*i.e.*, GSK199—repurposing can be foreseen as a valuable strategy, as it enables to accelerate the use of compounds with already known safety profiles. Moreover, treatments based on molecules with beneficial multi-target activities—a concept known as polypharmacology (Ravikumar and Aittokallio, 2018)—, which may help counteract multiple complications as those observed in COVID-19 patients, may show an increased antiviral spectrum.

In conclusion, our findings unveil an unprecedented role of citrullination in the replication of the two human coronaviruses HCoV-OC43 and SARS-CoV-2 in lung and kidney epithelial cells. We also provide evidence that increased PAD activity is required for β-HCoV replication, highlighting the potential use of PAD inhibitors as novel HTAs against β-HCoV infections. Experiments are ongoing to assess the target citrullinated proteins by proteomics approaches, as well as to test the anti-β-HCoV efficacy and safety of other PAD inhibitors in a wider range of cell lines that can more accurately represent the different tissues where the virus replicates *in vivo*.

Lastly, based on the current availability of different animal models to be exploited for SARS-CoV-2 replication (Lee and Lowen, 2021), including K18-hACE2 transgenic mice challenged with SARS-CoV-2 (Conforti et al., 2021), investigations are being performed to test the feasibility of our drug repurposing strategy *in vivo*.

Declaration of competing interest

The authors declare that they have no known competing financial interests or personal relationships that could have appeared to influence the work reported in this paper.

Acknowledgments

Appendix A. Supplementary data

Supplementary data to this article can be found online at https://doi.org/10.1016/j.antiviral.2022.105278.

References

Acharya, N.K., Nagele, E.P., Han, M., Coretti, N.J., DeMarshall, C., Kosciuk, M.C., Boulos, P.A., Nagele, R.G., 2012. Neuronal PAD4 expression and protein citrullination: possible role in production of autoantibodies associated with neurodegenerative disease. J. Autoimmun. 38, 369–380. https://doi.org/10.1016/j.jaut.2012.03.004.

Arisan, E.D., Uysal-Onganer, P., Lange, S., 2020. Putative roles for peptidylarginine deiminases in COVID-19. Int. J. Mol. Sci. 21, 1–29. https://doi.org/10.3390/ijms21134662.

Banerjee, A., El-Sayes, N., Budylowski, P., Jacob, R.A., Richard, D., Maan, H., Aguiar, J. A., Demian, W.L., Baid, K., D'Agostino, M.R., Ang, J.C., Murdza, T., Tremblay, B.J., Afkhami, S., Karimzadeh, M., Irving, A.T., Yip, L., Ostrowski, M., Hirota, J.A., Kozak, R., Capellini, T.D., Miller, M.S., Wang, B., Mubareka, S., McGeer, A.J., McArthur, A.G., Doxey, A.C., Mossman, K., 2021 May 21. Experimental and natural evidence of SARS-CoV-2-infection-induced activation of type I interferon responses. iScience 24 (5), 102477. https://doi.org/10.1016/j.isci.2021.102477. Epub 2021 Apr 26. PMID: 33937724; PMCID: PMC8074517.

Beigel, J.H., Tomashek, K.M., Dodd, L.E., Mehta, A.K., Zingman, B.S., Kalil, A.C., Hohmann, E., Chu, H.Y., Luetkemeyer, A., Kline, S., Lopez de Castilla, D., Finberg, R. W., Dierberg, K., Tapson, V., Hsieh, L., Patterson, T.F., Paredes, R., Sweeney, D.A., Short, W.R., Touloumi, G., Lye, D.C., Ohmagari, N., Oh, M., Ruiz-Palacios, G.M., Benfield, T., Fätkenheuer, G., Kortepeter, M.G., Atmar, R.L., Creech, C.B., Lundgren, J., Babiker, A.G., Pett, S., Neaton, J.D., Burgess, T.H., Bonnett, T., Green, M., Makowski, M., Osinusi, A., Nayak, S., Lane, H.C., 2020. Remdesivir for the treatment of Covid-19 — final report. N. Engl. J. Med. 383, 1813–1826. https://doi.org/10.1056/nejmoa2007764.

Biron, B.M., Chung, C.-S., O'brien, X.M., Chen, Y., Reichner, J.S., Ayala, A., 2016. In: E-mail Cl-Amidine Prevents Histone 3 Citrullination and Neutrophil Extracellular Trap Formation, and Improves Survival in a Murine Sepsis Model. https://doi.org/10.1159/000448808.

Casanova, V., Sousa, F.H., Shakamuri, P., Svoboda, P., Buch, C., D'Acremont, M., Christophorou, M.A., Pohl, J., Stevens, C., Barlow, P.G., 2020. Citrullination alters the antiviral and immunomodulatory activities of the human cathelicidin LL-37 during rhinovirus infection. Front. Immunol. 11 https://doi.org/10.3389/fimmu.2020.00085.

Chang, X., Han, J., Pang, L., Zhao, Y., Yang, Y., Shen, Z., 2009. Increased PADI4 expression in blood and tissues of patients with malignant tumors. BMC Cancer 9, 40. https://doi: 10.1186/1471-2407-9-40.

Chumanevich, A.A., Causey, C.P., Knuckley, B.A., Jones, J.E., Poudyal, D., Chumanevich, A.P., Davis, T., Matesic, L.E., Thompson, P.R., Hofseth, L.J., 2011. Suppression of colitis in mice by Cl-amidine: a novel peptidylarginine deiminase inhibitor. Am. J. Physiol. Gastrointest. Liver Physiol. 300, G929–G938. https://doi.org/10.1152/ajpgi.00435.2010.

Conforti, A., Marra, E., Palombo, F., Roscilli, G., Ravà, M., Fumagalli, V., Muzi, A., Maffei, M., Luberto, L., Lione, L., Salvatori, E., Compagnone, M., Pinto, E., Pavoni, E., Bucci, F., Vitagliano, G., Stoppoloni, D., Pacello, M.L., Cappelletti, M., Ferrara, F.F., D'Acunto, E., Chiarini, V., Arriga, R., Nyska, A., Di Lucia, P., Marotta, D., Bono, E., Giustini, L., Sala, E., Perucchini, C., Paterson, J., Ryan, K.A., Challis, A.-R., Matusali, G., Colavita, F., Caselli, E., Criscuolo, E., Clementi, N., Mancini, N., Groß, R., Seidel, A., Wettstein, L., Münch, J., Donnici, L., Conti, M., De Francesco, R., Kuka, M., Ciliberto, G., Castiletti, C., Capobianchi, M.R., Ippolito, G., Guidotti, L.G., Rovati, L., Iannacone, M., Aurisicchio, L., 2021. COVID-eVax, an electroporated DNA vaccine candidate encoding the SARS-CoV-2 RBD, elicits protective responses in animal models. Mol. Ther. S1525–0016 (21), 00466 https://doi.org/10.1016/j.ymthe.2021.09.011. –4.

Darrah, E., Andrade, F., 2018. Rheumatoid arthritis and citrullination. Curr. Opin. Rheumatol. 30, 72–78. https://doi.org/10.1097/BOR.0000000000000452.

De Wit, E., Van Doremalen, N., Falzarano, D., Munster, V.J., 2016. SARS and MERS: recent insights into emerging coronaviruses. Nat. Rev. Microbiol. 14, 523–534. https://doi.org/10.1038/nrmicro.2016.81.

Delorey, T.M., Ziegler, C.G.K., Heimberg, G., Normand, R., Yang, Y., Segerstolpe, A., Abbondanza, D., Fleming, S.J., Subramanian, A., Montoro, D.T., Jagadeesh, K.A., Dey, K.K., Sen, P., Slyper, M., Pita-Juárez, Y.H., Phillips, D., Biermann, J., Bloom-Ackermann, Z., Barkas, N., Ganna, A., Gomez, J., Melms, J.C., Katsyv, I., Normandin, E., Naderi, P., Popov, Y.V., Raju, S.S., Niezen, S., Tsai, L.T.-Y., Siddle, K. J., Sud, M., Tran, V.M., Vellarikkal, S.K., Wang, Y., Amir-Zilberstein, L., Atri, D.S., Beechem, J., Brook, O.R., Chen, J., Divakar, P., Dorceus, P., Engreitz, J.M., Essene, A., Fitzgerald, D.M., Fropf, R., Gazal, S., Gould, J., Grzyb, J., Harvey, T., Hecht, J., Hether, T., Jané-Valbuena, J., Leney-Greene, M., Ma, H., McCabe, C., McLoughlin, D.E., Miller, E.M., Muus, C., Niemi, M., Padera, R., Pan, L., Pant, D., Pe'er, C., Pfiffner-Borges, J., Pinto, C.J., Plaisted, J., Reeves, J., Ross, M., Rudy, M., Rueckert, E.H., Siciliano, M., Sturm, A., Todres, E., Waghray, A., Warren, S., Zhang, S., Zollinger, D.R., Cosimi, L., Gupta, R.M., Hacohen, N., Hibshoosh, H., Hide, W., Price, A.L., Rajagopal, J., Tata, P.R., Riedel, S., Szabo, G., Tickle, T.L., Ellinor, P.T., Hung, D., Sabeti, P.C., Novak, R., Rogers, R., Ingber, D.E., Jiang, Z.G., Juric, D., Babadi, M., Farhi, S.L., Izar, B., Stone, J.R., Vlachos, I.S., Solomon, I.H., Ashenberg, O., Porter, C.B.M., Li, B., Shalek, A.K., Villani, A.-C., Rozenblatt-Rosen, O., Regev, A., 2021. COVID-19 tissue atlases reveal SARS-CoV-2 pathology and cellular targets. Nature 595, 107–113. https://doi.org/10.1038/s41586-021-03570-8.

Desmyter, J., Melnick, J.L., Rawls, W.E., 1968. Defectiveness of interferon production and of rubella virus interference in a line of African green monkey kidney cells (Vero). J. Virol. 2 (10), 955–961. https://doi.org/10.1128/JVI.2.10.955-961.1968.

Dittmar, M., Lee, J.S., Whig, K., Segrist, E., Li, M., Kamalia, B., Castellana, L., Ayyanathan, K., Cardenas-Diaz, F.L., Morrisey, E.E., Truitt, R., Yang, W., Jurado, K., Samby, K., Ramage, H., Schultz, D.C., Cherry, S., 2021. Drug repurposing screens reveal cell-type-specific entry pathways and FDA-approved drugs active against SARS-Cov-2. Cell Rep. 35, 108959. https://doi.org/10.1016/j.celrep.2021.108959.

Elliott Jr., W., Guda, M.R., Asuthkar, S., Teluguakula, N., Prasad, D.V.R., Tsung, A.J., Velpula, K.K., 2021. PAD inhibitors as a potential treatment for SARS-CoV-2 immunothrombosis. Biomedicines 9 (12), 1867. https://doi.org/10.3390/biomedicines9121867.

Esposito, G., Vitale, A.M., Leijten, F.P., Strik, A.M., Koonen-Reemst, A.M., Yurttas, P., Robben, T.J., Coonrod, S., Gossen, J.A., 2007. Peptidylarginine deiminase (PAD) 6 is essential for oocyte cytoskeletal sheet formation and female fertility. Mol. Cell. Endocrinol. 273 (1–2), 25–31. https://doi: 10.1016/j.mce.2007.05.005.

Falcão, A.M., Meijer, M., Scaglione, A., Rinwa, P., Agirre, E., Liang, J., Larsen, S.C., Heskol, A., Frawley, R., Klingener, M., Varas-Godoy, M., Raposo, A.A.S.F., Ernfors, P., Castro, D.S., Nielsen, M.L., Casaccia, P., Castelo-Branco, G., 2019. PAD2-Mediated citrullination contributes to efficient oligodendrocyte differentiation and myelination. Cell Rep. 27 (4), 1090–1102 e10. https://doi: 10.1016/j.celrep.2019.03.108.

Fan, Y., Zhao, K., Shi, Z.L., Zhou, P., 2019. Bat coronaviruses in China. Viruses. https://doi.org/10.3390/v11030210.

Fischer, W., Eron, J.J., Holman, W., Cohen, M.S., Fang, L., Szewczyk, L.J., Sheahan, T.P., Baric, R., Mollan, K.R., Wolfe, C.R., Duke, E.R., Azizad, M.M., Borroto-Esoda, K., Wohl, D.A., Loftis, A.J., Alabanza, P., Lipansky, F., Painter, W.P., 2021. Molnupiravir, an Oral Antiviral Treatment for COVID-19. https://doi.org/10.1101/2021.06.17.21258639.

Ghosh, A.K., Miller, H., Knox, K., Kundu, M., Henrickson, K.J., Arav-Boger, R., 2021. Inhibition of human coronaviruses by antimalarial peroxides. ACS Infect. Dis. 7, 1985–1995. https://doi.org/10.1021/acsinfecdis.1c00053.

Griffante, G., Gugliesi, F., Pasquero, S., Dell'Oste, V., Biolatti, M., Salinger, A.J., Mondal, S., Thompson, P.R., Weerapana, E., Lebbink, R.J., Soppe, J.A., Stamminger, T., Girault, V., Pichlmair, A., Oroszlán, G., Coen, D.M., De Andrea, M., Landolfo, S., 2021. Human cytomegalovirus-induced host protein citrullination is crucial for viral replication. Nat. Commun. 12, 1–14. https://doi.org/10.1038/s41467-021-24178-6.

György, B., Tóth, E., Tarcsa, E., Falus, A., Buzás, E.I., 2006. Citrullination: a posttranslational modification in health and disease. Int. J. Biochem. Cell Biol. 38, 1662–1677. https://doi.org/10.1016/j.biocel.2006.03.008.

Hartenian, E., Nandakumar, D., Lari, A., Ly, M., Tucker, J.M., Glaunsinger, B.A., 2020. The molecular virology of coronaviruses. J. Biol. Chem. 295, 12910–12934. https://doi.org/10.1074/jbc.REV120.013930.

Hsu, J., 2020. Covid-19: what now for remdesivir? BMJ 371, m4457. https://doi.org/10.1136/bmj.m4457.

Jang, B., Kim, E., Choi, J.K., Jin, J.K., Kim, J.I., Ishigami, A., Maruyama, N., Carp, R.I., Kim, Y.S., Choi, E.K., 2008. Accumulation of citrullinated proteins by up-regulated peptidylarginine deiminase 2 in brains of scrapie-infected mice: a possible role in pathogenesis. Am. J. Pathol. 173 (4), 1129–1142. https://doi: 10.2353/ajpath.2008.080388.

Kan, R., Yurttas, P., Kim, B., Jin, M., Wo, L., Lee, B., Gosden, R., Coonrod, S.A., 2011. Regulation of mouse oocyte microtubule and organelle dynamics by PADI6 and the cytoplasmic lattices. Dev. Biol. 350 (2), 311–322. https://doi: 10.1016/j.ydbio.2010.11.033.

Kanno, T., Kawada, A., Yamanouchi, J., Yosida-Noro, C., Yoshiki, A., Shiraiwa, M., Kusakabe, M., Manabe, M., Tezuka, T., Takahara, H., 2000. Human peptidylarginine deiminase type III: molecular cloning and nucleotide sequence of the cDNA, properties of the recombinant enzyme, and immunohistochemical localization in human skin. J. Invest. Dermatol. 115 (5), 813–823. https://doi: 10.1046/j.1523-1747.2000.00131.x.

Knight, J.S., Subramanian, V., O'Dell, A.A., Yalavarthi, S., Zhao, W., Smith, C.K., Hodgin, J.B., Thompson, P.R., Kaplan, M.J., 2015. Peptidylarginine deiminase

inhibition disrupts NET formation and protects against kidney, skin and vascular disease in lupus-prone MRL/*lpr* mice. Ann. Rheum. Dis. 74, 2199–2206. https://doi.org/10.1136/annrheumdis-2014-205365.

Knuckley, B., Causey, C.P., Jones, J.E., Bhatia, M., Dreyton, C.J., Osborne, T.C., Takahara, H., Thompson, P.R., 2010. Substrate specificity and kinetic studies of PADs 1, 3, and 4 identify potent and selective inhibitors of protein arginine deiminase 3. Biochemistry 49 (23), 4852–4863. https://doi.org/10.1021/bi100363t.

Ksiazek, T.G., Erdman, D., Goldsmith, C.S., Zaki, S.R., Peret, T., Emery, S., Tong, S., Urbani, C., Comer, J.A., Lim, W., Rollin, P.E., Dowell, S.F., Ling, A.-E., Humphrey, C. D., Shieh, W.-J., Guarner, J., Paddock, C.D., Rota, P., Fields, B., DeRisi, J., Yang, J.-Y., Cox, N., Hughes, J.M., LeDuc, J.W., Bellini, W.J., Anderson, L.J., 2003. A novel coronavirus associated with severe acute respiratory syndrome. N. Engl. J. Med. 348, 1953–1966. https://doi.org/10.1056/nejmoa030781.

Leao, J.C., Gusmao, T.P. de L., Zarzar, A.M., Leao Filho, J.C., Barkokebas Santos de Faria, A., Morais Silva, I.H., Gueiros, L.A.M., Robinson, N.A., Porter, S., Carvalho, A. de A.T., 2020. Coronaviridae—Old Friends, New Enemy! Oral Diseases 0–3. https://doi.org/10.1111/odi.13447.

Ledet, M.M., Anderson, R., Harman, R., Muth, A., Thompson, P.R., Coonrod, S.A., Van de Walle, G.R., 2018. BB-Cl-Amidine as a novel therapeutic for canine and feline mammary cancer via activation of the endoplasmic reticulum stress pathway. BMC Cancer 18, 1–13. https://doi.org/10.1186/s12885-018-4323-8.

Lee, C.-Y., Lowen, A.C., 2021. Animal models for SARS-CoV-2. Curr. Opin. Virol. 48, 73–81. https://doi.org/10.1016/j.coviro.2021.03.009.

Lu, R., Zhao, X., Li, J., Niu, P., Yang, B., Wu, H., Wang, W., Song, H., Huang, B., Zhu, N., Bi, Y., Ma, X., Zhan, F., Wang, L., Hu, T., Zhou, H., Hu, Z., Zhou, W., Zhao, L., Chen, J., Meng, Y., Wang, J., Lin, Y., Yuan, J., Xie, Z., Ma, J., Liu, W.J., Wang, D., Xu, W., Holmes, E.C., Gao, G.F., Wu, G., Chen, W., Shi, W., Tan, W., 2020. Genomic characterisation and epidemiology of 2019 novel coronavirus: implications for virus origins and receptor binding. Lancet 395, 565–574. https://doi.org/10.1016/S0140-6736(20)30251-8.

Lewis, H.D., Liddle, J., Coote, J.E., Atkinson, S.J., Barker, M.D., Bax, B.D., Bicker, K.L., Bingham, R.P., Campbell, M., Chen, Y.H., Chung, C.W., Craggs, P.D., Davis, R.P., Eberhard, D., Joberty, G., Lind, K.E., Locke, K., Maller, C., Martinod, K., Patten, C., Polyakova, O., Rise, C.E., Rüdiger, M., Sheppard, R.J., Slade, D.J., Thomas, P., Thorpe, J., Yao, G., Drewes, G., Wagner, D.D., Thompson, P.R., Prinjha, R.K., Wilson, D.M., 2015. Inhibition of PAD4 activity is sufficient to disrupt mouse and human NET formation. Nat. Chem. Biol. 11 (3), 189–191. https://doi.org/10.1038/nchembio.1735.

Marcello, A., Civra, A., Milan Bonotto, R., Nascimento Alves, L., Rajasekharan, S., Giacobone, C., Caccia, C., Cavalli, R., Adami, M., Brambilla, P., Lembo, D., Poli, G., Leoni, V., 2020. The cholesterol metabolite 27-hydroxycholesterol inhibits SARS-CoV-2 and is markedly decreased in COVID-19 patients. Redox Biol. 36, 101682. https://doi.org/10.1016/j.redox.2020.101682.

Milani, M., Donalisio, M., Bonotto, R.M., Schneider, E., Arduino, I., Boni, F., Lembo, D., Marcello, A., Mastrangelo, E., 2021. Combined in silico and in vitro approaches identified the antipsychotic drug lurasidone and the antiviral drug elbasvir as SARS-CoV2 and HCoV-OC43 inhibitors. Antivir. Res. 189, 105055. https://doi.org/10.1016/j.antiviral.2021.105055.

Milewska, A., Kaminski, K., Ciejka, J., Kosowicz, K., Zeglen, S., Wojarski, J., Nowakowska, M., Szczubiałka, K., Pyrc, K., 2016. HTCC: broad range inhibitor of coronavirus entry. PLoS One 11, 1–17. https://doi.org/10.1371/journal.pone.0156552.

Mondal, S., Thompson, P.R., 2019. Protein arginine deiminases (PADs): biochemistry and chemical biology of protein citrullination. Acc. Chem. Res. 52, 818–832. https://doi.org/10.1021/acs.accounts.9b00024.

Mosca, J.D., Pitha, P.M., 1986. Transcriptional and posttranscriptional regulation of exogenous human beta interferon gene in simian cells defective in interferon synthesis. Mol. Cell Biol. 6 (6), 2279–2283. https://doi.org/10.1128/mcb.6.6.2279-2283.1986.

Musse, A.A., Li, Z., Ackerley, C.A., Bienzle, D., Lei, H., Poma, R., Harauz, G., Moscarello, M.A., Mastronardi, F.G., 2008. Peptidylarginine deiminase 2 (PAD2) overexpression in transgenic mice leads to myelin loss in the central nervous system. Dis. Model. Mech. (4–5), 229–240. https://doi.org/10.1242/dmm.000729.

Muth, A., Subramanian, V., Beaumont, E., Nagar, M., Kerry, P., McEwan, P., Srinath, H., Clancy, K., Parelkar, S., Thompson, P.R., 2017. Development of a selective inhibitor of protein arginine deiminase 2. J. Med. Chem. 60 (7), 3198–3211. https://doi.org/10.1021/acs.jmedchem.7b00274.

Nachat, R., Méchin, M.C., Charveron, M., Serre, G., Constans, J., Simon, M., 2005. Peptidylarginine deiminase isoforms are differentially expressed in the anagen hair follicles and other human skin appendages. J. Invest. Dermatol. 125 (1), 34–41. https://doi.org/10.1111/j.0022-202X.2005.23763.x.

Ogando, N.S., Dalebout, T.J., Zevenhoven-Dobbe, J.C., Limpens, R.W.A.L., van der Meer, Y., Caly, L., Druce, J., de Vries, J.J.C., Kikkert, M., Bárcena, M., Sidorov, I., Snijder, E.J., 2020. SARS-coronavirus-2 replication in Vero E6 cells: replication kinetics, rapid adaptation and cytopathology. J. Gen. Virol. 101, 925–940. https://doi.org/10.1099/jgv.0.001453.

Parisi, O.I., Dattilo, M., Patitucci, F., Malivindi, R., Delbue, S., Ferrante, P., Parapini, S., Galeazzi, R., Cavarelli, M., Cilurzo, F., Franzè, S., Perrotta, I., Pezzi, V., Selmin, F., Ruffo, M., Puoci, F., 2021. Design and development of plastic antibodies against SARS-CoV-2 RBD based on molecularly imprinted polymers that inhibit *in vitro* virus infection. Nanoscale 13 (40), 16885–16899. https://doi.org/10.1039/d1nr03727g.

Paules, C.I., Marston, H.D., Fauci, A.S., 2020. Coronavirus infections-more than just the common cold. J. Am. Med. Assoc. https://doi.org/10.1001/jama.2020.0757.

Pratesi, F., Tommasi, C., Anzilotti, C., Chimenti, D., Migliorini, P., 2006. Deiminated Epstein-Barr virus nuclear antigen 1 is a target of anti-citrullinated protein antibodies in rheumatoid arthritis. Arthritis Rheum. 54, 733–741. https://doi.org/10.1002/art.21629.

Pratesi, F., Tommasi, C., Anzilotti, C., Puxeddu, I., Sardano, E., Di Colo, G., Migliorini, P., 2011. Antibodies to a new viral citrullinated peptide, VCP2: fine specificity and correlation with anti-cyclic citrullinated peptide (CCP) and anti-VCP1 antibodies. Clin. Exp. Immunol. 164, 337–345. https://doi.org/10.1111/j.1365-2249.2011.04378.x.

Ravikumar, B., Aittokallio, T., 2018. Improving the efficacy-safety balance of polypharmacology in multi-target drug discovery. Expet Opin. Drug Discov. 13, 179–192. https://doi.org/10.1080/17460441.2018.1413089.

Senshu, T., Akiyama, K., Ishigami, A., Nomura, K., 1999. Studies on specificity of peptidylarginine deiminase reactions using an immunochemical probe that recognizes an enzymatically deiminated partial sequence of mouse keratin K1. J. Dermatol. Sci. 21, 113–126. https://doi: 10.1016/s0923-1811(99)00026-2.

Slack, J.L., Causey, C.P., Thompson, P.R., 2011. Protein arginine deiminase 4: a target for an epigenetic cancer therapy. Cell. Mol. Life Sci. 68, 709–720. https://doi.org/10.1007/s00018-010-0480-x.

Sokolove, J., Brennan, M.J., Sharpe, O., Lahey, L.J., Kao, A.H., Krishnan, E., Edmundowicz, D., Lepus, C.M., Wasko, M.C., Robinson, W.H., 2013. Brief report: citrullination within the atherosclerotic plaque: a potential target for the anti-citrullinated protein antibody response in rheumatoid arthritis. Arthritis Rheum. 65, 1719–1724. https://doi.org/10.1002/art.37961.

Su, S., Wong, G., Shi, W., Liu, J., Lai, A.C.K., Zhou, J., Liu, W., Bi, Y., Gao, G.F., 2016. Epidemiology, Genetic Recombination, and Pathogenesis of Coronaviruses. https://doi.org/10.1016/j.tim.2016.03.003.

Trier, N.H., Holm, B.E., Heiden, J., Slot, O., Locht, H., Lindegaard, H., Svendsen, A., Nielsen, C.T., Jacobsen, S., Theander, E., Houen, G., 2018. Antibodies to a strain-specific citrullinated Epstein-Barr virus peptide diagnoses rheumatoid arthritis. Sci. Rep. 8, 3684. https://doi.org/10.1038/s41598-018-22058-6.

van Venrooij, W.J., van Beers, J.J.B.C., Pruijn, G.J.M., 2011. Anti-CCP antibodies: the past, the present and the future. Nat. Rev. Rheumatol. 7, 391–398. https://doi.org/10.1038/nrrheum.2011.76.

Valesini, G., Gerardi, M.C., Iannuccelli, C., Pacucci, V.A., Pendolino, M., Shoenfeld, Y., 2015. Citrullination and autoimmunity. Autoimmun. Rev. 14, 490–497. https://doi.org/10.1016/j.autrev.2015.01.013.

Vossenaar, E.R., Zendman, A.J.W., Van Venrooij, W.J., Pruijn, G.J.M., 2003. PAD, a growing family of citrullinating enzymes: genes, features and involvement in disease. Bioessays 25, 1106–1118. https://doi.org/10.1002/bies.10357.

Wang, S., Wang, Y., 2013. Peptidylarginine deiminases in citrullination, gene regulation, health and pathogenesis. Biochim. Biophys. Acta 1126–1135. https://doi.org/10.1016/j.bbagrm.2013.07.003, 1829.

Warren, T.K., Jordan, R., Lo, M.K., Ray, A.S., Mackman, R.L., Soloveva, V., Siegel, D., Perron, M., Bannister, R., Hui, H.C., Larson, N., Strickley, R., Wells, J., Stuthman, K. S., Van Tongeren, S.A., Garza, N.L., Donnelly, G., Shurtleff, A.C., Retterer, C.J., Gharaibeh, D., Zamani, R., Kenny, T., Eaton, B.P., Grimes, E., Welch, L.S., Gomba, L., Wilhelmsen, C.L., Nichols, D.K., Nuss, J.E., Nagle, E.R., Kugelman, J.R., Palacios, G., Doerffler, E., Neville, S., Carra, E., Clarke, M.O., Zhang, L., Lew, W., Ross, B., Wang, Q., Chun, K., Wolfe, L., Babusis, D., Park, Y., Stray, K.M., Trancheva, I., Feng, J.Y., Barauskas, O., Xu, Y., Wong, P., Braun, M.R., Flint, M., McMullan, L.K., Chen, S.S., Fearns, R., Swaminathan, S., Mayers, D.L., Spiropoulou, C.F., Lee, W.A., Nichol, S.T., Cihlar, T., Bavari, S., 2016. Therapeutic efficacy of the small molecule GS-5734 against Ebola virus in rhesus monkeys. Nature 531, 381–385. https://doi.org/10.1038/nature17180.

Weiss, S.R., Navas-Martin, S., 2005. Coronavirus pathogenesis and the emerging pathogen severe acute respiratory syndrome coronavirus. Microbiol. Mol. Biol. Rev. 69, 635–664. https://doi.org/10.1128/MMBR.69.4.635-664.2005.

Willis, V.C., Banda, N.K., Cordova, K.N., Chandra, P.E., Robinson, W.H., Cooper, D.C., Lugo, D., Mehta, G., Taylor, S., Tak, P.P., Prinjha, R.K., Lewis, H.D., Holers, V.M., 2017. Protein arginine deiminase 4 inhibition is sufficient for the amelioration of collagen-induced arthritis. Clin. Exp. Immunol. 188, 263–274. https://doi.org/10.1111/cei.12932.

Willis, V.C., Gizinski, A.M., Banda, N.K., Causey, C.P., Knuckley, B., Cordova, K.N., Luo, Y., Levitt, B., Glogowska, M., Chandra, P., Kulik, L., Robinson, W.H., Arend, W. P., Thompson, P.R., Holers, V.M., 2011. N-α-Benzoyl-N5-(2-Chloro-1-Iminoethyl)-l-Ornithine amide, a protein arginine deiminase inhibitor, reduces the severity of murine collagen-induced arthritis. J. Immunol. 186, 4396–4404. https://doi.org/10.4049/jimmunol.1001620.

Wing, P.A.C., Keeley, T.P., Zhuang, X., Lee, J.Y., Prange-Barczynska, M., Tsukuda, S., Morgan, S.B., Harding, A.C., Argles, I.L.A., Kurlekar, S., Noerenberg, M., Thompson, C.P., Huang, K.Y.A., Balfe, P., Watashi, K., Castello, A., Hinks, T.S.C., James, W., Ratcliffe, P.J., Davis, I., Hodson, E.J., Bishop, T., McKeating, J.A., 2021. Hypoxic and pharmacological activation of HIF inhibits SARS-CoV-2 infection of lung epithelial cells. Cell Rep. 35, 109020. https://doi.org/10.1016/j.celrep.2021.109020.

Witalison, E.E., Thompson, P.R., Hofseth, L.J., 2015. Protein arginine deiminases and associated citrullination: physiological functions and diseases associated with dysregulation. Curr. Drug Targets 16, 700–710. https://doi.org/10.2174/1389450116666150202160954.

Wu, F., Zhao, S., Yu, B., Chen, Y.M., Wang, W., Song, Z.G., Hu, Y., Tao, Z.W., Tian, J.H., Pei, Y.Y., Yuan, M.L., Zhang, Y.L., Dai, F.H., Liu, Y., Wang, Q.M., Zheng, J.J., Xu, L., Holmes, E.C., Zhang, Y.Z., 2020. A new coronavirus associated with human respiratory disease in China. Nature 579, 265–269. https://doi.org/10.1038/s41586-020-2008-3.

Yang, L., Tan, D., Piao, H., 2016. Myelin basic protein citrullination in multiple sclerosis: a potential therapeutic target for the pathology. Neurochem. Res. 41, 1845–1856. https://doi.org/10.1007/s11064-016-1920-2.

Ying, S., Dong, S., Kawada, A., Kojima, T., Chavanas, S., Méchin, M.C., Adoue, V., Serre, G., Simon, M., Takahara, H., 2009. Transcriptional regulation of peptidylarginine deiminase expression in human keratinocytes. J. Dermatol. Sci. 53 (1), 2–9. https://doi: 10.1016/j.jdermsci.2008.09.009.

Yuzhalin, A.E., 2019. Citrullination in cancer. Cancer Res. 79, 1274–1284. https://doi.org/10.1158/0008-5472.CAN-18-2797.

Zaki, A.M., van Boheemen, S., Bestebroer, T.M., Osterhaus, A.D.M.E., Fouchier, R.A.M., 2012. Isolation of a novel coronavirus from a man with pneumonia in Saudi Arabia. N. Engl. J. Med. 367, 1814–1820. https://doi.org/10.1056/nejmoa1211721.

Zhang, X., Liu, X., Zhang, M., Li, T., Muth, A., Thompson, P.R., Coonrod, S.A., Zhang, X., 2016. Peptidylarginine deiminase 1-catalyzed histone citrullination is essential for early embryo development. Sci. Rep. 6, 38727. http://doi: 10.1038/srep38727.

Zhao, T., Pan, B., Alam, H.B., Liu, B., Bronson, R.T., Deng, Q., Wu, E., Li, Y., 2016. Protective effect of Cl-amidine against CLP-induced lethal septic shock in mice. Sci. Rep. 6, 36696. https://doi.org/10.1038/srep36696.

Review

HPV Meets APOBEC: New Players in Head and Neck Cancer

Giuseppe Riva [1] , Camilla Albano [2] , Francesca Gugliesi [2] , Selina Pasquero [2] ,
Sergio Fernando Castillo Pacheco [2] , Giancarlo Pecorari [1] , Santo Landolfo [2] , Matteo Biolatti [2,*] and
Valentina Dell'Oste [2,*]

[1] Otorhinolaryngology Division, Department of Surgical Sciences, University of Turin, 10126 Turin, Italy;
giuseppe.riva@unito.it (G.R.); giancarlo.pecorari@unito.it (G.P.)

[2] Department of Public Health and Pediatric Sciences, University of Turin, 10126 Turin, Italy;
camilla.albano@unito.it (C.A.); francesca.gugliesi@unito.it (F.G.); selina.pasquero@unito.it (S.P.);
sergiofernando.castillopachecho@unito.it (S.F.C.P.); santo.landolfo@unito.it (S.L.)

* Correspondence: matteo.biolatti@unito.it (M.B.); valentina.delloste@unito.it (V.D.);
Tel.: +39-011-6705635 (M.B. & V.D.)

Abstract: Besides smoking and alcohol, human papillomavirus (HPV) is a factor promoting head and neck squamous cell carcinoma (HNSCC). In some human tumors, including HNSCC, a number of mutations are caused by aberrantly activated DNA-modifying enzymes, such as the apolipoprotein B mRNA editing enzyme catalytic polypeptide-like (APOBEC) family of cytidine deaminases. As the enzymatic activity of APOBEC proteins contributes to the innate immune response to viruses, including HPV, the role of APOBEC proteins in HPV-driven head and neck carcinogenesis has recently gained increasing attention. Ongoing research efforts take the cue from two key observations: (1) APOBEC expression depends on HPV infection status in HNSCC; and (2) APOBEC activity plays a major role in HPV-positive HNSCC mutagenesis. This review focuses on recent advances on the role of APOBEC proteins in HPV-positive vs. HPV-negative HNSCC.

Keywords: human papillomavirus; head and neck cancer; APOBEC; cytidine deaminase; squamous cell carcinoma

1. Introduction

Head and neck squamous cell carcinoma (HNSCC) include about 6% of all cases of tumors worldwide, representing the sixth most prevalent type of cancer. Its incidence is of 15.2 and 4.6 per 100,000 people in men and women, respectively [1].

Alcohol and tobacco abuse are the two main risk factors for HNSCC and seem to act in a synergistic fashion. However, in recent years, human papillomavirus (HPV) has emerged as an independent biological risk factor for the development of HNSCC. Indeed, in men younger than 50 years without a prior history of tobacco and alcohol consumption, HPV infection is directly associated with increased incidence of oropharyngeal tumors [2]. HPV-driven tumorigenesis appears to be particularly relevant in the oropharynx, where the base of the tongue and the tonsils are the most vulnerable sites. Furthermore, patients affected by HPV-related HNSCC have a different mutational profile and a better survival [3,4]. In particular, the discover of different mutational profiles in HPV-negative (HPV⁻) vs. HPV-positive (HPV⁺) HNSCC has raised the hypothesis that HPV infection may also play a role in gene regulation [3].

In certain human tumors, aberrantly activated DNA-modifying enzymes, such as the apolipoprotein B mRNA editing enzyme catalytic polypeptide-like (APOBEC) family of cytidine deaminases, have been linked to several DNA mutations [5–8]. Interestingly, APOBEC activation is also a well-established pathway in the innate immune response to viruses, including retroviruses, parvoviruses, hepatitis B virus (HBV), BK polyomaviruses, herpes simplex virus 1 (HSV-1), human cytomegalovirus (HCMV), Epstein–Barr virus (EBV), and HPV [9,10]. Indeed, APOBEC3A (A3A) and APOBEC3C (A3C) can hypermutate

the HPV-16 genome, hampering its infectivity [9]. In addition, APOBEC3B (A3B) has been involved in HPV$^+$ HNSCC mutagenesis [11]. Intriguingly, diminished exposure to exogenous carcinogens tends to favor APOBEC-mediated mutations of HPV$^+$ HNSCC, whereas HPV$^-$ HNSCC mostly retains a carcinogen-associated mutational profile [11–13].

This review will summarize and analyze our current understanding of the emerging role of APOBEC proteins in HNSCC pathogenesis, focusing on the mutagenic activity of this family of deaminases.

2. Head and Neck Squamous Cell Carcinoma

HNSCC is a highly heterogeneous tumor typically arising from the epithelial cells of the mucosa, with the oral cavity, oropharynx, hypopharynx, and larynx being the most frequently affected sites [2,3]. Besides smoking and alcohol abuse, high-risk HPV infection is the main biological risk factor of HNSCC development in the oropharyngeal area, including 22–47% of oropharyngeal HNSCCs [14], with approximately 90% of HPV-related oropharyngeal carcinomas being caused by HPV-16 [15]. Thus, depending on their HPV infection status, HNSCCs can either be HPV$^+$ or HPV$^-$, with each group characterized by specific clinical manifestations, incidence patterns, molecular signatures, and prognoses [3,16–19]. For instance, HPV$^+$ HNSCC has a tendency to present as a small primary tumor with large nodal metastases [20]. Furthermore, the incidence of HPV$^+$ HNSCC in non-smoking and non-drinking younger subjects is much higher than that of HPV$^-$ HNSCC. With regard to differences in their molecular profiles, while a smoking-associated mutational signature was detected in a sample of HPV$^-$ HNSCCs, reduced exposure to exogenous carcinogens in HPV$^+$ HNSCC patients correlated with an APOBEC mutational burden [11,12]. In terms of differences in overall survival, HPV$^+$ HNSCCs generally display a better response to chemoradiotherapy [21] and a more favorable prognosis [20].

The highest prevalence of HPV infection in HNSCC has been reported in South America and central, eastern, and northern Europe, whereas southern European regions tend to have much lower incidence rates [14]. Moreover, in the past decades, the proportion of HPV-related oropharyngeal tumors has increased approximately 4-fold—from 7.2% in 1990–1994 to 32.7% in 2010–2012—seemingly as a result of altered sexual behaviors, as HPV$^+$ tumors are linked to oral sex [22].

Non-oropharyngeal HNSCCs i.e., tumor affecting the oral cavity, larynx and hypopharynx, are less frequently related to HPV infection, with HPV DNA prevalence in oral and laryngeal tumors being 23.5% and 24.0%, respectively [15]. It is also interesting to point out that not all HPV$^+$ tumors are positive for HPV E6 and E7 gene expression, two viral oncogenes considered to be the most reliable biomarkers of HPV-mediated transformation [23]. For instance, HPV DNA and E6/E7 mRNA could only be detected in 21.8%, 3.9%, and 3.1% of oropharyngeal, oral, and laryngeal tumors, respectively [14].

HPV proteins E6 and E7 play a functional role in cancer development through inactivation of p53 and retinoblastoma protein (pRb) [23,24]. In particular, pRb loss upregulates p16 protein expression, which in turn shuts down cyclin D1/cyclin-dependent kinase 4/6 (CDK4/6) signaling, thereby blocking the G1/S transition. The fact that p16 is now widely used as a molecular marker of HPV infection has led to the recent modification of the oropharyngeal Tumor Node Metastasis (TNM) staging system so as to include p16 positivity among the criteria for predicting HPV status [20]. However, the observation that p16 overexpression does not always coincide with HPV DNA positivity has questioned the use of this protein as a marker of HPV infection in HNSCC [25,26].

As aforementioned, HPV positivity and negativity determine distinctive molecular signatures among HNSCCs. The following sections summarize our current knowledge of this clinically relevant phenomenon.

The majority of HPV$^-$ HNSCCs harbor loss of chromosomes 3p and 9p as well as tumor protein 53 (TP53) mutations [27]. In such tumors, the amplification of cyclin D1 and the loss of the tumor suppressor gene CDKN2A (p16INK4A) drive neoplastic cells through the G1/S checkpoint, contributing to DNA replication [28]. Moreover, p53-mediated cell

cycle arrest and apoptosis in response to DNA damage is defective in these tumors because TP53 is usually inactivated by missense mutations and allelic loss [27]. Fittingly, TP53 somatic mutations, present in 30–75% of HNSCCs, correlate with poor survival of patients with invasive carcinomas [29,30].

Approximately 15% of HPV⁻ HNSCCs harbor NOTCH1 mutations, which make this transmembrane receptor the second most frequently mutated gene in HNSCC [4,16]. NOTCH1 regulates normal cell differentiation, lineage commitment, and embryonic development, and besides acting as a transcriptional activator can function as a tumor suppressor [16,31]. Another gene structurally similar to NOTCH1 that is instead amplified in HPV⁻ HNSCC is the epidermal growth factor receptor (EGFR), which plays a well-established role in cell proliferation. Lastly, HPV⁻ HNSCCs often display amplification of the MET proto-oncogene receptor tyrosine kinase, which drives migration, invasion and angiogenesis of cancer cells when constitutively activated [32,33].

On the other hand, HPV⁺ HNSCCs contain a lower number of mutations per tumor in comparison with HPV⁻ HNSCCs and hardly ever display inactivating p16INK4A mutations [16,31,34,35]. Furthermore, most of those genes that are aberrantly expressed in HPV⁻ HNSCCs are usually unaffected in their HPV⁺ counterparts, as shown by several epigenetic and genomic studies [19]. For example, HPV⁺ HNSCCs generally express the wild-type conformation of the tumor suppressor gene TP53 [19].

Another difference between HPV⁻ and HPV⁺ HNSCCs lies in expression of the two PYHIN proteins IFI16 and AIM2, the former nuclear and the second cytoplasmic sensors of double strand (ds) DNA. More specifically, while IFI16 is generally upregulated in HPV⁺ HNSCC, AIM2 gene expression levels are usually found unchanged in HPV⁺ HNSCCs with respect to their HPV⁻ counterparts, where this gene is already expressed at high levels (10% vs. 50% of cases, respectively) [12,13].

Lastly, while HPV⁺ HNSCCs carry mutations in the helical domain of the PIK3CA gene, HPV⁻ HNSCC harbors mutations across the entire gene. PIK3CA encodes the catalytic subunit of phosphoinositide 3-kinase (PI3K) p110α, which triggers AKT signaling. PIK3CA amplification, and/or mutations have been found in 34% of HPV⁻ and 56% of HPV⁺ HNSCCs [16]. The recent observation that the helical domain of the PIK3CA gene is subject to APOBEC-induced mutations in multiple cancers has led to the hypothesis that APOBEC activity may play a key role in HPV-induced transformation [11]. This assumption is also supported by the fact that in HPV-related cancers induction of APOBEC mutagenesis may also be the result of gene amplification besides viral infection [6]. In this regard, the role of APOBEC3 family of cytidine deaminases has been recently demonstrated in HPV⁺ HNSCCs [12], in good agreement with previous findings showing how the mutational signature of APOBEC can determine a specific mutational profile in these tumors [36].

The role of APOBEC-mediated cytosine deamination in generating driver mutations is discussed in more detail below.

3. The APOBEC Family and Cytosine Deamination

AID (activation-induced deaminase)/APOBEC is a family of enzymes with cytidine deaminase activity capable of converting cytosines into uracils in either RNA and/or single strand (ss) DNA, thus inducing missense mutations or early stop codons.

The human AID/APOBEC protein family comprises the following 11 members: Activation-induced cytidine deaminases (AIDs) and APOBEC1 (A1) (genes located on chromosome 12), APOBEC2 (A2) (chromosome 6), 7 APOBEC3 (A3) proteins (i.e., A3A, A3B, A3C, A3D, A3F, A3G, and A3H) (chromosome 22), and APOBEC4 (A4) (chromosome 1) [8,37].

Each member of this family shares at least one zinc-dependent deaminase (ZDD) containing the consensus amino acid sequence H-X-E-X23-28-P-C-X2-4-C, where X represents any amino acid. While the histidine (H) and cysteine (C) residues bind zinc at the active site, the glutamic acid residue (E) regulates proton shuttling through deamination [37–39]. APOBECs catalyze cytosine deamination into uracil through a zinc-mediated hydrolytic

mechanism. Specifically, the conserved glutamic acid in its zinc-binding deaminase motif mediates water deprotonation. This results in a zinc-stabilized hydroxide ion that promotes nucleophilic substitution of the amine group of the cytosine at position 4 with a carbonyl group. Each of the APOBEC proteins deaminates cytosines at specific consensus sequences, with the amino acid sequence at the 5′ of the target cytosine being unique to each APOBEC enzyme—i.e., 5′ WRCY for AID1 (W = A or T; R = Purine), 5′ AC for A1, 5′ CC for A3G and 5′ TC for all the other A3 enzymes (A3A, A3B, A3C, A3D, A3F, and A3H) [40,41].

APOBEC cytosine deamination activity is mediated by the catalytic site cytidine deaminase (CDA) domain containing a highly conserved ZDD sequence motif comprising five β-strands stabilized by six α-helices (Figure 1).
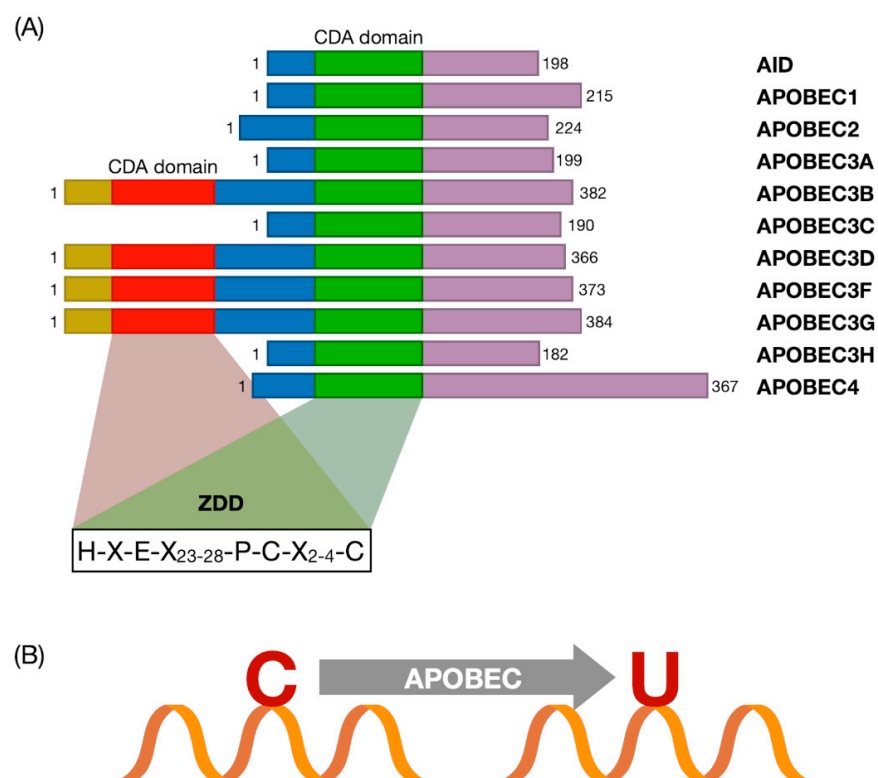

Figure 1. (**A**) Schematic representation of the apolipoprotein B mRNA editing enzyme catalytic polypeptide-like (APOBEC) family genes. The diagram shows the structural organization of APOBEC family proteins. The domains and position of the evolutionarily conserved residues are shown. The red box represents the catalytically inactive cytidine deaminase (CDA) domain, while the green box is the catalytically active CDA domain. The zinc-dependent deaminase (ZDD) consensus amino acid sequence (H-X-E-X23-28-P-C-X2-4-C) is shown. X represents any amino acid. Histidine (H) and cysteine (C) residues bind zinc at the active site, the glutamic acid residue (E) controls proton shuttling through deamination. CDA: Catalytic site cytidine deaminase. ZDD: Zinc-dependent deaminase. (Modified from [39]) (**B**) Reaction of the ssDNA cytosine deamination catalyzed by APOBEC family members.

The substrate specificity and function of the catalytic activity of APOBEC are influenced by the variations in the length, composition, and spatial distribution of these highly conserved secondary structures. Specifically, the conformation of the loops in proximity of the CDA regulates both substrate recognition and catalytic site interaction with the substrate. For instance, loop 7 contains a conserved sequence that, by interacting with loops 1, 3, and 5, determines the sequence targeting specificity of all AID/APOBEC enzymes [42]. Another example is the interaction of ssDNA/RNA with APOBECs, which occurs thanks to the combined action of shallow grooves on the protein surface and the catalytic site

rich in basic and hydrophobic residues capable of binding to negatively charged nucleic acids [41]. In addition, the catalytic activity of several APOBECs is determined by their ability to form high molecular weight homo and hetero complexes. For instance, APOBEC1 can heterodimerize with the A1 complementation factor (A1CF), an RNA binding protein co-factor, while AID is functionally active in both homodimer and monomer conformations. Interestingly, A3B, A3D, A3F, A3G, and A3H can only be detected as multimeric forms, whereas A2, A3A, and A3C can exclusively form monomers. Oligomers are then thought to influence the spatial orientation of the loops involved in ssDNA/RNA binding and catalytic site access, thereby regulating the deamination kinetics [43,44].

Each APOBEC family member exhibits different functions at the cellular level. For example, cytidine deamination by APOBEC proteins plays an important role in sensing endogenous and exogenous retroviruses and triggering innate and adaptive immunity. Furthermore, this catalytic activity is involved in the control of epigenetic mechanisms and lipid metabolism [45].

Another peculiar property of APOBEC is their ability to increase tumor mutations due to aberrant DNA editing [46–49]. APOBEC genes are quite often aberrantly regulated in cancer, which then leads to increased mutagenesis and genomic instability in cancer cells. Thus, there has been an increasing interest in determining whether altered expression profiles of APOBECs in tumor cells can increase the occurrence of somatic mutations. This may be in part supported by recent findings showing that germline variations of APOBECs are associated with increased mutagenic capacity, which then may promote tumorigenesis [39]. In this regard, whole exome and genome sequencing analyses have revealed the presence of an APOBEC mutation signature in multiple cancer types, including breast, bladder, thyroid, and cervix cancer, B cell lymphoma, lung adenocarcinoma (LUAD), acute lymphoblastic leukemia (ALL) and chronic lymphocytic leukemia (CLL), and multiple myelomas (MM). By contrast, other cancers, such as acute myeloid leukemia (AML) and colorectal and liver cancer, do not seem to contain any APOBEC signatures [50].

More recently, Burns et al. have reported high APOBEC3B mRNA levels in most of primary breast tumors and breast cancer cell lines examined. Of note, A3B expression and catalytic activity were associated with increased genomic uracil levels, dC > dT transition rates and mutation frequencies [51]. Finally, APOBEC3 proteins have been proposed to link viral infections to cancer development [39], an interesting aspect that will be further addressed in the following section.

4. APOBEC Genes vs. HPVs: Restriction Factors or DNA Editors?

Restriction factors (RFs) are the first line of defense against different viruses, including HPVs [52,53]. Among RFs, A3 genes have emerged as an integral part of intrinsic immunity: they are potently induced by interferons following viral infection and exert antiviral activities through deamination-independent and -dependent mechanisms [54], which has led many to hypothesize that an abnormal regulation of this response may trigger somatic mutagenesis in cancer cells.

APOBEC3 proteins were initially discovered for their activity against retroviruses [55], but later on, it became evident that they were also effective against a wide range of other viruses, such as parvoviruses [56], HBV [57,58], BK polyomaviruses [59,60], HSV-1 [61], HCMV [62], and EBV [63]. In this regard, our group has recently uncovered a novel mechanism of HCMV evasion from A3 restriction activity based on the progressive loss of APOBEC hot spots from its genome during evolution [10]. A3 inactivation as a means to evade host immune surveillance does not seem to be solely restricted to HCMV as other viruses, such as HSV-1 and Kaposi's sarcoma-associated herpesvirus (KSHV), can delocalize A3 proteins and, in doing so, neutralize their antiviral activity through a conserved ribonucleotide reductase (RNR)-dependent mechanism [64]. More recently, APOBECs have been involved in SARS-CoV-2 RNA editing [65]. Finally, a close relationship between APOBEC and HPV is suggested by the fact that APOBEC-driven mutations are frequent in cervical cancer, and that APOBEC expression is upregulated in HPV-infected

cells [11]. The first hint that A3s were restriction factors for HPVs came from in vitro studies showing that HPV pseudovirions, once packaged in 293T overexpressing A3A or A3C, displayed reduced infectivity in keratinocytes, an effect that could be reversed by A3A silencing [9,66,67]. An additional piece of evidence supporting the role of A3 proteins in HPV restriction was brought by experiments showing that catalytically inactive A3A mutants were unable to curb HPV infectivity in keratinocytes [68]. Importantly, the fact that HPV pseudovirion genomes isolated from A3A-overexpressing cells lack A3 RNA-editing activity further supports a mechanism by which A3 acts as a restriction factor for HPV in a deaminase-dependent fashion [68,69].

Among A3 genes, A3A is the more involved in HPV regulation, whereas A3B seems to have no effect on HPV infection [68]. More specifically, A3A expression negatively correlates with the number of encapsidated pseudovirions [68]. Interestingly, A3A, and also A3C, inhibit viral entry by binding to the HPV L1 capsid protein, suggesting that A3 species acts at different stages of the viral cycle [9].

A physiological process where the interplay between HPV and A3 is even more evident is the cell cycle. While HPV stimulates cell cycle progression through the S-phase, ectopic expression of A3A induces cell cycle arrest, probably as a result of the DNA damage triggered by its cytidine deaminase activity [70–72]. Thus, it seems that A3 can act in two different ways to restrict HPV replication: (i) Directly, by attacking the virus or (ii) indirectly, by inducing cell-cycle arrest. A direct effect of A3 on the HPV genome has been widely demonstrated in both in vitro and in vivo models. In particular, following A3A overexpression, HPV E2 appears to be one of main targets of A3 in the HPV-16$^+$ low-grade CIN (cervical intraepithelial neoplasia) lesion-derived cell line W12 [73] as well as in precancerous cervical lesions [74]. An enrichment of A3 editing events has also been observed in the LCR region of HPV-1$^+$ warts and HPV-16$^+$ precancerous cervical lesions [75,76]. Among A3 transcripts, A3A and A3C were prevalent, while A3B was expressed at a much lower levels in HPV-infected cervix. Given that A3-driven mutations are very frequently detected in CIN1 lesions, it is possible that A3 editing may preferentially occur during stages of productive infection, when HPV virions are being released [77].

In general, the frequency of HPV editing is significantly lower compared to other viruses, such as human immunodeficiency virus 1 (HIV-1) or HBV, which makes deamination an unlikely event during HPV restriction. This would not, however, preclude an involvement of A3 activity in driving HPV evolution through the introduction of variations that would otherwise be lacking in a DNA virus (e.g., HPV) that is duplicated with a much higher fidelity compared to any RNA virus. In this regard, the selective pressure exerted by A3-mediated editing has been proposed as the potential cause of TC dinucleotide depletion in high-risk α-HPV genomes [66]. On the other hand, A3A expression levels are significantly higher in mucosal tissue, the main target of α-HPV, compared to cutaneous skin, where β-HPVs are predominant [66]. Although such mutations may be deleterious for the virus, when they do not affect viral fitness, they might favor viral evasion from immune surveillance, thereby allowing positive selection of viral strains within the host. Thus, the HPV sequences present in cancer cells should not just be regarded as the result of A3 editing activity but also the consequence of the selective pressure against loss/enhancement of host cell fitness. Indeed, sequencing of HPV-16 genomes from 5570 samples representing productive, precancerous, and invasive lesions displayed a remarkable degree of inter-host variation that was more enhanced in productive lesions [78].

Another important aspect that should be considered is how HPVs regulate A3 genes. The first evidence of the existence of such mechanism came from the observation that A3B expression was upregulated by E6/E7 in keratinocytes in vitro [79]. Importantly, E7 from high-risk HPV types was later found to inhibit cullin-RING-based E3 ubiquitin ligase-mediated polyubiquitination and degradation of A3A. Furthermore, A3 genes, especially A3B, were found to be upregulated in precancerous cervical lesions, in good agreement with the aforementioned transactivation by E7 in keratinocytes [68,80,81]. Moreover, A3B upregulation relied on the presence of E6-responsive regions in the A3B promoter, which

in human keratinocytes made it inducible by E6 through the zinc finger protein ZNF384 and the TEA Domain Transcription Factor 4 (TEAD4) [82,83]. An additional piece to this complicated puzzle has been recently added by findings showing that both E6 and E7 from HPV-16 can independently upregulate A3B expression in immortalized keratinocytes, albeit through different mechanisms. E6 degrades p53, thus removing p53 repression of A3B [84], while E7 binds to pRB family members (pRB, p107, and p130) for degradation [85] (Figure 2).
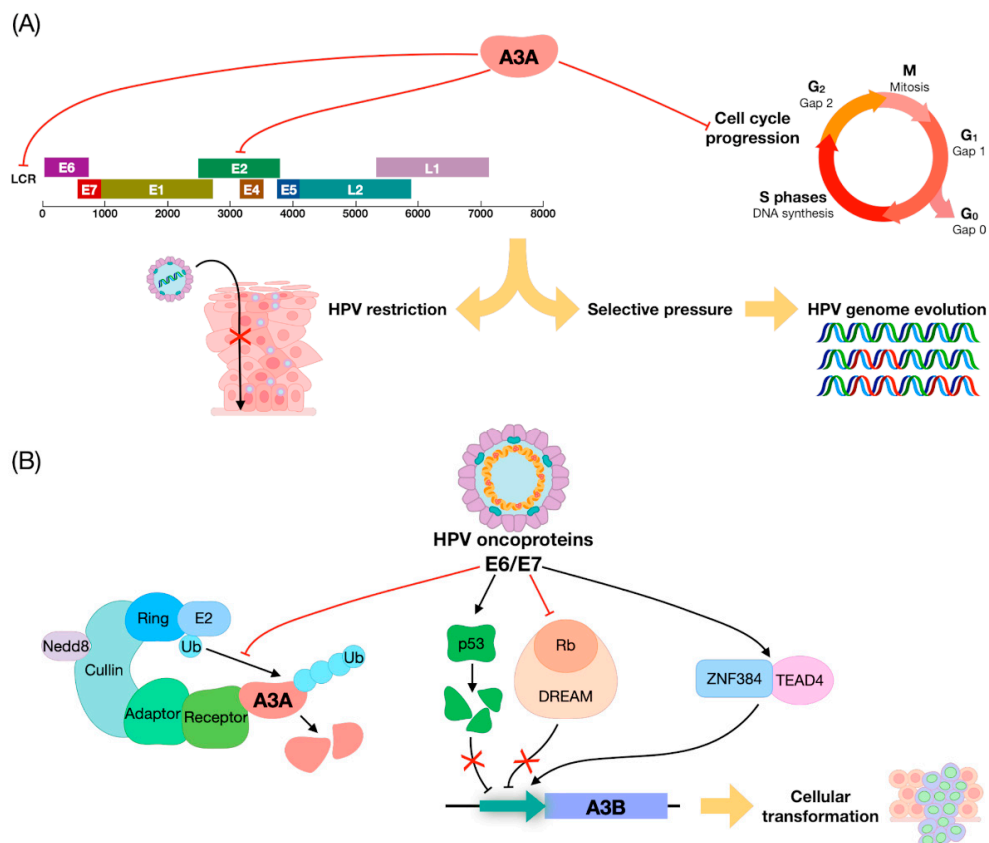

Figure 2. Summary of APOBEC3/HPV interplay. (**A**) Negative regulation exerted by A3A on human papillomavirus (HPV) gene expression and HPV-driven cell-cycle progression, leading to HPV restriction and genome evolution. (**B**) A3 modulation by HPV oncoproteins E6/E7: (i) cullin-RING-based E3 ubiquitin ligase-mediated polyubiquitination followed by A3A degradation; (ii) A3B upregulation through removal of the inhibitory activity exerted by p53 and Rb or through a direct effect of the zinc finger protein ZNF384 and TEAD4 on A3B promoter.

Overall, HPV-mediated upregulation of A3 genes may be linked to the evolutionary advantage that the virus would gain by inducing a certain level of A3 expression. In this regard, it is important to highlight that A3B, unlike A3A, does not inhibit HPV infectivity [68], indicating that the function of A3 in HPV restriction is entirely separate from its editing activity during tumor development, with the former mediated mainly by A3A and/or A3C and A3H, and the latter by A3B.

5. The Role of APOBEC in HNSCC

The hypothesis that APOBEC-driven mutagenesis is linked to cancer development derives from The Cancer Genome Atlas (TCGA) genome analyses showing that 68% of all mutations in bladder, cervical, breast, head and neck, and lung tumors are consistent with an APOBEC mutation pattern, and target cancer driver genes [6].

The functional role of APOBEC in HNSCC pathogenesis is supported by the following lines of evidence, summarized in Table 1.

Among HNSCCs, a higher APOBEC activity has been observed in HPV+ HNSCCs [11,12,86,87]. In particular, while 98% of HPV+ HNSCCs exhibit an APOBEC signature, this latter is only present in 76% of HPV- HNSCCs [86]. Indeed, as mentioned in Section 2 of this review, HPV- HNSCCs display a smoking-associated mutational signature, whereas HPV+ HNSCCs from patients less exposed to external carcinogens harbor a mutation pattern consistent with APOBEC DNA editing. Moreover, as previously discussed, APOBEC activity has been involved in the generation of helical domain hot spot mutations in the PIK3CA gene in HPV+ HNSCC [11].

Another important finding attesting the role of APOBEC in HNSCC development is that APOBEC enrichment directly correlates with the overall mutational burden of HPV+ HNSCC [7,88]. In particular, bioinformatics analysis of tumor exomes, transcriptomes, and germline exomes from 511 HNSCC patients from TCGA revealed a striking correlation between A3A expression and APOBEC mutation rate [7]. Consistently, enhanced expression of A3A was strongly correlated with the rate of HPV integration in oropharyngeal cancer biopsies [89]. Lastly, the observation that HPV16+ tumors have a higher proportion of APOBEC-related mutations compared to HPV33+ tumors (57% vs. 23%) suggests that the extent of APOBEC mutagenesis depends on the HPV serotype [90].

More evidence supporting a pro-tumorigenic role of APOBEC comes from immunohistochemistry and reverse transcription quantitative PCR analyses reporting higher expression levels of A3A and A3B in HPV+ vs. HPV- HNSCCs [12,87,89], with only one immunofluorescence-based study failing to detect enhanced A3 protein expression in HPV+ oropharyngeal cancers [91]. In particular, RT-qPCR of samples from tumor tissues and healthy mucosa showed low mRNA expression levels of A3A and A3B in HPV- HNSCC, whereas their expression was upregulated by 2–100 folds in HPV+ cancers [12]. Similar to A3A, A3H was found to be predominantly upregulated in HPV+ HNSCC [92].

Although A3A and A3B appear to be mainly overexpressed in HPV+ cancer, they have also been found to be upregulated in some subsets of HPV- HNSCCs [93–96]. In addition, the fact that low-grade HPV- oral dysplasia show intermediate levels of A3B protein expression, while high-grade oral dysplasia has much higher A3B protein levels, suggests that this gene may be progressively activated in HPV- oral cancers. Furthermore, the strong positive correlation between nuclear A3B and Ki67 scores observed in these tumors suggests a role of this gene in cell proliferation [95].

Cellular localization and tumor stage also appear to be important determinants of A3 protein expression. Immunohistochemistry of oral squamous cell carcinomas, which are predominantly HPV- tumors, has in fact revealed a more prominent cytoplasmic localization of A3B in a subgroup of tumor cells compared to normal oral epithelial cells, where A3B is mainly localized in the nucleus [96]. Besides A3B, also the expression pattern of AID changes according to tumor stage. In particular, AID expression is more frequently detected in early stage oral squamous cell carcinomas [97]. Moreover, a study on a Taiwanese sample reported a significantly higher expression of A3A in oral tumors carrying A3B-deletion alleles. The frequency of A3B-deletion germline polymorphism was found to be much higher in Taiwan in comparison with TCGA (50% vs. 5.8%). Although HPV status was not assessed, high levels of A3A expression were associated with better overall survival, especially among individuals carrying A3B-deletion alleles [93].

A correlation between APOBEC expression and other genes has been observed in RT-PCR-based investigations [12]. In HPV- HNSCC, statistically significant positive correlations were found between: (i) TP53 expression and A3A and A3F expression; (ii) NOTCH1 expression and A3B and A3F expression; and (iii) PD-L1 expression and A3A expression. In HPV+ HNSCC, positive correlations were found between (a) MET expression and A3A expression; (b) PD-L1 expression and A3F expression; and (c) IFI16 expression and A3A expression. However, following false discovery rate (FDR) adjustment, only the correlation between PD-L1 expression and A3F expression remained significant [12]. Another interesting association is between A3A and estrogen receptor α (ERα) expression in HPV+ oropharyngeal squamous cell carcinomas. In particular, A3A mRNA is induced by estrogen

in HPV$^+$ ERα^+ oropharyngeal carcinoma cells [98]. Lastly, head and neck tumors with high A3H levels exhibit a genome-wide DNA hypomethylation pattern [92].

More importantly, emerging evidence indicates that APOBEC-driven mutagenesis correlates with the initiation of several immune pathways in both HPV$^+$ and HPV$^-$ HN-SCC [7,99]. In particular, the activation of CD8$^+$ T cells was associated with APOBEC mutational burden, even when these cell populations were adjusted for HPV status. Moreover, overall T-cell populations along with eosinophil, dendritic, and cytotoxic cells and B-cell subsets correlated with APOBEC mutational burden. Interestingly, among these populations, cytotoxic T cells displayed the strongest correlation rate in HPV$^-$ HNSCC but were not associated with age and smoking, two well-established mutational signatures in HNSCC (see Section 2) [99]. Globally, such results demonstrate that APOBEC has a role in immune response, not only in HPV$^+$ HNSCC, but also in a subset of HPV$^-$ tumors.

HPV$^+$ HNSCC had the highest levels of IFN-γ, which is known to upregulate PD-L1 in tumors [100]. The fact that PD-L1 expression in HNSCC correlates with APOBEC mutations supports a potential role of APOBEC-dependent mutagenesis in immune checkpoint inhibition in cancer cells [12,100]. Indeed, tumor specific neoantigens (i.e., mutation-derived class I binding neoantigens), which correlates with response to immunotherapy, have been found to be significantly associated with APOBEC mutational burden, contrary to other sources of neoantigens [100]. Another important correlation found in HPV$^+$ HNSCC involves A3H expression and activation of the immune response. Specifically, A3H was shown to demethylate and upregulate CXCL10, thereby enhancing CD8$^+$ T cell tumor infiltration [92]. Lastly, an APOBEC-enriched subgroup with higher T-cell inflammation and immune checkpoint expression has been identified in HPV$^-$ HNSCC [99]. Globally, these results suggest a role of APOBEC in the response to cancer immunotherapy.

Survival analyses have shown that some members of APOBEC family affec overall survival (OS) [12,92,101]. In HPV$^+$ HNSCC, higher A3G or A3H expression correlates with better OS [92,101]. Moreover, APOBEC3s knockdown in HNSCC cells results in resistance to cisplatin and carboplatin as well as in increased rates of cisplatin-induced interstrand crosslink removal in HNSCC cells. These data support the hypothesis that APOBEC3s activate base excision repair in HNSCC, mediate repair of cisplatin-induced interstrand crosslinks, and consequently sensitize cells to cisplatin. Such effects contribute to the improved treatment responses observed in HPV$^+$ HNSCC patients [101]. On the other hand, in HPV$^-$ HNSCC, upregulation of A3F gene expression correlated with a worse prognosis, and patients displaying stable A3H expression levels had a lower OS [12]. The different impact of A3H expression on OS in HPV$^+$ vs. HPV$^-$ cancer patients may be related to the different mutational burden in these two tumor subgroups. Further studies are clearly needed to better understand this particular feature of A3H.

Table 1. Main features and role of APOBEC in HPV$^+$ and HPV$^-$ head and neck squamous cell carcinoma (HNSCC).

HPV$^+$	HPV$^-$
- Upregulation of A3A, A3B and A3H [12,87,89,92]. - Positive correlation with mutational burden [7,88,90]. - Generation of helical domain hot spot mutations in the PIK3CA gene [11]. - Correlation between A3A expression and integration of HPV DNA [89]. - Positive correlation between: PD-L1 and A3F expression [12,100]; A3A and Erα [98], IFI16 and MET [12] expression. - Association between A3H expression levels and genome-wide DNA hypomethylation pattern [92]. - Positive correlation between A3H and CD8$^+$ T cell infiltration [92]. - Higher A3G or A3H expression correlates with better overall survival [92,101].	- Upregulation of A3A and A3B in some subsets of tumors [93–96]. - Positive correlation between: A3A and A3F and TP53; A3B and A3F and TP53; A3A and PDL1 [12]; A3B and Ki67 [95]. - Higher T cell inflammation and immune checkpoint expression in an APOBEC-enriched subgroup [99]. - A3F upregulation correlates with a worse prognosis, whereas patients without changes in A3H expression have a lower overall survival [12].

6. Conclusions and Future Perspectives

In conclusion, emerging evidence from recent biochemical and bioinformatic analyses supports a functional role of APOBEC family members in both HPV+ and HPV- HNSCC pathogenesis. In particular, two of these genes, A3A and A3B, show distinct mutational signatures, with the former conferring a smoking-associated mutational signature to HPV- cancers, and the latter mainly acting as generator of driver mutations in HPV+ HNSCC under reduced exposure to exogenous carcinogens. In addition to influencing the mutational burden of cancer cells, APOBEC-driven mutagenesis is being increasingly involved in cancer immune response, cisplatin sensibility, and overall survival. The key finding that emerges from this review is that HNSCC patients with higher APOBEC expression levels tend to have a better response to chemotherapy and immunotherapy, which, given the positive correlation between HPV and A3 gene expression, may help explain the better survival of HPV+ vs. HPV- cancer patients. Further studies are thus urgently needed to conclusively determine whether A3 genes, especially A3H, are potential predictive biomarkers for cancer immunotherapy.

Author Contributions: G.R., V.D. and M.B. developed the ideas and drafted the manuscript. G.R., V.D., M.B., F.G. and S.P. wrote sections of the manuscript. C.A. and S.F.C.P. drew the figures. S.L. and G.P. critically reviewed the manuscript. All authors have read and agreed to the published version of the manuscript.

Conflicts of Interest: The authors declare no conflict of interest.

References

1. McDermott, J.D.; Bowles, D.W. Epidemiology of Head and Neck Squamous Cell Carcinomas: Impact on Staging and Prevention Strategies. *Curr. Treat. Options Oncol.* **2019**, *20*, 1–13. [CrossRef] [PubMed]
2. Chaturvedi, A.K.; Engels, E.A.; Pfeiffer, R.M.; Hernandez, B.Y.; Xiao, W.; Kim, E.; Jiang, B.; Goodman, M.T.; Sibug-Saber, M.; Cozen, W.; et al. Human papillomavirus and rising oropharyngeal cancer incidence in the United States. *J. Clin. Oncol.* **2011**, *29*, 4294–4301. [CrossRef] [PubMed]
3. Thariat, J.; Vignot, S.; Lapierre, A.; Falk, A.T.; Guigay, J.; Van Obberghen-Schilling, E.; Milano, G. Integrating genomics in head and neck cancer treatment: Promises and pitfalls. *Crit. Rev. Oncol. Hematol.* **2015**, *95*, 397–406. [CrossRef] [PubMed]
4. Lampri, E.S.; Chondrogiannis, G.; Ioachim, E.; Varouktsi, A.; Mitselou, A.; Galani, A.; Briassoulis, E.; Kanavaros, P.; Galani, V. Biomarkers of head and neck cancer, tools or a gordian knot? *Int. J. Clin. Exp. Med.* **2015**, *8*, 10340–10357. [PubMed]
5. Kuong, K.J.; Loeb, L.A. APOBEC3B mutagenesis in cancer. *Nat. Genet.* **2013**, *45*, 964–965. [CrossRef] [PubMed]
6. Roberts, S.A.; Lawrence, M.S.; Klimczak, L.J.; Grimm, S.A.; Fargo, D.; Stojanov, P.; Kiezun, A.; Kryukov, G.V.; Carter, S.L.; Saksena, G.; et al. An APOBEC cytidine deaminase mutagenesis pattern is widespread in human cancers. *Nat. Genet.* **2013**, *45*, 970–976. [CrossRef]
7. Faden, D.L.; Thomas, S.; Cantalupo, P.G.; Agrawal, N.; Myers, J.; DeRisi, J. Multi-modality analysis supports APOBEC as a major source of mutations in head and neck squamous cell carcinoma. *Oral Oncol.* **2017**, *74*, 8–14. [CrossRef] [PubMed]
8. Conticello, S.G. The AID/APOBEC family of nucleic acid mutators. *Genome Biol.* **2008**, *9*, 1–10. [CrossRef]
9. Monjurul, A.M.; Wakae, K.; Wang, Z.; Kitamura, K.; Liu, G.; Koura, M.; Imayasu, M.; Sakamoto, N.; Hanaoka, K.; Nakamura, M.; et al. APOBEC3A and 3C decrease human papillomavirus 16 pseudovirion infectivity. *Biochem. Biophys. Res. Commun.* **2015**, *457*, 295–299.
10. Pautasso, S.; Galitska, G.; Dell'Oste, V.; Biolatti, M.; Cagliani, R.; Forni, D.; De Andrea, M.; Gariglio, M.; Sironi, M.; Landolfo, S. Strategy of Human Cytomegalovirus to Escape Interferon Beta-Induced APOBEC3G Editing Activity. *J. Virol.* **2018**, *92*. [CrossRef]
11. Henderson, S.; Chakravarthy, A.; Su, X.; Boshoff, C.; Fenton, T.R. APOBEC-Mediated Cytosine Deamination Links PIK3CA Helical Domain Mutations to Human Papillomavirus-Driven Tumor Development. *Cell Rep.* **2014**, *7*, 1833–1841. [CrossRef] [PubMed]
12. Riva, G.; Pecorari, G.; Biolatti, M.; Pautasso, S.; Lo Cigno, I.; Garzaro, M.; Dell'Oste, V.; Landolfo, S. PYHIN genes as potential biomarkers for prognosis of human papillomavirus-positive or -negative head and neck squamous cell carcinomas. *Mol. Biol. Rep.* **2019**, *46*, 3333–3347. [CrossRef] [PubMed]
13. Riva, G.; Biolatti, M.; Pecorari, G.; Dell'Oste, V.; Landolfo, S. PYHIN Proteins and HPV: Role in the Pathogenesis of Head and Neck Squamous Cell Carcinoma. *Microorganisms* **2019**, *8*, 14. [CrossRef] [PubMed]

14. Castellsagué, X.; Alemany, L.; Quer, M.; Halec, G.; Quirós, B.; Tous, S.; Clavero, O.; Alòs, L.; Biegner, T.; Szafarowski, T.; et al. HPV Involvement in Head and Neck Cancers: Comprehensive Assessment of Biomarkers in 3680 Patients. *J. Natl. Cancer Inst.* **2016**, *108*, djv403. [CrossRef] [PubMed]

15. Kreimer, A.R.; Clifford, G.M.; Boyle, P.; Franceschi, S. Human papillomavirus types in head and neck squamous cell carcinomas worldwide: A systemic review. *Cancer Epidemiol. Biomarkers Prev.* **2005**, *14*, 467–475. [CrossRef]

16. Kang, H.; Kiess, A.; Chung, C.H. Emerging biomarkers in head and neck cancer in the era of genomics. *Nat. Rev. Clin. Oncol.* **2015**, *12*, 11–26. [CrossRef]

17. Braakhuis, B.J.M.; Snijders, P.J.F.; Keune, W.J.H.; Meijer, C.J.L.M.; Ruijter-Schippers, H.J.; Leemans, C.R.; Brakenhoff, R.H. Genetic patterns in head and neck cancers that contain or lack transcriptionally active human papillomavirus. *J. Natl. Cancer Inst.* **2004**, *96*, 998–1006. [CrossRef]

18. Slebos, R.J.C.; Yi, Y.; Ely, K.; Carter, J.; Evjen, A.; Zhang, X.; Shyr, Y.; Murphy, B.M.; Cmelak, A.J.; Burkey, B.B.; et al. Gene expression differences associated with human papillomavirus status in head and neck squamous cell carcinoma. *Clin. Cancer Res.* **2006**, *12*, 701–709. [CrossRef]

19. Lawrence, M.S.; Sougnez, C.; Lichtenstein, L.; Cibulskis, K.; Lander, E.; Gabriel, S.B.; Getz, G.; Ally, A.; Balasundaram, M.; Birol, I.; et al. Comprehensive genomic characterization of head and neck squamous cell carcinomas. *Nature* **2015**, *517*, 576–582.

20. Sahin, A.A.; Gilligan, T.D.; Caudell, J.J. Challenges With the 8th Edition of the AJCC Cancer Staging Manual for Breast, Testicular, and Head and Neck Cancers. *J. Natl. Compr. Canc. Netw.* **2019**, *17*, 560–564.

21. Colevas, A.D.; Yom, S.S.; Pfister, D.G.; Spencer, S.; Adelstein, D.; Adkins, D.; Brizel, D.M.; Burtness, B.; Busse, P.M.; Caudell, J.J.; et al. NCCN guidelines ®insights: Head and neck cancers, version 1.2018 featured updates to the NCCN guidelines. *JNCCN J. Natl. Compr. Cancer Netw.* **2018**, *16*, 479–490. [CrossRef] [PubMed]

22. D'Souza, G.; Kreimer, A.R.; Viscidi, R.; Pawlita, M.; Fakhry, C.; Koch, W.M.; Westra, W.H.; Gillison, M.L. Case–Control Study of Human Papillomavirus and Oropharyngeal Cancer. *N. Engl. J. Med.* **2007**, *356*, 1944–1956. [CrossRef] [PubMed]

23. Ndiaye, C.; Mena, M.; Alemany, L.; Arbyn, M.; Castellsagué, X.; Laporte, L.; Bosch, F.X.; de Sanjosé, S.; Trottier, H. HPV DNA, E6/E7 mRNA, and p16INK4a detection in head and neck cancers: A systematic review and meta-analysis. *Lancet Oncol.* **2014**, *15*, 1319–1331. [CrossRef]

24. Steenbergen, R.D.M.; Snijders, P.J.F.; Heideman, D.A.M.; Meijer, C.J.L.M. Clinical implications of (epi)genetic changes in HPV-induced cervical precancerous lesions. *Nat. Rev. Cancer* **2014**, *14*, 395–405. [CrossRef] [PubMed]

25. Meshman, J.; Wang, P.C.; Chin, R.; John, M.S.; Abemayor, E.; Bhuta, S.; Chen, A.M. Prognostic significance of p16 in squamous cell carcinoma of the larynx and hypopharynx. *Am. J. Otolaryngol. Head Neck Med. Surg.* **2017**, *38*, 31–37. [CrossRef] [PubMed]

26. Young, R.J.; Urban, D.; Angel, C.; Corry, J.; Lyons, B.; Vallance, N.; Kleid, S.; Iseli, T.A.; Solomon, B.; Rischin, D. Frequency and prognostic significance of p16 INK4A protein overexpression and transcriptionally active human papillomavirus infection in laryngeal squamous cell carcinoma. *Br. J. Cancer* **2015**, *112*, 1098–1104. [CrossRef]

27. Tabor, M.P.; Brakenhoff, R.H.; Ruijter-Schippers, H.J.; Van der Wal, J.E.; Snow, G.B.; Leemans, C.R.; Braakhuis, B.J.M. Multiple head and neck tumors frequently originate from a single preneoplastic lesion. *Am. J. Pathol.* **2002**, *161*, 1051–1060. [CrossRef]

28. Leemans, C.R.; Braakhuis, B.J.M.; Brakenhoff, R.H. The molecular biology of head and neck cancer. *Nat. Rev. Cancer* **2011**, *11*, 9–22. [CrossRef]

29. Kumar, B.; Cordell, K.G.; Lee, J.S.; Worden, F.P.; Prince, M.E.; Tran, H.H.; Wolf, G.T.; Urba, S.G.; Chepeha, D.B.; Teknos, T.N.; et al. EGFR, p16, HPV titer, Bcl-xL and p53, sex, and smoking as indicators of response to therapy and survival in oropharyngeal cancer. *J. Clin. Oncol.* **2008**, *26*, 3128–3137. [CrossRef]

30. Alsner, J.; Sørensen, S.B.; Overgaard, J. TP53 mutation is related to poor prognosis after radiotherapy, but not surgery, in squamous cell carcinoma of the head and neck. *Radiother. Oncol.* **2001**, *59*, 179–185. [CrossRef]

31. Agrawal, N.; Frederick, M.J.; Pickering, C.R.; Bettegowda, C.; Chang, K.; Li, R.J.; Fakhry, C.; Xie, T.X.; Zhang, J.; Wang, J.; et al. Exome sequencing of head and neck squamous cell carcinoma reveals inactivating mutations in NOTCH1. *Science (80-.)* **2011**, *333*, 1154–1157. [CrossRef] [PubMed]

32. Normanno, N.; De Luca, A.; Bianco, C.; Strizzi, L.; Mancino, M.; Maiello, M.R.; Carotenuto, A.; De Feo, G.; Caponigro, F.; Salomon, D.S. Epidermal growth factor receptor (EGFR) signaling in cancer. *Gene* **2006**, *366*, 2–16. [CrossRef] [PubMed]

33. Jiang, X.; Ye, J.; Dong, Z.; Hu, S.; Xiao, M. Novel genetic alterations and their impact on target therapy response in head and neck squamous cell carcinoma. *Cancer Manag. Res.* **2019**, *11*, 1321. [CrossRef] [PubMed]

34. Stransky, N.; Egloff, A.M.; Tward, A.D.; Kostic, A.D.; Cibulskis, K.; Sivachenko, A.; Kryukov, G.V.; Lawrence, M.S.; Sougnez, C.; McKenna, A.; et al. The mutational landscape of head and neck squamous cell carcinoma. *Science (80-.)* **2011**, *333*, 1157–1160. [CrossRef] [PubMed]

35. Kandoth, C.; McLellan, M.D.; Vandin, F.; Ye, K.; Niu, B.; Lu, C.; Xie, M.; Zhang, Q.; McMichael, J.F.; Wyczalkowski, M.A.; et al. Mutational landscape and significance across 12 major cancer types. *Nature* **2013**, *502*, 333–339. [CrossRef] [PubMed]

36. Hayes, D.N.; Van Waes, C.; Seiwert, T.Y. Genetic landscape of human papillomavirus-associated head and neck cancer and comparison to tobacco-related tumors. *J. Clin. Oncol.* **2015**, *33*, 3227–3234. [CrossRef]

37. Rebhandl, S.; Huemer, M.; Greil, R.; Geisberger, R. AID/APOBEC deaminases and cancer. *Oncoscience* **2015**, *2*, 320–333. [CrossRef]

38. Vieira, V.C.; Soares, M.A. The role of cytidine deaminases on innate immune responses against human viral infections. *Biomed. Res. Int.* **2013**, *2013*. [CrossRef]

39. Revathidevi, S.; Murugan, A.K.; Nakaoka, H.; Inoue, I.; Munirajan, A.K. APOBEC: A molecular driver in cervical cancer pathogenesis. *Cancer Lett.* **2021**, *496*, 104–116. [CrossRef]

40. Siriwardena, S.U.; Chen, K.; Bhagwat, A.S. Functions and Malfunctions of Mammalian DNA-Cytosine Deaminases. *Chem. Rev.* **2016**, *116*, 12688–12710. [CrossRef]

41. Salter, J.D.; Bennett, R.P.; Smith, H.C. The APOBEC Protein Family: United by Structure, Divergent in Function. *Trends Biochem. Sci.* **2016**, *41*, 578–594. [CrossRef] [PubMed]

42. Betts, L.; Xiang, S.; Short, S.A.; Wolfenden, R.; Carter, C.W. Cytidine deaminase. the 2.3 Å crystal structure of an enzyme: Transition-state analog complex. *J. Mol. Biol.* **1994**, *235*, 635–656. [CrossRef] [PubMed]

43. Li, J.; Chen, Y.; Li, M.; Carpenter, M.A.; McDougle, R.M.; Luengas, E.M.; Macdonald, P.J.; Harris, R.S.; Mueller, J.D. APOBEC3 multimerization correlates with HIV-1 packaging and restriction activity in living cells. *J. Mol. Biol.* **2014**, *426*, 1296–1307. [CrossRef] [PubMed]

44. Brar, S.S.; Sacho, E.J.; Tessmer, I.; Croteau, D.L.; Erie, D.A.; Diaz, M. Activation-induced deaminase, AID, is catalytically active as a monomer on single-stranded DNA. *DNA Repair (Amst)* **2008**, *7*, 77–87. [CrossRef] [PubMed]

45. Navaratnam, N.; Sarwar, R. An overview of cytidine deaminases. *Int. J. Hematol.* **2006**, *83*, 195–200. [CrossRef]

46. Suda, K.; Nakaoka, H.; Yoshihara, K.; Ishiguro, T.; Tamura, R.; Mori, Y.; Yamawaki, K.; Adachi, S.; Takahashi, T.; Kase, H.; et al. Clonal Expansion and Diversification of Cancer-Associated Mutations in Endometriosis and Normal Endometrium. *Cell Rep.* **2018**, *24*, 1777–1789. [CrossRef]

47. Moore, L.; Leongamornlert, D.; Coorens, T.H.H.; Sanders, M.A.; Ellis, P.; Dentro, S.C.; Dawson, K.J.; Butler, T.; Rahbari, R.; Mitchell, T.J.; et al. The mutational landscape of normal human endometrial epithelium. *Nature* **2020**, *580*, 640–646. [CrossRef]

48. Greenman, C.; Stephens, P.; Smith, R.; Dalgliesh, G.L.; Hunter, C.; Bignell, G.; Davies, H.; Teague, J.; Butler, A.; Stevens, C.; et al. Patterns of somatic mutation in human cancer genomes. *Nature* **2007**, *446*, 153–158. [CrossRef]

49. Nik-Zainal, S.; Davies, H.; Staaf, J.; Ramakrishna, M.; Glodzik, D.; Zou, X.; Martincorena, I.; Alexandrov, L.B.; Martin, S.; Wedge, D.C.; et al. Landscape of somatic mutations in 560 breast cancer whole-genome sequences. *Nature* **2016**, *534*, 47–54. [CrossRef]

50. Alexandrov, L.B.; Nik-Zainal, S.; Wedge, D.C.; Aparicio, S.A.J.R.; Behjati, S.; Biankin, A.V.; Bignell, G.R.; Bolli, N.; Borg, A.; Børresen-Dale, A.L.; et al. Signatures of mutational processes in human cancer. *Nature* **2013**, *500*, 415–421. [CrossRef]

51. Burns, M.B.; Lackey, L.; Carpenter, M.A.; Rathore, A.; Land, A.M.; Leonard, B.; Refsland, E.W.; Kotandeniya, D.; Tretyakova, N.; Nikas, J.B.; et al. APOBEC3B is an enzymatic source of mutation in breast cancer. *Nature* **2013**, *494*, 366–370. [CrossRef] [PubMed]

52. Carty, M.; Guy, C.; Bowie, A.G. Detection of viral infections by innate immunity. *Biochem. Pharmacol.* **2020**, *183*, 114316. [CrossRef] [PubMed]

53. Smith, N.J.; Fenton, T.R. The APOBEC3 genes and their role in cancer: Insights from human papillomavirus. *J. Mol. Endocrinol.* **2019**, *62*, R269–R287. [CrossRef] [PubMed]

54. Stavrou, S.; Ross, S.R. APOBEC3 Proteins in Viral Immunity. *J. Immunol.* **2015**, *195*, 4565–4570. [CrossRef] [PubMed]

55. Sheehy, A.M.; Gaddis, N.C.; Choi, J.D.; Malim, M.H. Isolation of a human gene that inhibits HIV-1 infection and is suppressed by the viral Vif protein. *Nature* **2002**, *418*, 646–650. [CrossRef]

56. Narvaiza, I.; Linfesty, D.C.; Greener, B.N.; Hakata, Y.; Pintel, D.J.; Logue, E.; Landau, N.R.; Weitzman, M.D. Deaminase-independent inhibition of parvoviruses by the APOBEC3A cytidine deaminase. *PLoS Pathog.* **2009**, *5*, e1000439. [CrossRef]

57. Turelli, P.; Mangeat, B.; Jost, S.; Vianin, S.; Trono, D. Inhibition of Hepatitis B Virus Replication by APOBEC3G. *Science (80-.)* **2004**, *303*, 1829. [CrossRef]

58. Suspène, R.; Guétard, D.; Henry, M.; Sommer, P.; Wain-Hobson, S.; Vartanian, J.P. Extensive editing of both hepatitis B virus DNA strands by APOBEC3 cytidine deaminases in vitro and in vivo. *Proc. Natl. Acad. Sci. USA* **2005**, *102*, 8321–8326. [CrossRef]

59. Peretti, A.; Geoghegan, E.M.; Pastrana, D.V.; Smola, S.; Feld, P.; Sauter, M.; Lohse, S.; Ramesh, M.; Lim, E.S.; Wang, D.; et al. Characterization of BK Polyomaviruses from Kidney Transplant Recipients Suggests a Role for APOBEC3 in Driving In-Host Virus Evolution. *Cell Host Microbe* **2018**, *23*, 628–635.e7. [CrossRef]

60. Verhalen, B.; Starrett, G.J.; Harris, R.S.; Jiang, M. Functional Upregulation of the DNA Cytosine Deaminase APOBEC3B by Polyomaviruses. *J. Virol.* **2016**, *90*, 6379–6386. [CrossRef]

61. Suspene, R.; Aynaud, M.-M.; Koch, S.; Pasdeloup, D.; Labetoulle, M.; Gaertner, B.; Vartanian, J.-P.; Meyerhans, A.; Wain-Hobson, S. Genetic Editing of Herpes Simplex Virus 1 and Epstein-Barr Herpesvirus Genomes by Human APOBEC3 Cytidine Deaminases in Culture and In Vivo. *J. Virol.* **2011**, *85*, 7594–7602. [CrossRef] [PubMed]

62. Weisblum, Y.; Oiknine-Djian, E.; Zakay-Rones, Z.; Vorontsov, O.; Haimov-Kochman, R.; Nevo, Y.; Stockheim, D.; Yagel, S.; Panet, A.; Wolf, D.G. APOBEC3A Is Upregulated by Human Cytomegalovirus (HCMV) in the Maternal-Fetal Interface, Acting as an Innate Anti-HCMV Effector. *J. Virol.* **2017**, *91*. [CrossRef] [PubMed]

63. Cheng, A.Z.; Yockteng-Melgar, J.; Jarvis, M.C.; Malik-Soni, N.; Borozan, I.; Carpenter, M.A.; McCann, J.L.; Ebrahimi, D.; Shaban, N.M.; Marcon, E.; et al. Epstein–Barr virus BORF2 inhibits cellular APOBEC3B to preserve viral genome integrity. *Nat. Microbiol.* **2019**, *4*, 78–88. [CrossRef] [PubMed]

64. Cheng, A.Z.; Moraes, S.N.; Attarian, C.; Yockteng-Melgar, J.; Jarvis, M.C.; Biolatti, M.; Galitska, G.; Dell'Oste, V.; Frappier, L.; Bierle, C.J.; et al. A Conserved Mechanism of APOBEC3 Relocalization by Herpesviral Ribonucleotide Reductase Large Subunits. *J. Virol.* **2019**, *93*. [CrossRef] [PubMed]

65. Di Giorgio, S.; Martignano, F.; Torcia, M.G.; Mattiuz, G.; Conticello, S.G. Evidence for host-dependent RNA editing in the transcriptome of SARS-CoV-2. *Sci. Adv.* **2020**, *6*, eabb5813. [CrossRef] [PubMed]

66. Warren, C.J.; Westrich, J.A.; Van Doorslaer, K.; Pyeon, D. Roles of APOBEC3A and APOBEC3B in human papillomavirus infection and disease progression. *Viruses* **2017**, *9*, 233. [CrossRef] [PubMed]

67. Pyeon, D.; Lambert, P.F.; Ahlquist, P. Production of infectious human papillomavirus independently of viral replication and epithelial cell differentiation. *Proc. Natl. Acad. Sci. USA* **2005**, *102*, 9311–9316. [CrossRef]

68. Warren, C.J.; Xu, T.; Guo, K.; Griffin, L.M.; Westrich, J.A.; Lee, D.; Lambert, P.F.; Santiago, M.L.; Pyeon, D. APOBEC3A Functions as a Restriction Factor of Human Papillomavirus. *J. Virol.* **2015**, *89*, 688–702. [CrossRef]

69. Sharma, S.; Patnaik, S.K.; Thomas Taggart, R.; Kannisto, E.D.; Enriquez, S.M.; Gollnick, P.; Baysal, B.E. APOBEC3A cytidine deaminase induces RNA editing in monocytes and macrophages. *Nat. Commun.* **2015**, *6*, 1–15. [CrossRef]

70. Landry, S.; Narvaiza, I.; Linfesty, D.C.; Weitzman, M.D. APOBEC3A can activate the DNA damage response and cause cell-cycle arrest. *EMBO Rep.* **2011**, *12*, 444–450. [CrossRef]

71. Land, A.M.; Law, E.K.; Carpenter, M.A.; Lackey, L.; Brown, W.L.; Harris, R.S. Endogenous APOBEC3A DNA cytosine deaminase is cytoplasmic and nongenotoxic. *J. Biol. Chem.* **2013**, *288*, 17253–17260. [CrossRef] [PubMed]

72. Mussil, B.; Suspène, R.; Aynaud, M.M.; Gauvrit, A.; Vartanian, J.P.; Wain-Hobson, S. Human APOBEC3A Isoforms Translocate to the Nucleus and Induce DNA Double Strand Breaks Leading to Cell Stress and Death. *PLoS ONE* **2013**, *8*, e73641. [CrossRef] [PubMed]

73. Stanley, M.A.; Browne, H.M.; Appleby, M.; Minson, A.C. Properties of a non-tumorigenic human cervical keratinocyte cell line. *Int. J. Cancer* **1989**, *43*, 672–676. [CrossRef] [PubMed]

74. Kukimoto, I.; Mori, S.; Aoyama, S.; Wakae, K.; Muramatsu, M.; Kondo, K. Hypermutation in the E2 gene of human papillomavirus type 16 in cervical intraepithelial neoplasia. *J. Med. Virol.* **2015**, *87*, 1754–1760. [CrossRef] [PubMed]

75. Vartanian, J.P.; Guétard, D.; Henry, M.; Wain-Hobson, S. Evidence for editing of human papillomavirus DNA by APOBEC3 in benign and precancerous lesions. *Science (80-.)* **2008**, *320*, 230–233. [CrossRef] [PubMed]

76. Wang, Z.; Wakae, K.; Kitamura, K.; Aoyama, S.; Liu, G.; Koura, M.; Monjurul, A.M.; Kukimoto, I.; Muramatsu, M. APOBEC3 Deaminases Induce Hypermutation in Human Papillomavirus 16 DNA upon Beta Interferon Stimulation. *J. Virol.* **2014**, *88*, 1308–1317. [CrossRef]

77. Hirose, Y.; Onuki, M.; Tenjimbayashi, Y.; Mori, S.; Ishii, Y.; Takeuchi, T.; Tasaka, N.; Satoh, T.; Morisada, T.; Iwata, T.; et al. Within-Host Variations of Human Papillomavirus Reveal APOBEC Signature Mutagenesis in the Viral Genome. *J. Virol.* **2018**, *92*. [CrossRef]

78. Mirabello, L.; Yeager, M.; Yu, K.; Clifford, G.M.; Xiao, Y.; Zhu, B.; Cullen, M.; Boland, J.F.; Wentzensen, N.; Nelson, C.W.; et al. HPV16 E7 Genetic Conservation Is Critical to Carcinogenesis. *Cell* **2017**, *170*, 1164–1174.e6. [CrossRef]

79. Westrich, J.A.; Warren, C.J.; Klausner, M.J.; Guo, K.; Liu, C.-W.; Santiago, M.L.; Pyeon, D. Human Papillomavirus 16 E7 Stabilizes APOBEC3A Protein by Inhibiting Cullin 2-Dependent Protein Degradation. *J. Virol.* **2018**, *92*. [CrossRef]

80. Chakravarthy, A.; Henderson, S.; Thirdborough, S.M.; Ottensmeier, C.H.; Su, X.; Lechner, M.; Feber, A.; Thomas, G.J.; Fenton, T.R. Human papillomavirus drives tumor development throughout the head and neck: Improved prognosis is associated with an immune response largely restricted to the Oropharynx. *J. Clin. Oncol.* **2016**, *34*, 4132–4141. [CrossRef]

81. Vieira, V.C.; Leonard, B.; White, E.A.; Starrett, G.J.; Temiz, N.A.; Lorenz, L.D.; Lee, D.; Soares, M.A.; Lambert, P.F.; Howley, P.M.; et al. Human papillomavirus E6 triggers upregulation of the antiviral and cancer genomic DNA deaminase APOBEC3B. *MBio* **2014**, *5*. [CrossRef] [PubMed]

82. Mori, S.; Takeuchi, T.; Ishii, Y.; Yugawa, T.; Kiyono, T.; Nishina, H.; Kukimoto, I. Human Papillomavirus 16 E6 Upregulates APOBEC3B via the TEAD Transcription Factor. *J. Virol.* **2017**, *91*. [CrossRef] [PubMed]

83. Mori, S.; Takeuchi, T.; Ishii, Y.; Kukimoto, I. Identification of APOBEC3B promoter elements responsible for activation by human papillomavirus type 16 E6. *Biochem. Biophys. Res. Commun.* **2015**, *460*, 555–560. [CrossRef] [PubMed]

84. Fischer, M.; Steiner, L.; Engeland, K. The transcription factor p53: Not a repressor, solely an activator. *Cell Cycle* **2014**, *13*, 3037–3058. [CrossRef] [PubMed]

85. Periyasamy, M.; Singh, A.K.; Gemma, C.; Kranjec, C.; Farzan, R.; Leach, D.A.; Navaratnam, N.; Pálinkás, H.L.; Vertessy, B.G.; Fenton, T.R.; et al. P53 controls expression of the DNA deaminase APOBEC3B to limit its potential mutagenic activity in cancer cells. *Nucleic Acids Res.* **2017**, *45*, 11056–11069. [CrossRef] [PubMed]

86. Cannataro, V.L.; Gaffney, S.G.; Sasaki, T.; Issaeva, N.; Grewal, N.K.S.; Grandis, J.R.; Yarbrough, W.G.; Burtness, B.; Anderson, K.S.; Townsend, J.P. APOBEC-induced mutations and their cancer effect size in head and neck squamous cell carcinoma. *Oncogene* **2019**, *38*, 3475–3487. [CrossRef] [PubMed]

87. Qin, T.; Zhang, Y.; Zarins, K.R.; Jones, T.R.; Virani, S.; Peterson, L.A.; McHugh, J.B.; Chepeha, D.; Wolf, G.T.; Rozek, L.S.; et al. Expressed HNSCC variants by HPV-status in a well-characterized Michigan cohort. *Sci. Rep.* **2018**, *8*, 1–11. [CrossRef] [PubMed]

88. Gillison, M.L.; Akagi, K.; Xiao, W.; Jiang, B.; Pickard, R.K.L.; Li, J.; Swanson, B.J.; Agrawal, A.D.; Zucker, M.; Stache-Crain, B.; et al. Human papillomavirus and the landscape of secondary genetic alterations in oral cancers. *Genome Res.* **2019**, *29*, 1–17. [CrossRef]

89. Kondo, S.; Wakae, K.; Wakisaka, N.; Nakanishi, Y.; Ishikawa, K.; Komori, T.; Moriyama-Kita, M.; Endo, K.; Murono, S.; Wang, Z.; et al. APOBEC3A associates with human papillomavirus genome integration in oropharyngeal cancers. *Oncogene* **2017**, *36*, 1687–1697. [CrossRef]

90. Chatfield-Reed, K.; Gui, S.; O'Neill, W.Q.; Teknos, T.N.; Pan, Q. HPV33+ HNSCC is associated with poor prognosis and has unique genomic and immunologic landscapes. *Oral Oncol.* **2020**, *100*, 104488. [CrossRef]

91. Kono, T.; Hoover, P.; Poropatich, K.; Paunesku, T.; Mittal, B.B.; Samant, S.; Laimins, L.A. Activation of DNA damage repair factors in HPV positive oropharyngeal cancers. *Virology* **2020**, *547*, 27–34. [CrossRef] [PubMed]

92. Liu, Q.; Luo, Y.W.; Cao, R.Y.; Pan, X.; Chen, X.J.; Zhang, S.Y.; Zhang, W.L.; Zhou, J.Y.; Cheng, B.; Ren, X.Y. Association between APOBEC3H-Mediated Demethylation and Immune Landscape in Head and Neck Squamous Carcinoma. *Biomed. Res. Int.* **2020**, *2020*. [CrossRef] [PubMed]

93. Chen, T.W.; Lee, C.C.; Liu, H.; Wu, C.S.; Pickering, C.R.; Huang, P.J.; Wang, J.; Chang, I.Y.F.; Yeh, Y.M.; Chen, C.D.; et al. APOBEC3A is an oral cancer prognostic biomarker in Taiwanese carriers of an APOBEC deletion polymorphism. *Nat. Commun.* **2017**, *8*, 1–13. [CrossRef] [PubMed]

94. Cho, R.J.; Alexandrov, L.B.; Den Breems, N.Y.; Atanasova, V.S.; Farshchian, M.; Purdom, E.; Nguyen, T.N.; Coarfa, C.; Rajapakshe, K.; Prisco, M.; et al. APOBEC mutation drives early-onset squamous cell carcinomas in recessive dystrophic epidermolysis bullosa. *Sci. Transl. Med.* **2018**, *10*. [CrossRef]

95. Argyris, P.P.; Wilkinson, P.E.; Jarvis, M.C.; Magliocca, K.R.; Patel, M.R.; Vogel, R.I.; Gopalakrishnan, R.; Koutlas, I.G.; Harris, R.S. Endogenous APOBEC3B overexpression characterizes HPV-positive and HPV-negative oral epithelial dysplasias and head and neck cancers. *Mod. Pathol.* **2020**. [CrossRef]

96. Fanourakis, G.; Tosios, K.; Papanikolaou, N.; Chatzistamou, I.; Xydous, M.; Tseleni-Balafouta, S.; Sklavounou, A.; Voutsinas, G.E.; Vastardis, H. Evidence for APOBEC3B mRNA and protein expression in oral squamous cell carcinomas. *Exp. Mol. Pathol.* **2016**, *101*, 314–319. [CrossRef]

97. Nakanishi, Y.; Kondo, S.; Wakisaka, N.; Tsuji, A.; Endo, K.; Murono, S.; Ito, M.; Kitamura, K.; Muramatsu, M.; Yoshizaki, T. Role of Activation-Induced Cytidine Deaminase in the Development of Oral Squamous Cell Carcinoma. *PLoS ONE* **2013**, *8*, e62066. [CrossRef]

98. Kano, M.; Kondo, S.; Wakisaka, N.; Wakae, K.; Aga, M.; Moriyama-Kita, M.; Ishikawa, K.; Ueno, T.; Nakanishi, Y.; Hatano, M.; et al. Expression of estrogen receptor alpha is associated with pathogenesis and prognosis of human papillomavirus-positive oropharyngeal cancer. *Int. J. Cancer* **2019**, *145*, 1547–1557. [CrossRef]

99. Messerschmidt, C.; Obermayer, B.; Klinghammer, K.; Ochsenreither, S.; Treue, D.; Stenzinger, A.; Glimm, H.; Fröhling, S.; Kindler, T.; Brandts, C.H.; et al. Distinct immune evasion in APOBEC-enriched, HPV-negative HNSCC. *Int. J. Cancer* **2020**, *147*, 2293–2302. [CrossRef]

100. Faden, D.L.; Ding, F.; Lin, Y.; Zhai, S.; Kuo, F.; Chan, T.A.; Morris, L.G.; Ferris, R.L. APOBEC mutagenesis is tightly linked to the immune landscape and immunotherapy biomarkers in head and neck squamous cell carcinoma. *Oral Oncol.* **2019**, *96*, 140–147. [CrossRef]

101. Conner, K.L.; Shaik, A.N.; Ekinci, E.; Kim, S.; Ruterbusch, J.J.; Cote, M.L.; Patrick, S.M. HPV induction of APOBEC3 enzymes mediate overall survival and response to cisplatin in head and neck cancer. *DNA Repair (Amst)* **2020**, *87*, 102802. [CrossRef] [PubMed]

Human Cytomegalovirus and Autoimmune Diseases: Where Are We?

Francesca Gugliesi [1,†] , Selina Pasquero [1,†] , Gloria Griffante [2] , Sara Scutera [1] , Camilla Albano [1] , Sergio Fernando Castillo Pacheco [1] , Giuseppe Riva [3] , Valentina Dell'Oste [1] and Matteo Biolatti [1,*]

[1] Department of Public Health and Pediatric Sciences, University of Turin, 10126 Turin, Italy; francesca.gugliesi@unito.it (F.G.); selina.pasquero@unito.it (S.P.); sara.scutera@unito.it (S.S.); camilla.albano@unito.it (C.A.); sergiofernando.castillopacheco@unito.it (S.F.C.P.); valentina.delloste@unito.it (V.D.)

[2] Department of Translational Medicine, Molecular Virology Unit, University of Piemonte Orientale Medical School, 28100 Novara, Italy; gloria.griffante@uniupo.it

[3] Otorhinolaryngology Division, Department of Surgical Sciences, University of Turin, 10126 Turin, Italy; giuseppe.riva@unito.it

* Correspondence: matteo.biolatti@unito.it; Tel.: +39-011-670-5635

† These authors contributed equally to this work.

Abstract: Human cytomegalovirus (HCMV) is a ubiquitous double-stranded DNA virus belonging to the β-subgroup of the herpesvirus family. After the initial infection, the virus establishes latency in poorly differentiated myeloid precursors from where it can reactivate at later times to cause recurrences. In immunocompetent subjects, primary HCMV infection is usually asymptomatic, while in immunocompromised patients, HCMV infection can lead to severe, life-threatening diseases, whose clinical severity parallels the degree of immunosuppression. The existence of a strict interplay between HCMV and the immune system has led many to hypothesize that HCMV could also be involved in autoimmune diseases (ADs). Indeed, signs of active viral infection were later found in a variety of different ADs, such as rheumatological, neurological, enteric disorders, and metabolic diseases. In addition, HCMV infection has been frequently linked to increased production of autoantibodies, which play a driving role in AD progression, as observed in systemic lupus erythematosus (SLE) patients. Documented mechanisms of HCMV-associated autoimmunity include molecular mimicry, inflammation, and nonspecific B-cell activation. In this review, we summarize the available literature on the various ADs arising from or exacerbating upon HCMV infection, focusing on the potential role of HCMV-mediated immune activation at disease onset.

Keywords: human cytomegalovirus; autoimmunity; autoimmune diseases

1. Introduction

The adaptive immune response recognizes external pathogens as non-self antigens as opposed to the antigens from one's own body, known as self-antigens. Dysregulation of this response can lead to the failure to distinguish self from non-self antigens, a phenomenon known as immune tolerance, acquired during fetal development, responsible for a variety of autoimmune diseases (ADs) [1].

ADs result from a complex interaction between genetic predisposition and environmental factors [2–4], which trigger immune responses leading to tissue destruction.

ADs comprise a family of more than 80 chronic illnesses affecting approximately 3–5% of the general population [5,6]. The concordance of ADs in identical twins, consistently less than 100% (12–67%), highlights the importance of epigenetic and environmental factors and, especially, infections in AD pathogenesis [5,7].

Human cytomegalovirus (HCMV) is a ubiquitous virus belonging to the *Herpesviridae* family. HCMV displays a double strand (ds) DNA genome, characterized by an enormous genome capacity, with estimates of more than 200 open reading frames (ORFs), even though

ribosome profiling and transcript analysis detected additional previously unidentified ORFs (~751 translated ORFs) [8]. HCMV infection is lifelong in the host, due to virus ability to establish latency. Even though one well characterized viral reservoir is hematopoietic cells, the exact latency site remains still elusive. Interestingly, and contrary to the classical perspective, it is becoming evident that latency-associated gene expression mirrors lytic viral patterns, albeit at much lower levels of expression [9].

Nowadays, also epigenetic modifications emerged as critical players in the regulation of active/latent HCMV infection [10]. During latency, in infected CD34+ progenitor cells and CD14+ monocytes, HCMV chromatin is associated with repressive markers, such as H3K9Me3, H3K27Me3, and transcriptional repressors, like heterochromatin protein 1 (HP1) and the KRAB-associated protein 1 (KAP1) [11]. During myeloid differentiation and activation, transcriptional repressors are downregulated, and the viral chromatin carries transcriptional active markers such as acetylated histones (AcH) and phosphorylated histone H3 [11]. Several evidences suggest that HCMV chronic infection accelerates age-related epigenetic changes, pointing out the interplay between HCMV and epigenetic machinery regulation [12]. At the same time, epigenetic events play a pivotal role in the pathophysiology of autoimmune/inflammatory conditions [13]. To date, the exact correlation of HCMV epigenetic modifications and development of ADs is still missing, and studies addressing the impact of HCMV on epigenetic modification on AD's onset are required.

A large body of evidence has shown how HCMV can use several of its genes to manipulate the innate and adaptive immune system of the infected subject [14–19]. This feature alongside many others, such as its wide tropism [20–23], its ability to persist in the host during phases of latency and reactivation, and, as already mentioned, its global distribution [24], makes HCMV a candidate etiological agent of ADs. A causative link between HCMV infection and ADs may appear difficult to determine epidemiologically given the widespread prevalence of HCMV and the rare occurrence of ADs. Mounting evidence has increasingly associated HCMV infection with rheumatologic diseases—e.g., systemic lupus erythematosus (SLE), systemic sclerosis (SSc), and rheumatoid arthritis (RA)—and neurological disorders—e.g., multiple sclerosis (MS), enteric disorders, and metabolic disorders, such as type 1 diabetes (T1D).

Despite the great effort, researchers have not yet been able to discriminate whether HCMV is an initiator of AD or an epiphenomenon that may simply exacerbate the course of ADs. In this regard, multiple mechanisms have been proposed to explain HCMV-induced autoimmunity. Through a mechanism defined as "molecular mimicry", viral epitopes that are highly similar to host determinants may induce the development of antibodies that attack the self at the level of specific tissues, as it has been hypothesized for the viral tegument protein pp65 in SLE patients [25]. Intriguingly, upon HCMV infection, immunocompetent hosts tend to develop an autoimmune reaction through the generation of autoantibodies, which occurs more frequently in those individuals with a systemic involvement [26]. HCMV-infected bone marrow transplant recipients quite often develop organ-specific autoantibodies against the human aminopeptidase CD13 [27,28] or common phospholipid [29], whereas solid organ transplant recipients develop non-organ-specific autoantibodies [30]. Accordingly, hypergammaglobulinemia, cryoglobulinemia, and autoantibody production are common features of HCMV-driven mononucleosis [31,32]. This unspecific hyperactivation of humoral immunity is thought to represent a mechanism of viral immune evasion, because it curbs host B-cell responses. Once the tissue is infected, activated antigen-presenting cells (APCs) are attracted to the infection site and release high levels of cytokines and chemokines that activate autoreactive T- or B-cells, leading to loss of tolerance, a phenomenon called "bystander activation". Several pieces of evidence suggest a role of HCMV infection in vascular damage and stenosis [33,34], an event that is quite frequent and fatal in patients with ADs [35].

There is also some evidence indicating that HCMV infection and ADs mutually affect each other. In particular, while primary or secondary HCMV infection can induce chronic, systemic type I inflammation, which may promote autoimmunity, eventually leading to

ADs [36], autoimmune flares can also trigger HCMV reactivation [36]. HCMV-induced immunosuppression, which has severe consequences in transplant recipients, may also play a protective role in the course of ADs [37].

This review aims to provide an updated overview on the role of HCMV in the etiopathogenesis of ADs, focusing on the underlying mechanism that has been proposed for each specific disorder.

2. Modulation of the Immune System by HCMV

HCMV has established a complex relationship with the host immune system, for both systemic dissemination and latency [38]. Indeed, primary and latent HCMV infection can be kept in check by the host immune system in a hierarchical and redundant way through type I and II interferons (IFNs), natural killer cells (NKs), and CD8$^+$ and CD4$^+$ T-cells [16,17,38]. Conversely, in different clinical settings, patients become immunocompromised, and high systemic inflammatory response, particularly driven by cytokines such as TNF-α, as well as diminished immune function has been detected. The inflammatory cascades can stimulate the HCMV major immediate early promoter (MIEP), followed by HCMV reactivation from latency [38]. HCMV reactivation is also frequently observed in immunocompetent seropositive adults, where it may exacerbate chronic illnesses, such as ADs. Vice versa, the inflammatory environment of ADs, described in detail in the paragraphs below, may induce reactivation of HCMV, forcing replication.

HCMV, thanks to its continuous co-evolution with the host, has developed an arsenal of immune escape mechanisms to counteract the immune system, particularly the "unwanted" inflammation [38–41]. These "viral gambits" are discussed below.

Adaptive immunity is critical for the control of primary HCMV infections, which can later on be enhanced by clonal expansion of activated CD4$^+$ and CD8$^+$ T-cells [41]. To counteract this response, HCMV employs five viral glycoproteins (i.e., US2, US3, US6, US10, and US11), all capable of interfering with the presentation of the major histocompatibility (MHC) class I antigen [42] and the recognition of antigenic peptides by CD8$^+$ T-cells. Concurrently, an important role in regulating the production of antigenic peptides and inhibiting the production of viral epitopes [43] is played by HCMV miR-US4-1, which, by targeting the endoplasmic reticulum aminopeptidase 1 (ERAP1), inhibits the CD8$^+$ T-cell response. Likewise, HCMV miR-UL112-5p appears to downregulate ERAP1 expression, thereby inhibiting the processing and presentation of HCMV pp65 to cytotoxic T lymphocytes (CTLs) [43,44]. Finally, upon THP-1 cell infection, HCMV pUL8 reduces the levels of pro-inflammatory factors so as to inhibit inflammation [45], whereas HCMV pUL10 mediates immunosuppression by reducing T-cell proliferation and cytokine production [46].

On the other hand, innate immunity represents the host's first line of defense against external pathogens [47]. The initial intracellular response is triggered by pattern recognition receptors (PRRs), which after detecting pathogen-associated molecular patterns (PAMPs) can activate a downstream signaling pathway leading to the production of type I IFN and the release of pro-inflammatory cytokines. Also in this case, HCMV has devised different strategies to circumvent innate immunity [40,48,49]. For instance, our group has recently shown that the HCMV tegument protein pp65—also known as pUL83—binds to cyclic guanosine monophosphate–adenosine monophosphate synthase (cGAS), thereby inhibiting its ability to stimulate IFN-β production [50]. Similarly, the tegument protein UL31 has been shown to interact with cGAS, thereby decreasing cGAMP production and type I IFN gene expression [51].

Consistent with an immune escape function of HCMV tegument proteins, two studies by Fu et al. have shown that pp71—also known as pUL82—can inhibit trafficking of the stimulator of IFN genes (STING) [52], and that UL42 is a negative regulator of the cGAS/STING pathway [53]. Another HMCV glycoprotein, known as US9, can downregulate IFN type I by interfering with the mitochondrial antiviral-signaling protein (MAVS) and STING pathways [54]. Furthermore, the HCMV immediate–early (IE) 86 kDa protein

(IE86) downmodulates IFN-β mRNA expression by preventing nuclear factor-κB (NF-κB)-mediated transactivation of IFN-β [55]. Interestingly, a new study by Kim et al. [56] has revealed that IE86 may also inhibit IFN-β promoter activation by inducing STING degradation through the proteasome.

The innate immune system also relies on the concerted anti-microbial action of NKs, dendritic cells, and macrophages [47]. In particular, NKs play a primary role in counteracting viral infection thanks to their ability to recognize virus-infected cells through activating or inhibitory receptors—e.g., NKG2D and NKp30. As a consequence, HCMV has evolved various immune evasion strategies that rely on the modulation of NK receptors [57,58]. For example, HCMV UL142, UL148a, US9, US18, and US20 have all been shown to downregulate—to different extents and sometimes in an allelic-specific manner—MHC class I polypeptide-related sequence A (MICA), one of the eight different NKG2D ligands [59,60]. In addition, miR-UL112 and UL16 can both inhibit the expression of MHC class I polypeptide-related sequence B (MICB). Besides MICB, UL16 can also downmodulate the expression of UL16-binding protein 1 (ULBP1), ULBP2, and ULBP6 [61–64]. ULBP3 is instead targeted by UL142, which can also act as a MICA inhibitor [65,66]. The ability to concurrently evade multiple cellular pathways has also been shown for US18 and US20, both capable of inhibiting MICA and the NKp30 ligand B7-H6 [67,68] (Figure 1).

Moreover, HCMV encodes a set of Fcγ binding glycoproteins (viral FcγRs, vFcγRs) that bind to the Fc region of host IgG and facilitate evasion from the host immune response [69]. Particularly four vFcγRs encoded by HCMV have been identified: gp68 (UL119-118), gp34 (RL11), gp95 (RL12), and gpRL13 (RL13) [70–73]. They are crucial for viral escape from both innate and adaptive immune responses, including antibody dependent cellular cytotoxicity (ADCC) [71].
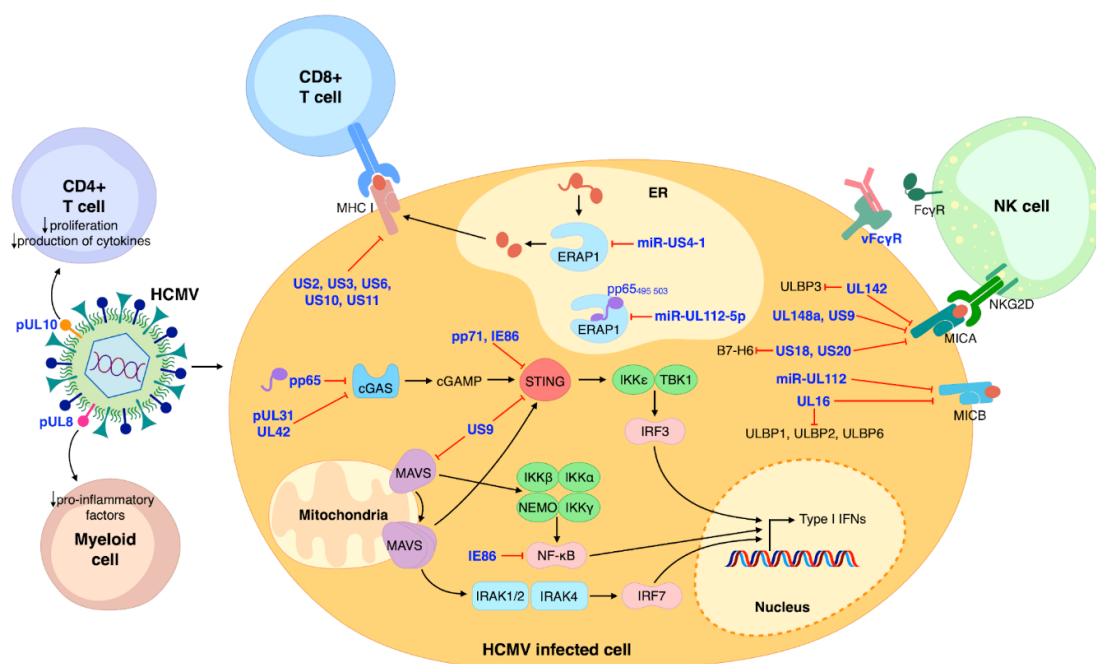
Figure 1. Schematic model summarizing the major aspects of HCMV modulation of the immune system. NK cells, CD8^{+} and CD4^{+} T-cells, and myeloid cells are the main protagonists of host immune control of HCMV infection. HCMV proteins are represented in blue. Black arrows indicate stimulation/activation; red lines represent inhibition.

Another strategy that HCMV has acquired is the ability to produce viral products homologs to cytokines, chemokines, and their receptors, which can alter the immune response and the clearance of the virus during the productive or the latent phase of the infection [15]. Among these factors, HCMV encodes an interleukin 10 (IL-10) homolog, known as cmvIL-10, which can modulate the immune response and induce replication and

persistence of the virus. cmvIL-10 can stimulate the differentiation of autoreactive B cells on one hand and on the other hand suppress pro-inflammatory factors, tilting the immune response and inducing a chronic productive infection. In different autoimmune disorders, IL-10 presents an altered expression due to polymorphisms in its promoter, and elevated levels of IL-10 have been detected in SLE and Sjögren's syndrome (SS) patients [74–76]. Although a direct relationship between HCMV, IL-10, and autoimmune disorders has not yet been recognized, further investigations are needed to better clarify a possible role of HCMV cytokine homologs in these diseases.

Interestingly, polymorphisms in cytokine signaling pathways might be involved in autoimmune disorders in association with viral infection. For example, the association between genetic polymorphisms related to cytokines, as single-nucleotide polymorphisms (SNPs) in signal transducer and activator of transcription 4 (STAT4) or interleukin 10 (IL-10), and different autoimmune disorders has been described [77–79], identifying IFN-α as an environmental modifier of the STAT4 risk allele and indicating a major risk to develop the disorder during a viral infection [80]. These results suggest that an altered function or expression of different cytokines can predispose to the autoimmune disease or modulate the disease manifestations.

3. Documented Mechanisms of HCMV-Induced Autoimmunity

HCMV can induce or perpetuate autoimmunity through different processes that can be divided into two categories: (1) antigen-specific (i.e., molecular mimicry) and (2) non-antigen-specific (i.e., bystander activation). From an immunopathological perspective, HCMV can trigger or sustain autoimmunity through the following three mechanisms: (i) autoantibodies production, (ii) enhanced inflammation, and (iii) vascular damage (Figure 2). These will be further discussed below.
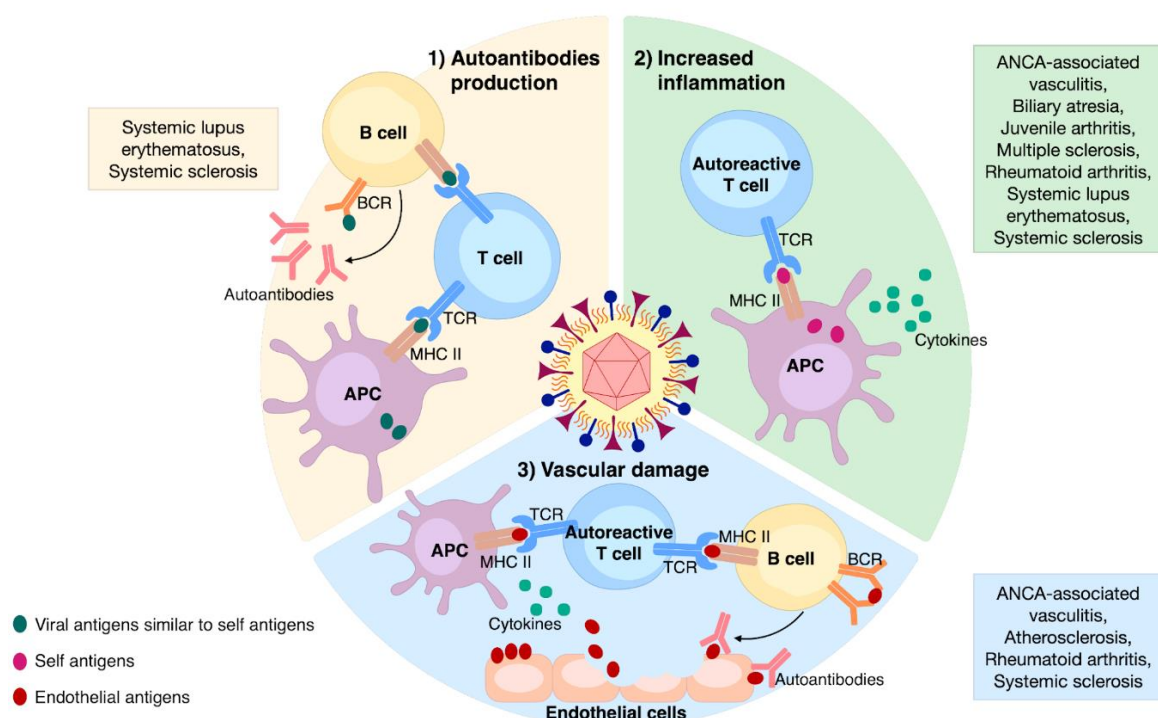
Figure 2. The main mechanisms involved in HCMV-induced autoimmunity and associated ADs. (**1**) Autoantibodies production: the occurrence of viral epitopes, structurally similar to self-ones, can induce the activation of both T- and B-cells through their presentation by APCs; (**2**) increased inflammation: non-specific anti-HCMV immune response leads to the release of self-antigens and cytokines from the affected tissue; those self-antigens presented by APCs can stimulate autoreactive T-cells; (**3**) vascular damage: enduring HCMV infection triggers vascular damaging; the release of endothelial antigens and cytokines induces the activation of autoreactive T-cells and B-cells, culminating in aggression of endothelial cells via specific autoantibodies.

3.1. Autoantibodies Production

This particularly harmful effect of HCMV is due to viral-induced molecular mimicry, which is a mechanism through which HCMV infection activates T-cells that are cross-reactive with self-antigens. Although among the *Herpesviridae* family, the Epstein–Barr virus (EBV) has been more extensively studied in this regard [81], HCMV has also been frequently involved in the generation of cross-reactive autoantibody in ADs. For example, patients affected by SSc express different autoantibodies able to recognize both cellular proteins and their homologous HCMV counterparts—e.g., anti-topoisomerase I/HCMV pUL70 [82] and anti-cell surface integrin–neuroblastoma-amplified gene (NAG)-2/HCMV pUL94 [83] antibodies. The association of HCMV infection with ADs does not appear to be solely restricted to SSc given that SLE patients can also express high levels of two anti-pp65 and anti-pp150 antibodies [25,84,85]. Consistent with a role of HCMV pp65 in autoimmunity, immunization of BALB/c mice with peptides derived from the C-terminus of this viral protein led to the generation of anti-dsDNA and antinuclear antibodies, inducing severe signs of glomerulonephritis [86]. More recently, SLE patients were also found to express high levels of IgG antibodies against the HCMV DNA-binding nuclear protein UL44 [87]. Intriguingly, this antibody was able to co-immunoprecipitate UL44 and nuclear SLE autoantigens during virus-induced apoptosis, suggesting a novel contribution of HCMV to humoral immunity in ADs. Other possible associations of antibodies against HCMV structures and self-antigens were speculated but not confirmed in other ADs [88,89].

Humoral autoimmunity can also be induced by non-specific B-cell activation, since HCMV can be considered a bona fide polyclonal B-cell activator. In this regard, HCMV can induce B-cell proliferation and favor autoantibody production by interacting with Toll-like receptor (TLR)7/9 in plasmacytoid dendritic cells (pDCs) [90]. More recently, cross-talk between B-cell-activating factor (BAFF) and TLR9 signaling has been shown to promote IgG secretion and survival of B-cells following HCMV infection [91].

3.2. Enhanced Inflammation

The mechanism behind this nonspecific antiviral immune response is best known as bystander activation, defined as the stimulation of autoreactive T-cells by self-antigens presented by APCs. The presence of terminally differentiated CD4$^+$CD28$^-$ T-cells is typical of HCMV-infected individuals [92,93], including patients with ADs, such as RA [94]. Reactivation and replication of HCMV in inflamed tissue has been found to induce T-cell differentiation of the pathogenic and dysregulated CD4$^+$CD28$^-$ subset under autoimmune conditions, albeit these cells do not seem to have a direct auto aggressive behavior, as described in detail by Bano et al. [95]. In this review, the authors also speculate that RA-infected synovial fibroblasts may directly or indirectly—through the release of non-infectious exosomes—present HCMV antigens to T-cells, thereby inducing their terminal differentiation. This hypothesis has been recently substantiated by a proof of concept study showing that, in antineutrophil cytoplasmic antibody (ANCA)-associated vasculitis (AAV), the expansion of CD28$^-$ T-cells was reduced by an antiviral therapy able to suppress HCMV subclinical reactivation, indicating that expansion of this clone was HCMV-dependent [96]. By contrast, Wu et al. [97] have more recently shown that the expansion of CD4$^+$ CD28$^-$ cells in SLE patients is negatively associated with disease activity—lupus low disease activity state is associated with lower anti-DNA levels—and that the polyfunctional CD8$^+$ T-cell response to HCMV pp65 is not impaired. Moreover, HCMV seropositive MS patients displayed not only an altered B-cell phenotype and function, but also a modulation of the IFNβ response and a reduced pro-inflammatory cytokine B-cell profile, indicating a putative protective role of HCMV [98].

In ADs characterized by high levels of inflammation and chronic immune stimulation, such as RA, a causative role of HCMV has also been hypothesized. For instance, after specific HCMVpp65 long-term stimulation, increased anti-HCMV IgG antibodies and intracellular IFN-γ-producing HCMVpp65-specific CD28$^-$CD8$^+$ T-cells were observed in RA and juvenile arthritis (JIA) patients vs. healthy controls (HCs), indicating a possible

enhancement of the inflammatory response following endogenous HCMV reactivation [99]. Moreover, an increased proportion of terminally differentiated immunoglobulin-like receptor 1 (LIR-1+) CD8+ T-cells was detected in HCMV seropositive RA patients. These cells were characterized by cytolytic activity, pro-inflammatory properties, and anti-infectious effector features, all distinctive characteristics of the so-called "chronic infection phenotype", probably involved in the inflammatory pathogenesis of RA [100].

A cause–effect relationship between HCMV infection and other systemic ADs, such as SLE and SSc, is supported by experiments testing the in vitro response to the HCMV antigen in T-cells from SLE and SSc patients. The enhanced expression levels of IFN-γ, IL-4, and IL-2 as well as the increased number of memory T-cells found in these patients led, in fact, the authors to conclude that exposure to HCMV may promote fibrosis and vascular damage [101].

In recent years, Arcangeletti and co-workers have taken a closer look at the interplay between HCMV and the immune response in SSc and inflammation. Interestingly, in HCMV-infected human dermal fibroblasts, this group was able to detect increased HCMV-specific CD8+ T-cell responses associated with disease parameters, which were paralleled by enhanced expression of several fibrosis- and apoptosis-associated factors involved in SSc pathogenesis [102,103].

HCMV can amplify inflammation through other mechanisms. For instance, the latency-associated gene US31 is expressed at higher levels in PBMCs from SLE patients vs. HCs. This upregulation may be relevant to AD pathogenesis, because US31, by acting through the non-canonical NF-κB pathway (NF-κB2), can alter the immunological properties of monocytes and macrophages and promote an M1 inflammatory phenotype [104].

With regard to the interplay between HCMV and MS, murine cytomegalovirus (MCMV) can promote EAE in resistant BALB/c mice by activating inflammatory APCs and CD8+ encephalitogenic-specific T-cells and promoting the M1 phenotype of microglia [105].

Biliary atresia (BA), classified as an autoimmune-mediated disease, is a disorder characterized by inflammation, fibrosis, and obstruction of the bile duct. To simulate BA, mice depleted of Treg cells were infected with low doses of MCMV, a condition that led to increased expression of IFN-γ-activated genes and inflammation, attesting an involvement of CMV in disease progression [106].

NKs play a crucial role in homeostasis and immune responses. Besides exerting a cytotoxic effect, NK activation can trigger the release of different pro-inflammatory cytokines, promoting excessive inflammation, which eventually leads to ADs. In this regard, distinct NK subsets are capable of reaching different tissues where they can exert a protective effect on immune homeostasis. Such an example is the expansion of adaptive NKG2C+ cells in acute HCMV infection or reactivation, inducing a protective effect [107]. Furthermore, higher percentages and absolute numbers of these cells are found in MS patients positive for HCMV, again indicating that HCMV may play a protective role in this autoimmune condition [108]. On the other hand, a study by Liu et al. revealed the existence of an antibody able to recognize HCMV pp150 across various ADs. The fact that this antibody was also able to recognize the single-pass membrane protein CIP2A and promoted cell death of CD56bright NKs, a subset whose expansion is frequently observed in autoimmunity, led to the conclusion that the generation of HCMV-induced autoantibodies may be responsible for the onset of ADs [85].

Unconventional γδ T-cells are potent inducers of cytotoxicity and have been recently identified as determinants of adaptive immunity against pathogens and tumors via APC activation and stimulation of other leukocytes [109]. Once activated, they trigger tissue repair, inflammation, and lysis of different cell types. In patients affected by the severe combined immunodeficiencies (SCID), an increase in γδ T-cells associated with HCMV infection and autoimmune cytopenia was observed, suggesting that HCMV may promote expansions of these cells [110]. However, the direct involvement of HCMV in the activation of γδ T-cells, as well as the direct role of these cells in ADs, has yet to be clarified.

3.3. Vascular Damage

HCMV plays an important role in vascular damage through endothelial cell (EC) apoptosis, infiltration of inflammatory cells, and smooth muscle cell proliferation. Lunardi and co-workers were the first to uncover a correlation between HCMV infection and endothelial damage in SSc [111]. The mechanism of HCMV-induced vascular damage was later linked to molecular mimicry characterized by auto aggression of ECs through release of specific autoantibodies against NAG-2/UL94 proteins, as described in Section 3.1. Indeed, the immunization of BALB/c mice with UL94 and NAG-2 peptides coupled with a carrier protein caused ischemic lesions on footpads and tails. Moreover, treatment of ECs with the same antibodies resulted in increased reactive oxygen species (ROS) production [33].

In atherosclerosis, an auto-inflammatory disorder with an autoimmune setting, HSP60 autoantibodies, which share homology with UL122 and US28 HCMV peptides, have been reported. These peptides present sequence homology also with different EC surface molecules [112]. DNA microarray-based experiments showed that these purified anti-HCMV antibodies can modulate the expression of various molecules (e.g., adhesion molecules, chemokines, molecules involved in inflammation, etc.) involved in EC activation and damage [113].

Finally, HCMV infection has been positively associated with $CD4^+CD28^-$ T-cell expansion and high cardiovascular disease (CVD) mortality risk among RA patients, further confirming a direct causal link between HCMV and vascular damage in AD [114,115]. The expansion of $CD4^+CD28^-$ T-cells in HCMV-positive/ANCA-associated vasculitis (AAV) patients, expressing a Th1 phenotype, with high levels of IFN-γ and TNF-α production and co-expression of different endothelial homing markers [96], further corroborates the role of HCMV in inducing AD-related vascular damage.

4. The Main Autoimmune Diseases Associated with HCMV Infection

4.1. Rheumatologic Diseases

4.1.1. Systemic Lupus Erythematosus

Systemic lupus erythematosus (SLE) is a chronic AD characterized by connective tissue inflammation and heterogeneous clinical manifestations, ranging from mere cutaneous and musculoskeletal features to kidney and/or central nervous system involvement, often associated with significant morbidity and mortality. Although the causes of SLE are not clearly understood, many have proposed that SLE may be due to a combination of genetic predisposition and environmental factors (e.g., UV exposure, infection, and stress) [116,117].

All SLE patients inevitably show abnormalities in monocytic lineage cells, which can lead to T-cell deficiencies, polyclonal B-cell activation, immune complex formation, and autoantibody production. In this regard, the peculiar ability of HCMV to establish lifetime latency and to periodically shift between the lytic and latent stage has been linked to the aberrant humoral response in SLE. Fittingly, augmented anti-HCMV IgM/IgG titer tends to correlate with clinical and immunological manifestations of SLE [118]. Studies that found an association between HCMV and SLE disease were often performed in European countries [119,120]. Additionally, differences in the prevalence of HCMV infection in SLE patients were reported by different research groups. For example, Takizawa et al. [121] found that 149 of 151 patients with rheumatologic disease were infected by HCMV, by pp65 antigenemia assay, and all 74 SLE patients were positive for HCMV infection. Newkirk et al. [122] found that the prevalence of HCMV infection in SLE patients was 60% by using ELISA kits to detect HCMV specific antibodies. After adjusting for the rheumatoid factor, Su et al. [123] found that 84 of 87 SLE patients (96.55%) were HCMV IgG-positive, and that nine (10.34%) were HCMV IgM-positive. On the other hand, several other studies did not observe a direct association between HCMV seroprevalence and SLE [124–126]. For examples, James et al. reported that HCMV infection was not related

to SLE [126]. Altogether, these results suggest that to date we do not have a complete understanding of the relationship between HCMV infection and SLE development.

A potential role of HCMV in SLE pathogenesis was initially proposed by several groups after identifying specific autoantigens induced upon HCMV infection [89,122]. Molecular mimicry has been described also for another member of the *Herpesviridae* family, i.e., EBV, that may be involved in the pathogenesis of SLE. Indeed, anti-Epstein–Barr nuclear antigen 1 (EBNA1) antibodies can recognize human proteins such as SmB and Ro60 [127].

As already mentioned, (see HCMV pp65, Section 3), HCMV can lead to the production of autoantibodies against nuclear proteins, such as in the case of the LA protein. Specifically, HCMV can directly—or indirectly, through molecular mimicry—induce cell surface expression of this small nuclear ribonucleoprotein, thereby leading to the production of autoantibodies in genetically susceptible individuals [122,128]. Subsequently, two independent groups [25,86] showed that immunization of previously non-autoimmune mice with peptides encompassing the HCMV epitope $pp65_{422-439}$ led to the appearance of autoantibodies against nuclear components while inducing early signs of nephritis resembling human SLE. Importantly, high levels of serum anti-$pp65_{422-439}$ antibodies were found in patients with SLE, suggesting that pp65 contained B-cell epitope(s) that could trigger autoimmunity in genetically predisposed individuals [25]. The same authors uncovered amino acid sequence homology between HCMV $pp65_{422-439}$ and the TATA-box binding protein associated factor 9 ($TAF9_{134-144}$) and detected the presence of specific antibodies against these epitopes in association with anti-nuclear and anti-dsDNA antibodies, typically found in SLE, alongside increased anti-TAF9 antibodies in sera from SLE patients [86].

More recently, Neo et al. have described a potential alternative process involving UL44, a DNA-binding phosphoprotein essential for HCMV DNA replication [87]. The observation that after translocation to the nucleus, UL44 interacted with other viral and host proteins to increase viral DNA replication efficiency led these authors to hypothesize that delayed clearance of apoptotic cellular material in genetically predisposed individuals may favor the presentation of intracellular self-antigens to humoral immunity. They succeeded in isolating a human UL44 antibody from the sera of SLE/HCMV IgG seropositive patients, showing that it could bind to UL44 complexed with cell-surface localized SLE autoantigens during virus-induced apoptosis. Thus, based on these findings, it is conceivable that HCMV may trigger and/or potentiate the host humoral immune response to nuclear self-antigens, predisposing infected individuals to SLE.

Genome-wide association studies (GWAS) have identified over 50 susceptibility loci for SLE in the population (mostly genes regulatory regions). Therefore, it is crucial to investigate the link between genetic susceptibility and viral infections in the development of SLE. For example, Harley and colleagues demonstrated that EBV gene products that serve as transcription factors have preferential interaction with loci containing risk alleles [127]. However, if any of the HCMV proteins preferentially bind SLE risk loci is still to be addressed.

Under a clinical point of view, dysfunction of the immune system has been long known to increase the risk of infection among SLE patients, accounting for approximately 50% of hospitalizations during the course of the disease [129], suggesting that a lifelong immunosuppression of an individual, as it is often the case for SLE patients, may favor HCMV reactivation [130]. This hypothesis was later on corroborated by findings from a 26-year retrospective study showing that infections, including those caused by HCMV, were amongst the top three causes of death in SLE patients [131], raising the important question of which risk factors are associated with HCMV disease in the SLE population. This question has been recently answered by a systematic review [132] identifying the following risk factors: (i) high viral load, which together with enhanced levels of HCMV antigenemia correlated with the development of life-threatening end-organ damage; (ii) lymphopenia, resulting in failure to mount a host cellular immune response against HCMV; and (iii) type

of treatment—HCMV disease progression correlated with higher corticosteroid doses and/or immunosuppressants [133].

HCMV infection is also known to trigger SLE flares through direct cytopathic effects and/or activation of inflammatory processes, thus causing both systemic and organ-specific disease. Lastly, the clinical features of HCMV infection themselves happen to mimic SLE flares, further complicating the clinical picture of SLE patients [134].

4.1.2. Systemic Sclerosis

Systemic sclerosis (SSc) is a chronic systemic inflammatory disease characterized by vasculopathy and extensive fibrosis. It has the highest mortality among ADs due to pulmonary hypertension and lung fibrosis. The etiology still remains unknown, although genetic predisposition, environmental factors, and infectious agents have all been considered as potential triggering factors [135–137]. The activation of the immune system plays a key role in SSc pathogenesis and is probably the link between initial vascular involvement and the end-stage of the disease (i.e., tissue fibrosis), raising the hypothesis that certain autoantibodies may not simply be epiphenomena but rather play a central role in disease pathogenesis. In particular, intracellular antigens autoantibodies have been associated with specific SSc subsets [138], whereas cell surface antigens autoantibodies production has been shown to cause EC damage and apoptosis and activation of fibroblasts, T lymphocytes, and macrophages. In turn, these activated cells tend to secrete higher levels of cytokines, leading to changes in the extracellular matrix, one of the hallmarks of SSc.

Among infective agents, herpesviruses have been suggested to be causative agents in the immunopathogenesis of SSc [139,140]. Indeed, antibodies against HCMV and EBV are more frequently detected in SSc than in healthy controls [141–143].

The statistically significant association with HCMV infection in Swiss SSc patients (59% seropositivity in SSc patients compared with 12–21% controls) [144] has not been observed in other studies so far [143,145], even though higher HCMV antibody concentrations have been found in SSc patients [146,147]. In this regard, future studies should clarify why a ubiquitous virus such as HCMV only triggers an autoimmune response in certain individuals, whereas in others it has no effect.

HCMV can maintain an active, persistent replication for the life span of the immunocompetent host, particularly thanks to its macrophage and endothelial tropism [148]. Starting from the observation that HCMV antibodies are prevalent in SSc patients [144] and that UL70 viral protein can be recognized by anti-topoisomerase I antibody, Lunardi et al. were the first to propose a novel pathogenesis mechanism of SSc based on HCMV molecular mimicry of the cellular protein NAG-2 expressed on ECs and fibroblasts, with the latter being involved in the so-called "scleroderma like phenotype" linked to SSc pathogenesis [33,83,111] (see Sections 3.1 and 3.3).

The most frequently found autoantibodies among SSc patients are those directed against centromere proteins (anti-CENPs), DNA topoisomerase I (anti-topo I), and RNA polymerase III (anti-RNA polIII). Of note, in SSc, there is a significant correlation between the expression of autoantibodies against RNA polIII and the presence of specific clinical features, such as high risk of diffuse cutaneous disease, short survival time, and renal involvement. Moreover, SSc patients expressing autoantibodies against anti-topo I are at high risk of developing pulmonary interstitial fibrosis, whereas patients with CENP autoantibodies have the best prognosis [138]. Lastly, a recent study [149] evaluating the relationship between the immune response of SSc patients to six major antigens of HCMV (i.e., UL57, UL83, UL55, UL44, p38, and UL99) and specific clinical and immunological characteristics of the disease found that the presence of anti-UL44 antibodies correlates with arthritis, a clinical feature of SSc. This finding supports the idea that anti HCMV antibodies may play an important role in breaking tolerance and triggering SSc pathogenesis.

4.1.3. Rheumatoid Arthritis

In spite of an increasing body of evidence, a functional role of HCMV in the pathogenesis of rheumatoid arthritis (RA) has not yet been conclusively proven due to controversial findings, whereas a correlation between EBV and RA has already been found. There are several examples of molecular mimicry between EBV and self-antigens relevant to RA, such as HLA-DRB1 polymorphisms, human interleukin (h IL)-10, and a CXC chemochine receptors [150]. While some early studies found high HCMV seroprevalence among RA patients [120,151,152], other investigations could not establish a clear association between HCMV infection and RA [144,153–155]. In support of a role of HCMV in RA, some authors have more recently reported the presence of HCMV replication in synovial specimens from RA patients, which correlated with increased disease severity, revealing a higher incidence of HCMV infection in RA patients than previously thought [152,156]. However, the fact that immunosuppressive therapy can lead to HCMV reactivation does not allow drawing any definitive conclusions as to whether HCMV may be involved in RA initiation rather than its exacerbation.

The term "rheumatoid arthritis" was defined in 1859 by Alfred Baring Garrod to distinguish this chronic systemic autoimmune disease from other forms of arthritis (e.g., osteoarthritis, spondyloarthritis, etc.) [157]. RA affects 0.5–1% of the worldwide population, with higher prevalence in the elderly [158], with a female to male ratio of 3:1 [159]. RA is a T-cell-driven autoimmune disease, accompanied by autoantibody production that affects primarily the lining of the synovial joints, leading to destructive synovitis, progressive disability, and even to premature death due to extra-articular manifestations, such as vasculitis [160,161]. The chronic inflammation and subsequent tissue damage of the joints is caused by the deposition of immune complexes (ICs) composed of autoantibodies bound to their cognate autoantigens, which attract innate immune cells to the site of deposition, with subsequent release of proteolytic enzymes, slowly degrading the synovial tissue in an endless vicious cycle [160]. Autoantibodies isolated from patients with RA were shown to recognize citrullinated proteins (anti-citrullinated peptide antibodies, ACPAs) and IgG (rheumatoid factor, RF) [162]. Interestingly, these autoantibodies were found to be already present in a subset of RA patients years before the disease onset and could predict a more aggressive and severe progression [163,164].

Citrullination is a post-translational modification catalyzed by a family of peptidylarginine deiminases (PADs) that convert peptidylarginine into peptidylcitrulline, whose aberrant dysregulation has been linked to several inflammatory conditions, such as ADs, cancer, and neurodegenerative diseases [165–169]. The theory that citrullination is involved in the etiopathogenesis of RA has been supported by several lines of evidence [170–173], but the mechanisms that trigger citrullination and, therefore, initiate RA development are still unknown. Interestingly, many genetic and environmental factors have been associated with RA pathogenesis, especially among ACPA-positive patients. According to the so-called "two hit" model, in genetically predisposed individuals, the first hit is represented by environmental triggers, such as smoking or infection, which induce citrullination of peptides that are successively presented to autoreactive T-cells, leading to the generation of high-affinity anti-citrullinated peptide antibodies. These events are thought to occur years before the onset of the disease. During the second hit, synovitis and further citrullination together with pre-existing ACPA lead to the development of chronic inflammation due to persistent formation of ICs [174]. Intriguingly, three independent studies [175–177] have shown that citrullination of EBV proteins may create epitopes that are recognized by ACPA isolated from RA patients, indicating that ACPAs can indeed react with a viral deiminated protein and suggesting that herpes viruses, such as EBV, are environmental factors contributing to the onset and/or development of RA. Due to the lack of direct evidence, we cannot however make a similar claim about HCMV species. In this regard, it would be interesting to investigate whether viral infections are directly involved in PAD activation and whether subsequent citrullination of cellular and/or viral proteins is dysregulated in AD. Very recently, Casanova et al. [178] have reported citrullination of human cathelicidin

LL37, a host defense peptide, in human rhinovirus (HRV)-infected bronchial epithelial cells, which negatively affects the antimicrobial and antiviral activity of this peptide, suggesting that citrullination may constitute a viral immune evasion mechanism.

On the other hand, an immune response to latent HCMV has been shown play a critical role in the progression of inflammation and structural damage of joints in RA patients [179]. In this regard, it is important to point out that RA patients tend to display expansion of a particular subset of T-cells CD4$^+$ lacking the costimulatory molecule CD28, required for T-cell activation and survival [180,181] (see Sections 3.2 and 3.3). Intriguingly, the frequency rate of this clonal expansion, which rarely exceeds 1% in the elderly, quite often reaches values between 5% and 10% in RA patients, where it is associated with extra-articular manifestations, such as early atherosclerotic vessel damage [94], probably due to the ability of CD4$^+$CD28$^-$ T-cells to exert a cytotoxic activity and directly attack the vascular tissue [182]. As it correlates with disease severity and the extent of extra-articular involvement, the frequency rate of CD4$^+$CD28$^-$ T-cells in RA has been proposed to be a predictor of future acute coronary events. Intriguingly, HCMV infection is a major trigger of CD4$^+$CD28$^-$ T-cells expansion [92]. The fact that these T-cells are only found in HCMV-positive RA patients and respond to HCMV antigen stimulation in vitro suggests that HCMV infection contributes to increased inflammation and RA aggravation by accelerating extra manifestations, such as coronary damage. The detection of CD4$^+$CD28$^-$ T-cells in other inflammatory conditions, such as psoriatic arthritis, MS, inflammatory bowel diseases (IBDs), cardiovascular diseases, chronic rejection, ankylosing spondylitis, and Wegener's granulomatosis, has led to the hypothesis that HCMV-mediate induction of CD4$^+$CD28$^-$ T-cells may be a shared mechanism of ADs [92,93,183,184]. Eventually, CD4$^+$CD28$^-$ T-cells may respond to autoantigens in the synovium and produce cytotoxic molecules or activate macrophages to release pro-inflammatory cytokines that leads to cartilage erosion [95]. As already mentioned, HCMV DNA, specific antigens, and infectious virus particles have all been detected in synovial tissue and fluid from the joints of 10% to 50% RA patients [156,185–188]. Interestingly, HCMV has been associated with a significantly increased risk of cardiovascular disease also in non-RA patients [189–191], which is not so surprising in light of mounting evidence supporting the ability of HCMV to manipulate the host cell metabolism to favor viral growth [192].

Increased RA disease activities in HCMV-seropositive individuals may also be linked to the expansion of another specific of CD8$^+$ T-cell subset, which preferentially expresses the inhibitory NK cell receptor LIR-1 and exerts a cytolytic effect [100]. Indeed, expression of LIR-1 on CD8$^+$ T-cells is upregulated following HCMV infection [193] and results in reduced T-cell proliferation [194]. LIR-1 is also considered a marker of premature immune senescence, since its upregulation may limit tissue damage otherwise caused by persistent anti-HCMV immune response [195].

In conclusion, emerging evidence indicates that HCMV may contribute to the development of RA by exacerbating and/or accelerating disease severity, especially in patients with vascular manifestations. However, there is disagreement on whether HCMV infection is an initiating event or just an epiphenomenon.

4.2. Neurological Diseases

Multiple Sclerosis

Multiple sclerosis (MS) is a chronic autoimmune inflammatory disease affecting the central nervous system (CNS) characterized by the destruction of neuronal axonal myelin. It mainly affects young adults, with a higher prevalence in females, often leading to non-traumatic neurological disabilities. The progressive deterioration of motor, sensory, and cognitive functions is characterized by specific histopathological markers, such as demyelination, leukocyte infiltration, neurodegeneration, and reactive gliosis of the CNS [196]. Although the precise etiology of MS is not yet clear, it is thought to occur in genetically susceptible individuals following interaction with one or more environmental factors. The most common environmental risk factors are sunlight exposure, vitamin D levels, cigarette

smoke, and infectious agents [197]. In particular, several epidemiological studies have reported a significant association of herpesvirus infections with MS pathogenesis. Among herpesviruses, EBV, which infects about 95% of the global adult population, has often been proposed as the major culprit candidate [198,199]. Although no other pathogens have been as strongly associated with MS as EBV, many studies have looked at a possible correlation between MS susceptibility and infection with other herpesviruses, in particular HCMV. One of the peculiarities of HCMV is that of being able to establish a permanent latent infection whose prevalence appears to be inversely related to the socioeconomic development of the population in question—in good agreement with the broader "hygiene hypothesis", according to which the correlation between HCMV and MS may be indirectly linked to exposure to other environmental factors [200]. Contrary to this assumption, others have proposed that the immunopathology of MS can in fact be influenced by HCMV, as the impact of this latter on the immune system ultimately interferes with the host immune response to other pathogens (i.e., heterologous immunity) [201].

With regard to molecular evidence supporting a relationship between MS and HCMV infection, two different studies found higher HCMV DNA loads in a cohort of MS patients compared to HCs [202,203]. Moreover, the same authors detected positivity for anti-HCMV IgG antibodies in almost 80% of the MS patients examined. However, the fact that there were no significant differences in anti-HCMV antibody concentration between MS patients and HCs led the authors to conclude that the presence of these antibodies alone was not a significant marker for MS development. Finally, the hypothesis that the risk of developing MS increases due to systemic HCMV infection is also supported by some MS cases where opportunistic reactivation of HCMV infection has been linked to worsening of pre-existing MS [204,205].

By contrast, other studies have shown a negative correlation between the development of MS and HCMV seropositivity [200,201], although skeptics argue that this may not be the result of a direct protective effect but simply an epiphenomenon related to the adoption of a Western lifestyle or to early viral infections. In this regard, Alari-Pahissa and colleagues [200] conducted a study aimed to determine whether the serological status of HCMV in early MS patients was different from that observed in non-early MS patients, in particular by looking at the putative association of this virus with the clinical course of the disease and the humoral immune response against other herpesviruses. In a nutshell, the authors found that HCMV increased not only the production of pro-inflammatory cytokines (e.g., TNF-α and IFN-γ) but also the antibody-dependent cellular cytotoxicity mediated by adaptive NKs, an activity that is known to influence the host immune response to other pathogens [206,207]. Since anti-EBNA-1 antibody levels had been previously shown to directly correlate with increased MS disease activity [208], the authors asked whether they could establish an association between a specific humoral response in MS patients and HCMV positivity. Interestingly, they observed a decrease in the EBNA-1 index related to disease duration in HCMV-positive MS patients aged 40 years or younger [200,209]. Moreover, the same patients displayed an increased proportion of end-differentiating T-cells. Thus, altogether these findings indicate that HCMV seropositive individuals close to MS onset tend to develop an inflammatory process involving a pool of more differentiated T-cells with respect to HCMV seronegative individuals. In this setting, persistent HCMV infection might divert immunological resources, reducing the risk of autoimmunity, in line with the hypothesis that it may be protective for MS development. A more recent study has recorded lower anti-HCMV IgG seroprevalence rates in MS patients—either younger or older than 40 years—compared to HCs [209]. Of note, these patients had relapsing MS and were not subjected to any steroid or disease-modifying treatments at the time of sampling. Overall, these findings indicate that, in MS patients, HCMV infection not only modulates the immune response by reducing the severity of the disease, but may also affect the response against EBV infection.

A very recent study has instead examined the possibility that HCMV may also induce changes in the peripheral B-cell compartment in MS patients. Both B-cell phenotype

and function were found to be influenced by HCMV infection, promoting early stages of differentiation in relapsing–remitting MS (RRMS) and reducing the pro-inflammatory cytokine profile in advanced MS. Overall, the results of this study argue in favor of the hypothesis that HCMV infection modulates B-cell subset distribution and IFN-β response in MS patients. Furthermore, they indicate that HCMV infection is associated with a reduced pro-inflammatory cytokine profile in progressive MS (PMS), thereby providing mechanistic insights into the alleged protective action of HCMV in MS [98].

In conclusion, the relationships and associations of HCMV infection with the development and progression of MS appear physiologically relevant and, thus, worthy of further investigation. Even though it is currently difficult to say with any certainty whether HCMV exerts a beneficial or harmful effect on MS, the latest findings seem to concur that there is a correlation between HCMV infection and a lower susceptibility to MS.

4.3. Enteropathies

In recent years, the role of HCMV in the pathogenesis of gastrointestinal diseases has gained increasing attention. A large body of literature has in fact documented that epithelial cells of the intestinal mucosa are the primary sites of HCMV replication both in vivo [210] and in vitro [211,212]. Moreover, HCMV has also been pinpointed as the main cause of graft failure after intestinal/multivisceral transplantation [213,214].

Among autoimmune diseases of the gastrointestinal tract, IBDs, in particular Crohn's disease (CD) and ulcerative colitis (UC), are those where a strict interplay with HCMV infection has been demonstrated [215]. CD and UC differ in the type of lesions affecting the digestive tract. Indeed, while UC is characterized by constant damage to the rectum and variable and continuous lesions to the colon, CD displays discontinuous lesions of the digestive tract [216]. Activation of IFN-γ-releasing T helper cells (Th1/Th17) and CTL is a common marker of CD, thought to counteract HCMV activity. Conversely, UC is characterized by a Th2/Th9 profile that does not inhibit HCMV replication [217,218]. These key immunological differences may offer some clues as to why HCMV reactivation is an infrequent event during CD flares, whereas it is recurrent in patients affected by UC.

A correlation between HCMV and IBDs was first proposed over 50 years ago [219] on the basis of the observation that treatment of inflamed colonic mucosa with immunosuppressive drugs, such as corticosteroids, favored HCMV reactivation. A role of HCMV in IBD has been very recently corroborated by findings showing that HCMV infection may also complicate UC or CD hospitalizations in terms of increased inpatient mortality, length of stay, and hospital charges [220].

HCMV-induced bowel inflammation follows a general pattern consisting of three phases. The first phase (initiation) involves the release of soluble mediators of inflammation from the mucosa, which serves as a way to recruit latently infected monocytes. In the second phase (reactivation), monocyte activation, and differentiation trigger viral reactivation. In the final phase (consolidation), HCMV starts replicating predominantly in ECs, exacerbating the inflammatory response [221–225]. Although the reported prevalence of HCMV infection in active IBD is highly variable, HCMV infection is regarded by many as an important risk factor for the occurrence and exacerbation of IBD [226]. However, the contribution of HCMV in IBD flare-ups has been recently questioned. While some authors have argued in favor of a significant contribution of the virus in promoting inflammatory flares, others have endorsed a role of HCMV as passive bystander [227–229]. For instance, two cohorts of HCMV-positive and HCMV-negative patients showed similar rates of colectomy, and the specific markers of infection spontaneously disappeared in HCMV-positive patients [230]. In contrast, another group found an association between HCMV infection and enhanced risk of steroid resistance, but no undeniable consensus was actually reached [231,232]. These discrepancies can be to a certain extent reconciled by the fact that the patients enrolled in those studies were affected by different inflammatory diseases (UC or CD), displayed heterogeneous clinical scores, and underwent different treatments. Additionally, inappropriate HCMV detection methods were employed. In-

terestingly, episodes of HCMV-related enterocolitis tend to decrease among IBD patients, suggesting that shifting from a corticosteroid-based maintenance therapy to more effective agents that do not trigger viral reactivation may lessen the risk of HCMV colitis [233].

Additionally, the findings related to HCMV prevalence appear to be highly heterogeneous. For example, a meta-analysis demonstrated that HCMV infection occurred in a percentage of IBD patients ranging from 0.5–100% [234]. Furthermore, an inconsistent percentage of HCMV antigen positivity (10–90%) was reported by three IBD biopsy studies [235–237]. In particular, HCMV tissue infection was observed in 11% of steroid-refractory CD patients vs. 38% of UC patients [238,239]. Moreover, markers of HCMV infection are rarely found in patients with inactive or mild-to-moderate UC [226,240–242], whereas active HCMV infection occurs in 20% to 40% of steroid-refractory UC [243–250], suggesting that HCMV exacerbates inflammation.

The molecular mechanisms underlying the interplay between HCMV and IBD seem to be related to TNF-α, an inflammatory cytokine important for the pathophysiology of IBD. Fittingly, different studies have shown how effective anti-TNFα agents can be in treating IBDs refractory to medical therapy [251,252]. Interestingly, upon binding to the TNF receptor (TNFR), TNF-α promotes NF-κB-mediate transactivation of the IE gene, thereby triggering the differentiation of HCMV latently infected cells and boosting the overall virus growth [253].

The relationship between IBD and HCMV has been studied in more detail using TCR-αKO mice latently infected with MCMV [254,255], a condition thought to replicate HCMV latency. TCR-αKO mice are prone to develop colitis, during which an increase in MCMV replication rates is typically observed. Interestingly, infected cells were identified mostly in the perivascular stroma region (i.e., pericytes) and inflamed colonic mucosa, in good agreement with reports showing that HCMV infection is more pronounced when an inflammatory status coexists [226]. In these sites, neutrophil migration and M1 macrophage presence were detected, further corroborating the notion that HCMV can induce these events in vitro as well [256].

The diagnostic protocol employed to differentiate HCMV-induced colitis from colitis associated with the inflammatory disease itself requires the analysis of viral markers, as clinical or endoscopic symptoms are not sufficient for the differential diagnosis [257–259].

Different methods are now available for the diagnosis of HCMV infection, either indirect (e.g., IgM and IgG detection) or direct ones (e.g., detection of the virus or its components), even though sometimes it is difficult to demonstrate HCMV reactivation from its intestinal reservoir (reviewed in [228,260]). Probably, the most useful method to distinguish refractory from non-refractory IBD is to quantify the HCMV load, since refractory patients display HCMV DNA values higher than 10^3 copies/10^5 cells—either enterocytes or immune cells—in the damaged mucosa [261,262], thus enabling the differentiation of HCMV colitis from mucosal infection.

HCMV infection is a critical issue to be taken into account also when it comes to therapeutic options for IBD patients. Corticosteroids are the first-line therapy for moderate-to-severe IBD flare-ups, but they enhance HCMV reactivation. Another treatment option for UC patients is represented by antivirals. Antiviral therapy is considered the most appropriate approach for moderate-to-severe, steroid-refractory relapse with high viral load values [263]. The main difficulty with applying the appropriate antiviral therapy is the distinction of HCMV reactivation from HCMV colitis as inflammation of the colonic mucosa of UC patients may contribute to reactivating HCMV replication [227,264]. Antiviral treatment allows some patients with steroid-resistant UC and active HCMV infection to avoid colectomy, even though they are poor responder to conventional IBD therapies [265], sometimes restoring the response to immunosuppressive therapies [266]. The response rate with antiviral therapy in patients with steroid-refractory disease showing HCMV reactivation is 72% (range 50–83%) [231,242,244,248]. These data should not be considered as univocal, because most of these patients were simultaneously treated with cyclosporine or granulocytapheresis and antivirals. In addition, those HCMV positive patients who were not treated

with antivirals also showed clinical improvements [230,236,244,267]. Many authors argue that antiviral treatment should be given concomitantly with immunosuppressive therapy to achieve a synergistic effect on both inflammation and viral replication [268,269], especially in the case of anti-TNF-α therapy [228,254]. Finally, an alternative option to treat UC patients with HCMV colitis is represented by the administration of granulocyte/monocyte adsorptive apheresis [244,270] or tacrolimus [230,244,271].

4.4. Metabolic Diseases
Type 1 Diabetes

Type 1 diabetes (T1D) is a chronic disease, characterized by the destruction of pancreatic β-cells, resulting in insulin deficiency. Autoimmune processes triggered by virus infections, combined with genetic susceptibility and environmental factors, have been implicated in the complex pathogenesis of T1D [272,273].

Attempts carried out by different groups to understand if HCMV is involved in the etiology of T1D gave controversial results.

For example, two independent Finnish studies did not establish an association between HCMV and T1D in young children [274,275]. These results confirm a Swedish prospective study about T1D prevalence in congenitally infected infants [276]. Conversely, a strong correlation between positivity for the HCMV genome and autoantibodies against islet cells has been found in PBMCs of Canadian T1D patients [88] as well as in a congenitally HCMV infected child, who developed T1D already at the age of 13 months [277]. Among herpesviruses, also EBV has been suggested to be related to the development of T1D [278]. A more recent paper investigating the relationship between HCMV and EBV with T1D revealed a higher percentage of IgM against HCMV and EBV in T1D patients compared to the control group [279]. These studies collectively suggested that HCMV, and also EBV, could represent a co-factor, rather than a major player, in the development of T1D.

Finally, HCMV is also generally considered an independent risk factor for early developing new-onset posttransplantation diabetes mellitus (PTDM), supported by the observation of its ability to induce the immunological damage of β-cells [280].

5. Conclusions

In recent years, HCMV has gained increasing attention from researchers due to its harmful effects on immunocompromised patients. The tremendous research effort undertaken to understand the mechanisms of HCMV pathogenesis and develop new diagnostic techniques and antiviral drugs has however led to the discovery of novel functions of this virus in other pathophysiological processes such as autoimmunity. In this review, we have summarized past and current literature on the emerging role of HCMV in several ADs, elucidating mechanisms (Figure 2) and related clinical manifestations (Table 1).

Overall, the evidence herein described clearly highlights the widespread ability of HCMV to manipulate the immune system, which may lead to self-tolerance breakdown in genetically predisposed individuals. Many hypotheses support that HCMV infection have a role in ADs. HCMV display a high seroprevalence in adults; in the USA, Europe and Australia, HCMV seroprevalence is variable, ranging between 36% and 77%, while in developing countries and in particular sub-Saharan Africa, HCMV is highly endemic with a seropositivity rate up to 100% [281]. A strengthening explanation for the high incidence of HCMV in AD patients in developing countries could be related to the high prevalence of ADs in the general population and the endemic state of HCMV with a rate approaching 100% in some areas [281].

Primary and secondary HCMV infections seem to be highly effective in shifting the balance toward immune dysregulation, which eventually triggers the initiation or perpetuation of ADs. There are also a few studies claiming a protective role of HCMV in ADs, such as in the case of MS [98], which may be easily explained by the fact that HCMV during the course of evolution has devised a number of strategies that limit inflammation and tissue damage of the host to preserve virus–host coexistence [282].

Overall, the development of new diagnostic markers to detect the presence of HCMV in AD patients may help clinicians better predict the type of clinical manifestations and the extent of disease progression. Furthermore, it is envisaged that the adoption of antivirals against HCMV in combination with immunosuppressive therapy may represent a viable therapeutic solution for certain ADs.

As large epidemiological studies are clearly needed to draw any definitive conclusions on the role of HCMV in AD pathogenesis, the availability of effective HCMV vaccines, currently in clinical development, could not only unravel the impact of HCMV on Ads, but also improve the quality of life of AD patients.

Table 1. Autoimmune diseases which have been triggered by or associated with HCMV.

Autoimmune Diseases	References *
Rheumatologic diseases	
Systemic Lupus Erythematosus	[86,87,89,118–124,126,128–134]
Systemic sclerosis	[33,83,111,138–141,143–147,149]
Rheumatoid arthritis	[92,95,100,144,151–156,179,183,185]
Neurological diseases	
Multiple sclerosis	[98,200–205,209]
Enteropathies	
Crohn disease & ulcerative colitis	[217–256,263–271]
Metabolic diseases	
Type 1 diabetes	[88,274–280]

* References cite case reports, studies or aspects of pathogenesis in each case.

References

1. Wang, L.; Wang, F.-S.; Gershwin, M.E. Human Autoimmune Diseases: A Comprehensive Update. *J. Intern. Med.* **2015**, *278*, 369–395. [CrossRef]
2. Selmi, C.; Mayo, M.J.; Bach, N.; Ishibashi, H.; Invernizzi, P.; Gish, R.G.; Gordon, S.C.; Wright, H.I.; Zweiban, B.; Podda, M.; et al. Primary Biliary Cirrhosis in Monozygotic and Dizygotic Twins: Genetics, Epigenetics, and Environment. *Gastroenterology* **2004**, *127*, 485–492. [CrossRef] [PubMed]
3. Perricone, C.; Versini, M.; Ben-Ami, D.; Gertel, S.; Watad, A.; Segel, M.J.; Ceccarelli, F.; Conti, F.; Cantarini, L.; Bogdanos, D.P.; et al. Smoke and Autoimmunity: The Fire behind the Disease. *Autoimmun. Rev.* **2016**, *15*, 354–374. [CrossRef] [PubMed]
4. Lammert, C. Genetic and Environmental Risk Factors for Autoimmune Hepatitis. *Clin. Liver Dis.* **2019**, *14*, 29–32. [CrossRef] [PubMed]
5. Deitiker, P.; Atassi, M.Z. Non-MHC Genes Linked to Autoimmune Disease. *Crit. Rev. Immunol.* **2012**, *32*, 193–285. [CrossRef]
6. Hu, X.; Daly, M. What Have We Learned from Six Years of GWAS in Autoimmune Diseases, and What Is Next? *Curr. Opin. Immunol.* **2012**, *24*, 571–575. [CrossRef]
7. Fairweather, D.; Rose, N.R. Women and Autoimmune Diseases. *Emerg. Infect. Dis.* **2004**, *10*, 2005–2011. [CrossRef]
8. Stern-Ginossar, N.; Weisburd, B.; Michalski, A.; Le, V.T.K.; Hein, M.Y.; Huang, S.-X.; Ma, M.; Shen, B.; Qian, S.-B.; Hengel, H.; et al. Decoding Human Cytomegalovirus. *Science* **2012**, *338*, 1088–1093. [CrossRef]
9. Shnayder, M.; Nachshon, A.; Krishna, B.; Poole, E.; Boshkov, A.; Binyamin, A.; Maza, I.; Sinclair, J.; Schwartz, M.; Stern-Ginossar, N. Defining the Transcriptional Landscape during Cytomegalovirus Latency with Single-Cell RNA Sequencing. *mBio* **2018**, *9*. [CrossRef]
10. DiNardo, A.R.; Netea, M.G.; Musher, D.M. Postinfectious Epigenetic Immune Modifications—A Double-Edged Sword. *N. Engl. J. Med.* **2021**, *384*, 261–270. [CrossRef] [PubMed]

11. Liu, X.; Hummel, M.; Abecassis, M. Epigenetic Regulation of Cellular and Cytomegalovirus Genes during Myeloid Cell Development. *Intern. Med. Rev.* **2017**, *3*. [CrossRef]

12. Kananen, L.; Nevalainen, T.; Jylhävä, J.; Marttila, S.; Hervonen, A.; Jylhä, M.; Hurme, M. Cytomegalovirus Infection Accelerates Epigenetic Aging. *Exp. Gerontol.* **2015**, *72*, 227–229. [CrossRef] [PubMed]

13. Surace, A.E.A.; Hedrich, C.M. The Role of Epigenetics in Autoimmune/Inflammatory Disease. *Front. Immunol.* **2019**, *10*, 1525. [CrossRef]

14. Dunn, W.; Chou, C.; Li, H.; Hai, R.; Patterson, D.; Stolc, V.; Zhu, H.; Liu, F. Functional Profiling of a Human Cytomegalovirus Genome. *Proc. Natl. Acad. Sci. USA* **2003**, *100*, 14223–14228. [CrossRef]

15. McSharry, B.P.; Avdic, S.; Slobedman, B. Human Cytomegalovirus Encoded Homologs of Cytokines, Chemokines and Their Receptors: Roles in Immunomodulation. *Viruses* **2012**, *4*, 2448–2470. [CrossRef]

16. Halenius, A.; Hengel, H. Human Cytomegalovirus and Autoimmune Disease. *Biomed. Res. Int.* **2014**, *2014*, 472978. [CrossRef]

17. Galitska, G.; Biolatti, M.; De Andrea, M.; Leone, A.; Coscia, A.; Bertolotti, L.; Ala, U.; Bertino, E.; Dell'Oste, V.; Landolfo, S. Biological Relevance of Cytomegalovirus Genetic Variability in Congenitally and Postnatally Infected Children. *J. Clin. Virol.* **2018**, *108*, 132–140. [CrossRef] [PubMed]

18. Gugliesi, F.; Coscia, A.; Griffante, G.; Galitska, G.; Pasquero, S.; Albano, C.; Biolatti, M. Where Do We Stand after Decades of Studying Human Cytomegalovirus? *Microorganisms* **2020**, *8*, 685. [CrossRef]

19. Berry, R.; Watson, G.M.; Jonjic, S.; Degli-Esposti, M.A.; Rossjohn, J. Modulation of Innate and Adaptive Immunity by Cytomegaloviruses. *Nat. Rev. Immunol.* **2020**, *20*, 113–127. [CrossRef]

20. Sinzger, C.; Schmidt, K.; Knapp, J.; Kahl, M.; Beck, R.; Waldman, J.; Hebart, H.; Einsele, H.; Jahn, G. Modification of Human Cytomegalovirus Tropism through Propagation in Vitro Is Associated with Changes in the Viral Genome. *J. Gen. Virol.* **1999**, *80*, 2867–2877. [CrossRef] [PubMed]

21. Sinzger, C.; Digel, M.; Jahn, G. Cytomegalovirus Cell Tropism. *Curr. Top. Microbiol. Immunol.* **2008**, *325*, 63–83.

22. Nguyen, C.C.; Kamil, J.P. Pathogen at the Gates: Human Cytomegalovirus Entry and Cell Tropism. *Viruses* **2018**, *10*, 704. [CrossRef]

23. Gerna, G.; Kabanova, A.; Lilleri, D. Human Cytomegalovirus Cell Tropism and Host Cell Receptors. *Vaccines* **2019**, *7*, 70. [CrossRef] [PubMed]

24. Zuhair, M.; Smit, G.S.A.; Wallis, G.; Jabbar, F.; Smith, C.; Devleesschauwer, B.; Griffiths, P. Estimation of the Worldwide Seroprevalence of Cytomegalovirus: A Systematic Review and Meta-Analysis. *Rev. Med. Virol.* **2019**, *29*, e2034. [CrossRef] [PubMed]

25. HoHsieh, A.; Wang, C.M.; Wu, Y.-J.J.; Chen, A.; Chang, M.-I.; Chen, J.-Y. B Cell Epitope of Human Cytomegalovirus Phosphoprotein 65 (HCMV Pp65) Induced Anti-DsDNA Antibody in BALB/c Mice. *Arthritis Res.* **2017**, *19*, 65. [CrossRef] [PubMed]

26. Varani, S.; Mastroianni, A.; Frascaroli, G.; Tammik, C.; Rahbar, A.; Christensson, M.; Rossini, G.; Landini, M.P.; Söderberg-Nauclér, C. Generalized Wegener's Granulomatosis in an Immunocompetent Adult after Cytomegalovirus Mononucleosis and Bacterial Urinary Tract Infection. *Arthritis Rheum.* **2009**, *60*, 1558–1562. [CrossRef]

27. Giugni, T.D.; Söderberg, C.; Ham, D.J.; Bautista, R.M.; Hedlund, K.O.; Möller, E.; Zaia, J.A. Neutralization of Human Cytomegalovirus by Human CD13-Specific Antibodies. *J. Infect. Dis.* **1996**, *173*, 1062–1071. [CrossRef] [PubMed]

28. Soderberg, C.; Sumitran-Karuppan, S.; Ljungman, P.; Moller, E. CD13-Specific Autoimmunity in Cytomegalovirus-Infected Immunocompromised Patients. *Transplantation* **1996**, *61*, 594–600. [CrossRef] [PubMed]

29. Mengarelli, A.; Minotti, C.; Palumbo, G.; Arcieri, P.; Gentile, G.; Iori, A.P.; Arcese, W.; Mandelli, F.; Avvisati, G. High Levels of Antiphospholipid Antibodies Are Associated with Cytomegalovirus Infection in Unrelated Bone Marrow and Cord Blood Allogeneic Stem Cell Transplantation. *Br. J. Haematol.* **2000**, *108*, 126–131. [CrossRef]

30. Toyoda, M.; Galfayan, K.; Galera, O.A.; Petrosian, A.; Czer, L.S.; Jordan, S.C. Cytomegalovirus Infection Induces Anti-Endothelial Cell Antibodies in Cardiac and Renal Allograft Recipients. *Transplant. Immunol.* **1997**, *5*, 104–111. [CrossRef]

31. Wager, O.; Räsänen, J.A.; Hagman, A.; Klemola, E. Mixed Cryoimmunoglobulinaemia in Infectious Mononucleois and Cytomegalovirus Mononucleosis. *Int. Arch. Allergy Appl. Immunol.* **1968**, *34*, 345–361. [CrossRef]

32. Kantor, G.L.; Goldberg, L.S.; Johnson, B.L.; Derechin, M.M.; Barnett, E.V. Immunologic Abnormalities Induced by Postperfusion Cytomegalovirus Infection. *Ann. Intern. Med.* **1970**, *73*, 553–558. [CrossRef] [PubMed]

33. Lunardi, C.; Dolcino, M.; Peterlana, D.; Bason, C.; Navone, R.; Tamassia, N.; Beri, R.; Corrocher, R.; Puccetti, A. Antibodies against Human Cytomegalovirus in the Pathogenesis of Systemic Sclerosis: A Gene Array Approach. *PLoS Med.* **2006**, *3*, e2. [CrossRef] [PubMed]

34. Streblow, D.N.; Orloff, S.L.; Nelson, J.A. Acceleration of Allograft Failure by Cytomegalovirus. *Curr. Opin. Immunol.* **2007**, *19*, 577–582. [CrossRef]

35. Amaya-Amaya, J.; Montoya-Sánchez, L.; Rojas-Villarraga, A. Cardiovascular Involvement in Autoimmune Diseases. *Biomed. Res. Int.* **2014**, *2014*, 367359. [CrossRef] [PubMed]

36. van de Berg, P.J.; Heutinck, K.M.; Raabe, R.; Minnee, R.C.; Young, S.L.; van Donselaar-van der Pant, K.A.; Bemelman, F.J.; van Lier, R.A.; ten Berge, I.J. Human Cytomegalovirus Induces Systemic Immune Activation Characterized by a Type 1 Cytokine Signature. *J. Infect. Dis.* **2010**, *202*, 690–699. [CrossRef]

37. George, M.J.; Snydman, D.R.; Werner, B.G.; Griffith, J.; Falagas, M.E.; Dougherty, N.N.; Rubin, R.H. The Independent Role of Cytomegalovirus as a Risk Factor for Invasive Fungal Disease in Orthotopic Liver Transplant Recipients. Boston Center for Liver Transplantation CMVIG-Study Group. Cytogam, MedImmune, Inc. Gaithersburg, Maryland. *Am. J. Med.* **1997**, *103*, 106–113. [CrossRef]

38. Forte, E.; Zhang, Z.; Thorp, E.B.; Hummel, M. Cytomegalovirus Latency and Reactivation: An Intricate Interplay With the Host Immune Response. *Front. Cell Infect. Microbiol.* **2020**, *10*, 130. [CrossRef]

39. Dell'Oste, V.; Biolatti, M.; Galitska, G.; Griffante, G.; Gugliesi, F.; Pasquero, S.; Zingoni, A.; Cerboni, C.; De Andrea, M. Tuning the Orchestra: HCMV vs. Innate Immunity. *Front. Microbiol.* **2020**, *11*, 661. [CrossRef]

40. Ye, L.; Qian, Y.; Yu, W.; Guo, G.; Wang, H.; Xue, X. Functional Profile of Human Cytomegalovirus Genes and Their Associated Diseases: A Review. *Front. Microbiol.* **2020**, *11*, 2104. [CrossRef]

41. Manandhar, T.; Hò, G.-G.T.; Pump, W.C.; Blasczyk, R.; Bade-Doeding, C. Battle between Host Immune Cellular Responses and HCMV Immune Evasion. *Int. J. Mol. Sci.* **2019**, *20*, 3626. [CrossRef]

42. Hewitt, E.W. The MHC Class I Antigen Presentation Pathway: Strategies for Viral Immune Evasion. *Immunology* **2003**, *110*, 163–169. [CrossRef] [PubMed]

43. Kim, S.; Lee, S.; Shin, J.; Kim, Y.; Evnouchidou, I.; Kim, D.; Kim, Y.-K.; Kim, Y.-E.; Ahn, J.-H.; Riddell, S.R.; et al. Human Cytomegalovirus MicroRNA MiR-US4-1 Inhibits CD8(+) T Cell Responses by Targeting the Aminopeptidase ERAP1. *Nat. Immunol.* **2011**, *12*, 984–991. [CrossRef]

44. Romania, P.; Cifaldi, L.; Pignoloni, B.; Starc, N.; D'Alicandro, V.; Melaiu, O.; Li Pira, G.; Giorda, E.; Carrozzo, R.; Bergvall, M.; et al. Identification of a Genetic Variation in ERAP1 Aminopeptidase That Prevents Human Cytomegalovirus MiR-UL112-5p-Mediated Immunoevasion. *Cell Rep.* **2017**, *20*, 846–853. [CrossRef]

45. Pérez-Carmona, N.; Martínez-Vicente, P.; Farré, D.; Gabaev, I.; Messerle, M.; Engel, P.; Angulo, A. A Prominent Role of the Human Cytomegalovirus UL8 Glycoprotein in Restraining Proinflammatory Cytokine Production by Myeloid Cells at Late Times during Infection. *J. Virol.* **2018**, *92*. [CrossRef]

46. Bruno, L.; Cortese, M.; Monda, G.; Gentile, M.; Calò, S.; Schiavetti, F.; Zedda, L.; Cattaneo, E.; Piccioli, D.; Schaefer, M.; et al. Human Cytomegalovirus PUL10 Interacts with Leukocytes and Impairs TCR-Mediated T-Cell Activation. *Immunol Cell Biol.* **2016**, *94*, 849–860. [CrossRef] [PubMed]

47. Akira, S.; Uematsu, S.; Takeuchi, O. Pathogen Recognition and Innate Immunity. *Cell* **2006**, *124*, 783–801. [CrossRef]

48. Galitska, G.; Biolatti, M.; Griffante, G.; Gugliesi, F.; Pasquero, S.; Dell'Oste, V.; Landolfo, S. Catch Me If You Can: The Arms Race between Human Cytomegalovirus and the Innate Immune System. *Future Virol.* **2019**, *14*, 247–263. [CrossRef]

49. Biolatti, M.; Gugliesi, F.; Dell'Oste, V.; Landolfo, S. Modulation of the Innate Immune Response by Human Cytomegalovirus. *Infect. Genet. Evol.* **2018**, *64*, 105–114. [CrossRef] [PubMed]

50. Biolatti, M.; Dell'Oste, V.; Pautasso, S.; Gugliesi, F.; von Einem, J.; Krapp, C.; Jakobsen, M.R.; Borgogna, C.; Gariglio, M.; De Andrea, M.; et al. Human Cytomegalovirus Tegument Protein Pp65 (PUL83) Dampens Type I Interferon Production by Inactivating the DNA Sensor CGAS without Affecting STING. *J. Virol.* **2018**, *92*. [CrossRef] [PubMed]

51. Huang, Z.-F.; Zou, H.-M.; Liao, B.-W.; Zhang, H.-Y.; Yang, Y.; Fu, Y.-Z.; Wang, S.-Y.; Luo, M.-H.; Wang, Y.-Y. Human Cytomegalovirus Protein UL31 Inhibits DNA Sensing of CGAS to Mediate Immune Evasion. *Cell Host Microbe* **2018**, *24*, 69–80.e4. [CrossRef] [PubMed]

52. Fu, Y.-Z.; Su, S.; Gao, Y.-Q.; Wang, P.-P.; Huang, Z.-F.; Hu, M.-M.; Luo, W.-W.; Li, S.; Luo, M.-H.; Wang, Y.-Y.; et al. Human Cytomegalovirus Tegument Protein UL82 Inhibits STING-Mediated Signaling to Evade Antiviral Immunity. *Cell Host Microbe* **2017**, *21*, 231–243. [CrossRef] [PubMed]

53. Fu, Y.-Z.; Guo, Y.; Zou, H.-M.; Su, S.; Wang, S.-Y.; Yang, Q.; Luo, M.-H.; Wang, Y.-Y. Human Cytomegalovirus Protein UL42 Antagonizes CGAS/MITA-Mediated Innate Antiviral Response. *PLoS Pathog.* **2019**, *15*, e1007691. [CrossRef] [PubMed]

54. Choi, H.J.; Park, A.; Kang, S.; Lee, E.; Lee, T.A.; Ra, E.A.; Lee, J.; Lee, S.; Park, B. Human Cytomegalovirus-Encoded US9 Targets MAVS and STING Signaling to Evade Type I Interferon Immune Responses. *Nat. Commun.* **2018**, *9*, 125. [CrossRef] [PubMed]

55. Taylor, R.T.; Bresnahan, W.A. Human Cytomegalovirus IE86 Attenuates Virus- and Tumor Necrosis Factor Alpha-Induced NFkappaB-Dependent Gene Expression. *J. Virol.* **2006**, *80*, 10763–10771. [CrossRef] [PubMed]

56. Kim, J.-E.; Kim, Y.-E.; Stinski, M.F.; Ahn, J.-H.; Song, Y.-J. Human Cytomegalovirus IE2 86 KDa Protein Induces STING Degradation and Inhibits CGAMP-Mediated IFN-β Induction. *Front. Microbiol.* **2017**, *8*, 1854. [CrossRef]

57. Zingoni, A.; Molfetta, R.; Fionda, C.; Soriani, A.; Paolini, R.; Cippitelli, M.; Cerboni, C.; Santoni, A. NKG2D and Its Ligands: "One for All, All for One". *Front. Immunol.* **2018**, *9*, 476. [CrossRef] [PubMed]

58. Lam, V.C.; Lanier, L.L. NK Cells in Host Responses to Viral Infections. *Curr. Opin. Immunol.* **2017**, *44*, 43–51. [CrossRef] [PubMed]

59. Patel, M.; Vlahava, V.-M.; Forbes, S.K.; Fielding, C.A.; Stanton, R.J.; Wang, E.C.Y. HCMV-Encoded NK Modulators: Lessons From in Vitro and in Vivo Genetic Variation. *Front. Immunol.* **2018**, *9*, 2214. [CrossRef]

60. Schmiedel, D.; Mandelboim, O. Disarming Cellular Alarm Systems-Manipulation of Stress-Induced NKG2D Ligands by Human Herpesviruses. *Front. Immunol.* **2017**, *8*, 390. [CrossRef]

61. Cosman, D.; Müllberg, J.; Sutherland, C.L.; Chin, W.; Armitage, R.; Fanslow, W.; Kubin, M.; Chalupny, N.J. ULBPs, Novel MHC Class I-Related Molecules, Bind to CMV Glycoprotein UL16 and Stimulate NK Cytotoxicity through the NKG2D Receptor. *Immunity* **2001**, *14*, 123–133. [CrossRef]

62. Kubin, M.; Cassiano, L.; Chalupny, J.; Chin, W.; Cosman, D.; Fanslow, W.; Müllberg, J.; Rousseau, A.M.; Ulrich, D.; Armitage, R. ULBP1, 2, 3: Novel MHC Class I-Related Molecules That Bind to Human Cytomegalovirus Glycoprotein UL16, Activate NK Cells. *Eur. J. Immunol.* **2001**, *31*, 1428–1437. [CrossRef]

63. Rölle, A.; Mousavi-Jazi, M.; Eriksson, M.; Odeberg, J.; Söderberg-Nauclér, C.; Cosman, D.; Kärre, K.; Cerboni, C. Effects of Human Cytomegalovirus Infection on Ligands for the Activating NKG2D Receptor of NK Cells: Up-Regulation of UL16-Binding Protein (ULBP)1 and ULBP2 Is Counteracted by the Viral UL16 Protein. *J. Immunol.* **2003**, *171*, 902–908. [CrossRef]

64. Eagle, R.A.; Traherne, J.A.; Hair, J.R.; Jafferji, I.; Trowsdale, J. ULBP6/RAET1L Is an Additional Human NKG2D Ligand. *Eur. J. Immunol.* **2009**, *39*, 3207–3216. [CrossRef] [PubMed]

65. Ashiru, O.; Bennett, N.J.; Boyle, L.H.; Thomas, M.; Trowsdale, J.; Wills, M.R. NKG2D Ligand MICA Is Retained in the Cis-Golgi Apparatus by Human Cytomegalovirus Protein UL142. *J. Virol.* **2009**, *83*, 12345–12354. [CrossRef]

66. Bennett, N.J.; Ashiru, O.; Morgan, F.J.E.; Pang, Y.; Okecha, G.; Eagle, R.A.; Trowsdale, J.; Sissons, J.G.P.; Wills, M.R. Intracellular Sequestration of the NKG2D Ligand ULBP3 by Human Cytomegalovirus. *J. Immunol.* **2010**, *185*, 1093–1102. [CrossRef]

67. Fielding, C.A.; Weekes, M.P.; Nobre, L.V.; Ruckova, E.; Wilkie, G.S.; Paulo, J.A.; Chang, C.; Suárez, N.M.; Davies, J.A.; Antrobus, R.; et al. Control of Immune Ligands by Members of a Cytomegalovirus Gene Expansion Suppresses Natural Killer Cell Activation. *Elife* **2017**, *6*. [CrossRef]

68. Charpak-Amikam, Y.; Kubsch, T.; Seidel, E.; Oiknine-Djian, E.; Cavaletto, N.; Yamin, R.; Schmiedel, D.; Wolf, D.; Gribaudo, G.; Messerle, M.; et al. Human Cytomegalovirus Escapes Immune Recognition by NK Cells through the Downregulation of B7-H6 by the Viral Genes US18 and US20. *Sci. Rep.* **2017**, *7*, 8661. [CrossRef]

69. Jenks, J.A.; Goodwin, M.L.; Permar, S.R. The Roles of Host and Viral Antibody Fc Receptors in Herpes Simplex Virus (HSV) and Human Cytomegalovirus (HCMV) Infections and Immunity. *Front. Immunol.* **2019**, *10*. [CrossRef]

70. Atalay, R.; Zimmermann, A.; Wagner, M.; Borst, E.; Benz, C.; Messerle, M.; Hengel, H. Identification and Expression of Human Cytomegalovirus Transcription Units Coding for Two Distinct Fcγ Receptor Homologs. *J. Virol.* **2002**, *76*, 8596–8608. [CrossRef]

71. Corrales-Aguilar, E.; Trilling, M.; Hunold, K.; Fiedler, M.; Le, V.T.K.; Reinhard, H.; Ehrhardt, K.; Mercé-Maldonado, E.; Aliyev, E.; Zimmermann, A.; et al. Human Cytomegalovirus Fcγ Binding Proteins Gp34 and Gp68 Antagonize Fcγ Receptors I, II and III. *PLoS Pathog.* **2014**, *10*, e1004131. [CrossRef]

72. Cortese, M.; Calò, S.; D'Aurizio, R.; Lilja, A.; Pacchiani, N.; Merola, M. Recombinant Human Cytomegalovirus (HCMV) RL13 Binds Human Immunoglobulin G Fc. *PLoS ONE* **2012**, *7*, e50166. [CrossRef]

73. Sprague, E.R.; Reinhard, H.; Cheung, E.J.; Farley, A.H.; Trujillo, R.D.; Hengel, H.; Bjorkman, P.J. The Human Cytomegalovirus Fc Receptor Gp68 Binds the Fc CH2-CH3 Interface of Immunoglobulin G. *J. Virol.* **2008**, *82*, 3490–3499. [CrossRef]

74. Perrier, S.; Serre, A.F.; Dubost, J.J.; Beaujon, G.; Plazonnet, M.P.; Albuisson, E.; Sauvezie, B. Increased Serum Levels of Interleukin 10 in Sjögren's Syndrome; Correlation with Increased IgG1. *J. Rheumatol.* **2000**, *27*, 935–939.

75. Elazeem, M.I.A.; Mohammed, R.A.; Abdallah, N.H. Correlation of Serum Interleukin-10 Level with Disease Activity and Severity in Systemic Lupus Erythematosus. *Egypt Rheumatol. Rehabil.* **2018**, *45*, 25–33. [CrossRef]

76. Manolova, I.; Ivanova, M.; Stanilova, S. Gene Polymorphisms of Immunoregulatory Cytokines IL-10 and TGF-B1 in Systemic Lupus Erythematosus. *Genes Autoimmun. Intracell. Signal. Microbiome Contrib.* **2013**. [CrossRef]

77. Colafrancesco, S.; Ciccacci, C.; Priori, R.; Latini, A.; Picarelli, G.; Arienzo, F.; Novelli, G.; Valesini, G.; Perricone, C.; Borgiani, P. STAT4, TRAF3IP2, IL10, and HCP5 Polymorphisms in Sjögren's Syndrome: Association with Disease Susceptibility and Clinical Aspects. Available online: https://www.hindawi.com/journals/jir/2019/7682827/ (accessed on 2 February 2021).

78. Ciccacci, C.; Perricone, C.; Ceccarelli, F.; Rufini, S.; Fusco, D.D.; Alessandri, C.; Spinelli, F.R.; Cipriano, E.; Novelli, G.; Valesini, G.; et al. A Multilocus Genetic Study in a Cohort of Italian SLE Patients Confirms the Association with STAT4 Gene and Describes a New Association with HCP5 Gene. *PLoS ONE* **2014**, *9*, e111991. [CrossRef] [PubMed]

79. Ji, J.D.; Lee, W.J.; Kong, K.A.; Woo, J.H.; Choi, S.J.; Lee, Y.H.; Song, G.G. Association of STAT4 Polymorphism with Rheumatoid Arthritis and Systemic Lupus Erythematosus: A Meta-Analysis. *Mol. Biol. Rep.* **2010**, *37*, 141–147. [CrossRef] [PubMed]

80. Hagberg, N.; Rönnblom, L. Interferon-α Enhances the IL-12-Induced STAT4 Activation Selectively in Carriers of the STAT4 SLE Risk Allele Rs7574865[T]. *Ann. Rheum. Dis.* **2019**, *78*, 429–431. [CrossRef]

81. Nagata, K.; Hayashi, K. Epstein-Barr Virus Reactivation-Induced Immunoglobulin Production: Significance on Autoimmunity. *Microorganisms* **2020**, *8*, 1875. [CrossRef]

82. Muryoi, T.; Kasturi, K.N.; Kafina, M.J.; Cram, D.S.; Harrison, L.C.; Sasaki, T.; Bona, C.A. Antitopoisomerase I Monoclonal Autoantibodies from Scleroderma Patients and Tight Skin Mouse Interact with Similar Epitopes. *J. Exp. Med.* **1992**, *175*, 1103–1109. [CrossRef]

83. Lunardi, C.; Bason, C.; Navone, R.; Millo, E.; Damonte, G.; Corrocher, R.; Puccetti, A. Systemic Sclerosis Immunoglobulin G Autoantibodies Bind the Human Cytomegalovirus Late Protein UL94 and Induce Apoptosis in Human Endothelial Cells. *Nat. Med.* **2000**, *6*, 1183–1186. [CrossRef] [PubMed]

84. Chang, M.; Pan, M.-R.; Chen, D.-Y.; Lan, J.-L. Human Cytomegalovirus Pp65 Lower Matrix Protein: A Humoral Immunogen for Systemic Lupus Erythematosus Patients and Autoantibody Accelerator for NZB/W F1 Mice. *Clin. Exp. Immunol.* **2006**, *143*, 167–179. [CrossRef] [PubMed]

85. Liu, Y.; Mu, R.; Gao, Y.-P.; Dong, J.; Zhu, L.; Ma, Y.; Li, Y.-H.; Zhang, H.-Q.; Han, D.; Zhang, Y.; et al. A Cytomegalovirus Peptide-Specific Antibody Alters Natural Killer Cell Homeostasis and Is Shared in Several Autoimmune Diseases. *Cell Host Microbe* **2016**, *19*, 400–408. [CrossRef]

86. Hsieh, A.-H.; Jhou, Y.-J.; Liang, C.-T.; Chang, M.; Wang, S.-L. Fragment of Tegument Protein Pp65 of Human Cytomegalovirus Induces Autoantibodies in BALB/c Mice. *Arthritis Res.* **2011**, *13*, R162. [CrossRef] [PubMed]

87. Neo, J.Y.J.; Wee, S.Y.K.; Bonne, I.; Tay, S.H.; Raida, M.; Jovanovic, V.; Fairhurst, A.-M.; Lu, J.; Hanson, B.J.; MacAry, P.A. Characterisation of a Human Antibody That Potentially Links Cytomegalovirus Infection with Systemic Lupus Erythematosus. *Sci. Rep.* **2019**, *9*, 9998. [CrossRef]

88. Pak, C.Y.; Cha, C.Y.; Rajotte, R.V.; McArthur, R.G.; Yoon, J.W. Human Pancreatic Islet Cell Specific 38 Kilodalton Autoantigen Identified by Cytomegalovirus-Induced Monoclonal Islet Cell Autoantibody. *Diabetologia* **1990**, *33*, 569–572. [CrossRef]

89. Curtis, H.A.; Singh, T.; Newkirk, M.M. Recombinant Cytomegalovirus Glycoprotein GB (UL55) Induces an Autoantibody Response to the U1-70 KDa Small Nuclear Ribonucleoprotein. *Eur. J. Immunol.* **1999**, *29*, 3643–3653. [CrossRef]

90. Varani, S.; Cederarv, M.; Feld, S.; Tammik, C.; Frascaroli, G.; Landini, M.P.; Söderberg-Nauclér, C. Human Cytomegalovirus Differentially Controls B Cell and T Cell Responses through Effects on Plasmacytoid Dendritic Cells. *J. Immunol.* **2007**, *179*, 7767–7776. [CrossRef]

91. Xu, H.; Dong, P.; Ma, X.; Song, D.; Xue, D.; Xu, R.; Lu, H.; He, X. B Cell-Activating Factor Regulates the Survival of B Lymphocytes Infected with Human Cytomegalovirus. *Immunol. Lett.* **2017**, *187*, 1–6. [CrossRef]

92. van Leeuwen, E.M.M.; Remmerswaal, E.B.M.; Vossen, M.T.M.; Rowshani, A.T.; Wertheim-van Dillen, P.M.E.; van Lier, R.A.W.; ten Berge, I.J.M. Emergence of a CD4+CD28- Granzyme B+, Cytomegalovirus-Specific T Cell Subset after Recovery of Primary Cytomegalovirus Infection. *J. Immunol.* **2004**, *173*, 1834–1841. [CrossRef]

93. Fasth, A.E.R.; Dastmalchi, M.; Rahbar, A.; Salomonsson, S.; Pandya, J.M.; Lindroos, E.; Nennesmo, I.; Malmberg, K.-J.; Söderberg-Nauclér, C.; Trollmo, C.; et al. T Cell Infiltrates in the Muscles of Patients with Dermatomyositis and Polymyositis Are Dominated by CD28null T Cells. *J. Immunol.* **2009**, *183*, 4792–4799. [CrossRef] [PubMed]

94. Gerli, R.; Schillaci, G.; Giordano, A.; Bocci, E.B.; Bistoni, O.; Vaudo, G.; Marchesi, S.; Pirro, M.; Ragni, F.; Shoenfeld, Y.; et al. CD4+CD28− T Lymphocytes Contribute to Early Atherosclerotic Damage in Rheumatoid Arthritis Patients. *Circulation* **2004**, *109*, 2744–2748. [CrossRef]

95. Bano, A.; Pera, A.; Almoukayed, A.; Clarke, T.H.S.; Kirmani, S.; Davies, K.A.; Kern, F. CD28null CD4 T-Cell Expansions in Autoimmune Disease Suggest a Link with Cytomegalovirus Infection. *F1000Res* **2019**, *8*, 327. [CrossRef]

96. Chanouzas, D.; Sagmeister, M.; Faustini, S.; Nightingale, P.; Richter, A.; Ferro, C.J.; Morgan, M.D.; Moss, P.; Harper, L. Subclinical Reactivation of Cytomegalovirus Drives CD4+CD28null T-Cell Expansion and Impaired Immune Response to Pneumococcal Vaccination in Antineutrophil Cytoplasmic Antibody-Associated Vasculitis. *J. Infect. Dis.* **2019**, *219*, 234–244. [CrossRef]

97. Wu, C.-S.; Chyuan, I.-T.; Chiu, Y.-L.; Chen, W.-L.; Shen, C.-Y.; Hsu, P.-N. Preserved Specific Anti-Viral T-Cell Response but Associated with Decreased Lupus Activity in SLE Patients with Cytomegalovirus Infection. *Rheumatology* **2020**, *59*, 3340–3349. [CrossRef] [PubMed]

98. Zabalza, A.; Vera, A.; Alari-Pahissa, E.; Munteis, E.; Moreira, A.; Yélamos, J.; Llop, M.; López-Botet, M.; Martínez-Rodríguez, J.E. Impact of Cytomegalovirus Infection on B Cell Differentiation and Cytokine Production in Multiple Sclerosis. *J. Neuroinflammation* **2020**, *17*, 161. [CrossRef]

99. Almanzar, G.; Schmalzing, M.; Trippen, R.; Höfner, K.; Weißbrich, B.; Geissinger, E.; Meyer, T.; Liese, J.; Tony, H.-P.; Prelog, M. Significant IFNγ Responses of CD8+ T Cells in CMV-Seropositive Individuals with Autoimmune Arthritis. *J. Clin. Virol.* **2016**, *77*, 77–84. [CrossRef]

100. Rothe, K.; Quandt, D.; Schubert, K.; Rossol, M.; Klingner, M.; Jasinski-Bergner, S.; Scholz, R.; Seliger, B.; Pierer, M.; Baerwald, C.; et al. Latent Cytomegalovirus Infection in Rheumatoid Arthritis and Increased Frequencies of Cytolytic LIR-1+CD8+ T Cells. *Arthritis Rheumatol.* **2016**, *68*, 337–346. [CrossRef] [PubMed]

101. Janahi, E.M.A.; Das, S.; Bhattacharya, S.N.; Haque, S.; Akhter, N.; Jawed, A.; Wahid, M.; Mandal, R.K.; Lohani, M.; Areeshi, M.Y.; et al. Cytomegalovirus Aggravates the Autoimmune Phenomenon in Systemic Autoimmune Diseases. *Microb. Pathog.* **2018**, *120*, 132–139. [CrossRef]

102. Arcangeletti, M.-C.; Maccari, C.; Vescovini, R.; Volpi, R.; Giuggioli, D.; Sighinolfi, G.; De Conto, F.; Chezzi, C.; Calderaro, A.; Ferri, C. A Paradigmatic Interplay between Human Cytomegalovirus and Host Immune System: Possible Involvement of Viral Antigen-Driven CD8+ T Cell Responses in Systemic Sclerosis. *Viruses* **2018**, *10*, 508. [CrossRef]

103. Arcangeletti, M.-C.; D'Accolti, M.; Maccari, C.; Soffritti, I.; Conto, F.D.; Chezzi, C.; Calderaro, A.; Ferri, C.; Caselli, E. Impact of Human Cytomegalovirus and Human Herpesvirus 6 Infection on the Expression of Factors Associated with Cell Fibrosis and Apoptosis: Clues for Implication in Systemic Sclerosis Development. *Int. J. Mol. Sci.* **2020**, *21*, 6397. [CrossRef] [PubMed]

104. Guo, G.; Ye, S.; Xie, S.; Ye, L.; Lin, C.; Yang, M.; Shi, X.; Wang, F.; Li, B.; Li, M.; et al. The Cytomegalovirus Protein US31 Induces Inflammation through Mono-Macrophages in Systemic Lupus Erythematosus by Promoting NF-KB2 Activation. *Cell Death Dis.* **2018**, *9*, 104. [CrossRef] [PubMed]

105. Milovanovic, J.; Popovic, B.; Milovanovic, M.; Kvestak, D.; Arsenijevic, A.; Stojanovic, B.; Tanaskovic, I.; Krmpotic, A.; Arsenijevic, N.; Jonjic, S.; et al. Murine Cytomegalovirus Infection Induces Susceptibility to EAE in Resistant BALB/c Mice. *Front. Immunol.* **2017**, *8*, 192. [CrossRef] [PubMed]

106. Wen, J.; Xiao, Y.; Wang, J.; Pan, W.; Zhou, Y.; Zhang, X.; Guan, W.; Chen, Y.; Zhou, K.; Wang, Y.; et al. Low Doses of CMV Induce Autoimmune-Mediated and Inflammatory Responses in Bile Duct Epithelia of Regulatory T Cell-Depleted Neonatal Mice. *Lab. Investig.* **2015**, *95*, 180–192. [CrossRef]

107. Zitti, B.; Bryceson, Y.T. Natural Killer Cells in Inflammation and Autoimmunity. *Cytokine Growth Factor Rev.* **2018**, *42*, 37–46. [CrossRef]

108. Martínez-Rodríguez, J.E.; Cobo-Calvo, A.; Villar, L.M.; Munteis, E.; Blanco, Y.; Rasal, R.; Vera, A.; Muntasell, A.; Alvarez-Lafuente, R.; Saiz, A.; et al. Adaptive Natural Killer Cell Response to Cytomegalovirus and Disability Progression in Multiple Sclerosis. *Mult. Scler.* **2016**, *22*, 741–752. [CrossRef]

109. McCarthy, N.E.; Eberl, M. Human Γδ T-Cell Control of Mucosal Immunity and Inflammation. *Front. Immunol.* **2018**, *9*. [CrossRef] [PubMed]

110. Tometten, I.; Felgentreff, K.; Hönig, M.; Hauck, F.; Albert, M.H.; Niehues, T.; Perez, R.; Ghosh, S.; Picard, C.; Stary, J.; et al. Increased Proportions of Γδ T Lymphocytes in Atypical SCID Associate with Disease Manifestations. *Clin. Immunol.* **2019**, *201*, 30–34. [CrossRef]

111. Lunardi, C.; Bason, C.; Corrocher, R.; Puccetti, A. Induction of Endothelial Cell Damage by HCMV Molecular Mimicry. *Trends Immunol.* **2005**, *26*, 19–24. [CrossRef]

112. Bason, C.; Corrocher, R.; Lunardi, C.; Puccetti, P.; Olivieri, O.; Girelli, D.; Navone, R.; Beri, R.; Millo, E.; Margonato, A.; et al. Interaction of Antibodies against Cytomegalovirus with Heat-Shock Protein 60 in Pathogenesis of Atherosclerosis. *Lancet* **2003**, *362*, 1971–1977. [CrossRef]

113. Dolcino, M.; Puccetti, A.; Barbieri, A.; Bason, C.; Tinazzi, E.; Ottria, A.; Patuzzo, G.; Martinelli, N.; Lunardi, C. Infections and Autoimmunity: Role of Human Cytomegalovirus in Autoimmune Endothelial Cell Damage. *Lupus* **2015**, *24*, 419–432. [CrossRef]

114. Broadley, I.; Pera, A.; Morrow, G.; Davies, K.A.; Kern, F. Expansions of Cytotoxic CD4+CD28- T Cells Drive Excess Cardiovascular Mortality in Rheumatoid Arthritis and Other Chronic Inflammatory Conditions and Are Triggered by CMV Infection. *Front. Immunol.* **2017**, *8*, 195. [CrossRef] [PubMed]

115. Pera, A.; Broadley, I.; Davies, K.A.; Kern, F. Cytomegalovirus as a Driver of Excess Cardiovascular Mortality in Rheumatoid Arthritis: A Red Herring or a Smoking Gun? *Circ. Res.* **2017**, *120*, 274–277. [CrossRef]

116. Di Battista, M.; Marcucci, E.; Elefante, E.; Tripoli, A.; Governato, G.; Zucchi, D.; Tani, C.; Alunno, A. One Year in Review 2018: Systemic Lupus Erythematosus. *Clin. Exp. Rheumatol.* **2018**, *36*, 763–777. [PubMed]

117. Luo, S.; Long, H.; Lu, Q. Recent Advances in Understanding Pathogenesis and Therapeutic Strategies of Systemic Lupus Erythematosus. *Int. Immunopharmacol.* **2020**, *89*, 107028. [CrossRef] [PubMed]

118. Pérez-Mercado, A.E.; Vilá-Pérez, S. Cytomegalovirus as a Trigger for Systemic Lupus Erythematosus. *J. Clin. Rheumatol.* **2010**, *16*, 335–337. [CrossRef]

119. Bendiksen, S.; Van Ghelue, M.; Rekvig, O.P.; Gutteberg, T.; Haga, H.J.; Moens, U. A Longitudinal Study of Human Cytomegalovirus Serology and Viruria Fails to Detect Active Viral Infection in 20 Systemic Lupus Erythematosus Patients. *Lupus* **2000**, *9*, 120–126. [CrossRef] [PubMed]

120. Rider, J.R.; Ollier, W.E.; Lock, R.J.; Brookes, S.T.; Pamphilon, D.H. Human Cytomegalovirus Infection and Systemic Lupus Erythematosus. *Clin. Exp. Rheumatol.* **1997**, *15*, 405–409.

121. Takizawa, Y.; Inokuma, S.; Tanaka, Y.; Saito, K.; Atsumi, T.; Hirakata, M.; Kameda, H.; Hirohata, S.; Kondo, H.; Kumagai, S.; et al. Clinical Characteristics of Cytomegalovirus Infection in Rheumatic Diseases: Multicentre Survey in a Large Patient Population. *Rheumatology* **2008**, *47*, 1373–1378. [CrossRef]

122. Newkirk, M.M.; van Venrooij, W.J.; Marshall, G.S. Autoimmune Response to U1 Small Nuclear Ribonucleoprotein (U1 SnRNP) Associated with Cytomegalovirus Infection. *Arthritis Res.* **2001**, *3*, 253–258. [CrossRef] [PubMed]

123. Su, B.Y.-J.; Su, C.-Y.; Yu, S.-F.; Chen, C.-J. Incidental Discovery of High Systemic Lupus Erythematosus Disease Activity Associated with Cytomegalovirus Viral Activity. *Med. Microbiol. Immunol.* **2007**, *196*, 165–170. [CrossRef] [PubMed]

124. McClain, M.T.; Poole, B.D.; Bruner, B.F.; Kaufman, K.M.; Harley, J.B.; James, J.A. An Altered Immune Response to Epstein-Barr Nuclear Antigen 1 in Pediatric Systemic Lupus Erythematosus. *Arthritis Rheum.* **2006**, *54*, 360–368. [CrossRef] [PubMed]

125. Parks, C.G.; Cooper, G.S.; Hudson, L.L.; Dooley, M.A.; Treadwell, E.L.; St.Clair, E.W.; Gilkeson, G.S.; Pandey, J.P. Association of Epstein-Barr Virus with Systemic Lupus Erythematosus: Effect Modification by Race, Age, and Cytotoxic T Lymphocyte–Associated Antigen 4 Genotype. *Arthritis Rheum.* **2005**, *52*, 1148–1159. [CrossRef]

126. James, J.A.; Neas, B.R.; Moser, K.L.; Hall, T.; Bruner, G.R.; Sestak, A.L.; Harley, J.B. Systemic Lupus Erythematosus in Adults Is Associated with Previous Epstein-Barr Virus Exposure. *Arthritis Rheum.* **2001**, *44*, 1122–1126. [CrossRef]

127. Harley, J.B.; James, J.A. Epstein-Barr Virus Infection Induces Lupus Autoimmunity. *Bull. Nyu Hosp. Jt Dis.* **2006**, *64*, 45–50. [PubMed]

128. Baboonian, C.; Venables, P.J.; Booth, J.; Williams, D.G.; Roffe, L.M.; Maini, R.N. Virus Infection Induces Redistribution and Membrane Localization of the Nuclear Antigen La (SS-B): A Possible Mechanism for Autoimmunity. *Clin. Exp. Immunol.* **1989**, *78*, 454–459.

129. Bouza, E.; Moya, J.G.; Muñoz, P. Infections in Systemic Lupus Erythematosus and Rheumatoid Arthritis. *Infect. Dis. Clin. North. Am.* **2001**, *15*, 335–361. [CrossRef]

130. Bertsias, G.; Ioannidis, J.P.A.; Boletis, J.; Bombardieri, S.; Cervera, R.; Dostal, C.; Font, J.; Gilboe, I.M.; Houssiau, F.; Huizinga, T.; et al. EULAR Recommendations for the Management of Systemic Lupus Erythematosus. Report of a Task Force of the EULAR Standing Committee for International Clinical Studies Including Therapeutics. *Ann. Rheum. Dis.* **2008**, *67*, 195–205. [CrossRef] [PubMed]

131. Fei, Y.; Shi, X.; Gan, F.; Li, X.; Zhang, W.; Li, M.; Hou, Y.; Zhang, X.; Zhao, Y.; Zeng, X.; et al. Death Causes and Pathogens Analysis of Systemic Lupus Erythematosus during the Past 26 Years. *Clin. Rheumatol.* **2014**, *33*, 57–63. [CrossRef]

132. Choo, H.M.C.; Cher, W.Q.; Kwan, Y.H.; Fong, W.W.S. Risk Factors for Cytomegalovirus Disease in Systemic Lupus Erythematosus (SLE): A Systematic Review. *Adv. Rheumatol.* **2019**, *59*, 12. [CrossRef]

133. Xue, Y.; Jiang, L.; Wan, W.-G.; Chen, Y.-M.; Zhang, J.; Zhang, Z.-C. Cytomegalovirus Pneumonia in Patients with Rheumatic Diseases After Immunosuppressive Therapy: A Single Center Study in China. *Chin. Med. J.* **2016**, *129*, 267–273. [CrossRef]

134. Qin, L.; Qiu, Z.; Hsieh, E.; Geng, T.; Zhao, J.; Zeng, X.; Wan, L.; Xie, J.; Ramendra, R.; Routy, J.P.; et al. Association between Lymphocyte Subsets and Cytomegalovirus Infection Status among Patients with Systemic Lupus Erythematosus: A Pilot Study. *Medicine* **2019**, *98*, e16997. [CrossRef] [PubMed]

135. Elhai, M.; Meune, C.; Avouac, J.; Kahan, A.; Allanore, Y. Trends in Mortality in Patients with Systemic Sclerosis over 40 Years: A Systematic Review and Meta-Analysis of Cohort Studies. *Rheumatology* **2012**, *51*, 1017–1026. [CrossRef] [PubMed]

136. Marie, I.; Gehanno, J.-F. Environmental Risk Factors of Systemic Sclerosis. *Semin. Immunopathol.* **2015**, *37*, 463–473. [CrossRef]

137. Gyftaki-Venieri, D.A.; Abraham, D.J.; Ponticos, M. Insights into Myofibroblasts and Their Activation in Scleroderma: Opportunities for Therapy? *Curr. Opin. Rheumatol.* **2018**, *30*, 581–587. [CrossRef]

138. Harvey, G.R.; McHugh, N.J. Serologic Abnormalities in Systemic Sclerosis. *Curr. Opin. Rheumatol.* **1999**, *11*, 495–502. [CrossRef] [PubMed]

139. Radić, M.; Martinović Kaliterna, D.; Radić, J. Infectious Disease as Aetiological Factor in the Pathogenesis of Systemic Sclerosis. *Neth. J. Med.* **2010**, *68*, 348–353.

140. Randone, S.B.; Guiducci, S.; Cerinic, M.M. Systemic Sclerosis and Infections. *Autoimmun. Rev.* **2008**, *8*, 36–40. [CrossRef]

141. Bilgin, H.; Kocabaş, H.; Keşli, R. The Prevalence of Infectious Agents in Patients with Systemic Sclerosis. *Turk. J. Med. Sci.* **2015**, *45*, 1192–1197. [CrossRef] [PubMed]

142. Trombetta, A.C.; Tomatis, V.; Alessandri, E.; Paolino, S.; Pizzorni, C.; Ghio, M.; Ruaro, B.; Patane, M.; Gotelli, E.; Goegan, F.; et al. AB0723 Seroprevalence of Epstein-Barr Virus and Cytomegalovirus in Systemic Sclerosis Patients: Preliminary Results. *Ann. Rheum. Dis.* **2018**, *77*, 1500–1501. [CrossRef]

143. Esen, B.A.; Yılmaz, G.; Uzun, S.; Ozdamar, M.; Aksözek, A.; Kamalı, S.; Türkoğlu, S.; Gül, A.; Ocal, L.; Aral, O.; et al. Serologic Response to Epstein-Barr Virus Antigens in Patients with Systemic Lupus Erythematosus: A Controlled Study. *Rheumatol. Int.* **2012**, *32*, 79–83. [CrossRef] [PubMed]

144. Neidhart, M.; Kuchen, S.; Distler, O.; Brühlmann, P.; Michel, B.A.; Gay, R.E.; Gay, S. Increased Serum Levels of Antibodies against Human Cytomegalovirus and Prevalence of Autoantibodies in Systemic Sclerosis. *Arthritis Rheum.* **1999**, *42*, 389–392. [CrossRef]

145. Pandey, J.P. Immunoglobulin GM Genes and IgG Antibodies to Cytomegalovirus in Patients with Systemic Sclerosis. *Clin. Exp. Rheumatol.* **2004**, *22*, S35–S37.

146. Arnson, Y.; Amital, H.; Guiducci, S.; Matucci-Cerinic, M.; Valentini, G.; Barzilai, O.; Maya, R.; Shoenfeld, Y. The Role of Infections in the Immunopathogensis of Systemic Sclerosis–Evidence from Serological Studies. *Ann. N. Y. Acad. Sci.* **2009**, *1173*, 627–632. [CrossRef] [PubMed]

147. Vaughan, J.H.; Shaw, P.X.; Nguyen, M.D.; Medsger, T.A.; Wright, T.M.; Metcalf, J.S.; Leroy, E.C. Evidence of Activation of 2 Herpesviruses, Epstein-Barr Virus and Cytomegalovirus, in Systemic Sclerosis and Normal Skins. *J. Rheumatol.* **2000**, *27*, 821–823. [PubMed]

148. Jarvis, M.A.; Nelson, J.A. Human Cytomegalovirus Persistence and Latency in Endothelial Cells and Macrophages. *Curr. Opin. Microbiol.* **2002**, *5*, 403–407. [CrossRef]

149. Efthymiou, G.; Dardiotis, E.; Liaskos, C.; Marou, E.; Scheper, T.; Meyer, W.; Daponte, A.; Daoussis, D.; Hadjigeorgiou, G.; Bogdanos, D.P.; et al. A Comprehensive Analysis of Antigen-Specific Antibody Responses against Human Cytomegalovirus in Patients with Systemic Sclerosis. *Clin. Immunol.* **2019**, *207*, 87–96. [CrossRef]

150. Balandraud, N.; Roudier, J. Epstein-Barr Virus and Rheumatoid Arthritis. *Jt. Bone Spine* **2018**, *85*, 165–170. [CrossRef] [PubMed]

151. Musiani, M.; Zerbini, M.; Ferri, S.; Plazzi, M.; Gentilomi, G.; La Placa, M. Comparison of the Immune Response to Epstein-Barr Virus and Cytomegalovirus in Sera and Synovial Fluids of Patients with Rheumatoid Arthritis. *Ann. Rheum. Dis.* **1987**, *46*, 837–842. [CrossRef]

152. Bassyouni, R.H.; Dwedar, R.A.; Ezzat, E.M.; Marzaban, R.N.; Nassr, M.H.; Rashid, L. Elevated Cytomegalovirus and Epstein-Barr Virus Burden in Rheumatoid Arthritis: A True Pathogenic Role or Just a Coincidence? *Egypt. Rheumatol.* **2019**, *41*, 255–259. [CrossRef]

153. Pierer, M.; Rothe, K.; Quandt, D.; Schulz, A.; Rossol, M.; Scholz, R.; Baerwald, C.; Wagner, U. Association of Anticytomegalovirus Seropositivity with More Severe Joint Destruction and More Frequent Joint Surgery in Rheumatoid Arthritis. *Arthritis Rheum.* **2012**, *64*, 1740–1749. [CrossRef] [PubMed]

154. Alvarez-Lafuente, R.; Fernández-Gutiérrez, B.; de Miguel, S.; Jover, J.A.; Rollin, R.; Loza, E.; Clemente, D.; Lamas, J.R. Potential Relationship between Herpes Viruses and Rheumatoid Arthritis: Analysis with Quantitative Real Time Polymerase Chain Reaction. *Ann. Rheum. Dis.* **2005**, *64*, 1357–1359. [CrossRef] [PubMed]

155. Mourgues, C.; Henquell, C.; Tatar, Z.; Pereira, B.; Nourisson, C.; Tournadre, A.; Soubrier, M.; Couderc, M. Monitoring of Epstein-Barr Virus (EBV)/Cytomegalovirus (CMV)/Varicella-Zoster Virus (VZV) Load in Patients Receiving Tocilizumab for Rheumatoid Arthritis. *Jt. Bone Spine* **2016**, *83*, 412–415. [CrossRef] [PubMed]

156. Mehraein, Y.; Lennerz, C.; Ehlhardt, S.; Remberger, K.; Ojak, A.; Zang, K.D. Latent Epstein-Barr Virus (EBV) Infection and Cytomegalovirus (CMV) Infection in Synovial Tissue of Autoimmune Chronic Arthritis Determined by RNA- and DNA-in Situ Hybridization. *Mod. Pathol.* **2004**, *17*, 781–789. [CrossRef] [PubMed]

157. Garrod, A.B. On Gout and Rheumatism. The Differential Diagnosis, and the Nature of the so-Called Rheumatic Gout. *Med. Chir. Trans.* **1854**, *37*, 181–220. [CrossRef] [PubMed]

158. Silman, A.J.; Pearson, J.E. Epidemiology and Genetics of Rheumatoid Arthritis. *Arthritis Res.* **2002**, *4* (Suppl. 3), S265–S272. [CrossRef]

159. Wolfe, A.M.; Kellgren, J.H.; Masi, A.T. The Epidemiology of Rheumatoid Arthritis: A Review. II. Incidence and Diagnostic Criteria. *Bull. Rheum Dis.* **1968**, *19*, 524–529. [PubMed]

160. Firestein, G.S. Evolving Concepts of Rheumatoid Arthritis. *Nature* **2003**, *423*, 356–361. [CrossRef]

161. Cojocaru, M.; Cojocaru, I.M.; Silosi, I.; Vrabie, C.D.; Tanasescu, R. Extra-Articular Manifestations in Rheumatoid Arthritis. *Maedica* **2010**, *5*, 286–291.

162. Taylor, P.; Gartemann, J.; Hsieh, J.; Creeden, J. A Systematic Review of Serum Biomarkers Anti-Cyclic Citrullinated Peptide and Rheumatoid Factor as Tests for Rheumatoid Arthritis. *Autoimmune Dis.* **2011**, *2011*, 815038. [CrossRef] [PubMed]

163. Nishimura, K.; Sugiyama, D.; Kogata, Y.; Tsuji, G.; Nakazawa, T.; Kawano, S.; Saigo, K.; Morinobu, A.; Koshiba, M.; Kuntz, K.M.; et al. Meta-Analysis: Diagnostic Accuracy of Anti-Cyclic Citrullinated Peptide Antibody and Rheumatoid Factor for Rheumatoid Arthritis. *Ann. Intern. Med.* **2007**, *146*, 797–808. [CrossRef] [PubMed]

164. Bizzaro, N.; Bartoloni, E.; Morozzi, G.; Manganelli, S.; Riccieri, V.; Sabatini, P.; Filippini, M.; Tampoia, M.; Afeltra, A.; Sebastiani, G.; et al. Anti-Cyclic Citrullinated Peptide Antibody Titer Predicts Time to Rheumatoid Arthritis Onset in Patients with Undifferentiated Arthritis: Results from a 2-Year Prospective Study. *Arthritis Res.* **2013**, *15*, R16. [CrossRef]

165. Vossenaar, E.R.; van Venrooij, W.J. Citrullinated Proteins: Sparks That May Ignite the Fire in Rheumatoid Arthritis. *Arthritis Res.* **2004**, *6*, 107–111. [CrossRef]

166. Acharya, N.K.; Nagele, E.P.; Han, M.; Coretti, N.J.; DeMarshall, C.; Kosciuk, M.C.; Boulos, P.A.; Nagele, R.G. Neuronal PAD4 Expression and Protein Citrullination: Possible Role in Production of Autoantibodies Associated with Neurodegenerative Disease. *J. Autoimmun.* **2012**, *38*, 369–380. [CrossRef]

167. Knight, J.S.; Subramanian, V.; O'Dell, A.A.; Yalavarthi, S.; Zhao, W.; Smith, C.K.; Hodgin, J.B.; Thompson, P.R.; Kaplan, M.J. Peptidylarginine Deiminase Inhibition Disrupts NET Formation and Protects against Kidney, Skin and Vascular Disease in Lupus-Prone MRL/Lpr Mice. *Ann. Rheum. Dis.* **2015**, *74*, 2199–2206. [CrossRef]

168. Yang, L.; Tan, D.; Piao, H. Myelin Basic Protein Citrullination in Multiple Sclerosis: A Potential Therapeutic Target for the Pathology. *Neurochem. Res.* **2016**, *41*, 1845–1856. [CrossRef] [PubMed]

169. Yuzhalin, A.E. Citrullination in Cancer. *Cancer Res.* **2019**, *79*, 1274–1284. [CrossRef] [PubMed]

170. Suzuki, A.; Yamada, R.; Chang, X.; Tokuhiro, S.; Sawada, T.; Suzuki, M.; Nagasaki, M.; Nakayama-Hamada, M.; Kawaida, R.; Ono, M.; et al. Functional Haplotypes of PADI4, Encoding Citrullinating Enzyme Peptidylarginine Deiminase 4, Are Associated with Rheumatoid Arthritis. *Nat. Genet.* **2003**, *34*, 395–402. [CrossRef]

171. Kuhn, K.A.; Kulik, L.; Tomooka, B.; Braschler, K.J.; Arend, W.P.; Robinson, W.H.; Holers, V.M. Antibodies against Citrullinated Proteins Enhance Tissue Injury in Experimental Autoimmune Arthritis. *J. Clin. Investig.* **2006**, *116*, 961–973. [CrossRef] [PubMed]

172. Foulquier, C.; Sebbag, M.; Clavel, C.; Chapuy-Regaud, S.; Al Badine, R.; Méchin, M.-C.; Vincent, C.; Nachat, R.; Yamada, M.; Takahara, H.; et al. Peptidyl Arginine Deiminase Type 2 (PAD-2) and PAD-4 but Not PAD-1, PAD-3, and PAD-6 Are Expressed in Rheumatoid Arthritis Synovium in Close Association with Tissue Inflammation. *Arthritis Rheum.* **2007**, *56*, 3541–3553. [CrossRef]

173. Willis, V.C.; Gizinski, A.M.; Banda, N.K.; Causey, C.P.; Knuckley, B.; Cordova, K.N.; Luo, Y.; Levitt, B.; Glogowska, M.; Chandra, P.; et al. N-α-Benzoyl-N5-(2-Chloro-1-Iminoethyl)-L-Ornithine Amide, a Protein Arginine Deiminase Inhibitor, Reduces the Severity of Murine Collagen-Induced Arthritis. *J. Immunol.* **2011**, *186*, 4396–4404. [CrossRef]

174. Klareskog, L.; Stolt, P.; Lundberg, K.; Källberg, H.; Bengtsson, C.; Grunewald, J.; Rönnelid, J.; Harris, H.E.; Ulfgren, A.-K.; Rantapää-Dahlqvist, S.; et al. A New Model for an Etiology of Rheumatoid Arthritis: Smoking May Trigger HLA-DR (Shared Epitope)-Restricted Immune Reactions to Autoantigens Modified by Citrullination. *Arthritis Rheum.* **2006**, *54*, 38–46. [CrossRef] [PubMed]

175. Deo, S.S.; Shetty, R.R.; Mistry, K.J.; Chogle, A.R. Detection of Viral Citrullinated Peptide Antibodies Directed Against EBV or VCP: In Early Rheumatoid Arthritis Patients of Indian Origin. *J. Lab. Physicians* **2010**, *2*, 93–99. [CrossRef]

176. Kraal, L.J.N.; Nijland, M.L.; Germar, K.L.; Baeten, D.L.P.; ten Berge, I.J.M.; Fehres, C.M. Anti-Citrullinated Protein Antibody Response after Primary EBV Infection in Kidney Transplant Patients. *PLoS ONE* **2018**, *13*, e0197219. [CrossRef]

177. Trier, N.H.; Holm, B.E.; Heiden, J.; Slot, O.; Locht, H.; Lindegaard, H.; Svendsen, A.; Nielsen, C.T.; Jacobsen, S.; Theander, E.; et al. Antibodies to a Strain-Specific Citrullinated Epstein-Barr Virus Peptide Diagnoses Rheumatoid Arthritis. *Sci. Rep.* **2018**, *8*, 3684. [CrossRef] [PubMed]

178. Casanova, V.; Sousa, F.H.; Shakamuri, P.; Svoboda, P.; Buch, C.; D'Acremont, M.; Christophorou, M.A.; Pohl, J.; Stevens, C.; Barlow, P.G. Citrullination Alters the Antiviral and Immunomodulatory Activities of the Human Cathelicidin LL-37 During Rhinovirus Infection. *Front. Immunol.* **2020**, *11*. [CrossRef] [PubMed]

179. Davis, J.M.; Knutson, K.L.; Skinner, J.A.; Strausbauch, M.A.; Crowson, C.S.; Therneau, T.M.; Wettstein, P.J.; Matteson, E.L.; Gabriel, S.E. A Profile of Immune Response to Herpesvirus Is Associated with Radiographic Joint Damage in Rheumatoid Arthritis. *Arthritis Res.* **2012**, *14*, R24. [CrossRef]

180. Martens, P.B.; Goronzy, J.J.; Schaid, D.; Weyand, C.M. Expansion of Unusual CD4+ T Cells in Severe Rheumatoid Arthritis. *Arthritis Rheum.* **1997**, *40*, 1106–1114. [CrossRef] [PubMed]

181. Pawlik, A.; Ostanek, L.; Brzosko, I.; Brzosko, M.; Masiuk, M.; Machalinski, B.; Gawronska-Szklarz, B. The Expansion of CD4+CD28− T Cells in Patients with Rheumatoid Arthritis. *Arthritis Res.* **2003**, *5*, R210–R213. [CrossRef]
182. Namekawa, T.; Wagner, U.G.; Goronzy, J.J.; Weyand, C.M. Functional Subsets of CD4 T Cells in Rheumatoid Synovitis. *Arthritis Rheum.* **1998**, *41*, 2108–2116. [CrossRef]
183. Hooper, M.; Kallas, E.G.; Coffin, D.; Campbell, D.; Evans, T.G.; Looney, R.J. Cytomegalovirus Seropositivity Is Associated with the Expansion of CD4+CD28− and CD8+CD28− T Cells in Rheumatoid Arthritis. *J. Rheumatol.* **1999**, *26*, 1452–1457.
184. Lamprecht, P.; Gross, W.L. Wegener's Granulomatosis. *Herz* **2004**, *29*, 47–56. [CrossRef]
185. Hamerman, D.; Gresser, I.; Smith, C. Isolation of Cytomegalovirus from Synovial Cells of a Patient with Rheumatoid Arthritis. *J. Rheumatol.* **1982**, *9*, 658–664. [PubMed]
186. Einsele, H.; Steidle, M.; Müller, C.A.; Fritz, P.; Zacher, J.; Schmidt, H.; Saal, J.G. Demonstration of Cytomegalovirus (CMV) DNA and Anti-CMV Response in the Synovial Membrane and Serum of Patients with Rheumatoid Arthritis. *J. Rheumatol.* **1992**, *19*, 677–681.
187. Murayama, T.; Jisaki, F.; Ayata, M.; Sakamuro, D.; Hironaka, T.; Hirai, K.; Tsuchiya, N.; Ito, K.; Furukawa, T. Cytomegalovirus Genomes Demonstrated by Polymerase Chain Reaction in Synovial Fluid from Rheumatoid Arthritis Patients. *Clin. Exp. Rheumatol.* **1992**, *10*, 161–164.
188. Xu, X.; Estekizadeh, A.; Davoudi, B.; Varani, S.; Malmström, V.; Rahbar, A.; Söderberg-Nauclér, C. Detection of Human Cytomegalovirus in Synovial Neutrophils Obtained from Patients with Rheumatoid Arthritis. *Scand. J. Rheumatol.* **2020**, 1–6. [CrossRef]
189. Melnick, J.L.; Hu, C.; Burek, J.; Adam, E.; DeBakey, M.E. Cytomegalovirus DNA in Arterial Walls of Patients with Atherosclerosis. *J. Med. Virol.* **1994**, *42*, 170–174. [CrossRef]
190. Xenaki, E.; Hassoulas, J.; Apostolakis, S.; Sourvinos, G.; Spandidos, D.A. Detection of Cytomegalovirus in Atherosclerotic Plaques and Nonatherosclerotic Arteries. *Angiology* **2009**, *60*, 504–508. [CrossRef] [PubMed]
191. Wang, H.; Peng, G.; Bai, J.; He, B.; Huang, K.; Hu, X.; Liu, D. Cytomegalovirus Infection and Relative Risk of Cardiovascular Disease (Ischemic Heart Disease, Stroke, and Cardiovascular Death): A Meta-Analysis of Prospective Studies Up to 2016. *J. Am. Heart Assoc.* **2017**, *6*. [CrossRef] [PubMed]
192. Shenk, T.; Alwine, J.C. Human Cytomegalovirus: Coordinating Cellular Stress, Signaling, and Metabolic Pathways. *Annu. Rev. Virol.* **2014**, *1*, 355–374. [CrossRef]
193. Northfield, J.; Lucas, M.; Jones, H.; Young, N.T.; Klenerman, P. Does Memory Improve with Age? CD85j (ILT-2/LIR-1) Expression on CD8 T Cells Correlates with "memory Inflation" in Human Cytomegalovirus Infection. *Immunol. Cell Biol.* **2005**, *83*, 182–188. [CrossRef] [PubMed]
194. Wagner, C.S.; Walther-Jallow, L.; Buentke, E.; Ljunggren, H.-G.; Achour, A.; Chambers, B.J. Human Cytomegalovirus-Derived Protein UL18 Alters the Phenotype and Function of Monocyte-Derived Dendritic Cells. *J. Leukoc. Biol.* **2008**, *83*, 56–63. [CrossRef]
195. Saverino, D.; Fabbi, M.; Ghiotto, F.; Merlo, A.; Bruno, S.; Zarcone, D.; Tenca, C.; Tiso, M.; Santoro, G.; Anastasi, G.; et al. The CD85/LIR-1/ILT2 Inhibitory Receptor Is Expressed by All Human T Lymphocytes and down-Regulates Their Functions. *J. Immunol.* **2000**, *165*, 3742–3755. [CrossRef] [PubMed]
196. Compston, A.; Coles, A. Multiple Sclerosis. *Lancet* **2008**, *372*, 1502–1517. [CrossRef]
197. Olsson, T.; Barcellos, L.F.; Alfredsson, L. Interactions between Genetic, Lifestyle and Environmental Risk Factors for Multiple Sclerosis. *Nat. Rev. Neurol.* **2017**, *13*, 25–36. [CrossRef]
198. Lucas, R.M.; Hughes, A.M.; Lay, M.-L.J.; Ponsonby, A.-L.; Dwyer, D.E.; Taylor, B.V.; Pender, M.P. Epstein-Barr Virus and Multiple Sclerosis. *J. Neurol. Neurosurg. Psychiatry* **2011**, *82*, 1142–1148. [CrossRef]
199. Ascherio, A. Environmental Factors in Multiple Sclerosis. *Expert Rev. Neurother.* **2013**, *13*, 3–9. [CrossRef]
200. Alari-Pahissa, E.; Moreira, A.; Zabalza, A.; Alvarez-Lafuente, R.; Munteis, E.; Vera, A.; Arroyo, R.; Alvarez-Cermeño, J.C.; Villar, L.M.; López-Botet, M.; et al. Low Cytomegalovirus Seroprevalence in Early Multiple Sclerosis: A Case for the 'Hygiene Hypothesis'? *Eur. J. Neurol.* **2018**, *25*, 925–933. [CrossRef]
201. White, D.W.; Suzanne Beard, R.; Barton, E.S. Immune Modulation during Latent Herpesvirus Infection. *Immunol. Rev.* **2012**, *245*, 189–208. [CrossRef]
202. Sanadgol, N.; Ramroodi, N.; Ahmadi, G.A.; Komijani, M.; Moghtaderi, A.; Bouzari, M.; Rezaei, M.; Kardi, M.T.; Dabiri, S.; Moradi, M.; et al. Prevalence of Cytomegalovirus Infection and Its Role in Total Immunoglobulin Pattern in Iranian Patients with Different Subtypes of Multiple Sclerosis. *New Microbiol.* **2011**, *34*, 263–274. [PubMed]
203. Najafi, S.; Ghane, M.; Poortahmasebi, V.; Jazayeri, S.M.; Yousefzadeh-Chabok, S. Prevalence of Cytomegalovirus in Patients With Multiple Sclerosis: A Case-Control Study in Northern Iran. *Jundishapur J. Microbiol.* **2016**, *9*, e36582. [CrossRef]
204. Vanheusden, M.; Stinissen, P.; 't Hart, B.A.; Hellings, N. Cytomegalovirus: A Culprit or Protector in Multiple Sclerosis? *Trends Mol. Med.* **2015**, *21*, 16–23. [1.002CrossRef] [PubMed]
205. Clerico, M.; De Mercanti, S.; Artusi, C.A.; Durelli, L.; Naismith, R.T. Active CMV Infection in Two Patients with Multiple Sclerosis Treated with Alemtuzumab. *Mult. Scler.* **2017**, *23*, 874–876. [CrossRef] [PubMed]
206. Costa-Garcia, M.; Vera, A.; Moraru, M.; Vilches, C.; López-Botet, M.; Muntasell, A. Antibody-Mediated Response of NKG2Cbright NK Cells against Human Cytomegalovirus. *J. Immunol.* **2015**, *194*, 2715–2724. [CrossRef] [PubMed]

207. López-Montañés, M.; Alari-Pahissa, E.; Sintes, J.; Martínez-Rodríguez, J.E.; Muntasell, A.; López-Botet, M. Antibody-Dependent NK Cell Activation Differentially Targets EBV-Infected Cells in Lytic Cycle and Bystander B Lymphocytes Bound to Viral Antigen-Containing Particles. *J. Immunol.* **2017**, *199*, 656–665. [CrossRef] [PubMed]
208. Lünemann, J.D.; Tintoré, M.; Messmer, B.; Strowig, T.; Rovira, A.; Perkal, H.; Caballero, E.; Münz, C.; Montalban, X.; Comabella, M. Elevated Epstein-Barr Virus-Encoded Nuclear Antigen-1 Immune Responses Predict Conversion to Multiple Sclerosis. *Ann. Neurol.* **2010**, *67*, 159–169. [CrossRef]
209. Maple, P.A.C.; Tanasescu, R.; Gran, B.; Constantinescu, C.S. A Different Response to Cytomegalovirus (CMV) and Epstein-Barr Virus (EBV) Infection in UK People with Multiple Sclerosis (PwMS) Compared to Controls. *J. Infect.* **2020**, *80*, 320–325. [CrossRef]
210. Baroco, A.L.; Oldfield, E.C. Gastrointestinal Cytomegalovirus Disease in the Immunocompromised Patient. *Curr. Gastroenterol. Rep.* **2008**, *10*, 409–416. [CrossRef]
211. Esclatine, A.; Lemullois, M.; Servin, A.L.; Quero, A.M.; Geniteau-Legendre, M. Human Cytomegalovirus Infects Caco-2 Intestinal Epithelial Cells Basolaterally Regardless of the Differentiation State. *J. Virol.* **2000**, *74*, 513–517. [CrossRef]
212. Jarvis, M.A.; Wang, C.E.; Meyers, H.L.; Smith, P.P.; Corless, C.L.; Henderson, G.J.; Vieira, J.; Britt, W.J.; Nelson, J.A. Human Cytomegalovirus Infection of Caco-2 Cells Occurs at the Basolateral Membrane and Is Differentiation State Dependent. *J. Virol.* **1999**, *73*, 4552–4560. [CrossRef]
213. Nagai, S.; Mangus, R.S.; Anderson, E.; Ekser, B.; Kubal, C.A.; Fridell, J.A.; Tector, A.J. Cytomegalovirus Infection After Intestinal/Multivisceral Transplantation: A Single-Center Experience With 210 Cases. *Transplantation* **2016**, *100*, 451–460. [CrossRef]
214. Chiereghin, A.; Gabrielli, L.; Zanfi, C.; Petrisli, E.; Lauro, A.; Piccirilli, G.; Baccolini, F.; Dazzi, A.; Cescon, M.; Morelli, M.C.; et al. Monitoring Cytomegalovirus T-Cell Immunity in Small Bowel/Multivisceral Transplant Recipients. *Transplant. Proc.* **2010**, *42*, 69–73. [CrossRef]
215. Varani, S.; Landini, M.P. Cytomegalovirus-Induced Immunopathology and Its Clinical Consequences. *Herpesviridae* **2011**, *2*, 6. [CrossRef]
216. Ramos, G.P.; Papadakis, K.A. Mechanisms of Disease: Inflammatory Bowel Diseases. *Mayo Clin. Proc.* **2019**, *94*, 155–165. [CrossRef]
217. Jentzer, A.; Veyrard, P.; Roblin, X.; Saint-Sardos, P.; Rochereau, N.; Paul, S.; Bourlet, T.; Pozzetto, B.; Pillet, S. Cytomegalovirus and Inflammatory Bowel Diseases (IBD) with a Special Focus on the Link with Ulcerative Colitis (UC). *Microorganisms* **2020**, *8*, 1078. [CrossRef] [PubMed]
218. Strober, W.; Fuss, I.J. Proinflammatory Cytokines in the Pathogenesis of Inflammatory Bowel Diseases. *Gastroenterology* **2011**, *140*, 1756–1767. [CrossRef]
219. Powell, R.D.; Warner, N.E.; Levine, R.S.; Kirsner, J.B. Cytomegalic Inclusion Disease and Ulcerative Colitis: Report of a Case in a Young Adult. *Am. J. Med.* **1961**, *30*, 334–340. [CrossRef]
220. Hendler, S.A.; Barber, G.E.; Okafor, P.N.; Chang, M.S.; Limsui, D.; Limketkai, B.N. Cytomegalovirus Infection Is Associated with Worse Outcomes in Inflammatory Bowel Disease Hospitalizations Nationwide. *Int. J. Colorectal. Dis.* **2020**, *35*, 897–903. [CrossRef]
221. Taylor-Wiedeman, J.; Sissons, J.G.; Borysiewicz, L.K.; Sinclair, J.H. Monocytes Are a Major Site of Persistence of Human Cytomegalovirus in Peripheral Blood Mononuclear Cells. *J. Gen. Virol.* **1991**, *72*, 2059–2064. [CrossRef] [PubMed]
222. Söderberg-Nauclér, C.; Fish, K.N.; Nelson, J.A. Reactivation of Latent Human Cytomegalovirus by Allogeneic Stimulation of Blood Cells from Healthy Donors. *Cell* **1997**, *91*, 119–126. [CrossRef]
223. Reeves, M.B.; Lehner, P.J.; Sissons, J.G.P.; Sinclair, J.H. An in Vitro Model for the Regulation of Human Cytomegalovirus Latency and Reactivation in Dendritic Cells by Chromatin Remodelling. *J. Gen. Virol.* **2005**, *86*, 2949–2954. [CrossRef] [PubMed]
224. Hommes, D.W.; Sterringa, G.; van Deventer, S.J.H.; Tytgat, G.N.J.; Weel, J. The Pathogenicity of Cytomegalovirus in Inflammatory Bowel Disease: A Systematic Review and Evidence-Based Recommendations for Future Research. *Inflamm. Bowel. Dis.* **2004**, *10*, 245–250. [CrossRef]
225. Julka, K.; Surawicz, C.M. Cytomegalovirus in Inflammatory Bowel Disease: Time for Another Look? *Gastroenterology* **2009**, *137*, 1163–1166. [CrossRef] [PubMed]
226. Kuwabara, A.; Okamoto, H.; Suda, T.; Ajioka, Y.; Hatakeyama, K. Clinicopathologic Characteristics of Clinically Relevant Cytomegalovirus Infection in Inflammatory Bowel Disease. *J. Gastroenterol.* **2007**, *42*, 823–829. [CrossRef]
227. Lawlor, G.; Moss, A.C. Cytomegalovirus in Inflammatory Bowel Disease: Pathogen or Innocent Bystander? *Inflamm. Bowel. Dis.* **2010**, *16*, 1620–1627. [CrossRef]
228. Pillet, S.; Pozzetto, B.; Roblin, X. Cytomegalovirus and Ulcerative Colitis: Place of Antiviral Therapy. *World J. Gastroenterol.* **2016**, *22*, 2030–2045. [CrossRef] [PubMed]
229. Mourad, F.H.; Hashash, J.G.; Kariyawasam, V.C.; Leong, R.W. Ulcerative Colitis and Cytomegalovirus Infection: From A to Z. *J. Crohns Colitis* **2020**, *14*, 1162–1171. [CrossRef]
230. Matsuoka, K.; Iwao, Y.; Mori, T.; Sakuraba, A.; Yajima, T.; Hisamatsu, T.; Okamoto, S.; Morohoshi, Y.; Izumiya, M.; Ichikawa, H.; et al. Cytomegalovirus Is Frequently Reactivated and Disappears without Antiviral Agents in Ulcerative Colitis Patients. *Am. J. Gastroenterol.* **2007**, *102*, 331–337. [CrossRef]
231. Domènech, E.; Vega, R.; Ojanguren, I.; Hernández, A.; Garcia-Planella, E.; Bernal, I.; Rosinach, M.; Boix, J.; Cabré, E.; Gassull, M.A. Cytomegalovirus Infection in Ulcerative Colitis: A Prospective, Comparative Study on Prevalence and Diagnostic Strategy. *Inflamm. Bowel Dis.* **2008**, *14*, 1373–1379. [CrossRef]

232. Lv, Y.-L.; Han, F.-F.; Jia, Y.-J.; Wan, Z.-R.; Gong, L.-L.; Liu, H.; Liu, L.-H. Is Cytomegalovirus Infection Related to Inflammatory Bowel Disease, Especially Steroid-Resistant Inflammatory Bowel Disease? A Meta-Analysis. *Infect. Drug Resist.* **2017**, *10*, 511–519. [CrossRef] [PubMed]

233. Hissong, E.; Chen, Z.; Yantiss, R.K. Cytomegalovirus Reactivation in Inflammatory Bowel Disease: An Uncommon Occurrence Related to Corticosteroid Dependence. *Mod. Pathol.* **2019**, *32*, 1210–1216. [CrossRef] [PubMed]

234. Criscuoli, V.; Rizzuto, M.-R.; Cottone, M. Cytomegalovirus and Inflammatory Bowel Disease: Is There a Link? *World J. Gastroenterol.* **2006**, *12*, 4813–4818. [CrossRef] [PubMed]

235. Rahbar, A.; Boström, L.; Lagerstedt, U.; Magnusson, I.; Söderberg-Naucler, C.; Sundqvist, V.-A. Evidence of Active Cytomegalovirus Infection and Increased Production of IL-6 in Tissue Specimens Obtained from Patients with Inflammatory Bowel Diseases. *Inflamm. Bowel Dis.* **2003**, *9*, 154–161. [CrossRef] [PubMed]

236. Kim, J.J.; Simpson, N.; Klipfel, N.; Debose, R.; Barr, N.; Laine, L. Cytomegalovirus Infection in Patients with Active Inflammatory Bowel Disease. *Dig. Dis. Sci.* **2010**, *55*, 1059–1065. [CrossRef]

237. Dimitroulia, E.; Spanakis, N.; Konstantinidou, A.E.; Legakis, N.J.; Tsakris, A. Frequent Detection of Cytomegalovirus in the Intestine of Patients with Inflammatory Bowel Disease. *Inflamm. Bowel Dis.* **2006**, *12*, 879–884. [CrossRef]

238. Roblin, X.; Pillet, S.; Berthelot, P.; Del Tedesco, E.; Phelip, J.-M.; Chambonnière, M.-L.; Peyrin-Biroulet, L.; Pozzetto, B. Prevalence of Cytomegalovirus Infection in Steroid-Refractory Crohn's Disease. *Inflamm. Bowel Dis.* **2012**, *18*, E1396–E1397. [CrossRef]

239. Römkens, T.E.H.; Bulte, G.J.; Nissen, L.H.C.; Drenth, J.P.H. Cytomegalovirus in Inflammatory Bowel Disease: A Systematic Review. *World J. Gastroenterol.* **2016**, *22*, 1321–1330. [CrossRef]

240. Knösel, T.; Schewe, C.; Petersen, N.; Dietel, M.; Petersen, I. Prevalence of Infectious Pathogens in Crohn's Disease. *Pathol. Res. Pract.* **2009**, *205*, 223–230. [CrossRef]

241. Takahashi, Y.; Tange, T. Prevalence of Cytomegalovirus Infection in Inflammatory Bowel Disease Patients. *Dis. Colon Rectum.* **2004**, *47*, 722–726. [CrossRef] [PubMed]

242. Papadakis, K.A.; Tung, J.K.; Binder, S.W.; Kam, L.Y.; Abreu, M.T.; Targan, S.R.; Vasiliauskas, E.A. Outcome of Cytomegalovirus Infections in Patients with Inflammatory Bowel Disease. *Am. J. Gastroenterol.* **2001**, *96*, 2137–2142. [CrossRef] [PubMed]

243. Kojima, T.; Watanabe, T.; Hata, K.; Shinozaki, M.; Yokoyama, T.; Nagawa, H. Cytomegalovirus Infection in Ulcerative Colitis. *Scand. J. Gastroenterol.* **2006**, *41*, 706–711. [CrossRef]

244. Yoshino, T.; Nakase, H.; Ueno, S.; Uza, N.; Inoue, S.; Mikami, S.; Matsuura, M.; Ohmori, K.; Sakurai, T.; Nagayama, S.; et al. Usefulness of Quantitative Real-Time PCR Assay for Early Detection of Cytomegalovirus Infection in Patients with Ulcerative Colitis Refractory to Immunosuppressive Therapies. *Inflamm. Bowel Dis.* **2007**, *13*, 1516–1521. [CrossRef]

245. Wada, Y.; Matsui, T.; Matake, H.; Sakurai, T.; Yamamoto, J.; Kikuchi, Y.; Yorioka, M.; Tsuda, S.; Yao, T.; Yao, S.; et al. Intractable Ulcerative Colitis Caused by Cytomegalovirus Infection: A Prospective Study on Prevalence, Diagnosis, and Treatment. *Dis. Colon. Rectum.* **2003**, *46*, S59-65. [CrossRef]

246. Minami, M.; Ohta, M.; Ohkura, T.; Ando, T.; Ohmiya, N.; Niwa, Y.; Goto, H. Cytomegalovirus Infection in Severe Ulcerative Colitis Patients Undergoing Continuous Intravenous Cyclosporine Treatment in Japan. *World J. Gastroenterol.* **2007**, *13*, 754–760. [CrossRef] [PubMed]

247. Kambham, N.; Vij, R.; Cartwright, C.A.; Longacre, T. Cytomegalovirus Infection in Steroid-Refractory Ulcerative Colitis: A Case-Control Study. *Am. J. Surg. Pathol.* **2004**, *28*, 365–373. [CrossRef] [PubMed]

248. Cottone, M.; Pietrosi, G.; Martorana, G.; Casà, A.; Pecoraro, G.; Oliva, L.; Orlando, A.; Rosselli, M.; Rizzo, A.; Pagliaro, L. Prevalence of Cytomegalovirus Infection in Severe Refractory Ulcerative and Crohn's Colitis. *Am. J. Gastroenterol.* **2001**, *96*, 773–775. [CrossRef] [PubMed]

249. Barahona-Garrido, J.; Martínez-Benítez, B.; Espinosa-Cárdenas, E.; Sarti, H.M.; Gutiérrez-Manjarrez, J.I.; Aguirre-Gutiérrez, R.; Tellez-Avila, F.I.; Coss-Adame, E.; García-Juárez, I.; Yamamoto-Furusho, J.K. Cytomegalovirus Infection in Patients Who Required Colectomy for Toxic Megacolon or Severe Steroid-Refractory Ulcerative Colitis. *Dig. Dis. Sci.* **2010**, *55*, 867–868. [CrossRef] [PubMed]

250. Maher, M.M.; Nassar, M.I. Acute Cytomegalovirus Infection Is a Risk Factor in Refractory and Complicated Inflammatory Bowel Disease. *Dig. Dis. Sci.* **2009**, *54*, 2456–2462. [CrossRef]

251. Dignass, A.; Lindsay, J.O.; Sturm, A.; Windsor, A.; Colombel, J.-F.; Allez, M.; D'Haens, G.; D'Hoore, A.; Mantzaris, G.; Novacek, G.; et al. Second European Evidence-Based Consensus on the Diagnosis and Management of Ulcerative Colitis Part 2: Current Management. *J. Crohns. Colitis* **2012**, *6*, 991–1030. [CrossRef] [PubMed]

252. Campos, S.T.; Portela, F.A.; Tomé, L. Cytomegalovirus, Inflammatory Bowel Disease, and Anti-TNFα. *Int. J. Colorectal. Dis.* **2017**, *32*, 645–650. [CrossRef]

253. Stein, J.; Volk, H.D.; Liebenthal, C.; Krüger, D.H.; Prösch, S. Tumour Necrosis Factor Alpha Stimulates the Activity of the Human Cytomegalovirus Major Immediate Early Enhancer/Promoter in Immature Monocytic Cells. *J. Gen. Virol.* **1993**, *74*, 2333–2338. [CrossRef]

254. Nakase, H.; Honzawa, Y.; Toyonaga, T.; Yamada, S.; Minami, N.; Yoshino, T.; Matsuura, M. Diagnosis and Treatment of Ulcerative Colitis with Cytomegalovirus Infection: Importance of Controlling Mucosal Inflammation to Prevent Cytomegalovirus Reactivation. *Intest. Res.* **2014**, *12*, 5–11. [CrossRef]

255. Matsumura, K.; Nakase, H.; Kosugi, I.; Honzawa, Y.; Yoshino, T.; Matsuura, M.; Kawasaki, H.; Arai, Y.; Iwashita, T.; Nagasawa, T.; et al. Establishment of a Novel Mouse Model of Ulcerative Colitis with Concomitant Cytomegalovirus Infection: In Vivo Identification of Cytomegalovirus Persistent Infected Cells. *Inflamm. Bowel Dis.* **2013**, *19*, 1951–1963. [CrossRef]

256. Chang, W.L.W.; Barry, P.A.; Szubin, R.; Wang, D.; Baumgarth, N. Human Cytomegalovirus Suppresses Type I Interferon Secretion by Plasmacytoid Dendritic Cells through Its Interleukin 10 Homolog. *Virology* **2009**, *390*, 330–337. [CrossRef]

257. Park, S.C.; Jeen, Y.M.; Jeen, Y.T. Approach to Cytomegalovirus Infections in Patients with Ulcerative Colitis. *Korean J. Intern. Med.* **2017**, *32*, 383–392. [CrossRef]

258. Fakhreddine, A.Y.; Frenette, C.T.; Konijeti, G.G. A Practical Review of Cytomegalovirus in Gastroenterology and Hepatology. *Gastroenterol. Res. Pract.* **2019**, *2019*, 6156581. [CrossRef]

259. Yerushalmy-Feler, A.; Padlipsky, J.; Cohen, S. Diagnosis and Management of CMV Colitis. *Curr. Infect. Dis. Rep.* **2019**, *21*, 5. [CrossRef] [PubMed]

260. Yokoyama, Y.; Yamakawa, T.; Hirano, T.; Kazama, T.; Hirayama, D.; Wagatsuma, K.; Nakase, H. Current Diagnostic and Therapeutic Approaches to Cytomegalovirus Infections in Ulcerative Colitis Patients Based on Clinical and Basic Research Data. *Int. J. Mol. Sci.* **2020**, *21*, 2438. [CrossRef] [PubMed]

261. Ciccocioppo, R.; Racca, F.; Paolucci, S.; Campanini, G.; Pozzi, L.; Betti, E.; Riboni, R.; Vanoli, A.; Baldanti, F.; Corazza, G.R. Human Cytomegalovirus and Epstein-Barr Virus Infection in Inflammatory Bowel Disease: Need for Mucosal Viral Load Measurement. *World J. Gastroenterol.* **2015**, *21*, 1915–1926. [CrossRef] [PubMed]

262. Ciccocioppo, R.; Racca, F.; Scudeller, L.; Piralla, A.; Formagnana, P.; Pozzi, L.; Betti, E.; Vanoli, A.; Riboni, R.; Kruzliak, P.; et al. Differential Cellular Localization of Epstein-Barr Virus and Human Cytomegalovirus in the Colonic Mucosa of Patients with Active or Quiescent Inflammatory Bowel Disease. *Immunol. Res.* **2016**, *64*, 191–203. [CrossRef]

263. Jones, A.; McCurdy, J.D.; Loftus, E.V.; Bruining, D.H.; Enders, F.T.; Killian, J.M.; Smyrk, T.C. Effects of Antiviral Therapy for Patients with Inflammatory Bowel Disease and a Positive Intestinal Biopsy for Cytomegalovirus. *Clin. Gastroenterol. Hepatol.* **2015**, *13*, 949–955. [CrossRef]

264. Beswick, L.; Ye, B.; van Langenberg, D.R. Toward an Algorithm for the Diagnosis and Management of CMV in Patients with Colitis. *Inflamm. Bowel Dis.* **2016**, *22*, 2966–2976. [CrossRef]

265. Shukla, T.; Singh, S.; Loftus, E.V.; Bruining, D.H.; McCurdy, J.D. Antiviral Therapy in Steroid-Refractory Ulcerative Colitis with Cytomegalovirus: Systematic Review and Meta-Analysis. *Inflamm. Bowel Dis.* **2015**, *21*, 2718–2725. [CrossRef]

266. Roblin, X.; Pillet, S.; Oussalah, A.; Berthelot, P.; Del Tedesco, E.; Phelip, J.-M.; Chambonnière, M.-L.; Garraud, O.; Peyrin-Biroulet, L.; Pozzetto, B. Cytomegalovirus Load in Inflamed Intestinal Tissue Is Predictive of Resistance to Immunosuppressive Therapy in Ulcerative Colitis. *Am. J. Gastroenterol.* **2011**, *106*, 2001–2008. [CrossRef]

267. Lévêque, N.; Brixi-Benmansour, H.; Reig, T.; Renois, F.; Talmud, D.; Brodard, V.; Coste, J.-F.; De Champs, C.; Andréoletti, L.; Diebold, M.-D. Low Frequency of Cytomegalovirus Infection during Exacerbations of Inflammatory Bowel Diseases. *J. Med. Virol.* **2010**, *82*, 1694–1700. [CrossRef]

268. Hommel, C.; Pillet, S.; Rahier, J.-F. Comment on: "Resolution of CMV Infection in the Bowel on Vedolizumab Therapy". *J. Crohns Colitis* **2020**, *14*, 148–149. [CrossRef] [PubMed]

269. Kopylov, U.; Papamichael, K.; Katsanos, K.; Waterman, M.; Bar-Gil Shitrit, A.; Boysen, T.; Portela, F.; Peixoto, A.; Szilagyi, A.; Silva, M.; et al. Impact of Infliximab and Cyclosporine on the Risk of Colectomy in Hospitalized Patients with Ulcerative Colitis Complicated by Cytomegalovirus-A Multicenter Retrospective Study. *Inflamm. Bowel Dis.* **2017**, *23*, 1605–1613. [CrossRef] [PubMed]

270. Sands, B.E.; Sandborn, W.J.; Panaccione, R.; O'Brien, C.D.; Zhang, H.; Johanns, J.; Adedokun, O.J.; Li, K.; Peyrin-Biroulet, L.; Van Assche, G.; et al. Ustekinumab as Induction and Maintenance Therapy for Ulcerative Colitis. *N. Engl. J. Med.* **2019**, *381*, 1201–1214. [CrossRef] [PubMed]

271. Henmi, Y.; Kakimoto, K.; Inoue, T.; Nakazawa, K.; Kubota, M.; Hara, A.; Mikami, T.; Naka, Y.; Hirata, Y.; Hirata, Y.; et al. Cytomegalovirus Infection in Ulcerative Colitis Assessed by Quantitative Polymerase Chain Reaction: Risk Factors and Effects of Immunosuppressants. *J. Clin. Biochem. Nutr.* **2018**, *63*, 246–251. [CrossRef] [PubMed]

272. Faulkner, C.L.; Luo, Y.X.; Isaacs, S.; Rawlinson, W.D.; Craig, M.E.; Kim, K.W. The Virome in Early Life and Childhood and Development of Islet Autoimmunity and Type 1 Diabetes: A Systematic Review and Meta-Analysis of Observational Studies. *Rev. Med. Virol.* **2020**, e2209. [CrossRef]

273. Mine, K.; Yoshikai, Y.; Takahashi, H.; Mori, H.; Anzai, K.; Nagafuchi, S. Genetic Susceptibility of the Host in Virus-Induced Diabetes. *Microorganisms* **2020**, *8*, 1133. [CrossRef]

274. Aarnisalo, J.; Veijola, R.; Vainionpää, R.; Simell, O.; Knip, M.; Ilonen, J. Cytomegalovirus Infection in Early Infancy: Risk of Induction and Progression of Autoimmunity Associated with Type 1 Diabetes. *Diabetologia* **2008**, *51*, 769–772. [CrossRef] [PubMed]

275. Hiltunen, M.; Hyöty, H.; Karjalainen, J.; Leinikki, P.; Knip, M.; Lounamaa, R.; Akerblom, H.K. Serological Evaluation of the Role of Cytomegalovirus in the Pathogenesis of IDDM: A Prospective Study. The Childhood Diabetes in Finland Study Group. *Diabetologia* **1995**, *38*, 705–710. [CrossRef] [PubMed]

276. Ivarsson, S.A.; Lindberg, B.; Nilsson, K.O.; Ahlfors, K.; Svanberg, L. The Prevalence of Type 1 Diabetes Mellitus at Follow-up of Swedish Infants Congenitally Infected with Cytomegalovirus. *Diabet Med.* **1993**, *10*, 521–523. [CrossRef]

277. Ward, K.P.; Galloway, W.H.; Auchterlonie, I.A. Congenital Cytomegalovirus Infection and Diabetes. *Lancet* **1979**, *1*, 497. [CrossRef]

278. Hyöoty, H.; Räasäanen, L.; Hiltunen, M.; Lehtinen, M.; Huupponen, T.; Leinikki, P. Decreased Antibody Reactivity to Epstein-Barr Virus Capsid Antigen in Type 1 (Insulin-Dependent) Diabetes Mellitus. *Apmis* **1991**, *99*, 359–363. [CrossRef]

279. Saber, A.Z.A.B.I.; Mohammed, A.H. The Roles of Human Cytomegalovirus and Epstein-Barr Virus in Type 1 Diabetes Mellitus. *Ann. Trop. Med. Health* **2019**, *22*, 90–99. [CrossRef]

280. Hjelmesæth, J.; Müller, F.; Jenssen, T.; Rollag, H.; Sagedal, S.; Hartmann, A. Is There a Link between Cytomegalovirus Infection and New-Onset Posttransplantation Diabetes Mellitus? Potential Mechanisms of Virus Induced β-Cell Damage. *Nephrol. Dial. Transplant.* **2005**, *20*, 2311–2315. [CrossRef]

281. Adland, E.; Klenerman, P.; Goulder, P.; Matthews, P.C. Ongoing Burden of Disease and Mortality from HIV/CMV Coinfection in Africa in the Antiretroviral Therapy Era. *Front. Microbiol.* **2015**, *6*, 1016. [CrossRef]

282. Clement, M.; Humphreys, I.R. Cytokine-Mediated Induction and Regulation of Tissue Damage During Cytomegalovirus Infection. *Front. Immunol.* **2019**, *10*, 78. [CrossRef]

Strigolactone Analogs Are Promising Antiviral Agents for the Treatment of Human Cytomegalovirus Infection

Matteo Biolatti [1] , **Marco Blangetti** [2] , **Giulia D'Arrigo** [3] , **Francesca Spyrakis** [3] ,
Paola Cappello [4] , **Camilla Albano** [1] , **Paolo Ravanini** [5] , **Santo Landolfo** [1] ,
Marco De Andrea [1,6,*] , **Cristina Prandi** [2] and **Valentina Dell'Oste** [1,*]

1   Department of Public Health and Pediatric Sciences, University of Turin, 10126 Turin, Italy;
    matteo.biolatti@unito.it (M.B.); camilla.albano@unito.it (C.A.); santo.landolfo@unito.it (S.L.)
2   Department of Chemistry, University of Turin, 10125 Turin, Italy; marco.blangetti@unito.it (M.B.);
    cristina.prandi@unito.it (C.P.)
3   Department of Molecular Biotechnology and Health Sciences, University of Turin, 10126 Turin, Italy;
    giulia.darrigo@unito.it (G.D.); francesca.spyrakis@unito.it (F.S.)
4   Department of Drug Science and Technology, University of Turin, 10125 Turin, Italy; paola.cappello@unito.it
5   Laboratory Medicine Department, Laboratory of Molecular Virology, "Maggiore della Carità" Hospital,
    28100 Novara, Italy; paolo.ravanini@gmail.com
6   Center for Translational Research on Autoimmune and Allergic Disease-CAAD, 28100 Novara, Italy
*   Correspondence: marco.deandrea@unito.it (M.D.A.); valentina.delloste@unito.it (V.D.);
    Tel.: +39-011-6705647 (M.D.A.); +39-011-6705631 (V.D.)

Abstract: The human cytomegalovirus (HCMV) is a widespread pathogen and is associated with severe diseases in immunocompromised individuals. Moreover, HCMV infection is the most frequent cause of congenital malformation in developed countries. Although nucleoside analogs have been successfully employed against HCMV, their use is hampered by the occurrence of serious side effects. There is thus an urgent clinical need for less toxic, but highly effective, antiviral drugs. Strigolactones (SLs) are a novel class of plant hormones with a multifaceted activity. While their role in plant-related fields has been extensively explored, their effects on human cells and their potential applications in medicine are far from being fully exploited. In particular, their antiviral activity has never been investigated. In the present study, a panel of SL analogs has been assessed for antiviral activity against HCMV. We demonstrate that TH-EGO and EDOT-EGO significantly inhibit HCMV replication in vitro, impairing late protein expression. Moreover, we show that the SL-dependent induction of apoptosis in HCMV-infected cells is a contributing mechanism to SL antiviral properties. Overall, our results indicate that SLs may be a promising alternative to nucleoside analogs for the treatment of HCMV infections.

Keywords: human cytomegalovirus; strigolactone analogs; antiviral activity; apoptosis

1. Introduction

Human cytomegalovirus (HCMV), which is part of the *Betaherpesvirinae* subfamily, is one of the most significant opportunistic human pathogens. Although HCMV rarely causes symptomatic clinical manifestations in immunocompetent individuals, it induces severe morbidity and mortality in the immunocompromised population, following either primary infection or reactivation, leading to gastro-intestinal diseases, pneumonia, retinitis and other organ infections [1]. Moreover, HCMV is the most common cause of congenital malformations in developed countries, resulting in neurodevelopmental delay, fetal and neonatal death, and most frequently sensorineural hearing loss [2,3].

Clinically available drugs for anti-HCMV therapy are currently mainly composed of nucleoside, nucleotide and non-nucleotide inhibitors of viral DNA synthesis [4]. However, these agents suffer from several drawbacks, including the induction of adverse side effects, especially in the treatment of congenital infections, and the selection of single- or multi-resistant HCMV mutants [2]. Therefore, there is a burning need to develop new compounds against HCMV diseases.

Strigolactones (SLs) are a newly emerged class of plant hormones with many functions. They are made up of a tricyclic ABC core bound to a fourth butenolide ring, commonly known as the D-ring, that is generally thought to be responsible for the bioactivity of SLs [5]. SLs contribute to defining plant morphology, even in response to environmental conditions, and are involved in the setup of communication with organisms in the rhizosphere. For instance, they regulate shoot branching and serve as rhizosphere signals for the control of host-plant interactions with heterologous organisms, including symbiotic arbuscular mycorrhizal fungi and parasitic weeds [6]. In recent years, SLs have become a cutting-edge topic in plant biology and agronomy as they hold great potential for the development of modern agriculture [7].

While their role in plant-related fields has been thoroughly investigated, the effects of SLs on human cells and their use in medicine are both still poorly defined. The most significant data reported thus far refer to the effect of SLs on cancer cells [8–10]. Indeed, it has been demonstrated that synthetic analogs of SLs induce G2/M arrest and apoptosis in a variety of human cancer cells, while having minimal influence on the growth and viability of non-transformed cells, such as human fibroblasts, mammary epithelial cells and normal primary prostate cells [11,12]. Interestingly, cancer cells with stem-like properties are more sensitive to the inhibitory effects of SL analogs than the heterogeneous population of cancer cells [11]. The SL anti-proliferative effects displayed on cancer cells have also been confirmed by the finding that SLs induce DNA double-strand breaks (DSBs), and impair cellular DNA-repair [13].

Finally, recent papers have reported the promising anti-inflammatory effects that SLs exert by inhibiting the release of inflammatory molecules, i.e., nitric oxide (NO), tumor necrosis factor-alpha (TNF-α) and interleukin-6 (IL-6), and the migration of neutrophils and macrophages in fluorescent-protein-labeled zebrafish larvae [14], as well as by triggering the expression of detoxifying enzymes, such as heme-oxygenase (HO-1) and NAD(P)H dehydrogenase [quinone] 1 (NQO1) [15].

As the antiviral activity of SLs has never been investigated, we have screened a panel of SL analogs in order to identify new druggable targets for anti-HCMV therapy. We show, for the first time, that the SLs TH-EGO and EDOT-EGO and their derivatives that lack the butenolide ring (TH-ABC and EDOT-ABC) (see Table 1) markedly inhibit the replication of different HCMV strains in vitro. Moreover, we demonstrate that SLs do not affect the first steps of HCMV infection, i.e., attachment and entry, rather, they exert their role on the late phases of the viral cycle. In particular, we show that an SL-dependent apoptotic trigger may be a novel strategy against HCMV infection.

Finally, *in silico* molecular docking simulations have been used to predict the interactions between the SL analogs and the modeled structure of the putative target IE1, which is known to inhibit apoptosis [16–18].

2. Materials and Methods

2.1. Compounds

The SL analogs TH-EGO, EDOT-EGO and EGO-10 were synthesized as previously described [19]. TH-ABC and EDOT-ABC were synthesized according to the cited procedure, with the exception that the last synthetic sequence step was omitted. GR24 was purchased from Strigolab srl.

The SL analogs were dissolved in dimethyl sulfoxide (DMSO) (Sigma-Aldrich, Milan, Italy) at stock concentrations of 20 mM and used as racemic mixtures. Cells were treated at the indicated doses by diluting the compounds to the required highest concentration in the appropriate culture medium.

2.2. Cells and Viruses

Primary human foreskin fibroblasts (HFFs, ATCC SCRC-1041™, American Type Culture Collection, Manassas, VA, USA) and African green monkey kidney cells (VEROs, ATCC CCL-81™) were cultured in Dulbecco's Modified Eagle's Medium supplemented with 10% heat inactivated fetal bovine serum (FBS), 2 mM glutamine, 1 mM sodium pyruvate, 100 U/mL penicillin and 100 µg/mL streptomycin sulfate (Sigma-Aldrich, Milan, Italy). The HCMV laboratory strain Merlin was kindly provided by Klaus Hamprecht and Gerhard Jahn (University Hospital of Tübingen, Germany) [20]; the VR1814 isolate was provided by Giuseppe Gerna (University of Pavia, Italy) [21]; the AD169 (ATCC VR538, American Type Culture Collection, Manassas, VA, USA) HCMV strain was already available at the Laboratory of Pathogenesis of Viral Infections (University of Turin, Italy). All HCMV strains were propagated and titrated on HFFs using a standard plaque assay [22]. Clinical isolates of HSV-1 and HSV-2 were a generous gift from Valeria Ghisetti, "Amedeo di Savoia" Hospital, Turin, Italy. They were propagated and titrated by plaque assay on Vero cells, as previously described [23].

2.3. Antiviral Assays

2.3.1. Virus Yield Reduction Assay

HFF or VERO cells were seeded in 24-well plates and pre-treated, after 24 h, with different concentrations of SL analogs or the vehicle control (DMSO) for 2 h at 37 °C. They were then infected with HCMV or HSV, respectively, at MOI of 0.1 PFU/cell in the presence of SLs. Following virus adsorption (2 h at 37 °C), the viral inoculum was removed, and the cultures were maintained in medium that contained the corresponding molecule for 144 h (HCMV) or 48 h (HSV). The cells and supernatants were then harvested and disrupted using three freeze (liquid nitrogen)/thaw (37 °C) cycles. The extent of virus replication was subsequently assessed by titrating the infectivity of the supernatants of the cell suspensions in HFF or VERO cells, as previously described [23,24]. Plaques were microscopically counted, and the mean plaque counts for each drug concentration were expressed as a percentage of the mean plaque count of DMSO. The number of plaques was plotted as a function of drug concentration, and the concentration that produced a 50% reduction in plaque formation (IC_{50}) was determined for each test by a nonlinear regression (curve fitting analysis) in GraphPad Prism software.

2.3.2. Attachment Assay

HFFs were seeded in 24-well plates and, after 24 h, the cultures were chilled over ice for 20 min and washed three times with a 4 °C pre-chilled medium. Pre-chilled cell monolayers were then treated with either serial dilutions of compounds or DMSO for 30 min at 4 °C, then infected with on ice pre-cooled HCMV (MOI 0.1) and incubated for 2 h at 4 °C to ensure viral attachment, but not entry. After two gentle washes with cold DMEM to remove any unattached virus and compounds, cells were overlaid with 0.8% methylcellulose medium and shifted to 37 °C for 72 h. At the end of the incubation, plates were fixed and colored with crystal violet, and the plaques were microscopically counted. Subsequently, one lane per plate was used as a control to confirm that incubation at 4 °C allowed viral attachment, but not viral entry. In order to establish this, the cells to which the virus had been pre-attached at 4 °C were treated with cold (4 °C) acidic glycine (100 mM glycine, 150 mM NaCl [pH 3]) for 2 min to inactivate any attached, but not yet penetrated, virus, before being overlaid with 0.8% methylcellulose. This resulted in 100% inhibition of plaque formation in untreated cells, indicating that no virus had entered the cells during the attachment period.

2.3.3. Entry Assay

HCMV (MOI of 0.1) was adsorbed for 2 h at 4 °C on pre-chilled (4 °C) confluent HFFs to allow viral attachment. Cells were then washed with cold DMEM three times to remove any unbound virus, treated with different concentrations of either the compounds or DMSO, and incubated for 2 h at

37 °C. Any un-penetrated virus was inactivated with acidic glycine for 2 min at room temperature, as previously described. Subsequently, the cells were washed three times with medium pre-warmed at 37 °C to return the pH to neutral, overlaid with 0.8% methylcellulose and incubated for 72 h at 37 °C. Plates were then fixed and colored with crystal violet, and plaques were microscopically counted.

2.4. Cytotoxicity Assay

To determine SL cytotoxicity, HFF and VERO cells were seeded in a 96-well culture plate and exposed to increasing concentrations of either SLs or vehicle (DMSO) the following day. After 144 h or 48 h, respectively, of incubation, the number of viable cells was determined using the 3-(4,5-dimethylthiazol-2-yl)-2,5-diphenyltetrazolium bromide (MTT) (Sigma-Aldrich, Milan, Italy) assay, as previously described [15].

2.5. Western Blot Analysis

After treatment, cells were washed with PBS, and cell lysis was carried out using Radioimmunoprecipitation Assay (RIPA) buffer to obtain total cell lysate. An equal amount of the cell extracts was fractionated by electrophoresis on sodium dodecyl sulfate polyacrylamide gels and transferred to Immobilon-P membranes (Biorad, Milan, Italy). After blocking with 5% nonfat dry milk in TBS-Tween 0.05%, membranes were incubated overnight at 4 °C with the appropriate primary antibodies. The following primary antibodies were used: mouse monoclonal antibodies anti-IEA (IE1 and IE2, clone CH160) (Virusys, Taneytown, MD, USA, P1215), UL44 (clone (CH13) (Virusys, Taneytown, MD, USA, P1202-1), pp28 (clone 5C3) (Virusys, Taneytown, MD, USA, CA004-100) and anti-α-Tubulin (clone 5-B-1-2) (Active-Motif, La Hulpe, Belgium, 39527) (all at 1:1000 dilution in 5% nonfat dry milk, TBS-Tween 0.05%). After washing with TBST buffer (500 mM NaCl, 20 mM Tris pH 7.4, 0.05% Tween 20), the membrane was incubated with an HRP-conjugated anti-mouse secondary antibody (GE Healthcare, Chicago, IL, USA) for 1 h at room temperature, and visualized using an enhanced chemiluminescence detection kit (SuperSignal West Pico Chemiluminescent Substrate, Thermo SCIENTIFIC, Waltham, MA, USA).

2.6. Apoptosis Detection

2.6.1. Annexin V Analysis

To distinguish apoptotic from necrotic cells, double staining was performed for exposed phosphatidylserine and propidium iodide (PI) exclusion using the Annexin V-FITC Apoptosis Detection Kit (Calbiochem, San Diego, CA, USA). Experiments were performed according to the manufacturer's instructions. Briefly, the different compounds (12.5 µM) were added to the HFFs, and the cells were then infected and processed 24 or 48 h after treatment. The cells were washed in PBS, trypsinized and then resuspended in a binding buffer (10 mM HEPES/NaOH, pH 7.4, 140 mM NaCl, 2.5 mM CaCl$_2$). Annexin V-FITC was added to a final concentration of 100 ng/mL, and the cells were incubated in the dark for 10 min, then washed again in PBS and resuspended in 300 µL of the binding buffer. In total, 40 µg/mL of PI was added to each sample before the flow cytometric analyses. Cells were analyzed using a FACSCalibur flow cytometer (BD Biosciences, Franklin Lakes, NJ, USA). Data analysis was performed using standard ModFit LT software (BD Biosciences, Franklin Lakes, NJ, USA). Unstained cells, cells stained with Annexin V-FITC only and cells stained with PI only were used as controls to establish compensation and quadrants. Cells were gated according to their light-scatter properties to exclude cell debris.

2.6.2. In-Vitro Analysis of Caspase-3 Activity

Caspase-3 activity was assessed using the SensoLyte AFC Caspase Sampler Kit "Fluorimetric" (Anaspec, CA, USA). Experiments were performed according to the manufacturer's instructions. After 1 h of incubation at 25 °C, fluorescence was measured at an excitation wavelength of 405 nm and

an emission wavelength of 500 nm using the VICTOR3 1420 multilabel counter (Perkin–Elmer, Milan, Italy). Protease activity was expressed as RFU (relative units of fluorescence).

2.7. Molecular Modeling

The HCMV IE1 (UL123) structure was modeled by means of the homology modeling service SWISS-MODEL [25]. The crystal structure of the IE1 of the rhesus macaque cytomegalovirus (PDB code 4wic) was used as a template to construct the model of the IE1 of HCMV (Merlin strain). The identity sequence was 25% and the coverage 74%. The stereochemical validation of the model was performed by building the Ramachandran plot of the protein-backbone using the RAMPAGE server (http://mordred.bioc.cam.ac.uk/~{}rapper/rampage.php). Possible druggable pockets were identified in the protein model using the FLAP*site* algorithm, which was implemented in the FLAP software (Molecular Discovery Ltd., Borehamwood, UK) [26]. The molecular docking of SL analogs was performed using GOLD suite version 5.5 (The Cambridge Crystallographic Data Centre, CCDC, Software Ltd., Cambridge, UK) [27]. The region of interest was defined within 10 Å from a reference atom (HB2 on Arg72). GOLD default parameters were set, and the compounds were subjected to 15 genetic algorithm runs using the CHEMPLP fitness function. Pictures were prepared using PyMOL version 1.7.6.4.

2.8. Statistical Analysis

All statistical tests were performed using GraphPad Prism version 5.00 for Windows (GraphPad Software, La Jolla, CA, USA). Data are presented as means ± standard deviations (SD). Means were compared using two-way analysis of variance (ANOVA) with Bonferroni's post-tests. Differences were considered to be statistically significant for $p < 0.05$ (*, $p < 0.05$; **, $p < 0.01$; ***, $p < 0.001$).

3. Results

3.1. Effects of SL Analogs on HCMV Productive Infection

In order to identify novel compounds that are capable of inhibiting HCMV replication in vitro, we screened a series of SL analogs, named TH-EGO, EDOT-EGO, EGO-10 and GR24, which had previously been characterized for their anti-proliferative [11,12] and anti-inflammatory activities [13–15]. Their chemical characteristics are reported in Table 1.

Although the stereochemistry of SLs at the 2' position of the butenolide ring and the fact that it plays a crucial role in bioactivity effectiveness have been well explored, we decided to start our preliminary screening with racemic mixtures of the compounds [28].
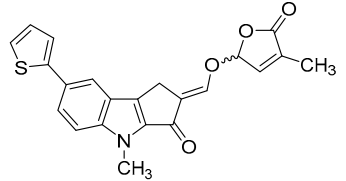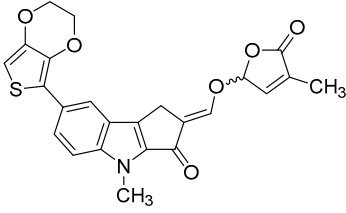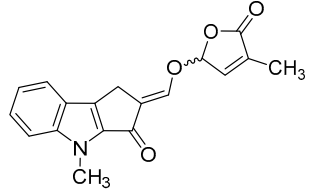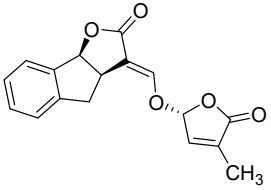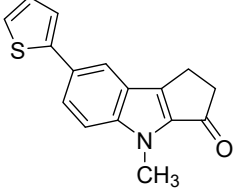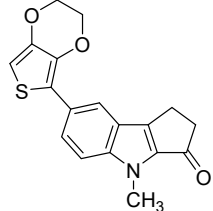
Prior to the assessment of the antiviral activity of SL analogs, a standard MTT viability assay was performed to rule out the possibility that the drugs may have cytotoxic effects on the HFF cells. To this end, different concentrations of each molecule were tested, and the compounds were only considered non-toxic if they maintained at least 70% cell viability after 144 h of treatment. This parameter indicated that the cytotoxicity of the compounds shown in Figure 1A (i.e., TH-EGO, EDOT-EGO, EGO-10 and GR24) for primary HFFs was low or undetectable at concentrations of up to 25 µM as ~90% of treated cells were viable after 144 h (Figure 1A).

TH-EGO, EDOT-EGO, EGO-10 and GR24 were then analyzed for their antiviral activity against a range of HCMV strains, i.e., Merlin, AD169 and VR1814, at a concentration of 25 µM, which was the minimum effective dose that did not show particular cytotoxicity. A series of time-of-addition assays were performed to show which phase of the HCMV replication cycle is targeted by SL analogs. Briefly, the compounds were added to the cells as follows: (i) before infection (pre-adsorption stage, from 2 h prior to infection); (ii) during infection (adsorption stage, 2 h); (iii) after infection (post-adsorption stage, from 0 to 144 hpi); or (iv) before, during, and after infection (Figure 1B). The virus yield reduction assay revealed that TH-EGO, EDOT-EGO and to a lesser extent GR24 demonstrated significant activity against HCMV when added before, during and after infection (Figure 1C). Finally, the inhibition of HCMV replication was limited to the higher doses tested or was absent in the pre-treatment or

post-treatment assays, meaning that IC$_{50}$ values could not be determined (data not shown). Two of the SL analyzed, namely TH-EGO and EDOT-EGO, inhibited HCMV replication by over 90% and were, thus, selected for further analysis. Interestingly, the inhibitory activity of SLs was not strain specific, as was observed in HFFs infected with different HCMV strains (Figure 1C).

A more detailed analysis with serial dilutions of the two compounds (3–25 µM) revealed that TH-EGO and EDOT-EGO specifically inhibited HCMV replication (the Merlin strain was used in all of the subsequent experiments, because its background resembles clinical isolates [29]) in a dose-dependent manner, with inhibitory concentration (IC$_{50}$) values of 12.04 and 9.13 µM, respectively (Figure 1D).

Table 1. Strigolactone (SL) compounds used in this study.

| Chemical Structure	Compound	IUPAC Name
	TH-EGO	(±)(*E*)-4-methyl-2-(((4-methyl-5-oxo-2,5-dihydrofuran-2-yl)oxy)methylene)-7-(thiophen-2-yl)-1,4-dihydrocyclopenta[b]indol-3(2*H*)-one
	EDOT-EGO	(±)(*E*)-7-(2,3-dihydrothieno[3,4-b][1,4]dioxin-5-yl)-4-methyl-2-(((4-methyl-5-oxo-2,5-dihydrofuran-2-yl)oxy)methylene)-1,4-dihydrocyclopenta[b]indol-3(2*H*)-one
	EGO-10	(±)(*E*)-4-methyl-2-(((4-methyl-5-oxo-2,5-dihydrofuran-2-yl)oxy)methylene)-1,4-dihydrocyclopenta[b]indol-3(2*H*)-one
	GR24	(±)(3a*R*,8b*S*,*E*)-3-((((*R*)-4-methyl-5-oxo-2,5-dihydrofuran-2-yl)oxy)methylene)-3,3a,4,8b-tetrahydro-2*H*-indeno[1,2-b]furan-2-one
	TH-ABC	4-methyl-7-(thiophen-2-yl)-1,4-dihydrocyclopenta[b]indol-3(2*H*)-one
	EDOT-ABC	7-(2,3-dihydrothieno[3,4-b][1,4]dioxin-5-yl)-4-methyl-1,4-dihydrocyclopenta[b]indol-3(2*H*)-one
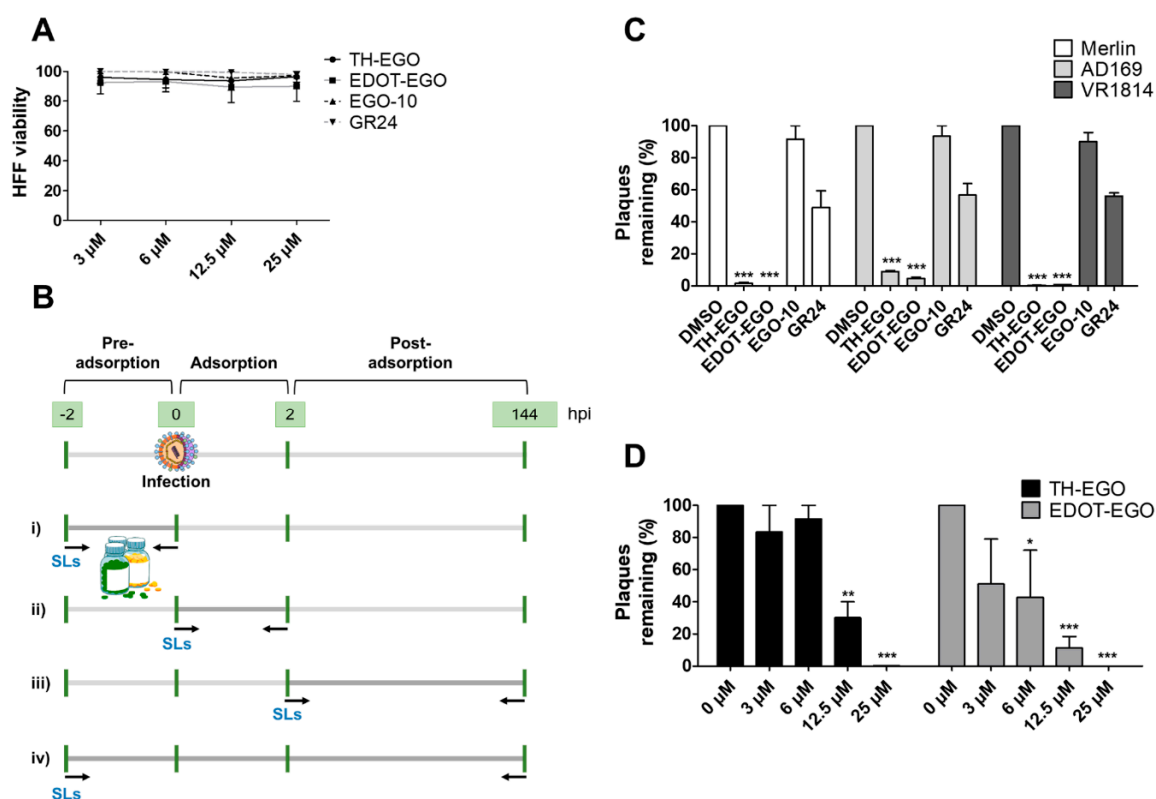
Figure 1. SL analogs antiviral activity against the human cytomegalovirus (HCMV). (**A**) Cell viability was measured using the 3-(4,5-dimethylthiazol-2-yl)-2,5-diphenyltetrazolium bromide (MTT) assay. Confluent human foreskin fibroblast (HFF) cultures seeded in 96-well plates were incubated with different concentrations of the indicated SLs for 144 h. Graphs are representative of three independent experiments with duplicate replicate wells for each analysis. (**B**) Flow-charts of time-of-addition assays. (**C**) Identification of SL-analogs with anti-HCMV activity. HFF cells were cultivated in 24-well plates and pre-treated with 25 μM of the indicated SLs for 2 h. Subsequently, cells were infected with the indicated HCMV strains (MOI of 0.1) and, following virus adsorption (2 h at 37 °C), the viral inoculum was removed; cultures were exposed to SLs during the infection, for 144 h. Dimethyl sulfoxide (DMSO) was used as the vehicle control. The extent of HCMV replication was then assessed by titrating the infectivity of supernatants and cell-associated viruses—obtained from freeze (liquid nitrogen)/thaw (37 °C) cycles—and combined using a standard plaque assay in HFFs. Plaques were microscopically counted, and the mean plaque counts for each molecule were expressed as a percentage of the mean plaque count of the control. Three independent experiments were performed, and one representative experiment is shown (***, $p < 0.001$, two-way ANOVA followed by Bonferroni's post-tests). (**D**) HFFs were infected with HCMV (Merlin strain, MOI of 0.1) and, where indicated, the cells were treated with increasing concentrations of TH-EGO, EDOT-EGO or DMSO, before and during virus adsorption. These remained in the culture media throughout the experiment. The extent of HCMV replication was then assessed by titrating the infectivity of supernatants and cell-associated viruses—obtained from freeze (liquid nitrogen)/thaw (37 °C) cycles—and combined using a standard plaque assay. Plaques were microscopically counted, and the mean plaque counts for each drug concentration were expressed as a percentage of the mean count of the control. The number of plaques was plotted as a function of drug concentration. Three independent experiments were performed, and one representative experiment is shown (*, $p < 0.05$; **, $p < 0.01$; ***, $p < 0.001$, two-way ANOVA followed by Bonferroni's post-tests).

To further evaluate whether the antiviral activity of the SL analogs was limited to HCMV or whether it could be extended to other members of the *Herpesviridae* family, we assessed their efficacy against herpes simplex type 1 (HSV-1) and type 2 (HSV-2) (Figure S1). MTT viability assays on VERO cells after 48 h of treatment were used to establish that a dose of 12.5 μM was associated with low

or undetectable cytotoxicity for all of the compounds tested (Figure S1, panel A). We confirmed that TH-EGO and EDOT-EGO were the most powerful SL analogs against both HSV-1 and HSV-2, with IC_{50} values of 5.71 and 11.80 for TH-EGO, and 4.16 and 3.81 for EDOT-EGO, respectively (Figure S1, panel B and C).

3.2. The Butenolide Ring Is Critical for the Antiviral Activity of TH-EGO and EDOT-EGO

Since TH-EGO and EDOT-EGO displayed the most potent anti-HCMV activity, we sought to unveil the functional group responsible for this antiviral property. Two SL analogs that lack an enol ether bridge on the butenolide ring, named TH-ABC and EDOT-ABC, were then synthesized and evaluated for their antiviral activity (Table 1). As shown in Figure 2A, the modified compounds also did not affect (TH-ABC, ~90%) or slightly affect (EDOT-ABC, ~70%) cell viability up to 25 μM. Interestingly, they partially retained antiviral activity against HCMV in vitro, although it was lower than that of the original compounds, suggesting that the presence of an enol ether bridge on the butenolide ring is critical for the antiviral activity of TH-EGO and EDOT-EGO (Figure 2B).

Interestingly, the efficacy of the SL derivatives that lack the enol ether bridge on the butenolide ring (TH-ABC and EDOT-ABC) were highly compromised for both HSV-1 and HSV-2, confirming that this structure is critical to the antiviral activity of TH-EGO and EDOT-EGO (Figure S1, panel C).
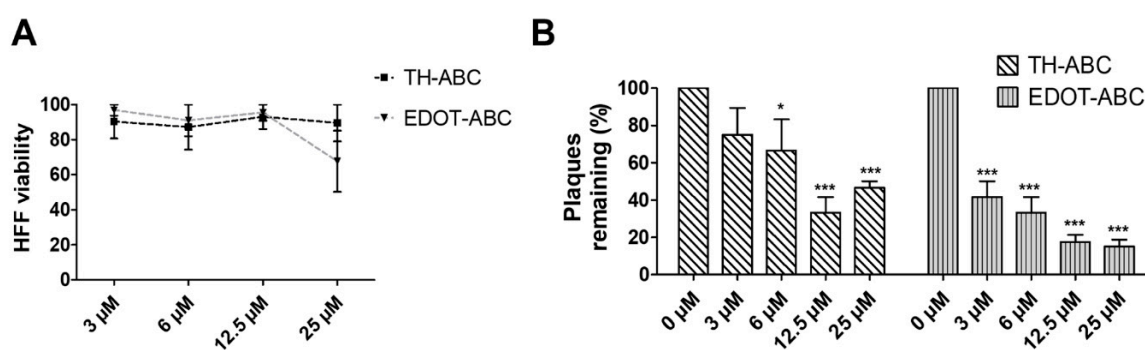

Figure 2. SL derivatives antiviral activity against HCMV. (**A**) Viability was measured using the MTT assay. Confluent HFF cultures were seeded in 96-well plates and incubated with different concentrations of SLs for 144 h. Graphs are representative of three independent experiments with duplicate replicate wells for each analysis. (**B**) Antiviral activity of TH-ABC and EDOT-ABC on HCMV replication. HFF cells were pre-treated with the indicated dilutions of SLs for 2 h. Subsequently, the HFFs were infected with the HCMV Merlin strain (MOI of 0.1) and, following virus adsorption (2 h at 37 °C), the viral inoculum was removed and the cultures were exposed to increasing dilutions of either the SLs or vehicle (DMSO) and incubated for 144 h. Supernatants and cell-associated viruses—obtained from freeze (liquid nitrogen)/thaw (37 °C) cycles—were combined, and virus infectivity titers were determined by plaque assay. Plaques were microscopically counted, and the mean plaque counts for each compound concentration were expressed as a percentage of the mean count of the control (*, $p < 0.05$; ***, $p < 0.001$, two-way ANOVA followed by Bonferroni's post-tests).

3.3. TH-EGO and EDOT-EGO Inhibit an Early-Late Event in the HCMV Replication Cycle

In order to gain more insight into the nature of the antiviral activity of the selected SL analogs, the effects of TH-EGO and EDOT-EGO were investigated during the HCMV replication cycle. To investigate if the compounds may target the early steps of the virus life cycle, i.e., virus attachment and entry into cells, an attachment assay was first carried out under experimental conditions in which the virus was allowed to bind to the surface of the host cells, in the presence or absence of SLs, but did not undergo cell entry. Briefly, pre-chilled HFF monolayers were infected with HCMV in the presence of the SLs, for 2 h at 4 °C. Cells were washed to remove the compounds and any unabsorbed viral particles, and a 0.8% methylcellulose solution was then added to measure the infectivity of the particles that had

successfully attached to the cells. As shown in Figure 3A, TH-EGO and EDOT-EGO barely impaired the attachment of HCMV in a concentration-independent manner.
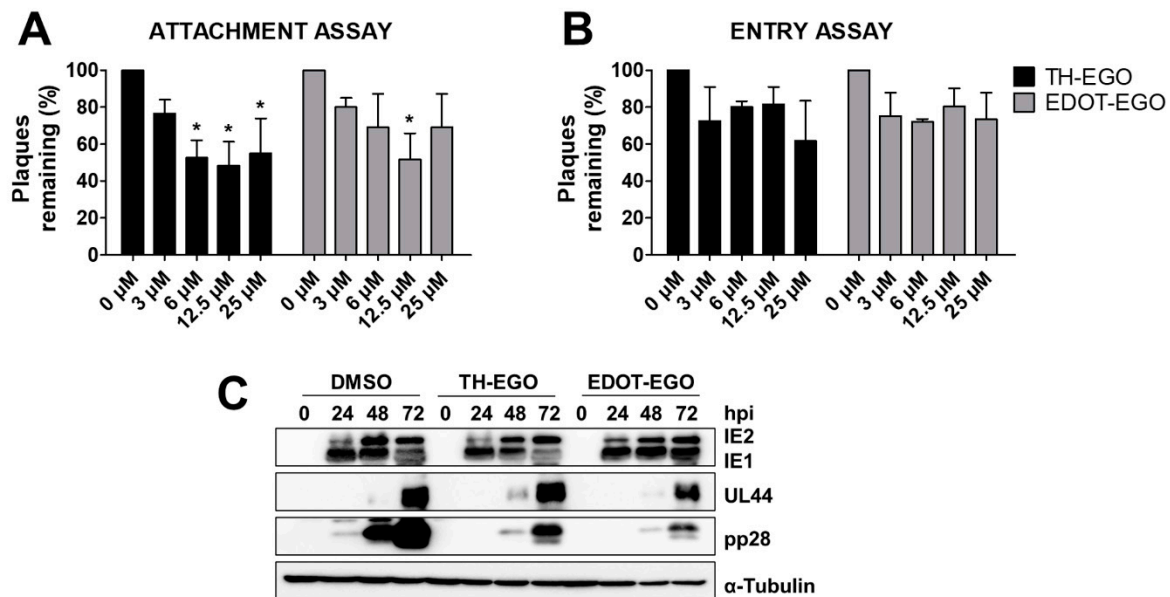

Figure 3. Inhibitory effect on individual stages of viral protein production. (**A**) Attachment assay. HFF cells were infected with HCMV Merlin (MOI of 0.1) in the presence of serial dilutions of either the SLs or vehicle (DMSO); inoculated cultures were then kept for 2 h at 4 °C in presence of SL analogs to allow virus attachment, but not entry, to occur, which were then tested using plaque reduction assays. Plaques were microscopically counted, and the mean plaque counts for each drug concentration were expressed as a percentage of the mean count of the control (*, $p < 0.05$, two-way ANOVA followed by Bonferroni's post-tests) (**B**) Entry assay. HFFs were infected in the absence of SLs and kept at 4 °C for 2 h to allow virus attachment to occur; serial dilutions of the compound were added to washed cells and the temperature was then shifted to 37 °C to allow entry to occur. After a single wash with acidic glycine to remove virus particles from the cell surface, cells were overlaid with methylcellulose-containing medium. Data are presented as a percentage of the mean count of the control (two-way ANOVA followed by Bonferroni's post-tests). (**C**) HFFs were treated with TH-EGO, EDOT-EGO (12.5 μM) or with equal volumes of DMSO solvent 1 h before infection and for the entire duration of the infection, and infected with HCMV at a MOI of 0.3. Lysates were prepared at the indicated time-points and subjected to Western blot analyses for IEA (IE1 + IE2), UL44, pp28 and α-Tubulin, which was used as a loading control.

To test whether the inhibitory activities of the SL analogs were due to the inhibition of HCMV entry into cells, pre-chilled HFF monolayers were infected with HCMV for 2 h at 4 °C. TH-EGO, EDOT-EGO and DMSO (used as a vehicle negative control) were then added, and the cells were further incubated at 37 °C to allow viral entry. These experimental conditions allow synchronized virus penetration to occur following attachment at low temperatures. After 2 h at 37 °C, SL analogs were removed, and acidic glycine treatment was performed to inactivate any residual HCMV particles that were attached to the cell surface. The cells were then overlaid with 0.8% methylcellulose to measure the infectivity of HCMV that had successfully entered the cells. As shown in Figure 3B, SL analogs only weakly affected HCMV entry under the examined concentrations. Taken together, these findings suggest that TH-EGO and EDOT-EGO are not able to interfere with viral attachment and entry, indicating that the initial steps of HCMV replication are not the main targets for SLs.

Finally, in order to identify the phase of the HCMV replication program that is affected by SL analogs, the effects of TH-EGO and EDOT-EGO on viral gene expression were investigated in HCMV-infected cells. To this end, total protein cell extracts were prepared from HCMV-infected

HFFs that had been treated with the indicated compounds for various lengths of time post infection. The expression patterns of IEA (IE1 and IE2), UL44 and pp28 were then examined via immunoblotting with specific antibodies and were used as a reflection of the levels of immediate-early, early and late viral products, respectively. As shown in Figure 3C, TH-EGO and EDOT-EGO decreased the expression of the late tegument protein pp28 at every time point, whereas the IEA and UL44 proteins were not affected. These results indicate that the SL analogs interfere with a molecular event that occurs in an early-late stage of the HCMV replication cycle, i.e., a stage that follows the onset of IE gene expression and viral DNA replication.

3.4. Virolysis as the Mechanism for TH-EGO and EDOT-EGO Antiviral Activity

It has been previously reported that SL analogs induce apoptosis in the osteosarcoma cell line U2OS [13]. As apoptosis is also one of the major mechanisms by which hosts evade viral infection [18,30], we assessed the capability of SL analogs to modulate cell-death pathways in HCMV-infected cells via dual staining with annexin V and PI. The binding of Annexin V to phosphatidyl serine is a marker of early apoptosis, while PI only stains the chromatin of cells with compromised plasma membrane and is, therefore, a marker of necrosis. As shown in Figure 4A, at 48 hpi, a significant increase in early apoptosis (annexin+/PI−) and necrosis (annexin+/PI+) was detected in cells treated with TH-EGO (40.39 vs. 5.66; 11.33 vs. 9.05) and EDOT-EGO (39.40 vs. 5.66; 17.42 vs. 9.05) compared to vehicle-treated cells. Moreover, we compared the activity of caspase-3, the final executor of the apoptotic cascade, in cells treated with either TH-EGO, EDOT-EGO or DMSO at different time points after HCMV infection to definitively corroborate the pro-apoptotic effect of SLs on infected cells, as caspases play a central role in mediating various apoptotic responses. Interestingly, significant differences in the ability to activate caspase-3 were observed in SL-treated, infected and non-infected cells (Figure 4B), suggesting that the SLs may specifically trigger caspase activity and promote the apoptotic process only during the course of HCMV infection.

3.5. Identification of Putative Drug-Binding Target Proteins Using In-Silico Docking Simulations

We decided to use an *in silico* structure-based approach to get clues on the possible molecular targets of the SL-analogs, performing molecular docking simulations on possibly relevant HCMV targets. In the series of HCMV proteins involved in apoptosis inhibition, it was found that vMIA (UL37, prevents the pro-apoptotic cascade), vICA (UL36, prevents caspase-8 activation), UL38 (inhibits apoptosis and facilitates viral replication), IE1 (UL123) and IE2 (UL122) play a key role in initiating lytic cycle gene regulation pathways [16]. We searched the Protein Data Bank [31] for the crystallographic structure of the listed proteins and did not find any of them. Therefore, we tried to model the structures of the missing proteins using homology modeling, and were only able to obtain reliable models for IE1 (see Materials and Methods for further details on IE1). The obtained models were analyzed using the FLAP*site* algorithm [26] for the identification of possible binding sites, and the SL analogs were docked in most druggable pockets using GOLD software [32]. Herein, we only report the results that were obtained upon docking the most active SLs, TH-EGO and EDOT-EGO, in IE1. The IE1 structure was modeled on the IE1 of rhesus macaque cytomegalovirus (PDD code 4wic), with which it shares low sequence identity (25%) but high coverage (74%). The model Ramachandran plot reported that 98% of the residues were in favored regions (see Figure S2). The protein model is shown in Figure 5A and displays a relatively elongated structure. The unique pocket, which is large enough to accommodate SL analogs, was identified between helix 2 and the loop connecting helices 3 and 4. TH-EGO and EDOT-EGO were docked in the pocket and their binding pose is reported in Figure 5B,C. Considering that, currently, all the known natural SLs have been shown to have a (*R*)-configuration at the 2′ position where the D-ring is bound to the rest of the molecule [33], in both cases the (*R*)-enantiomer of our synthesized analogues was chosen. The score, which was assigned to the poses using the CHEMPLP scoring function, as implemented in the GOLD software, was quite high ([67 and 70, respectively]; [34]) and supported the reliability of the prediction.
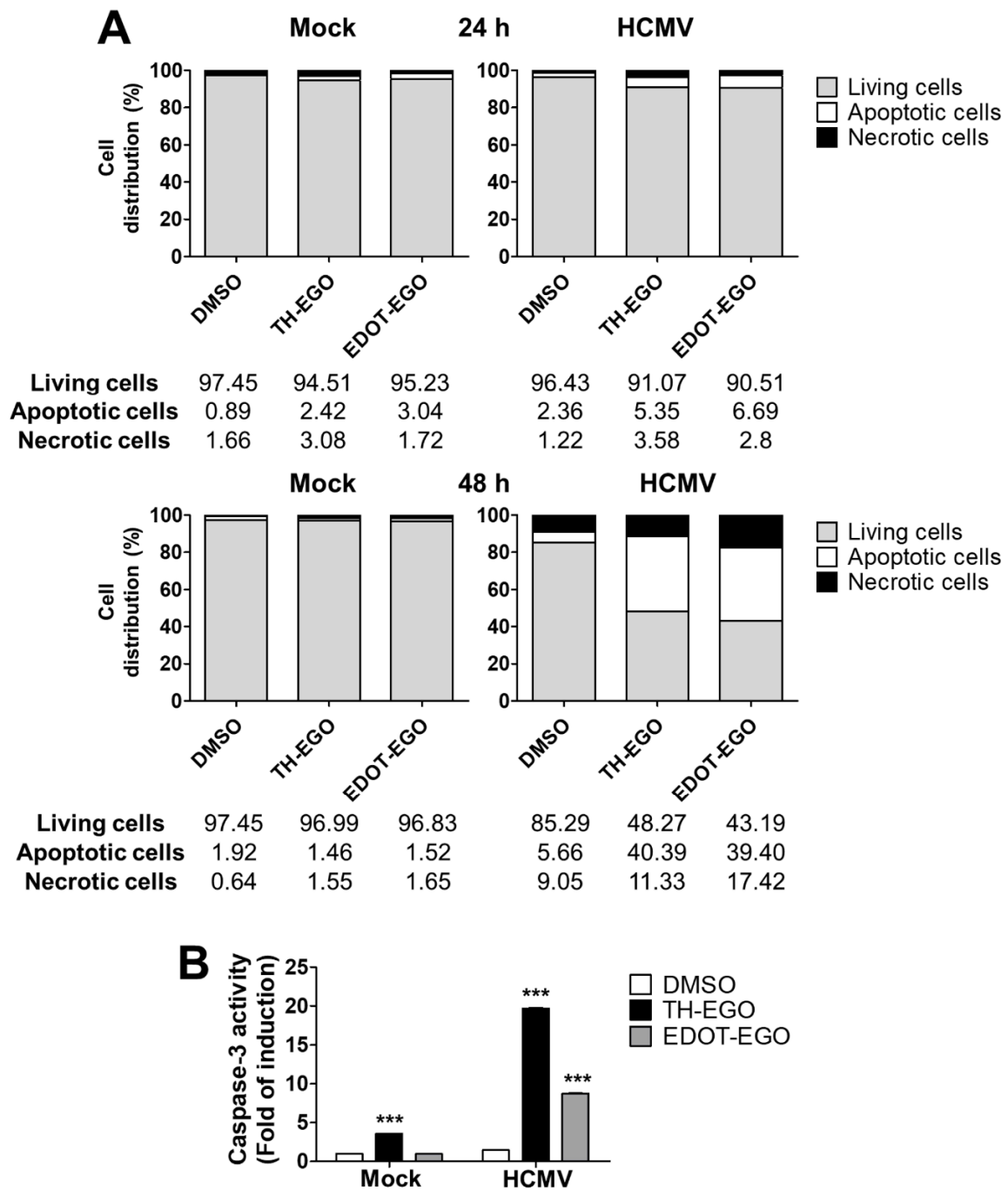
Figure 4. Interplay between apoptosis and SL analogs. (**A**) HFFs were treated with TH-EGO, EDOT-EGO (12.5 μM) or with equal volumes of DMSO solvent 1 h before infection and for the entire duration of the infection, and infected with HCMV (Merlin strain, MOI 1). After 24 h (upper panel) and 48 h (lower panel), cells were processed for Annexin V/propidium iodide (PI) flow cytometric analysis. Annexin−/PI− cells indicated living cells, Annexin+/PI− apoptotic cells and Annexin+/PI+ necrotic cells. Values were plotted as the percentage of cell distribution across the three different conditions. (**B**) HFFs were treated as described in (**A**) for 24 h with either SL TH-EGO, EDOT-EGO (12.5 μM) or with the solvent DMSO, in the absence or the presence of HCMV (Merlin strain, MOI 1) and processed via fluorimetric assay for caspase-3 activation. Fluorescence intensity is reported as RFU values (relative fluorescence units). Fold changes were calculated after the normalization of the SL-analogs vs. DMSO-treated cells, in mock or HCMV-infected cells. Data are shown as mean ± SD (***, $p < 0.001$, two-way ANOVA followed by Bonferroni's post-tests).
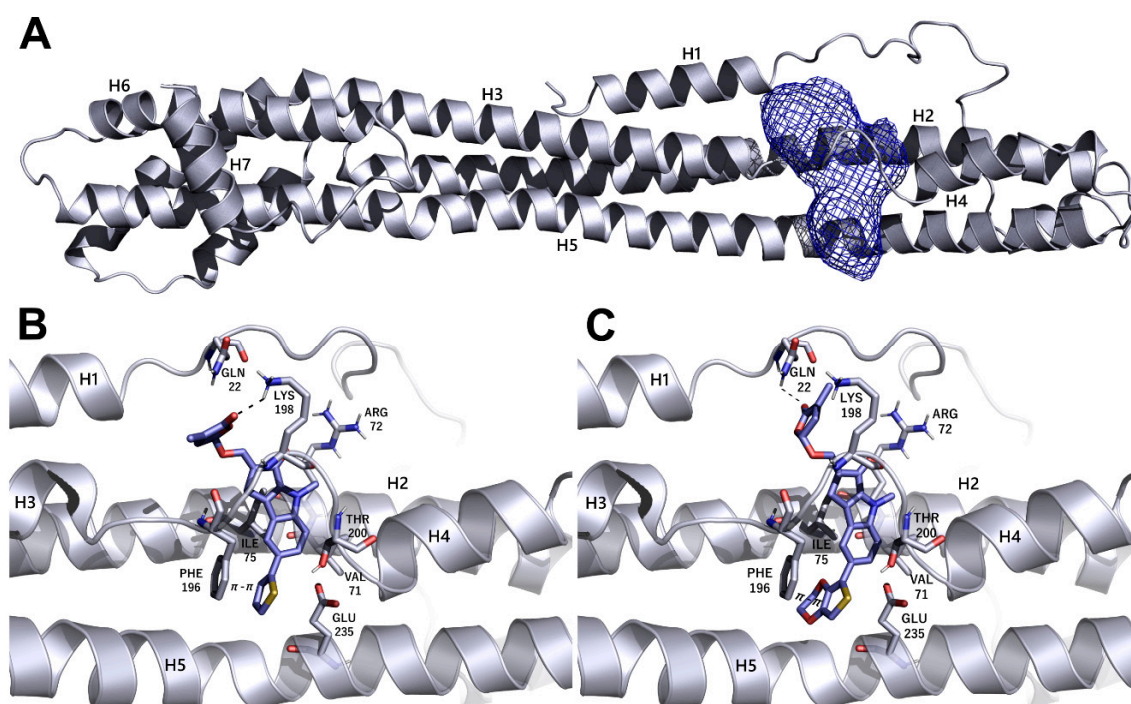
Figure 5. Modeling of the possible complexes formed by IE1 and the most active SL analogs TH-EGO and EDOT-EGO. (**A**) Homology model of IE1. The protein is represented as a cartoon and the selected binding site as a mesh contour. (**B**,**C**) Predicted binding pose of TH-EGO and EDOT-EGO in the protein pocket. Hydrogen bonds are shown as black dashed lines. The SLs and the residues lining the pocket are displayed as lilac and grey capped sticks, respectively.

The best poses obtained for the two compounds are quite similar. In the case of TH-EGO, the butenolide ring forms a hydrogen bond with Lys198, while the thiophen moiety is involved in $\pi-\pi$ stacking contact with the aromatic ring of Phe196. Hydrophobic interactions are formed between the tricyclic ring ABC and Val71 and Ile75 (Figure 5B). EDOT-EGO hydrogen bonds through the butenolide ring to Gln22. Indeed, the orientation of the butenolide ring is different than that of TH-EGO, and this is the only difference between the poses of the two SL analogs. As for EDOT-EGO, $\pi-\pi$ stacking is formed between the ethylenedioxythienyl group and the Phe196 side-chain, and the tricyclic ring ABC forms hydrophobic contact with the same Val71 and Ile75 (Figure 5C). The other SL analogs only maintained the π-π interaction with Phe196, while the hydrogen bonds with the upper part of the binding site are lost. The corresponding CHEMPLP scores were 57 for TH-ABC, 62 for EDOT-ABC, 57 for EGO-10 and 53 for GR24. We believe that the loss of such a polar interaction could be an explanation for the lower activity of the other SLs analogs (Figure S3).

4. Discussion

The identification and validation of new antiviral drugs against HCMV replication is a priority for the clinical management of HCMV infections. HCMV is the principal pathogen in transplant recipients and is recognized as the leading viral cause of birth defects [1–3]. The standard therapy for HCMV disease is associated with adverse side effects, and prolonged treatment may lead to the emergence of drug-resistant mutants [35]. Moreover, the antivirals that are currently used are not able to prevent the reactivation of latent HCMV, and no vaccine is currently available. Therefore, there is an urgent need for new first-line anti-HCMV drugs with novel mechanisms of action that can be safely administered without causing major adverse effects.

Known for their pleiotropic regulatory roles in plant growth and development, SL analogs are attractive new antiviral candidates that display features that are promising for pharmacology, as shown in the treatment of a variety of solid and non-solid tumors [7].

To the best of our knowledge, this is the first study that demonstrates that SLs have an antiviral effect against various members of the *Herpesviridae* family, including HCMV, HSV-1 and HSV-2. Of the SL analogs analyzed, TH-EGO and EDOT-EGO showed a significant dose-dependent effect upon infection with a range of HCMV strains. Moreover, we have demonstrated herein that their antiviral activity relies on the butenolide ring, as the TH-EGO and EDOT-EGO derivatives that lack this domain displayed lower activity than the unmodified compounds.

A detailed analysis performed over the time course of the infection process has allowed us to demonstrate that the SLs analogs did not affect the very first steps of HCMV replication (attachment and entry). Accordingly, the expression levels of immediate early and early viral proteins were not inhibited by the treatment of HFF with TH-EGO and EDOT-EGO. By contrast, late viral proteins, the paradigm of which is the UL99 gene product (pp28 protein), were significantly affected by the same compounds. Since HCMV replication is a complex process that is regulated by the precisely coordinated interplay of several viral and cellular proteins, our findings support the view that, even if SLs possess inhibitory effects on viral events, the exploitation of other cellular processes may be a suitable strategy with which to identify the cellular pathways targeted by SLs. In this context, further investigations on physiologically important targets for HCMV infection, such as endothelial and epithelial cells, and on cells that do not progress to a lytic infection, such as monocytes, will be crucial to corroborate and expand the data obtained on HFFs.

SL analogs have displayed pro-apoptotic activity in a variety of human cancer cells, but not in non-transformed human fibroblasts [11–13]. In this context, the pro-apoptotic activity of SLs relies on their ability to induce the activation of p38 and stress-response pathways [11,12]. Accordingly, we have demonstrated herein that SLs trigger caspase induction and an apoptotic phenotype in HCMV-infected fibroblasts, thus specifically favoring the elimination of infected cells.

During the course of evolution, HCMV has established a complex scenario of viral mechanisms of escape from apoptosis, involving several viral proteins, such as vMIA (UL37 exon 1), vICA (UL36), UL38, IE1 and IE2 [18]. We therefore hypothesized that SL-triggered apoptosis in infected cells relies on specific binding to viral cell-death inhibitors. Molecular docking studies, performed on the homology model of IE1, support the hypothesis that SLs may directly target antiapoptotic proteins when exerting their antiviral activity. The binding poses obtained for TH-EGO and EDOT-EGO in IE1 are consistent, and the estimated energy of interaction is reliable for the formation of a stable protein-ligand complex [34]. However, our findings do not preclude the possibility that SLs may target other antiapoptotic proteins, such as vMIA, cICA, UL38 and IE2, for which no structure, nor even a template to be used for homology modeling, is available. Indeed, structure-based drug design simulations are strongly limited by the availability of a target model. Moreover, other HCMV proteins that we are currently not able to model may be contemporaneously targeted by SLs.

5. Conclusions

In summary, our results indicate that TH-EGO and EDOT-EGO are attractive candidates for a new class of antiviral drugs. Antiviral therapy that is based on molecules exerting their effects by targeting cellular proteins instead of specific viral proteins is a promising solution, as they are not associated to drug resistance. The potent SL in vitro antiviral activity warrants further in vivo studies that can validate the potential use of SLs in the prevention and/or control of HCMV infections.

6. Patents

Patent "Strigolattoni per uso nella prevenzione e/o trattamento di infezioni da virus della famiglia Herpesviridae" (No: 102018000010142, University of Turin, Italy).

References

1. Griffiths, P.; Baraniak, I.; Reeves, M. The pathogenesis of human cytomegalovirus. *J. Pathol.* **2015**, *235*, 288–297. [CrossRef] [PubMed]

2. Rawlinson, W.D.; Boppana, S.B.; Fowler, K.B.; Kimberlin, D.W.; Lazzarotto, T.; Alain, S.; Daly, K.; Doutré, S.; Gibson, L.; Giles, M.L.; et al. Congenital cytomegalovirus infection in pregnancy and the neonate: Consensus recommendations for prevention, diagnosis, and therapy. *Lancet Infect. Dis.* **2017**, *17*, e177–e188. [CrossRef]

3. Britt, W.J. Maternal Immunity and the Natural History of Congenital Human Cytomegalovirus Infection. *Viruses* **2018**, *10*, 405. [CrossRef] [PubMed]

4. Britt, W.J.; Prichard, M.N. New therapies for human cytomegalovirus infections. *Antiviral Res.* **2018**, *159*, 153–174. [CrossRef]

5. Zwanenburg, B.; Blanco-Ania, D. Strigolactones: New plant hormones in the spotlight. *J. Exp. Bot.* **2018**, *69*, 2205–2218. [CrossRef] [PubMed]

6. Koltai, H.; Prandi, C. Strigolactones: Past, present and future. *Planta* **2016**, *243*, 1309. [CrossRef]

7. Makhzoum, A.; Yousefzadi, M.; Malik, S.; Gantet, P.; Tremouillaux-Guiller, J. Strigolactone biology: Genes, functional genomics, epigenetics and applications. *Crit. Rev. Biotechnol.* **2017**, *37*, 151–162. [CrossRef]

8. Mayzlish-Gati, E.; Laufer, D.; Grivas, C.F.; Shaknof, J.; Sananes, A.; Bier, A.; Ben-Harosh, S.; Belausov, E.; Johnson, M.D.; Artuso, E.; et al. Strigolactone analogs act as new anti-cancer agents in inhibition of breast cancer in xenograft model. *Cancer Biol. Ther.* **2015**, *16*, 1682–1688. [CrossRef]

9. Hasan, M.N.; Razvi, S.S.I.; Kuerban, A.; Balamash, K.S.; Al-Bishri, W.M.; Abulnaja, K.O.; Choudhry, H.; Khan, J.A.; Moselhy, S.S.; M, Z.; et al. Strigolactones-a novel class of phytohormones as anti-cancer agents. *J. Pestic. Sci.* **2018**, *43*, 168–172. [CrossRef]

10. Hasan, M.N.; Choudhry, H.; Razvi, S.S.; Moselhy, S.S.; Kumosani, T.A.; Zamzami, M.A.; Omran, Z.; Halwani, M.A.; Al-Babili, S.; Abualnaja, K.O.; et al. Synthetic strigolactone analogues reveal anti-cancer activities on hepatocellular carcinoma cells. *Bioorg. Med. Chem. Lett.* **2018**, *28*, 1077–1083. [CrossRef]

11. Pollock, C.B.; Koltai, H.; Kapulnik, Y.; Prandi, C.; Yarden, R.I. Strigolactones: A novel class of phytohormones that inhibit the growth and survival of breast cancer cells and breast cancer stem-like enriched mammosphere cells. *Breast Cancer Res. Treat.* **2012**, *134*, 1041–1055. [CrossRef] [PubMed]

12. Pollock, C.B.; McDonough, S.; Wang, V.S.; Lee, H.; Ringer, L.; Li, X.; Prandi, C.; Lee, R.J.; Feldman, A.S.; Koltai, H.; et al. Strigolactone analogues induce apoptosis through activation of p38 and the stress response pathway in cancer cell lines and in conditionally reprogrammed primary prostate cancer cells. *Oncotarget* **2014**, *5*, 1683–1698. [CrossRef] [PubMed]

13. Croglio, M.P.; Haake, J.M.; Ryan, C.P.; Wang, V.S.; Lapier, J.; Schlarbaum, J.P.; Dayani, Y.; Artuso, E.; Prandi, C.; Koltai, H.; et al. Analogs of the novel phytohormone, strigolactone, trigger apoptosis and synergize with PARP inhibitors by inducing DNA damage and inhibiting DNA repair. *Oncotarget* **2016**, *7*, 13984–14001. [CrossRef] [PubMed]

14. Zheng, J.-X.; Han, Y.-S.; Wang, J.-C.; Yang, H.; Kong, H.; Liu, K.-J.; Chen, S.-Y.; Chen, Y.-R.; Chang, Y.-Q.; Chen, W.-M.; et al. Strigolactones: A plant phytohormone as novel anti-inflammatory agents. *Medchemcomm* **2018**, *9*, 181–188. [CrossRef]

15. Tumer, T.B.; Yılmaz, B.; Ozleyen, A.; Kurt, B.; Tok, T.T.; Taskin, K.M.; Kulabas, S.S. GR24, a synthetic analog of Strigolactones, alleviates inflammation and promotes Nrf2 cytoprotective response: In vitro and in silico evidences. *Comput. Biol. Chem.* **2018**, *76*, 179–190. [CrossRef]

16. Zhu, H.; Shen, Y.; Shenk, T. Human cytomegalovirus IE1 and IE2 proteins block apoptosis. *J. Virol.* **1995**, *69*, 7960–7970. [CrossRef]

17. Yu, Y.; Alwine, J.C. Human cytomegalovirus major immediate-early proteins and simian virus 40 large T antigen can inhibit apoptosis through activation of the phosphatidylinositide 3′-OH kinase pathway and the cellular kinase Akt. *J. Virol.* **2002**, *76*, 3731–3738. [CrossRef]

18. Brune, W.; Andoniou, C.E. Die Another Day: Inhibition of Cell Death Pathways by Cytomegalovirus. *Viruses* **2017**, *9*, 249. [CrossRef]

19. Prandi, C.; Occhiato, E.G.; Tabasso, S.; Bonfante, P.; Novero, M.; Scarpi, D.; Bova, M.E.; Miletto, I. New Potent Fluorescent Analogues of Strigolactones: Synthesis and Biological Activity in Parasitic Weed Germination and Fungal Branching. *Eur. J. Org. Chem.* **2011**, *2011*, 3781–3793. [CrossRef]

20. Dolan, A.; Cunningham, C.; Hector, R.D.; Hassan-Walker, A.F.; Lee, L.; Addison, C.; Dargan, D.J.; McGeoch, D.J.; Gatherer, D.; Emery, V.C.; et al. Genetic content of wild-type human cytomegalovirus. *J. Gen. Virol.* **2004**, *85*, 1301–1312. [CrossRef]

21. Grazia Revello, M.; Baldanti, F.; Percivalle, E.; Sarasini, A.; De-Giuli, L.; Genini, E.; Lilleri, D.; Labò, N.; Gerna, G. In vitro selection of human cytomegalovirus variants unable to transfer virus and virus products from infected cells to polymorphonuclear leukocytes and to grow in endothelial cells. *J. Gen. Virol.* **2001**, *82*, 1429–1438. [CrossRef] [PubMed]

22. Gariano, G.R.; Dell'Oste, V.; Bronzini, M.; Gatti, D.; Luganini, A.; De Andrea, M.; Gribaudo, G.; Gariglio, M.; Landolfo, S. The intracellular DNA sensor IFI16 gene acts as restriction factor for human cytomegalovirus replication. *PLoS Pathog.* **2012**, *8*, e1002498. [CrossRef] [PubMed]

23. Luganini, A.; Nicoletto, S.F.; Pizzuto, L.; Pirri, G.; Giuliani, A.; Landolfo, S.; Gribaudo, G. Inhibition of herpes simplex virus type 1 and type 2 infections by peptide-derivatized dendrimers. *Antimicrob. Agents Chemother.* **2011**, *55*, 3231–3239. [CrossRef] [PubMed]

24. Biolatti, M.; Dell'Oste, V.; Pautasso, S.; von Einem, J.; Marschall, M.; Plachter, B.; Gariglio, M.; De Andrea, M.; Landolfo, S. Regulatory Interaction between the Cellular Restriction Factor IFI16 and Viral pp65 (pUL83) Modulates Viral Gene Expression and IFI16 Protein Stability. *J. Virol.* **2016**, *90*, 8238–8250. [CrossRef] [PubMed]

25. Waterhouse, A.; Bertoni, M.; Bienert, S.; Studer, G.; Tauriello, G.; Gumienny, R.; Heer, F.T.; de Beer, T.A.P.; Rempfer, C.; Bordoli, L.; et al. SWISS-MODEL: Homology modelling of protein structures and complexes. *Nucleic Acids Res.* **2018**, *46*, W296–W303. [CrossRef] [PubMed]

26. Baroni, M.; Cruciani, G.; Sciabola, S.; Perruccio, F.; Mason, J.S. A common reference framework for analyzing/comparing proteins and ligands. Fingerprints for Ligands and Proteins (FLAP): Theory and application. *J. Chem. Inf. Model.* **2007**, *47*, 279–294. [CrossRef] [PubMed]

27. Jones, G.; Willett, P.; Glen, R.C.; Leach, A.R.; Taylor, R. Development and validation of a genetic algorithm for flexible docking. *J. Mol. Biol.* **1997**, *267*, 727–748. [CrossRef]

28. Artuso, E.; Ghibaudi, E.; Lace, B.; Marabello, D.; Vinciguerra, D.; Lombardi, C.; Koltai, H.; Kapulnik, Y.; Novero, M.; Occhiato, E.G.; et al. Stereochemical Assignment of Strigolactone Analogues Confirms Their Selective Biological Activity. *J. Nat. Prod.* **2015**, *78*, 2624–2633. [CrossRef]

29. Kalser, J.; Adler, B.; Mach, M.; Kropff, B.; Puchhammer-Stöckl, E.; Görzer, I. Differences in Growth Properties among Two Human Cytomegalovirus Glycoprotein O Genotypes. *Front. Microbiol.* **2017**, *8*, 1609. [CrossRef]

30. Collins-McMillen, D.; Chesnokova, L.; Lee, B.-J.; Fulkerson, H.L.; Brooks, R.; Mosher, B.S.; Yurochko, A.D. HCMV Infection and Apoptosis: How Do Monocytes Survive HCMV Infection? *Viruses* **2018**, *10*, 533. [CrossRef]

31. Berman, H.M.; Battistuz, T.; Bhat, T.N.; Bluhm, W.F.; Bourne, P.E.; Burkhardt, K.; Feng, Z.; Gilliland, G.L.; Iype, L.; Jain, S.; et al. The Protein Data Bank. *Acta Crystallogr. D Biol. Crystallogr.* **2002**, *58*, 899–907. [CrossRef] [PubMed]

32. Jones, T.R.; Sun, L. Human cytomegalovirus US2 destabilizes major histocompatibility complex class I heavy chains. *J. Virol.* **1997**, *71*, 2970–2979. [CrossRef] [PubMed]

33. Koltai, H.; Prandi, C. *Strigolactones—Biology and Applications*; Springer International Publishing: New York City, NY, USA, 2019; ISBN 978-3-030-12152-5.

34. Spyrakis, F.; Felici, P.; Bayden, A.S.; Salsi, E.; Miggiano, R.; Kellogg, G.E.; Cozzini, P.; Cook, P.F.; Mozzarelli, A.; Campanini, B. Fine tuning of the active site modulates specificity in the interaction of O-acetylserine sulfhydrylase isozymes with serine acetyltransferase. *Biochim. Biophys. Acta* **2013**, *1834*, 169–181. [CrossRef] [PubMed]

35. James, S.H.; Kimberlin, D.W. Advances in the prevention and treatment of congenital cytomegalovirus infection. *Curr. Opin. Pediatr.* **2016**, *28*, 81–85. [CrossRef] [PubMed]

Where do we Stand after Decades of Studying Human Cytomegalovirus?

Francesca Gugliesi [1,†], **Alessandra Coscia** [2,†], **Gloria Griffante** [1], **Ganna Galitska** [1], **Selina Pasquero** [1], **Camilla Albano** [1] **and Matteo Biolatti** [1,*]

[1] Laboratory of Pathogenesis of Viral Infections, Department of Public Health and Pediatric Sciences, University of Turin, 10126 Turin, Italy; francesca.gugliesi@unito.it (F.G.); gloria.griffante@unito.it (G.G.); ganna.galitska@unito.it (G.G.); selina.pasquero@unito.it (S.P.); camilla.albano@unito.it (C.A.)

[2] Complex Structure Neonatology Unit, Department of Public Health and Pediatric Sciences, University of Turin, 10126 Turin, Italy; alessandra.coscia@unito.it

[*] Correspondence: matteo.biolatti@unito.it

[†] These authors contributed equally to this work.

Abstract: Human cytomegalovirus (HCMV), a linear double-stranded DNA betaherpesvirus belonging to the family of Herpesviridae, is characterized by widespread seroprevalence, ranging between 56% and 94%, strictly dependent on the socioeconomic background of the country being considered. Typically, HCMV causes asymptomatic infection in the immunocompetent population, while in immunocompromised individuals or when transmitted vertically from the mother to the fetus it leads to systemic disease with severe complications and high mortality rate. Following primary infection, HCMV establishes a state of latency primarily in myeloid cells, from which it can be reactivated by various inflammatory stimuli. Several studies have shown that HCMV, despite being a DNA virus, is highly prone to genetic variability that strongly influences its replication and dissemination rates as well as cellular tropism. In this scenario, the few currently available drugs for the treatment of HCMV infections are characterized by high toxicity, poor oral bioavailability, and emerging resistance. Here, we review past and current literature that has greatly advanced our understanding of the biology and genetics of HCMV, stressing the urgent need for innovative and safe anti-HCMV therapies and effective vaccines to treat and prevent HCMV infections, particularly in vulnerable populations.

Keywords: human cytomegalovirus; genetic variability; viral dissemination; pathogenesis; antiviral therapy

1. Introduction

Human cytomegalovirus (HCMV), also called human herpesvirus 5 (HHV-5), is one of the nine herpesviruses capable of successfully infecting humans. HCMV belongs to the Group I of the Baltimore classification, and specifically to the subfamily *Betaherpesvirinae* within the *Herpesviridae* family (Table 1) [1].

Table 1. Classification of human herpesviruses.

Subfamily	Genus	Species	Tropism	Global Prevalence (%)
Alphaherpesvirinae	Simplexvirus	Human herpesvirus 1 (HHV-1)/Herpes simplex virus type 1 (HSV-1)	Mucoepithelial cells (mainly oro-facial tract), neurons	40–90
		Human herpesvirus 2 (HHV-2)/Herpes simplex virus type 2 (HSV-2)	Mucoepithelial cells (mainly genital tract), neurons	10–60
	Varicellovirus	Human herpesvirus 3 (HHV-3)/Varicella zoster virus (VZV)	Mucoepithelial cells, T cells, neurons	50–95
Betaherpesvirinae	Cytomegalovirus	Human herpesvirus 5 (HHV-5)/Human cytomegalovirus (HCMV)	Epithelial cells, monocytes, lymphocytes, fibroblasts, and more	56–94
	Roseolovirus	Human herpesvirus 6A (HHV-6A)	Epithelial cells, T cells, fibroblasts	60–100
		Human herpesvirus 6B (HHV-6B)	Epithelial cells, T cells, fibroblasts	40–100
		Human herpesvirus 7 (HHV-7)	Epithelial cells, T cells, fibroblasts	44–98
Gammaherpesvirinae	Lymphocryptovirus	Human herpesvirus 4 (HHV-4)/Epstein-Barr virus (EBV)	Mucoepithelial cells, B cells	80–100
	Rhadinovirus	Human herpesvirus 8 (HHV-8)/Kaposi's sarcoma associated herpesvirus (KSHV)	Lymphocytes	6–50

The expression of HCMV genes, similar to that of all other herpesviruses, occurs in a temporal cascade consisting of immediate-early (IE), early (E), and late (L) genes. The viral particles are formed by a double-stranded DNA (dsDNA) genome (~230 kb), an icosahedral capsid, followed by the tegument (a proteinaceous layer), and a coating known as pericapsid or envelope, which confers the virion a quasi-spherical shape (Figure 1), a feature shared with all other herpesviruses.
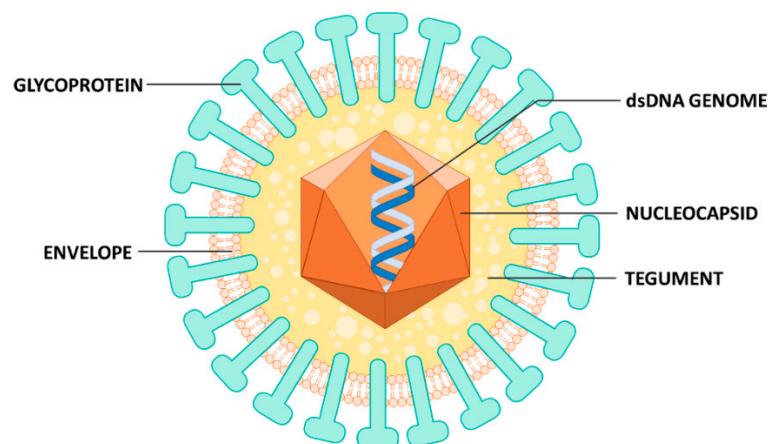

Figure 1. Structure of HCMV virion. Mature virions are coated by an envelope, from which viral glycoproteins protrude, and contain a double-stranded DNA genome enclosed within an icosahedral symmetry capsid, that is surrounded by tegument.

HCMV can infect a broad cell range that includes epithelial cells of glandular and mucous tissues, smooth muscle cells, fibroblasts, macrophages, hepatocytes, dendritic cells, and vascular endothelial cells (ECs) [2]. After primary infection, similar to other members of the herpesvirus family, HCMV can establish latency in the host that can be reversed even after many years by any number of stimuli [3,4].

A typical characteristic of HCMV, which originally granted the virus its name, is that of forming in the infected cell a voluminous intranuclear inclusion body and one or more intra-cytoplasmic inclusion bodies, the so-called "owl's eye" inclusions, made up of clusters of newly formed viruses and lysosomes. The formation of such bodies generally results in increased cellular volume, a phenomenon defined as cytomegaly. Studies on HCMV began in the early 1900s when particular attention was paid to the owl's eyes found in biopsies from stillborn fetuses and later in the kidneys and parathyroid gland cells of organ transplant patients [4].

HCMV efficiently spreads through infected body fluids, and it can also be transmitted vertically from the mother to the fetus through the placenta, causing congenital pathologies. Furthermore, even when the primary infection is resolved by an effective cellular immune response, a population of latently infected myeloid cells can persist in bone marrow monocyte precursors, thereby contributing to the risk of transferring HCMV along with organs and tissues following transplantation.

HCMV is a common pathogen of global clinical relevance, with worldwide seroprevalence ranging from 56% to 94% [5]. The viral spread in the global population is enormous, mainly due to the asymptomatic mode of infection, followed by a constant shedding of the virus through body fluids (e.g., milk, saliva, cervical secretions, and tears), which can last for months or even years.

HCMV is particularly dangerous for the following target categories of individuals [6]: (i) immunocompetent hosts, where it causes asymptomatic infections or a slight form of mononucleotic-like pathology; (ii) immunocompromised individuals such as patients suffering from human immunodeficiency virus (HIV) or undergoing bone or organ transplants; and (iii) congenitally infected newborns, who can be infected in utero, postnatally, or via breastfeeding. Of note, the prevalence of congenital HCMV (cHCMV) disease is much higher than that of Down syndrome, spina bifida, or fetal alcohol syndrome [7].

The host immune status ultimately determines the outcome of the infection as immunocompromised conditions predispose the patient to a primary infection or determine the reactivation of a latent one. In this regard, HCMV is notoriously famous for its ability to cause congenital anomalies and long-term neurological sequelae in newborns. Furthermore, it can also trigger the development of serious pathologies in solid organ or stem cell transplant recipients that are not always resolved by currently available antivirals, thereby leading in some cases to death [8].

This review provides a summary of the general characteristics of HCMV as well as its strain variability, dissemination, latency, reactivation, pathogenesis, prevention, and treatment.

2. Pathogenesis

HCMV pathogenesis and clinical features of infection in various patient populations are summarized below (Figure 2).
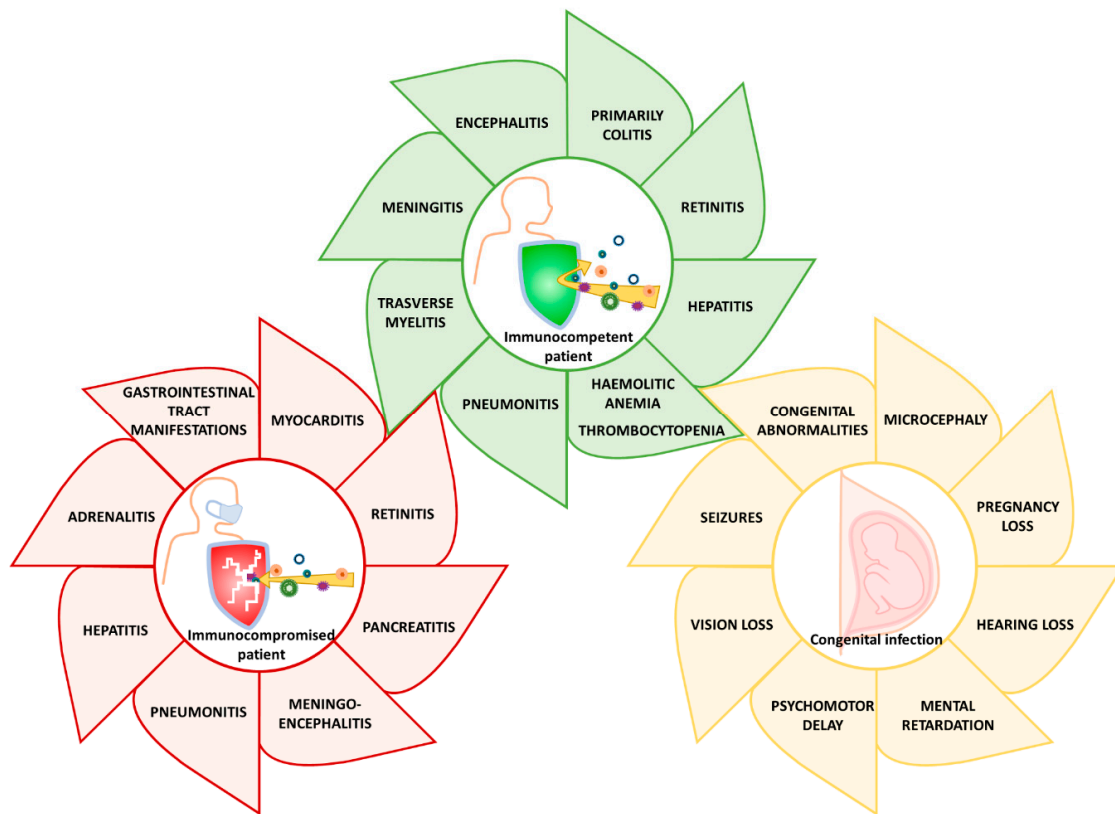
Figure 2. HCMV clinical manifestations in immunocompetent individuals with severe HCMV infection, in immunocompromised people, especially in acquired immune deficiency syndrome (AIDS) patients, transplant recipients, and upon congenital infection.

2.1. Infection of Immunocompetent Adults

HCMV infection commonly occurs in healthy adults and children, with a prevalence gradually increasing with age [9]. When symptomatic, it results in a mononucleosis-like syndrome with a less prominent cervical lymphadenopathy than that caused by the Epstein-Barr virus (EBV) [10]. One of the symptoms is rash, which only manifests in 30% of HCMV mononucleosis cases [11]. Noteworthy, a minority of primary HCMV infections result in relapsing symptoms (i.e., fever, night sweats, fatigue, myalgia, arthralgia, and transaminitis), which can last for several weeks [10] or, less frequently, lead to multi-organ failure [12,13], even though the severe tissue-invasive disease is usually limited to critically ill or immunodeficient patients [14]. A study describing the various clinical manifestations of 290 immunocompetent patients with severe HCMV infection showed that the gastrointestinal tract is the preferential organ affected, primarily in the form of colitis, followed by morbidities of the central nervous system (CNS) (i.e., meningitis, encephalitis, and transverse myelitis), hematological abnormalities (i.e., hemolytic anemia, and thrombocytopenia), the involvement of the eye (uveitis and retinitis), liver (hepatitis), and lung (pneumonitis), and thrombosis of the arterial and venous system [15]. Although several studies have reported a rapid clinical improvement in immunocompetent patients with severe HCMV infection after anti-HCMV therapy, criteria for specific antiviral pharmacological treatments are not well established [12]. Randomized controlled trials should therefore be conducted to determine in which cases anti-HCMV therapy in immunocompetent patients with symptomatic HCMV infections is needed.

2.2. Infection of Immunocompromised Patients

In the immunocompetent host, HCMV and immunity coexist in a delicate balance. When the host immune system is compromised—i.e., in individuals with acquired immune deficiency syndrome

(AIDS) and other immune diseases, post-transplant and intensive care unit (ICU) patients, and, to some extent, elderly people—the virus can exert its full pathogenic potential. Its reactivation in immunocompetent hosts, which occurs intermittently throughout life, triggers a lifelong IgG-mediated immunologic response that keeps in check viral replication. In contrast, uncontrolled viral replication occurs when populations of HCMV-specific CD4$^+$ and CD8$^+$ T cells are not well preserved, as observed in immunocompromised hosts, leading to severe clinical disease [16].

2.3. Cytomegalovirus and HIV

HIV-infected individuals are generally co-infected with HCMV [17]. Prior to the introduction of highly active antiretroviral therapy (HAART) in developed countries, about 40% of HIV-infected patients would suffer from severe HCMV disease [18]. Currently, durable suppression of HIV viremia has increased the overall patient life quality and expectancy and reduced to a minimum the pathologies associated with HCMV viral reactivation. Nevertheless, comorbidities remain problematic for HIV patients. In this regard, a close relationship between HCMV infection and HIV persistence has been reported. This is probably due to the fact that HIV-driven CD4$^+$ T-cell loss and dysfunction may lead to HCMV replication and subsequent expansion of CD8$^+$ T cells. Indeed, an elevated number of CD8$^+$ T cells and a low CD4$^+$/CD8$^+$ T-cell ratio have been observed in individuals co-infected with both viruses but not in patients infected with HIV or HCMV alone [19]. Fittingly, Hunt et al. [20] demonstrated that CD8 T-cell activation could be reduced in HAART-treated HIV patients with incomplete CD4 T-cell recovery by administering anti-HCMV drugs, attesting that HCMV plays a significant role in immune activation in HIV patients. Moreover, persistent HCMV replication modulated longevity and proliferation of HIV-infected cells, improved the recruitment of new HIV target cells, and stimulated HIV transcription, thereby creating an HIV reservoir favoring AIDS progression. Clinically, retinitis has been shown to be the predominant pathology in AIDS patients (20–30%), and it usually appears at the late stages of the syndrome in patients with low CD4 count [21]. HCMV retinitis in HIV patients is commonly observed in two different forms: fulminant or indolent, both characterized by minimal or completely absent vitreous and anterior chamber inflammation [22]. If left untreated, HCMV infection of retinal cells may cause subacute retinal destruction, which can result in irreversible blindness. Paradoxically, HAART therapy while restoring the patient immune system can lead to a new pathology, known as immune recovery uveitis (IRU), which is equally destructive to the host tissue and deleterious to the quality of the patient's life [23]. Following retinitis, the most prevalent clinical manifestations are the following: colitis(in the US, 5–10% of HIV patients with low CD4 lymphocyte counts were affected by enterocolitis prior to the availability of HAART therapy [24]), esophagitis (most commonly due to co-infection with either herpes simplex virus or *Candida albicans*), pneumonitis, encephalitis, hepatitis, and adrenalitis [25].

2.4. Cytomegalovirus and Transplant Patients

HCMV is one of the most frequently encountered opportunistic viral pathogens in transplant patients: a primary infection can occur in seronegative individuals after organ transplantation while a latent infection can be reactivated in seropositive individuals due to immunosuppressive treatment. The risks of HCMV-related complications in transplant recipients (R) vary according to the serostatus of the donor (D): HCMV D$^-$/R$^-$ transplantation is classified as low-risk, HCMV D$^+$/R$^+$ or D$^-$/R$^+$ as medium-risk, and HCMV D$^+$/R$^-$ as high-risk [26,27]. The most prevalent clinical manifestations in HCMV-transplanted patients are gastrointestinal symptoms, mainly affecting the upper digestive tract, whereas diarrhea is a rare occurrence indicative of colon involvement. Meningoencephalitis, clinical hepatitis, myocarditis, and pancreatitis are more common than respiratory symptoms, which in fact indicate more severe disease and may require admission to an ICU. Transplant patients without HCMV prophylaxis may display a spectrum of clinical manifestations that vary in severity from patient to patient, depending on additional personal illness risk factors, type of transplant procedure, the immunological match between donor and recipient, and immunosuppressive drugs being

administered. For instance, patients treated with mammalian target of rapamycin (mTOR) inhibitors display a very low incidence of HCMV. The incidence of HCMV also correlates with the type of transplant: about 50% among pancreas or kidney–pancreas recipients, 50–75% in lung or heart–lung recipients, 9–23% in heart recipients, 22–29% in liver recipients, and 8–32% in kidney recipients [28,29]. Moreover, in patients undergoing allogeneic hematopoietic stem cell transplantation (HSCT), HCMV can lead to fatal infectious complications related to host immune recovery—about 30–70% of non-autologous and 5% of autologous HSCT-patients develop HCMV disease. Pneumonia is the disease most highly associated with HCMV infection of HSCT patients, frequently leading to death despite aggressive treatment with antiviral agents and adjunctive therapies [30]. The reasons for the development of different clinical sequelae among all the aforementioned types of transplanted patients is probably due to a combination of the following factors: (i) the nature of the proinflammatory cytokine cocktail arising after organ transplantation; (ii) the duration of HCMV replication—most transplant recipients display acute HCMV infection, which subsequently results in disease in a relatively short time frame, whereas, for example, congenitally infected infants and HIV patients can display high levels of HCMV replication for several months; and (iii) the status of the immune system response. For instance, HCMV pneumonitis only occurs when patients can activate their immune system [31].

Interestingly, conflicting results have been reported regarding the association between early cytomegalovirus reactivation and relapse after HSCT. Some studies suggest that HCMV replication after transplantation is associated with a decreased relapse risk [32–37], while others highlight that HCMV's protective effect is restricted to patients with acute myeloid leukemia (AML) [38,39] and cannot be extended to patients with acute lymphoblastic leukemia (ALL) [40], lymphoma [41], myelodysplastic syndrome (MDS) [42], or observed in pediatric leukemias [43]. Furthermore, a more recent study by Peric et al. [44] reports that the protective HCMV effect has been pronounced in patients with myeloproliferative malignancies, while, at the same time, confirming the fact that such effect has not been observed in patients with lymphoproliferative disorders, in concordance with other studies [40,41]. Moreover, the same study highlights a significant reduction of relapse in patients with myeloproliferative neoplasms (MPN) associated with early CMV reactivation [44]. Finally, some evidence suggests that the beneficial effect of HCMV is mostly related to the conditioning regimen and restricted only to patients who receive myeloablative chemotherapy (MAC) before undergoing HSCT [45]. Despite the mounting evidence, the impact of HCMV reactivation on the patients' overall survival (OS) has been largely regarded as controversial due to its known negative effect on non-relapse mortality (NRM). Thus, it remains largely unclear whether these conflicting reports can provide a more detailed insight into the distinct protective mechanism or they simply reflect other variables, including the sample size of the studied transplant groups. Therefore, larger prospective studies with a significant follow-up on all patients with different malignancies, monitored and treated in a homogeneous manner are needed to fully elucidate the underlying mechanism responsible for the exact effect of HCMV reactivation. These findings may ultimately lead to a significant improvement in patient management, donor selection strategies, or more personalized preemptive treatment of HCMV infection in posttransplant patients with particular malignancies.

2.5. Congenital and Neonatal Infection

HCMV is the major infectious cause of congenital abnormalities. The incidence of cHCMV infection due to primary and non-primary maternal HCMV infection is ~0.4–0.8% in developed countries. In general, the risk of transmission correlated with the stage of pregnancy is higher in later stages and lower in earlier ones, but in either case HCMV infection is generally associated with severe clinical sequelae in the fetus. In developed countries, ~40% of women in reproductive age are HCMV seronegative, 1–3% of whom may contract primary HCMV infection during pregnancy. The most vulnerable groups include adolescents, mothers, and caregivers in close contact with young children (e.g., teachers, nurses, etc.). Primary maternal HCMV infection has a 30–40% risk of transmission to the

fetus. Importantly, HCMV reactivation or reinfection can also occur in women who are seropositive prior to pregnancy, but, in such cases, the rate of HCMV transmission is only ~1% [46,47].

The hypothesis that pre-existing maternal immunity may favor low HCMV transmission rates has long been debated. In this regard, Coppola et al. [48] performed a systemic review of the literature using Preferred Reporting Items for Systematic Review and Meta-Analyses (PRISMA) [49] guidelines and identified 19 studies assessing congenital HCMV birth prevalence in HCMV-seropositive mothers. All these studies reported low levels of congenital HCMV birth prevalence (0.4–0.6%) in seropositive mothers, in good agreement with previous findings by Lanzieri et al. [50], who systematically reviewed postnatal HCMV prevalence in developing countries. Moreover, 11 studies reported HCMV maternal seroprevalence and HCMV birth prevalence rates of 84–100% and 0.6–6.1%, respectively.

Even though most infants with cHCMV are asymptomatic, they may develop health problems at birth or later. In the most severe cases, cHCMV can cause the death of the unborn baby. In all other cases, the most clinically relevant signs at birth may include microcephaly, hepatosplenomegaly, retinitis, intrauterine growth restriction, seizures, rash, and jaundice. Some children with cHCMV infection may also suffer from long-term health problems, such as hearing loss, which can be present at birth or may develop later even in asymptomatic infants, developmental and motor delay, vision loss, and seizures. Cognitive impairment and retinitis have also been observed in asymptomatic children but at much lower rates compared to symptomatic children [51]. Prevention of HCMV remains elusive given the lack of drugs capable of treating HCMV infection in pregnant women. This aspect, together with the fact that maternal immunity has a protective role against cHCMV infection, suggests that vaccine development remains the most viable option to avoid HCMV vertical transmission.

3. Dissemination

HCMV exploits both vertical and horizontal transmission. Vertical transmission occurs through the placenta [52–54], during birth (with genital secretions), or postnatally through breast milk [55–57]. Horizontal transmission takes place via organ transplant [58,59], blood transfusion, or direct contact with contaminated body fluids, such as urine, breast milk, and genital secretions [60–62].

In most of these cases, because they cover all body surfaces, epithelial cells of the skin and internal mucosa are the first site of HCMV infection. For instance, infection through breastfeeding starts from the oral mucosa, moves to the gastrointestinal tract, which can support a productive infection, and eventually disseminates throughout the body. In contrast, studies using murine CMV (MCMV) have shown that, after oral/intranasal inoculation, the infection can only evolve in the upper respiratory tract but not in the gut [63]. It remains a matter of debate how HCMV disseminates from the upper respiratory tract throughout the body.

It is widely acknowledged that HCMV can spread systemically via leucocytes, a process associated with short-duration viremia, during which infection of the lungs, liver, and spleen occurs primarily through viral dissemination [64]. Subsequent secondary dissemination leads to the infection of salivary glands, breast, and kidneys, all secretion-producing organs that release the virus into the environment for months, even years, favoring intra-host transmission [64]. According to a model whereby primary dissemination produces many viral particles that then infect other organs generating even more virus progeny, it would be expected a gradual increase in viral burden during primary infection [64] (Figure 3).
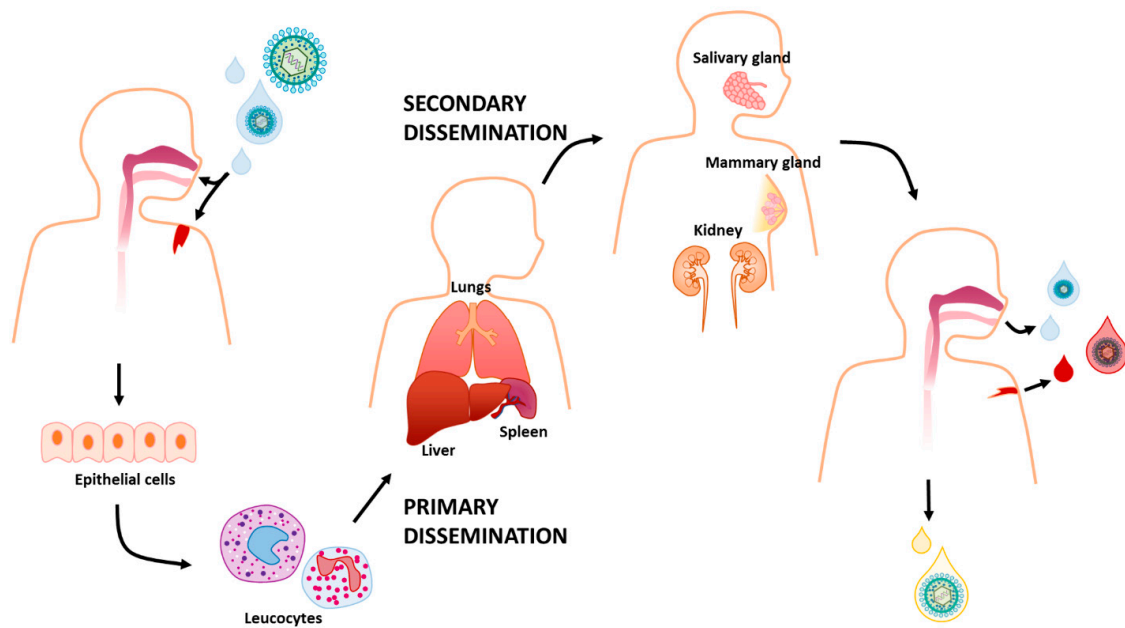
Figure 3. HCMV can be transmitted directly from person to person through bodily fluids including saliva, urine, cervical, and vaginal secretions, breast milk, semen, blood, and tears. It infects a new host usually by getting in through the upper gastrointestinal gastrointestinal tract or the respiratory tract. Here, the epithelial cells are often the first site of infection and from there HCMV infects leucocytes that traffic around the body. This is correlated with a process called primary viral dissemination that leads to the infection of multiple tissues, such as lungs, liver, and spleen. Afterwards, secondary viral dissemination spreads the infection to secretion-producing organs, such as salivary and mammary glands and kidneys, which shed the virus.

However, animal studies using the MCMV model showed a biphasic rather than a gradual increase in viremia, suggesting a much more complex scenario [65].

Recently, Jackson and Sparer [66] demonstrated that cells of the upper respiratory tract, once infected, release not only viral progeny but also chemotactic factors. According to the proposed model, these chemokines trigger the recruitment of innate immune cells, which after being infected further spread the virus to secondary organs and body fluids [66]. Fittingly, HCMV DNA has never been found in the form of free circulating viral particles, except for highly fragmented DNA [67]. Consistent with the lack of free circulating HCMV, leukocyte-depleted blood from seropositive donors prior to blood transfusion prevents HCMV transfer [68,69], indicating that HCMV viremia is mostly cell-associated. More recently, Farrell et al. [63] showed that the first cells to be infected after nasal inoculation with MCMV are alveolar macrophages and type 2 alveolar epithelial cells. Entry into epithelial cells and macrophages occurs through endocytosis and is followed by subsequent pH-dependent fusion with the endosomal membrane, mediated by the viral envelope glycoproteins gB and gH/gL/gO and the pentameric complex formed by gH/gL/UL128, UL130 and UL131A [70,71]. Then, the local spread is thought to occur through direct cell-to-cell transmission, mediated in part by the HCMV gene *US28* [72].

The main cell types contributing to hematogenous dissemination, albeit to different extents, include polymorphonuclear cells (PMNs), monocytes, ECs, and dendritic cells. After recruitment to the first site of infection, these cells are highly prone to infection themselves, thereby becoming potential vehicles for HCMV transmission, even though most of them are unable to support a complete viral replication cycle [73–76]. Consistently, HCMV is frequently found in PMNs from immunocompromised patients [74], in which viral replication is generally abortive and non-productive [73]. The infection of PMNs most likely occurs by transient microfusion between ECs and PMNs after an initial direct contact mediated by the pentameric complex. Successively, infected PMNs transfer the virus particles

to other cell types [77]. On the other hand, other studies using MCMV do not seem to support the hypothesis that neutrophils play a role in HCMV dissemination, since their depletion did not alter primary or secondary viral diffusion [78], whereas depletion of monocytes, macrophages, and NK led to reduced viral dissemination [63,79,80]. However, it is important to point out that there are substantial differences between human and murine CMV, exemplified by the lack of the MCMV CXC chemokine homolog involved in neutrophil migration [78].

HCMV carries two genes, *UL146* and *UL147*, which encode for the two chemokine homologs vCXCL-1 and vCXCL-2, respectively, involved in the recruitment of innate immune cells [81–84]. pUL128, a key component of the pentameric complex, is an important chemokine that, once released in the extracellular milieu, regulates monocyte migration [85]. Likewise, MCK2 in MCMV acts as a strong attractant of monocytes, which appear to be conserved dissemination vehicles across species [86,87]. Monocyte-driven hematogenous spread is probably the result of the close proximity of these cells to the vascular epithelium, which renders them particularly susceptible to infection with viral particles originating from productively infected ECs. Once fully differentiated into tissue macrophages [75], they can, in turn, spread the infection to the organs where they transmigrated [88–90].

Infected ECs also play a fundamental and active role in HCMV dissemination. In fact, HCMV infection of ECs supports viral replication and promotes the enhanced expression of the adhesion molecules ICAM-1 and vCAM-1 [91,92], as well as increased vascular permeability, which promotes recruitment of leucocytes, direct contact [92] and migration through the endothelial layer.

Dendritic cells (DCs) are antigen-presenting cells that keep in check foreign pathogens by influencing T-cell activation and differentiation in the draining lymph node through different mechanisms [93]. Immature DCs localize in all mucosal and epidermal surfaces of the body where they uptake HCMV infectious particles, thereby initiating the maturation process during their migration to the draining lymph node. Upon localization in this new site, the newly mature and permissive DCs are capable of transferring the virus to other cells [94].

In summary, there is still certainly a long way to go before we can fully understand the pathogenesis of HCMV infection, but the aforementioned mechanism of HCMV dissemination proposed by Jackson and Sparer [66] appears to be putting together many pieces of the puzzle.

4. Latency

Viral latency is defined as the maintenance of the viral genome without any production of infectious progeny until this dormant genome can reactivate in response to specific stimuli and initiate a productive infection. It is, therefore, becoming increasingly clear that a better understanding of latency and subsequent reactivation may be crucial to elucidate HCMV pathogenesis and develop therapeutics targeting latent virus reservoirs. This is a particularly important aspect given that all commercially available drugs for the treatment of HCMV diseases only target lytic but not latent infections.

For decades, latency was considered as a silent state of the infection, characterized by overall suppression of viral gene expression aimed at preventing the detection and activation of the immune system. However, several recent studies have shown latency to be a dynamic phase of the infection, where viral gene expression triggers a transcriptional cascade responsible for subverting host cell functions, such as cell survival, genome carriage, and immune evasion [95–97].

The main site where HCMV is known to establish latency is in cells of the myeloid lineage. The idea that infectious viral particles could be carried by white blood cells came from the observation that blood transfer from healthy seropositive donors to immunosuppressed seronegative recipients often resulted in HCMV disease [98–100], and that transfusion of leukocyte-depleted blood reduced the incidence of HCMV disease [101].

However, it was only thanks to the increased sensitivity of the PCR technique that HCMV DNA could be found in naturally latently infected peripheral blood mononuclear cells (PBMCs), in particular monocytes and CD34$^+$ progenitor cells isolated from the bone marrow [102,103]. Consistent with the

notion of myeloid cells being a bona fide site of latency, HCMV IE RNA expression has also recently been detected in DCs isolated from peripheral blood of healthy individuals [104].

Investigations on viral gene expression during natural infection are limited by the fact that only 0.004–0.01% of mononuclear cells from seropositive granulocyte colony-stimulating factor (G-CSF)-stimulated donors carry viral genomes, with a low copy number of 2–13 genomes per infected cell, as judged by PCR-driven in situ hybridization [105]. For this and other reasons, leukemic cell line models such as THP-1 and CD34+ Kasumi 3, as well as several embryonic stem cell lines, have been preferentially used as bona fide and low-cost models to study latency and reactivation in vitro [106–109].

As CD34+ cells are also lymphoid cell progenitors, several studies have tried to explain why myeloid cells are then the only cell lineage able to carry latent viral genome. By performing experimentally latent HCMV infection of CD34+ progenitor cells, Poole et al. [110] observed an increase in the cellular transcription factor GATA-2, a key regulator of myeloid differentiation, suggesting that the virus may only engage myeloid-committed cells, promoting their survival. GATA-2 is also involved in the differentiation of hematopoietic progenitors along the endothelial lineage. However, HCMV DNA could not be detected by PCR in ECs from the saphenous vein of healthy individuals, contrary to the hypothesis that microvasculature is a site of HCMV latency [111].

To establish latency, HCMV must stop the production of infectious viral particles through suppression of viral gene expression and, at the same time, induce the expression of latency-associated viral genes [112–116]. One of the key events required to initiate a state of latency involves the repression of the viral major immediate-early promoter (MIEP), which is sufficient to prevent the expression of E and late L genes as well. Transcriptional inactivation of this region is achieved through induction of repressive chromatin marks—e.g., histones methylation and recruitment of heterochromatin protein 1 (HP-1)—and repressive transcription factors [117]. Concurrently, differentiation of latent CD34+ cells or monocytes to macrophages or DCs induces re-activation of the promoter through histone acetylation and loss of HP-1, with subsequent expression of *IE* genes and re-entry into the lytic cycle [76,104,118,119], indicating that dynamic regulation of the MIEP is a first and crucial step to control latency/reactivation.

One of the most widely accepted hypotheses is that the virus gene expression upon latency is mainly characterized by a robust suppression and shut down of almost all viral genes, an expression profile similar to that of the late lytic cycle. In this regard, it has been proposed that, in latently infected cells, the timely transcriptional cascade of productive infection may be prematurely interrupted by cellular mechanisms. Alternatively, there could be, right after viral entry, early induction of viral gene expression followed by massive repression of viral transcription [120].

As mentioned above, rather than being quiescent, latent HCMV infection induces the expression of a certain amount of viral genes. The most sophisticated mechanism for modulating the host cell environment without attracting an immune response is mediated by non-immunogenic molecules, such as small RNA transcripts. Assessing both experimentally and naturally latent infected cells by next-generation sequencing, Rossetto et al. [121] identified two long non-coding (nc) RNAs (lncRNAs), RNA4.9 and RNA2.7, and mRNAs encoding replication factors UL84 and UL44. Of note, RNA lnc4.9 in concert with latently expressed *UL84* was shown to interact with members of the polycomb repressor complex 2 (PRC2), which potentially represents an additional step of silencing of the MIEP through their histone methyltransferase activity [122].

Across its genome, HCMV also encodes at least 20 viral microRNAs (miRNAs) identified first in lytically-infected cells [123], but also in latently-infected cells THP-1 by Meshesha et al. [124], using deep-sequencing analysis. More recently, two similar studies were performed using instead primary latently-infected cells that more resemble the in vivo situation, even though they showed conflicting results to some extent [125,126]. The advantage of using miRNAs, besides their non-immunogenic state, stems from their ability to modulate the expression of multiple targets involved in immune evasion, survival, and proliferation of HCMV-infected cells, as well as virus

reactivation [127]. One example is the miR-UL148D that during the lytic cycle promotes T-cell chemotaxis by targeting CCL5 (RANTES), while during latency it may trigger activin signaling, thereby inhibiting pro-inflammatory cytokine secretion [126,128]. In addition, even cellular miRNAome was shown to be widely affected by HCMV latent infection [129].

A restricted amount of viral proteins is detected in naturally latent infected cells, even though their exact role in latency is only partially clear. These include: US28, a constitutively activated chemokine receptor acting as a chemokine sink [130]; viral IL-10, which can downregulate MHC II surface expression and modulate CD4$^+$ T-cell recognition [131], UL144, a decoy tumor necrosis factor receptor (TNFR), which inhibits T cell proliferation in vitro [132] and subverts the TH1 immune response in a TNF ligand-independent fashion [133]; LUNA (latency unique natural antigen), a protein required for reactivation [134]; and UL138, which maintains latent infection and suppresses reactivation [115]. Interestingly, this latter is a potentially druggable target in latently infected cells as it inhibits a cellular drug transporter [134].

As latency appears to be a very complex phenomenon, reactivation is often the result of a closely intertwined crosstalk between cellular and viral signals triggering multiple pathways. Indeed, *IE* gene expression alone does not seem to be sufficient to induce the production of infectious particles [76]. In this regard, the observation that differentiation of experimentally latently infected monocytes into monocyte-derived macrophages can lead to a fully permissive phenotype [88,89] implies that the differentiation status is a critical determinant of reactivation. In addition, mounting evidence indicates that inflammation may also play a role in HCMV reactivation. For instance, virus reactivation has been observed in several progenitor cell types under a variety of inflammatory conditions [135–137], and HCMV disease prevalence is directly associated with highly inflammatory environments [137–139].

In light of the above, it is becoming increasingly evident how a multiplicity of latency and reactivation pathways can determine the course of HCMV infection. These pathways appear to be independent of the clinical strains but seemingly dependent on a combination of viral and cellular factors working cooperatively to cross the threshold for reactivation of latently infected cells (Figure 4).
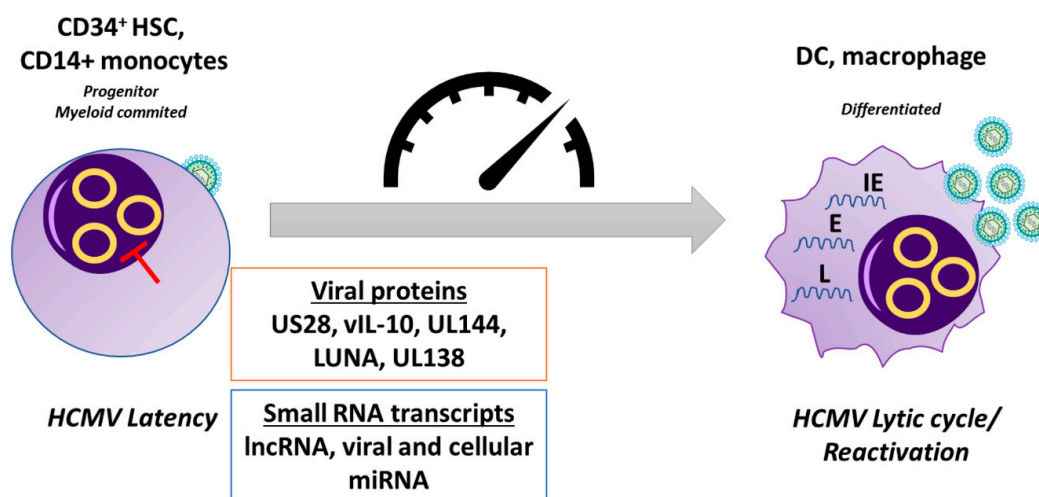

Figure 4. Latency. Following primary infection, HCMV can establish latency in CD34$^+$ myeloid progenitor cells and is carried down the myeloid lineage. In latently-infected CD34$^+$ cells and monocytes, there is a targeted suppression of lytic viral gene expression. HCMV utilizes several viral proteins and small RNA transcripts, including viral and cellular miRNAs, during latent infection to alter the signaling environment within the cell to maintain the status of latency. Differentiation of these cells to macrophages and DCs causes the derepression of the MIEP and allows initiation of the lytic transcription program, which involves a temporal cascade of viral gene transcription, allowing reactivation of de novo virus production. HCMV, human cytomegalovirus; DC, dendritic cell; HSC, hematopoietic stem cell; lncRNA, long non-coding RNA; IE, immediate-early; E, early; L, late.

5. HCMV Strain Variation

The massive spread of HCMV infection and the wide spectrum of disease manifestations in infected patients sparked a major interest in determining the origin and mechanisms of HCMV pathogenicity. It has been 66 years since Margaret Gladys Smith isolated for the first time MCMV from salivary glands and propagated the virus in mouse cell culture—such strain is still in use and commonly called "Smith strain" [140]. One year later, she succeeded in growing submaxillary salivary-derived HCMV in human cell culture. As early as 1960, Thomas Weller isolated the so-called David strain from a liver biopsy and managed to identify serological differences between cytomegalic inclusion disease (CID) isolates [141].. Subsequently, five different HCMV clinical isolates were sequenced (FIX GenBank AC146907; TR GenBank KF021605; PH GenBank AC146904; Toledo GenBank AC146905; Merlin GenBank AY446894). The pioneering work on sequencing of the complete genome of an HCMV laboratory strain (AD169 GenBank AC146999) [142], along with numerous in vitro findings and data from several vaccine studies, revealed the existence of a substantial genetic variation among HCMV strains. In particular, the highly passaged laboratory strains AD169 and Towne (GenBank FJ616285) appeared attenuated when administered as vaccine candidates [143,144]. By contrast, the Toledo strain, which had only been passaged several times in culture, caused disease when administered to seropositive individuals [145]. Taken together, these findings suggest that the pathogenic potential of HCMV was correlated with the genetic composition of each distinct strain.

The differences among the widely used laboratory strains AD169, Towne, and Toledo were localized to multiple ORFs in the UL/b′ region of the genome, encoding viral proteins with immunomodulatory or evasive functions [145,146]. Those genes that were lost upon extensive passaging in vitro played a crucial role in promoting viral replication and immune manipulation in vivo [147]. Consistently, extensive culture passaging led to the selection of HCMV mutants lacking these genes within weeks of propagation, and it also gave rise to variations between commonly used laboratory strains [146,148–150].

In the following years, with the development of more sensitive sequencing techniques, such as Sanger and high-throughput sequencing [151,152], a higher number of HCMV genomes were sequenced from bacterial artificial chromosomes [153–155], virion DNA [156], or overlapping PCR amplicons [148]. The widespread implementation of these new techniques allowed assessing different aspects of HCMV genome variation in clinical HCMV isolates from different cohorts of infected patients, thus providing novel insights into the genetic variation upon natural infection. Up to date, the complete genomes of 351 full-length HCMV strains have been published and analyzed (National Institute of Allergy and Infectious Diseases (NIAID)-sponsored Virus Pathogen Database and Analysis Resource (ViPR) [157]) [158]. Interestingly, these sequencing data show that HCMV can be highly polymorphic among and within hosts [159–161], with a high level of intra-host variability comparable to that of RNA viruses [159]. Given the fact that HCMV is a large double-stranded DNA virus, a high degree of genetic variation contradicted the logical expectation that the virus would retain high genome stability [162]. This unexpected intra-host HCMV diversity was initially attributed to the rapid occurrence of de novo mutations [159,160]—i.e. new mutations occur every time the virus infects a new host, thereby giving rise to a unique viral strain for each infected individual. Eventually, HCMV infection triggers a selection event where a new genotype becomes dominant due to the selective pressure of the immune response [159]. An alternative explanation was based on the evidence that viral and host factors can contribute to the onset of HCMV genome mutations, thus fostering virus genetic drift upon infection [163,164]. However, more recent data indicate that in non-mixed infections the mutation rate of HCMV is no different from that of other DNA viruses, while HCMV acquires a high degree of variability upon mixed infections [165–167], extensive recombination [152,166–168], or reactivation of the latent virus within a single individual. Many of these genetic alterations may in turn influence HCMV cell tropism, immune evasion, and disease outcomes. Indeed, the contribution of superinfection and recombination to viral genetic variability, an intensively debated topic, could have important ramifications in viral evolution, immune adaptation, and pathogenesis, especially in congenital or transplant patients [169,170].

Substantial efforts have been undertaken by various groups to correlate infection outcomes with variation in HCMV-specific genes [145,171,172]. Even though the selection of these genes was based on data supporting their potential role in viral pathogenicity and dissemination, these studies were only limited to Sanger sequencing of polymerase chain reaction (PCR) amplicons and often focused on a small number of polymorphic (hypervariable) genes. Furthermore, in such cases, low-abundance viral populations might have been missed, and the overall viral diversity underestimated. Thus, future studies should take advantage of high-throughput sequencing for fast detection and characterization of multiple-strain infections. Ideally, as recently put forward by Davison and co-workers, the definition of HCMV natural populations should be carried out by whole genome sequencing of HCMV strains directly from clinical samples [166].

6. Prevention

Although the development of an HCMV vaccine had already started in the 1970s, research in HCMV vaccine discovery received a major push when in 2000 the US Institute of Medicine placed HCMV among the top priorities for vaccine development [173]. Despite these increasing efforts, an effective vaccine against HCMV is currently missing, de facto leaving high-risk populations, chiefly immunocompromised patients and immunocompetent seronegative pregnant mothers, exposed to primary infection [174]. Given that one of the main obstacles to the development of an efficient vaccine against HCMV is the lack of protection against HCMV re-infection and/or reactivation, the first objective of a newly designed HCMV vaccine should be that of shielding vulnerable populations from primary infection. The long-range goal would then be to grant permanent protection against new infections with other HCMV strains and reactivated infections, which can occur repeatedly throughout life. To reach these goals, the ideal HCMV vaccine should be able to trigger a strong humoral response, in the form of binding and neutralizing antibodies, and an HCMV-specific CD8$^+$ and CD4$^+$ T-cell response. With this in mind, the experimental and clinical results achieved so far predict that the ideal HCMV vaccine should include: (i) gB, promoting both humoral—primarily antibody-binding—and T-cell-mediated response [164]; (ii) pp65, triggering a potent T-cell response; and (iii) the pentameric complex (PC), which prompts a quite strong neutralizing antibody (NAb) response [175]. Indeed, PC-induced NAbs are powerful cell-to-cell spread viral inhibitors in numerous cell types, not just fibroblasts. In the following sections, we summarize the most relevant approaches for designing effective HCMV vaccines (Table 2).

Table 2. HCMV Vaccines. NAb, Neutralizing Antibody; HELF, human embryonic lung fibroblasts; PC, pentameric complex; VLPs, virus like particles.

Live HCMV Vaccine	Description	Clinical Trials
Towne vaccine	HCMV attenuated strain.	Phase I/II clinical studies evidences: (a) no virus excretion; (b) no virus latency; (c) NAb induction; (d) generation of both HCM-specific CD4 and CD8 T-cell; (e) partial protection against a secondary infection.
Towne-Toledo chimera vaccines	Genetic recombinant Towne and Toledo.	In Phase I clinical trials they were well tolerated and with no virus excretion. One chimera was more immunogenic than Towne.
AD169 vaccine	HCMV attenuated strain.	Patients did not to display cell-mediated immunity depression or any systemic reactions.

Live HCMV Vaccine	Description	Clinical Trials
V160 vaccine	Replication-defective virus vaccine based on strain AD169.	Phase I study showed that V160-immunized HCMV-seronegative patients have features comparable in quality to those from seropositive subjects.
Viral vectored vaccines	Heterologous viral vectors used to deliver HCMV-encoded antigens: (a) canarypox virus vector; (b) alphavirus vector [Venezuelan equine encephalitis (VEE) virus]; (c) lymphocyte choriomeningitis virus vector; (d) modified vaccinia Ankara virus (MVA) vector; (e) adenovirus type 6 vector.	Many of them were tested in Phase I/II trials. While viral vectors cannot replicate completely when injected into humans, they have an optimal safety profile.
Non-living HCMV Vaccines		
gB subunit vaccines	Combination of the recombinant glycoprotein gB with an adjuvant.	Many Phase II studies showed that gB/MF59 vaccine had a certain degree of protection against HCMV infection through the mucosal route, but the antibody response was short-lived and disappeared within a year.
DNA based vaccines	Single or mixed combination of plasmids encoding viral antigens such as pp65, gB and IE1.	The most promising DNA-based plasmid vaccine, called ASP0113 divalent DNA vaccine, is currently in Phase III clinical trials.
RNA based vaccines	Different strategies: (a) synthetic self-amplifying mRNA expressing a pp65-IE1 construct and gB; (b) mRNA-based multiantigenic vaccine including pp65, gB and PC; (c) lipid nanoparticle (LNP)-encapsulated nucleoside-modified mRNA encoding full-length gB.	Currently they have been all tested only on animal models.
VLPs vaccines	Enveloped virus-like particles (VLPs) which exhibit on their surface gB and, in some cases, PC.	Different variations of VLPs have shown some success in animal immunization tests.
Dense body vaccines	Dense bodies purified from HCMV infected cell.	DB-injected mice did display both T-cell and NAb responses

6.1. Live HCMV Vaccines

The first attempts to develop an HCMV vaccine were focused on two attenuated strains: the AD169 and the Towne strain, both developed at the beginning of the 1970s by Elek and Stern in London and Plotkin in Philadelphia [176,177]. Their results show the vaccine to be very safe due to the absence of virus excretions—this was true even for vaccinated kidney transplant patients on chronic immunosuppression. Furthermore, these patients did not display cell-mediated immunity depression or any systemic reactions. Concerning immunogenicity, NAbs were present at levels similar to those found in the serum of patients infected with the wild type virus. Although the vaccine was able to generate both HCMV-specific CD8^{+} and CD4^{+} T-cell response, the immunity induced by vaccination

did not prevent secondary infection in pregnant women, while mucosal immunity induced by natural infection did. Thus, immunization was deemed incomplete [178]. A reason for this only partial success is probably related to the fact that the two HCMV strains used to obtain the vaccines, when propagated on fibroblasts in vitro, are known to acquire mutations in *UL128L*, a subunit of the pentameric complex. In particular, the Towne strain undergoes a 2-bp insertion (TT), causing a frameshift mutation in *UL130* [154]. This event is particularly important if we consider that a functional PC is required for the virus entry into epithelial cells or ECs, whereas gB and the gH/gL dimer are sufficient for entry into fibroblasts [179]. Consistently, epithelial-neutralizing antibodies against Towne strain, harboring a mutation in PC, were 28-fold lower than those induced by natural infection [180].

To develop a live HCMV vaccine with the same safety of the Towne's one but more protective and immunogenic, four genetic recombinants of Towne and Toledo, a low-passage HCMV strain, were subsequently generated. The chimera vaccine candidates were tested in Phase I clinical trials and found to be well tolerated and with no virus excretions in saliva or urine, with two chimeras (2 and 4) being more immunogenic than Towne [181].

In 2012, a replication-defective virus strategy was put in place for the first time. It consisted of restoring a mutated PC through serial passages of AD169-infected ECs. Subsequently, the two HCMV proteins IE1/2 and UL51 were linked to a protein domain that rendered their stability dependent on the synthetic compound Shield 1 (Shld1). That meant that HCMV could replicate normally in the presence of Shld1, whereas in the absence of such molecule viral replication was abortive due to the IE1/2 and UL51 degradation. As later confirmed in several studies, this defective virus, named V160, retained its ability to express all other AD169-specific proteins, including PC and gB, thereby eliciting both T cell and humoral responses in non-human primates as well as in humans [182]. A recently concluded Phase I study showed that sera from V160-immunized HCMV-seronegative patients have features similar in quality to those from seropositive subjects, justifying future clinical trials on this vaccine [183].

Finally, several viral vectored vaccines against HCMV have been formulated and tested in Phase I/II trials. These strategies for vaccine development employ heterologous viral vectors to deliver HCMV-encoded antigens such as gB, pp65, IE1, and, in some cases, PC proteins. While viral vectors cannot replicate completely when injected into humans, they have an optimal safety profile and can efficiently carry the desired viral antigens. The following heterologous viral vectors were tested as HCMV vaccines: canarypox virus vector, alphavirus vector (Venezuelan equine encephalitis (VEE) virus), lymphocyte choriomeningitis virus vector, modified vaccinia Ankara virus (MVA) vector, and adenovirus type 6 vector [184].

In conclusion, although consistent progress has been made over the past 45 years, and several potential candidates have emerged, an effective live HCMV vaccine has yet to be successfully developed.

6.2. Non-Living HCMV Vaccines

The simplest non-living HCMV vaccines are the so-called subunit vaccines, obtained by combining subunit immunogens with an adjuvant. The first one was made with the recombinant glycoprotein gB with the microfluidized adjuvant 59 (MF59) [185]. Several Phase II clinical trials in both adults and toddlers showed that after three doses given at 0, 1, and 6 months gB/MF59 was able to induce a reasonable NAb titer. Even though these studies showed that gB when injected alone as a vaccine had a certain degree of protection against HCMV infection through the mucosal route, the antibody response was short-lived and disappeared within a year [186].

A different strategy for non-living vaccines is based on genetic programming of host cells—via uptake of naked DNA or RNA—to express the desired immunogens in vivo. In this regard, a plasmid-based DNA vaccine, called the ASP0113 bivalent DNA vaccine, managed to reach Phase III clinical trials. This vaccine was obtained using two plasmids: VCL-6365, encoding the extracellular domain of gB, and VCL-6368, encoding a modified pp65 protein kinase gene [187].

Likewise, the use of self-replicating RNA to express viral proteins has made progress in recent years. Specifically, an mRNA-based multiantigenic vaccine containing gB, pp65, and PC injected in mice was capable of inducing potent cell-mediated and humoral immune responses. Although an effective cell response to pp65 was hampered by the presence of other HCMV antigens, it could be restored by sequential immunization of pp65 followed by PC + gB + pp65 [188]. In a very recent study a new RNA-based vaccine, consisting of lipid nanoparticle (LNP)-encapsulated nucleoside-modified mRNA encoding full-length gB, was tested on a group of young New Zealand White rabbits. The gB nucleoside-modified mRNA-LNP vaccines were highly immunogenic with similar kinetics and comparable peak gB-binding and functional antibody responses induced by gB/MF59 subunit vaccine. However, rabbits immunized with nucleoside-modified mRNA-LNP showed significantly longer duration of vaccine-induced antibody responses [189].

Other heavily studied approaches include the use of HCMV peptides, to elicit cellular immunity in transplant patients, and enveloped virus-like particles (VLPs) in order to stimulate wild type viruses in the absence of viral DNA, with VLPs exhibiting on their surface gB and, in some cases, PC different variations of VLPs have had some success in animal immunization tests [190,191].

One different approach involves the purification of dense bodies (DBs), including virion tegument and envelope proteins but not viral genome, produced by HCMV-infected cells. DB-injected mice did display both T-cell and NAb responses [192].

In summary, the antigens needed for successful vaccination against HCMV are well known from the literature. Thus, further effort will be required in combining such antigens to achieve a durable response that would protect an individual for an extended time.

7. Treatment

The high incidence and clinical manifestations of HCMV infection underscore the need for efficient antiviral therapies in treating disease in immunocompromised patients and congenitally infected infants.

Four compounds are currently approved for systemic treatment or prophylaxis of HCMV infections: ganciclovir (GCV) and its oral prodrug valganciclovir (VGCV), cidofovir (CDV), foscarnet (FOS), and, more recently, letermovir (LTV) [193,194] (Table 3).

Table 3. Antiviral agents approved for treatment or prevention of HCMV infections.

Agent	Compound Information	Viral Target	Mechanism of Action	Route of Administration	Dosage	Toxicities
Ganciclovir (Cytovene®)	Acyclic nucleoside analogue of guanine	UL54	When phosphorylated to Ganciclovir triphosphate inhibits the viral DNA polymerase UL54	Intravenous Oral	Induction: 5 mg/kg every 12 hours for 7–14 days Maintenance: 5 mg/kg for 100–120 days after transplant FDA approved for maintenance therapy only using 1 mg three times a day	Neutropenia Thrombocytopenia Neurotoxicity
Valganciclovir (Valcyte®)	L-Valyl ester of Ganciclovir	UL54	Converted to Ganciclovir in intestine and liver, inhibits the viral DNA polymerase	Oral	Induction: 900 mg twice a day for 21 days Maintenance: 900 mg once per day	Granulocytopenia Anemia Thrombocytopenia
Cidofovir (Vistide®)	Deoxycytidine acyclic nucleotide phosphonate analog	UL54	When phosphorylated to Cidofovir biphosphate inhibits the viral DNA polymerase	Intravenous	Induction: 5 mg/kg weekly for 2 weeks Maintenance: 5 mg/kg every 2 weeks	Nephrotoxicity Metabolic acidosis Ocular hypotony

Table 3. *Cont.*

Agent	Compound Information	Viral Target	Mechanism of Action	Route of Administration	Dosage	Toxicities
Foscarnet (Foscavir®)	Synthetic organic analogue of inorganic pyrophosphate	UL54	Inhibits activity of pyrophosphate binding site on viral DNA polymerase UL54	Intravenous	Induction: 60 mg/kg every 8 hours for 14–21 days Maintenance: 90–120 mg/kg everyday	Nephrotoxicity Hypocalcemia Electrolytes imbalance Genital ulceration
Letermovir (Prevymis®)	Non-nucleoside, 3,4-dihydroquinazolinyl acetic	pUL56	Binds pUL56 subunit of the HCMV terminase complex preventing the cleavage of concatemeric DNA	Intravenous Oral	Prophylaxis: 480 mg once a day, through 100 days post-transplant	

Among the latter, GCV, CDV, and FOS exhibit similar activities, as they target viral DNA polymerases, consequently inhibiting the synthesis of HCMV DNA [195]. In contrast, LTV blocks DNA packaging in the viral capsid by interfering with the viral terminase complex [196]. Furthermore, in the late 1990s, a fifth antiviral compound, fomivirsen, also known as Vitravene, was approved for the treatment of HCMV infection by the Food and Drug Administration (FDA) and the European Agency for the Evaluation of Medicinal Products (EMEA). Fomivirsen, an antisense 21-mer phosphorothioate oligonucleotide (5′-GCGTTTGCTCTTCTTCTTGCG-3′) complementary to the mRNA encoding the IE-2 protein, is used to treat HCMV-induced retinopathy in immunocompromised subjects [197]. Prophylactic treatment with acyclovir has also been approved in some countries, although the effectiveness of this approach is moderate.

The front-line therapy for HCMV infections is GCV, which was approved for medical use in 1988 and is now routinely used to treat congenitally HCMV-infected infants [198] and immunocompromised hosts with HCMV disease [199] or given as a prophylactic agent to prevent HCMV disease [194,200,201]. GCV, a monosodium salt of 9-(1,3-dihydroxy-2-propoxymethyl)-guanine, is an acyclic nucleoside analog administered by intravenous infusion that, when phosphorylated to form GCV triphosphate (GCV-TP), inhibits the viral UL54 DNA polymerase and, by competing with deoxyguanosine (dGTP), curbs the elongation of viral DNA. GCV is administered in an inactive form and is selectively phosphorylated in the infected cells by the HCMV UL97 kinase [202]. This kinase is responsible for the conversion of GCV to GCV monophosphate (GCV-MP), while the subsequent phosphorylation steps generating the active form of the drug (GCV-TP) are controlled by cellular kinases [203]. However, its moderate antiviral activity and dose-limiting toxicity hinder its efficacy and may lead to the development of drug-resistant infections, mainly in immunocompromised patients [204]. Specifically, GCV-induced cytotoxicity may result in thrombocytopenia and neutropenia in transplant recipients [205].

Secondary therapies for HCMV infections consist of CDV and FOS, which can both cause nephrotoxicity and give rise to resistant infections [193,194].

CDV was approved in 1996 for the treatment of HCMV retinitis in AIDS patients and is available only intravenously. Cidofovir, 1-[(S)-3-hydroxy-2-(phosphonomethoxy) propyl]cytosine, is an acyclic phosphonate nucleoside (ANP) acting as an analog of CMP (cytidine monophosphate). CDV presents a broad spectrum of antiviral activity; in particular, it acts against most DNA viruses (e.g., herpesviruses, adenovirus, polyomavirus, and orthopoxvirus) [206]. Since CDV is a monophosphate analog, it does not require the initial activating phosphorylation by the UL97 viral kinase. Nevertheless, to be active, CDV needs to be diphosphorylated by the pyruvate kinase, creatine kinase and nucleoside diphosphate kinase, all present at high levels in infected HCMV cells. Once activated, CDV competes with deoxycytidine triphosphate and is incorporated in the DNA as an alternative substrate of the viral DNA polymerase where it acts as a non-mandatory chain terminator [206]. CDV resistance is

only associated with viral DNA polymerase mutations and occurs at a frequency comparable to that of GCV [206].

FOS was approved for the treatment of HCMV infections in 1991. Similar to CDV, FOS inhibits the replication of several types of DNA viruses (e.g., several herpes family viruses, hepatitis B virus, and HIV), but it is primarily used for the treatment of HCMV retinitis [207]. FOS is a synthetic organic analog of inorganic pyrophosphate, which reversibly inhibits the activity of the UL54 DNA polymerase. FOS resistance during long-term therapy occurs at similar rates to those displayed by CDV and GCV. However, FOS can be particularly useful against some GCV-resistant infections as the frequency of GCV cross-resistance is much lower than that observed for CDV and GCV, even though renal toxicity may limit its usefulness [208]. Combination therapy with GCV has also been investigated, but it does not seem to be more efficient than GCV alone. Despite the above limitations, the broad spectrum of antiviral activity of FOS makes this compound useful for the treatment of some GCV-resistant infections. Of note, FOS has also been approved for the treatment of ACV-resistant HSV infections. Lastly, because this agent crosses the blood-brain barrier, it is indicated for the treatment of viral infections involving the central nervous system.

Drug resistance results from the development of single or multiple mutations leading to different levels of resistance that can reduce the efficacy of the antiviral treatments. Since all these drugs, except of fomivirsen, target, directly or indirectly, viral DNA polymerase, the emergence of drug-resistant HCMV strains, often due to mutations in UL97 and/or UL54, has increasingly hampered disease management [209]. Therefore, there is an urgent medical need for new anti-HCMV agents with new mechanisms of action and fewer side effects.

Currently, a promising new class of riboside analogs with strong and specific antiviral activity against HCMV is being tested in a clinical trial. One of these drugs is maribavir, a benzimidazole riboside characterized by a novel mechanism of action based on its ability to inhibit UL97, a viral enzyme that blocks nuclear egress of viral capsids, and to interfere with viral DNA synthesis. Even though clinical trials with maribavir have not yet been conclusive, the drug is still being evaluated as a potential preventive treatment of HCMV infection [210,211].

BAY 38-4766, also called tomeglovir, is a non-nucleoside antiviral. The antiviral activity of BAY 38-4766 is due to its ability to hinder DNA maturation most likely by targeting the UL89 and UL56 genes encoding for the subunits of a multiprotein complex involved in HCMV termination [212]. Interestingly, in a guinea pig model, after infection and treatment, measurable amounts of the compound were detected in fetal blood, attesting that the drug is capable of crossing the placenta in pregnant animals [213]. BAY 38-4766 is in clinical development and has shown a positive safety profile in healthy male volunteers at single oral doses of up to 2000 mg. However, no recent studies have highlighted the current state of clinical development of this drug or related compounds in the series [213].

GW275175X is a new benzimidazole riboside class of HCMV inhibitors that can block the maturational cleavage of high molecular weight HCMV DNA by interacting with pUL56 and pUL89, the two subunits of the HCMV terminase complex [214]. GW275175X was advanced to Phase I clinical trial with an increasing dose of safety, pharmacokinetics, and tolerability, but was later set aside to prioritize maribavir testing. The clinical potential of this antiviral still requires further study.

Brincidofovir (CMX001), a prodrug of CDV, is an oral lipid-drug conjugate quickly absorbed into cells whereupon the lipid side chain is cleaved, releasing CDV to be further phosphorylated by intracellular kinases to CDV diphosphate. Since brincidofovir is not a substrate for the oxyanion transporter in the kidney, kidney damage should be reduced. Nonetheless, CDV may lead to gastrointestinal toxicity, which is quite often dose-limiting [215].

In 2017, LTV became the latest FDA-approved drug for prophylaxis of HCMV infections in allogeneic HSCT recipients [216]. LTV is a non-nucleoside 3,4-dihydroquinazolinyl acetic acid, which can be administered orally or intravenously infused. LTV acts as an inhibitor of the HCMV DNA terminase complex by interacting with the pUL56 subunit of such complex and preventing the cleavage of concatemeric DNA into monomeric genome length DNA, which ultimately inhibits DNA

packaging into the virion. LVT displays good efficacy against different clinical isolates of HCMV, including GCV-resistant strains, and is ineffective against all other herpesviruses [217].

To sum up, evidence from the literature indicates that currently available anti-HCMV drugs, despite being able to interfere with viral replication through different mechanisms of action, are often associated with multiple side effects such as drug toxicity, poor oral bioavailability, and drug resistance. Therefore, innovative compounds targeting new virus components with fewer adverse effects are urgently needed to improve patient outcomes.

8. Conclusions

HCMV is the leading cause of congenital infections resulting in severe morbidity and mortality among newborns worldwide. This virus is highly polymorphic, particularly in genes contributing to immune modulation. Despite a large amount of HCMV research over the past few decades, the mechanisms and virulence factors contributing to HCMV pathogenesis and particular clinical outcomes remain unclear. To make matters worse, to date, no safe vaccines against HCMV infections exist and current antiviral therapies are quite unsatisfactory due to the frequent occurrence of drug resistance and toxicity.

Overall, the lack of advances in the treatment of HCMV-driven diseases clearly clashes with the widespread notion that HCMV poses "a greater threat to infants than other viruses". Thus, an in-depth understanding of HCMV-host interactions, especially at the individual level, will be instrumental to develop new diagnostic/therapeutic tools for the clinical management of this viral disease.

References

1. Arvin, A.; Campadelli-Fiume, G.; Mocarski, E.; Moore, P.S.; Roizman, B.; Whitley, R.; Yamanishi, K. *Human Herpesviruses: Biology, Therapy, and Immunoprophylaxis*; Cambridge University Press: Cambridge, UK, 2007; ISBN 978-0-521-82714-0.

2. Sinzger, C.; Digel, M.; Jahn, G. Cytomegalovirus cell tropism. *Curr. Top. Microbiol. Immunol.* **2008**, *325*, 63–83. [CrossRef]

3. Griffiths, P.; Baraniak, I.; Reeves, M. The pathogenesis of human cytomegalovirus. *J. Pathol.* **2015**, *235*, 288–297. [CrossRef] [PubMed]

4. Landolfo, S.; Gariglio, M.; Gribaudo, G.; Lembo, D. The human cytomegalovirus. *Pharmacol. Ther.* **2003**, *98*, 269–297. [CrossRef]

5. Zuhair, M.; Smit, G.S.A.; Wallis, G.; Jabbar, F.; Smith, C.; Devleesschauwer, B.; Griffiths, P. Estimation of the worldwide seroprevalence of cytomegalovirus: A systematic review and meta-analysis. *Rev. Med. Virol.* **2019**, *29*, e2034. [CrossRef] [PubMed]

6. Crough, T.; Khanna, R. Immunobiology of human cytomegalovirus: From bench to bedside. *Clin. Microbiol. Rev.* **2009**, *22*, 76–98. [CrossRef]

7. Mestas, E. Congenital Cytomegalovirus. *Adv. Neonat. Care* **2016**, *16*, 60–65. [CrossRef]

8. Mocarski, E.S.; Shenk, T.; Pass, R. Cytomegaloviruses. In *Fields Virology*; Knipe, D.M., Howley, P.M., Eds.; Lippincott Williams & Wilkins: Philadelphia, PA, USA, 2007; pp. 2701–2772.

9. Bate, S.L.; Dollard, S.C.; Cannon, M.J. Cytomegalovirus seroprevalence in the United States: The national health and nutrition examination surveys, 1988–2004. *Clin. Infect. Dis.* **2010**, *50*, 1439–1447. [CrossRef]

10. Horwitz, C.A.; Henle, W.; Henle, G.; Snover, D.; Rudnick, H.; Balfour, H.H.; Mazur, M.H.; Watson, R.; Schwartz, B.; Muller, N. Clinical and laboratory evaluation of cytomegalovirus-induced mononucleosis in previously healthy individuals. Report of 82 cases. *Medicine* **1986**, *65*, 124–134. [CrossRef]

11. Cohen, J.I.; Corey, G.R. Cytomegalovirus infection in the normal host. *Medicine* **1985**, *64*, 100–114. [CrossRef]

12. Nangle, S.; Mitra, S.; Roskos, S.; Havlichek, D. Cytomegalovirus infection in immunocompetent adults: Is observation still the best strategy? *IDCases* **2018**, *14*, e00442. [CrossRef]

13. Urbano, J.; Moreira-Silva, S.; Frioes, F.; Almeida, J.; Abreu, C.; Pimenta, J. Cytomegalic Infection in an Immunocompetent Patient: A Case With Multiple Organ Dysfunction. *J. Med. Cases* **2015**, *6*, 480–482. [CrossRef]

14. Fakhreddine, A.Y.; Frenette, C.T.; Konijeti, G.G. A Practical Review of Cytomegalovirus in Gastroenterology and Hepatology. *Gastroenterol. Res. Pract.* **2019**, *2019*, 6156581. [CrossRef] [PubMed]

15. Rafailidis, P.I.; Mourtzoukou, E.G.; Varbobitis, I.C.; Falagas, M.E. Severe cytomegalovirus infection in apparently immunocompetent patients: A systematic review. *Virol. J.* **2008**, *5*, 47. [CrossRef] [PubMed]

16. Dioverti, M.V.; Razonable, R.R. Cytomegalovirus. *Microbiol. Spectr.* **2016**, *4*. [CrossRef] [PubMed]

17. Gianella, S.; Massanella, M.; Wertheim, J.O.; Smith, D.M. The Sordid Affair Between Human Herpesvirus and HIV. *J. Infect. Dis.* **2015**, *212*, 845–852. [CrossRef] [PubMed]

18. Steininger, C.; Puchhammer-Stöckl, E.; Popow-Kraupp, T. Cytomegalovirus disease in the era of highly active antiretroviral therapy (HAART). *J. Clin. Virol.* **2006**, *37*, 1–9. [CrossRef] [PubMed]

19. Freeman, M.L.; Mudd, J.C.; Shive, C.L.; Younes, S.-A.; Panigrahi, S.; Sieg, S.F.; Lee, S.A.; Hunt, P.W.; Calabrese, L.H.; Gianella, S.; et al. CD8 T-Cell Expansion and Inflammation Linked to CMV Coinfection in ART-treated HIV Infection. *Clin. Infect. Dis.* **2016**, *62*, 392–396. [CrossRef]

20. Hunt, P.W.; Martin, J.N.; Sinclair, E.; Epling, L.; Teague, J.; Jacobson, M.A.; Tracy, R.P.; Corey, L.; Deeks, S.G. Valganciclovir reduces T cell activation in HIV-infected individuals with incomplete CD4+ T cell recovery on antiretroviral therapy. *J. Infect. Dis.* **2011**, *203*, 1474–1483. [CrossRef]

21. Chiotan, C.; Radu, L.; Serban, R.; Cornăcel, C.; Cioboata, M.; Anghel, A. Cytomegalovirus retinitis in HIV/AIDS patients. *J. Med. Life* **2014**, *7*, 237–240.

22. Ho, M.; Invernizzi, A.; Zagora, S.; Tsui, J.; Oldani, M.; Lui, G.; McCluskey, P.; Young, A.L. Presenting Features, Treatment and Clinical Outcomes of Cytomegalovirus Retinitis: Non-HIV Patients Vs HIV Patients. *Ocul. Immunol. Inflamm.* **2019**, 1–8. [CrossRef]

23. Jabs, D.A. Cytomegalovirus retinitis and the acquired immunodeficiency syndrome—Bench to bedside: LXVII Edward Jackson Memorial Lecture. *Am. J. Ophthalmol.* **2011**, *151*, 198–216.e1. [CrossRef] [PubMed]

24. Meiselman, M.S.; Cello, J.P.; Margaretten, W. Cytomegalovirus colitis. Report of the clinical, endoscopic, and pathologic findings in two patients with the acquired immune deficiency syndrome. *Gastroenterology* **1985**, *88*, 171–175. [CrossRef]

25. Springer, K.L.; Weinberg, A. Cytomegalovirus infection in the era of HAART: Fewer reactivations and more immunity. *J. Antimicrob. Chemother.* **2004**, *54*, 582–586. [CrossRef] [PubMed]

26. Humar, A.; Snydman, D. AST Infectious Diseases Community of Practice Cytomegalovirus in solid organ transplant recipients. *Am. J. Transplant.* **2009**, *9*, S78–S86. [CrossRef] [PubMed]

27. Azevedo, L.S.; Pierrotti, L.C.; Abdala, E.; Costa, S.F.; Strabelli, T.M.V.; Campos, S.V.; Ramos, J.F.; Latif, A.Z.A.; Litvinov, N.; Maluf, N.Z.; et al. Cytomegalovirus infection in transplant recipients. *Clinics* **2015**, *70*, 515–523. [CrossRef]

28. Simon, D.M.; Levin, S. Infectious complications of solid organ transplantations. *Infect. Dis. Clin. North Am.* **2001**, *15*, 521–549. [CrossRef]

29. Razonable, R.R.; Humar, A. Cytomegalovirus in solid organ transplant recipients-Guidelines of the American Society of Transplantation Infectious Diseases Community of Practice. *Clin. Transplant.* **2019**, *33*, e13512. [CrossRef]

30. Cho, S.-Y.; Lee, D.-G.; Kim, H.-J. Cytomegalovirus Infections after Hematopoietic Stem Cell Transplantation: Current Status and Future Immunotherapy. *Int. J. Mol. Sci.* **2019**, *20*, 2666. [CrossRef]

31. Travi, G.; Pergam, S.A. Cytomegalovirus pneumonia in hematopoietic stem cell recipients. *J. Intensiv. Care Med.* **2014**, *29*, 200–212. [CrossRef]

32. Lönnqvist, B.; Ringdèn, O.; Ljungman, P.; Wahren, B.; Gahrton, G. Reduced risk of recurrent leukaemia in bone marrow transplant recipients after cytomegalovirus infection. *Br. J. Haematol.* **1986**, *63*, 671–679. [CrossRef]

33. Kollman, C.; Howe, C.W.; Anasetti, C.; Antin, J.H.; Davies, S.M.; Filipovich, A.H.; Hegland, J.; Kamani, N.; Kernan, N.A.; King, R.; et al. Donor characteristics as risk factors in recipients after transplantation of bone marrow from unrelated donors: The effect of donor age. *Blood* **2001**, *98*, 2043–2051. [CrossRef] [PubMed]

34. Ljungman, P.; Brand, R.; Einsele, H.; Frassoni, F.; Niederwieser, D.; Cordonnier, C. Donor CMV serologic status and outcome of CMV-seropositive recipients after unrelated donor stem cell transplantation: An EBMT megafile analysis. *Blood* **2003**, *102*, 4255–4260. [CrossRef] [PubMed]

35. Behrendt, C.E.; Rosenthal, J.; Bolotin, E.; Nakamura, R.; Zaia, J.; Forman, S.J. Donor and recipient CMV serostatus and outcome of pediatric allogeneic HSCT for acute leukemia in the era of CMV-preemptive therapy. *Biol. Blood Marrow Transplant.* **2009**, *15*, 54–60. [CrossRef] [PubMed]

36. Farina, L.; Bruno, B.; Patriarca, F.; Spina, F.; Sorasio, R.; Morelli, M.; Fanin, R.; Boccadoro, M.; Corradini, P. The hematopoietic cell transplantation comorbidity index (HCT-CI) predicts clinical outcomes in lymphoma and myeloma patients after reduced-intensity or non-myeloablative allogeneic stem cell transplantation. *Leukemia* **2009**, *23*, 1131–1138. [CrossRef] [PubMed]

37. Schmidt-Hieber, M.; Labopin, M.; Beelen, D.; Volin, L.; Ehninger, G.; Finke, J.; Socié, G.; Schwerdtfeger, R.; Kröger, N.; Ganser, A.; et al. CMV serostatus still has an important prognostic impact in de novo acute leukemia patients after allogeneic stem cell transplantation: A report from the Acute Leukemia Working Party of EBMT. *Blood* **2013**, *122*, 3359–3364. [CrossRef]

38. Elmaagacli, A.H.; Steckel, N.K.; Koldehoff, M.; Hegerfeldt, Y.; Trenschel, R.; Ditschkowski, M.; Christoph, S.; Gromke, T.; Kordelas, L.; Ottinger, H.D.; et al. Early human cytomegalovirus replication after transplantation is associated with a decreased relapse risk: Evidence for a putative virus-versus-leukemia effect in acute myeloid leukemia patients. *Blood* **2011**, *118*, 1402–1412. [CrossRef]

39. Jang, J.E.; Kim, S.J.; Cheong, J.-W.; Hyun, S.Y.; Kim, Y.D.; Kim, Y.R.; Kim, J.S.; Min, Y.H. Early CMV replication and subsequent chronic GVHD have a significant anti-leukemic effect after allogeneic HSCT in acute myeloid leukemia. *Ann. Hematol.* **2015**, *94*, 275–282. [CrossRef]

40. Green, M.L.; Leisenring, W.M.; Xie, H.; Walter, R.B.; Mielcarek, M.; Sandmaier, B.M.; Riddell, S.R.; Boeckh, M. CMV reactivation after allogeneic HCT and relapse risk: Evidence for early protection in acute myeloid leukemia. *Blood* **2013**, *122*, 1316–1324. [CrossRef]

41. Mariotti, J.; Maura, F.; Spina, F.; Roncari, L.; Dodero, A.; Farina, L.; Montefusco, V.; Carniti, C.; Sarina, B.; Patriarca, F.; et al. Impact of cytomegalovirus replication and cytomegalovirus serostatus on the outcome of patients with B cell lymphoma after allogeneic stem cell transplantation. *Biol. Blood Marrow Transplant.* **2014**, *20*, 885–890. [CrossRef]

42. Yanada, M.; Yamamoto, K.; Emi, N.; Naoe, T.; Suzuki, R.; Taji, H.; Iida, H.; Shimokawa, T.; Kohno, A.; Mizuta, S.; et al. Cytomegalovirus antigenemia and outcome of patients treated with pre-emptive ganciclovir: Retrospective analysis of 241 consecutive patients undergoing allogeneic hematopoietic stem cell transplantation. *Bone Marrow Transplant.* **2003**, *32*, 801–807. [CrossRef]

43. Jeljeli, M.; Guérin-El Khourouj, V.; Porcher, R.; Fahd, M.; Leveillé, S.; Yakouben, K.; Ouachée-Chardin, M.; LeGoff, J.; Cordeiro, D.J.; Pédron, B.; et al. Relationship between cytomegalovirus (CMV) reactivation, CMV-driven immunity, overall immune recovery and graft-versus-leukaemia effect in children. *Br. J. Haematol.* **2014**, *166*, 229–239. [CrossRef] [PubMed]

44. Peric, Z.; Wilson, J.; Durakovic, N.; Ostojic, A.; Desnica, L.; Vranjes, V.R.; Marekovic, I.; Serventi-Seiwerth, R.; Vrhovac, R. Early human cytomegalovirus reactivation is associated with lower incidence of relapse of myeloproliferative disorders after allogeneic hematopoietic stem cell transplantation. *Bone Marrow Transplant.* **2018**, *53*, 1450–1456. [CrossRef] [PubMed]

45. Manjappa, S.; Bhamidipati, P.K.; Stokerl-Goldstein, K.E.; DiPersio, J.F.; Uy, G.L.; Westervelt, P.; Liu, J.; Schroeder, M.A.; Vij, R.; Abboud, C.N.; et al. Protective effect of cytomegalovirus reactivation on relapse after allogeneic hematopoietic cell transplantation in acute myeloid leukemia patients is influenced by conditioning regimen. *Biol. Blood Marrow Transplant.* **2014**, *20*, 46–52. [CrossRef] [PubMed]

46. Wang, C.; Zhang, X.; Bialek, S.; Cannon, M.J. Attribution of congenital cytomegalovirus infection to primary versus non-primary maternal infection. *Clin. Infect. Dis.* **2011**, *52*, e11–e13. [CrossRef] [PubMed]

47. Goderis, J.; De Leenheer, E.; Smets, K.; Van Hoecke, H.; Keymeulen, A.; Dhooge, I. Hearing loss and congenital CMV infection: A systematic review. *Pediatrics* **2014**, *134*, 972–982. [CrossRef] [PubMed]

48. Coppola, T.; Mangold, J.F.; Cantrell, S.; Permar, S.R. Impact of Maternal Immunity on Congenital Cytomegalovirus Birth Prevalence and Infant Outcomes: A Systematic Review. *Vaccines* **2019**, *7*, 129. [CrossRef]

49. PRISMA. Available online: http://www.prisma-statement.org/ (accessed on 23 April 2020).

50. Lanzieri, T.M.; Dollard, S.C.; Bialek, S.R.; Grosse, S.D. Systematic review of the birth prevalence of congenital cytomegalovirus infection in developing countries. *Int. J. Infect. Dis.* **2014**, *22*, 44–48. [CrossRef]

51. Fowler, K.B.; Boppana, S.B. Congenital cytomegalovirus infection. *Semin. Perinatol.* **2018**, *42*, 149–154. [CrossRef]

52. Stagno, S.; Pass, R.F.; Dworsky, M.E.; Britt, W.J.; Alford, C.A. Congenital and perinatal cytomegalovirus infections: Clinical characteristics and pathogenic factors. *Birth Defects Orig. Artic. Ser.* **1984**, *20*, 65–85.

53. Schopfer, K.; Lauber, E.; Krech, U. Congenital cytomegalovirus infection in newborn infants of mothers infected before pregnancy. *Arch. Dis. Child.* **1978**, *53*, 536–539. [CrossRef]

54. Diosi, P.; Babusceac, L.; Nevinglovschi, O.; Kun-Stoicu, G. Cytomegalovirus infection associated with pregnancy. *Lancet* **1967**, *2*, 1063–1066. [CrossRef]

55. Dworsky, M.; Yow, M.; Stagno, S.; Pass, R.F.; Alford, C. Cytomegalovirus infection of breast milk and transmission in infancy. *Pediatrics* **1983**, *72*, 295–299. [PubMed]

56. Hamprecht, K.; Maschmann, J.; Vochem, M.; Dietz, K.; Speer, C.P.; Jahn, G. Epidemiology of transmission of cytomegalovirus from mother to preterm infant by breastfeeding. *Lancet* **2001**, *357*, 513–518. [CrossRef]

57. Stagno, S.; Reynolds, D.W.; Pass, R.F.; Alford, C.A. Breast milk and the risk of cytomegalovirus infection. *N. Engl. J. Med.* **1980**, *302*, 1073–1076. [CrossRef] [PubMed]

58. Meyers, J.D. Cytomegalovirus infection following marrow transplantation: Risk, treatment, and prevention. *Birth Defects Orig. Artic. Ser.* **1984**, *20*, 101–117.

59. Van den Berg, A.P.; van Son, W.J.; Jiwa, N.M.; van der Bij, W.; Schirm, J.; van der Giessen, M.; The, T.H. Recent advances in the diagnosis of active cytomegalovirus infection after organ transplantation. *Transplant. Proc.* **1990**, *22*, 226–228. [PubMed]

60. Adler, S.P. Cytomegalovirus and child day care: Risk factors for maternal infection. *Pediatr. Infect. Dis. J.* **1991**, *10*, 590–594. [CrossRef]

61. Staras, S.A.S.; Dollard, S.C.; Radford, K.W.; Flanders, W.D.; Pass, R.F.; Cannon, M.J. Seroprevalence of cytomegalovirus infection in the United States, 1988–1994. *Clin. Infect. Dis.* **2006**, *43*, 1143–1151. [CrossRef]

62. Handsfield, H.H.; Chandler, S.H.; Caine, V.A.; Meyers, J.D.; Corey, L.; Medeiros, E.; McDougall, J.K. Cytomegalovirus infection in sex partners: Evidence for sexual transmission. *J. Infect. Dis.* **1985**, *151*, 344–348. [CrossRef]

63. Farrell, H.E.; Lawler, C.; Tan, C.S.E.; MacDonald, K.; Bruce, K.; Mach, M.; Davis-Poynter, N.; Stevenson, P.G. Murine Cytomegalovirus Exploits Olfaction To Enter New Hosts. *MBio* **2016**, *7*, e00251-16. [CrossRef]

64. Britt, W. Virus entry into host, establishment of infection, spread in host, mechanisms of tissue damage. In *Human Herpesviruses: Biology, Therapy and Immunoprophylaxis*; Arvin, A., Campadelli-Fiume, G., Mocarski, E., Moore, P.S., Roizman, B., Whitley, R., Yamanishi, K., Eds.; Cambridge University Press: Cambridge, UK, 2007; ISBN 978-0-521-82714-0.

65. Collins, T.M.; Quirk, M.R.; Jordan, M.C. Biphasic viremia and viral gene expression in leukocytes during acute cytomegalovirus infection of mice. *J. Virol.* **1994**, *68*, 6305–6311. [CrossRef] [PubMed]

66. Jackson, J.W.; Sparer, T. There Is Always Another Way! Cytomegalovirus' Multifaceted Dissemination Schemes. *Viruses* **2018**, *10*, 383. [CrossRef] [PubMed]

67. Boom, R.; Sol, C.J.A.; Schuurman, T.; Van Breda, A.; Weel, J.F.L.; Beld, M.; Ten Berge, I.J.M.; Wertheim-Van Dillen, P.M.E.; De Jong, M.D. Human cytomegalovirus DNA in plasma and serum specimens of renal transplant recipients is highly fragmented. *J. Clin. Microbiol.* **2002**, *40*, 4105–4113. [CrossRef] [PubMed]

68. Chen, X.Y.; Hou, P.F.; Bi, J.; Ying, C.M. Detection of human cytomegalovirus DNA in various blood components after liver transplantation. *Braz. J. Med. Biol. Res.* **2014**, *47*, 340–344. [CrossRef]

69. Eisenfeld, L.; Silver, H.; McLaughlin, J.; Klevjer-Anderson, P.; Mayo, D.; Anderson, J.; Herson, V.; Krause, P.; Savidakis, J.; Lazar, A. Prevention of transfusion-associated cytomegalovirus infection in neonatal patients by the removal of white cells from blood. *Transfusion* **1992**, *32*, 205–209. [CrossRef]

70. Heldwein, E.E. gH/gL supercomplexes at early stages of herpesvirus entry. *Curr. Opin. Virol.* **2016**, *18*, 1–8. [CrossRef]

71. Ryckman, B.J.; Jarvis, M.A.; Drummond, D.D.; Nelson, J.A.; Johnson, D.C. Human cytomegalovirus entry into epithelial and endothelial cells depends on genes UL128 to UL150 and occurs by endocytosis and low-pH fusion. *J. Virol.* **2006**, *80*, 710–722. [CrossRef]

72. Noriega, V.M.; Gardner, T.J.; Redmann, V.; Bongers, G.; Lira, S.A.; Tortorella, D. Human cytomegalovirus US28 facilitates cell-to-cell viral dissemination. *Viruses* **2014**, *6*, 1202–1218. [CrossRef]

73. Grefte, A.; Harmsen, M.C.; van der Giessen, M.; Knollema, S.; van Son, W.J.; The, T.H. Presence of human cytomegalovirus (HCMV) immediate early mRNA but not ppUL83 (lower matrix protein pp65) mRNA in polymorphonuclear and mononuclear leukocytes during active HCMV infection. *J. Gen. Virol.* **1994**, *75*, 1989–1998. [CrossRef]

74. Gerna, G.; Zipeto, D.; Percivalle, E.; Parea, M.; Revello, M.G.; Maccario, R.; Peri, G.; Milanesi, G. Human cytomegalovirus infection of the major leukocyte subpopulations and evidence for initial viral replication in polymorphonuclear leukocytes from viremic patients. *J. Infect. Dis.* **1992**, *166*, 1236–1244. [CrossRef]

75. Sinzger, C.; Jahn, G. Human cytomegalovirus cell tropism and pathogenesis. *Intervirology* **1996**, *39*, 302–319. [CrossRef] [PubMed]

76. Taylor-Wiedeman, J.; Sissons, P.; Sinclair, J. Induction of endogenous human cytomegalovirus gene expression after differentiation of monocytes from healthy carriers. *J. Virol.* **1994**, *68*, 1597–1604. [CrossRef] [PubMed]

77. Gerna, G.; Percivalle, E.; Baldanti, F.; Sozzani, S.; Lanzarini, P.; Genini, E.; Lilleri, D.; Revello, M.G. Human cytomegalovirus replicates abortively in polymorphonuclear leukocytes after transfer from infected endothelial cells via transient microfusion events. *J. Virol.* **2000**, *74*, 5629–5638. [CrossRef] [PubMed]

78. Dogra, P.; Miller-Kittrell, M.; Pitt, E.; Jackson, J.W.; Masi, T.; Copeland, C.; Wu, S.; Miller, W.E.; Sparer, T. A little cooperation helps murine cytomegalovirus (MCMV) go a long way: MCMV co-infection rescues a chemokine salivary gland defect. *J. Gen. Virol.* **2016**, *97*, 2957–2972. [CrossRef]

79. Selgrade, M.K.; Osborn, J.E. Role of macrophages in resistance to murine cytomegalovirus. *Infect. Immun.* **1974**, *10*, 1383–1390. [CrossRef]

80. Farrell, H.E.; Davis-Poynter, N.; Bruce, K.; Lawler, C.; Dolken, L.; Mach, M.; Stevenson, P.G. Lymph Node Macrophages Restrict Murine Cytomegalovirus Dissemination. *J. Virol.* **2015**, *89*, 7147–7158. [CrossRef]

81. Heo, J.; Dogra, P.; Masi, T.J.; Pitt, E.A.; de Kruijf, P.; Smit, M.J.; Sparer, T.E. Novel Human Cytomegalovirus Viral Chemokines, vCXCL-1s, Display Functional Selectivity for Neutrophil Signaling and Function. *J. Immunol.* **2015**, *195*, 227–236. [CrossRef]

82. Penfold, M.E.; Dairaghi, D.J.; Duke, G.M.; Saederup, N.; Mocarski, E.S.; Kemble, G.W.; Schall, T.J. Cytomegalovirus encodes a potent alpha chemokine. *Proc. Natl. Acad. Sci. USA* **1999**, *96*, 9839–9844. [CrossRef]

83. Yamin, R.; Lecker, L.S.M.; Weisblum, Y.; Vitenshtein, A.; Le-Trilling, V.T.K.; Wolf, D.G.; Mandelboim, O. HCMV vCXCL1 Binds Several Chemokine Receptors and Preferentially Attracts Neutrophils over NK Cells by Interacting with CXCR2. *Cell Rep.* **2016**, *15*, 1542–1553. [CrossRef]

84. Hassan-Walker, A.F.; Okwuadi, S.; Lee, L.; Griffiths, P.D.; Emery, V.C. Sequence variability of the alpha-chemokine UL146 from clinical strains of human cytomegalovirus. *J. Med. Virol.* **2004**, *74*, 573–579. [CrossRef]

85. Zheng, Q.; Tao, R.; Gao, H.; Xu, J.; Shang, S.; Zhao, N. HCMV-encoded UL128 enhances TNF-α and IL-6 expression and promotes PBMC proliferation through the MAPK/ERK pathway in vitro. *Viral. Immunol.* **2012**, *25*, 98–105. [CrossRef] [PubMed]

86. Saederup, N.; Lin, Y.C.; Dairaghi, D.J.; Schall, T.J.; Mocarski, E.S. Cytomegalovirus-encoded beta chemokine promotes monocyte-associated viremia in the host. *Proc. Natl. Acad. Sci. USA* **1999**, *96*, 10881–10886. [CrossRef]

87. Saederup, N.; Aguirre, S.A.; Sparer, T.E.; Bouley, D.M.; Mocarski, E.S. Murine cytomegalovirus CC chemokine homolog MCK-2 (m131-129) is a determinant of dissemination that increases inflammation at initial sites of infection. *J. Virol.* **2001**, *75*, 9966–9976. [CrossRef]

88. Ibanez, C.E.; Schrier, R.; Ghazal, P.; Wiley, C.; Nelson, J.A. Human cytomegalovirus productively infects primary differentiated macrophages. *J. Virol.* **1991**, *65*, 6581–6588. [CrossRef] [PubMed]

89. Lathey, J.L.; Spector, S.A. Unrestricted replication of human cytomegalovirus in hydrocortisone-treated macrophages. *J. Virol.* **1991**, *65*, 6371–6375. [CrossRef] [PubMed]

90. Waldman, W.J.; Knight, D.A.; Huang, E.H.; Sedmak, D.D. Bidirectional transmission of infectious cytomegalovirus between monocytes and vascular endothelial cells: An in vitro model. *J. Infect. Dis.* **1995**, *171*, 263–272. [CrossRef]

91. Bentz, G.L.; Jarquin-Pardo, M.; Chan, G.; Smith, M.S.; Sinzger, C.; Yurochko, A.D. Human cytomegalovirus (HCMV) infection of endothelial cells promotes naive monocyte extravasation and transfer of productive virus to enhance hematogenous dissemination of HCMV. *J. Virol.* **2006**, *80*, 11539–11555. [CrossRef]

92. Gerna, G.; Baldanti, F.; Revello, M.G. Pathogenesis of human cytomegalovirus infection and cellular targets. *Hum. Immunol.* **2004**, *65*, 381–386. [CrossRef]

93. Théry, C.; Amigorena, S. The cell biology of antigen presentation in dendritic cells. *Curr. Opin. Immunol.* **2001**, *13*, 45–51. [CrossRef]

94. Shenk, T.E.; Stinski, M.F. Human cytomegalovirus. In *Current Topics in Microbiology and Immunology*; Springer: Berlin/Heidelberg, Germany, 2008; ISBN 978-3-540-77348-1.

95. Sinclair, J.H.; Reeves, M.B. Human cytomegalovirus manipulation of latently infected cells. *Viruses* **2013**, *5*, 2803–2824. [CrossRef]

96. Sinclair, J. Manipulation of dendritic cell functions by human cytomegalovirus. *Expert Rev. Mol. Med.* **2008**, *10*, e35. [CrossRef] [PubMed]

97. Sinclair, J. Human cytomegalovirus: Latency and reactivation in the myeloid lineage. *J. Clin. Virol.* **2008**, *41*, 180–185. [CrossRef] [PubMed]

98. Yeager, A.S. Transfusion-acquired cytomegalovirus infection in newborn infants. *Am. J. Dis. Child.* **1974**, *128*, 478–483. [CrossRef] [PubMed]

99. Adler, S.P. Transfusion-associated cytomegalovirus infections. *Rev. Infect. Dis.* **1983**, *5*, 977–993. [CrossRef] [PubMed]

100. Tolpin, M.D.; Stewart, J.A.; Warren, D.; Mojica, B.A.; Collins, M.A.; Doveikis, S.A.; Cabradilla, C.; Schauf, V.; Raju, T.N.; Nelson, K. Transfusion transmission of cytomegalovirus confirmed by restriction endonuclease analysis. *J. Pediatr.* **1985**, *107*, 953–956. [CrossRef]

101. Thiele, T.; Krüger, W.; Zimmermann, K.; Ittermann, T.; Wessel, A.; Steinmetz, I.; Dölken, G.; Greinacher, A. Transmission of cytomegalovirus (CMV) infection by leukoreduced blood products not tested for CMV antibodies: A single-center prospective study in high-risk patients undergoing allogeneic hematopoietic stem cell transplantation (CME). *Transfusion* **2011**, *51*, 2620–2626. [CrossRef]

102. Taylor-Wiedeman, J.; Sissons, J.G.; Borysiewicz, L.K.; Sinclair, J.H. Monocytes are a major site of persistence of human cytomegalovirus in peripheral blood mononuclear cells. *J. Gen. Virol.* **1991**, *72*, 2059–2064. [CrossRef]

103. Mendelson, M.; Monard, S.; Sissons, P.; Sinclair, J. Detection of endogenous human cytomegalovirus in CD34$^+$ bone marrow progenitors. *J. Gen. Virol.* **1996**, *77*, 3099–3102. [CrossRef]

104. Reeves, M.B.; MacAry, P.A.; Lehner, P.J.; Sissons, J.G.P.; Sinclair, J.H. Latency, chromatin remodeling, and reactivation of human cytomegalovirus in the dendritic cells of healthy carriers. *Proc. Natl. Acad. Sci. USA* **2005**, *102*, 4140–4145. [CrossRef]

105. Slobedman, B.; Mocarski, E.S. Quantitative analysis of latent human cytomegalovirus. *J. Virol.* **1999**, *73*, 4806–4812. [CrossRef]

106. Saffert, R.T.; Kalejta, R.F. Human cytomegalovirus gene expression is silenced by Daxx-mediated intrinsic immune defense in model latent infections established in vitro. *J. Virol.* **2007**, *81*, 9109–9120. [CrossRef] [PubMed]

107. Yee, L.-F.; Lin, P.L.; Stinski, M.F. Ectopic expression of HCMV IE72 and IE86 proteins is sufficient to induce early gene expression but not production of infectious virus in undifferentiated promonocytic THP-1 cells. *Virology* **2007**, *363*, 174–188. [CrossRef] [PubMed]

108. O'Connor, C.M.; Murphy, E.A. A Myeloid Progenitor Cell Line Capable of Supporting Human Cytomegalovirus Latency and Reactivation, Resulting in Infectious Progeny. *J. Virol.* **2012**, *86*, 9854–9865. [CrossRef] [PubMed]

109. Penkert, R.R.; Kalejta, R.F. Human embryonic stem cell lines model experimental human cytomegalovirus latency. *MBio* **2013**, *4*, e00298-13. [CrossRef]

110. Poole, E.; McGregor Dallas, S.R.; Colston, J.; Joseph, R.S.V.; Sinclair, J. Virally induced changes in cellular microRNAs maintain latency of human cytomegalovirus in CD34$^+$ progenitors. *J. Gen. Virol.* **2011**, *92*, 1539–1549. [CrossRef]

111. Reeves, M.B.; Coleman, H.; Chadderton, J.; Goddard, M.; Sissons, J.G.P.; Sinclair, J.H. Vascular endothelial and smooth muscle cells are unlikely to be major sites of latency of human cytomegalovirus in vivo. *J. Gen. Virol.* **2004**, *85*, 3337–3341. [CrossRef]

112. Kondo, K.; Kaneshima, H.; Mocarski, E.S. Human cytomegalovirus latent infection of granulocyte-macrophage progenitors. *Proc. Natl. Acad. Sci. USA* **1994**, *91*, 11879–11883. [CrossRef]

113. Avdic, S.; Cao, J.Z.; Cheung, A.K.L.; Abendroth, A.; Slobedman, B. Viral interleukin-10 expressed by human cytomegalovirus during the latent phase of infection modulates latently infected myeloid cell differentiation. *J. Virol.* **2011**, *85*, 7465–7471. [CrossRef]

114. Bego, M.; Maciejewski, J.; Khaiboullina, S.; Pari, G.; St. Jeor, S. Characterization of an Antisense Transcript Spanning the UL81-82 Locus of Human Cytomegalovirus. *J. Virol.* **2005**, *79*, 11022–11034. [CrossRef]

115. Goodrum, F.; Reeves, M.; Sinclair, J.; High, K.; Shenk, T. Human cytomegalovirus sequences expressed in latently infected individuals promote a latent infection in vitro. *Blood* **2007**, *110*, 937–945. [CrossRef]

116. Hargett, D.; Shenk, T.E. Experimental human cytomegalovirus latency in CD14+ monocytes. *Proc. Natl. Acad. Sci. USA* **2010**, *107*, 20039–20044. [CrossRef] [PubMed]

117. Elder, E.; Sinclair, J. HCMV latency: What regulates the regulators? *Med. Microbiol. Immunol.* **2019**, *208*, 431–438. [CrossRef] [PubMed]

118. Murphy, J.C.; Fischle, W.; Verdin, E.; Sinclair, J.H. Control of cytomegalovirus lytic gene expression by histone acetylation. *EMBO J.* **2002**, *21*, 1112–1120. [CrossRef] [PubMed]

119. Reeves, M.B.; Lehner, P.J.; Sissons, J.G.P.; Sinclair, J.H. An in vitro model for the regulation of human cytomegalovirus latency and reactivation in dendritic cells by chromatin remodelling. *J. Gen. Virol.* **2005**, *86*, 2949–2954. [CrossRef] [PubMed]

120. Schwartz, M.; Stern-Ginossar, N. The Transcriptome of Latent Human Cytomegalovirus. *J. Virol.* **2019**, *93*. [CrossRef]

121. Rossetto, C.C.; Tarrant-Elorza, M.; Pari, G.S. Cis and trans acting factors involved in human cytomegalovirus experimental and natural latent infection of CD14 (+) monocytes and CD34 (+) cells. *PLoS Pathog.* **2013**, *9*, e1003366. [CrossRef]

122. Margueron, R.; Reinberg, D. The Polycomb complex PRC2 and its mark in life. *Nature* **2011**, *469*, 343–349. [CrossRef]

123. Stark, T.J.; Arnold, J.D.; Spector, D.H.; Yeo, G.W. High-resolution profiling and analysis of viral and host small RNAs during human cytomegalovirus infection. *J. Virol.* **2012**, *86*, 226–235. [CrossRef]

124. Meshesha, M.K.; Bentwich, Z.; Solomon, S.A.; Avni, Y.S. In vivo expression of human cytomegalovirus (HCMV) microRNAs during latency. *Gene* **2016**, *575*, 101–107. [CrossRef]

125. Pan, C.; Zhu, D.; Wang, Y.; Li, L.; Li, D.; Liu, F.; Zhang, C.-Y.; Zen, K. Human Cytomegalovirus miR-UL148D Facilitates Latent Viral Infection by Targeting Host Cell Immediate Early Response Gene 5. *PLoS Pathog.* **2016**, *12*, e1006007. [CrossRef]

126. Lau, B.; Poole, E.; Krishna, B.; Sellart, I.; Wills, M.R.; Murphy, E.; Sinclair, J. The Expression of Human Cytomegalovirus MicroRNA MiR-UL148D during Latent Infection in Primary Myeloid Cells Inhibits Activin A-triggered Secretion of IL-6. *Sci Rep* **2016**, *6*, 31205. [CrossRef] [PubMed]

127. Diggins, N.L.; Hancock, M.H. HCMV miRNA Targets Reveal Important Cellular Pathways for Viral Replication, Latency, and Reactivation. *Noncoding RNA* **2018**, *4*, 29. [CrossRef] [PubMed]

128. Kim, Y.; Lee, S.; Kim, S.; Kim, D.; Ahn, J.-H.; Ahn, K. Human cytomegalovirus clinical strain-specific microRNA miR-UL148D targets the human chemokine RANTES during infection. *PLoS Pathog.* **2012**, *8*, e1002577. [CrossRef] [PubMed]

129. Fu, M.; Gao, Y.; Zhou, Q.; Zhang, Q.; Peng, Y.; Tian, K.; Wang, J.; Zheng, X. Human cytomegalovirus latent infection alters the expression of cellular and viral microRNA. *Gene* **2014**, *536*, 272–278. [CrossRef]

130. Beisser, P.S.; Laurent, L.; Virelizier, J.L.; Michelson, S. Human cytomegalovirus chemokine receptor gene US28 is transcribed in latently infected THP-1 monocytes. *J. Virol.* **2001**, *75*, 5949–5957. [CrossRef]

131. Cheung, A.K.L.; Gottlieb, D.J.; Plachter, B.; Pepperl-Klindworth, S.; Avdic, S.; Cunningham, A.L.; Abendroth, A.; Slobedman, B. The role of the human cytomegalovirus UL111A gene in down-regulating CD4+ T-cell recognition of latently infected cells: Implications for virus elimination during latency. *Blood* **2009**, *114*, 4128–4137. [CrossRef]

132. Cheung, T.C.; Humphreys, I.R.; Potter, K.G.; Norris, P.S.; Shumway, H.M.; Tran, B.R.; Patterson, G.; Jean-Jacques, R.; Yoon, M.; Spear, P.G.; et al. Evolutionarily divergent herpesviruses modulate T cell activation by targeting the herpesvirus entry mediator cosignaling pathway. *Proc. Natl. Acad. Sci. USA* **2005**, *102*, 13218–13223. [CrossRef]

133. Poole, E.; Groves, I.; MacDonald, A.; Pang, Y.; Alcami, A.; Sinclair, J. Identification of TRIM23 as a cofactor involved in the regulation of NF-kappaB by human cytomegalovirus. *J. Virol.* **2009**, *83*, 3581–3590. [CrossRef]

134. Keyes, L.R.; Hargett, D.; Soland, M.; Bego, M.G.; Rossetto, C.C.; Almeida-Porada, G.; St Jeor, S. HCMV protein LUNA is required for viral reactivation from latently infected primary CD14⁺ cells. *PLoS ONE* **2012**, *7*, e52827. [CrossRef]

135. Weekes, M.P.; Tan, S.Y.L.; Poole, E.; Talbot, S.; Antrobus, R.; Smith, D.L.; Montag, C.; Gygi, S.P.; Sinclair, J.H.; Lehner, P.J. Latency-associated degradation of the MRP1 drug transporter during latent human cytomegalovirus infection. *Science* **2013**, *340*, 199–202. [CrossRef]

136. Hahn, G.; Jores, R.; Mocarski, E.S. Cytomegalovirus remains latent in a common precursor of dendritic and myeloid cells. *Proc. Natl. Acad. Sci. USA* **1998**, *95*, 3937–3942. [CrossRef] [PubMed]

137. Reeves, M.B.; Compton, T. Inhibition of inflammatory interleukin-6 activity via extracellular signal-regulated kinase-mitogen-activated protein kinase signaling antagonizes human cytomegalovirus reactivation from dendritic cells. *J. Virol.* **2011**, *85*, 12750–12758. [CrossRef]

138. Söderberg-Nauclér, C.; Fish, K.N.; Nelson, J.A. Reactivation of latent human cytomegalovirus by allogeneic stimulation of blood cells from healthy donors. *Cell* **1997**, *91*, 119–126. [CrossRef]

139. Humar, A.; St Louis, P.; Mazzulli, T.; McGeer, A.; Lipton, J.; Messner, H.; MacDonald, K.S. Elevated serum cytokines are associated with cytomegalovirus infection and disease in bone marrow transplant recipients. *J. Infect. Dis.* **1999**, *179*, 484–488. [CrossRef] [PubMed]

140. Tong, C.Y.; Bakran, A.; Williams, H.; Cuevas, L.E.; Peiris, J.S.; Hart, C.A. Association of tumour necrosis factor alpha and interleukin 6 levels with cytomegalovirus DNA detection and disease after renal transplantation. *J. Med. Virol.* **2001**, *64*, 29–34. [CrossRef] [PubMed]

141. Smith, M.G. Propagation of salivary gland virus of the mouse in tissue cultures. *Proc. Soc. Exp. Biol. Med.* **1954**, *86*, 435–440. [CrossRef]

142. Craig, J.M.; Macauley, J.C.; Weller, T.H.; Wirth, P. Isolation of intranuclear inclusion producing agents from infants with illnesses resembling cytomegalic inclusion disease. *Proc. Soc. Exp. Biol. Med.* **1957**, *94*, 4–12. [CrossRef]

143. Chee, M.S.; Bankier, A.T.; Beck, S.; Bohni, R.; Brown, C.M.; Cerny, R.; Horsnell, T.; Hutchison, C.A.; Kouzarides, T.; Martignetti, J.A. Analysis of the protein-coding content of the sequence of human cytomegalovirus strain AD169. *Curr. Top. Microbiol. Immunol.* **1990**, *154*, 125–169. [CrossRef]

144. Neff, B.J.; Weibel, R.E.; Buynak, E.B.; McLean, A.A.; Hilleman, M.R. Clinical and laboratory studies of live cytomegalovirus vaccine Ad-169. *Proc. Soc. Exp. Biol. Med.* **1979**, *160*, 32–37. [CrossRef]

145. Plotkin, S.A.; Farquhar, J.; Horberger, E. Clinical trials of immunization with the Towne 125 strain of human cytomegalovirus. *J. Infect. Dis.* **1976**, *134*, 470–475. [CrossRef]

146. Quinnan, G.V.; Delery, M.; Rook, A.H.; Frederick, W.R.; Epstein, J.S.; Manischewitz, J.F.; Jackson, L.; Ramsey, K.M.; Mittal, K.; Plotkin, S.A. Comparative virulence and immunogenicity of the Towne strain and a nonattenuated strain of cytomegalovirus. *Ann. Intern. Med.* **1984**, *101*, 478–483. [CrossRef]

147. Cha, T.A.; Tom, E.; Kemble, G.W.; Duke, G.M.; Mocarski, E.S.; Spaete, R.R. Human cytomegalovirus clinical isolates carry at least 19 genes not found in laboratory strains. *J. Virol.* **1996**, *70*, 78–83. [CrossRef] [PubMed]

148. Prichard, M.N.; Penfold, M.E.; Duke, G.M.; Spaete, R.R.; Kemble, G.W. A review of genetic differences between limited and extensively passaged human cytomegalovirus strains. *Rev. Med. Virol.* **2001**, *11*, 191–200. [CrossRef] [PubMed]

149. Dargan, D.J.; Douglas, E.; Cunningham, C.; Jamieson, F.; Stanton, R.J.; Baluchova, K.; McSharry, B.P.; Tomasec, P.; Emery, V.C.; Percivalle, E.; et al. Sequential mutations associated with adaptation of human cytomegalovirus to growth in cell culture. *J. Gen. Virol.* **2010**, *91*, 1535–1546. [CrossRef] [PubMed]

150. Wilkinson, G.W.G.; Davison, A.J.; Tomasec, P.; Fielding, C.A.; Aicheler, R.; Murrell, I.; Seirafian, S.; Wang, E.C.Y.; Weekes, M.; Lehner, P.J.; et al. Human cytomegalovirus: Taking the strain. *Med. Microbiol. Immunol.* **2015**, *204*, 273–284. [CrossRef]

151. Bradley, A.J.; Lurain, N.S.; Ghazal, P.; Trivedi, U.; Cunningham, C.; Baluchova, K.; Gatherer, D.; Wilkinson, G.W.G.; Dargan, D.J.; Davison, A.J. High-throughput sequence analysis of variants of human cytomegalovirus strains Towne and AD169. *J. Gen. Virol.* **2009**, *90*, 2375–2380. [CrossRef]

152. Jung, G.S.; Kim, Y.Y.; Kim, J.I.; Ji, G.Y.; Jeon, J.S.; Yoon, H.W.; Lee, G.-C.; Ahn, J.H.; Lee, K.M.; Lee, C.H. Full genome sequencing and analysis of human cytomegalovirus strain JHC isolated from a Korean patient. *Virus Res.* **2011**, *156*, 113–120. [CrossRef]

153. Sijmons, S.; Thys, K.; Mbong Ngwese, M.; Van Damme, E.; Dvorak, J.; Van Loock, M.; Li, G.; Tachezy, R.; Busson, L.; Aerssens, J.; et al. High-throughput analysis of human cytomegalovirus genome diversity highlights the widespread occurrence of gene-disrupting mutations and pervasive recombination. *J. Virol.* **2015**, *89*, 7673–7695. [CrossRef]

154. Dunn, W.; Chou, C.; Li, H.; Hai, R.; Patterson, D.; Stolc, V.; Zhu, H.; Liu, F. Functional profiling of a human cytomegalovirus genome. *Proc. Natl. Acad. Sci. USA* **2003**, *100*, 14223–14228. [CrossRef]

155. Murphy, E.; Yu, D.; Grimwood, J.; Schmutz, J.; Dickson, M.; Jarvis, M.A.; Hahn, G.; Nelson, J.A.; Myers, R.M.; Shenk, T.E. Coding potential of laboratory and clinical strains of human cytomegalovirus. *Proc. Natl. Acad. Sci. USA* **2003**, *100*, 14976–14981. [CrossRef]

156. Sinzger, C.; Hahn, G.; Digel, M.; Katona, R.; Sampaio, K.L.; Messerle, M.; Hengel, H.; Koszinowski, U.; Brune, W.; Adler, B. Cloning and sequencing of a highly productive, endotheliotropic virus strain derived from human cytomegalovirus TB40/E. *J. Gen. Virol.* **2008**, *89*, 359–368. [CrossRef] [PubMed]

157. Dolan, A.; Cunningham, C.; Hector, R.D.; Hassan-Walker, A.F.; Lee, L.; Addison, C.; Dargan, D.J.; McGeoch, D.J.; Gatherer, D.; Emery, V.C.; et al. Genetic content of wild-type human cytomegalovirus. *J. Gen. Virol.* **2004**, *85*, 1301–1312. [CrossRef] [PubMed]

158. Virus Pathogen Database and Analysis Resource (ViPR)—Genome Database with Visualization and Analysis Tools. Available online: https://www.viprbrc.org/brc/home.spg?decorator=vipr (accessed on 23 April 2020).

159. Pickett, B.E.; Sadat, E.L.; Zhang, Y.; Noronha, J.M.; Squires, R.B.; Hunt, V.; Liu, M.; Kumar, S.; Zaremba, S.; Gu, Z.; et al. ViPR: An open bioinformatics database and analysis resource for virology research. *Nucleic Acids Res.* **2012**, *40*, D593–D598. [CrossRef] [PubMed]

160. Renzette, N.; Bhattacharjee, B.; Jensen, J.D.; Gibson, L.; Kowalik, T.F. Extensive genome-wide variability of human cytomegalovirus in congenitally infected infants. *PLoS Pathog.* **2011**, *7*, e1001344. [CrossRef] [PubMed]

161. Renzette, N.; Gibson, L.; Jensen, J.D.; Kowalik, T.F. Human cytomegalovirus intrahost evolution-a new avenue for understanding and controlling herpesvirus infections. *Curr. Opin. Virol.* **2014**, *8*, 109–115. [CrossRef] [PubMed]

162. Renzette, N.; Pfeifer, S.P.; Matuszewski, S.; Kowalik, T.F.; Jensen, J.D. On the Analysis of Intrahost and Interhost Viral Populations: Human Cytomegalovirus as a Case Study of Pitfalls and Expectations. *J. Virol.* **2017**, *91*. [CrossRef]

163. Peck, K.M.; Lauring, A.S. Complexities of Viral Mutation Rates. *J. Virol.* **2018**, *92*. [CrossRef]

164. Vabret, N.; Bhardwaj, N.; Greenbaum, B.D. Sequence-Specific Sensing of Nucleic Acids. *Trends Immunol.* **2017**, *38*, 53–65. [CrossRef]

165. Christensen, M.H.; Paludan, S.R. Viral evasion of DNA-stimulated innate immune responses. *Cell. Mol. Immunol.* **2017**, *14*, 4–13. [CrossRef]

166. Hage, E.; Wilkie, G.S.; Linnenweber-Held, S.; Dhingra, A.; Suárez, N.M.; Schmidt, J.J.; Kay-Fedorov, P.C.; Mischak-Weissinger, E.; Heim, A.; Schwarz, A.; et al. Characterization of Human Cytomegalovirus Genome Diversity in Immunocompromised Hosts by Whole-Genome Sequencing Directly From Clinical Specimens. *J. Infect. Dis.* **2017**, *215*, 1673–1683. [CrossRef]

167. Suárez, N.M.; Wilkie, G.S.; Hage, E.; Camiolo, S.; Holton, M.; Hughes, J.; Maabar, M.; Vattipally, S.B.; Dhingra, A.; Gompels, U.A.; et al. Human Cytomegalovirus Genomes Sequenced Directly From Clinical Material: Variation, Multiple-Strain Infection, Recombination, and Gene Loss. *J. Infect. Dis.* **2019**, *220*, 781–791. [CrossRef] [PubMed]

168. Cudini, J.; Roy, S.; Houldcroft, C.J.; Bryant, J.M.; Depledge, D.P.; Tutill, H.; Veys, P.; Williams, R.; Worth, A.J.J.; Tamuri, A.U.; et al. Human cytomegalovirus haplotype reconstruction reveals high diversity due to superinfection and evidence of within-host recombination. *Proc. Natl. Acad. Sci. USA* **2019**, *116*, 5693–5698. [CrossRef] [PubMed]

169. Lassalle, F.; Depledge, D.P.; Reeves, M.B.; Brown, A.C.; Christiansen, M.T.; Tutill, H.J.; Williams, R.J.; Einer-Jensen, K.; Holdstock, J.; Atkinson, C.; et al. Islands of linkage in an ocean of pervasive recombination reveals two-speed evolution of human cytomegalovirus genomes. *Virus Evol.* **2016**, *2*, vew017. [CrossRef] [PubMed]

170. Houldcroft, C.J.; Cudini, J.; Goldstein, R.A.; Breuer, J. Reply to Jensen and Kowalik: Consideration of mixed infections is central to understanding HCMV intrahost diversity. *Proc. Natl. Acad. Sci. USA* **2020**, *117*, 818–819. [CrossRef] [PubMed]

171. Jensen, J.D.; Kowalik, T.F. A consideration of within-host human cytomegalovirus genetic variation. *Proc. Natl. Acad. Sci. USA* **2020**, *117*, 816–817. [CrossRef]

172. Paradowska, E.; Jabłońska, A.; Studzińska, M.; Kasztelewicz, B.; Zawilińska, B.; Wiśniewska-Ligier, M.; Dzierżanowska-Fangrat, K.; Woźniakowska-Gęsicka, T.; Kosz-Vnenchak, M.; Leśnikowski, Z.J. Cytomegalovirus glycoprotein H genotype distribution and the relationship with hearing loss in children. *J. Med. Virol.* **2014**, *86*, 1421–1427. [CrossRef]

173. Bradley, A.J.; Kovács, I.J.; Gatherer, D.; Dargan, D.J.; Alkharsah, K.R.; Chan, P.K.S.; Carman, W.F.; Dedicoat, M.; Emery, V.C.; Geddes, C.C.; et al. Genotypic analysis of two hypervariable human cytomegalovirus genes. *J. Med. Virol.* **2008**, *80*, 1615–1623. [CrossRef]

174. Stratton, K.R.; Durch, J.S.; Lawrence, R.S. *Vaccines for the 21st Century: A Tool for Decisionmaking*; Institute of Medicine (US) Committee to Study Priorities for Vaccine Development; National Academies Press: Washington, DC, USA, 2000; ISBN 978-0-309-05646-5.

175. Picone, O.; Vauloup-Fellous, C.; Cordier, A.G.; Guitton, S.; Senat, M.V.; Fuchs, F.; Ayoubi, J.M.; Grangeot Keros, L.; Benachi, A. A series of 238 cytomegalovirus primary infections during pregnancy: Description and outcome. *Prenat. Diagn.* **2013**, *33*, 751–758. [CrossRef]

176. Fouts, A.E.; Chan, P.; Stephan, J.-P.; Vandlen, R.; Feierbach, B. Antibodies against the gH/gL/UL128/UL130/UL131 complex comprise the majority of the anti-cytomegalovirus (anti-CMV) neutralizing antibody response in CMV hyperimmune globulin. *J. Virol.* **2012**, *86*, 7444–7447. [CrossRef]

177. Elek, S.D.; Stern, H. Development of a vaccine against mental retardation caused by cytomegalovirus infection in utero. *Lancet* **1974**, *1*, 1–5. [CrossRef]

178. Plotkin, S.A.; Furukawa, T.; Zygraich, N.; Huygelen, C. Candidate cytomegalovirus strain for human vaccination. *Infect. Immun.* **1975**, *12*, 521–527. [CrossRef] [PubMed]

179. Plotkin, S.A. Is there a formula for an effective CMV vaccine? *J. Clin. Virol.* **2002**, *25*, S13–S21. [CrossRef]

180. Wang, D.; Shenk, T. Human cytomegalovirus virion protein complex required for epithelial and endothelial cell tropism. *Proc. Natl. Acad. Sci. USA* **2005**, *102*, 18153–18158. [CrossRef] [PubMed]

181. Cui, X.; Meza, B.P.; Adler, S.P.; McVoy, M.A. Cytomegalovirus vaccines fail to induce epithelial entry neutralizing antibodies comparable to natural infection. *Vaccine* **2008**, *26*, 5760–5766. [CrossRef] [PubMed]

182. Adler, S.P.; Manganello, A.-M.; Lee, R.; McVoy, M.A.; Nixon, D.E.; Plotkin, S.; Mocarski, E.; Cox, J.H.; Fast, P.E.; Nesterenko, P.A.; et al. A Phase 1 Study of 4 Live, Recombinant Human Cytomegalovirus Towne/Toledo Chimera Vaccines in Cytomegalovirus–Seronegative Men. *J. Infect. Dis.* **2016**, *214*, 1341–1348. [CrossRef]

183. Wang, D.; Freed, D.C.; He, X.; Li, F.; Tang, A.; Cox, K.S.; Dubey, S.A.; Cole, S.; Medi, M.B.; Liu, Y.; et al. A replication-defective human cytomegalovirus vaccine for prevention of congenital infection. *Sci. Transl. Med.* **2016**, *8*, 362ra145. [CrossRef]

184. Liu, Y.; Freed, D.C.; Li, L.; Tang, A.; Li, F.; Murray, E.M.; Adler, S.P.; McVoy, M.A.; Rupp, R.E.; Barrett, D.; et al. A Replication-Defective Human Cytomegalovirus Vaccine Elicits Humoral Immune Responses Analogous to Those with Natural Infection. *J. Virol.* **2019**, *93*. [CrossRef]

185. Gerna, G.; Lilleri, D. Human cytomegalovirus (HCMV) infection/re-infection: Development of a protective HCMV vaccine. *New Microbiol.* **2019**, *42*, 1–20.

186. Gonczol, E.; Ianacone, J.; Ho, W.Z.; Starr, S.; Meignier, B.; Plotkin, S. Isolated gA/gB glycoprotein complex of human cytomegalovirus envelope induces humoral and cellular immune-responses in human volunteers. *Vaccine* **1990**, *8*, 130–136. [CrossRef]

187. Mitchell, D.K.; Holmes, S.J.; Burke, R.L.; Duliege, A.M.; Adler, S.P. Immunogenicity of a recombinant human cytomegalovirus gB vaccine in seronegative toddlers. *Pediatr. Infect. Dis. J.* **2002**, *21*, 133–138. [CrossRef]

188. Selinsky, C.; Luke, C.; Wloch, M.; Geall, A.; Hermanson, G.; Kaslow, D.; Evans, T. A DNA-based vaccine for the prevention of human cytomegalovirus-associated diseases. *Hum. Vaccin.* **2005**, *1*, 16–23. [CrossRef] [PubMed]

189. John, S.; Yuzhakov, O.; Woods, A.; Deterling, J.; Hassett, K.; Shaw, C.A.; Ciaramella, G. Multi-antigenic human cytomegalovirus mRNA vaccines that elicit potent humoral and cell-mediated immunity. *Vaccine* **2018**, *36*, 1689–1699. [CrossRef] [PubMed]

190. Nelson, C.S.; Jenks, J.A.; Pardi, N.; Goodwin, M.; Roark, H.; Edwards, W.; McLellan, J.S.; Pollara, J.; Weissman, D.; Permar, S.R. Human Cytomegalovirus Glycoprotein B Nucleoside-Modified mRNA Vaccine Elicits Antibody Responses with Greater Durability and Breadth than MF59-Adjuvanted gB Protein Immunization. *J. Virol.* **2020**, *94*. [CrossRef] [PubMed]

191. La Rosa, C.; Longmate, J.; Lacey, S.F.; Kaltcheva, T.; Sharan, R.; Marsano, D.; Kwon, P.; Drake, J.; Williams, B.; Denison, S.; et al. Clinical evaluation of safety and immunogenicity of PADRE-cytomegalovirus (CMV) and tetanus-CMV fusion peptide vaccines with or without PF03512676 adjuvant. *J. Infect. Dis.* **2012**, *205*, 1294–1304. [CrossRef] [PubMed]

192. Kirchmeier, M.; Fluckiger, A.-C.; Soare, C.; Bozic, J.; Ontsouka, B.; Ahmed, T.; Diress, A.; Pereira, L.; Schödel, F.; Plotkin, S.; et al. Enveloped virus-like particle expression of human cytomegalovirus glycoprotein B antigen induces antibodies with potent and broad neutralizing activity. *Clin. Vaccine Immunol.* **2014**, *21*, 174–180. [CrossRef] [PubMed]

193. Cayatte, C.; Schneider-Ohrum, K.; Wang, Z.; Irrinki, A.; Nguyen, N.; Lu, J.; Nelson, C.; Servat, E.; Gemmell, L.; Citkowicz, A.; et al. Cytomegalovirus vaccine strain towne-derived dense bodies induce broad cellular immune responses and neutralizing antibodies that prevent infection of fibroblasts and epithelial cells. *J. Virol.* **2013**, *87*, 11107–11120. [CrossRef] [PubMed]

194. Britt, W.J.; Prichard, M.N. New therapies for human cytomegalovirus infections. *Antivir. Res.* **2018**, *159*, 153–174. [CrossRef]

195. El Helou, G.; Razonable, R.R. Safety considerations with current and emerging antiviral therapies for cytomegalovirus infection in transplantation. *Expert Opin. Drug Saf.* **2019**, *18*, 1017–1030. [CrossRef]

196. Poole, C.L.; James, S.H. Antiviral Therapies for Herpesviruses: Current Agents and New Directions. *Clin. Ther.* **2018**, *40*, 1282–1298. [CrossRef]

197. Kim, E.S. Letermovir: First Global Approval. *Drugs* **2018**, *78*, 147–152. [CrossRef]

198. Stein, C.A.; Castanotto, D. FDA-Approved Oligonucleotide Therapies in 2017. *Mol. Ther.* **2017**, *25*, 1069–1075. [CrossRef] [PubMed]

199. Kimberlin, D.W.; Jester, P.M.; Sánchez, P.J.; Ahmed, A.; Arav-Boger, R.; Michaels, M.G.; Ashouri, N.; Englund, J.A.; Estrada, B.; Jacobs, R.F.; et al. Valganciclovir for symptomatic congenital cytomegalovirus disease. *N. Engl. J. Med.* **2015**, *372*, 933–943. [CrossRef] [PubMed]

200. Kotton, C.N.; Kumar, D.; Caliendo, A.M.; Huprikar, S.; Chou, S.; Danziger-Isakov, L.; Humar, A. The Transplantation Society International CMV Consensus Group The Third International Consensus Guidelines on the Management of Cytomegalovirus in Solid-organ Transplantation. *Transplantation* **2018**, *102*, 900–931. [CrossRef] [PubMed]

201. Green, M.L.; Leisenring, W.; Xie, H.; Mast, T.C.; Cui, Y.; Sandmaier, B.M.; Sorror, M.L.; Goyal, S.; Özkök, S.; Yi, J.; et al. Cytomegalovirus viral load and mortality after haemopoietic stem cell transplantation in the era of pre-emptive therapy: A retrospective cohort study. *Lancet Haematol.* **2016**, *3*, e119–e127. [CrossRef]

202. Littler, E.; Stuart, A.D.; Chee, M.S. Human cytomegalovirus UL97 open reading frame encodes a protein that phosphorylates the antiviral nucleoside analogue ganciclovir. *Nature* **1992**, *358*, 160–162. [CrossRef]

203. Gentry, B.G.; Gentry, S.N.; Jackson, T.L.; Zemlicka, J.; Drach, J.C. Phosphorylation of antiviral and endogenous nucleotides to di- and triphosphates by guanosine monophosphate kinase. *Biochem. Pharmacol.* **2011**, *81*, 43–49. [CrossRef]

204. Chou, S. Approach to drug-resistant cytomegalovirus in transplant recipients. *Curr. Opin. Infect. Dis.* **2015**, *28*, 293–299. [CrossRef]

205. Lischka, P.; Zimmermann, H. Antiviral strategies to combat cytomegalovirus infections in transplant recipients. *Curr. Opin. Pharmacol.* **2008**, *8*, 541–548. [CrossRef]

206. De Clercq, E.; Holý, A. Acyclic nucleoside phosphonates: A key class of antiviral drugs. *Nat. Rev. Drug Discov.* **2005**, *4*, 928–940. [CrossRef]

207. Wagstaff, A.J.; Bryson, H.M. Foscarnet. A reappraisal of its antiviral activity, pharmacokinetic properties and therapeutic use in immunocompromised patients with viral infections. *Drugs* **1994**, *48*, 199–226. [CrossRef]

208. Torres-Madriz, G.; Boucher, H.W. Immunocompromised hosts: Perspectives in the treatment and prophylaxis of cytomegalovirus disease in solid-organ transplant recipients. *Clin. Infect. Dis.* **2008**, *47*, 702–711. [CrossRef] [PubMed]

209. Razonable, R.R. Drug-resistant cytomegalovirus: Clinical implications of specific mutations. *Curr. Opin. Organ Transplant.* **2018**, *23*, 388–394. [CrossRef] [PubMed]

210. Stern, A.; Papanicolaou, G.A. CMV Prevention and Treatment in Transplantation: What's New in 2019. *Curr. Infect. Dis. Rep.* **2019**, *21*, 45. [CrossRef]

211. Maertens, J.; Cordonnier, C.; Jaksch, P.; Poiré, X.; Uknis, M.; Wu, J.; Wijatyk, A.; Saliba, F.; Witzke, O.; Villano, S. Maribavir for Preemptive Treatment of Cytomegalovirus Reactivation. *N. Engl. J. Med.* **2019**, *381*, 1136–1147. [CrossRef] [PubMed]

212. Buerger, I.; Reefschlaeger, J.; Bender, W.; Eckenberg, P.; Popp, A.; Weber, O.; Graeper, S.; Klenk, H.D.; Ruebsamen-Waigmann, H.; Hallenberger, S. A novel nonnucleoside inhibitor specifically targets cytomegalovirus DNA maturation via the UL89 and UL56 gene products. *J. Virol.* **2001**, *75*, 9077–9086. [CrossRef] [PubMed]

213. Schleiss, M.R.; Bernstein, D.I.; McVoy, M.A.; Stroup, G.; Bravo, F.; Creasy, B.; McGregor, A.; Henninger, K.; Hallenberger, S. The non-nucleoside antiviral, BAY 38-4766, protects against cytomegalovirus (CMV) disease and mortality in immunocompromised guinea pigs. *Antivir. Res.* **2005**, *65*, 35–43. [CrossRef]

214. Underwood, M.R.; Ferris, R.G.; Selleseth, D.W.; Davis, M.G.; Drach, J.C.; Townsend, L.B.; Biron, K.K.; Boyd, F.L. Mechanism of action of the ribopyranoside benzimidazole GW275175X against human cytomegalovirus. *Antimicrob. Agents Chemother.* **2004**, *48*, 1647–1651. [CrossRef]

215. Kotton, C.N. Updates on antiviral drugs for cytomegalovirus prevention and treatment. *Curr. Opin. Organ Transplant.* **2019**, *24*, 469–475. [CrossRef]

216. El Helou, G.; Razonable, R.R. Letermovir for the prevention of cytomegalovirus infection and disease in transplant recipients: An evidence-based review. *Infect. Drug Resist.* **2019**, *12*, 1481–1491. [CrossRef]

217. Vaismoradi, M.; Logan, P.A.; Jordan, S.; Sletvold, H. Adverse Drug Reactions in Norway: A Systematic Review. *Pharmacy* **2019**, *7*, 102. [CrossRef]